I. Synthesis of P-Chiral Phosphines and Methylphosphonate Oligonucleotides Enabled by a P(V) Reagent;

II. Convergent Total Synthesis of (–)-Cyclopamine

A thesis presented

by

Dongmin Xu

to

The Scripps Research Institute Graduate Program

in partial fulfillment of the requirements

for the degree of

Doctor of Philosophy

in the subject of

Chemistry

for

The Scripps Research Institute

La Jolla, California

November 2023

© Copyright 2023 by Dongmin Xu

All rights reserved.

Scripps Research

La Jolla, California
Jupiter, Florida

November 22, 2023

As members of the committee appointed to evaluate the thesis of **Dongmin Xu** we have read his thesis and found it to be acceptable without revision in partial fulfillment of The Scripps Research Institute's requirements for granting of the doctoral degree. Therefore, we the undersigned are satisfied that **Dongmin Xu** has met the requirements for the Doctorate of Philosophy Degree with respect to the written thesis, thesis presentation, and examination by this Committee.

Keary M. Engle, Ph.D., Chair

Phil S. Baran, Ph.D., Advisor

Ryan A. Shenvi, Ph.D.

Jin-Quan Yu, Ph.D.

Tian Qin, Ph.D., External Examiner
University of Texas Southwestern Medical Center

Office of Graduate Studies
10550 N. Torrey Pines Rd., TRY 10 • La Jolla, CA 92037 • p (858) 784-8469 • f (858) 784-2802
130 Scripps Way, 3B2 Jupiter, FL 33458 • p (561) 228-2370 • f (561) 228-3073
http://education.scripps.edu

Acknowledgements

Phil: You were such an amazing mentor to me during my PhD, and I cannot thank you enough for everything in the past five years. Thank you for taking me in, with no funding and despite me botching the visiting weekend interview by asking silly questions, and giving me the opportunity to work on projects I was truly interested in. Thank you for being supportive when I decided to switch to total synthesis in my 2nd year of PhD – a lot of PI's would have said no – and for being patient with me while I learned my way around. I will be forever grateful to you for that. From the big picture to experimental details, I know I can always turn to you for suggestions and you never hesitated to give them away. Your ability to approach a synthetic problem and quickly identify creative solutions for it is awe-inspiring, and I really appreciate the way you taught me to manage a total synthesis project – knowing when to push forward and when to regroup and test alternative strategies. Thank you for all the lessons and support throughout my PhD years!

Keary, Ryan, and Jin-Quan: Thank you for agreeing to serve as my committee members and for always being there to support me. I really appreciate all the valuable suggestions that you gave me in our committee meetings. It has been an absolute pleasure learning from you in the past five years!

Tian: Thank you for agreeing to serve as my external examiner. Even though we only overlapped for a month in the Baran lab when I just got started, you have taught me so much about chemistry and life over the years and I will always be grateful for that. I vividly remember the advice you gave me during my first week in the Baran lab, which

unfortunately must be translated from mandarin to English and loses most of its elegance, “Baran lab is a free space, but it is no place to goof around either. Work hard, learn as much as you can, give it your best effort, and you will certainly thrive as a chemist.” In retrospect, this is probably the best advice anyone could have ever given me for graduate school. Thank you and I know we will keep you touch!

Shelly: Thanks for being such an amazing lab admin Shelly. I still cannot wrap my head around how you manage this huge group on a daily basis. You were incredibly kind to everyone and I knew I can always count on you whenever I needed help. Wish you all the best!

Manolis: Manny! Man, where do I even start. Thank you for being such an amazing friend and collaborator throughout the years; you were the world’s best teammate someone could ever hope for. I always admired your work ethics, your positive attitude, your uncanny ability to come up with creative solutions to synthetic problems in the most unexpected yet reasonable way, and your impeccable taste for coffee and espresso. Words cannot possibly capture my gratitude for everything I have learned from you in the past three years, from little experimental tricks to big picture route design. I’m also going to miss our little coffee breaks in the afternoon where we share conversations about everything: chemistry, life, personal matters, geography, history, politics, and so much more. Thank you for everything Manolis, and I wish you nothing but the best as you start your new life back in Europe with Iro!

Anthony: Captain Rodriguez! Thank you for also being such an amazing collaborator and friend over the years. You're probably one of the most talented younger students I have ever seen. From your first day of joining the cyclopamine project I knew you were built different – you came in with a killer instinct and was ready to get to work. I was immensely impressed with the way you quickly absorbed all the new information and started to come up with your own ideas while also pumping out results and grams of materials in the hood from day 1. You also have incredible creativity and a sharp intuition when it comes to retrosynthetic analysis, as you always manage to come up with new and imaginative ways to make a molecule. Use them well and your next molecule will be smooth sailing for you! Besides chemistry, I'm going to miss all those fun anecdotes and cute pictures of Cooper and Barry. I was never really a dog person but they completely changed my mind haha. Best of luck on your next synthesis project and the rest of your PhD!

Benedikt: You were such an incredibly kind person and an amazing chemist; I don't think we would have done so much in the electrochemical cross coupling if it weren't for your help. I also really appreciate all the random conversations we had about literally anything, from Oktoberfest to our favorite Ghibli movies to which instant ramen tastes the best. Best of luck with your PhD, I will visit you in Munich when I have the chance!

Kyle K.: It was a great pleasure working with you on the P(V) project during my early years in the Baran lab. You were everyone's go-to person for any P(V) problems, and I cannot thank you enough for all the great suggestions and help you have given me while I

was learning my way around P(V) chemistry and graduate-level research in general. Wish you all the best in your future endeavors!

Julien: JV! It has been a privilege to work with you on the P(V) project and witness your tenure as a staff scientist in the Baran lab. Thank you for your constant support and understanding as I learned my way around, and for helping me find my footing in this lab when I just got started; I will be forever grateful to you for that. Best of luck with your independent career, and I wish you all the best with your new life in France. It's a shame that I cannot visit you and other friends in Europe in the near future due to my visa situation, but I guess *c'est la vie*!

Nazaret & Natalia: Thank you so much for helping me out on the P(V) paper! As a first-year student I was clueless about how to wrap up a project; thank you for showing me how it's done with flying colors. Both of you were always incredibly nice to me and I really enjoyed our collaboration together. I hope everything is going well back in Spain!

Cheng: The man, the mystery, the lawbreaker, the smooth criminal, the tattoo lover, the gym rat, the underground car racer, what is up my man. It's such an incredible experience to share my grad school years with a cool dude like you. You were such an amazing all-around chemist, both literature and experiment-wise, that I knew I can always turn to you for help. I have huge respect for your "full gas ahead" attitude towards chemistry and life, tackling one of the toughest molecules out there from your first day, putting in insane numbers of hours in the lab, running crazy scale-up's (that got safer as the years progressed,

let's say), and never once gave up even when the going got tough. You were also an extremely kind person who never hesitated to provide help and suggestions to those who needed them, including me. I missed sharing an office with you in our first year, cranking away in the lab together until the wee hours and then having a mini drag race down Genesee Avenue as we drove home. All in all, I think it's safe to say I've never met anyone like you before, and I don't think I will ever again. Continue to be yourself Cheng, I wish you all the best in Boston!

Max: We've known each other since our very first chemistry class at Boston College, and it has been an absolute pleasure to share so much of this journey with you. Echoing back to what you wrote in your thesis acknowledgement: I also remember that lab class where we made aspirin together, although it pains me to say that as an international student in his freshman year with broken English, I literally couldn't understand much of what you were saying that evening haha. Nevertheless, we somehow made it work and ended up with these perfect aspirin crystals! Little did I know back then that four years later both of us will be joining the Baran lab, and yet another four to five years later we would be getting our PhDs. Also, thanks for being such an amazing roommate during our first year in graduate school, even though we almost never saw each other in the apartment because of our drastically different biological clocks. I'm going to miss going to Leucadia with you on Sunday nights, sharing a pizza and washing it down with a cold one. It has been a blast knowing you for so many years – best of luck to you in Boston my old friend, shoot me a text if you're in town!

Jess: The Big Sister! It's been a pleasure sharing all these conversations with you while we were working late nights in the lab. I really enjoyed the stories of your adventures back in Peking University, and I will also forever remember how you smashed and outdrank everyone on the first night of our cabin trip to Big Bear. Best of luck at Neurocrine, and I am certain that you are in a happier place now.

Brendyn: Thanks for being an incredible hoodmate in the past three years Brendyn! We share the same kind of particularness when it comes to keeping the hood and bench area clean, which was probably why we got along so well when it comes to shared space and stuff. I really enjoyed the many chemistry "Sharpie talks" that we had right on our fume hood sashes; it was incredibly fun and rewarding to have someone to talk chemistry with and bounce ideas off each other while waiting for a TLC or running a column. Besides chemistry, I am also a huge fan of your taste for minigames (Geoguessr: the best 200 hours of my life I have ever wasted) and your ever-changing arsenal of catchphrases (phenomenal, right?). Chemistry hasn't been treating you well in recent years, but you are now very close and I'm sure you will finish this molecule in no time. Best of luck to the final year of your PhD; you'll soon be able to start this new life that you've always dreamed of!

Junchen: Greetings, master Tang. You're truly one of the most talented chemists I have ever seen, finishing portimines without breaking a sweat and still having enough gas in your tank afterwards to pursue a postdoc career in a different field. You are a quiet person in the lab but I did enjoy our occasional conversations, whether it was about chemistry or

our failing abilities to speak the Shanghainese dialect. I wish you all the best in the Parker lab; just remember to drive safely!

Kelly: I still can't get over the fact that I grabbed a cabbage instead of lettuces when we went shopping for the cabin trip at Vons, but hey it actually tasted not that bad in a sandwich. Thanks for organizing so many lab activities over the years and always keeping the fruit snacks in stock, all while you were slogging through the swamp of total synthesis like everyone else. Finishing daro and dyno was no easy feat! I also appreciate you answering all of my questions about job talks and what it's like working in a pharma. Wish you all the best and enjoy your final year of PhD!

Alex R.: I don't think I told you this but ever since the lab barbeque last year, Yi kept raving about "that cool girl with tats that also rode motorcycles." You're always super energetic in the lab and your enthusiasm for chemistry and life was contagious. You're also incredibly nice to everyone and never hesitated to help out those in need. Good luck with your project, I'm sure you and Fabian will finish it in no time!

Tim G.: I really missed sharing an office with you Tim. You were always incredibly kind to everyone and we've had so many great conversations in that office over the years. I also have fond memories of some quite sweaty bootcamp molecules that we tried to tackle together; even though it was miserable for everyone back then, your energy and constant positive attitude made it so much better. Wish you all the best with your next chapter of life!

Alex P.: Yee-haw, am I right? You are one of the most talented chemists I've seen in this lab, and I always admired your courage to choose to tackle the toughest synthetic problems out there, all on your own and since your first day in this lab. I also enjoyed all these morning conversations we had over coffee in the 439 office, after Manolis, Anthony and I got out of the LEO meetings. Even though you hit some rough patches early on in your PhD, you have proven yourself capable of taming even the baddest molecule in town. Best of luck with your total synthesis!

Christine: I still cannot believe you found my note at that boba shop. Now everyone knows my secret! Jokes aside, you are an amazing chemist and an incredibly nice person to everyone in this lab. I will miss going to the Thai food truck with you and the rest of the gang, and also you teaching me the subtle differences in Cantonese pronunciations ("shrimp dumpling" vs. "black dog" is still difficult for me but I think I'm getting there). Good luck with your project, I'm sure it'll be smooth sailing for someone with your talent and determination!

Philipp: I hope I didn't waste too much of your time forcing conversations on you while I was waiting for the solvent system haha. You're an incredibly talented chemist with a first-author publication already at such an early stage of your PhD. Just keep working hard and you'll get more in no time!

Pranali: You were such an incredibly kind person to everyone and I will really miss going to the Thai food truck or the coffee cart with you and the usual gang. I hope you're happy

in the Huang lab and I'm sure great things await you in the future. I know we will keep in touch!

Maithili, Mahdi, and Yiheng (Anna): Even though we only overlapped for a short amount of time, it is clear to me that all three of you are extremely talented chemists who are ready for whatever this lab may throw your way. Best of luck to your projects! If you need anything from me, don't hesitate to reach out.

Matteo: Despite what we say to each other every day (the world does not need to know the content of the sticky notes we left on each other's desks) you are one of my closest friends in the lab. Thank you for listening to my incessant complaints about everything inside or outside the lab; I hope I returned the favor by telling you about all the good Chinese restaurants in San Diego. I will miss all the fun we had in the 436 office, from conversations where we attempted to educate each other on the cultural difference between our home countries, to the office ball tournament where I unfortunately dominated you from the very beginning. Wish you all the best my friend, let's keep in touch!

Tamara: You have made everyone's life so much easier (except Max) and I don't think we ever thanked you enough for that. I still remember your first day in the lab: I was giving you safety training as the safety officer while thinking to myself, "there's no way this is gonna work; she'll need to do the work of several people!" Boy was I wrong – you were truly a superwoman. You took over the most tedious group jobs, ordered and unpacked mountains of consumables every week, managed to improve our horrendous chemical

inventory, and yet still found time to teach yourself flow chemistry and contribute to several projects in the lab. Thank you for being an incredible lab manager Tamara, we honestly don't deserve you. Wish you all the best!

Chi: The legend of Baran lab! It was a privilege to get to know you since my first day in the lab, and also sharing the 436 office with you for two years. You were such an incredible chemist with three finished natural products under your belt just during your postdoc years (!), and I can never thank you enough for all the chemistry wisdom you have imparted to me over the years. I will also miss sneaking into the basketball court of the nearby Hilton and playing pick-up games with you and the rest of the group. Best of luck at BMS, I wish you and your family all the best!

John: Bring it in, my Clash buddy! You clearly have what it takes to succeed in graduate school – you work hard, think deep, and always keep your composure through the toughest situations. I'm sure you will get all the offers you want this coming application season, and I can't wait to see you starting your next chapter of life!

Alberto: Let's go Celtics! I really enjoyed chatting with you about basketball and talking smack about the Lakers over the years. It's such a coincidence that a Spanish and a Chinese person share a connection over Boston's sports teams, but here we are and it has been an absolute blast. You were also one of the kindest people I've ever met in this lab, always being nice to everyone and never letting the stress and pressure of this lab affect your demeanors. I wish you and Simona all the best as you start your new life in Switzerland!

Benxiang: Thank you so much for helping us troubleshoot the DDCC reaction. It has been a privilege working in the same bay as you – I really enjoyed our conversations about chemistry and life while we were waiting for rotavaps or using the balances. Wish you all the best with your future endeavors!

Fabian: You have such encyclopedic knowledge of both terpene synthesis and peptide natural products that I know I can always turn to you for help. I really enjoyed our chemistry conversations in the office, and I will miss our "paper shaming" sessions in the afternoon where we check out the recent ASAP papers and dish out "fair" judgements of them. Wish you all the best with your project!

Jiawei: It has been an absolute pleasure sitting next to you in the 436 office! I will miss all the conversations we had about chemistry and your graduate school years, as well as the tips and tricks you learned from your recent fishing trips. Best of luck with your project!

You-Chen: It has been a privilege for me to work next to you in the past three years and get a front-row seat to the total syntheses of darobactin and dynobactin. Thank you for teaching me so much about peptide chemistry, and for giving me invaluable tips and suggestions about the job search process. I wish you and your family all the best, and since both of us are staying in San Diego we will definitely stay in touch!

Nate: I never thought I would find another PC enthusiast in the lab. It has been a blast talking with you about some random tech news and complaining about how Apple overcharges everything. You were also such an amazing chemist with a killer total synthesis

from your PhD; you and Brendyn make one hell of a team and I'm sure you will finish this molecule in no time. Best of luck, you are in the home stretch!

Debby: You were always incredibly kind to everyone in the lab and I really enjoyed our conversations throughout the years. I will miss the stories of your adventures back in Italy or your progress in figure skating classes. Best of luck at Takeda, and I know we will stay in touch!

Karolina: Thank you for being such an amazing hoodmate during your time in the Baran lab! You were always so kind to me and I really enjoyed our random conversations, from Polish culture to the best way to grab Fastpasses at Disneyland. I also remember the day we fixed the vacuum pump together and got it to go below 1 torr for the first time (and also probably the last time, unfortunately). It has been a blast knowing you and I wish you nothing but the best!

Kevin: I *really* tried to beat your high score in Aim Lab (after you made sure I see it by posting that screenshot on my fume hood) but I guess we will never see that day coming. You were such an amazing chemist and I always admired your constantly positive attitude and your ability to keep your composure even in the toughest situations. Best of luck at Gilead; shoot me a message on Steam anytime if you want to play Counter-Strike!

Kawa: Thanks for being such an amazing staff scientist throughout the years Kawa. You were ultra-efficient in the lab and always got straight to the point, and your passion for

chemistry was contagious to everyone around you. Thanks for putting up with my naïve electrochemistry related questions when I was working with the DDCC reaction. Congrats on baby number two, and I wish you and your family all the best!

Pengfei: Professor Hu! It has been an absolute blast working in the same shift as you during the tough COVID years. Thank you so much for all your valuable suggestions when I was still finding my footing after switching to a total synthesis project. I hope I was able to return the favor by helping you improve your driving haha. Best of luck at Westlake University, they are lucky to have someone with your talent and passion for chemistry.

Ming (Big Mike): Thank you so much for being an amazing senior student even after you left the lab. I really appreciate you taking me and Cheng to dinners when we were still first years; it was extremely helpful to get advice from a Baran lab veteran when I was still learning my way around this lab and chemistry research in general. Best of luck with law school, I know we will keep in touch!

All Baran lab members, former and current: I cannot possibly list everyone that I have crossed path with in the past five years in the Baran lab – I will need a separate word document for that! But I am truly thankful to everyone who taught me something, helped me out, had a nice conversation with me, or maybe shared a laugh or two together, at any point over the years. All of you made the Baran lab a truly special place for research and personal growth, and I will forever cherish all these memories. Thank you!

Mom and Dad: Everything I have achieved to this day I owe so much of it to your love and support. You were never like the traditional/stereotypical Chinese parents; thank you so much for creating a free space for me and raising me to be an independent person while always being there to support me at the same time. I don't think I will ever be able to repay you for everything you have done for me. I love you both!

Yi: Saving the best for the last. Words simply cannot capture how much I owe you for everything that I have achieved today. I cannot even imagine being in this place right now without your constant love and support throughout this ordeal. You are my best friend, my soul mate, and the only person that really understands me. I wish I could go back to the moment we met, four years ago at Scripps at that end-of-first-year celebration, and tell my younger self what an amazing women you are. I am so excited that both of us will be getting our PhD's and planning our future life together soon. My original plan was to pop the question after I graduate, but I couldn't even wait that long. Thanks for saying yes, I love you so much and can't wait to spend the rest of my life with you.

Table of Contents

Abstract **1**

List of abbreviations **3**

Chapter 1. Synthesis of P-Chiral Phosphines and Methylphosphonate Oligonucleotides Enabled by a P(V) Reagent **10**

Introduction **10**

Figure 1.1. Background and Introduction to the Π Reagent Platform 11

Stereospecific C–P Bond Formation: Reagent Development **13**

Figure 1.2 Initial Explorations and Reagent Development 13

Modular Assembly of P-Chiral Phosphines **14**

Table 1.1 Leaving Group Optimization for the Final Displacement Reaction 15

Figure 1.3. Scope of Π-Based Chiral Phosphine / Phosphine Oxide Synthesis 16

A Solution to Stereospecific MPO Synthesis **18**

Figure 1.4. Workflow and Optimization for Π-based MPO Synthesis 18

Figure 1.5. Scope of Π-Based Chiral MPO Synthesis 20

Conclusion and Outlook **21**

Figure 1.6. Stereochemical Roadmap of the P(V) Reagents 22

References **23**

Experimental **29**

Synthesis of Π Reagents 30

Table S1.1: X-ray crystal structure of 1.1b 34

Initial Exploration with Π Reagents 35

Table S1.2: X-Ray crystal structure of dead-end product 1.4 35

Stereochemical Assignments 37

Table S1.3: X-ray crystal structure of 1.8a 38

Table S1.4: X-ray crystal structure of 1.11a 39
Table S1.5: X-ray crystal structure of 1.34a 40
Synthesis of Grignard and Organolithium Reagents..... 42
General Procedure A: P-Chiral Phosphine Synthesis – Loading 44
General Procedures B and C: P-Chiral Phosphine Synthesis – Coupling 58
General Procedure D: P-Chiral Phosphine Synthesis – Leaving Group Installation 76
Table S1.6: Optimization Table of OMe Installation 77
General Procedures E, F, and G: P-Chiral Phosphine Synthesis – Displacement 85
Stereospecific Reduction of Phosphine Oxides 120
List of Failed Substrates..... 122
General Procedure G: Synthesis of 3'-O-Protected Nucleosides..... 123
General Procedure H: MPO Synthesis – Loading 125
General Procedure I: MPO Synthesis – Coupling 134
Ψ Activation of MPO Dimers 160
P-Chiral Phosphine: Inversed-Order Loading and Coupling Experiment 163
MPO: Inversed-Order Loading and Coupling Experiment..... 164
Chapter 1 Experimental References..... 166
NMR Spectra..... 168
Distribution of Credit 367
Chapter 2. Convergent Total Synthesis of (–)-Cyclopamine 368
Background 368
Figure 2.1 Cyclopamine and Related Natural Products..... 369
Figure 2.2. Cyclopropanation/Ring-Expansion *En Route* to Saridegib (IPI-926) .. 370
Previous Syntheses and Progress-Towards Studies 371
Figure 2.3 Masamune's Synthesis of Jervine..... 371

Figure 2.4 Giannis's Semisynthesis of Cyclopamine 372

1st Generation Route 374

Figure 2.5 Retrosynthetic Plan for the 1st Generation Route 374

Figure 2.6 Early-Stage Explorations for the 1st Generation Route. 375

Figure 2.7 Addition of Alkenyl Nucleophiles to the DHEA Scaffold. 376

Figure 2.8 Final Efforts Towards the 1st Generation Route 378

2nd Generation Route 380

Figure 2.9 Retrosynthetic Plan for the 2nd Generation Route 381

Figure 2.10 Unsuccessful HAT Cyclization *En Route* to the ABC Fragment..... 382

Figure 2.11 Synthetic Strategies Towards Enantiopure 2.63 383

Figure 2.12 Synthesis of the ABC Fragment and Endgame Model Studies 384

Figure 2.13 Preparation of the *O*-Benzyl Variant of the ABC Fragment 386

Figure 2.14 Synthesis of the Lactone Intermediate *En Route* to the EF Fragment. 387

Figure 2.15 Attempts to Elaborate the Lactone to the EF Fragment 389

Figure 2.16. Synthesis of the EF Fragment *via* Tsuji-Trost Cyclization..... 390

Figure 2.17. Endgame Sequence of the 2nd Generation Route 391

3rd Generation Routes 393

Figure 2.18 Doubly Decarboxylative Cross Coupling (DDCC) Strategy..... 393

Figure 2.19 Alternative DDCC Substrates and Control Experiments..... 394

Figure 2.20. A Prins Approach Towards the Endgame Sequence 396

Figure 2.21. Other Potential Prins Substrates 398

4th Generation/Final Route 399

Figure 2.22. Retrosynthetic Analysis of the 4th Generation Route 400

Figure 2.23 Synthesis of the ABC Fragment 401

Figure 2.24 Synthesis of the EF Fragment..... 402

Figure 2.25 Completion of the Total Synthesis of (–)-Cyclopamine 405

References 408

Experimental 416

Route Details and Optimization Tables 417

Detailed Synthesis of the ABC Fragment 417

Detailed Synthesis of the EF Fragment 418

Detailed Endgame Sequence 419

Calculation of Ideality Percentage 420

Table S2.1 Optimization of Enone Alkylation 421

Table S2.2 Optimization of the Doubly Decarboxylative Cross Coupling 422

Table S2.3 Optimization of Prins Cyclization 423

Table S2.4 Optimization of Enone 1,4-Reduction 424

Table S2.5 Optimization of Aza-Michael/Zn Reduction 425

Table S2.6 Optimization of Halocyclization 426

Table S2.7 Model Studies of the 1,2-Addition to the EF Enone 427

Table S2.8 Optimization of Tsuji-Trost Cyclization 428

Table S2.9 Optimization of RCM 430

Reaction Protocols and Characterization Data 431

Spectra Comparison Between Synthetic and Natural Cyclopamine 462

Chapter 2 Experimental References 469

NMR Spectra 471

X-Ray Crystallography Data 513

Distribution of Credit 588

Abstract

Chapter 1: Synthesis of P-Chiral Phosphines and Methylphosphonate Oligonucleotides Enabled by a P(V) Reagent

(*J. Am. Chem. Soc.* **2020**, *142*, 5785–5792.)

P-chiral phosphines represent an important class of ligands for asymmetric catalysis, one notable example being the DIPAMP ligand for an asymmetric hydrogenation reaction in the *L*-DOPA process. On the other hand, methylphosphonate oligonucleotides is an under-explored nucleotide modification that leads to unique chemical and biological properties but is plagued by difficulty in its synthesis. Herein we present a unified approach to access these two distinctive chemical spaces: utilization of a limonene-based P(V) reagent nicknamed Π (Phosphorous Incorporation, PI) for the modular, scalable, and stereospecific synthesis of P-chiral phosphines and methylphosphonate oligonucleotides. Synthesized from *trans*-limonene oxide, this reagent exhibited a different reactivity profile from that of the *cis*-limonene-derived Ψ reagents (Phosphorous–Sulfur Incorporation, PSI) previously disclosed. Essentially a chiral $POCl_3$ equivalent, Π can undergo addition of three carbon nucleophiles and a stereospecific reduction to afford P-chiral phosphines, or addition of a methyl nucleophile followed by two nucleosides to yield stereodefined methylphosphonate oligonucleotides. While both (+) and (–)-Π are available, only one is required to access both enantiomers of the final product: the stereospecific nature of each addition resulted in an enantiodivergent design where the order of addition dictated the stereochemical outcome.

Chapter 2: Convergent Total Synthesis of (–)-Cyclopamine

(*J. Am. Chem. Soc.* **2023**, *145*, 21760–21765.)

The *Veratrum* alkaloid cyclopamine was first known for (and named after) the grotesque birth defects it caused to new-born lambs, where they were found only with one eye (cyclopia) and died shortly after. Studies have shown that cyclopamine is a potent inhibitor of the hedgehog (hh) signaling pathway, which is essential for the correct differentiation of embryos during their development. For this reason, cyclopamine was quickly recognized as a potential anti-cancer agent and numerous medicinal analogs were reported, such as the semi-synthetic analog Saridegib (IPI-926). Prior efforts towards the synthesis of cyclopamine and its related family members relied heavily on semi-synthetic strategies, where a steroid progenitor with most of the carbon skeleton in place was further elaborated to the target structure. However, the unique structure of cyclopamine often necessitated intricate skeletal rearrangements and labor-intensive downstream functionalizations. This thesis discloses a concise and enantioselective total synthesis of (–)-cyclopamine with a 16-step longest linear sequence (LLS). Notable features of this work include a *de novo* synthesis of the EF ring system *via* a strain-inducing halocyclization process, a key Tsuji-Trost cyclization to construct the fully substituted, spirocyclic THF motif with exquisite diastereocontrol, and a late-stage ring-closing metathesis (RCM) reaction to forge the central tetrasubstituted olefin.

List of abbreviations

[O]	oxidation
°	degree
9-BBN	9-Borabicyclo[3.3.1]nonane
A	adenine
AAA	asymmetric allylic alkylation
Ac	acetate
acac	acetylacetonate
AcOH	acetic acid
Ad	1-adamantyl
AIBN	azobisisobutyronitrile
aq.	aqueous
Ar	aryl
ASO	anti-sense oligonucleotide
B(pin)	boronic pinacol ester
Bn	benzyl
Boc	*tert*-butyloxycarbonyl
Bs	benzenesulfonyl
Bz	benzoyl
C	cytosine
cat.	catalytic
CBS	Corey-Bakshi-Shibata
Cbz	carboxybenzyl

$CDCl_3$	chloroform-*d*
Chx	cyclohexyl
conc.	concentrated
conv.	conversion
CoPc	cobalt(II) phthalocyanine
Cp	cyclopentadienyl
Cy	cyclohexyl
d	days
d.r. or *dr*	diastereomeric ratio
dA	deoxyadenosine
dba	dibenzylideneacetonate
DBU	1,8-diazabicyclo(5.4.0)undec-7-ene
dC	deoxycytidine
DC	direct current
DCM	dichloromethane
DDCC	doubly decarboxylative cross coupling
DDQ	2,3-dichloro-5,6-dicyano-1,4-benzoquinone
decomp.	decomposition
dG	deoxyguanosine
DHEA	dehydroepiandrosterone
DIBAL-H	diisobutylaluminium hydride
DIC	N,N'-Diisopropylcarbodiimide

DIPAMP	(ethane-1,2-diyl)bis[(2-methoxyphenyl)(phenyl)phosphane]
DME	dimethoxyethane
DMF	dimethylformamide
DMI	1,3-dimethyl-2-imidazolidinone
DMS	dimethylsulfide
DMTr	dimethoxytrityl
DNA	deoxyribonucleic acid
dpm	dipivaloylmethanato
DPPA	diphenylphosphoryl azide
dppbz	1,2-bis(diphenylphosphino)benzene
dppf	1,1'-bis(diphenylphosphino)ferrocene
dppp	1,3-bis(diphenylphosphino)propane
dT	deoxythymidine
eq. or equiv.	equivalents
ESI	electron-spray ionization
Et	ethyl
Et_2O	diethyl ether
EtOAc	ethyl acetate
Fc	ferrocenyl
FG	functional group
G	guanine
G-II	Grubbs 2nd generation catalyst

h	hours
HAT	hydrogen-atom transfer
HG-II	Hoveyda-Grubbs 2nd generation catalyst
hh	hedgehog
HMDS	hexamethyldisilazane
HMPA	hexamethylphosphoramide
HPLC	high performance liquid chromatography
HRMS	high resolution mass spectrometry
HWE	Horner-Wadsworth-Emmons
Hz	Hertz
hν	light
Ipc	isopinocampheyl
*i*Pr	isopropyl
KHMDS	potassium hexamethyldisilazide
L-DOPA	*L*-3,4-dihyroxyphenylalanine
LAH	lithium aluminum hydride
LCMS	liquid chromatography mass spectrometry
LDA	lithium diisopropylamide
LHMDS	lithium hexamethyldisilazide
LiDBB	lithium 4,4'-di-*tert*-butylbiphenylide
LLS	longest linear sequence
M	molar
mA	milliamp

Me	methyl
MeCN	acetonitrile
MeOH	methanol
MePh	toluene
mg	milligram
mmol	millimole
MOA	mechanism of action
mol	mole
MOM	methoxymethyl
MPO	methylphosphonate oligonucleotides
NaHMDS	sodium hexamethyldisilazide
NBS	*N*-bromosuccinimide
*n*Bu	*n*-butyl
NHK	Nozaki-Hiyama-Kishi
NHPI	*N*-hydroxyphthalimide
NIS	*N*-iodosuccinimide
NMO	*N*-methylmorpholine
NMP	*N*-methyl-2-pyrrolidone
NMR	nuclear magnetic resonance
NOESY	nuclear Overhauser effect spectroscopy
Nu	nucleophile
OAc	acetate
OTf	triflate

P(III)	phosphorus (III)
P(V)	phosphorus (V)
PBS	phosphate buffer system
PG	protecting group
Ph	phenyl
PI	phosphorus incorporation
PMB	*p*-methoxybenzyl
PMHS	poly(methylhydrosiloxane)
ppm	parts per million
PSI	phosphorus sulfur incorporation
pTLC	preparative thin-layer chromatography
*p*TSA	*p*-toluenesulfonic acid
pyr	pyridine
quant.	quantitative
RAE	redox-active ester
rAP	rapid alternating polarity
RCM	ring-closing metathesis
ref.	reference
R_f	retention factor
RNA	ribonucleic acid
rt	room temperature
T	thymine
TBAF	tetra-*n*-butylammonium fluoride

TBDPS	*tert*-butyldiphenylsilyl
TBHP	*tert*-butylhydroperoxide
TBS	*tert*-butyldimethylsilyl
*t*Bu	*tert*-butyl
TCNHPI	3,4,5,6-tetrachloro-*N*-hydroxyphthalimide
TEMPO	(2,2,6,6-tetramethylpiperidin-1-yl)oxyl
TES	triethylsilyl
Tf	trifluoromethanesulfonyl
TFA	trifluoroacetic acid
THF	tetrahydrofuran
TLC	thin-layer chromatography
TMS	trimethylsilyl
TOF	time-of-flight
TPAP	tetrapropylammonium perruthenate

Chapter 1. Synthesis of P-Chiral Phosphines and Methylphosphonate Oligonucleotides Enabled by a P(V) Reagent

Introduction

Though identified nearly a century after the discovery of plane polarized light rotation,[1] phosphorus asymmetry is now rivaled only by carbon in terms of research interest. One important example is found in the emergence of anti-sense oligonucleotide (ASO) therapeutics, wherein the stereogenic identity of phosphorothioate linkages can influence physical properties.[2] In continuation of our collaborative work, we recently reported a method for the precise stereochemical control of phosphorothioate oligonucleotides using P(V)-based Phosphorus−Sulfur Incorporation (PSI, abbreviated Ψ) reagents.[3] In contrast to standard P(III) phosphoramidite reagents, Ψ-enabled ASO synthesis is redox-economic and relies on air- and moisture-tolerant building blocks. Methylphosphonate oligonucleotides (MPOs, Figure 1.1A), a related class of compounds, comprise a chiral phosphorus backbone that serves to achieve unique pharmacological effects, including superior resistance to phosphodiesterase degradation.[4,5] The absence of non-bridging oxygen atoms lends to a charge-neutral spine, thereby minimizing hydrogen bonding and preventing potentially destabilizing (or unwanted stabilizing) effects on formation of DNA−RNA duplexes.[4a−c] Indeed, one of the first ASO analogs featured an MPO linkage.[6] As with phosphorothioate ASOs, MPOs introduce phosphorus asymmetry, with *S*p and *R*p isomers that may differ in binding affinities and biological activities.[5b] To our knowledge, there exist no methods to access MPOs with complete stereocontrol, and all known

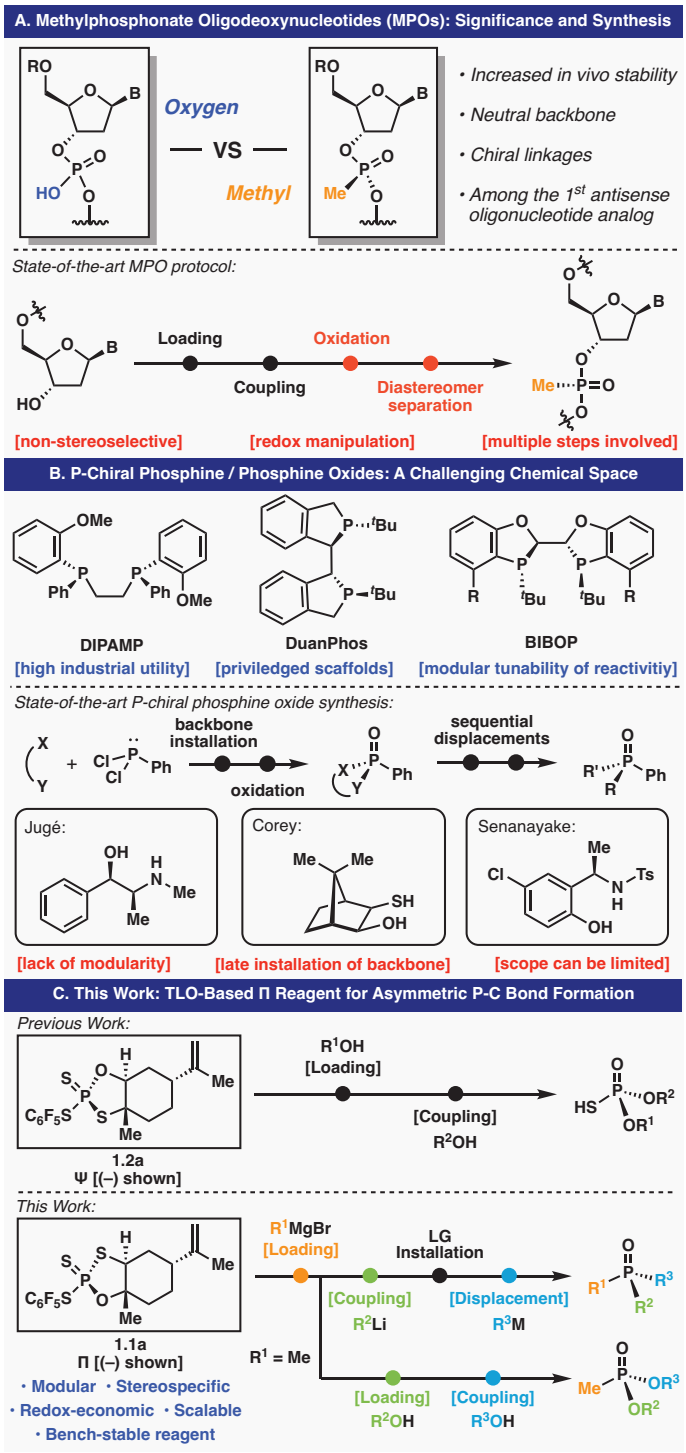


Figure 1.1. Background and Introduction to the Π Reagent Platform

(A) Utility of MPO and limitations of its current synthetic protocols; (B) Precedents, synthetic challenges, and current state-of-the-art syntheses of P-chiral phosphines; and (C) A divergent, Π reagent-based approach to address both challenges.

approaches are curiously underdeveloped.[5,7,8] Moreover, the typical preparation of MPO-based building blocks is wedded to a P(III) strategy that requires tedious separation of diastereomers.[7] Separately, another class of seemingly unrelated compounds drew our attention – namely, the chiral phosphines that form the basis of some of the most important ligands known (Figure 1.1B).[9–11] DIPAMP, for example, was among the first chiral phosphines used for asymmetric hydrogenation and made possible the renowned *L*-DOPA process, work that eventually led to a Nobel Prize in Chemistry.[9] Numbers of useful ligand scaffolds have since emerged, including DuanPhos[10] and BIBOP[11]. Despite this impressive scope of reactivity, a simple and modular approach for the synthesis of P-chiral phosphines remains elusive. Typical preparative routes are often lengthy, are non-redoxeconomic [P(III) → P(V) → P(III)], require separation of diastereomers, and/or are case-specific.[9–11] The most practical of these, introduced by Jugé (Figure 1.1B), relies on the chiral auxiliary ephedrine.[12] Though a classic approach, the scope is limited, the e.r. inconsistent, and the redox economy poor. Shortly thereafter, Corey reported a camphor-based chiral auxiliary that provides extremely high e.r., but is again limited by scope (2 examples) and redox economy.[13] Senanayake then improved on the Jugé approach, using both a P(V) starting material (for phenyl-substituted phosphines) and a more reactive auxiliary.[14] While high yields and e.r. are observed across a range of substrates, the auxiliary requires a six-step preparation sequence. We therefore sought to design a simple method to control phosphorus stereochemistry, foreseeing potential applications in two distinct fields: oligonucleotide chemistry and asymmetric synthesis. Herein, we trace the realization of a reagent pair that enables modular and enantiodivergent access to these markedly different classes of molecules (Figure 1.1C).

Stereospecific C–P Bond Formation: Reagent Development

Exploration of carbon nucleophile addition into a P(V) reagent platform commenced with Ψ (**1.2**), a compound class originally developed for stereospecific phosphorothioate synthesis (Figure 1.2A). As previously reported, Ψ derives from *cis*-limonene oxide, and initial success was realized using oxygen nucleophiles (specifically, a nucleoside hydroxyl group) in both the "loading" and "coupling" steps. Synthesis of the coupled product was found to be remarkably efficient and afforded a variety of phosphorothioate dinucleotides with perfect stereocontrol.[3] Early attempts to load carbon nucleophiles onto (−)-Ψ (**1.2a**) using Grignard reagents (e.g., PhMgBr) furnished adduct **1.3** in 50% yield after only 15 min. In contrast to the coupling of oxygen nucleophiles, addition of a second carbon nucleophile (*t*BuLi) to **1.3** resulted in a counterproductive P−O cleavage (compound **1.4**, 76% yield). Indeed, the subsequent thiirane-limonene

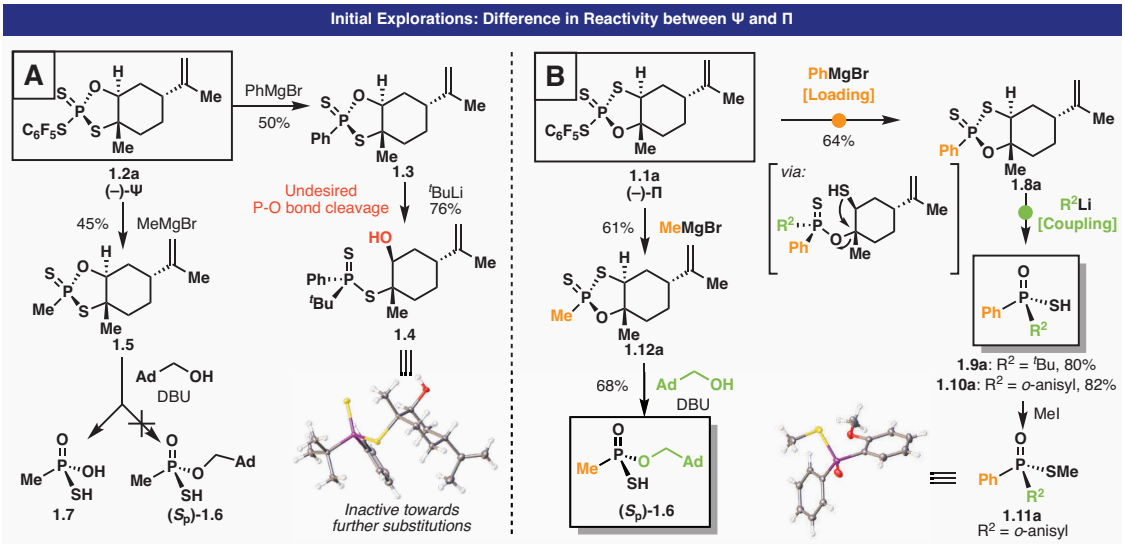


Figure 1.2 Initial Explorations and Reagent Development

(A) Initial exploration with Ψ ended in undesired P−O bond cleavage; (B) Π gave desired P−S bond cleavage and subsequent limonene backbone immolation.

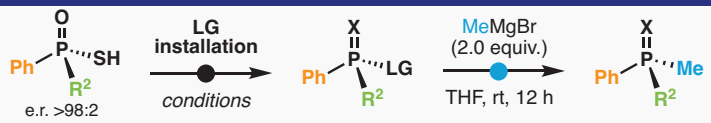
immolation event – which renders the sequence traceless – was effectively terminated. Similarly, **1.2a** was treated with MeMgBr to afford **1.5** (45% yield), a potential MPO precursor. Efforts to then couple 1-adamantylmethanol (a nucleoside alcohol model) proved futile, providing only hydrolysis product **1.7**. Our limited success with Ψ compelled investigation of the regioisomeric *trans*-limonene oxide-based analog. This new compound, Phosphorus Incorporation (PI, abbreviated Π) reagent (**1.1**), was hypothesized to have a starkly different reactivity profile than the cis-limonene oxide counterpart (Figure 1.2B). As with **1.2a**, the loading of (−)-Π (**1.1a**) with PhMgBr rapidly delivered adduct **1.8a** in 64% yield. To our delight, coupling with both *t*BuLi and o-anisyllithium saw successful thiirane−limonene excision to deliver **1.9a** and **1.10a** (80% and 82%, respectively). Anisyl-derived thiophosphinic acid **1.10a** was also readily methylated to give **1.11a**, the absolute configuration of which was verified by X-ray crystallography. The same promising reactivity was observed in methylated **1.12a**, with the addition of 1-adamantylmethanol delivering (R_p)-**1.6** (68% yield after *S*-benzylation with BnBr, see Experimental section). These investigations laid the necessary groundwork for chiral phosphine and MPO synthesis, as described below.

Modular Assembly of P-Chiral Phosphines

With enantiopure thiophosphinic acids [$R_1R_2P(O)SH$] in hand, search for the optimal leaving group to allow the final displacement reaction commenced (Table 1.1). Notably, chlorophosphine sulfide (entry 1) was unresponsive to nucleophilic attack, while chlorophosphine oxide (entry 2) reacted readily but saw diminished e.r. Moreover, the presence of electron-rich aromatic rings proved problematic (entry 3) and resulted in arene

chlorination. In a move away from chlorinated species, we predicted that thiophosphinic acid esters (–SH alkylation products) would function as competent leaving groups. Indeed, while moderately successful (entries 4–6), erosion of e.r. was again observed (see Experimental section for details). However, a simple leaving group exchange from thioalkoxy to methoxy (stereochemical information preserved) boosted the e.r. of the subsequent displacement to 98:2 while maintaining high reactivity (entry 7). In a final attempt, the more activated leaving group phenoxy (entry 8) led to phosphorous racemization. With the most promising results, methoxy was deemed the optimal candidate.

Leaving Group Optimization for the Final Displacement



Entry	X	R^2	Leaving group (conditions)	Yield	e.r.
1	S	^{t}Bu	Cl ($SOCl_2$)	no rxn	/
2	O	^{t}Bu	Cl (MeI, then SO_2Cl_2)	65%	67:33
3	O	*o*-anisyl	Cl (MeI, then SO_2Cl_2)	mixture	/
4	O	*o*-anisyl	SMe (MeI)	88%	94:6
5	O	*o*-anisyl	SEt (EtI)	43%	94:6
6	O	*o*-anisyl	SBn (BnBr)	43%	94:6
7	O	*o*-anisyl	OMe (MeI, then NaOMe)	77%	98:2
8	O	*o*-anisyl	OPh (MeI, then NaOPh)	80%	50:50

Table 1.1 Leaving Group Optimization for the Final Displacement Reaction

Figure 1.3 below illustrates the scope and sequence of Π-enabled phosphine synthesis; net stereoretention for each step was unequivocally confirmed by X-ray crystallography. As shown in Figure 1.3A variety of groups can be installed during loading, including methyl (**1.12**), aryl (**1.8**, **1.13, 1.14**, **1.16**, and **1.17**), biaryl (**1.15**), vinyl (**1.18**) and alkynyl (**1.19**) moieties. The coupling step is similarly versatile, enabling the addition

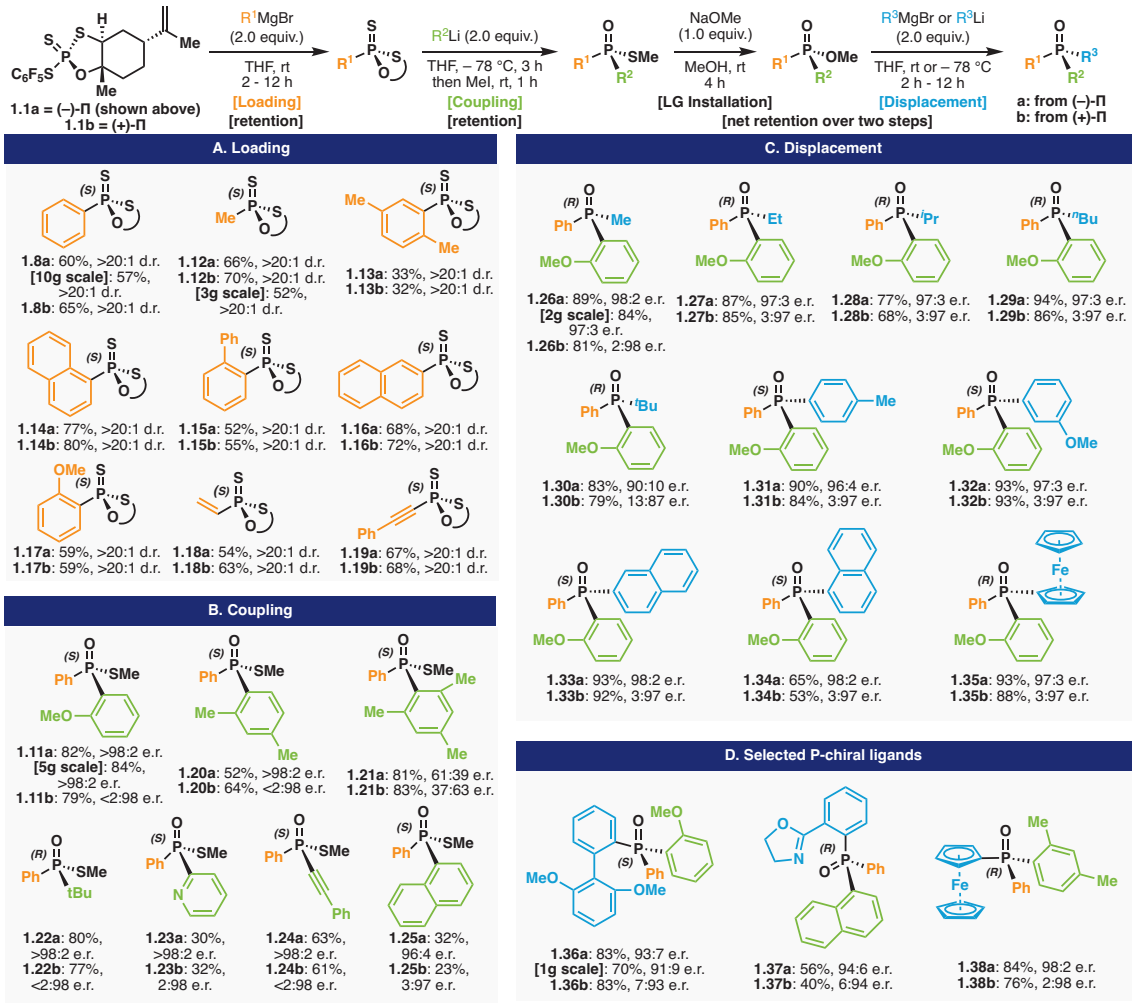
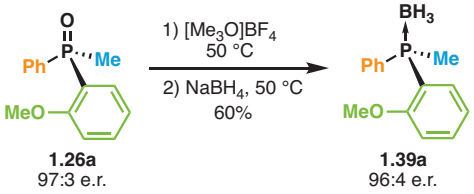


Figure 1.3. Scope of Π-Based Chiral Phosphine / Phosphine Oxide Synthesis

[All structures and stereochemistry shown in the scope refer to the corresponding compounds derived from (–)-Π (*i.e.* with suffix **a**)].

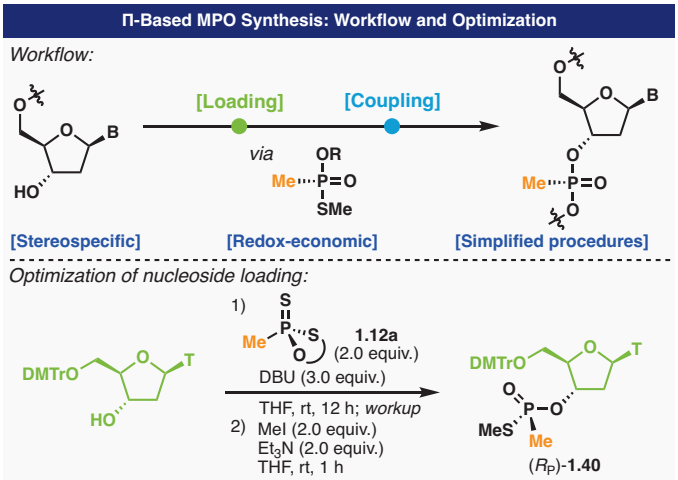
of 3° alkyl (**1.22**), aryl (**1.11, 1.20, 1.21,** and **1.25**), heteroaryl (**1.23**) and alkynyl (**1.24**) groups. In the final displacement, addition of alkyl (**1.26**–**30**), aryl (**1.31**–**34**), and ferrocenyl (**1.35**) groups were successful. Compounds originating from either (–)- or (+)-Π are denoted by suffixes **a** and **b**, respectively. Importantly, the absolute configuration of the final product is determined by the order of addition (*vide infra*). Among the notable substrates accessed through this route is **1.26** (PAMPO), a precursor to important ligand scaffolds DIPAMP[9a] and JoshPhos[15]. Likewise, compounds **1.27** and **1.29**, previously prepared through diastereomeric separation, are used in the enantioselective synthesis of allylic alcohols and phenyl sulfides.[16] Racemic versions of ligands like **1.36** (Buchwald-type) have been prepared previously,[17] and the enantioselective variants hold promise for asymmetric synthesis. PHOX-type ligands such as **1.37** have been widely used in palladium catalysis, including asymmetric allylic substitution.[18] Traditionally, preparation of these ligands rely on racemic phosphorus reagents and existing oxazoline stereocenters to achieve diastereomeric induction, thereby restricting access to select isomers. Ferrocenyl-containing ligand scaffolds such as **1.38** have been used in alkyne–aldehyde reductive couplings[19] and are typically prepared using Jugé's method (91:9 e.r. prior to recrystallization, compared to 98:2 using the current approach).

To be sure, there exist many literature methods for the stereospecific reduction of chiral phosphine oxides to phosphines. Examples include the use of $HSiCl_3$ (Et_3N is optional),[20] $HSiCl_3$ with sacrificial PPh_3,[21] polymethylhydrosiloxane (PMHS) and $Ti(O\textit{i}Pr)_4$,[14] and MeOTf/Meerwein's salt and $NaBH_4$.[22] As an example (see below), $NaBH_4$ and Meerwein's salt were enlisted to reduce PAMPO (**1.26a**) to PAMP (**1.39a**). Indeed, the reaction proceeded smoothly in 60% yield and 96:4 e.r.



A Solution to Stereospecific MPO Synthesis

We then looked to the development of the first stereocontrolled synthesis of MPO building blocks. A simple workflow wherein a nucleoside is loaded onto reagent **1.12,** followed by coupling with a second nucleoside, was proposed (Figure 1.4). Success here hinged on high stereospecificity in both reactions; fortunately, literature review suggested that methylphosphonothioates, previously prepared through tedious separation of diastereomers, could be cleanly coupled with high stereocontrol.[23]



Entry	Deviation from above	Yield	d.r.
1	none	88%	>20:1
2	1.3 equiv. of **1.12a**	71% + free dT	>20:1
3	MeCN as solvent	85%	7:1
4	10 equiv. DBU, 4 h	82%	5:1
5	direct MeI quench	methylation of T	/
6	column after each step	50%	>20:1

Figure 1.4. Workflow and Optimization for Π-based MPO Synthesis

Optimization of the loading step commenced using 5'-DMTr-dT as a model substrate. When a direct MeI quench is performed (i.e., without workup of step 1), methylation of the thymine nucleobase was observed (entry 5). The use of 1.3 equiv. of **1.12** (entry 2) resulted in lower yields, incomplete conversion, and a challenging purification process. Alternatively, when MeCN is used as solvent (entry 3), similar yields, but diminished d.r. (7:1), is returned. A large excess of DBU (10 equiv., entry 4) accelerates the reaction (full conversion of dT in 4 h), but likewise leads to erosion of d.r. (5:1). The two-step telescoped process proved advantageous over a stepwise approach (entry 6), as the highly polar thiophosphonic acid contributes to significant product loss on purification. In the optimal iteration, the nucleoside was first mixed with 2 equiv. of **1.12** and 3 equiv. of DBU in THF for 12 h. Following workup with a PBS buffer solution, residuals were re-dissolved in THF and treated with MeI and Et_3N to afford (R_p)-**1.40** in 88% yield and >20:1 d.r. (Figure 1.4).

A full exploration of the reaction scope was then carried out. Figure 1.5A outlines the stereochemical path of MPO synthesis, with phosphorous stereoretention in the loading step and inversion in coupling step. The four canonical DNA bases were readily loaded (Figure 1.5B); dA, dT and dC proceed in 72–90% yield and $\geqslant$ 20:1 dr, while dG sees diminished yields (46–59%) and $\geqslant$ 20:1 dr. In accord with Stec's observations,[23] all coupling reactions proceed smoothly to afford the corresponding dinucleotides in 39–91% yields and excellent d.r. (>20:1, Figure 1.5C). Notably, no significant difference in the reactivity of S_p and R_p isomers was recorded.

Finally, a chimeric sequence bearing both MPO and chiral phosphorothioates was also prepared (Figure 1.5C). As proof of concept, Ψ activation of a dT–dT dimer was

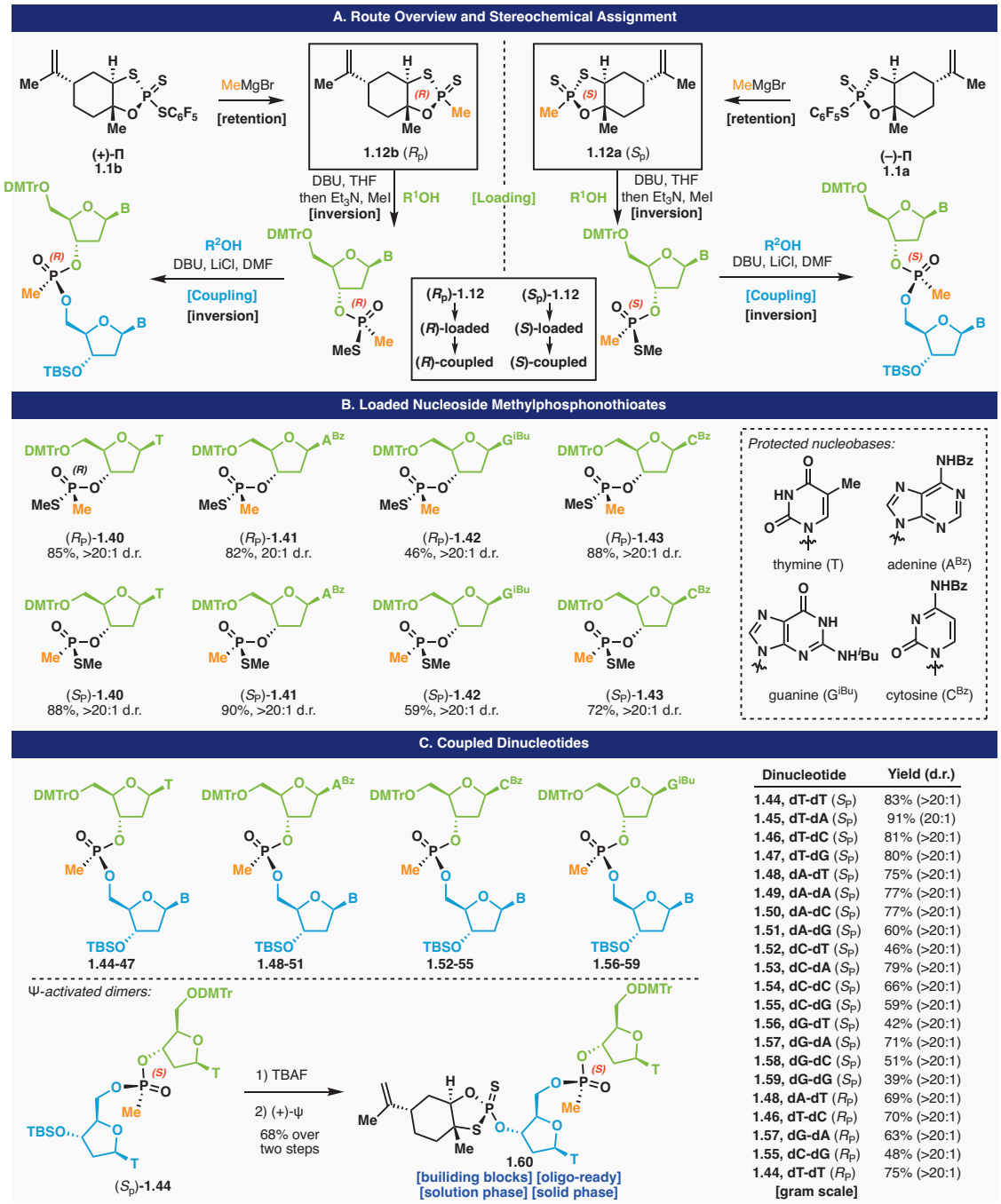


Figure 1.5. Scope of Π-Based Chiral MPO Synthesis

A) Stereochemical map of Π-based MPO synthesis. B) Scope of loaded nucleoside methylphosphonothioates. C) Scope of coupled dinucleotides and further applications.

demonstrated. Following TBS deprotection of (R_p)-**1.44**, the 3'-OH of the dT–dT dimer was successfully loaded onto (+)-Ψ to afford activated dimer **1.60**. Controlled alternation of phosphorotioate and methylphosphonate linkages is now within reach, opening the door for unexplored oligonucleotide architectures.

Conclusion and Outlook

A summary of our growing library of limonene-based P(V) reagents is outlined in Figure 1.6A. As with Ψ, the Π reagents are inexpensive and trivial to prepare, while boasting the same benefits of redox economy and benchtop practicality. A salient feature of this class is true enantiodivergence: choreography of nucleophile addition precisely controls stereochemical outcome (Figure 1.6B). In a powerful example, either enantiomer of thiophosphinic acid ester **1.11** can be procured by simply changing the order of nucleophile addition to (–)-Π. Similarly, prudent ordering of the loading/coupling partners with MPO-precursor **1.12** provides either (R_p)-**1.44** or (S_p)- **1.44** with equally minimal effort.

The product MPOs can be further activated for incorporation into oligonucleotides, a process facilitated by the inherent stability of P(V) reagents. By effectively serving as a formal surrogate for "chiral $POCl_3$" through a tunable sequence, the Π-reagent platform provides broad admission to otherwise challenging sectors of chemical space. The full capability of Π-reagents is yet to be revealed as we are still far from exhausting all the possible permutations of products that can be synthesized.

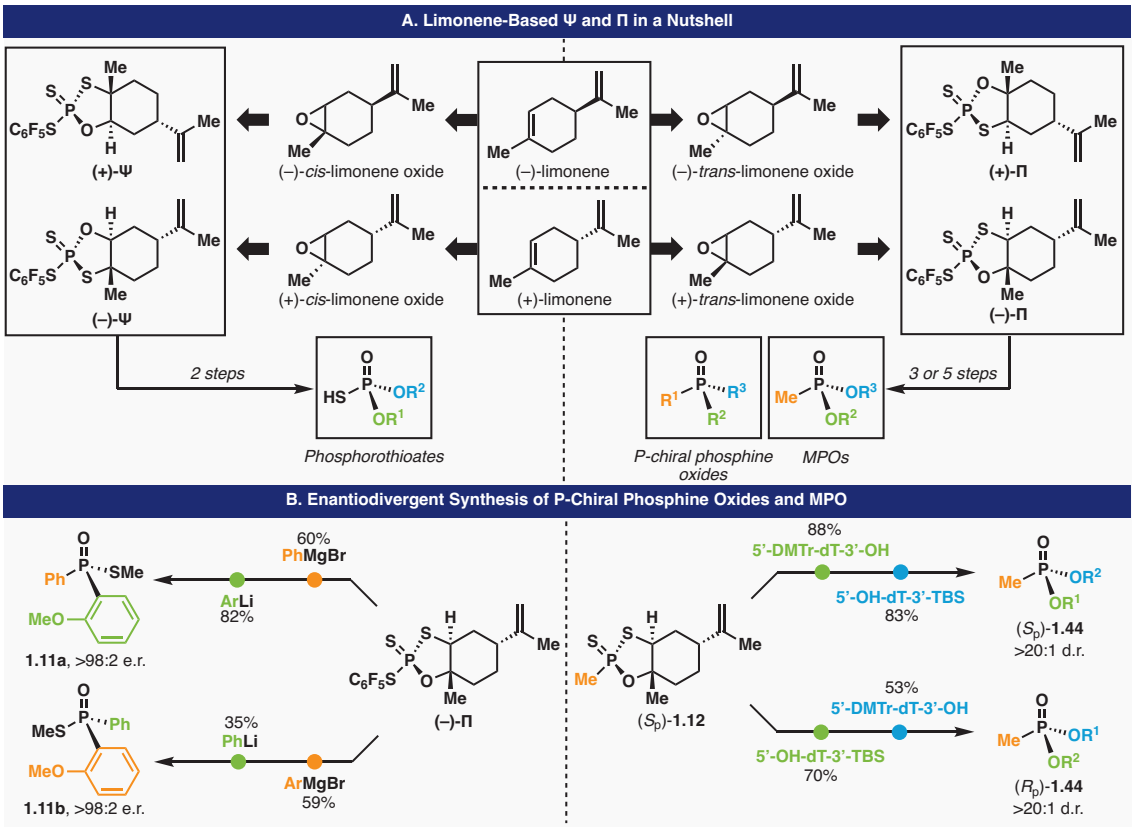


Figure 1.6. Stereochemical Roadmap of the P(V) Reagents

(A) Painting the full picture for limonene-based Ψ and Π reagents. (B) Enantiodivergent nature of the Π-based chiral phosphine and MPO syntheses. Ar = *o*-anisyl. OR^1 = 5'-DMTr-dT-3'-OH. OR^2 = 5'-OH-dT-3'-TBS.

References

1. Meisenheimer, J; Lichtenstadt, L., *Ber. dtsch. chem. Ges* **1911**, *44*, 356–359.
2. (a) Bohr, H. G.; Shim, I.; Stein, C.; Ørum, H.; Hansen, H. F.; Koch, T., Electronic Structures of LNA Phosphorothioate Oligonucleotides. *Mol. Ther. Nucleic Acids* **2017,** *8*, 428–441. (b) Iwamoto, N.; Butler, D. C. D.; Svrzikapa, N.; Mohapatra, S.; Zlatev, I.; Sah, D. W. Y.; Meena; Standley, S. M.; Lu, G.; Apponi, L. H.; Frank-Kamenetsky, M.; Zhang, J. J.; Vargeese, C.; Verdine, G. L., Control of phosphorothioate stereochemistry substantially increases the efficacy of antisense oligonucleotides. *Nat. Biotechnol.* **2017,** *35*, 845–851.
3. Knouse, K. W.; deGruyter, J. N.; Schmidt, M. A.; Zheng, B.; Vantourout, J. C.; Kingston, C.; Mercer, S. E.; McDonald, I. M.; Olson, R. E.; Zhu, Y.; Hang, C.; Zhu, J.; Yuan, C.; Wang, Q.; Park, P.; Eastgate, M. D.; Baran, P. S., Unlocking P(V): Reagents for chiral phosphorothioate synthesis. *Science* **2018,** *361*, 1234–1238.
4. (a) Pritchard, C. E.; Grasby, J. A.; Hamy, F.; Zacharek, A. M.; Singh, M.; Karn, J.; Gait, M. J., Methylphosphonate mapping of phosphate contacts critical for RNA recognition by the human immunodeficiency virus tat and rev proteins. *Nucleic Acids Res.* **1994,** *22*, 2592–2600. (b) Koch, M.; Flür, S.; Kreutz, C.; Ennifar, E.; Micura, R.; Polacek, N., Role of a ribosomal RNA phosphate oxygen during the EF-G–triggered GTP hydrolysis. *Proc. Natl. Acad. Sci.* **2015,** *112*, E2561. (c) Hamma, T.; Miller, P. S., Interactions of Hairpin Oligo-2′-O-Methylribonucleotides Containing Methylphosphonate Linkages with HIV TAR RNA. *Antisense and Nucleic Acid Drug Dev.* **2003,** *13*, 19–30.

5. (a) Agrawal, S.; Goodchild, J., Oligodeoxynucleoside methylphosphonates: synthesis and enzymic degradation. *Tetrahedron Lett.* **1987,** *28*, 3539–3542. (b) Reynolds, M. A.; Hogrefe, R. I.; Jaeger, J. A.; Schwartz, D. A.; Riley, T. A.; Marvin, W. B.; Daily, W. J.; Vaghefi, M. M.; Beck, T. A.; Knowles, S. K.; Klem, R. E.; Arnold, L. J., Jr., Synthesis and Thermodynamics of Oligonucleotides Containing Chirally Pure R P Methylphosphonate Linkages. *Nucleic Acids Res.* **1996,** *24*, 4584–4591.
6. Miller, P. S., Oligonucleoside Methylphosphonates as Antisense Reagents. *Bio/Technology* **1991,** *9*, 358–362.
7. For precedents of non-stereoselective MPO syntheses, see (a) Miller, P. S.; Yano, J.; Yano, E.; Carroll, C.; Jayaraman, K.; Ts'o, P. O. P., Nonionic nucleic acid analogs. Synthesis and characterization of dideoxyribonucleoside methylphosphonates. *Biochemistry* **1979,** *18*, 5134–5143. (b) Engels, J.; Jäger, A., Eine neue Synthese von Nukleosidmethylphosphonaten. *Angew. Chem. Int. Ed. Eng.* **1982,** *21*, 201–2015. (c) Lebedev, A. V.; Wenzinger, G. R.; Wickstrom, E., A new DMAP-catalyzed phosphonamidite coupling reaction for synthesis of oligonucleotide methylphosphonate derivatives. *Tetrahedron Lett.* **1990,** *31*, 851–854. (d) Heliński, J.; Dąbkowski, W.; Michalski, J., *N*,*N*-diisopropyl-O-P-nitrophenyl-P-methylphosphonoamidite: novel difunctional PIII reagent in oligonucleoside methylphosphonate synthesis containing 4-nitrophenoxy group. *Tetrahedron Lett.* **1991,** *32*, 4981–4984.
8. For stereoselective MPO syntheses with moderate d.r., see (a) Schell, P.; Engels, J. W., Rp-Diastereoselective synthesis of dinucleoside methylphosphonates by the

phosphoramidite approach. *Tetrahedron Lett.* **1998,** *39*, 8629–8632. (b) Rosmanitz, P.; Eisenhardt, S.; Bats, J. W.; Engels, J. W., New proline derived chiral building blocks for nucleoside methylphosphonate synthesis. *Tetrahedron* **1994,** *50*, 5719–5734.

9. (a) Vineyard, B. D.; Knowles, W. S.; Sabacky, M. J.; Bachman, G. L.; Weinkauff, D. J., Asymmetric hydrogenation. Rhodium chiral bisphosphine catalyst. *J. Am. Chem. Soc.* **1977,** *99*, 5946–5952. (b) Knowles, W. S., Asymmetric Hydrogenations (Nobel Lecture 2001). *Adv. Synth. Catal.* **2003,** *345*, 3–13.
10. (a) Liu, D.; Zhang, X., Practical P-Chiral Phosphane Ligand for Rh-Catalyzed Asymmetric Hydrogenation. *Eur. J. Org. Chem.* **2005,** *2005*, 646–649. (b) Gao, W.; Lv, H.; Zhang, X., Rh/DuanPhos-Catalyzed Asymmetric Hydrogenation of β-Acetylamino Vinylsulfides: An Approach to Chiral β-Acetylamino Sulfides. *Org. Lett.* **2017,** *19*, 2877–2880.
11. Tang, W.; Qu, B.; Capacci, A. G.; Rodriguez, S.; Wei, X.; Haddad, N.; Narayanan, B.; Ma, S.; Grinberg, N.; Yee, N. K.; Krishnamurthy, D.; Senanayake, C. H., Novel, Tunable, and Efficient Chiral Bisdihydrobenzooxaphosphole Ligands for Asymmetric Hydrogenation. *Org. Lett.* **2010,** *12*, 176–179.
12. (a) Juge, S.; Genet, J. P., Asymmetric synthesis of phosphinates, phosphine oxides and phosphines by Michaelis Arbuzov rearrangement of chiral oxazaphospholidine. *Tetrahedron Lett.* **1989,** *30*, 2783–2786. (b) Juge, S.; Stephan, M.; Laffitte, J. A.; Genet, J. P., Efficient asymmetric synthesis of optically pure tertiary mono and diphosphine ligands. *Tetrahedron Lett.* **1990,** *31*, 6357–6360.

13. Corey, E. J.; Chen, Z.; Tanoury, G. J., A new and highly enantioselective synthetic route to P-chiral phosphines and diphosphines. *J. Am. Chem. Soc.* **1993,** *115*, 11000–11001.

14. Han, Z. S.; Goyal, N.; Herbage, M. A.; Sieber, J. D.; Qu, B.; Xu, Y.; Li, Z.; Reeves, J. T.; Desrosiers, J.-N.; Ma, S.; Grinberg, N.; Lee, H.; Mangunuru, H. P. R.; Zhang, Y.; Krishnamurthy, D.; Lu, B. Z.; Song, J. J.; Wang, G.; Senanayake, C. H., Efficient Asymmetric Synthesis of P-Chiral Phosphine Oxides via Properly Designed and Activated Benzoxazaphosphinine-2-oxide Agents. *J. Am. Chem. Soc.* **2013,** *135*, 2474–2477.

15. Sieber, J. D.; Chennamadhavuni, D.; Fandrick, K. R.; Qu, B.; Han, Z. S.; Savoie, J.; Ma, S.; Samankumara, L. P.; Grinberg, N.; Lee, H.; Song, J. J.; Senanayake, C. H., Development of New P-Chiral P,π-Dihydrobenzooxaphosphole Hybrid Ligands for Asymmetric Catalysis. *Org. Lett.* **2014,** *16*, 5494–5497.

16. Harmat, N. J. S.; Warren, S., Chiral synthesis of Z-2-butylidenecyclohexan-1-ol and -1-yl phenylsulphide from optically active phosphine oxides. *Tetrahedron Lett.* **1990,** *31*, 2743–2746.

17. For examples, see (a) Yuen, O. Y.; Leung, M. P.; So, C. M.; Sun, R. W.-Y.; Kwong, F. Y., Palladium-Catalyzed Direct Arylation of Polyfluoroarenes for Accessing Tetra-ortho-Substituted Biaryls: Buchwald-type Ligand Having Complementary −PPh2 Moiety Exhibits Better Efficiency. *J. Org. Chem.* **2018,** *83*, 9008–9017. (b) Pedroni, J.; Boghi, M.; Saget, T.; Cramer, N., Access to β-Lactams by Enantioselective Palladium (0)-Catalyzed C (sp^3)-H Alkylation. *Angew. Chem. Int. Ed.* **2014,** *53*, 9064–9067.

18. (a) von Matt, P.; Pfaltz, A., Chiral phosphino-aryldihydrooxazoles as ligands in asymmetric catalysis: Pd-catalyzed allylic substitution. *Angew. Chem. Int. Ed. Engl.* **1993,** *32*, 566–568. (b) Sprinz, J.; Helmchen, G., Phosphinoaryl- and phosphinoalkyloxazolines as new chiral ligands for enantioselective catalysis: Very high enantioselectivity in palladium catalyzed allylic substitutions. *Tetrahedron Lett.* **1993,** *34*, 1769–1772.

19. (a) Chan, J.; Jamison, T. F., Enantioselective Synthesis of (−)-Terpestacin and Structural Revision of Siccanol Using Catalytic Stereoselective Fragment Couplings and Macrocyclizations. *J. Am. Chem. Soc.* **2004,** *126*, 10682–10691. (b) Colby, E. A.; Jamison, T. F., P-Chiral, Monodentate Ferrocenyl Phosphines, Novel Ligands for Asymmetric Catalysis. *J. Org. Chem.* **2003,** *68*, 156–166.

20. (a) Naumann, K.; Zon, G.; Mislow, K., Use of hexa-chlorodisilane as a reducing agent. Stereospecific deoxygenation of acyclic phosphine oxides. *J. Am. Chem. Soc.* **1969,** *91*, 7012–7023. (b) Horner, L.; Balzer, W. D., Phosphororganische verbindungen IXL zum sterischen verlauf der desoxygenierung von tertiären phosphinoxyden zu tertiären phosphinen mit trichlorsilan. *Tetrahedron Lett.* **1965,** *6*, 1157–1162.

21. Wu, H.-C.; Yu, J.-Q.; Spencer, J. B., Stereospecific Deoxygenation of Phosphine Oxides with Retention of Configuration Using Triphenylphosphine or Triethyl Phosphite as an Oxygen Acceptor. *Org. Lett.* **2004,** *6*, 4675–4678.

22. Rajendran, K. V.; Gilheany, D. G., Simple unprecedented conversion of phosphine oxides and sulfides to phosphine boranes using sodium borohydride. *Chem. Comm.* **2012,** *48*, 817–819.

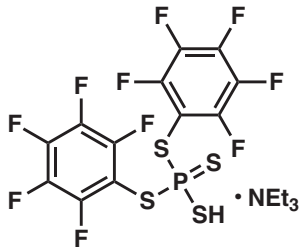
23. (a) Woźniak, L. A.; Wieczorek, M.; Pyzowski, J.; Majzner, W.; Stec, W. J., Stereochemistry of the DBU/LiCl-Assisted Nucleophilic Substitution at Phosphorus in Nucleoside-3‘-O-(Se-methyl Methanephosphonoselenolate)s. *J. Org. Chem.* **1998,** *63*, 5395–5402. (b) Pyzowski, J.; Wozniak, L. A.; Stec, W. J., Oligomeric Building Block Approach to the Synthesis of Diastereomerically Pure Pentathymidine 3‘,5‘-Methanephosphonates. *Org. Lett.* **2000,** *2*, 771–773.

Experimental

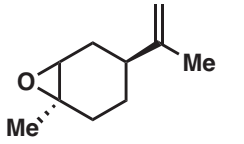
Tetrahydrofuran (THF), *N,N*-dimethylformamide (DMF), dicloromethane (DCM), acetonitrile (MeCN) and methanol (MeOH) were obtained by passing the previously degassed solvents through an activated alumina column. All 5'-DMTr protected nucleosides carrying conventional nucleobase protections (T = none, A = benzoyl, G = isobutyryl, C = benzoyl) were purchased from Chem-Impex. All reagents were purchased at the highest commercial quality and used without further purification unless otherwise stated. Yields refer to chromatographically and spectroscopically homogeneous material. Reactions were monitored by thin layer chromatography (TLC), GC/MS, GC/FID, or LC/MS. TLC was performed using 0.25 mm E. Merck silica plates (60F-254), using short-wave UV light as the visualizing agent, and $KMnO_4$ and heat as developing agents. NMR spectra were recorded on Bruker DRX-600, DRX-500, and AMX-400 instruments and are calibrated using residual undeuterated solvent ($CHCl_3$, acetone at 7.26, 2.05 ppm for ^1H NMR, and 77.16, 29.84 ppm for ^{13}C NMR, respectively). The following abbreviations were used to explain multiplicities: s = singlet, d = doublet, t = triplet, q = quartet, m = multiplet, br = broad. Column chromatography was performed using E. Merck silica gel (60, particle size 0.043–0.063 mm), and preparative TLC (pTLC) was performed on Merck silica plates (60F-254). High-resolution mass spectra (HRMS) were recorded on an Agilent LC/MSD TOF mass spectrometer by electrospray ionization time of flight reflectron experiments. Melting points were recorded on a Fisher-Johns 12-144 melting point apparatus and are uncorrected. The enantiomeric ratios were determined with Waters UPC2 SFC equipped with a photodiode array detector or an Agilent Technologies 1220 Infinity II LC HPLC. Optical rotation data was recorded on an Anton Paar 100 Modular Circular Polarimeter.

Synthesis of Π Reagents

Compounds **SI-1.1**[1] and **SI-1.2** (both enantiomers)[2] were synthesized according to published procedures.

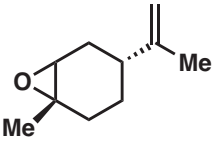


SI-1.1



(–)-*trans*-limonene oxide

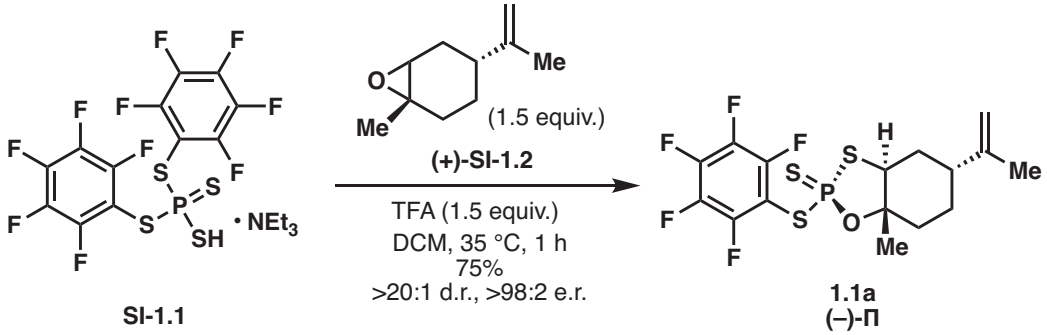
(–)-SI-1.2



(+)-*trans*-limonene oxide

(+)-SI-1.2

Synthesis of (–)-Π (1.1a):



SI-1.1 **1.1a (–)-Π**

Synthesis of **(–)-Π** follows an analogous procedure to the previously reported synthesis of Ψ reagents[1], where detailed pictorial guides can be found. To a solution of **SI-1.1** (1.00 g, 1.68 mmol, 1.0 equiv.) and trans-(+)-limonene oxide **SI-1.2** (0.383 g, 2.52 mmol, 1.5 equiv.) in dichloromethane (5.0 mL) was added trifluoroacetic acid (0.19 mL, 2.52 mmol, 1.5 equiv.) The reaction was warmed to 35 °C and allowed to stir for 1 hour. The reaction mixture was cooled to ambient temperature, and hexane (10 mL) was added into the batch to form a biphasic mixture. The stream was washed with water (5 mL), saturated $NaHCO_3$ (10 mL), and KH_2PO_4 (10% aqueous, 3 mL). The organic phase was filtered through a $MgSO_4$ pad and concentrated to ~3 mL. Methanol (5 mL) was added, the batch was

concentrated to ~3 mL; this procedure was repeated twice. The mixture was cooled to 5–10 °C and stirred for 5 min. The resulting slurry was filtered and the reactor and cake were washed with cold methanol (1 mL). The filter cake was dried *in vacuo* to afford **1.1a [(–)-Π]** as a crystalline white solid (0.56 g, 75% yield, >20:1 d.r., >98:2 e.r.).

Physical state: white crystalline solid

m.p. = 104–106 °C

$[\alpha]^{25}_{D}$ = -125° (c = 1.00 in $CHCl_3$)

R_f = 0.50 (hexane:toluene = 1:1)

^{1}H NMR (600 MHz, $CDCl_3$) δ 4.96 (s, 1H), 4.70 (d, *J* = 2.1 Hz, 1H), 2.90 (dd, *J* = 13.4, 2.9 Hz, 1H), 2.42 (s, 1H), 2.10 (ddp, *J* = 13.7, 6.4, 2.2 Hz, 2H), 2.02 (ddd, *J* = 12.5, 4.3, 2.7 Hz, 1H), 1.77 – 1.66 (m, 2H), 1.65 (s, 3H), 1.64 (s, 3H), 1.52 (td, *J* = 13.3, 4.2 Hz, 1H).

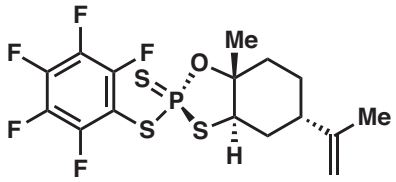
^{13}C NMR (151 MHz, $CDCl_3$) δ 148.86, 147.19, 144.69, 144.02, 142.28, 138.75, 137.05, 111.83, 104.30, 93.64, 93.60, 58.65, 58.64, 38.81, 34.21, 34.13, 28.39, 28.32, 24.89, 22.18, 18.74.

^{19}F NMR (376 MHz, $CDCl_3$) δ -128.54 (dd, *J* = 20.7, 4.6 Hz, 2F), -146.87 (ddd, *J* = 25.5, 14.7, 6.0 Hz, 1F), -159.16 – -160.51 (m, 2F).

^{31}P NMR (162 MHz, $CDCl_3$) δ 102.08.

HRMS (ESI-TOF): calc'd for $C_{16}H_{17}F_5OPS_3$ $[M+H]^+$: 447.0094, found: 447.0093.

Synthesis of (+)-Π (1.1b):

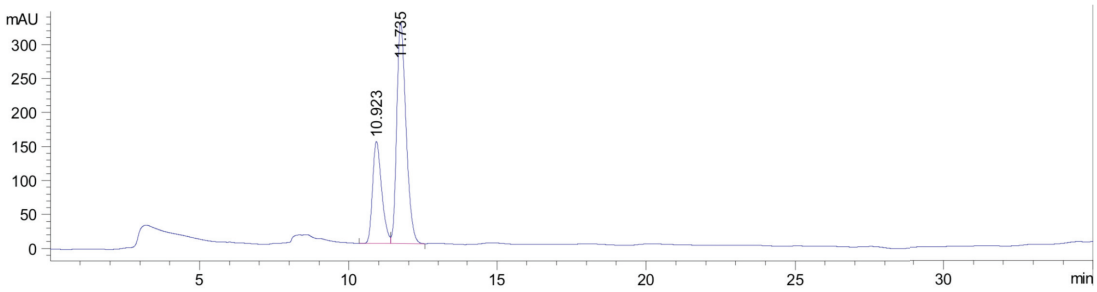


1b
(+)-Π

Synthesis of **1.1b** followed the same procedures outlined for **1.1a**. All characterization data were identical except the optical rotation, $[\alpha]^{25}_{D}$ = +124° (c = 1.00 in $CHCl_3$)

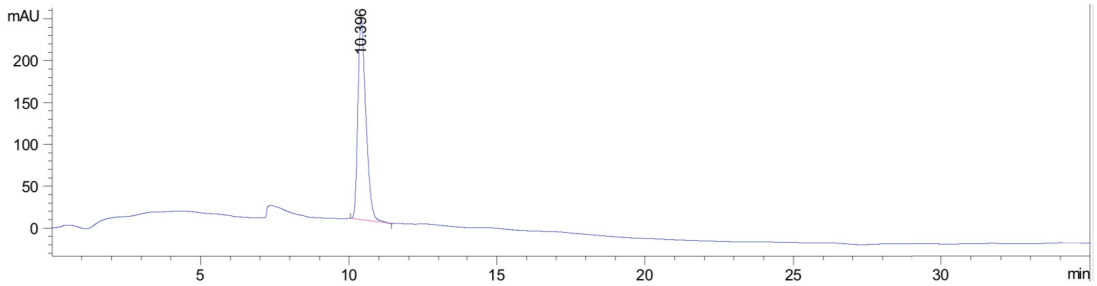
Chiral HPLC: Chiralpak AD-H column; 0.5% IPA in hexane, 0.5 mL/min, 254 nm.

Racemic:



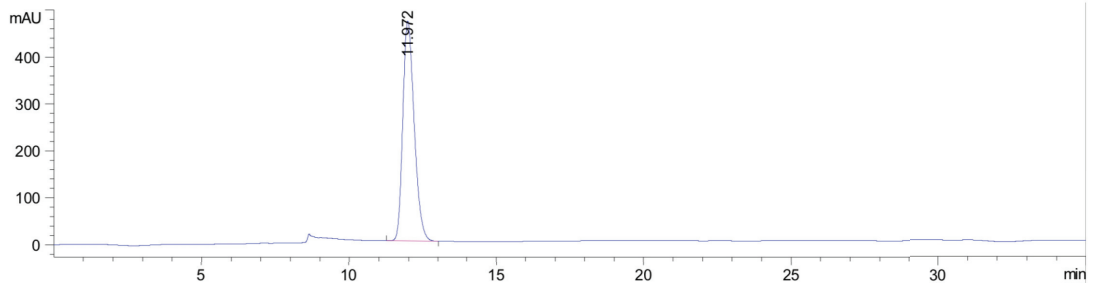
Peak #	RetTime [min]	Type	Width [min]	Area [mAU*s]	Height [mAU]	Area %
1	10.923	BV	0.3213	3182.84375	150.13548	31.1526
2	11.735	VB	0.3324	7034.11133	325.13907	68.8474

(–)-П:



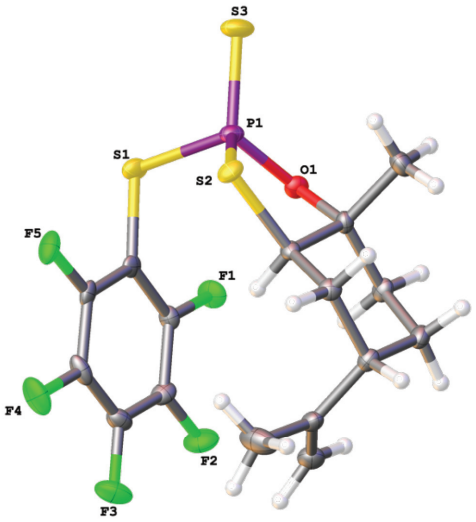
Peak #	RetTime [min]	Type	Width [min]	Area [mAU*s]	Height [mAU]	Area %
1	10.396	BB	0.2812	4508.61084	239.96260	100.0000

(+)-П:



Peak #	RetTime [min]	Type	Width [min]	Area [mAU*s]	Height [mAU]	Area %
1	11.972	BB	0.4147	1.25689e4	468.99081	100.0000

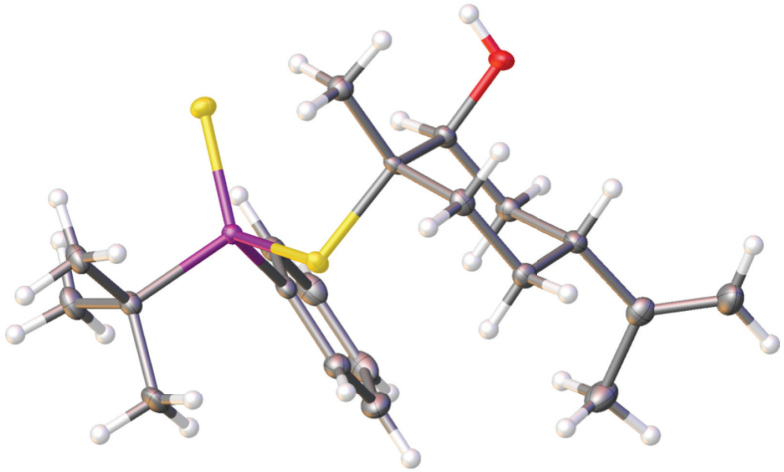
Table S1.1: X-ray crystal structure of 1.1b



Identification code	Baran636_01_a	
Empirical formula	C16 H16 F5 O P S3	
Formula weight	446.44	
Temperature	100.0 K	
Wavelength	0.71073 Å	
Crystal system	Orthorhombic	
Space group	$P2_12_12_1$	
Unit cell dimensions	a = 9.8755(7) Å	α= 90°.
	b = 11.4069(5) Å	β= 90°.
	c = 16.8121(10) Å	γ= 90°.
Volume	1893.86(19) $Å^3$	
Z	4	
Density (calculated)	1.566 Mg/m^3	
Absorption coefficient	0.526 mm^{-1}	
F(000)	912	
Crystal size	0.33 x 0.33 x 0.31 mm^3	
Theta range for data collection	2.158 to 27.479°.	
Index ranges	-12<=h<=12, -14<=k<=14, -21<=l<=17	
Reflections collected	11671	
Independent reflections	4341 [R(int) = 0.0279]	
Completeness to theta = 25.242°	99.9 %	
Absorption correction	Semi-empirical from equivalents	
Max. and min. transmission	0.6942 and 0.6421	
Refinement method	Full-matrix least-squares on F^2	
Data / restraints / parameters	4341 / 0 / 245	
Goodness-of-fit on F^2	1.039	
Final R indices [I>2sigma(I)]	R1 = 0.0247, wR2 = 0.0576	
R indices (all data)	R1 = 0.0280, wR2 = 0.0594	
Absolute structure parameter	-0.01(3)	
Extinction coefficient	n/a	
Largest diff. peak and hole	0.213 and -0.185 $e.Å^{-3}$	

Initial Exploration with Π Reagents

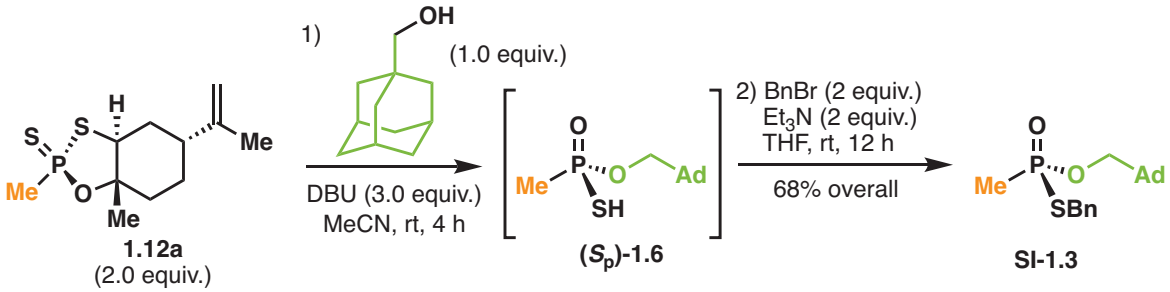
Table S1.2: X-Ray crystal structure of dead-end product 1.4



Identification code	baran695	
Empirical formula	C20 H31 O P S2	
Molecular formula	C20 H31 O P S2	
Formula weight	382.54	
Temperature	100.0 K	
Wavelength	0.71073 Å	
Crystal system	Monoclinic	
Space group	P 1 21 1	
Unit cell dimensions	a = 9.2918(4) Å	α= 90°.
	b = 10.4856(4) Å	β= 94.5610(10)°.
	c = 10.8907(4) Å	γ = 90°.
Volume	1057.72(7) $Å^3$	
Z	2	
Density (calculated)	1.201 Mg/m^3	
Absorption coefficient	0.332 mm^{-1}	
F(000)	412	
Crystal size	0.15 x 0.1 x 0.085 mm^3	
Crystal color, habit	colorless block	
Theta range for data collection	1.876 to 26.372°.	
Index ranges	-10<=h<=11, -13<=k<=13, -13<=l<=13	
Reflections collected	9611	
Independent reflections	4293 [R(int) = 0.0300]	
Completeness to theta = 25.242°	100.0 %	
Absorption correction	Semi-empirical from equivalents	
Max. and min. transmission	0.4910 and 0.4514	
Refinement method	Full-matrix least-squares on F^2	
Data / restraints / parameters	4293 / 1 / 223	
Goodness-of-fit on F^2	1.035	
Final R indices [I>2sigma(I)]	R1 = 0.0265, wR2 = 0.0644	
R indices (all data)	R1 = 0.0274, wR2 = 0.0651	
Absolute structure parameter	0.04(3)	
Largest diff. peak and hole	0.272 and -0.181 $e.Å^{-3}$	

All other characterizations can be found *vide infra.*

MPO [Synthesis of SI-1.3 *via* (S_p)-1.6]



To a flame-dried culture tube under argon was charged 1-adamantanemethanol (16.6 mg, 0.1 mmol, 1.0 equiv.), **1.12a** (52.5 mg, 0.2 mmol, 2.0 equiv.), and MeCN (1 mL). DBU (0.05 mL, 3.0 mmol, 3.0 equiv.) was added and the resulting solution was stirred for 4 h at rt. 2 mL of 1X PBS solution was added, and the mixture was extracted with DCM (3 x 3 mL). The combined organics were washed with brine (1 mL), dried over Na_2SO_4, filtered and concentrated. The resulting crude oil was dissolved in THF (1 mL). Et_3N (2 equiv.) and BnBr (2 equiv.) were added, and the resulting mixture was stirred for 12 h. The reaction was quenched with 1 mL of water and extracted with EtOAc (3 x 3 mL). The combined organics were dried over Na_2SO_4, filtered and concentrated. Purification by silica gel chromatography (hexane/EtOAc = 5:2) afforded 24.0 mg (69%) of compound **SI-1.3**.

Physical State: colorless oil

R_f = 0.40 (hexane/EtOAc = 5:2)

^{1}H NMR (400 MHz, $CDCl_3$) δ 7.41–7.22 (m, 5H), 4.14–3.97 (m, 2H), 3.65 (dd, *J* = 9.6, 6.5 Hz, 1H), 3.46 (dd, *J* = 9.7, 6.8 Hz, 1H), 1.98 (s, 3H), 1.77–1.57 (m, 9H), 1.50 (d, *J* = 2.9 Hz, 6H).

^{13}C NMR (151 MHz, $CDCl_3$) δ 138.13, 138.11, 129.05, 128.82, 127.64, 74.81, 74.76, 39.02, 37.03, 34.68, 34.65, 33.68, 33.63, 28.10, 20.35, 19.62.

^{31}P NMR (162 MHz, $CDCl_3$) δ 53.64.

HRMS (ESI-TOF): calc'd for $C19H28O_2PS$ [M+H]+: 351.1548, found: 351.1546.

Stereochemical Assignments

P-chiral phosphine workflow:

Compound **1.34a** was selected as the model substrate. X-ray crystal structures (see below) of **1.34a** and upstream intermediates **1.11a** and **1.8a** indicated stereoretention at phosphorus for each step.

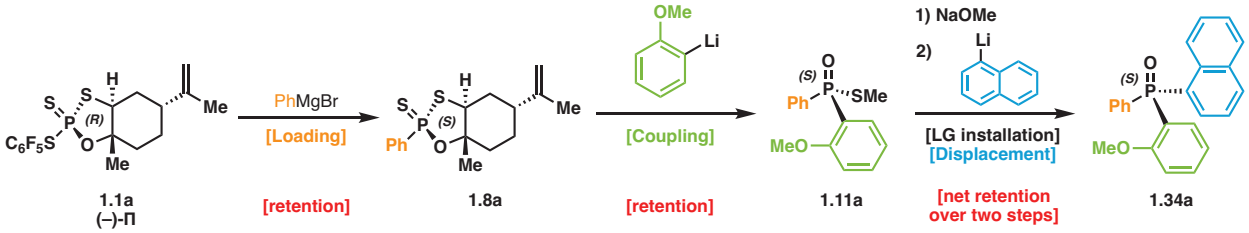
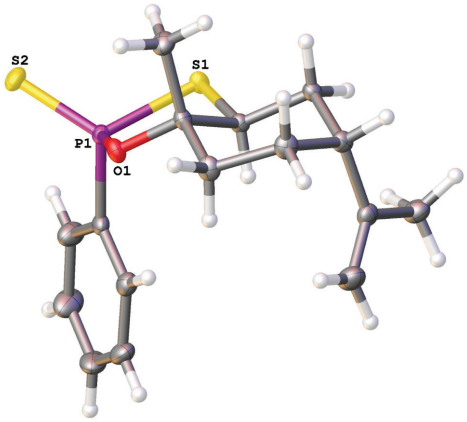
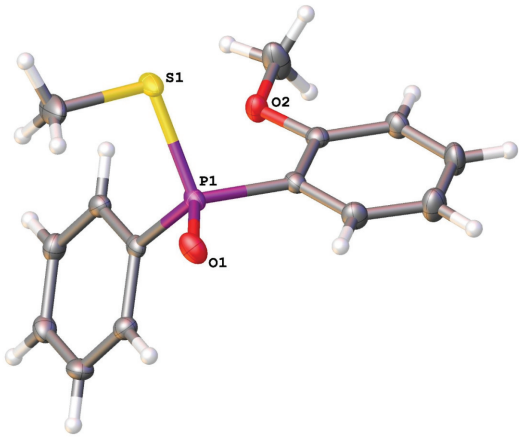


Table S1.3: X-ray crystal structure of 1.8a



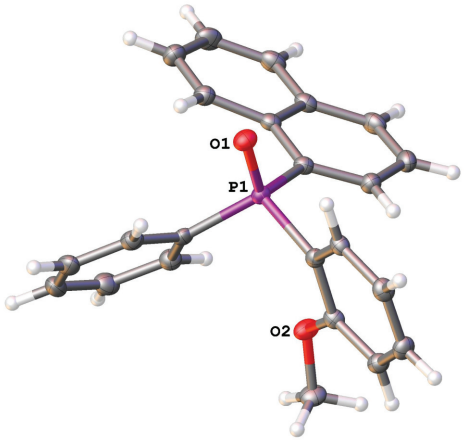
Identification code	Baran746	
Empirical formula	C16 H21 O P S2	
Formula weight	324.42	
Temperature	100.0 K	
Wavelength	1.54178 Å	
Crystal system	Orthorhombic	
Space group	$P2_12_12_1$	
Unit cell dimensions	a = 10.50020(10) Å	α= 90°.
	b = 10.57590(10) Å	β= 90°.
	c = 15.1419(2) Å	γ = 90°.
Volume	1681.49(3) $Å^3$	
Z	4	
Density (calculated)	1.281 Mg/m^3	
Absorption coefficient	3.705 mm^{-1}	
F(000)	688	
Crystal size	0.33 x 0.13 x 0.09 mm^3	
Theta range for data collection	5.101 to 71.088°.	
Index ranges	-12<=h<=12, -12<=k<=10, -18<=l<=18	
Reflections collected	14357	
Independent reflections	3224 [R(int) = 0.0232]	
Completeness to theta = 67.679°	100.0 %	
Absorption correction	Semi-empirical from equivalents	
Max. and min. transmission	0.7534 and 0.5643	
Refinement method	Full-matrix least-squares on F^2	
Data / restraints / parameters	3224 / 0 / 184	
Goodness-of-fit on F^2	1.073	
Final R indices [I>2sigma(I)]	R1 = 0.0199, wR2 = 0.0531	
R indices (all data)	R1 = 0.0200, wR2 = 0.0532	
Absolute structure parameter	-0.007(5)	
Extinction coefficient	0.00037(13)	
Largest diff. peak and hole	0.302 and -0.218 $e.Å^{-3}$	

Table S1.4: X-ray crystal structure of 1.11a



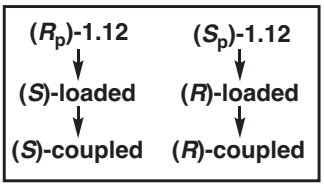
Identification code	Baran747	
Empirical formula	C14 H15 O2 P S	
Formula weight	278.29	
Temperature	100.0 K	
Wavelength	1.54178 Å	
Crystal system	Orthorhombic	
Space group	$P2_12_12_1$	
Unit cell dimensions	a = 8.38980(10) Å	α= 90°.
	b = 11.69970(10) Å	β= 90°.
	c = 14.1048(2) Å	γ = 90°.
Volume	1384.50(3) $Å^3$	
Z	4	
Density (calculated)	1.335 Mg/m^3	
Absorption coefficient	3.099 mm^{-1}	
F(000)	584	
Crystal size	0.12 x 0.1 x 0.08 mm^3	
Theta range for data collection	4.911 to 68.222°.	
Index ranges	-8<=h<=10, -13<=k<=14, -16<=l<=16	
Reflections collected	12841	
Independent reflections	2532 [R(int) = 0.0234]	
Completeness to theta = 67.679°	100.0 %	
Absorption correction	Semi-empirical from equivalents	
Max. and min. transmission	0.7534 and 0.6560	
Refinement method	Full-matrix least-squares on F^2	
Data / restraints / parameters	2532 / 0 / 166	
Goodness-of-fit on F^2	1.108	
Final R indices [I>2sigma(I)]	R1 = 0.0210, wR2 = 0.0584	
R indices (all data)	R1 = 0.0212, wR2 = 0.0586	
Absolute structure parameter	0.003(6)	
Extinction coefficient	0.0006(3)	
Largest diff. peak and hole	0.344 and -0.252 $e.Å^{-3}$	

Table S1.5: X-ray crystal structure of 1.34a



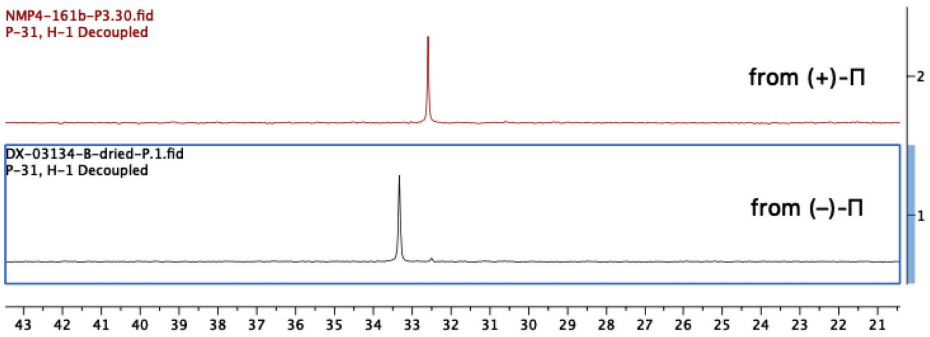
Identification code	Baran748	
Empirical formula	C23 H19 O2 P	
Formula weight	358.35	
Temperature	100.0 K	
Wavelength	1.54178 Å	
Crystal system	Monoclinic	
Space group	P 1 21 1	
Unit cell dimensions	a = 9.6822(2) Å	α= 90°.
	b = 8.56510(10) Å	β= 93.4740(10)°.
	c = 10.6603(2) Å	γ = 90°.
Volume	882.42(3) $Å^3$	
Z	2	
Density (calculated)	1.349 Mg/m^3	
Absorption coefficient	1.489 mm^{-1}	
F(000)	376	
Crystal size	0.17 x 0.08 x 0.06 mm^3	
Theta range for data collection	4.155 to 71.270°.	
Index ranges	-11<=h<=11, -10<=k<=10, -12<=l<=12	
Reflections collected	9893	
Independent reflections	3236 [R(int) = 0.0192]	
Completeness to theta = 67.500°	100.0 %	
Absorption correction	Semi-empirical from equivalents	
Max. and min. transmission	0.7535 and 0.6267	
Refinement method	Full-matrix least-squares on F^2	
Data / restraints / parameters	3236 / 1 / 236	
Goodness-of-fit on F^2	1.031	
Final R indices [I>2sigma(I)]	R1 = 0.0248, wR2 = 0.0667	
R indices (all data)	R1 = 0.0249, wR2 = 0.0668	
Absolute structure parameter	0.002(8)	
Extinction coefficient	n/a	
Largest diff. peak and hole	0.331 and -0.249 $e.Å^{-3}$	

MPO workflow:



The absolute stereochemistry outcome was determined by the following logic:

1. Addition of MeMgBr to Π occurs in stereoretention (see previous section).
2. The coupling step occurs with inversion at phosphorus, as is reported in literature.[3]
3. The net stereochemical outcome after loading and coupling is determined by comparing the ^{31}P NMR chemical shifts of dT-dT dimers (**1.44**) originating from either (–)- or (+)-Π:



   a. dT-dT dimer from (+)-Π: ^{31}P NMR (162 MHz, Acetone-d_6) δ 32.59.
   b. dT-dT dimer from (–)-Π: ^{31}P NMR (162 MHz, Acetone-d_6) δ 33.33.

4. According to literature [3]:
   a. dT-dT dimer with (R_p) MPO linkage: δ 33.00
   b. dT-dT dimer with (S_p) MPO linkage: δ 34.14
5. Thus, the downfield dT-dT dimer originating from (–)-Π carries a S_p MPO linkage, *vice versa*. In other words, net retention is observed after loading and coupling. Since coupling gives inversion (step 2), the loading step must occur with inversion too.

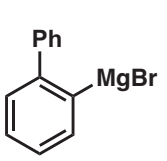
Synthesis of Grignard and Organolithium Reagents

All Grignard reagents were prepared from aryl bromides via Mg insertion in the presence of LiCl or purchased from commercial sources.

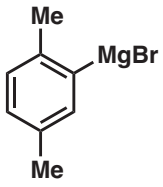
General procedure for Mg insertion:

LiCl (0.530 g, 12.5 mmol, 1.25 equiv.) was flame-dried under vacuum. After cooling, the flask was placed under Ar atmosphere, and Mg turnings (0.608 g, 25 mmol, 2.5 equiv.), iodine (a few grains) and THF (2 mL) were added. In a separate flask under Ar atmosphere, a solution of aryl bromide (10 mmol, 1.0 equiv.) in THF (8 mL) was prepared. A few drops of the aryl bromide solution in THF was added to the flask containing Mg, and the mixture was gently heated with a heat gun until the solution color changed from brown to colorless. The remaining aryl bromide solution was then slowly added. Upon complete addition, the mixture was placed in an oil bath (55 °C) and heated for 1-2 hr. The Grignard was titrated against iodine/LiCl before use following Knochel's published procedures.[4]

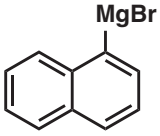
The following Grignard reagents were synthesized using the above procedures:



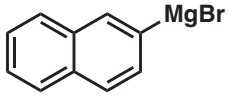
SI-1.4



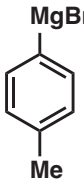
SI-1.5



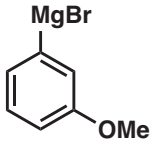
SI-1.6



SI-1.7

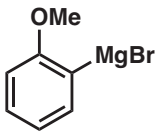


SI-1.8



SI-1.9

The following Grignard reagents were directly purchased from Sigma-Aldrich:

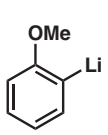
PhMgBr	MeMgBr	EtMgBr			
1.0 M	3.0 M	3.0 M	1.0 M	1.0 M	1.0 M
SI-1.10	SI-1.11	SI-1.12	SI-1.13	SI-1.14	SI-1.15

Unless otherwise stated, all organolithium reagents were freshly prepared by lithium-halogen exchange with aryl bromides, *via* direct deprotonation of terminal alkynes, or purchased from commercial sources. Ferrocenyllithium was prepared according to a published procedure.[5]

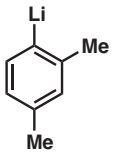
General procedure for lithium-halogen exchange:

To a flame dried round-bottom flask under argon atmosphere was charged aryl bromide (11 mmol, 1.1 equiv.) and THF (40 mL). The mixture was cooled to –78 °C and *n*BuLi solution (10 mmol, 1.0 equiv.) was added dropwise. The resulting mixture was allowed to stir for 30 min at –78 °C and used directly.

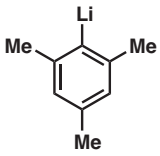
The following organolithium reagents were synthesized using the above method:



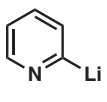
SI-1.16



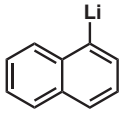
SI-1.17



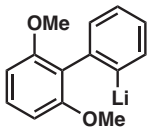
SI-1.18



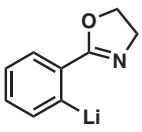
SI-1.19



SI-1.20



SI-1.21



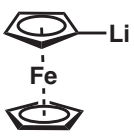
SI-1.22

Direct deprotonation of terminal alkynes follows the same procedure as lithium-halogen exchange. The following organolithium reagent was synthesized by direct deprotonation:



SI-1.23

Synthesis of FcLi (SI-1.24): [5]



SI-1.24

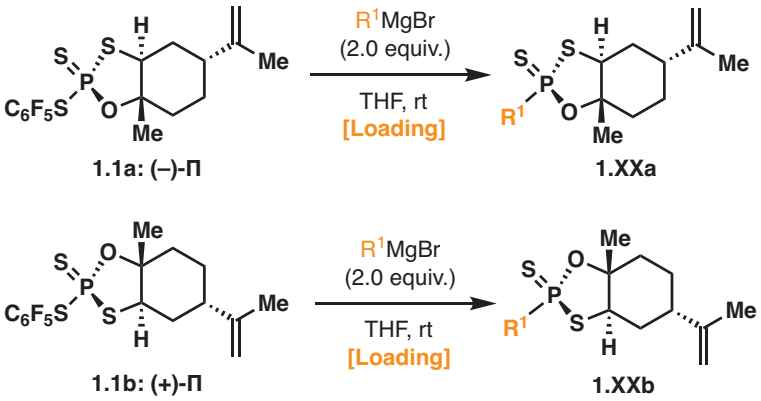
Following a literature procedure, a flame dried round-bottom flask under argon atmosphere was charged with ferrocene (186 mg, 1 mmol, 1.0 equiv.), ^{t}BuOK (0.15 mL, 1.0 M, 0.15 mmol, 0.15 equiv.) and THF (8 mL). The reaction was cooled to –78 °C and ^{t}BuLi (1.18 mL, 1.7 M, 2 mmol, 2.0 equiv.) was added

dropwise. The resulting mixture was allowed to stir at –78 °C for 1 h, brought to 0 °C for 30 min, and then used directly.

Finally, the following organolithium reagents were purchased from Sigma-Aldrich:

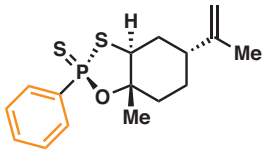
^{i}PrLi	^{n}BuLi	^{t}BuLi
0.7 M	2.5 M	1.6 M
SI-1.25	SI-1.26	SI-1.27

General Procedure A: P-Chiral Phosphine Synthesis – Loading



To a flamed-dried 250 mL round-bottom flask was charged **1.1** (4.46 g, 10 mmol, 1 equiv.). The flask was evacuated and backfilled with argon, after which anhydrous THF (100 mL, 0.1 M) was introduced. Grignard reagent (20 mmol, 2 equiv.) was then added dropwise and the resulting solution was allowed to stir at room temperature until ^{31}P NMR showed complete consumption of starting material. The reaction was quenched with slow addition of saturated aqueous NH_4Cl solution (20 mL) and diluted with water (80 mL) and EtOAc (150 mL). The two layers were separated, and the aqueous layer was washed twice with EtOAc (2 X 80 mL). The combined organic layers were washed with saturated aqueous $NaHCO_3$ solution (50 mL), brine (50 mL), and dried over anhydrous Na_2SO_4. The mixture was then filtered, concentrated *in vacuo*, and purified by silica gel chromatography to afford the desired product.

Compound 1.8a:



Following **General Procedure A** on 10 mmol scale with **1.1a** and Grignard reagent **SI-1.10**. Reaction time 2 h. Purification by silica gel column chromatography (hexane/toluene = 2:1 to 1:2) afforded 1.93 g (60%, >20:1 d.r.) of the title compound **1.8a**. On 50 mmol scale, 9.20 g (57%, >20:1 d.r.) of **1.8a** was obtained after purification.

Physical State: white solid

m.p. = 108–110 °C

$[\alpha]^{25}_{D}$ = -27.3° (c = 1.00 in $CHCl_3$)

R_f = 0.35 (hexane/toluene = 1:2)

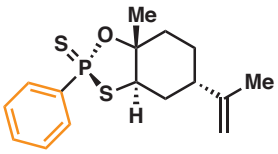
^{1}H NMR (400 MHz, $CDCl_3$) δ 7.87 (ddd, *J* = 15.2, 8.1, 1.5 Hz, 2H), 7.56 – 7.40 (m, 3H), 4.98 (s, 1H), 4.89 (s, 1H), 3.86 (dd, *J* = 13.2, 3.1 Hz, 1H), 2.50 (s, 1H), 2.26 – 2.09 (m, 3H), 2.08 – 1.84 (m, 2H), 1.83 (s, 3H), 1.73 (s, 3H).

^{13}C NMR (126 MHz, $CDCl_3$) δ 145.45, 138.93, 138.02, 132.21, 132.19, 130.30, 130.20, 128.70, 128.58, 111.94, 92.62, 92.59, 57.25, 57.24, 39.00, 34.91, 34.82, 29.05, 28.98, 25.36, 22.83, 19.33.

^{31}P NMR (162 MHz, $CDCl_3$) δ 97.21.

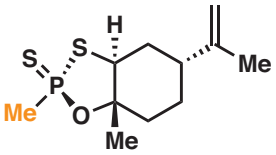
HRMS (ESI-TOF): calc'd for $C16H22OPS_2$ [M+H]+: 325.0850, found: 325.0849.

Compound 1.8b:



Following **General Procedure A** on 10 mmol scale with **1.1b** and Grignard reagent **SI-1.10**. Reaction time 2 h. Purification by silica gel column chromatography (hexane/toluene = 2:1 to 1:2) afforded 2.11 g (65%, >20:1 d.r.) of the title compound **1.8b**. All physical and spectroscopic properties are identical with **1.8a** except for the optical rotation: $[\alpha]^{25}_{D}$ = +31.6° (c = 1.00 in $CHCl_3$).

Compound 1.12a:



Following **General Procedure A** on 10 mmol scale with **1.1a** and Grignard reagent **SI-1.11**. Reaction time 2 h. Purification by silica gel column chromatography (hexane/toluene/EtOAc = 1:1:0 to 1:2:0 to 1:2:0.05) afforded 1.73 g (66%, >20:1 d.r.) of the title compound **1.12a**.

Physical State: white solid

m.p. = 102–105 °C

$[\alpha]^{25}_{D}$ = +136.4° (c = 0.50 in $CHCl_3$)

R_f = 0.20 (hexane/toluene = 1:2)

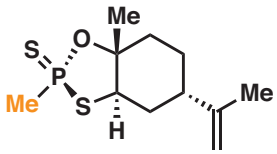
^{1}H NMR (400 MHz, $CDCl_3$) δ 5.01 (s, 1H), 4.89 (s, 1H), 3.74 (dd, *J* = 13.3, 3.1 Hz, 1H), 2.48 (s, 1H), 2.23 (d, *J* = 13.8 Hz, 1H), 2.20 (s, 3H), 2.17 (d, *J* = 0.8 Hz, 3H), 2.11 (d, *J* = 11.2 Hz, 1H), 2.06 – 2.00 (m, 1H), 1.80 (d, *J* = 8.1 Hz, 3H), 1.76 (s, 3H), 1.68 (s, 3H).

^{13}C NMR (151 MHz, $CDCl_3$) δ 145.25, 112.07, 92.26, 92.23, 56.99, 56.97, 38.93, 35.16, 35.08, 31.27, 30.74, 28.99, 28.93, 25.21, 22.78, 18.85.

^{31}P NMR (162 MHz, $CDCl_3$) δ 106.19.

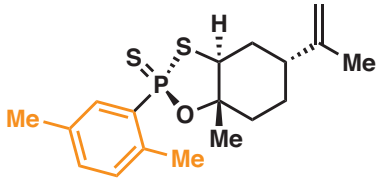
HRMS (ESI-TOF): calc'd for $C_{11}H_{20}OPS_2$ [M+H]+: 263.0693, found: 263.0697.

Compound 1.12b:



Following **General Procedure A** on 5 mmol scale with **1.1b** and Grignard reagent **SI-1.11**. Reaction time 2 h. Purification by silica gel column chromatography (hexane/toluene/EtOAc = 1:1:0 to 1:2:0 to 1:2:0.05) afforded 923 mg (70%, >20:1 d.r.) of the title compound **1.12b**. On 25 mmol scale, 3.41 g (52%, >20:1 d.r.) of **1.12b** was obtained after purification. All physical and spectroscopic properties are identical with **1.12a** except for the **$[\alpha]^{25}_{D}$** = -130.2° (c = 0.50 in $CHCl_3$).

Compound 1.13a:



Following **General Procedure A** on 0.5 mmol scale with **1.1a** and Grignard reagent **SI-1.5**. Reaction time 12 h. Purification by silica gel column chromatography (hexane/toluene = 2:1 to 1:2) afforded 60 mg (33%, >20:1 d.r.) of the title compound **1.13a**.

Physical State: colorless gel

$[\alpha]^{25}_{D}$ = -25.0° (c = 0.70 in $CHCl_3$)

R_f = 0.41 (hexane/EtOAc = 92:8)

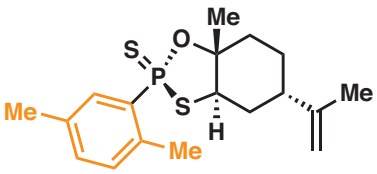
^{1}H NMR (400 MHz, $CDCl_3$) δ 7.51 (dd, *J* = 15.2, 1.8 Hz, 1H), 7.23 – 7.09 (m, 2H), 4.85 (d, *J* = 1.4 Hz, 1H), 4.78 (s, 1H), 3.55 (ddd, *J* = 13.3, 3.2, 1.6 Hz, 1H), 2.70 (s, 3H), 2.44 (t, *J* = 5.3 Hz, 1H), 2.33 (s, 3H), 2.23 – 2.06 (m, 3H), 2.02 – 1.81 (m, 3H), 1.79 (s, 3H), 1.66 (s, 3H).

^{13}C NMR (151 MHz, $CDCl_3$) δ 145.29, 137.41, 136.73, 136.68, 136.63, 135.04, 134.95, 132.36, 132.34, 132.29, 132.19, 129.44, 129.38, 111.88, 92.48, 92.44, 77.37, 77.16, 77.08, 76.95, 56.19, 56.17, 38.89, 34.78, 34.71, 28.96, 28.89, 25.35, 22.78, 21.56, 21.53, 21.13, 19.69.

^{31}P NMR (162 MHz, $CDCl_3$) δ 94.99.

HRMS (ESI-TOF): calc'd for $C18H26OPS_2$ [M+H]+: 353.1163, found: 353.1168.

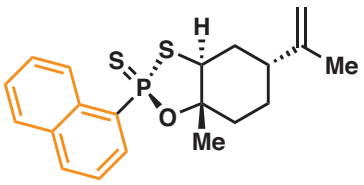
Compound 1.13b:



Following **General Procedure A** on 0.5 mmol scale with **1.1b** and Grignard reagent **SI-1.5**. Reaction time 12 h. Purification by silica gel column chromatography (hexane/toluene = 2:1 to 1:2) afforded 58 mg (32%, >20:1 d.r.) of the title compound **1.13b**. All physical

and spectroscopic properties are identical with **1.13a** except for the optical rotation: $[\alpha]^{25}_{D}$ = +31° (c = 0.60 in $CHCl_3$).

Compound 1.14a:



Following **General Procedure A** on 1 mmol scale with **1.1a** and Grignard reagent **SI-1.6**. Reaction time 12 h. Purification by silica gel column chromatography (hexane/toluene = 2:1 to 1:2) afforded 292 mg (77%, >20:1 d.r.) of the title compound **1.14a**.

Physical State: light yellow solid

m.p. = 114–116°C

$[\alpha]^{25}_{D}$ = -121.8° (c = 1.00 in $CHCl_3$)

R_f = 0.24 (hexane/Et_2O = 9:1)

^{1}H NMR (500 MHz, $CDCl_3$) δ 8.84 (dd, *J* = 8.4, 0.9 Hz, 1H), 8.03 – 7.83 (m, 3H), 7.65 (ddd, *J* = 8.5, 6.9, 1.4 Hz, 1H), 7.56 (ddd, *J* = 8.1, 6.9, 1.2 Hz, 1H), 7.47 (ddd, *J* = 8.1, 7.3, 3.6 Hz, 1H), 4.80 (d, *J* = 1.4 Hz, 1H), 4.73 (s, 1H), 3.57 (ddd, *J* = 13.3, 3.2, 1.6 Hz, 1H), 2.44 (d, *J* = 6.0 Hz, 1H), 2.22 (ddd, *J* = 12.4, 4.4, 2.8 Hz, 1H), 2.16 – 2.08 (m, 2H), 2.02 – 1.78 (m, 3H), 1.86 (s, 3H), 1.62 (d, *J* = 1.3 Hz, 3H).

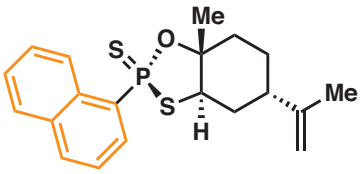
^{13}C NMR (151 MHz, $CDCl_3$) δ 163.86, 163.74, 159.73, 159.72, 145.52, 145.34, 145.15, 136.41, 136.32, 134.58, 133.59, 131.03, 130.99, 129.45, 129.43, 129.17, 129.08, 128.80, 127.79, 114.09, 114.07, 114.03, 97.12, 87.93, 87.76, 87.69, 86.90, 86.86, 85.92, 85.89,

75.87, 75.84, 72.60, 65.22, 65.18, 63.37, 55.55, 42.11, 40.79, 40.77, 26.16, 18.50, 12.25, 11.30, -4.52, -4.65.

^{31}P NMR (162 MHz, $CDCl_3$) δ 92.77.

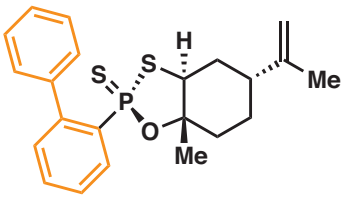
HRMS (ESI-TOF): calc'd for $C_{20}H_{24}OPS_2$ $[M+H]^+$: 375.1006, found: 375.1006.

Compound 1.14b:



Following **General Procedure A** on 0.5 mmol scale with **1.1b** and Grignard reagent **SI-1.6**. Reaction time 12 h. Purification by silica gel column chromatography (hexane/toluene = 2:1 to 1:2) afforded 152 mg (80%, >20:1 d.r.) of the title compound **1.14b**. All physical and spectroscopic properties are identical with **1.14a** except for the optical rotation: **$[\alpha]^{25}_D$** = +125.1° (c = 0.35 in DCM).

Compound 1.15a:



Following **General Procedure A** on 0.5 mmol scale with **1.1a** and Grignard reagent **SI-1.4**. Reaction time 12 h. Purification by silica gel column chromatography (hexane/toluene = 2:1 to 1:2) afforded 104 mg (52%, >20:1 d.r.) of the title compound **1.15a**.

Physical State: light yellow gel

$[\alpha]^{25}_D$ = -83.8° (c = 0.22 in DCM)

R_f = 0.31 (hexane/Et_2O = 9:1)

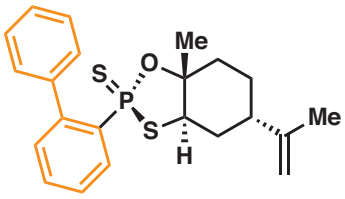
^{1}H NMR (400 MHz, $CDCl_3$) δ 7.44 (dd, *J* = 7.6, 1.4 Hz, 1H), 7.40 – 7.27 (m, 8H), 4.95 (d, *J* = 1.4 Hz, 1H), 4.89 – 4.82 (m, 1H), 3.74 (ddd, *J* = 13.3, 3.2, 1.6 Hz, 1H), 2.50 (s, 1H), 2.25 – 2.10 (m, 3H), 1.97 – 1.77 (m, 3H), 1.75 (s, 3H), 1.74 – 1.71 (m, 3H).

^{13}C NMR (151 MHz, $CDCl_3$) δ 145.07, 143.68, 140.20, 131.89, 131.05, 129.01, 128.55, 128.41, 128.25, 127.68, 112.31, 93.62, 93.59, 56.99, 56.97, 38.84, 34.76, 34.68, 28.76, 28.69, 25.31, 22.78, 19.60.

^{31}P NMR (162 MHz, $CDCl_3$) δ 77.83.

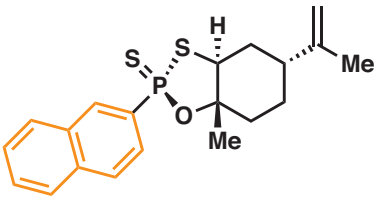
HRMS (ESI-TOF): calc'd for $C_{22}H_{26}OPS_2$ [M+H]+: 401.1163, found: 401.1157.

Compound 1.15b:



Following **General Procedure A** on 4 mmol scale with **1.1b** and Grignard reagent **SI-1.4**. Reaction time 12 h. Purification by silica gel column chromatography (hexane/toluene = 2:1 to 1:2) afforded 882 mg (55%, >20:1 d.r.) of the title compound **1.15b**. All physical and spectroscopic properties are identical with **1.15a** except for the optical rotation: **$[\alpha]^{25}_D$** = +95.7° (c = 1.00 in $CHCl_3$).

Compound 1.16a:



Following **General Procedure A** on 0.5 mmol scale with **1.1a** and Grignard reagent **SI-1.7**. Reaction time 12 h. Purification by silica gel column chromatography (hexane/toluene = 2:1) afforded 126 mg (68%, >20:1 d.r.) of the title compound **1.16a**.

Physical State: light yellow gel

$[\alpha]^{25}_{D}$ = -48.8° (c = 0.50 in $CHCl_3$)

R_f = 0.2 (hexane/toluene = 2:1)

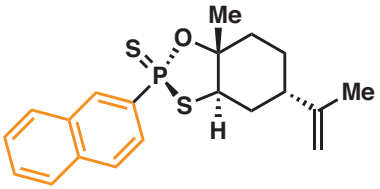
^{1}H NMR (400 MHz, $CDCl_3$) δ 8.41 (d, *J* = 17.9 Hz, 1H), 7.95 – 7.81 (m, 4H), 7.63 – 7.53 (m, 2H), 4.99 (d, *J* = 1.4 Hz, 1H), 4.92 (s, 1H), 3.95 (dd, *J* = 13.3, 3.1 Hz, 1H), 2.51 (s, 1H), 2.26 – 2.15 (m, 3H), 2.09 (td, *J* = 13.3, 12.6, 4.1 Hz, 1H), 1.99 – 1.88 (m, 2H), 1.87 (s, 3H), 1.73 (s, 3H).

^{13}C NMR (151 MHz, $CDCl_3$) δ 144.93, 135.15, 134.39, 134.31, 134.29, 131.82, 131.71, 131.46, 131.38, 128.80, 128.20, 128.10, 127.93, 127.29, 126.61, 124.81, 124.72, 111.35, 92.14, 92.11, 56.73, 56.72, 38.47, 34.38, 34.31, 28.49, 28.43, 24.82, 22.26, 18.84.

^{31}P NMR (162 MHz, $CDCl_3$) δ 97.21.

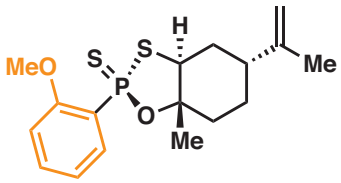
HRMS (ESI-TOF): calc'd for $C_{20}H_{24}OPS_2$ [M+H]+: 375.1006, found: 375.0999.

Compound 1.16b:



Following **General Procedure A** on 0.5 mmol scale with **1.1b** and Grignard reagent **SI-1.7**. Reaction time 12 h. Purification by silica gel column chromatography (hexane/toluene = 2:1) afforded 137 mg (72%, >20:1 d.r.) of the title compound **1.16b**. All physical and spectroscopic properties are identical with **1.16a** except for the optical rotation: $[\alpha]^{25}_{D}$ = +40.1° (c = 0.21 in DCM).

Compound 1.17a:



Following **General Procedure A** on 2 mmol scale with **1.1a** and Grignard reagent **SI-1.13**. Reaction time 12 h. Purification by silica gel column chromatography (hexane/toluene/EtOAc = 2:1:0 to 1:1:0 to 1:1:0.05) afforded 420 mg (59%, >20:1 d.r.) of the title compound **1.17a**.

Physical State: colorless oil

$[\alpha]^{25}_{D}$ = -38.2° (c = 0.50 in DCM)

R_f = 0.22 (hexane/Et_2O = 9:1)

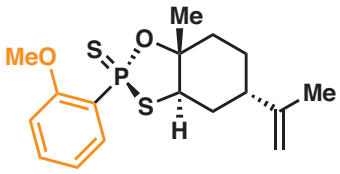
^{1}H NMR (400 MHz, $CDCl_3$) δ 7.98 (ddd, *J* = 17.3, 7.7, 1.7 Hz, 1H), 7.52 – 7.42 (m, 1H), 7.01 (tdd, *J* = 7.6, 3.4, 1.0 Hz, 1H), 6.95 (ddd, *J* = 8.2, 7.1, 0.9 Hz, 1H), 4.95 (q, *J* = 1.4 Hz, 1H), 4.88 (s, 1H), 3.98 (ddd, *J* = 13.5, 3.1, 0.7 Hz, 1H), 3.92 (s, 3H), 2.48 (s, 1H), 2.25 – 2.07 (m, 3H), 2.00 – 1.84 (m, 3H), 1.82 (s, 3H), 1.73 (dt, *J* = 1.4, 0.7 Hz, 3H).

^{13}C NMR (151 MHz, $CDCl_3$) δ 159.92, 159.89, 145.68, 134.24, 134.22, 134.07, 134.01, 125.12, 124.37, 120.49, 120.39, 111.99, 111.94, 111.88, 92.25, 92.22, 56.65, 56.64, 55.93, 39.05, 34.93, 34.85, 28.82, 28.76, 25.26, 22.78, 19.49.

^{31}P NMR (162 MHz, $CDCl_3$) δ 93.72.

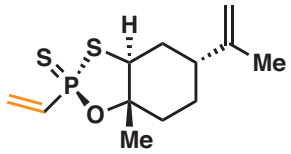
HRMS (ESI-TOF): calc'd for $C_{17}H_{24}O_2PS_2$ [M+H]+: 355.0955, found: 355.0951.

Compound 1.17b:



Following **General Procedure A** on 2.5 mmol scale with **1.1b** and Grignard reagent **SI-1.13**. Reaction time 12 h. Purification by silica gel column chromatography (hexane/toluene/EtOAc = 2:1:0 to 1:1:0 to 1:1:0.05) afforded 525 mg (59%, >20:1 d.r.) of the title compound **1.17b**. All physical and spectroscopic properties are identical with **1.17a** except for the optical rotation: **$[\alpha]^{25}_D$** = +50.8° (c = 1.00 in $CHCl_3$).

Compound 1.18a:



Following **General Procedure A** on 1 mmol scale with **1.1a** and Grignard reagent **SI-1.15**. Reaction time 0.5 h. Purification by silica gel column chromatography (hexane/toluene = 2:1 to 1:1) afforded 146 mg (54%, >20:1 d.r.) of the title compound **1.18a**.

Physical State: colorless oil

$[\alpha]^{25}_D$ = +12.5° (c = 0.28 in $CHCl_3$)

R_f = 0.41 (hexane/Et_2O = 9:1)

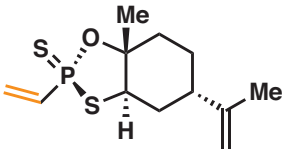
^{1}H NMR (500 MHz, $CDCl_3$) δ 6.38 (ddd, *J* = 29.8, 17.7, 11.4 Hz, 1H), 6.20 (ddd, *J* = 29.4, 17.7, 1.3 Hz, 1H), 5.98 (ddd, *J* = 57.5, 11.4, 1.3 Hz, 1H), 4.99 (d, *J* = 1.5 Hz, 1H), 4.88 (s, 1H), 3.74 (dd, *J* = 13.3, 3.2 Hz, 1H), 2.48 (s, 1H), 2.22 (dd, *J* = 13.8, 1.8 Hz, 1H), 2.16 – 2.09 (m, 1H), 2.06 (dd, *J* = 7.3, 4.7 Hz, 1H), 1.92 – 1.77 (m, 3H), 1.75 (dt, *J* = 1.5, 0.8 Hz, 3H), 1.72 (s, 3H).

^{13}C NMR (151 MHz, $CDCl_3$) δ 163.86, 163.74, 159.73, 159.72, 145.52, 145.34, 145.15, 136.41, 136.32, 134.58, 133.59, 131.03, 130.99, 129.45, 129.43, 129.17, 129.08, 128.80, 127.79, 114.09, 114.07, 114.03, 97.12, 87.93, 87.76, 87.69, 86.90, 86.86, 85.92, 85.89, 75.87, 75.84, 72.60, 65.22, 65.18, 63.37, 55.55, 42.11, 40.79, 40.77, 26.16, 18.50, 12.25, 11.30, -4.52, -4.65.

^{31}P NMR (162 MHz, $CDCl_3$) δ 93.96.

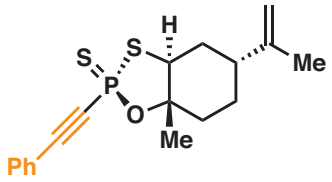
HRMS (ESI-TOF): calc'd for $C12H20OPS_2$ [M+H]+: 275.0693, found: 275.0695.

Compound 1.18b:



Following **General Procedure A** on 0.5 mmol scale with **1.1b** and Grignard reagent **SI-1.15**. Reaction time 0.5 h. Purification by silica gel column chromatography (hexane/toluene = 2:1 to 1:1) afforded 85 mg (63%, >20:1 d.r.) of the title compound **1.18b**. All physical and spectroscopic properties are identical with **1.18a** except for the optical rotation: **$[\alpha]^{25}_D$** = -7.96° (c = 0.21 in DCM).

Compound 1.19a:



Following **General Procedure A** on 1 mmol scale with **1.1a** and Grignard reagent **SI-1.14**. Reaction time 1 h. Purification by silica gel column chromatography (hexane/toluene = 2:1 to 1:2) afforded 232 mg (67%, >20:1 d.r.) of the title compound **1.19a**.

Physical State: light yellow solid

m.p. = 107–110 °C

$[\alpha]^{25}_{D}$ = +115.3° (c = 0.22 in DCM).

R_f = 0.24 (hexane/Et_2O = 9:1)

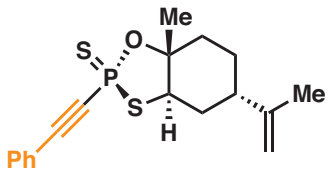
^{1}H NMR (500 MHz, $CDCl_3$) δ 7.57 – 7.49 (m, 2H), 7.48 – 7.40 (m, 1H), 7.40 – 7.33 (m, 2H), 5.02 (d, *J* = 1.5 Hz, 1H), 4.95 (s, 1H), 4.14 (dt, *J* = 13.2, 2.7 Hz, 1H), 2.51 (t, *J* = 6.0 Hz, 1H), 2.29 (ddd, *J* = 13.8, 3.4, 1.7 Hz, 1H), 2.15 (d, *J* = 15.0 Hz, 1H), 2.10 (ddd, *J* = 12.5, 4.4, 2.9 Hz, 1H), 2.03 – 1.86 (m, 2H), 1.85 – 1.79 (m, 1H), 1.78 (s, 3H), 1.67 (s, 3H).

^{13}C NMR (151 MHz, $CDCl_3$) δ 145.31, 132.66, 132.65, 130.72, 128.62, 120.06, 120.03, 112.15, 99.29, 99.03, 93.04, 93.01, 87.23, 85.86, 57.13, 57.10, 39.01, 35.14, 35.06, 29.03, 28.96, 25.49, 22.86, 19.79.

^{31}P NMR (162 MHz, $CDCl_3$) δ 60.28.

HRMS (ESI-TOF): calc'd for $C18H22OPS_2$ [M+H]+: 349.0850, found: 349.0841.

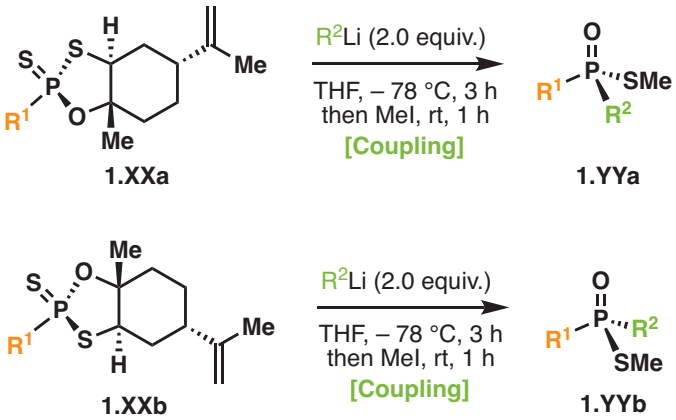
Compound 1.19b:



Following **General Procedure A** on 0.5 mmol scale with **1.1b** and Grignard reagent **SI-1.14**. Reaction time 1 h. Purification by silica gel column chromatography (hexane/toluene = 2:1 to 1:2) afforded 118 mg (68%, >20:1 d.r.) of the title compound **1.19b**. All physical and spectroscopic properties are identical with **1.19a** except for the optical rotation: $[\alpha]^{25}_{D}$ = -104.0° (c = 0.20 in DCM).

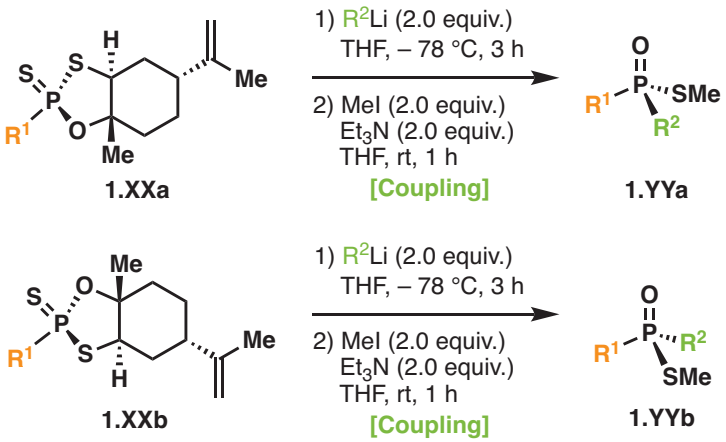
General Procedures B and C: P-Chiral Phosphine Synthesis – Coupling

General Procedure B (One-Pot MeI Quench):



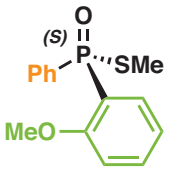
The organolithium reagent (4.0 mmol, 2.0 equiv., see **Synthesis of Grignard and Organolithium Reagents**) in 14 mL of THF was cooled to – 78 °C if not already at such temperature. A solution of the starting material (2.0 mmol, 1.0 equiv.) in 6 mL THF was prepared in a flame-dried flask under argon atmosphere, which was then added dropwise to the flask containing the organolithium reagent. The resulting mixture was stirred for 3 h while being kept at –78 °C. After ^{31}P NMR analysis of a small aliquot showed complete consumption of starting material, the reaction was quenched with an excess of methyl iodide (8.0 mmol, 4.0 equiv.), warmed to room temperature, and stirred for another hour. To the resulting mixture was added saturated aqueous NH_4Cl solution (20 mL) and EtOAc (40 mL). The layers were separated, and the aqueous layer was washed with EtOAc (2 x 20 mL). The combined organic layers were washed with brine (20 mL), dried over anhydrous Na_2SO_4, filtered and concentrated. The residue was purified by silica gel chromatography to afford the desired product.

General Procedure C (Stepwise):



The organolithium reagent (4.0 mmol, 2.0 equiv., see **Synthesis of Grignard and Organolithium Reagents**) in 14 mL of THF was cooled to – 78 °C if not already at such temperature. A solution of the starting material (2.0 mmol, 1.0 equiv.) in 6 mL THF was prepared in a flame-dried flask under argon atmosphere, which was then added dropwise to the flask containing the organolithium reagent. The resulting mixture was stirred for 3 h while being kept at –78 °C. After ^{31}P NMR analysis of a small aliquot showed complete consumption of starting material, the reaction was carefully quenched with slow addition of saturated aqueous NH_4Cl solution (20 mL) and then diluted with water (10 mL) and DCM (40 mL). The layers were separated, and the aqueous layer was washed with DCM (2 x 20 mL). The combined organic layers were washed with brine (20 mL), dried over anhydrous Na_2SO_4, filtered and concentrated. The residue was dissolved in THF (10 mL), to which Et_3N (4.0 mmol, 2.0 equiv.) and MeI (4.0 mmol, 2.0 equiv.) were added. After stirring for 1 h, the reaction was diluted with water (20 mL) and extracted with EtOAc (3 x 40 mL). The combined organic layers were washed with brine (20 mL), dried over anhydrous Na_2SO_4, filtered and concentrated. The residue was purified by silica gel chromatography to afford the desired product.

Compound 1.11a



Following **General Procedure B** on 4 mmol scale with **1.8a** and organolithium reagent **SI-1.16**. Purification by silica gel column chromatography (hexane/EtOAc = 2:1 to 1:2) afforded 916 mg (82%, >98:2 e.r.) of the title compound **1.11a**. On 20 mmol scale, 4.70 g (84%, >98:2 e.r.) of **1.11a** was obtained after purification.

Physical State: light yellow solid

m.p. = 89–92 °C

$[\alpha]^{25}_{D}$ = -13.1° (c = 1.00 in $CHCl_3$)

R_f = 0.42 (hexane/EtOAc = 1:2)

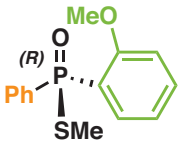
^{1}H NMR (400 MHz, $CDCl_3$) δ 7.97 (dddd, *J* = 14.2, 7.6, 1.8, 0.4 Hz, 1H), 7.94 – 7.86 (m, 2H), 7.55 – 7.40 (m, 4H), 7.08 (tdd, *J* = 7.5, 2.5, 0.9 Hz, 1H), 6.89 (ddd, *J* = 8.3, 6.1, 0.9 Hz, 1H), 3.71 (s, 3H), 2.27 (d, *J* = 12.3 Hz, 3H).

^{13}C NMR (126 MHz, $CDCl_3$) δ 160.45, 160.41, 134.73, 134.55, 134.53, 134.01, 133.95, 133.85, 131.89, 131.86, 131.53, 131.44, 128.36, 128.25, 121.66, 120.99, 120.89, 120.82, 111.66, 111.60, 55.57, 10.43, 10.41.

^{31}P NMR (162 MHz, $CDCl_3$) δ 41.34.

HRMS (ESI-TOF): calc'd for $C14H16O_2PS$ $[M+H]^+$: 279.0609, found: 279.0612.

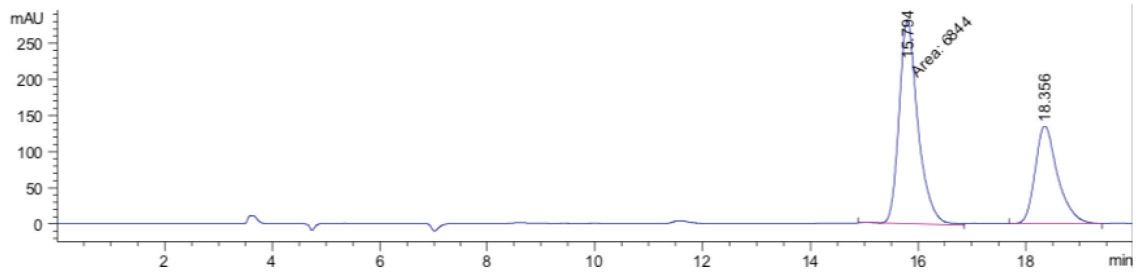
Compound 1.11b



Following **General Procedure B** on 5 mmol scale with **1.8b** and organolithium reagent **SI-1.16**. Purification by silica gel column chromatography (hexane/EtOAc = 2:1 to 1:2) afforded 1.07 g (77%, >98:2 e.r.) of the title compound **1.11b**. All physical and spectroscopic properties are identical with **1.11a** except for the optical rotation: $[\alpha]^{25}_{D}$ = +15.6 (c = 1.00 in $CHCl_3$).

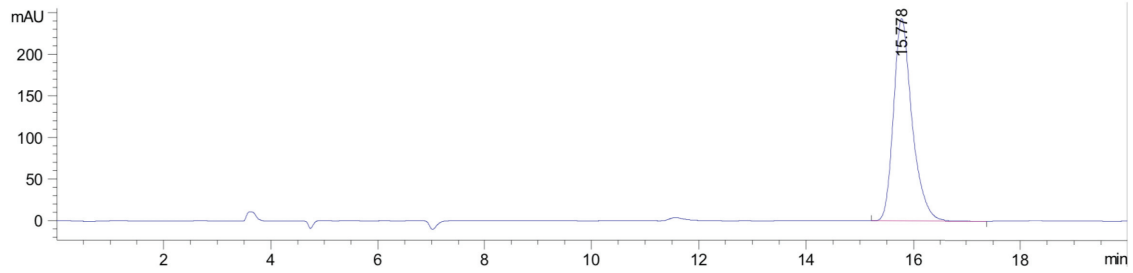
Chiral HPLC: Chiralpak AD-H column; IPA/hexane = 15:85, 0.8 mL/min, 280 nm.

Rac-1.11:



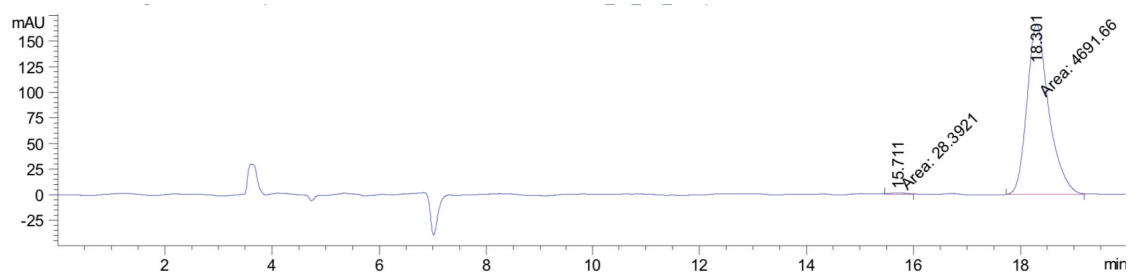
Peak #	RetTime [min]	Type	Width [min]	Area [mAU*s]	Height [mAU]	Area %
1	15.794	MM	0.4050	6843.99512	281.63220	63.7041
2	18.356	BB	0.4294	3899.41577	135.65712	36.2959

1.11a:



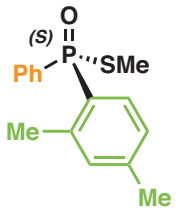
Peak #	RetTime [min]	Type	Width [min]	Area [mAU*s]	Height [mAU]	Area %
1	15.778	BB	0.3598	5829.13623	243.07790	100.0000

1.11b:



Peak #	Ret Time [min]	Type	Width [min]	Area [mAU*s]	Height [mAU]	Area %
1	15.711	MM	0.3689	28.39210	1.28263	0.6015
2	18.301	MM	0.4715	4691.66260	165.83667	99.3985

Compound 1.20a



Following **General Procedure B** on 0.5 mmol scale with **1.8a** and organolithium reagent **SI-1.17**. Purification by silica gel column chromatography (hexane/EtOAc = 3:1 to 1:1) afforded 72.0 mg (52%, >98:2 e.r.) of the title compound **1.20a**.

Physical State: white amorphous solid

$[\alpha]^{25}_D$ = +15.5 (c = 0.40 in $CHCl_3$)

R_f = 0.45 (hexane/EtOAc = 1:2)

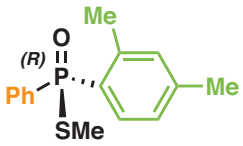
^{1}H NMR (400 MHz, $CDCl_3$) δ 7.85 – 7.76 (m, 2H), 7.65 (dd, *J* = 14.8, 8.3 Hz, 1H), 7.57 – 7.50 (m, 1H), 7.50 – 7.43 (m, 2H), 7.07 (ddd, *J* = 5.5, 1.6, 0.8 Hz, 2H), 2.49 (s, 1H), 2.35 (s, 4H), 2.27 (d, *J* = 11.9 Hz, 3H).

^{13}C NMR (126 MHz, $CDCl_3$) δ 143.15, 143.13, 142.59, 142.51, 134.02, 133.17, 133.14, 133.12, 133.04, 133.02, 132.22, 132.20, 131.68, 131.60, 128.81, 128.71, 127.83, 126.98, 126.46, 126.35, 21.65, 21.62, 21.50, 10.83, 10.81.

^{31}P NMR (162 MHz, $CDCl_3$) δ 46.50.

HRMS (ESI-TOF): calc'd for C15H18OPS [M+H]+: 277.0816, found: 277.0818.

Compound 1.20b

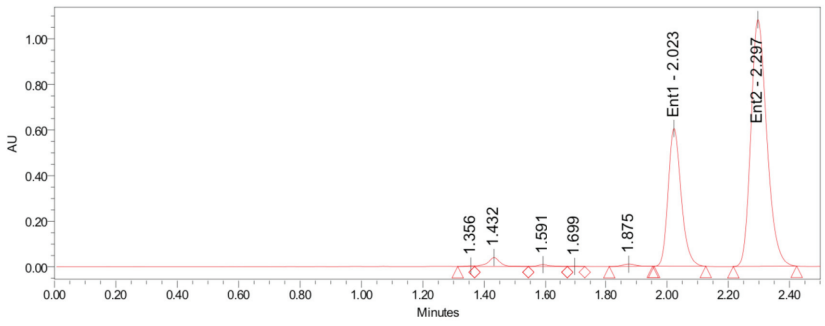


Following **General Procedure B** on 1 mmol scale with **1.8b** and organolithium reagent **SI-1.17**. Purification by silica gel column chromatography (hexane/EtOAc = 3:1 to 1:1) afforded 176 mg (64%, >98:2 e.r.) of the title compound **1.20b**. All physical and spectroscopic properties are identical with **1.20a** except for the optical rotation: **$[\alpha]^{25}_D$** = -15.1° (c = 0.40 in $CHCl_3$).

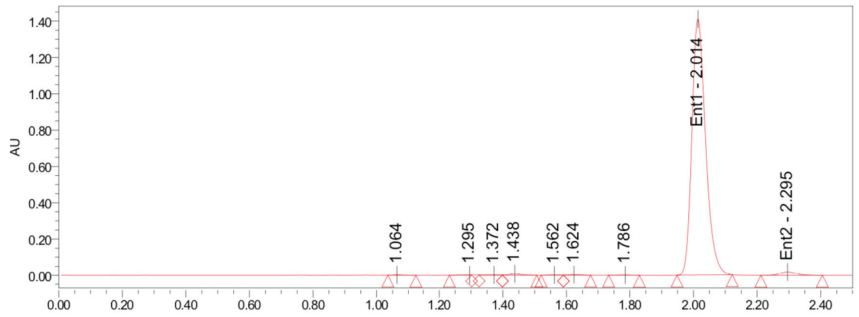
Chiral HPLC: The sample was analyzed on a Waters UPC2 SFC with a Daicel IG column (3 mm, 4.6x250 mm) under isocratic conditions (4 mL/min, 40% MeOH / CO_2, 1600 psi backpressure) at 30 °C. The enantiomers were detected by UV light (230 nm).

***Rac*-1.20:**

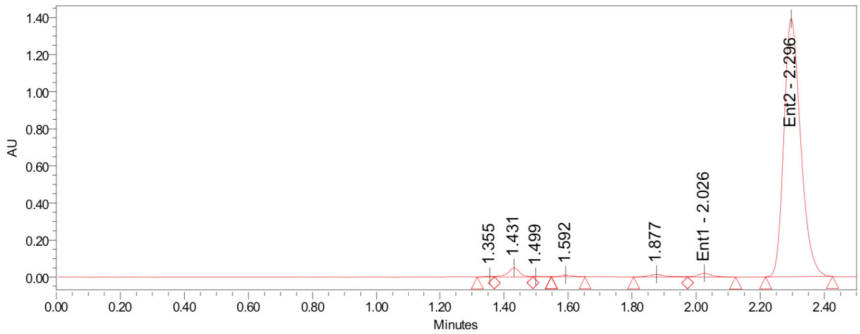
31.30	68.70



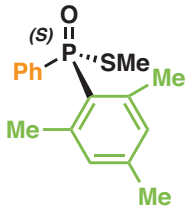
1.20a: 98.47 | 1.53



1.20b: 1.23 | 98.77



Compound 1.21a



Following **General Procedure C** on 0.2 mmol scale with **1.8a** and organolithium reagent **SI-1.18**. Purification by pTLC (hexane/EtOAc = 1:1) afforded 47 mg (81%, 61:39 e.r.) of the title compound **1.21a**.

Physical State: colorless oil

$[\alpha]^{25}_{D}$ = -4.9° (c = 0.45 in $CHCl_3$)

R_f = 0.45 (hexane/EtOAc = 1:2)

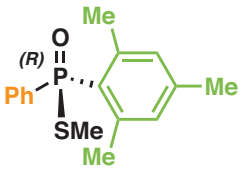
^{1}H NMR (400 MHz, $CDCl_3$) δ 7.82 – 7.73 (m, 2H), 7.53 – 7.39 (m, 3H), 6.89 (dd, *J* = 4.3, 0.6 Hz, 2H), 2.44 (s, 6H), 2.39 (d, *J* = 11.8 Hz, 3H), 2.29 (s, 3H).

^{13}C NMR (151 MHz, $CDCl_3$) δ 143.55, 143.48, 142.30, 142.28, 137.36, 136.66, 131.89, 131.87, 131.39, 131.31, 130.51, 130.44, 128.92, 128.83, 125.85, 125.16, 23.76, 23.74, 21.19, 21.18, 11.02, 11.00.

^{31}P NMR (162 MHz, $CDCl_3$) δ 47.36.

HRMS (ESI-TOF): calc'd for C16H20OPS [M+H]+: 291.0972, found: 291.0975.

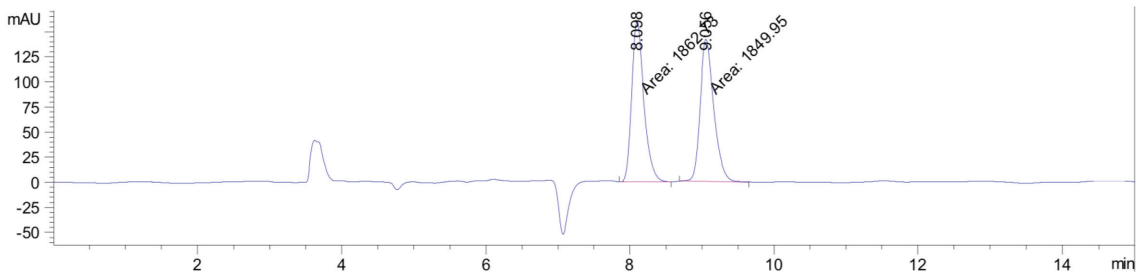
Compound 1.21b



Following **General Procedure C** on 0.2 mmol scale with **1.8b** and organolithium reagent **SI-1.18**. Purification by pTLC (hexane/EtOAc = 1:1) afforded 48 mg (83%, 37:63 e.r.) of the title compound **1.21b**. All physical and spectroscopic properties are identical with **1.21a** except for the optical rotation: $[\alpha]^{25}_{D}$ = +3.5° (c = 1.00 in $CHCl_3$).

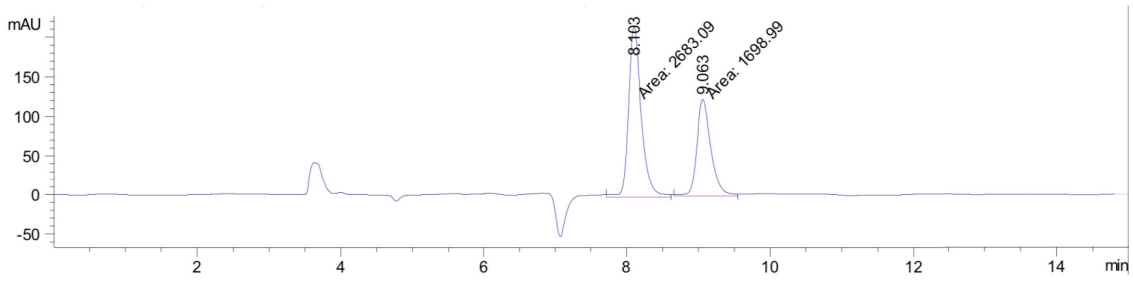
Chiral HPLC: Chiralpak AD-H column; IPA/hexane = 15:85, 0.8 mL/min, 280 nm.

***Rac*-1.21:**



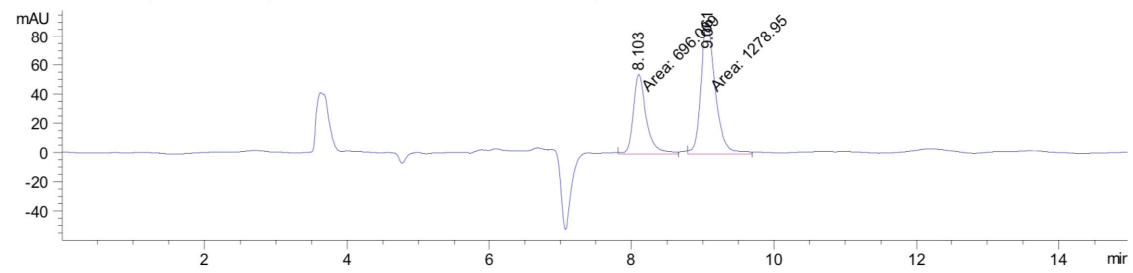
Peak #	RetTime [min]	Type	Width [min]	Area [mAU*s]	Height [mAU]	Area %
1	8.098	MM	0.1939	1862.72913	160.14670	50.1722
2	9.056	MM	0.2175	1849.94568	141.73521	49.8278

1.21a:



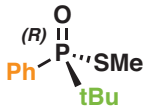
Peak #	RetTime [min]	Type	Width [min]	Area [mAU*s]	Height [mAU]	Area %
1	8.103	MM	0.2057	2683.08984	217.44278	61.2286
2	9.063	MM	0.2288	1698.99426	123.77626	38.7714

1.21b:



Peak #	RetTime [min]	Type	Width [min]	Area [mAU*s]	Height [mAU]	Area %
1	8.103	MM	0.2124	696.00922	54.62587	35.2417
2	9.061	MM	0.2307	1278.94836	92.38139	64.7583

Compound 1.22a



Following **General Procedure B** on 2 mmol scale with **1.8a** and organolithium reagent **SI-1.27**. Purification by silica gel column chromatography (hexane/EtOAc = 2:1 to 1:2) afforded 364 mg (80%, >98:2 e.r.) of the title compound **1.22a**.

Physical State: white solid

m.p. = 80–82 °C

$[\alpha]^{25}_D$ = +142.5° (c = 1.00 in $CHCl_3$)

R_f = 0.56 (hexane:EtOAc = 1:2)

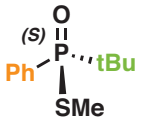
^{1}H NMR (400 MHz, $CDCl_3$) δ 7.92 – 7.85 (m, 2H), 7.56 – 7.44 (m, 3H), 2.12 (d, *J* = 10.5 Hz, 3H), 1.17 (d, *J* = 16.9 Hz, 9H).

^{13}C NMR (151 MHz, $CDCl_3$) δ 133.23, 133.17, 132.06, 132.04, 130.64, 130.03, 128.47, 128.39, 36.67, 36.20, 24.80, 9.61, 9.59.

^{31}P NMR (162 MHz, $CDCl_3$) δ 68.92.

HRMS (ESI-TOF): calc'd for C11H18OPS [M+H]+: 229.0806, found: 229.0818.

Compound 1.22b

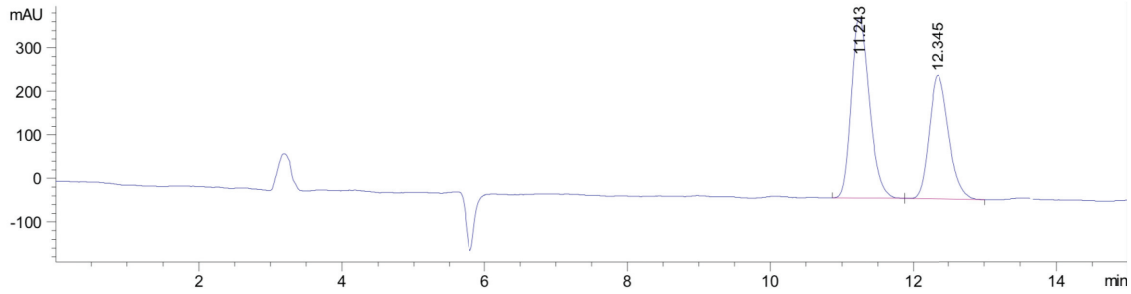


Following **General Procedure B** on 2 mmol scale with **1.8b** and organolithium reagent **SI-1.27**. Purification by silica gel column chromatography (hexane/EtOAc = 2:1 to 1:2) afforded 352 mg (77%, >98:2 e.r.) of the title compound **1.22b**. All physical and

spectroscopic properties are identical with **1.22a** except for the optical rotation: $[\alpha]^{25}_{D}$ = -135.2° (c = 1.00 in $CHCl_3$).

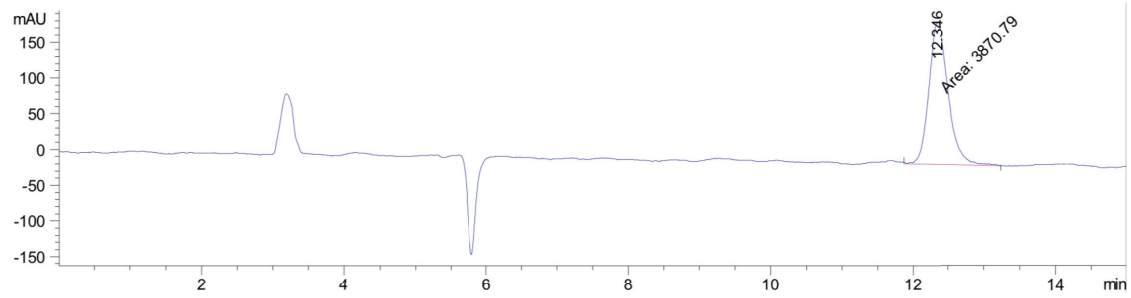
Chiral HPLC: Chiralpak AD-H column; IPA/hexane = 20:80, 1 mL/min, 210 nm.

***Rac*-1.22:**



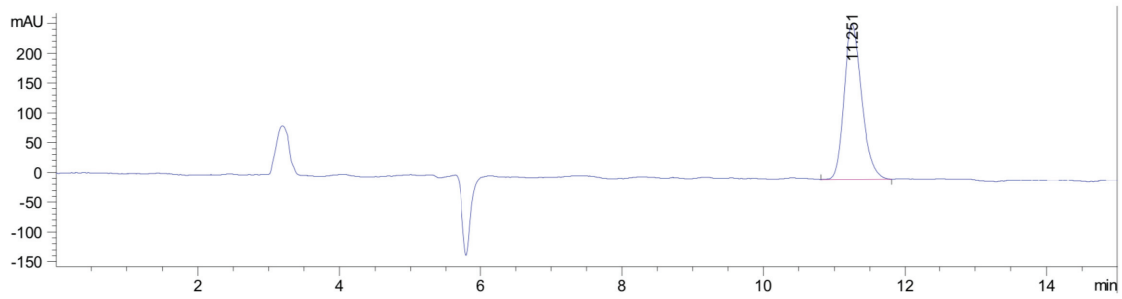
Peak #	RetTime [min]	Type	Width [min]	Area [mAU*s]	Height [mAU]	Area %
1	11.244	BV	0.2596	569.46625	33.62511	57.3140
2	12.348	VB	0.2883	424.12305	22.46315	42.6860

1.22a:



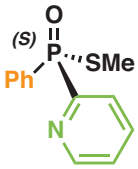
Peak #	RetTime [min]	Type	Width [min]	Area [mAU*s]	Height [mAU]	Area %
1	12.346	BB	0.2916	277.62958	14.48868	100.0000

1.22b:



Peak #	RetTime [min]	Type	Width [min]	Area [mAU*s]	Height [mAU]	Area %
1	11.249	BB	0.2603	316.60913	18.62310	100.0000

Compound 1.23a



Following **General Procedure C** on 0.2 mmol scale with **1.8a** and organolithium reagent **SI-1.19**. Purification by silica gel column chromatography (hexane/EtOAc = 1:2 to pure EtOAc) afforded 15.1 mg (30%, >98:2 e.r.) of the title compound **1.23a**.

Physical State: light yellow oil

$[\alpha]^{25}_{D}$ = -21.6° (c = 0.38 in $CHCl_3$)

R_f = 0.34 (hexane/EtOAc = 1:4)

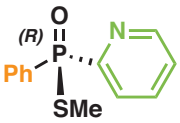
^{1}H NMR (600 MHz, $CDCl_3$) δ 8.81 (d, *J* = 4.7 Hz, 1H), 8.16 (ddt, *J* = 7.7, 5.5, 1.1 Hz, 1H), 8.12 – 8.02 (m, 2H), 7.83 (tdd, *J* = 7.7, 4.8, 1.7 Hz, 1H), 7.57 – 7.52 (m, 1H), 7.50 – 7.45 (m, 2H), 7.40 (dddd, *J* = 7.6, 4.8, 2.7, 1.3 Hz, 1H), 2.23 (d, *J* = 12.2 Hz, 3H).

^{13}C NMR (151 MHz, $CDCl_3$) δ 156.56, 155.64, 150.74, 150.60, 136.49, 136.42, 132.63, 132.61, 132.18, 132.14, 132.07, 131.48, 128.73, 128.66, 128.65, 128.15, 128.00, 125.92, 125.90, 10.21, 10.19.

^{31}P NMR (162 MHz, $CDCl_3$) δ 40.29.

HRMS (ESI-TOF): calc'd for C12H13NOPS [M+H]+: 250.0455, found: 250.0459

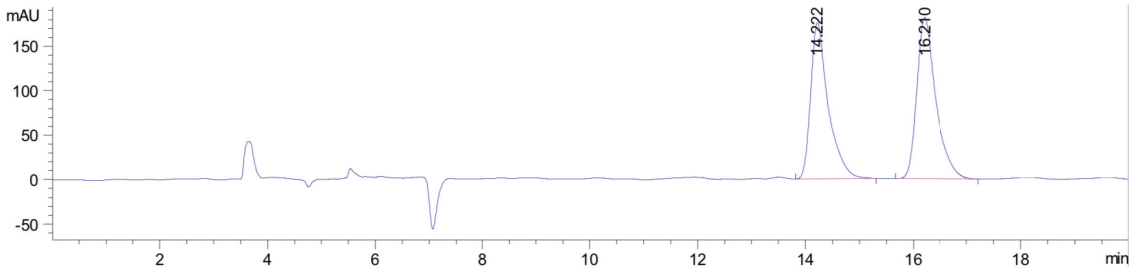
Compound 1.23b



Following **General Procedure C** on 0.2 mmol scale with **1.8b** and organolithium reagent **SI-1.19**. Purification by silica gel column chromatography (hexane/EtOAc = 1:2 to pure EtOAc) afforded 15.9 mg (32%, 98:2 e.r.) of the title compound **1.23b**. All physical and spectroscopic properties are identical with **1.23a** except for the optical rotation: **$[\alpha]^{25}_D$** = +24.1° (c = 0.80 in $CHCl_3$).

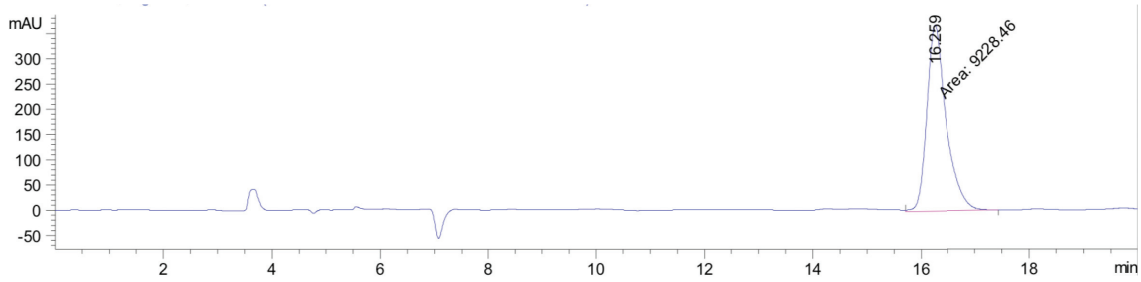
Chiral HPLC: Chiralpak AD-H column; IPA/hexane = 15:85, 0.8 mL/min, 254 nm.

***Rac*-1.23:**



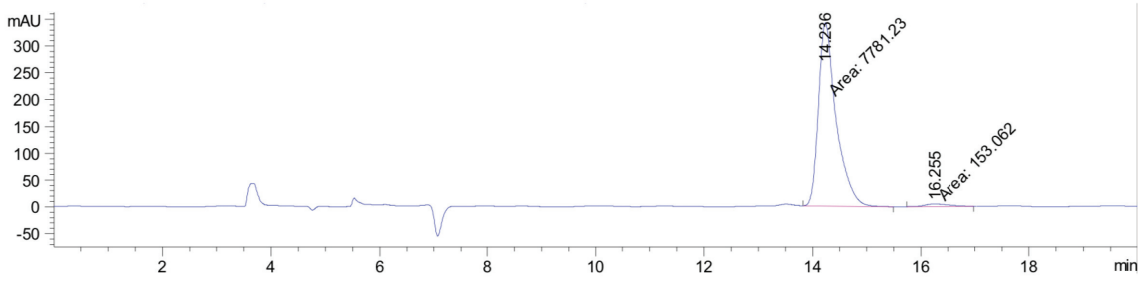
Peak #	RetTime [min]	Type	Width [min]	Area [mAU*s]	Height [mAU]	Area %
1	14.222	BB	0.3305	3980.13208	175.54428	46.8565
2	16.210	BB	0.3681	4514.16260	181.55713	53.1435

1.23a:



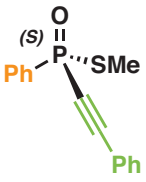
Peak #	RetTime [min]	Type	Width [min]	Area [mAU*s]	Height [mAU]	Area %
1	16.259	MM	0.4176	9228.45508	368.27570	100.0000

1.23b:



Peak #	RetTime [min]	Type	Width [min]	Area [mAU*s]	Height [mAU]	Area %
1	14.236	MM	0.3788	7781.22705	342.33466	98.0709
2	16.255	MM	0.5079	153.06165	5.02283	1.9291

Compound 1.24a



Following **General Procedure C** on 0.05 mmol scale with **1.8a** and organolithium reagent **SI-1.23**. Purification by pTLC (hexane/EtOAc = 1:1) afforded 8.6 mg (63%, >98:2 e.r.) of the title compound **1.24a**.

Physical State: white amorphous solid

$[\alpha]^{25}_D$ = -10.5° (c = 0.43 in $CHCl_3$)

R_f = 0.50 (hexane/EtOAc = 1:2)

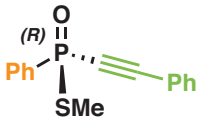
^{1}H NMR (500 MHz, $CDCl_3$) δ 8.01 (dd, *J* = 15.1, 8.4 Hz, 2H), 7.66 – 7.50 (m, 5H), 7.46 (t, *J* = 7.5 Hz, 1H), 7.38 (t, *J* = 8.1 Hz, 2H), 2.40 (d, *J* = 14.1 Hz, 3H).

^{13}C NMR (126 MHz, $CDCl_3$) δ 133.07, 133.04, 132.93, 132.76, 132.74, 131.90, 131.12, 131.03, 128.98, 128.86, 128.75, 119.75, 119.71, 104.97, 104.71, 83.08, 81.64, 11.56, 11.53.

^{31}P NMR (162 MHz, $CDCl_3$) δ 18.40.

HRMS (ESI-TOF): calc'd for C15H14OPS [M+H]+: 273.0503, found: 273.0508.

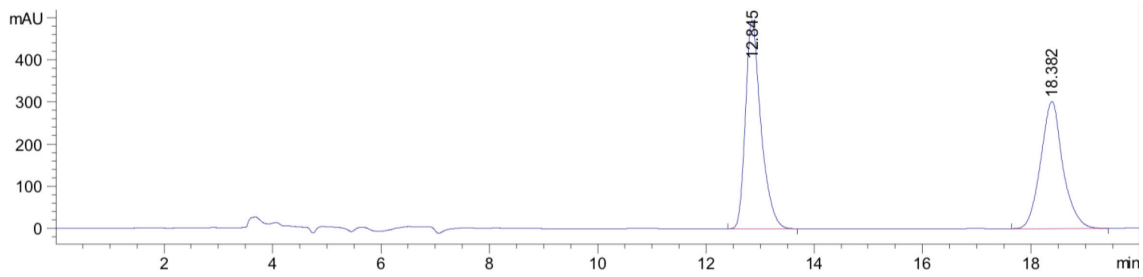
Compound 1.24b



Following **General Procedure C** on 0.05 mmol scale with **1.8b** and organolithium reagent **SI-1.23**. Purification by pTLC (hexane/EtOAc = 1:1) afforded 8.3 mg (61%, >98:2 e.r.) of the title compound **1.24b**. All physical and spectroscopic properties are identical with **1.24a** except for the optical rotation: **$[\alpha]^{25}_D$** = +11.9° (c = 0.42 in $CHCl_3$).

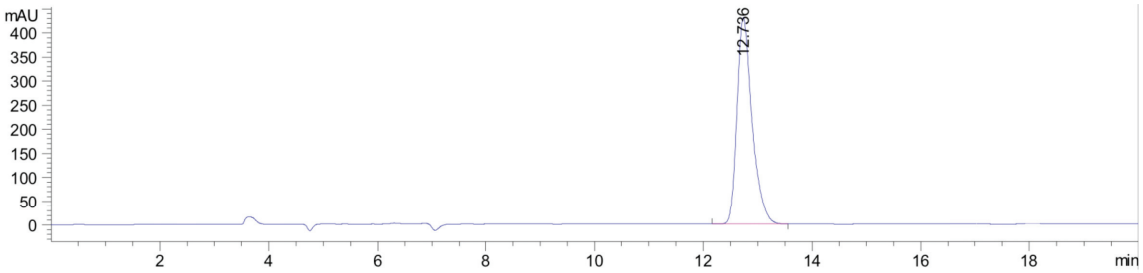
Chiral HPLC: Chiralpak AD-H column; IPA/hexane = 15:85, 0.8 mL/min, 280 nm.

***Rac*-1.24:**



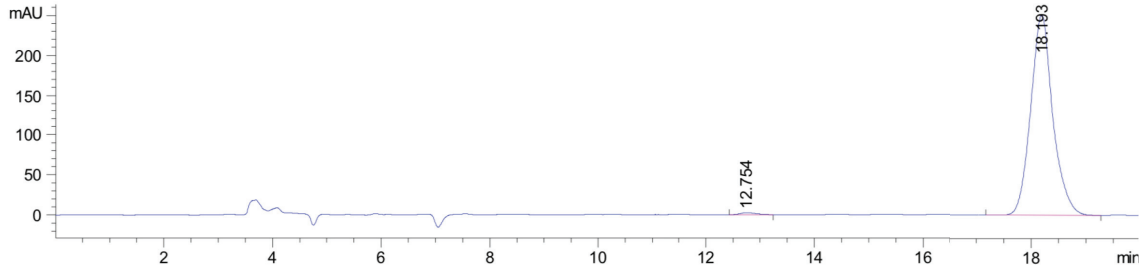
Peak #	RetTime [min]	Type	Width [min]	Area [mAU*s]	Height [mAU]	Area %
1	12.845	BB	0.2955	9812.92188	494.60172	53.5073
2	18.382	BB	0.4194	8526.50098	302.00214	46.4927

1.24a:



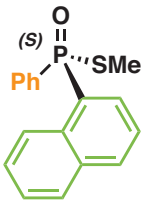
Peak #	RetTime [min]	Type	Width [min]	Area [mAU*s]	Height [mAU]	Area %
1	12.736	BB	0.2883	8265.87207	429.92844	100.0000

1.24b:



Peak #	RetTime [min]	Type	Width [min]	Area [mAU*s]	Height [mAU]	Area %
1	12.754	BB	0.2812	48.27975	2.50090	0.6828
2	18.193	BB	0.4151	7022.17871	250.43669	99.3172

Compound 1.25a



Following **General Procedure C** on 1 mmol scale with **1.8a** and organolithium reagent **SI-1.20**. Purification by silica gel column chromatography (hexane/EtOAc = 3:1 to 2:1) afforded 94 mg (32%, 96:4 e.r.) of the title compound **1.25a**.

Physical State: white amorphous solid

$[\alpha]^{25}_{D}$ = -39.2° (c = 0.24 in $CHCl_3$)

R_f = 0.44 (hexane/EtOAc = 1:1)

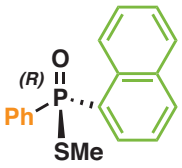
^{1}H NMR (400 MHz, $CDCl_3$) δ 8.78 – 8.72 (m, 1H), 8.08 – 7.98 (m, 2H), 7.94 – 7.84 (m, 3H), 7.60 – 7.44 (m, 6H), 2.34 (d, *J* = 12.1 Hz, 3H).

^{13}C NMR (151 MHz, $CDCl_3$) δ 134.17, 134.10, 133.94, 133.92, 133.67, 133.47, 133.40, 133.26, 133.20, 132.96, 132.53, 132.51, 131.83, 131.76, 129.02, 129.01, 128.97, 128.88, 128.82, 128.13, 127.51, 127.12, 127.09, 126.72, 124.58, 124.48, 11.19, 11.17.

^{31}P NMR (162 MHz, $CDCl_3$) δ 46.99.

HRMS (ESI-TOF): calc'd for C17H16OPS [M+H]+: 299.0659, found: 299.0662.

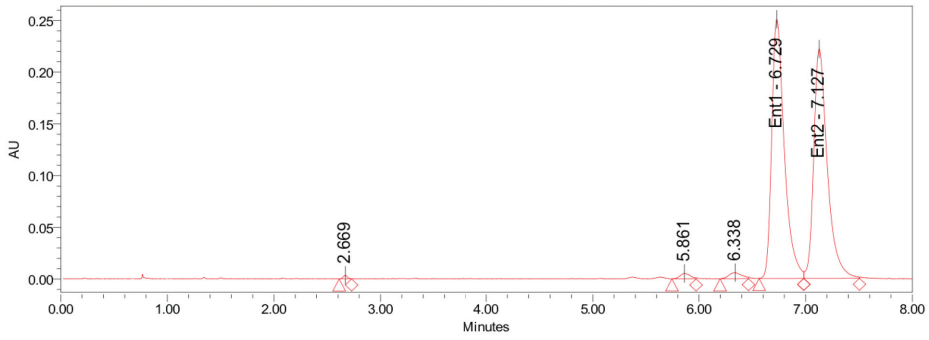
Compound 1.25b



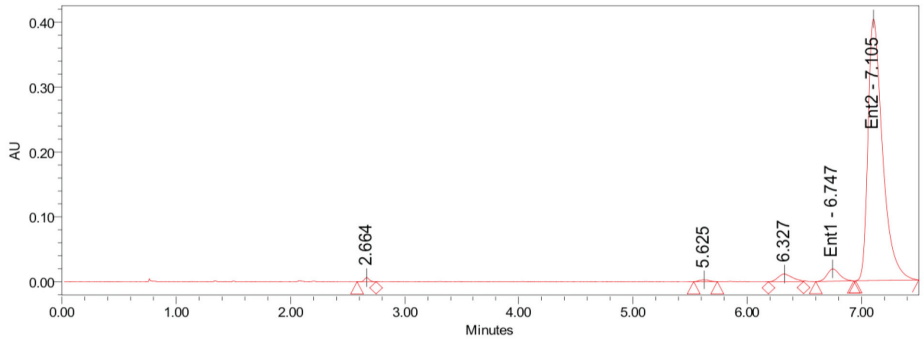
Following **General Procedure C** on 1 mmol scale with **1.8b** and organolithium reagent **SI-1.20**. Purification by silica gel column chromatography (hexane/EtOAc = 3:1 to 2:1) afforded 68 mg (23%, 97:3 e.r.) of the title compound **1.25b**. All physical and spectroscopic properties are identical with **1.25a** except for the optical rotation: **$[\alpha]^{25}_{D}$** = +37.5° (c = 1.00 in $CHCl_3$).

Chiral HPLC conditions: The sample was analyzed on a Waters UPC2 SFC with a Daicel IB column (3 mm, 4.6x250 mm) under isocratic conditions (4 mL/min, 15% IPA / CO_2, 1600 psi backpressure) at 30 °C. The enantiomers were detected by UV light (220 nm).

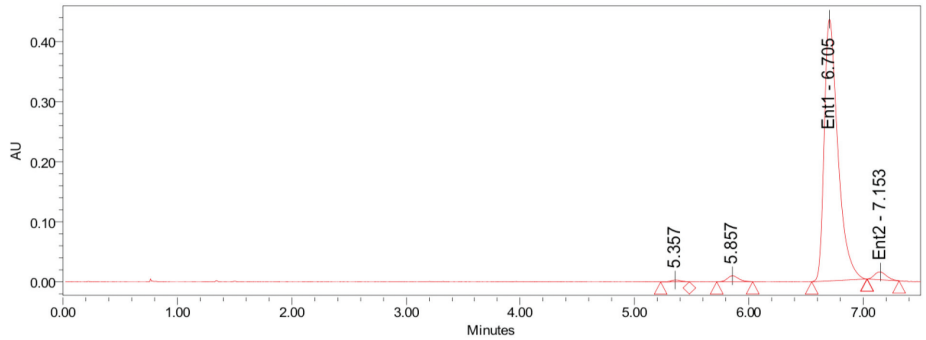
***Rac*-1.25: integration** 51.16 | 48.84



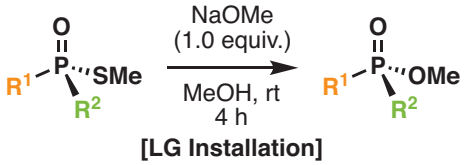
1.25a: integration 3.86 | 96.14



1.25b: integration 97.42 | 2.58



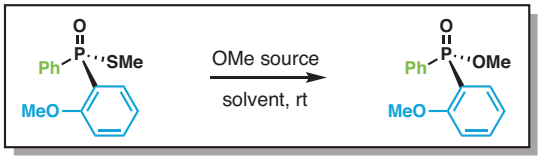
General Procedure D: P-Chiral Phosphine Synthesis – Leaving Group Installation



[LG Installation]

To a flame-dried 50 mL round-bottom flask was charged the starting material (1.0 mmol, 1.0 equiv.). The flask was evacuated and backfilled with argon, and then anhydrous methanol (8 mL) was introduced via syringe, followed by NaOMe (2.0 mL, 0.5 M solution in MeOH, 1.0 mmol, 1.0 equiv.). The resulting mixture was stirred at room temperature for 4 h, after which saturated aqueous NH_4Cl solution (10 mL) and EtOAc (20 mL) were added. The layers were separated, and the aqueous layer was washed with EtOAc (2 x 10 mL). The combined organic layers were washed with brine (10 mL), dried over anhydrous Na_2SO_4, filtered and concentrated. (Note: filter again if white precipitates are observed after concentration). The crude product was purified by silica gel chromatography to afford the desired product.

Table S1.6: Optimization Table of OMe Installation

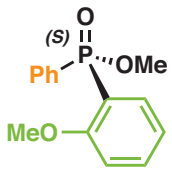


#	Source of OMe	equiv. of OMe	Time (h)	Solvent	Yield	e.r.
1	NaOMe (solid)	2	12	MeOH	80%	97:3
2	NaOMe (solid)	2	12	THF	<10% conv.	/
3	NaOMe (solid)	2	12	DMSO	<10% conv.	/
4	LiOMe	2	12	MeOH	79%	85:15
5	KOMe	2	12	MeOH	90%	78:22
6	MeOH + Et_3N	2	12	MeOH	no rxn	/
7	MeOH + DBU	2	12	MeOH	88%	95:5
8	MeOH + KO^{t}Bu	2	12	MeOH	89%	90:10
9	NaOMe + 15-crown-5	2	12	MeOH	81%	96:4
10	NaOMe (soln.)	20	12	MeOH	97%	50:50
11	NaOMe (soln.)	2	4	MeOH	78%	98:2
12	NaOMe (soln.)	5	4	MeOH	93%	96:4
13	NaOMe (soln.)	8	4	MeOH	97%	93:7
14	NaOMe (soln.)	10	4	MeOH	97%	90:10
15	NaOMe (soln.)	1.2	4	MeOH	81%	98:2
16	NaOMe (soln.)	1.0	4	MeOH	76%	98:2
17	NaOMe (soln.)	1.0	48	MeOH	90%	90:10

Notes: 1) All reactions were run on 0.05 mmol scale. **2)** Entry 15 gave higher yield than entry 16 but suffered from low reproducibility of e.r. in our hands. In contrary, the protocol of entry 16 was more robust in terms of e.r. and allowed more room for deviation (*e.g.* slight variations in reaction time), hence the optimal condition. **3)** The stereochemical outcome of LG installation is unclear because all compounds failed to produce satisfactory crystals for X-ray analysis. The structures below were drawn based on **the assumption that LG installation occurs with stereoretention at phosphorus**. To ensure clarity, the same **a** vs. **b** suffix convention was used to denote the origin of the compounds [**a** from

(–)-Π and **b** from (+)-Π]. As a side note, LG installation and final displacement gave net stereoretention over two steps (see **Stereochemical Assignment**).

Compound SI-1.28a



Following **General Procedure D** on 1 mmol scale with **1.11a**. Purification by silica gel column chromatography (hexane/EtOAc = 1:1 to 1:4) afforded 186 mg (70%, 98:2 e.r.) of the title compound **SI-1.28a**. On 16 mmol scale, 3.24g (77%, 97:3 e.r.) of **SI-1.28a** was obtained after purification.

Physical State: colorless oil

$[\alpha]^{25}_{D}$ = -16.5° (c = 0.84 in $CHCl_3$)

R_f = 0.25 (hexane/EtOAc = 1:3)

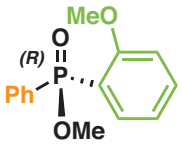
^{1}H NMR (400 MHz, $CDCl_3$) δ 7.98 (ddd, *J* = 13.3, 7.5, 1.8 Hz, 1H), 7.88 – 7.80 (m, 2H), 7.50 (dddd, *J* = 9.6, 6.8, 2.1, 1.1 Hz, 2H), 7.46 – 7.38 (m, 2H), 7.06 (tdd, *J* = 7.5, 2.6, 0.9 Hz, 1H), 6.87 (dd, *J* = 6.1, 2.2 Hz, 1H), 3.75 (d, *J* = 11.4 Hz, 3H), 3.71 (s, 3H).

^{13}C NMR (151 MHz, $CDCl_3$) δ 161.11, 161.08, 134.90, 134.86, 134.59, 134.57, 132.54, 131.93, 131.90, 131.87, 131.86, 131.59, 128.18, 128.10, 120.79, 120.71, 119.41, 118.51, 111.39, 111.34, 55.62, 51.53, 51.49.

^{31}P NMR (162 MHz, $CDCl_3$) δ 31.78.

HRMS (ESI-TOF): calc'd for $C14H16O_3P$ $[M+H]^+$: 263.0837, found: 263.0842.

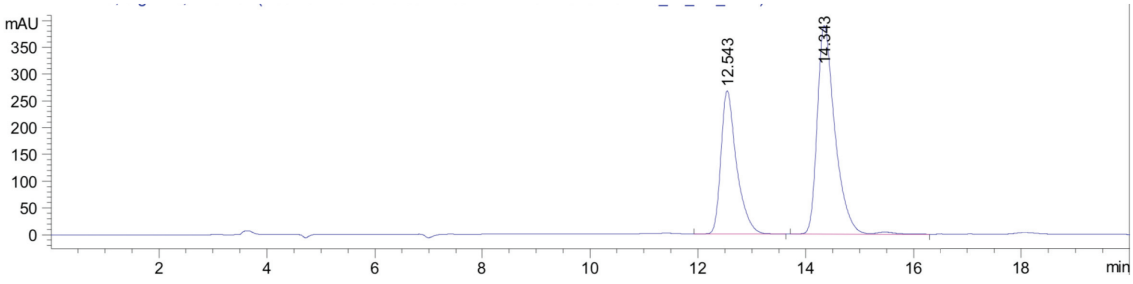
Compound SI-1.28b



Following **General Procedure D** on 0.9 mmol scale with **1.11b**. Purification by silica gel column chromatography (hexane/EtOAc = 1:1 to 1:4) afforded 151 mg (64%, 98:2 e.r.) of the title compound **SI-1.28b**. All physical and spectroscopic properties are identical with **SI-1.28a** except for the optical rotation: $[\alpha]^{25}_{D}$ = +19.2° (c = 0.91 in $CHCl_3$).

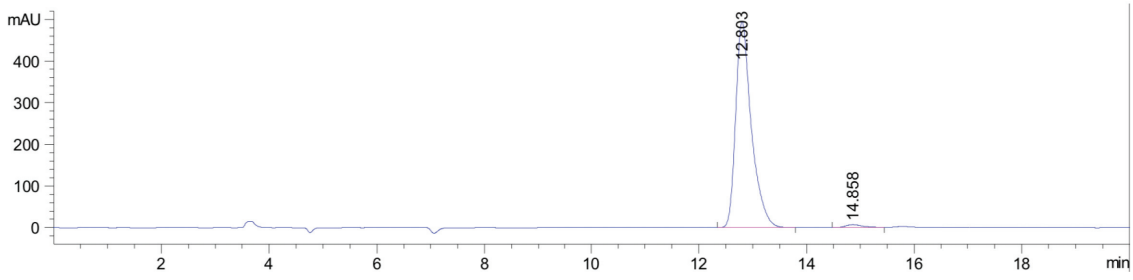
Chiral HPLC: Chiralpak AD-H column; IPA/hexane = 15:85, 0.8 mL/min, 280 nm.

***Rac*-SI-1.28:**



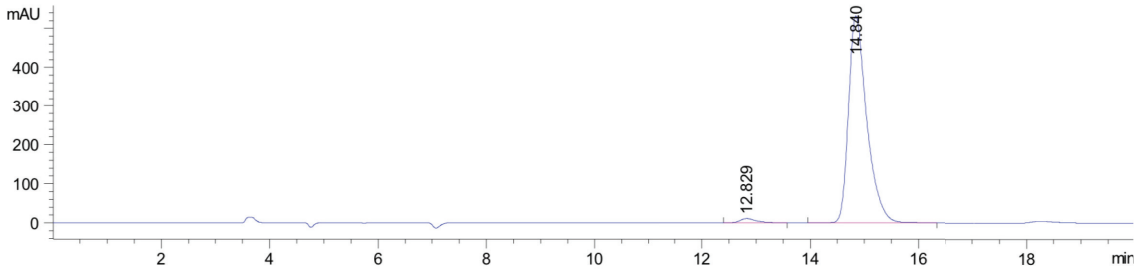
Peak #	RetTime [min]	Type	Width [min]	Area [mAU*s]	Height [mAU]	Area %
1	12.543	BB	0.2985	5364.15918	266.89676	37.6614
2	14.343	BV R	0.3398	8878.95508	388.78754	62.3386

SI-1.28a



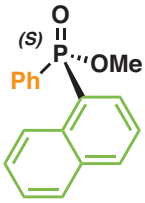
Peak #	RetTime [min]	Type	Width [min]	Area [mAU*s]	Height [mAU]	Area %
1	12.803	BB	0.2997	9992.37988	494.65460	98.4871
2	14.858	BB	0.3345	153.49863	6.87481	1.5129

SI-1.28b



Peak #	RetTime [min]	Type	Width [min]	Area [mAU*s]	Height [mAU]	Area %
1	12.829	BB	0.2955	217.58826	10.87355	1.7211
2	14.840	BB	0.3504	1.24246e4	532.07574	98.2789

Compound SI-1.29a



Following **General Procedure D** on 0.30 mmol scale with organolithium reagent **1.25a**. Purification by silica gel column chromatography (hexane:/EtOAc = 2:1 to 1:1) afforded 68.4 mg (80%, 92:8 e.r.) of the title compound **SI-1.29a**.

Physical State: white amorphous solid

$[\alpha]^{25}_{D}$ = -18.6° (c = 0.65 in $CHCl_3$)

R_f = 0.33 (hexane/EtOAc = 1:1)

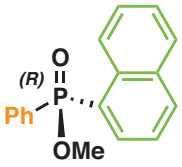
^{1}H NMR (600 MHz, $CDCl_3$) δ 8.55 – 8.48 (m, 1H), 8.21 (ddd, *J* = 14.8, 7.1, 1.3 Hz, 1H), 8.04 (d, *J* = 8.1 Hz, 1H), 7.91 – 7.85 (m, 1H), 7.85 – 7.77 (m, 2H), 7.56 (ddd, *J* = 8.3, 7.1, 2.8 Hz, 1H), 7.53 – 7.47 (m, 3H), 7.42 (td, *J* = 7.5, 3.1 Hz, 2H), 3.82 (d, *J* = 11.1 Hz, 3H).

^{13}C NMR (151 MHz, $CDCl_3$) δ 134.31, 134.26, 133.84, 133.80, 133.78, 133.77, 133.07, 132.99, 132.40, 132.30, 132.28, 131.56, 131.49, 129.03, 129.02, 128.73, 128.64, 127.64, 127.21, 126.47, 126.43, 126.33, 124.80, 124.70, 51.75, 51.71.

^{31}P NMR (162 MHz, $CDCl_3$) δ 34.77.

HRMS (ESI-TOF): calc'd for $C17H16O_2P$ [M+H]+: 283.0888, found: 283.0890.

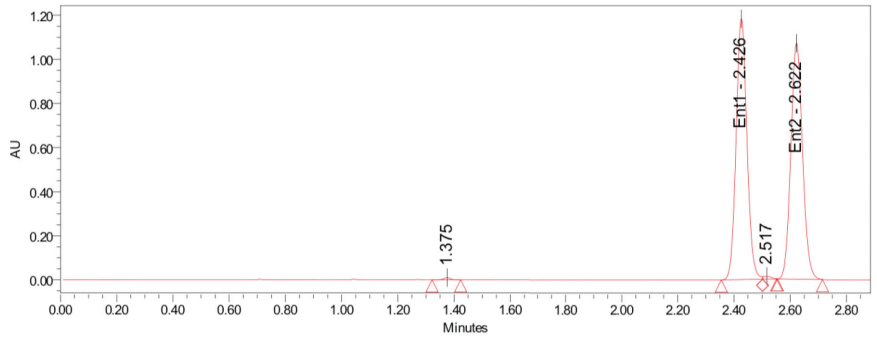
Compound SI-1.29b



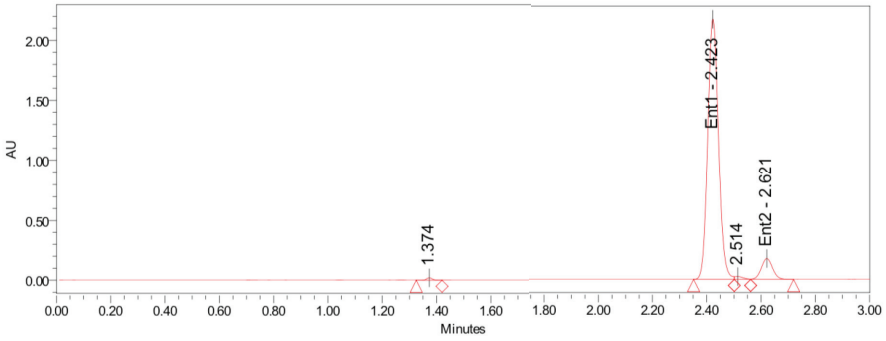
Following **General Procedure D** on 0.22 mmol scale with organolithium reagent **1.25b**. Purification by silica gel column chromatography (hexane/EtOAc = 2:1 to 1:1) afforded 50.6 mg (81%, 92:8 e.r.) of the title compound **SI-1.29b**. All physical and spectroscopic properties are identical with **SI-1.29a** except for the optical rotation: **$[\alpha]^{25}_{D}$** = +14.3° (c = 0.59 in $CHCl_3$).

Chiral HPLC conditions: The sample was analyzed on a Waters UPC2 SFC with a Daicel IBN column (3 mm, 4.6x250 mm) under isocratic conditions (4 mL/min, 15% MeOH / CO_2, 1600 psi backpressure) at 30 °C. The enantiomers were detected by UV light (220 nm).

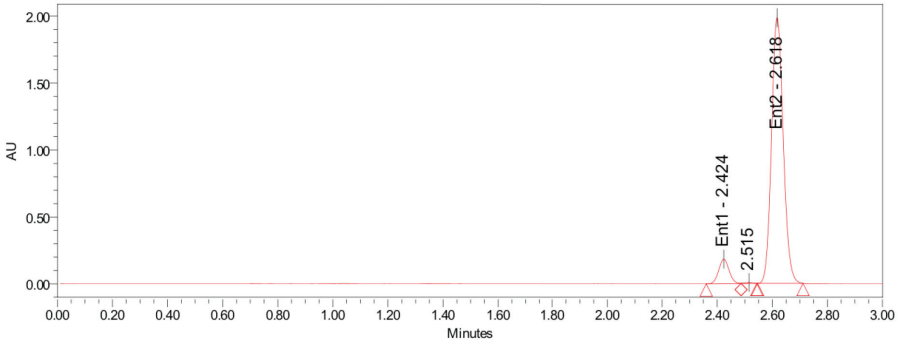
***Rac*-SI-1.29: integration** 50.51 | 49.49



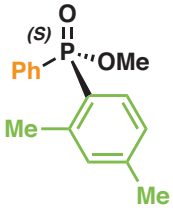
SI-1.29a: integration 92.28 | 7.72



SI-1.29b: integration 7.57 | 92.43



Compound SI-1.30a



Following **General Procedure D** on 0.66 mmol scale with organolithium reagent **1.20a**. Purification by silica gel column chromatography (hexane:EtOAc 2:1 to 1:1) afforded 97 mg (56%, 97:3 e.r.) of the title compound **SI-1.30a**.

Physical State: colorless oil

$[\alpha]^{25}_{D}$ = +16.1° (c = 0.80 in $CHCl_3$)

R_f = 0.30 (hexane/EtOAc = 1:2)

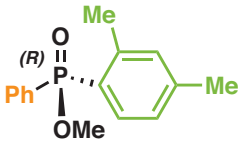
^{1}H NMR (400 MHz, $CDCl_3$) δ 7.83 – 7.68 (m, 3H), 7.55 – 7.48 (m, 1H), 7.48 – 7.38 (m, 2H), 7.10 (dt, *J* = 7.9, 2.2 Hz, 1H), 7.03 (d, *J* = 4.9 Hz, 1H), 3.74 (d, *J* = 11.1 Hz, 3H), 2.36 (s, 3H), 2.34 (s, 3H).

^{13}C NMR (126 MHz, $CDCl_3$) δ 143.07, 143.05, 142.03, 141.94, 133.66, 133.59, 132.53, 132.50, 132.43, 132.09, 132.07, 131.72, 131.64, 131.43, 128.63, 128.53, 126.47, 126.36, 125.26, 51.30, 51.25, 21.55, 21.26, 21.22.

^{31}P NMR (162 MHz, $CDCl_3$) δ 34.34.

HRMS (ESI-TOF): calc'd for $C_{15}H_{18}O_2P$ [M+H]+: 261.1044, found: 261.1050.

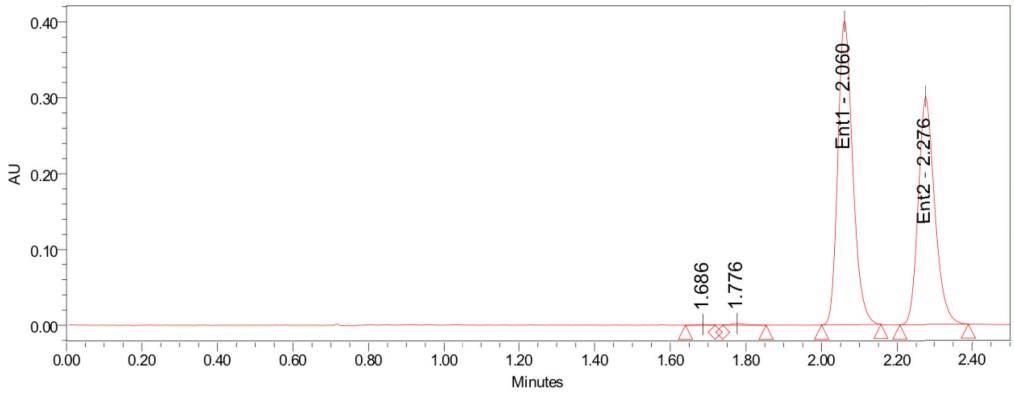
Compound SI-1.30b



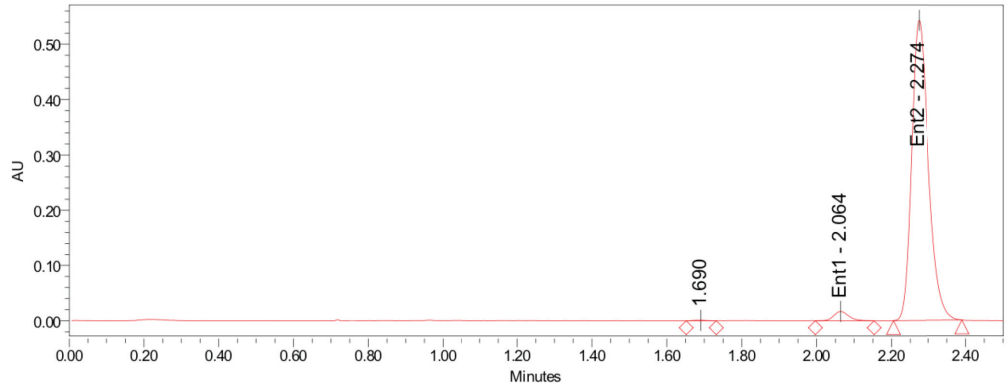
Following **General Procedure D** on 0.59 mmol scale with organolithium reagent **1.20b**. Purification by silica gel column chromatography (hexane:EtOAc 2:1 to 1:1) afforded 80 mg (52%, 98:2 e.r.) of the title compound **SI-1.30b**. All physical and spectroscopic properties are identical with **SI-1.30a** except for the optical rotation: **$[\alpha]^{25}_{D}$** = –16.9° (c = 0.80 in $CHCl_3$).

Chiral HPLC conditions: The sample was analyzed on a Waters UPC2 SFC with a Daicel IG column (3 mm, 4.6x250 mm) under isocratic conditions (4 mL/min, 25% MeOH / CO_2, 1600 psi backpressure) at 30 °C. The enantiomers were detected by UV light (240 nm)

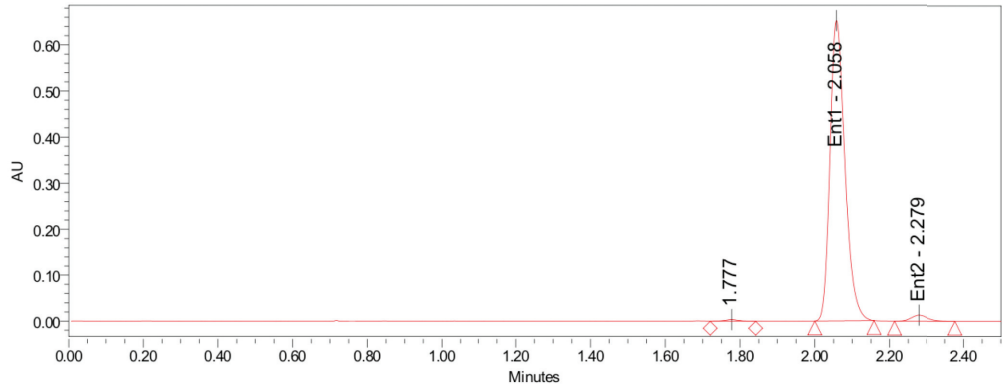
***Rac*-SI-1.30:** 53.43 | 46.57



SI-1.30a: 2.61 | 97.39

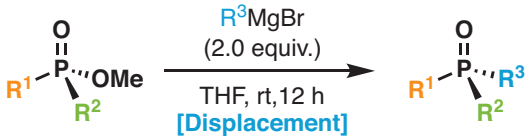


SI-1.30b: 97.80 | 2.20



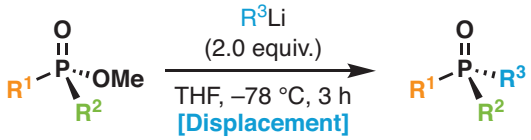
General Procedures E, F, and G: P-Chiral Phosphine Synthesis – Displacement

General Procedure E:



To a flame-dried 13 x 100 mm culture tube under argon was charged the starting material (0.05 mmol, 1.0 equiv.) in THF (0.5 mL). The Grignard reagent (0.10 mmol, 2.0 equiv., unless otherwise specified) was added dropwise, and the reaction was stirred for 12 h at. room temperature. Saturated aqueous NH_4Cl solution (1 mL) and EtOAc (2 mL) were added. The layers were separated, and the aqueous layer was washed with EtOAc (2 x 2 mL). The combined organic layers were washed with brine (1 mL), dried over anhydrous Na_2SO_4, filtered and concentrated. The crude product was purified by pTLC or silica gel chromatography to afford the desired product.

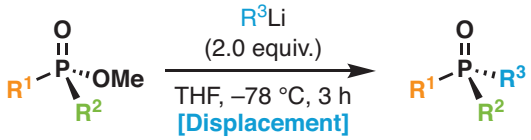
General Procedure F:



To a flame-dried 13 x 100 mm culture tube under argon was charged the starting material (0.05 mmol, 1.0 equiv.) in THF (0.5 mL) and cooled to –78 °C. The organolithium reagent (0.10 mmol, 2.0 equiv., unless otherwise specified) was added dropwise, and the reaction was stirred for 3 h at –78 °C. Saturated aqueous NH_4Cl solution (1 mL) and EtOAc (2 mL) were added. The layers were separated, and the aqueous layer was washed with EtOAc (2 x. 2 mL). The combined organic layers were washed with brine (1 mL), dried over

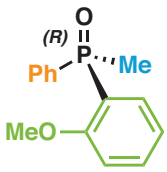
anhydrous Na_2SO_4, filtered and concentrated. The crude product was purified by pTLC or silica gel chromatography to afford the desired product.

General Procedure G:



The organolithium reagent (0.10 mmol, 2.0 equiv., unless otherwise specified) in 0.3 mL of THF was prepared in a flame-dried 13 x 100 mm culture tube under argon (see **Synthesis of Grignard and Organolithium Reagents**). The starting material (0.05 mmol, 1.0 equiv.) in 0.2 mL of THF was added dropwise, and the reaction was stirred for 3 h at –78 °C. Saturated aqueous NH_4Cl solution (1 mL) and EtOAc (2 mL) were added. The layers were separated, and the aqueous layer was washed with EtOAc (2 x 2 mL). The combined organic layers were washed with brine (1 mL), dried over anhydrous Na_2SO_4, filtered and concentrated. The crude product was purified by pTLC or silica gel chromatography to afford the desired product.

Compound 1.26a



Following **General Procedure E** on 0.05 mmol scale with **SI-1.28a** and Grignard reagent **SI-1.11**. Purification by pTLC (5% MeOH in EtOAc) afforded 10.9 mg (89%, 98:2 e.r.) of

the title compound **1.26a**. On 12 mmol scale, 2.54g (84%, 97:3 e.r.) of **1.26a** was obtained after purification.

Physical State: white solid

m.p. = 81–83 °C

$[\alpha]^{25}_{D}$ = +30.4° (c = 0.55 in $CHCl_3$)

R_f = 0.43 (5% MeOH in EtOAc)

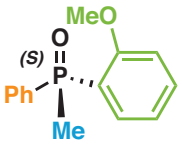
^{1}H NMR (400 MHz, $CDCl_3$) δ 7.95 (ddd, *J* = 13.1, 7.5, 1.8 Hz, 1H), 7.79 – 7.68 (m, 2H), 7.55 – 7.37 (m, 4H), 7.10 (t, *J* = 7.5 Hz, 1H), 6.88 (dd, *J* = 8.3, 5.2 Hz, 1H), 3.72 (s, 3H), 2.08 (d, *J* = 14.0 Hz, 3H).

^{13}C NMR (151 MHz, $CDCl_3$) δ 160.04, 160.01, 135.34, 134.67, 134.06, 134.05, 134.03, 131.42, 131.40, 130.40, 130.34, 128.38, 128.30, 121.80, 121.22, 121.15, 111.03, 110.99, 55.42, 16.53, 16.03.

^{31}P NMR (162 MHz, $CDCl_3$) δ 29.41.

HRMS (ESI-TOF): calc'd for $C_{14}H_{16}O_2P$ [M+H]+: 247.0888, found: 247.0889.

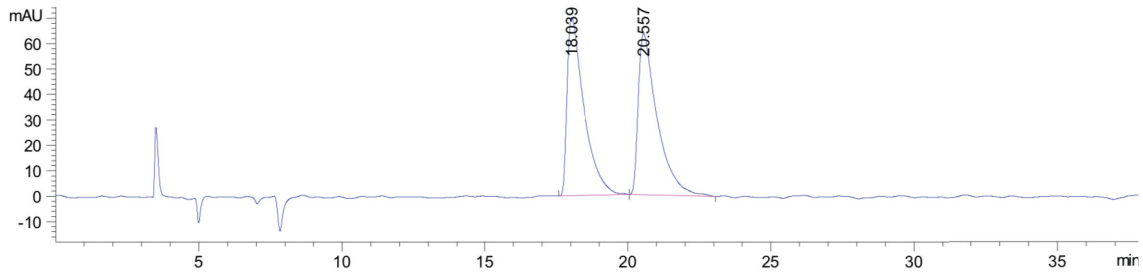
Compound 1.26b



Following **General Procedure E** on 0.05 mmol scale with **SI-1.28b** and Grignard reagent **SI-1.11**. Purification by pTLC (5% MeOH in EtOAc) afforded 10.0 mg (81%, 98:2 e.r.) of the title compound **1.26b**. All physical and spectroscopic properties are identical with **1.26a** except for the optical rotation: **$[\alpha]^{25}_{D}$** = -28.5° (c = 0.64 in $CHCl_3$).

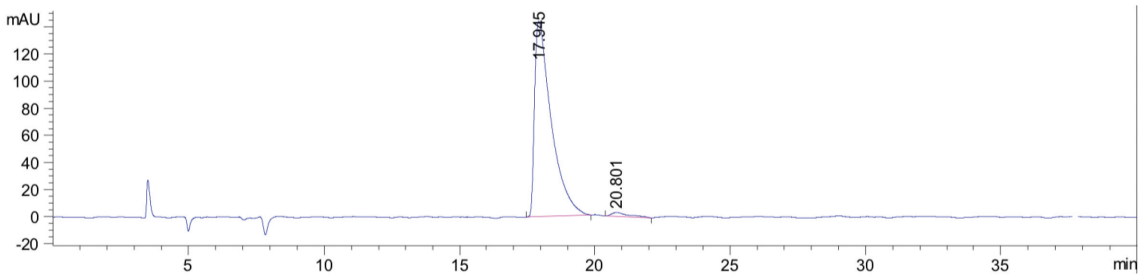
Chiral HPLC: Chiralpak IA-H column; IPA/hexane = 15:85, 0.8 mL/min, 254 nm.

***Rac*-1.26:**



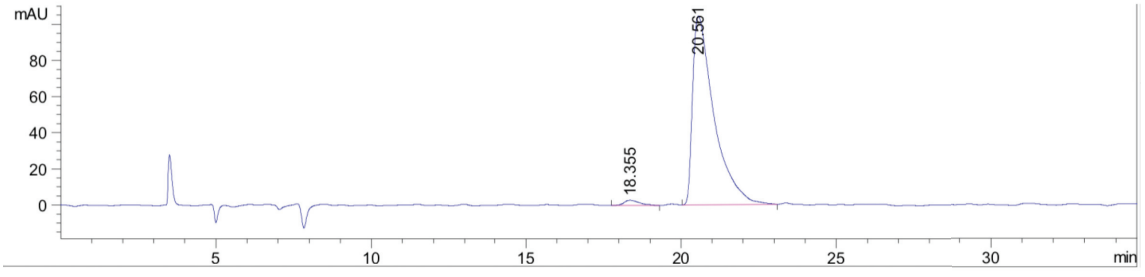
Peak #	RetTime [min]	Type	Width [min]	Area [mAU*s]	Height [mAU]	Area %
1	18.039	BB	0.6008	2902.60425	70.14416	49.8072
2	20.557	BB	0.6566	2925.07153	63.35460	50.1928

1.26a:



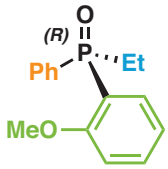
Peak #	RetTime [min]	Type	Width [min]	Area [mAU*s]	Height [mAU]	Area %
1	17.945	BB	0.6198	6178.07764	144.22162	97.8250
2	20.801	BB	0.6276	137.36038	2.92647	2.1750

1.26b:



Peak #	RetTime [min]	Type	Width [min]	Area [mAU*s]	Height [mAU]	Area %
1	18.355	BB	0.4847	103.97015	2.93907	2.0333
2	20.561	BB	0.7055	5009.37354	104.44637	97.9667

Compound 1.27a



Following **General Procedure E** on 0.05 mmol scale with **SI-1.28a** and Grignard reagent **SI-1.12**. Purification by pTLC (5% MeOH in EtOAc) afforded 11.4 mg (87%, 97:3 e.r.) of the title compound **1.27a**.

Physical State: white amorphous solid

$[\alpha]^{25}_{D}$ = +21.4° (c = 0.71 in $CHCl_3$)

R_f = 0.45 (5% MeOH in EtOAc)

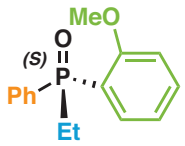
^{1}H NMR (400 MHz, $CDCl_3$) δ 7.99 (ddd, *J* = 12.7, 7.5, 1.8 Hz, 1H), 7.77 (ddd, *J* = 11.7, 8.2, 1.5 Hz, 2H), 7.54 – 7.36 (m, 4H), 7.10 (t, *J* = 7.5 Hz, 1H), 6.88 (dd, *J* = 8.1, 5.5 Hz, 1H), 3.75 (s, 3H), 2.52 – 2.29 (m, 2H), 1.15 (dt, *J* = 18.2, 7.7 Hz, 3H).

^{13}C NMR (151 MHz, $CDCl_3$) δ 159.90, 159.87, 134.78, 134.75, 134.25, 133.94, 133.92, 133.59, 131.38, 131.36, 130.83, 130.77, 128.35, 128.27, 121.33, 121.26, 120.58, 119.94, 110.86, 110.82, 55.38, 22.46, 21.97, 5.75, 5.72.

^{31}P NMR (162 MHz, $CDCl_3$) δ 34.63.

HRMS (ESI-TOF): calc'd for $C_{15}H_{18}O_2P$ [M+H]+: 261.1044, found: 261.1049.

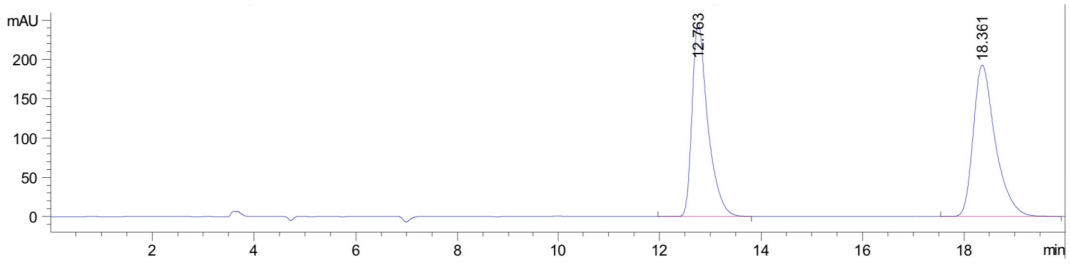
Compound 1.27b



Following **General Procedure E** on 0.03 mmol scale with **SI-1.28b** and Grignard reagent **SI-1.12**. Purification by pTLC (5% MeOH in EtOAc) afforded 6.6 mg (85%, 97:3 e.r.) of the title compound **1.27b**. All physical and spectroscopic properties are identical with **1.27a** except for the optical rotation: $[\alpha]^{25}_{D}$ = -18.1° (c = 0.33 in $CHCl_3$).

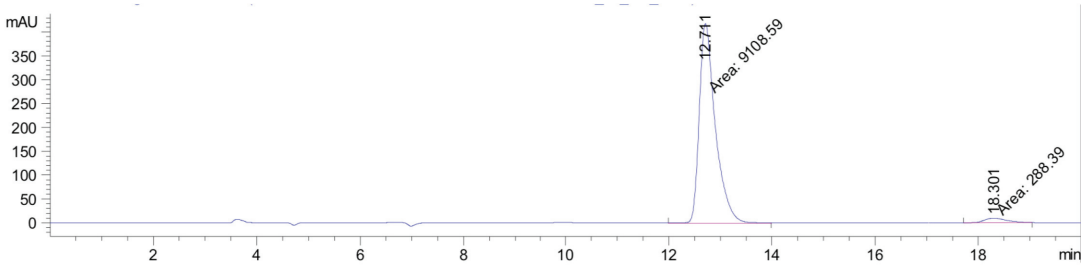
Chiral HPLC: Chiralpak AD-H column; IPA/hexane = 85:15, 0.8 mL/min, 280 nm.

***Rac*-1.27:**



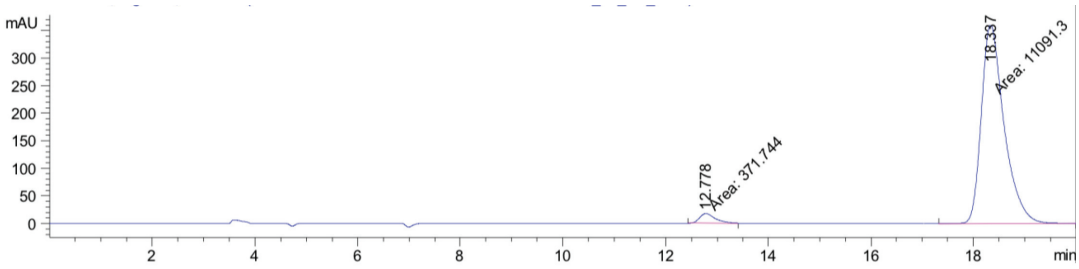
Peak #	RetTime [min]	Type	Width [min]	Area [mAU*s]	Height [mAU]	Area %
1	12.763	BB	0.3182	5298.26514	247.03671	47.6183
2	18.361	BB	0.4528	5828.26855	192.71062	52.3817

1.27a:



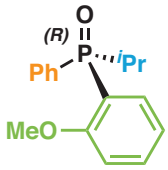
Peak #	RetTime [min]	Type	Width [min]	Area [mAU*s]	Height [mAU]	Area %
1	12.711	MM	0.3625	9108.58789	418.74292	96.9310
2	18.301	MM	0.4926	288.39041	9.75820	3.0690

1.27b:



Peak #	RetTime [min]	Type	Width [min]	Area [mAU*s]	Height [mAU]	Area %
1	12.711	MM	0.3625	9108.58789	418.74292	96.9310
2	18.301	MM	0.4926	288.39041	9.75820	3.0690

Compound 1.28a



Following **General Procedure F** on 0.05 mmol scale with **SI-1.28a** and organolithium reagent **SI-1.25**. Purification by pTLC (hexane/EtOAc = 1:3) afforded 10.5 mg (77%, 97:3 e.r.) of the title compound **1.28a**.

Physical State: white amorphous solid

$[\alpha]^{25}_{D}$ = +13.8° (c = 0.50 in $CHCl_3$)

R_f = 0.5 (EtOAc)

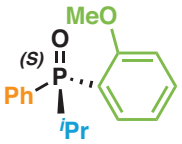
^{1}H NMR (400 MHz, $CDCl_3$) δ 8.08 (ddd, *J* = 12.4, 7.6, 1.8 Hz, 1H), 7.88 (ddd, *J* = 11.2, 7.9, 1.7 Hz, 2H), 7.52 – 7.36 (m, 4H), 7.09 (t, *J* = 7.7 Hz, 1H), 6.87 (dd, *J* = 8.3, 5.2 Hz, 1H), 3.83 (s, 3H), 2.87 (dq, *J* = 14.1, 7.1 Hz, 1H), 1.15 (ddd, *J* = 38.7, 17.0, 7.2 Hz, 6H).

^{13}C NMR (151 MHz, $CDCl_3$) δ 159.43, 159.39, 134.88, 134.85, 133.70, 133.65, 133.63, 133.07, 131.26, 131.24, 131.22, 131.20, 128.23, 128.16, 121.44, 121.37, 121.12, 120.50, 110.64, 110.59, 55.30, 26.66, 26.17, 15.45, 15.44, 15.09, 15.07.

^{31}P NMR (162 MHz, $CDCl_3$) δ 38.08.

HRMS (ESI-TOF): calc'd for $C_{16}H_{20}O_2P$ [M+H]+: 275.1201, found: 275.1203.

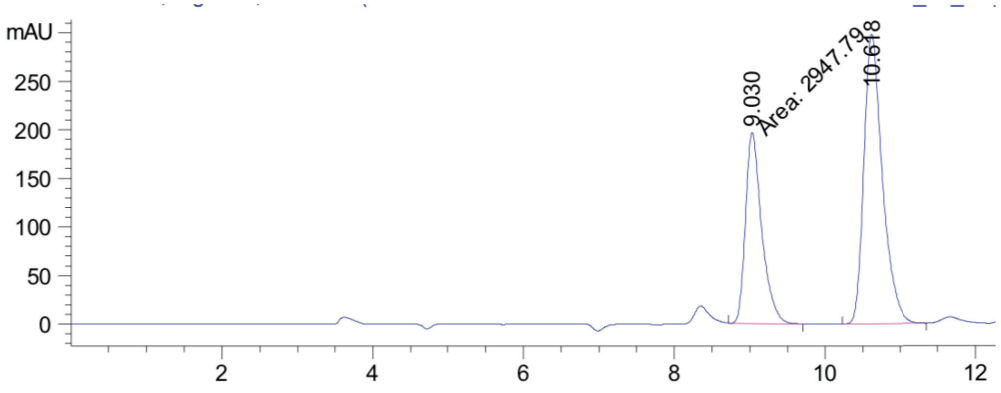
Compound 1.28b



Following **General Procedure F** on 0.03 mmol scale with **SI-1.28b** and organolithium reagent **SI-1.25**. Purification by pTLC (hexane/EtOAc = 1:3) afforded 5.6 mg (68%, >98:2 e.r.) of the title compound **1.28b**. All physical and spectroscopic properties are identical with **1.28a** except for the optical rotation: **$[\alpha]^{25}_D$** = +12.6° (c = 0.28 in $CHCl_3$).

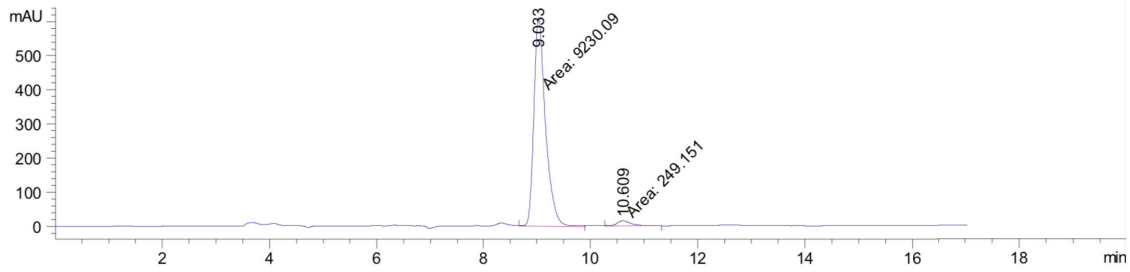
Chiral HPLC: Chiralpak AD-H column; IPA/hexane = 85:15, 0.8 mL/min, 280 nm.

***Rac*-1.28:**



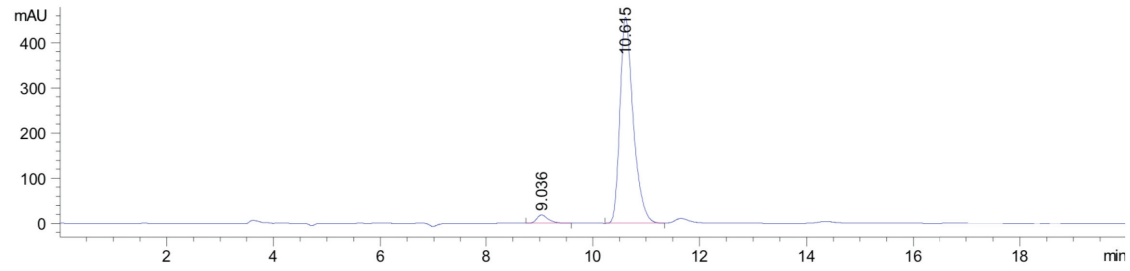
Peak #	RetTime [min]	Type	Width [min]	Area [mAU*s]	Height [mAU]	Area %
1	9.030	MM	0.2498	2947.79004	196.65530	36.6094
2	10.618	BB	0.2576	5104.21680	298.35754	63.3906

1.28a:



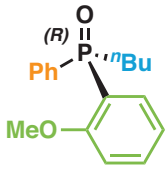
Peak #	RetTime [min]	Type	Width [min]	Area [mAU*s]	Height [mAU]	Area %
1	9.033	MM	0.2518	9230.09375	611.01166	97.3716
2	10.609	MM	0.2831	249.15092	14.66878	2.6284

1.28b:



Peak #	RetTime [min]	Type	Width [min]	Area [mAU*s]	Height [mAU]	Area %
1	9.036	BB	0.2237	276.11398	18.54888	3.3867
2	10.615	BV	0.2594	7876.84766	456.34201	96.6133

Compound 1.29a



Following **General Procedure F** on 0.05 mmol scale with **SI-1.28a** and organolithium reagent **SI-1.26**. Purification by pTLC (hexane/EtOAc = 1:3) afforded 13.6 mg (94%, 97:3 e.r.) of the title compound **1.29a**.

Physical State: colorless oil

$[\alpha]^{25}_D$ = +5.3° (c = 0.43 in $CHCl_3$)

R_f = 0.54 (EtOAc)

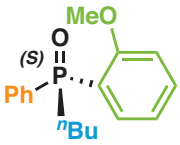
^{1}H NMR (600 MHz, Acetone-d_6) δ 8.01 – 7.94 (m, 1H), 7.88 – 7.80 (m, 2H), 7.57 – 7.41 (m, 4H), 7.14 – 7.09 (m, 1H), 7.09 – 7.04 (m, 1H), 3.85 (s, 3H), 2.51 – 2.40 (m, 1H), 2.38 – 2.26 (m, 1H), 1.61 – 1.48 (m, 1H), 1.47 – 1.35 (m, 3H), 0.90 – 0.81 (m, 3H).

^{13}C NMR (151 MHz, Acetone-d_6) δ 160.67, 160.64, 136.89, 136.23, 134.97, 134.94, 134.51, 134.50, 131.82, 131.81, 131.51, 131.45, 128.96, 128.89, 123.05, 122.43, 121.67, 121.60, 111.99, 111.94, 55.72, 29.77, 29.28, 24.64, 24.61, 24.58, 24.54, 13.95.

^{31}P NMR (162 MHz, Acetone-d_6) δ 29.39.

HRMS (ESI-TOF): calc'd for $C17H22O_2P$ [M+H]+: 289.1357, found: 289.1362.

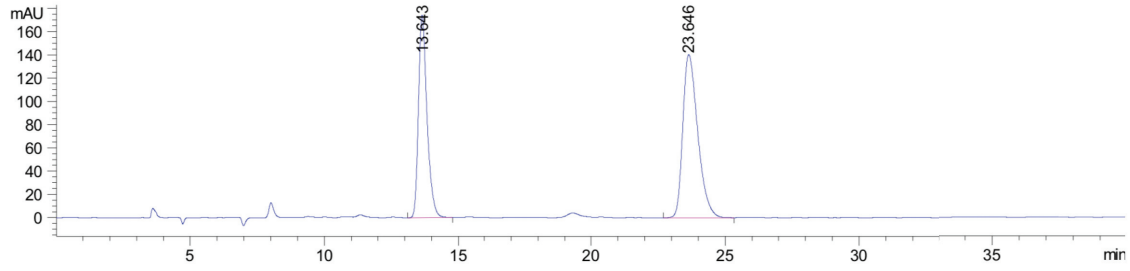
Compound 1.29b



Following **General Procedure F** on 0.03 mmol scale with **SI-1.28b** and organolithium reagent **SI-1.26**. Purification by pTLC (hexane/EtOAc = 1:3) afforded 7.4 mg (86%, 97:3 e.r.) of the title compound **1.29b**. All physical and spectroscopic properties are identical with **1.29a** except for the optical rotation: **$[\alpha]^{25}_D$** = -7.1° (c = 0.37 in $CHCl_3$).

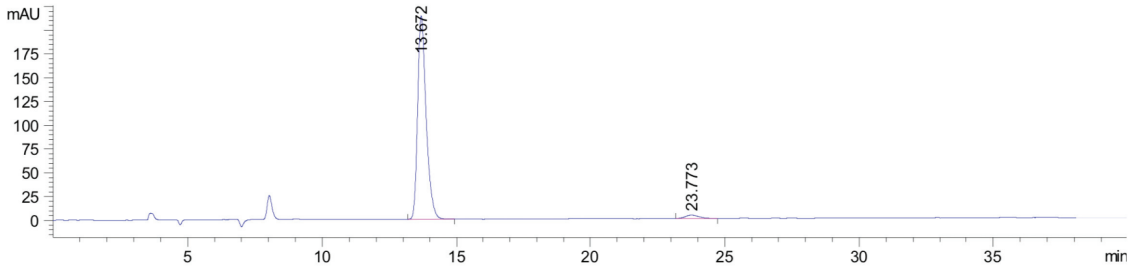
Chiral HPLC: Chiralpak AD-H column; IPA/hexane = 85:15, 0.8 mL/min, 280 nm.

***Rac*-1.29:**



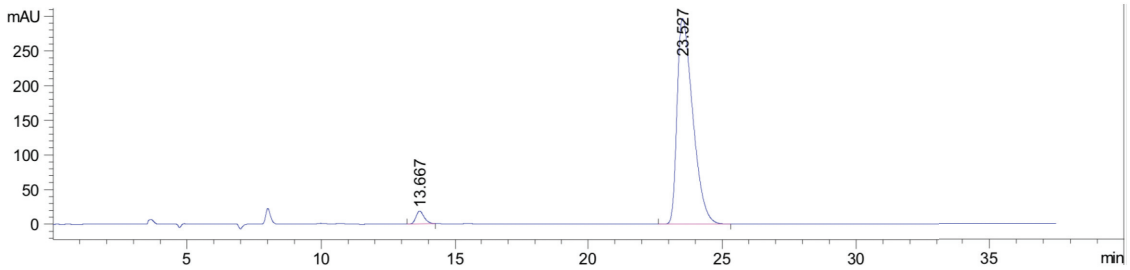
Peak #	RetTime [min]	Type	Width [min]	Area [mAU*s]	Height [mAU]	Area %
1	13.643	BB	0.3342	3859.52734	174.36667	41.4813
2	23.646	BB	0.5944	5444.73584	140.40887	58.5187

1.29a:



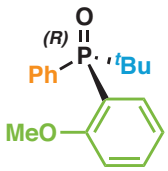
Peak #	RetTime [min]	Type	Width [min]	Area [mAU*s]	Height [mAU]	Area %
1	13.672	BB	0.3313	4685.98682	214.10204	97.4058
2	23.773	BB	0.4264	124.80049	3.51336	2.5942

1.29b:



Peak #	RetTime [min]	Type	Width [min]	Area [mAU*s]	Height [mAU]	Area %
1	13.667	BB	0.3206	390.29437	18.46751	3.1308
2	23.527	BB	0.6262	1.20758e4	297.07373	96.8692

Compound 1.30a



Following **General Procedure F** on 0.05 mmol scale with **SI-1.28a** and organolithium reagent **SI-1.27**. Purification by pTLC (hexane/EtOAc = 1:3) afforded 12.0 mg (83%, 90:10 e.r.) of the title compound **1.30a**.

Physical State: white amorphous solid

$[\alpha]^{25}_{D}$ = +10.7° (c = 0.27 in $CHCl_3$)

R_f = 0.53 (EtOAc)

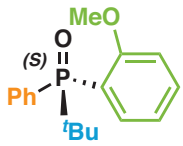
^{1}H NMR (400 MHz, $CDCl_3$) δ 8.16 (ddd, *J* = 12.1, 7.6, 1.8 Hz, 1H), 7.99 – 7.88 (m, 2H), 7.54 – 7.36 (m, 4H), 7.11 (tt, *J* = 7.5, 1.2 Hz, 1H), 6.91 (dd, *J* = 8.3, 5.1 Hz, 1H), 3.75 (s, 3H), 1.26 (d, *J* = 15.4 Hz, 9H).

^{13}C NMR (151 MHz, $CDCl_3$) δ 159.73, 159.70, 136.27, 136.24, 133.70, 133.69, 133.27, 132.65, 132.18, 132.12, 131.18, 131.16, 127.97, 127.89, 121.27, 121.20, 120.56, 119.97, 110.97, 110.93, 54.77, 35.10, 34.63, 26.11, 26.10.

^{31}P NMR (162 MHz, $CDCl_3$) δ 43.50.

HRMS (ESI-TOF): calc'd for $C17H22O_2P$ [M+H]+: 289.1357, found: 289.1361.

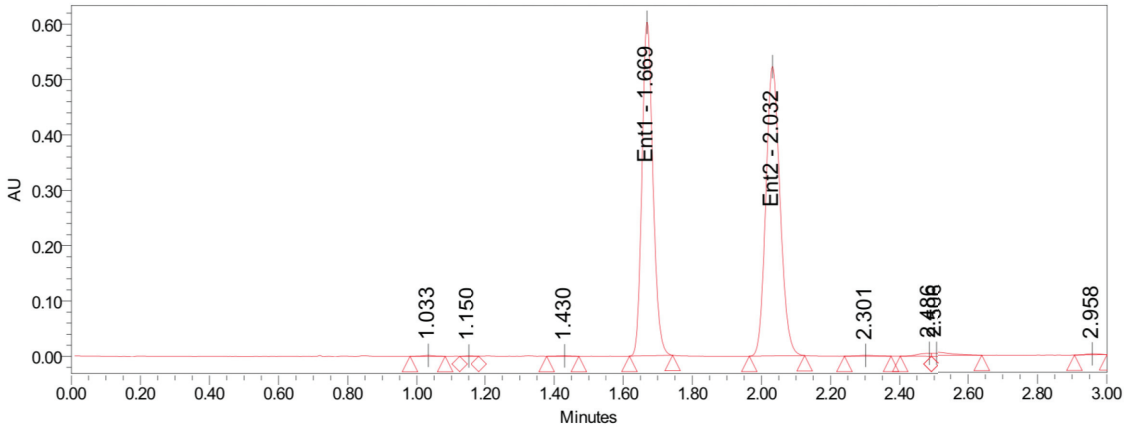
Compound 1.30b



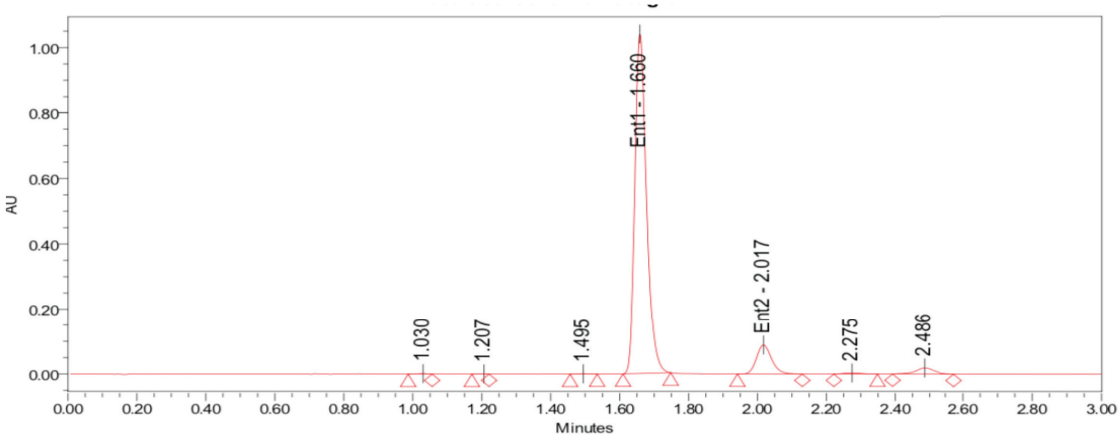
Following **General Procedure F** on 0.03 mmol scale with **SI-1.28b** and organolithium reagent **SI-1.27**. Purification by pTLC (hexane/EtOAc = 1:3) afforded 6.8 mg (79%, 87:13 e.r.) of the title compound **1.30b**. All physical and spectroscopic properties are identical with **1.30a** except for the optical rotation: $[\alpha]^{25}_{D}$ = -12.5° (c = 0.33 in $CHCl_3$).

Chiral HPLC conditions: The sample was analyzed on a Waters UPC2 SFC with a Daicel IG column (3 mm, 4.6x250 mm) under isocratic conditions (4 mL/min, 25% MeOH / CO_2, 1600 psi backpressure) at 30 °C. The enantiomers were detected by UV light (218 nm).

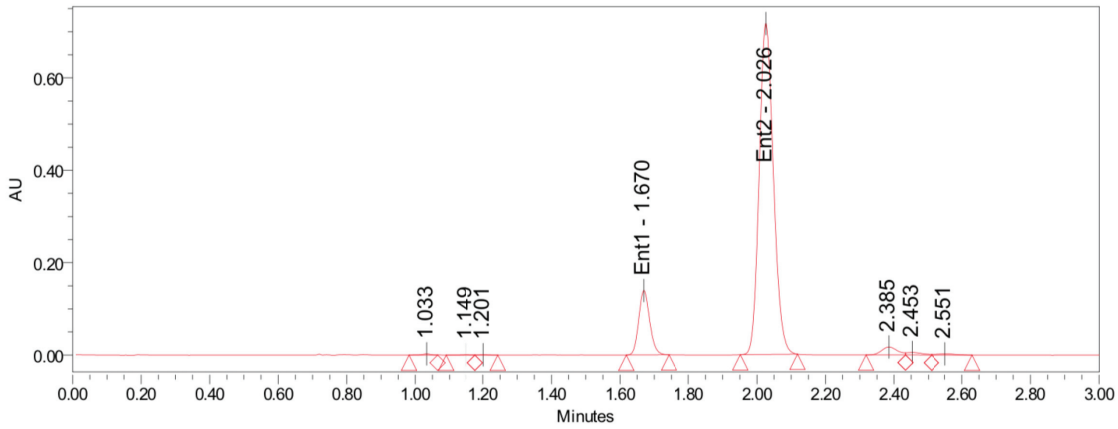
***Rac*-1.30:** 47.04 | 52.96



1.30a: 90.00 | 10.00



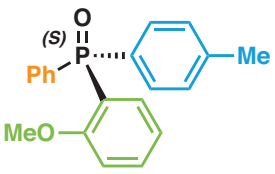
1.30b: 13.01 | 86.99



Discussion on diminished e.r.:

The exact reason for the drop in e.r. during the final displacement reaction, as we observed in compounds **1.30**, **1.36** and **1.37**, remains unclear to us. Our hypothesis is that LiOMe (the byproduct of the final displacement reaction) can start racemizing unreacted starting material *via* repeated addition-elimination if the desired substitution reaction is not fast enough. This would explain why the drop in e.r. was more significant when sterically hindered (tBuLi, **1.30**) or electronically stabilized (**1.36**, **1.37**) nucleophiles were used. Evidence supporting this hypothesis can be found in the optimization table of the LG group installation reaction (see **Table S1.6**), where using a large excess of NaOMe resulted in complete racemization of the $R_1R_2P(O)OMe$ product.

Compound 1.31a



Following **General Procedure E** on 0.05 mmol scale with **SI-1.28a** and Grignard reagent **SI-1.8** (4.0 equiv.). Purification by pTLC (hexane/EtOAc = 1:2) afforded 14.5 mg (90%, 96:4 e.r.) of the title compound **1.31a**.

Physical State: colorless gel

$[\alpha]^{25}_{D}$ = -6.7° (c = 0.73 in $CHCl_3$)

R_f = 0.35 (hexane/EtOAc = 1:3)

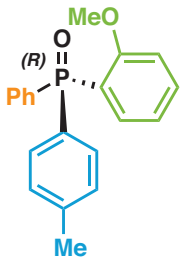
^{1}H NMR (400 MHz, $CDCl_3$) δ 7.75 (ddd, *J* = 13.4, 7.6, 1.8 Hz, 1H), 7.68 (ddd, *J* = 12.5, 8.2, 1.3 Hz, 2H), 7.59 (dd, *J* = 12.3, 8.0 Hz, 2H), 7.55 – 7.45 (m, 2H), 7.44 – 7.37 (m, 2H), 7.23 (dd, *J* = 8.3, 2.7 Hz, 2H), 7.10 – 7.02 (m, 1H), 6.90 (dd, *J* = 8.3, 5.2 Hz, 1H), 3.55 (s, 3H), 2.38 (s, 3H).

^{13}C NMR (126 MHz, $CDCl_3$) δ 161.01 (d, *J* = 3.2 Hz), 141.96 (d, *J* = 2.6 Hz), 135.08 (d, *J* = 7.1 Hz), 134.28 (d, *J* = 1.8 Hz), 133.67 (d, *J* = 107.6 Hz), 132.01 (d, *J* = 10.6 Hz), 131.88 (d, *J* = 10.2 Hz), 131.44 (d, *J* = 2.7 Hz), 129.85 (d, *J* = 109.8 Hz), 128.99 (d, *J* = 12.9 Hz), 128.16 (d, *J* = 12.4 Hz), 121.02 (d, *J* = 11.6 Hz), 120.62 (d, *J* = 103.8 Hz), 111.50 (d, *J* = 6.5 Hz), 55.37, 21.71.

^{31}P NMR (162 MHz, $CDCl_3$) δ 27.45.

HRMS (ESI-TOF): calc'd for $C_{20}H_{20}O_2P$ [M+H]+: 323.1201, found: 323.1200.

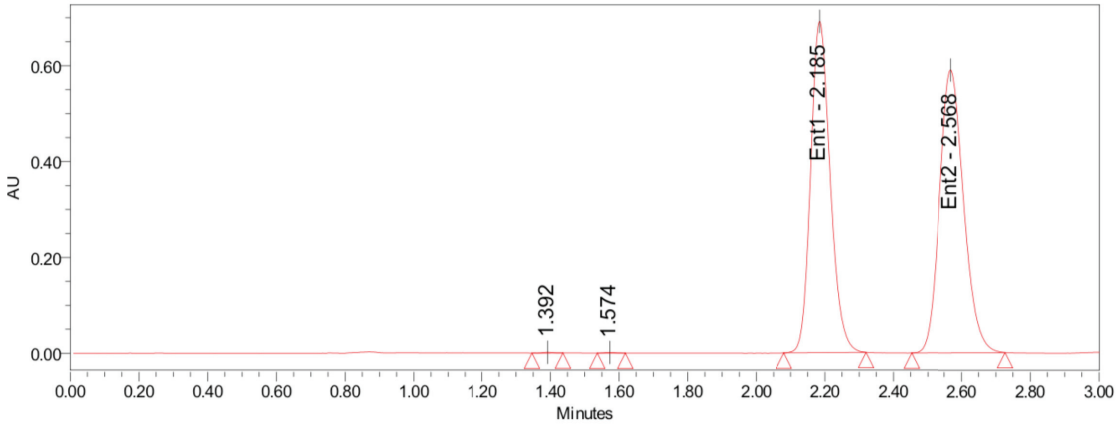
Compound 1.31b



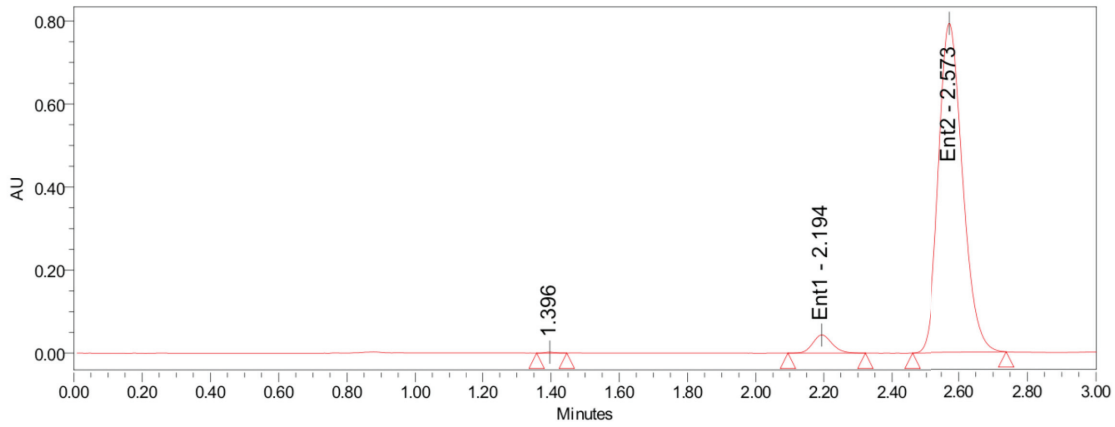
Following **General Procedure E** on 0.05 mmol scale with **SI-1.28b** and Grignard reagent **SI-1.8** (4.0 equiv.). Purification by pTLC (hexane/EtOAc = 1:2) afforded 13.6 mg (84%, 97:3 e.r.) of the title compound **1.31b**. All physical and spectroscopic properties are identical with **1.31a** except for the optical rotation: $[\alpha]^{25}_{D}$ = +6.5° (c = 0.68 in $CHCl_3$).

Chiral HPLC conditions: The sample was analyzed on a Waters UPC2 SFC with a Daicel IG column (3 mm, 4.6x250 mm) under isocratic conditions (4 mL/min, 40% MeOH / CO_2, 1600 psi backpressure) at 30 °C. The enantiomers were detected by UV light (230 nm).

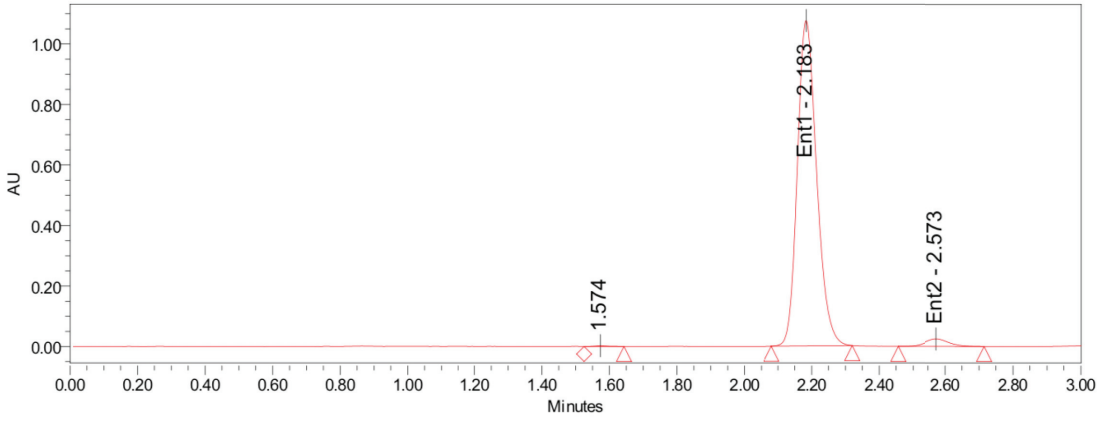
***Rac*-1.31:** 48.47 | 51.53



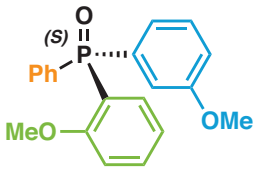
1.31a: 4.23 | 95.77



1.31b: 97.25 | 2.75



Compound 1.32a



Following **General Procedure E** on 0.05 mmol scale with **SI-1.28a** and Grignard reagent **SI-1.9**. Purification by pTLC (hexane/EtOAc = 1:3) afforded 15.8 mg (93%, 97:3 e.r.) of the title compound **1.32a**.

Physical State: white amorphous solid

$[\alpha]^{25}_{D}$ = -9.5° (c = 0.78 in $CHCl_3$)

R_f = 0.33 (hexane/EtOAc = 1:3)

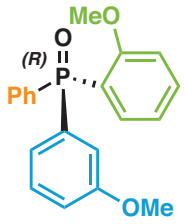
^{1}H NMR (400 MHz, $CDCl_3$) δ 7.76 – 7.64 (m, 3H), 7.56 – 7.46 (m, 2H), 7.45 – 7.38 (m, 2H), 7.36 – 7.28 (m, 2H), 7.22 (ddt, *J* = 12.1, 7.5, 1.2 Hz, 1H), 7.10 – 7.00 (m, 2H), 6.91 (dd, *J* = 8.2, 5.3 Hz, 1H), 3.78 (s, 3H), 3.57 (s, 3H).

^{13}C NMR (151 MHz, $CDCl_3$) δ 161.14, 161.12, 159.49, 159.39, 135.10, 135.05, 134.93, 134.44, 134.43, 134.23, 133.61, 132.89, 131.91, 131.85, 131.61, 131.59, 129.46, 129.36, 128.29, 128.20, 124.28, 124.22, 121.08, 121.00, 120.69, 120.01, 117.84, 117.82, 116.77, 116.69, 111.62, 111.57, 55.52, 55.44.

^{31}P NMR (162 MHz, $CDCl_3$) δ 27.38.

HRMS (ESI-TOF): calc'd for $C_{20}H_{20}O_3P$ [M+H]+: 339.1150, found: 339.1150.

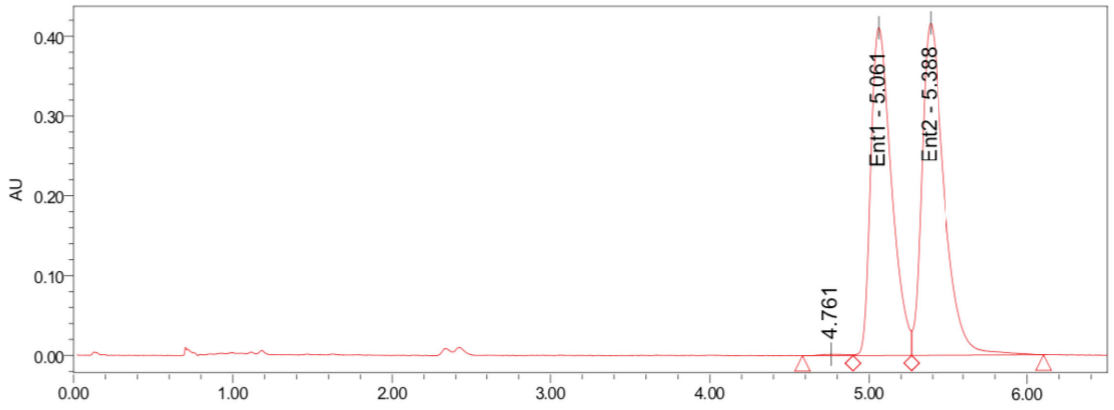
Compound 1.32b



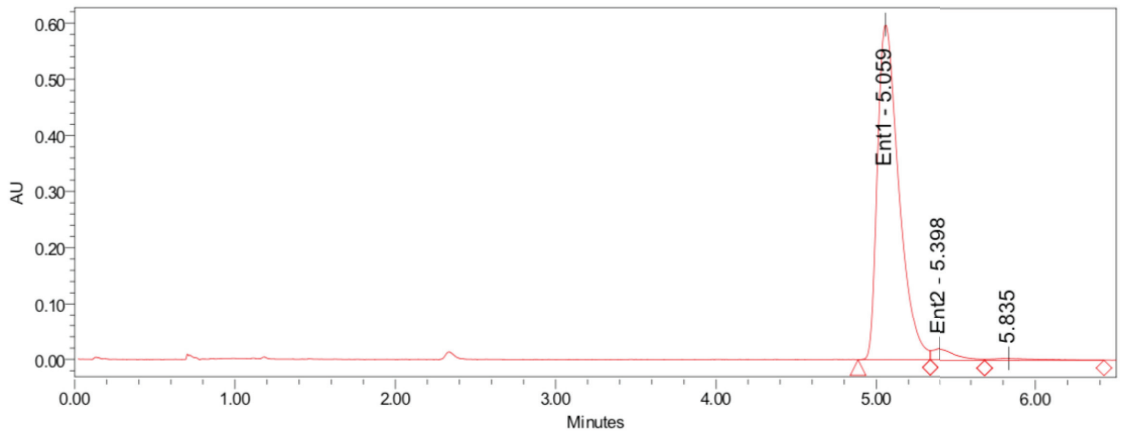
Following **General Procedure E** on 0.05 mmol scale with **SI-1.28b** and Grignard reagent **SI-1.9**. Purification by pTLC (hexane/EtOAc = 1:3) afforded 15.8 mg (93%, 97:3 e.r.) of the title compound **1.32b**. All physical and spectroscopic properties are identical with **1.32a** except for the optical rotation: $[\alpha]^{25}_{D}$ = +8.1° (c = 0.78 in $CHCl_3$).

Chiral HPLC conditions: The sample was analyzed on a Waters UPC2 SFC with a Daicel IA column (3 mm, 4.6x250 mm) under isocratic conditions (4 mL/min, 25% IPA / CO_2, 1600 psi backpressure) at 30 °C. The enantiomers were detected by UV light (212 nm).

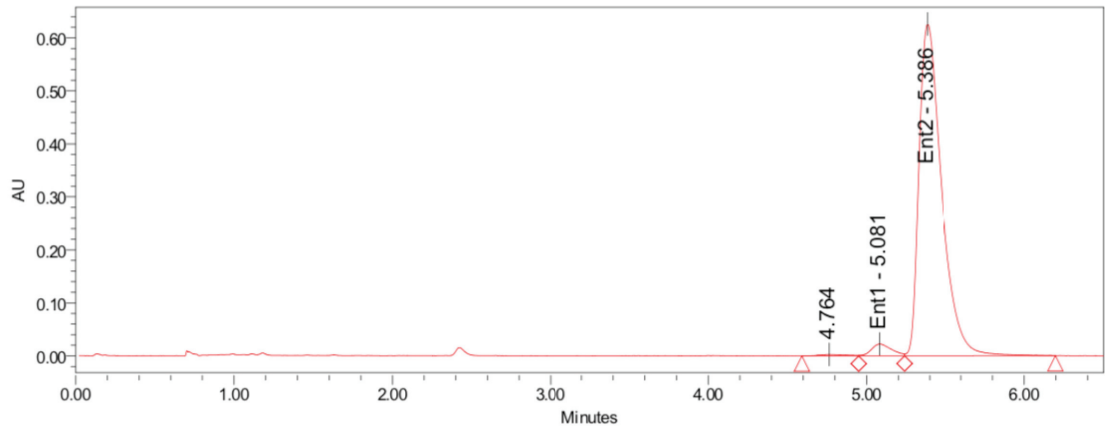
***Rac*-1.32:** 46.93 | 53.07



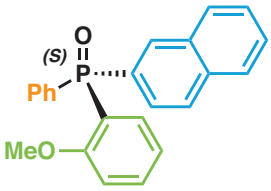
1.32a: 96.37 | 3.63



1.32b: 3.02 | 96.98



Compound 1.33a



Following **General Procedure E** on 0.05 mmol scale with **SI-1.28a** and Grignard reagent **SI-1.7** (10 equiv.). Purification by silica gel column chromatography (hexane/EtOAc = 1:2 to pure EtOAc) afforded 16.7 mg (93%, 98:2 e.r.) of the title compound **1.33a**.

Physical State: colorless gel

$[\alpha]^{25}_D$ = -7.6° (c = 0.50 in $CHCl_3$)

R_f = 0.37 (hexane/EtOAc = 1:4)

^{1}H NMR (600 MHz, $CDCl_3$) δ 8.37 – 8.31 (m, 1H), 7.90 – 7.83 (m, 3H), 7.76 (dddd, *J* = 23.9, 12.5, 8.0, 1.6 Hz, 3H), 7.67 (ddd, *J* = 10.2, 8.4, 1.5 Hz, 1H), 7.60 – 7.49 (m, 4H), 7.44 (ddd, *J* = 8.9, 7.0, 3.0 Hz, 2H), 7.12 – 7.05 (m, 1H), 6.96 – 6.90 (m, 1H), 3.55 (s, 3H).

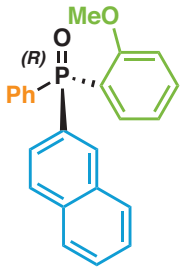
^{13}C NMR (151 MHz, $CDCl_3$) δ 161.14, 161.12, 135.19, 135.14, 134.75, 134.73, 134.50, 134.49, 133.79, 133.73, 133.02, 132.66, 132.57, 131.97, 131.90, 131.66, 131.64, 130.81,

130.09, 129.09, 128.36, 128.28, 128.03, 127.88, 127.86, 127.78, 127.20, 127.13, 126.76, 121.17, 121.09, 120.71, 120.02, 111.60, 111.56, 55.44.

^{31}P NMR (162 MHz, $CDCl_3$) δ 27.55.

HRMS (ESI-TOF): calc'd for $C_{23}H_{20}O_2P$ [M+H]+: 359.1201, found: 359.1205.

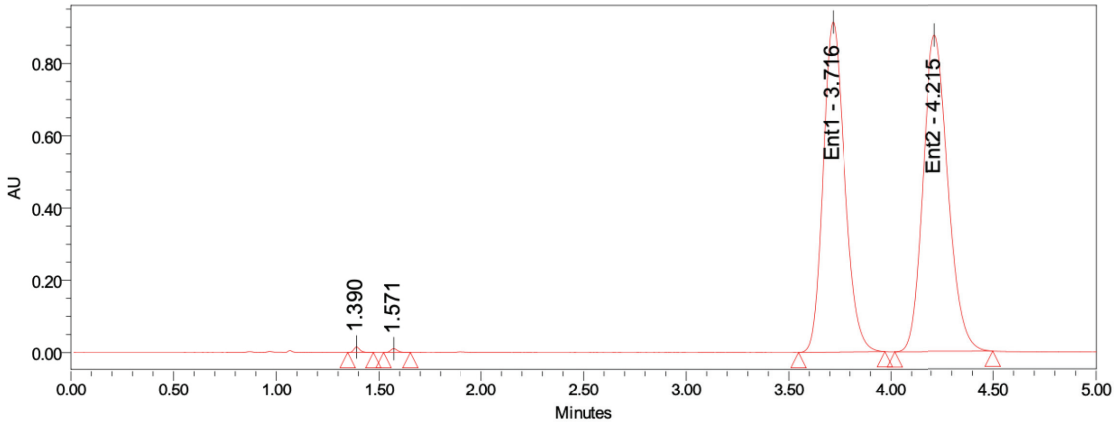
Compound 1.33b



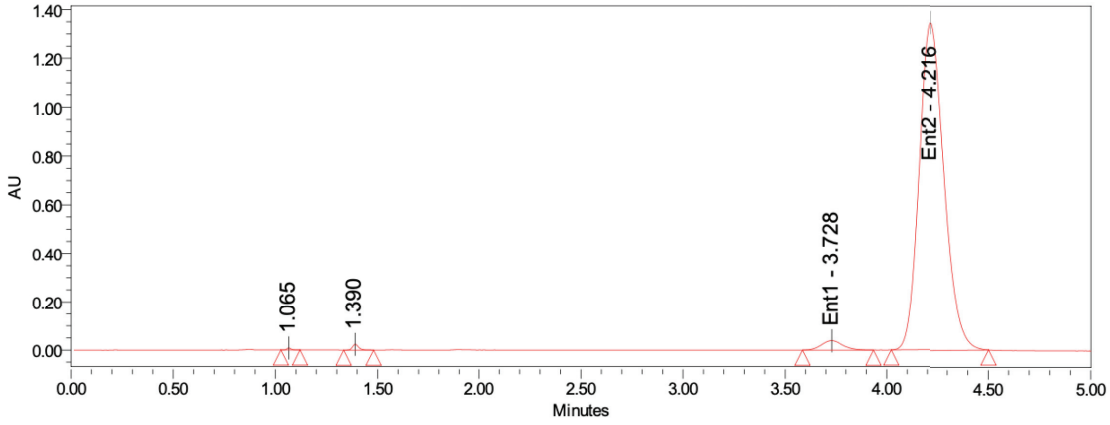
Following **General Procedure E** on 0.05 mmol scale with **SI-1.28b** and Grignard reagent **SI-1.7** (10 equiv.). Purification by silica gel column chromatography (hexane/EtOAc = 1:2 to pure EtOAc) afforded 16.5 mg (92%, 97:3 e.r.) of the title compound **1.33b**. All physical and spectroscopic properties are identical with **1.33a** except for the optical rotation: **$[\alpha]^{25}_D$** = +8.1° (c = 0.83 in $CHCl_3$).

Chiral HPLC conditions: The sample was analyzed on a Waters UPC2 SFC with a Daicel IBN column (3 mm, 4.6x250 mm) under isocratic conditions (4 mL/min, 15% MeOH / CO_2, 1600 psi backpressure) at 30 °C. The enantiomers were detected by UV light (220 nm).

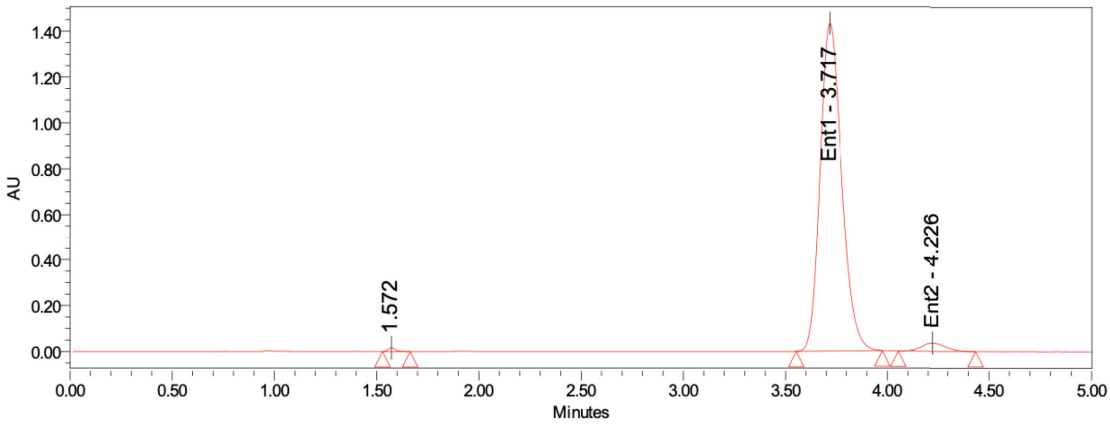
***Rac*-1.33:** 47.15 | 52.85



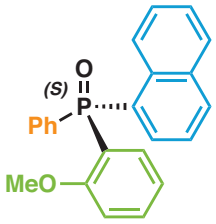
1.33a: 2.35 | 97.65



1.33b: 97.17 | 2.83



Compound 1.34a



Following **General Procedure G** on 0.05 mmol scale with **SI-1.28a** and organolithium reagent **SI-1.20**. Purification by pTLC (hexane/EtOAc = 1:3) afforded 11.7 mg (65%, 98:2 e.r.) of the title compound **1.34a**.

Physical State: white crystalline solid

m.p. = 167–169 °C

$[\alpha]^{25}_{D}$ = +21.3 (c = 0.52 in $CHCl_3$)

R_f = 0.36 (hexane/EtOAc = 1:3)

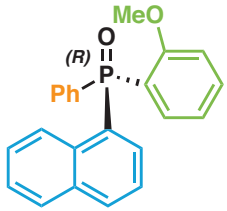
^{1}H NMR (400 MHz, $CDCl_3$) δ 8.57 (d, *J* = 8.5 Hz, 1H), 7.98 (d, *J* = 8.0 Hz, 1H), 7.87 (d, *J* = 8.2 Hz, 1H), 7.83 – 7.70 (m, 3H), 7.57 – 7.36 (m, 8H), 7.08 (tdd, *J* = 7.5, 2.1, 0.9 Hz, 1H), 6.91 (dd, *J* = 7.9, 5.3 Hz, 1H), 3.46 (s, 3H).

^{13}C NMR (151 MHz, $CDCl_3$) δ 161.17, 161.15, 134.99, 134.94, 134.36, 134.35, 134.05, 133.94, 133.88, 133.82, 133.34, 133.18, 133.10, 132.84, 132.82, 132.25, 132.18, 131.58, 131.56, 129.60, 128.89, 128.80, 128.79, 128.31, 128.23, 127.62, 127.58, 127.17, 126.32, 124.39, 124.29, 121.42, 121.29, 121.22, 120.74, 111.75, 111.71, 55.45.

^{31}P NMR (162 MHz, $CDCl_3$) δ 30.93.

HRMS (ESI-TOF): calc'd for $C23H20O_2P$ [M+H]+: 359.1201, found: 359.1197.

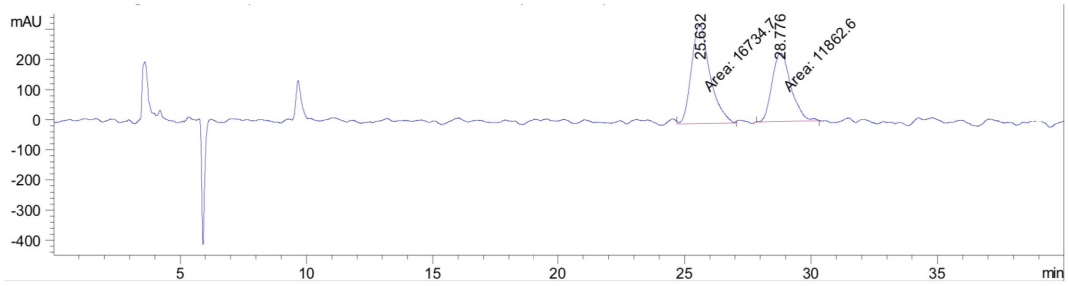
Compound 1.34b



Following **General Procedure G** on 0.03 mmol scale with **SI-1.28b** and organolithium reagent **SI-1.20**. Purification by pTLC (hexane/EtOAc = 1:3) afforded 5.7 mg (53%, 97:3 e.r.) of the title compound **1.34b**. All physical and spectroscopic properties are identical with **1.34a** except for the optical rotation: $[\alpha]^{25}_{D}$ = -22.5° (c = 0.29 in $CHCl_3$).

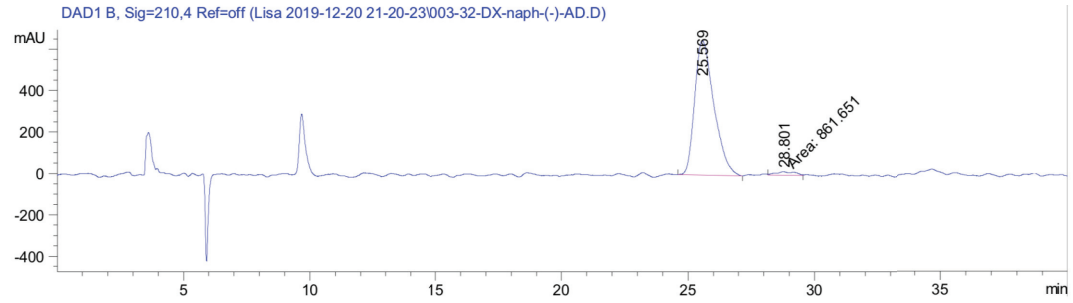
Chiral HPLC: Chiralpak AD-H column; isopropanol/hexane = 80:20, 0.8 mL/min, 280 nm.

***Rac*-1.34:**



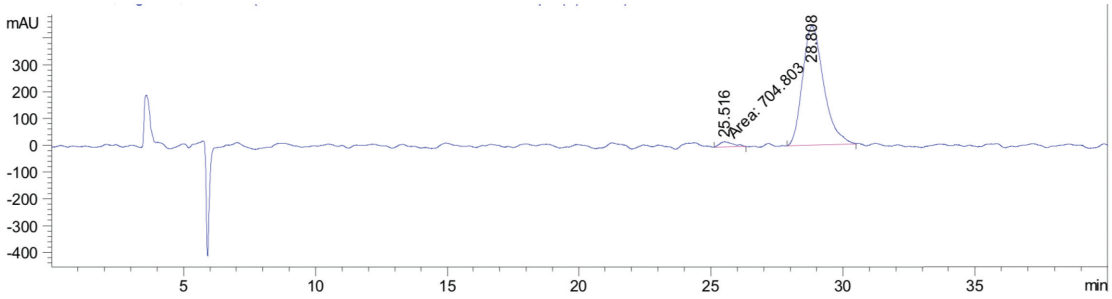
Peak #	RetTime [min]	Type	Width [min]	Area [mAU*s]	Height [mAU]	Area %
1	25.632	MM	0.8476	1.67347e4	329.05856	58.5186
2	28.776	MM	0.8689	1.18626e4	227.53297	41.4814

1.34a:



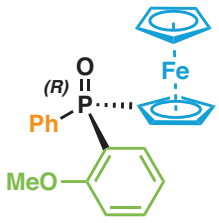
Peak #	RetTime [min]	Type	Width [min]	Area [mAU*s]	Height [mAU]	Area %
1	25.569	BB	0.6337	3.44452e4	650.53851	97.5595
2	28.801	MM	0.8695	861.65088	16.51578	2.4405

1.34b:



Peak #	RetTime [min]	Type	Width [min]	Area [mAU*s]	Height [mAU]	Area %
1	25.516	MM	0.5912	704.80267	19.87043	2.7648
2	28.808	BV R	0.6577	2.47873e4	445.12915	97.2352

Compound 1.35a



Following **General Procedure G** on 0.05 mmol scale with **SI-1.28a** and organolithium reagent **SI-1.24**. Purification by pTLC (hexane/EtOAc = 1:3) afforded 19.3 mg (93%, 97:3 e.r.) of the title compound **1.35a**.

Physical State: orange gel

$[\alpha]^{25}_D$ = -38.2° (c = 0.10 in $CHCl_3$)

R_f = 0.29 (hexane/EtOAc = 1:3)

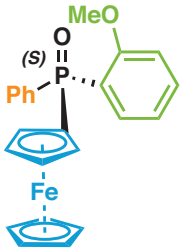
^{1}H NMR (400 MHz, $CDCl_3$) δ 7.95 (ddd, *J* = 13.4, 7.5, 1.8 Hz, 1H), 7.71 – 7.62 (m, 2H), 7.54 – 7.45 (m, 1H), 7.44 (td, *J* = 7.2, 1.6 Hz, 1H), 7.41 – 7.34 (m, 2H), 7.10 (tdd, *J* = 7.5, 1.8, 0.9 Hz, 1H), 6.87 (dd, *J* = 8.3, 5.3 Hz, 1H), 4.59 (s, 1H), 4.47 (s, 1H), 4.44 (s, 2H), 4.12 (s, 5H), 3.51 (s, 3H).

^{13}C NMR (126 MHz, $CDCl_3$) δ 160.44, 160.41, 136.23, 135.35, 134.48, 134.43, 133.84, 133.83, 131.00, 130.98, 130.90, 127.90, 127.80, 123.26, 122.42, 120.92, 120.83, 111.64, 111.59, 73.41, 72.97, 72.87, 72.45, 72.29, 72.19, 71.42, 71.33, 71.17, 71.08, 69.69, 55.35.

^{31}P NMR (162 MHz, $CDCl_3$) δ 27.37.

HRMS (ESI-TOF): calc'd for $C_{23}H_{22}{}^{54}FeO_2P$ [M+H]+: 415.0754, found: 415.0747.

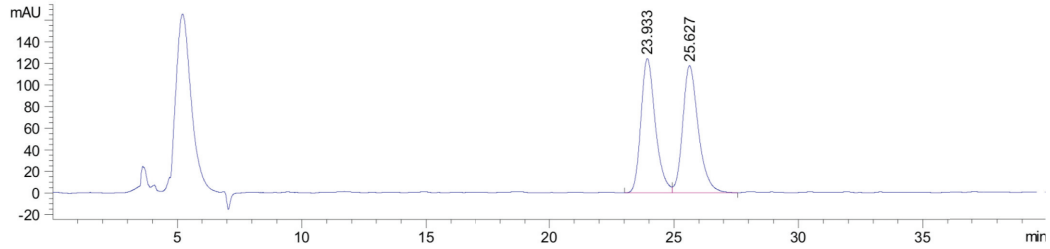
Compound 1.35b



Following **General Procedure G** on 0.05 mmol scale with **SI-1.28b** and organolithium reagent **SI-1.24**. Purification by pTLC (hexane:EtOAc = 1:3) afforded 18.3 mg (88%, 97:3 e.r.) of the title compound **1.35b**. All physical and spectroscopic properties are identical with **1.35a** except for the optical rotation: **$[\alpha]^{25}_D$** = +39.0 (c = 0.10 in $CHCl_3$).

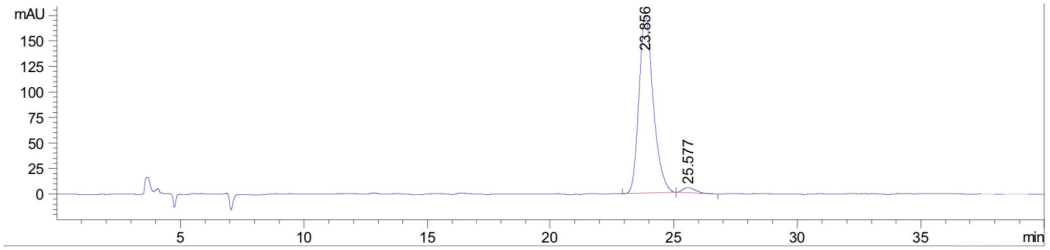
Chiral HPLC: Chiralpak AD-H column; IPA/hexane = 85:15, 0.8 mL/min, 280 nm.

***Rac*-1.35:**



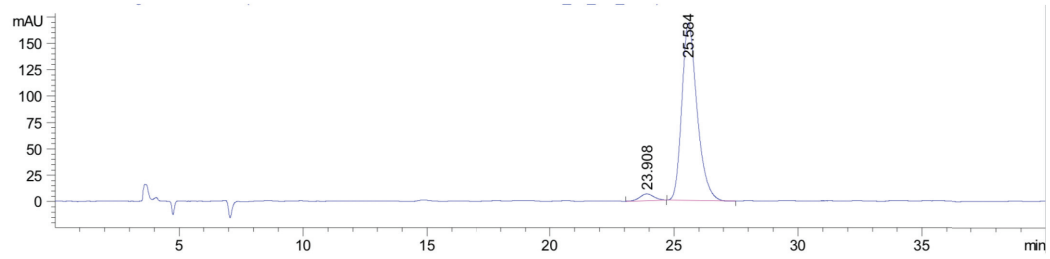
Peak #	RetTime [min]	Type	Width [min]	Area [mAU*s]	Height [mAU]	Area %
1	23.933	BV	0.6103	5013.09375	124.34603	49.3424
2	25.627	VB	0.6618	5146.71387	117.78574	50.6576

1.35a:



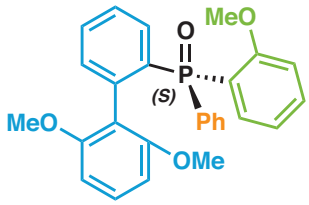
Peak #	RetTime [min]	Type	Width [min]	Area [mAU*s]	Height [mAU]	Area %
1	23.856	BB	0.6067	6963.61084	174.07208	97.3413
2	25.577	BB	0.5148	190.19843	5.19951	2.6587

1.35b:



Peak #	RetTime [min]	Type	Width [min]	Area [mAU*s]	Height [mAU]	Area %
1	23.908	BB	0.5442	244.94312	6.34717	3.2983
2	25.584	BB	0.6456	7181.36475	168.38510	96.7017

Compound 1.36a



Following **General Procedure G** on 0.05 mmol scale with **SI-1.28a** and organolithium reagent **SI-1.21**. Purification by pTLC (hexane/EtOAc = 1:3) afforded 18.3 mg (83%, 93:7 e.r.) of the title compound **1.36a**.

Physical State: white solid

m.p. = 187– 189 °C

$[\alpha]^{25}_{D}$ = +49.6° (c = 0.74 in $CHCl_3$)

R_f = 0.25 (hexane/EtOAc = 1:3)

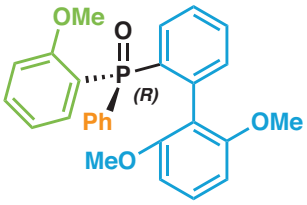
^{1}H NMR (400 MHz, $CDCl_3$) δ 7.70 – 7.58 (m, 3H), 7.55 – 7.45 (m, 2H), 7.41 – 7.30 (m, 3H), 7.30 – 7.24 (m, 2H), 7.19 (dddd, *J* = 7.6, 4.2, 1.3, 0.5 Hz, 1H), 7.03 (t, *J* = 8.3 Hz, 1H), 6.89 (tdd, *J* = 7.5, 2.0, 0.9 Hz, 1H), 6.76 (dd, *J* = 8.0, 5.2 Hz, 1H), 6.28 (dd, *J* = 8.4, 0.8 Hz, 1H), 6.19 (dd, *J* = 8.4, 0.8 Hz, 1H), 3.52 (s, 3H), 3.50 (s, 3H), 3.43 (s, 3H).

^{13}C NMR (126 MHz, $CDCl_3$) δ 160.58, 160.55, 157.95, 157.61, 139.20, 139.13, 134.76, 134.70, 134.35, 133.66, 133.56, 133.50, 133.27, 133.26, 132.70, 132.56, 132.48, 132.11, 132.03, 131.01, 130.99, 130.70, 130.68, 129.22, 127.51, 127.41, 126.39, 126.28, 122.33, 121.51, 120.60, 120.50, 117.83, 117.80, 111.02, 110.97, 103.04, 102.92, 55.37, 55.28, 55.12.

^{31}P NMR (162 MHz, $CDCl_3$) δ 26.90.

HRMS (ESI-TOF): calc'd for $C_{27}H_{26}O_4P$ [M+H]+: 445.1569, found: 445.1565.

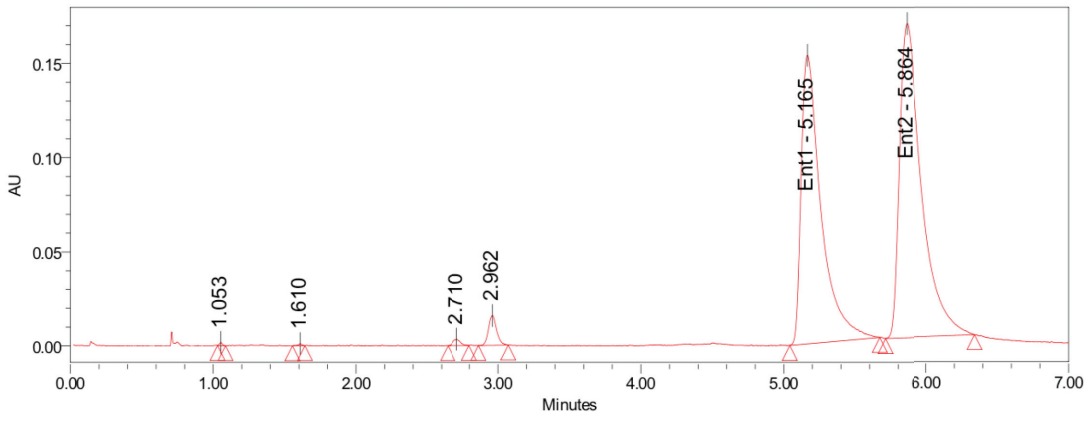
Compound 1.36b



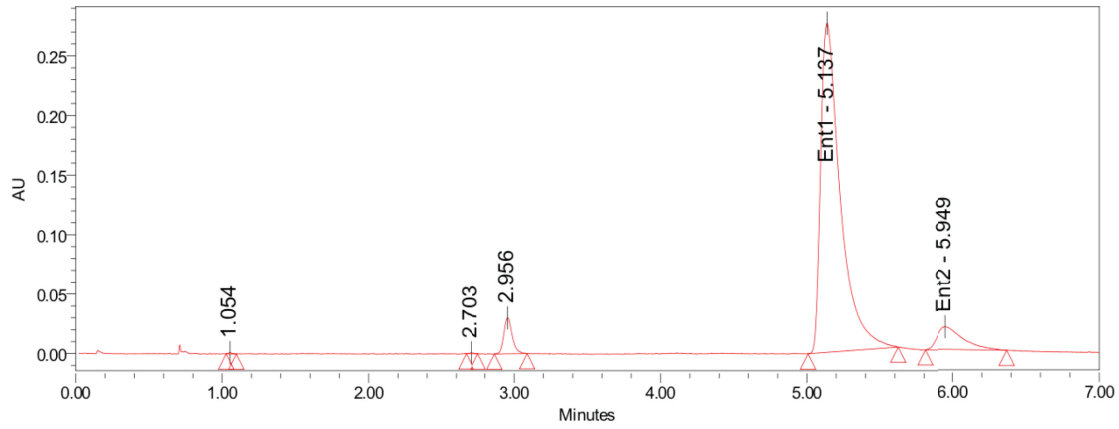
Following **General Procedure G** on 0.05 mmol scale with **SI-1.28b** and organolithium reagent **SI-1.21**. Purification by pTLC (hexane/EtOAc = 1:3) afforded 18.3 mg (83%, 93:7 e.r.) of the title compound **1.36b**. All physical and spectroscopic properties are identical with **1.36a** except for the optical rotation: $[\alpha]^{25}_{D} = -44.5°$ (c = 1.00 in $CHCl_3$).

Chiral HPLC conditions: The sample was analyzed on a Waters UPC2 SFC with a Daicel IBN column (3 mm, 4.6x250 mm) under isocratic conditions (4 mL/min, 20% IPA / CO_2, 1600 psi backpressure) at 30 °C. The enantiomers were detected by UV light (220 nm).

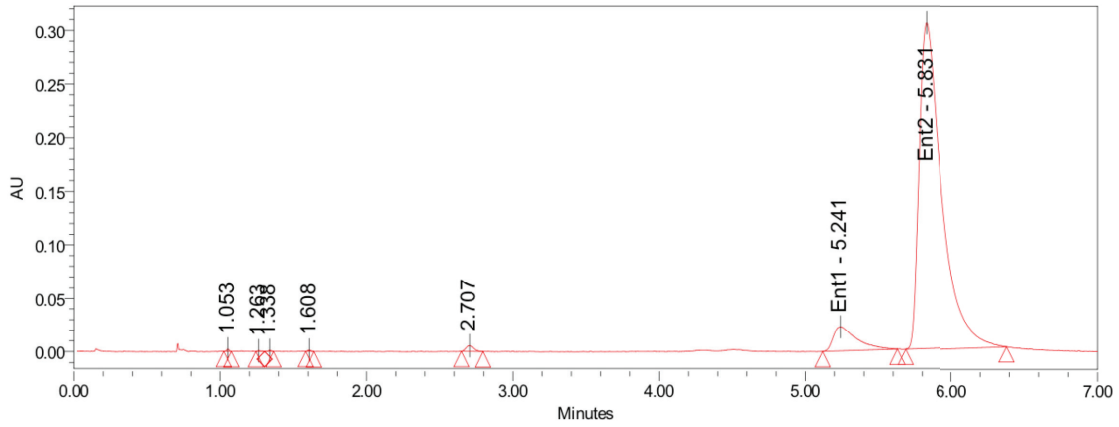
***Rac*-1.36:** 44.89 | 55.11



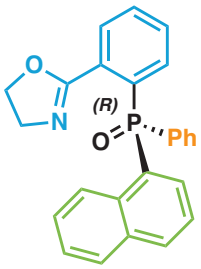
1.36a: 91.61 | 8.39



1.36b: 7.01 | 92.99 |



Compound 1.37a



Following **General Procedure G** on 0.05 mmol scale with **SI-1.29a** and organolithium reagent **SI-1.22** (4 equiv.). Purification by pTLC (hexane/EtOAc = 1:2) afforded 11.4 mg (56%, 94:6 e.r.) of the title compound **1.37a**.

Physical State: yellow amorphous solid

$[\alpha]^{25}_D$ = -23.5° (c = 0.38 in $CHCl_3$)

R_f = 0.40 (hexane/EtOAc = 1:2)

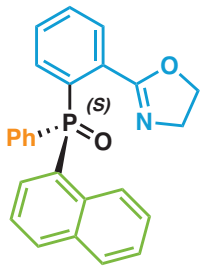
^{1}H NMR (400 MHz, Acetone-d_6) δ 8.65 (d, *J* = 8.6 Hz, 1H), 8.12 (d, *J* = 8.2 Hz, 1H), 8.00 (d, *J* = 8.3 Hz, 1H), 7.79 – 7.70 (m, 3H), 7.67 (tt, *J* = 7.6, 1.6 Hz, 1H), 7.64 – 7.47 (m, 7H), 7.45 – 7.36 (m, 2H), 3.91 (ddd, *J* = 10.1, 8.8, 7.7 Hz, 1H), 3.80 (ddd, *J* = 10.5, 8.4, 7.7 Hz, 1H), 3.65 – 3.48 (m, 2H).

^{13}C NMR (151 MHz, Acetone-d_6) δ 164.58, 164.56, 135.47, 134.90, 134.84, 134.76, 134.71, 134.64, 134.61, 134.56, 134.15, 134.11, 134.10, 134.02, 133.34, 133.32, 133.11, 133.04, 132.45, 132.43, 132.38, 132.36, 131.66, 131.27, 131.21, 130.97, 130.83, 130.75, 129.63, 129.63, 129.15, 129.07, 128.59, 128.56, 127.45, 127.16, 125.25, 125.15, 68.28, 55.74.

^{31}P NMR (162 MHz, Acetone-d_6) δ 32.05.

HRMS (ESI-TOF): calc'd for $C_{25}H_{21}NO_2P$ [M+H]+: 398.1310, found: 398.1306.

Compound 1.37b

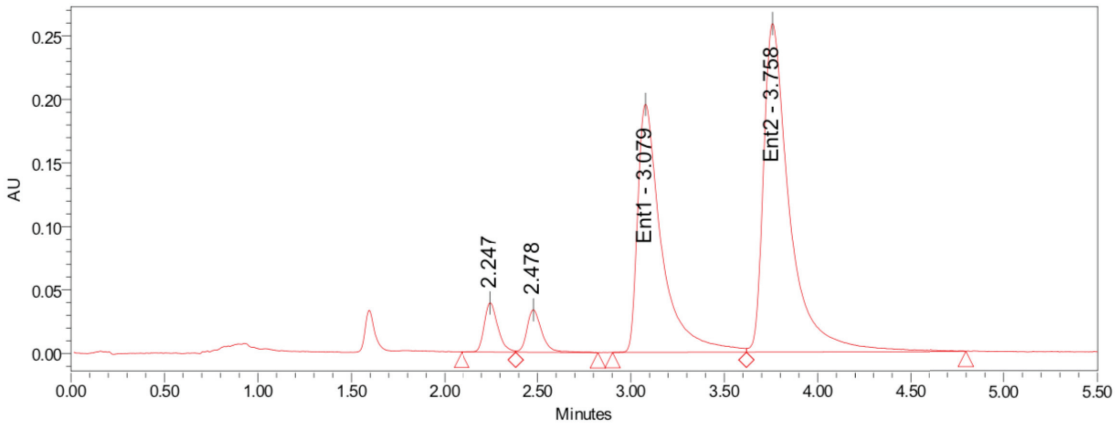


Following **General Procedure G** on 0.05 mmol scale with **SI-1.29b** and organolithium reagent **SI-1.22** (4 equiv.). Purification by pTLC (hexane/EtOAc = 1:2) afforded 8.0 mg (40%, e.r. between 89:11 to 94:6, unsatisfactory chiral HPLC separation, *vide infra*) of the

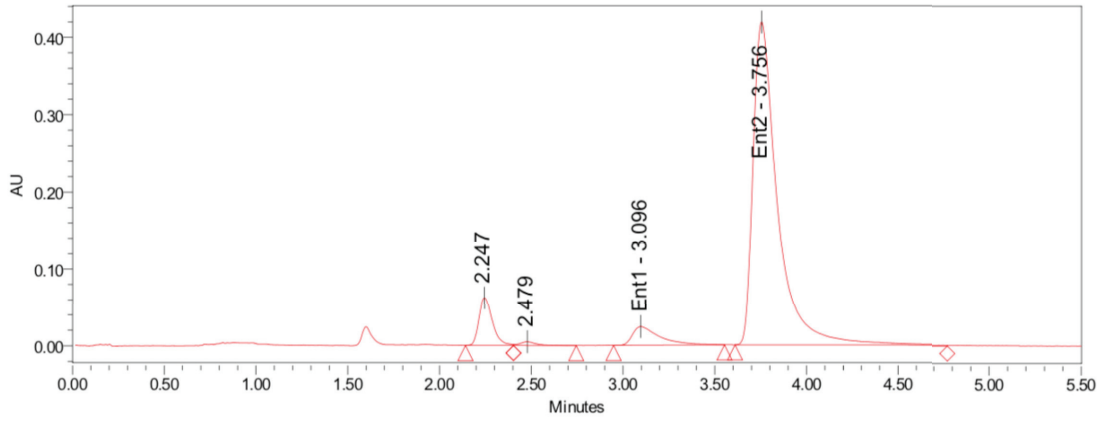
title compound **1.37b**. All physical and spectroscopic properties are identical with **1.37a** except for the optical rotation: $[\alpha]^{25}_{D}$ = +22.8° (c = 0.40 in $CHCl_3$).

Chiral HPLC conditions: The sample was analyzed on a Waters UPC2 SFC with a Daicel IA column (3 mm, 4.6x250 mm) under isocratic conditions (4 mL/min, 40% IPA / CO_2, 1600 psi backpressure) at 30 °C. The enantiomers were detected by UV light (212 nm).

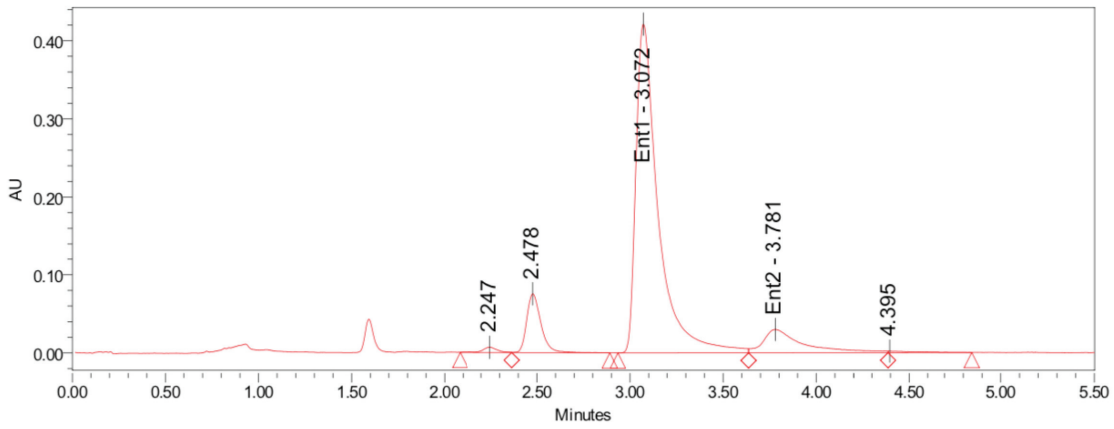
***Rac*-1.37:** 40.91 | 59.09



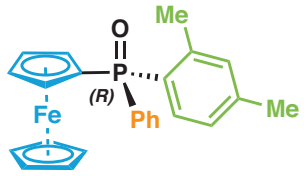
1.37a: 5.98 | 94.02



1.37b: 88.90 | 11.10



Compound 1.38a



Following **General Procedure G** on 0.05 mmol scale with **SI-1.30a** and organolithium reagent **SI-1.24**. Purification by pTLC (hexane/EtOAc = 1:3) afforded 16.6 mg (84%, 98:2 e.r.) of the title compound **1.38a**.

Physical State: orange amorphous solid

$[\alpha]^{25}_{D}$ = +88.0° (c = 0.10 in $CHCl_3$)

R_f = 0.35 (hexane/EtOAc = 1:3)

^{1}H NMR (400 MHz, $CDCl_3$) δ 7.76 – 7.67 (m, 2H), 7.51 (dtd, *J* = 16.2, 8.6, 8.1, 6.2 Hz, 3H), 7.11 (dd, *J* = 14.0, 7.8 Hz, 1H), 6.99 (s, 1H), 6.92 (d, *J* = 7.9 Hz, 1H), 4.72 (s, 1H), 4.54 (s, 1H), 4.40 (s, 1H), 4.21 (s, 5H), 3.93 (s, 1H), 2.30 (d, *J* = 4.1 Hz, 6H).

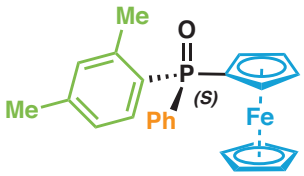
^{13}C NMR (151 MHz, $CDCl_3$) δ 142.33, 142.27, 142.10, 142.08, 134.78, 134.09, 133.58, 133.49, 132.56, 132.49, 131.45, 131.43, 131.32, 131.26, 130.16, 129.45, 128.33, 128.25,

125.79, 125.71, 74.30, 73.52, 72.84, 72.75, 72.35, 72.28, 71.97, 71.90, 71.33, 71.26, 69.81, 21.47, 21.39, 21.36.

^{31}P NMR (162 MHz, $CDCl_3$) δ 31.77.

HRMS (ESI-TOF): calc'd for $C_{24}H_{24}{}^{54}FeOP$ [M+H]+: 413.0961, found: 413.0954.

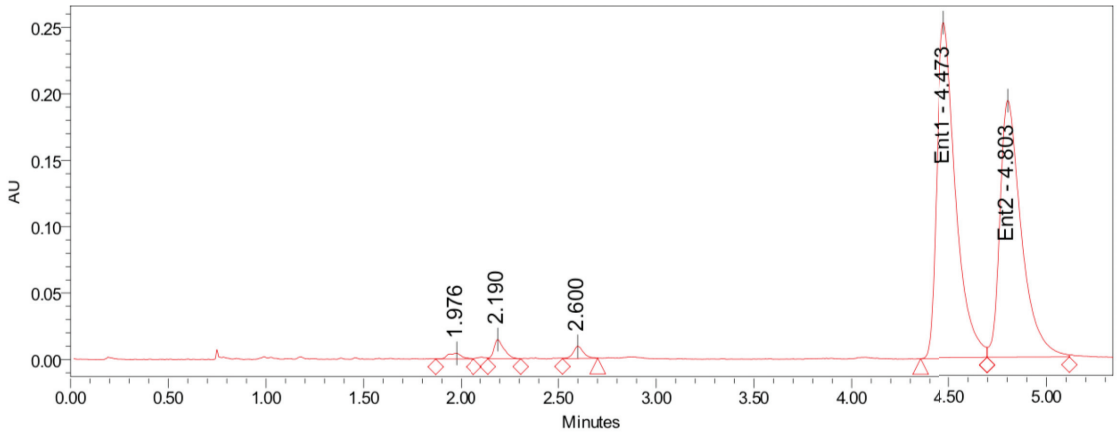
Compound 1.38b



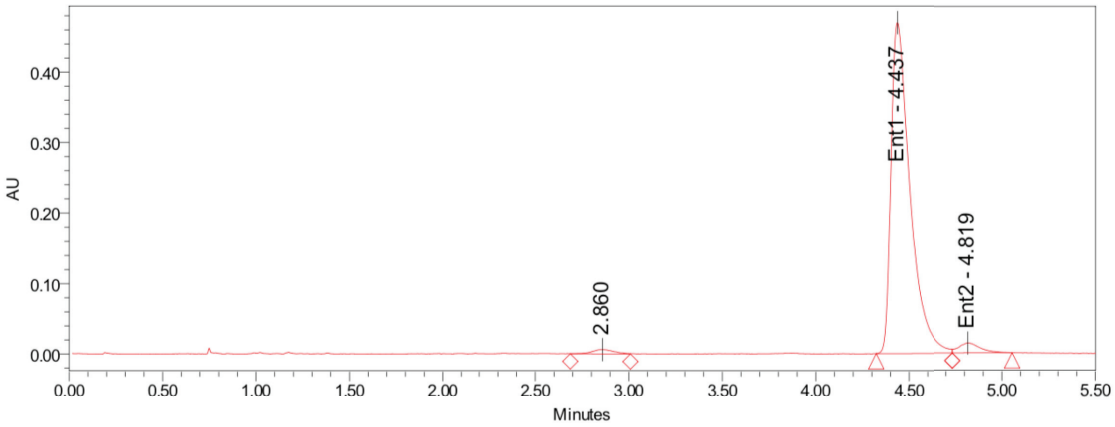
Following **General Procedure G** on 0.05 mmol scale with **SI-1.30b** and organolithium reagent **SI-1.24**. Purification by pTLC (hexane/EtOAc = 1:3) afforded 15.8 mg (76%, between 97:3 and 98:2 e.r., unsatisfactory chiral HPLC separation, *vide infra*) of the title compound **1.38b**. All physical and spectroscopic properties are identical with **1.38a** except for the optical rotation: **$[\alpha]^{25}_D$** = –79.0° (c = 0.10 in $CHCl_3$).

Chiral HPLC conditions: The sample was analyzed on a Waters UPC2 SFC with a Daicel IB column (3 mm, 4.6x250 mm) under isocratic conditions (4 mL/min, 20% IPA / CO_2, 1600 psi backpressure) at 30 °C. The enantiomers were detected by UV light (220 nm).

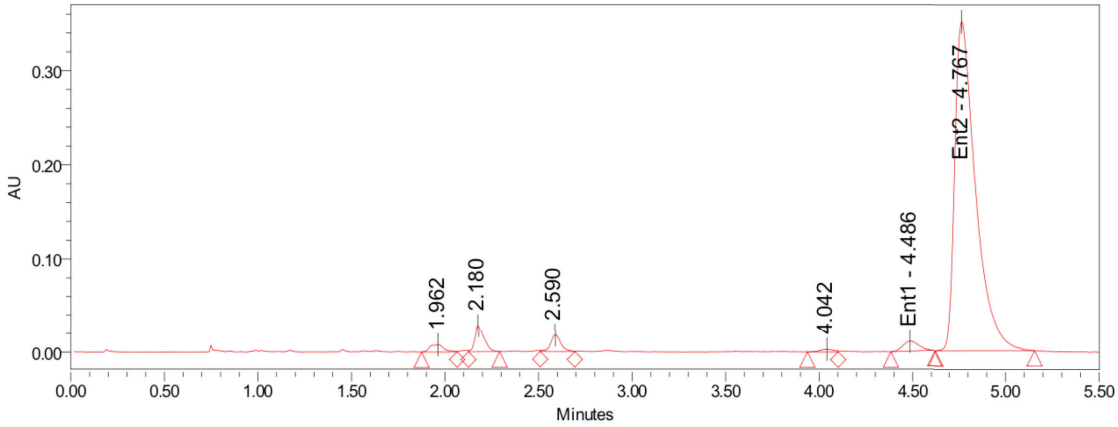
***Rac*-1.38:** 53.91 | 46.09



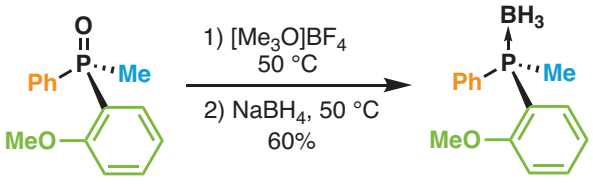
1.38a: 96.69 | 3.31



1.38b: 2.29 | 97.71



Stereospecific Reduction of Phosphine Oxides

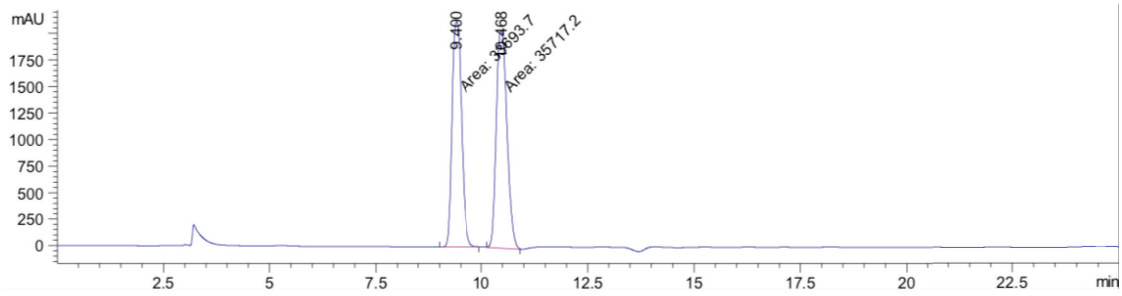


1.26a
97:3 e.r.

1.39a
96:4 e.r.

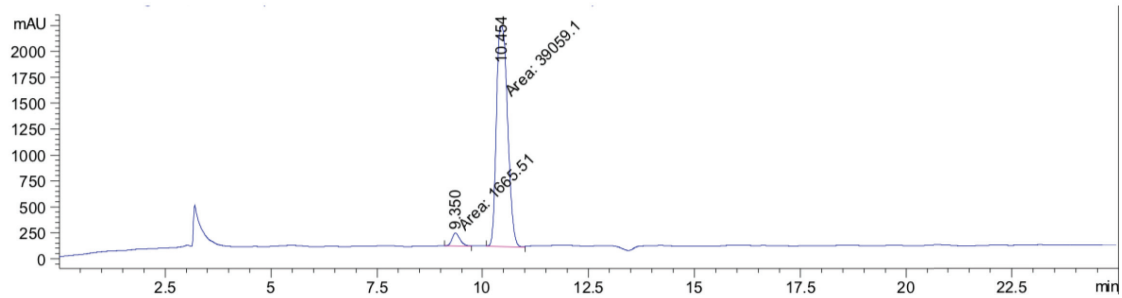
Reduction of chiral phosphine follows a reported procedure [6]: A solution of **1.26a** (0.5 mmol, 1.0 equiv.) in DCM (1 mL) was added dropwise at room temperature to a stirred solution of Meerwein's salt (0.5 mmol, 1.0 equiv.) in DCM (1 mL) under argon atmosphere. The reaction mixture was refluxed gently for 2 h at which point ^{31}P NMR showed the complete conversion of phosphine oxide to the alkoxyphosphonium salt. After cooling to room temperature, sodium borohydride (3 mmol, 6.0 equiv.) dissolved in diglyme (1 mL) was added dropwise to the reaction mixture. This mixture was refluxed gently for 2 h. Once the ^{31}P NMR showed the full conversion of salt to phosphine borane the reaction mixture was washed with water (5 mL), and the isolated organic layer was dried over anhydrous $MgSO_4$. The drying agent was removed by filtration, and the solvent was removed in vacuo to give a colorless oil, which was purified by silica gel chromatography (hexane/EtOAc = 4:1) to yield **1.39a** (60%, 96:4 e.r.) as a white solid. All spectroscopic data were identical with literature. Enantiomeric ratio was measured with a Chiralpak AD-H column with 2% isopropanol in hexane as eluent and 1 mL/min as the flow rate.

Racemic **1.39**:



Peak #	RetTime [min]	Type	Width [min]	Area [mAU*s]	Height [mAU]	Area %
1	9.400	MM	0.2641	3.36937e4	2126.38135	48.5424
2	10.468	MM	0.2903	3.57172e4	2050.31763	51.4576

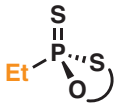
Enantioenriched **1.39a**:



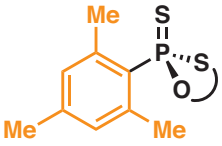
Peak #	RetTime [min]	Type	Width [min]	Area [mAU*s]	Height [mAU]	Area %
1	9.350	MM	0.2215	1665.51257	125.34003	4.0897
2	10.454	MM	0.3062	3.90591e4	2126.23096	95.9103

List of Failed Substrates

Section A: Loading:

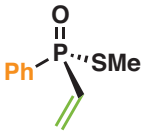


full conv. of SM
inseparable mixture

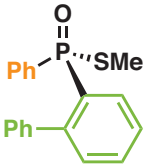


<5% conv.

Section B: Coupling:

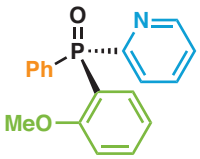


complex mixture

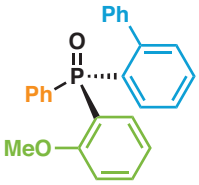


<5% conv.

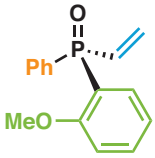
Section C: Displacement:



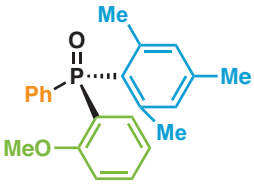
With RLi:
full conv. to $R_2P(O)H$



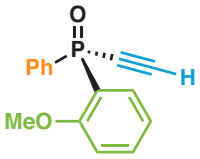
With RMgX: <5% conv.
With RLi: complex mixture



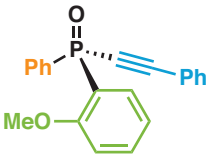
With RMgX: <5% conv.
With RLi: <5% conv.



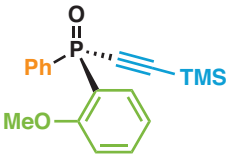
With RLi: <5% conv.



With RMgX: no rxn

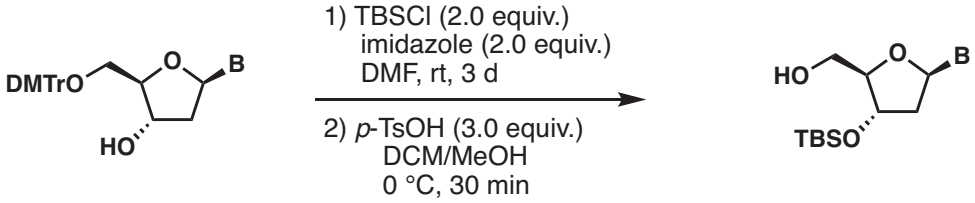


With RLi: <5% conv.



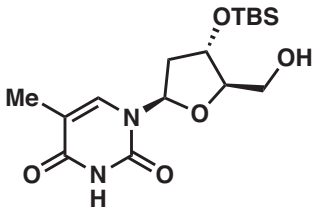
With RLi: <5% conv.

General Procedure G: Synthesis of 3'-O-Protected Nucleosides



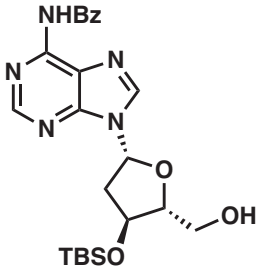
Synthetic methods of 3'-*O*-TBS protected nucleosides were adapted from literature procedures.[1, 7] A solution of 5′-O-DMTr protected nucleoside (10 mmol, 1.0 equiv.) and imidazole (3.14 g, 46.2 mmol, 2.0 equiv.) in DMF (30 mL) was cooled to 0 °C, to which TBSCl (20 mmol, 2.0 equiv.) was added. The reaction was stirred at room temperature for 3 days, and then diluted with EtOAc (80 mL) and washed with water (100 mL x 3). The organic layer was dried over $MgSO_4$ and the solvent was removed *in vacuo*. The residue was dissolved in 100 mL of DCM and 40 mL of MeOH, then cooled to 0 °C. A solution of *p*-toluenesulfonic acid (20 mmol, 2.0 equiv.) in 10 mL of MeOH was added, and the reaction was stirred at 0 °C for 30 min. Pyridine (1 mL) was added to neutralize the excess acid. The crude reaction mixture was evaporated to dryness, diluted in EtOAc (100 mL) and washed with saturated $NaHCO_3$ (50 mL) and brine (50 mL). The organic layer was dried over Na_2SO_4, filtered and concentrated *in vacuo*. The crude product was purified by silica gel chromatography (pure DCM to 5% MeOH in DCM gradient) to afford the desired product.

Compound SI-1.31



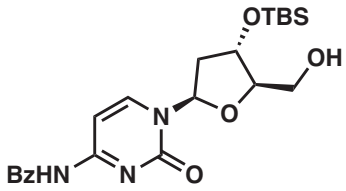
Following **General Procedure G** on 10 mmol scale with 5′-O-(4,4′-dimethoxytrityl) thymidine. **SI-1.31** (2.8 g, 79%) was isolated as a white foam with identical spectroscopic properties as reported in literature.[8]

Compound SI-1.32



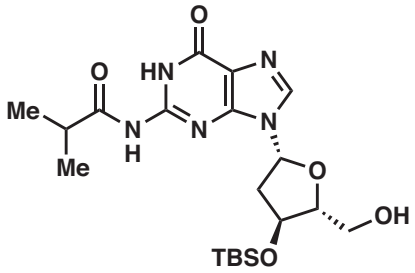
Following **General Procedure G** on 10 mmol scale with N^6-benzoyl-5'-O- (4,4'-dimethoxytrityl)-2'-deoxyadenosine. **SI-1.32** (3.8 g, 81%) was isolated as a white foam with identical spectroscopic properties as reported in literature.[9]

Compound SI-1.33



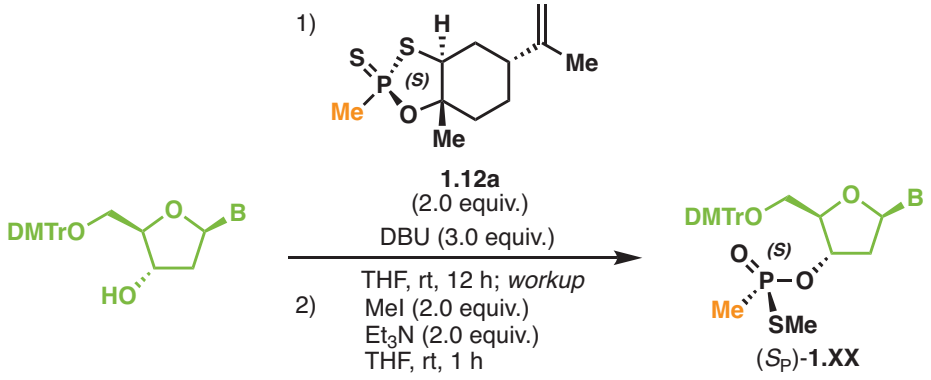
Following **General Procedure G** on 10 mmol scale with N^4-benzoyl-5′- *O*-(4,4′-dimethoxytrityl)-2′-deoxycytidine. **SI-1.33** (3.7 g, 83%) was isolated as a white foam with identical spectroscopic properties as reported in literature.[8]

Compound SI-1.34



Following **General Procedure G** on 10 mmol scale with N^2-isobutyryl-5′-O-(4,4′-dimethoxytrityl)-2′-deoxyguanosine. **SI-1.34** (3.3 g, 72%) was isolated as a white foam with identical spectroscopic properties as reported in literature.[8]

General Procedure H: MPO Synthesis – Loading

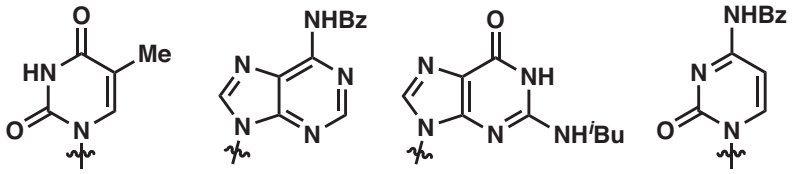


To a flame-dried 50 mL round bottom flask under argon was charged nucleoside (1.0 mmol, 1.0 equiv.), **12** (524.6 mg, 2.0 mmol, 2.0 equiv.), and THF (10 mL). DBU (3.0 mmol, 3.0 equiv.) was added dropwise, and the resulting solution was stirred for 12 h at rt. The reaction was then quenched with 20 mL of 1X PBS solution and extracted with DCM (3 x 30 mL). The combined organic layers were washed with saturated aqueous $NaHCO_3$ solution (10 mL), brine (10 mL), dried over Na_2SO_4, filtered and concentrated. The residue was re-dissolved in THF (5 mL). Et_3N (2 equiv.) and MeI (2 equiv.) were added, and the

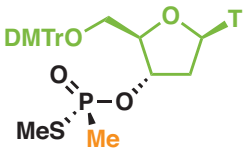
heterogeneous mixture was stirred vigorously for 1 h. The reaction was quenched with 10 mL of water and extracted with EtOAc (3 x 20 mL). The combined organic layers were dried over Na_2SO_4, filtered and concentrated. The residue was purified by silica gel chromatography to afford the desired product.

Nucleobase Nomenclature:

Unless otherwise stated, the following nucleobase abbreviations will be adopted *vide infra*.



Compound (R_p)-1.40



Following **General Procedure H** on 0.5 mmol scale with **1.12b** and 5′-O-(4,4′-dimethoxytrityl) thymidine. Purification by silica gel column chromatography (2% to 5% MeOH in DCM) afforded 275 mg (85%, >20:1 d.r.) of the title compound (R_p)-**1.40**.

Physical State: white foam

R_f = 0.3 (EtOAc)

^{1}H NMR (600 MHz, Acetone-d_6) δ 10.01 (s, 1H), 7.58 (d, J = 1.3 Hz, 1H), 7.53 – 7.47 (m, 2H), 7.41 – 7.31 (m, 6H), 7.30 – 7.23 (m, 1H), 6.95 – 6.89 (m, 4H), 6.38 (dd, J = 8.3, 6.0 Hz, 1H), 5.32 (ddt, J = 10.9, 5.3, 2.5 Hz, 1H), 4.23 (q, J = 3.2 Hz, 1H), 3.79 (s, 6H), 3.49

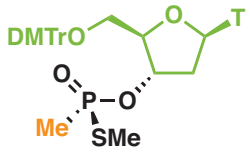
– 3.40 (m, 2H), 2.63 – 2.57 (m, 2H), 2.18 (d, J = 13.1 Hz, 3H), 1.82 (d, J = 15.7 Hz, 3H), 1.50 (d, J = 1.2 Hz, 3H).

^{13}C NMR (151 MHz, Acetone-d_6) δ 164.22, 159.94, 159.93, 151.35, 145.81, 138.60, 136.58, 136.44, 136.24, 131.13, 130.15, 129.86, 129.14, 129.13, 128.90, 128.88, 128.39, 127.95, 127.51, 126.23, 114.18, 113.71, 111.44, 87.82, 85.26, 85.21, 85.19, 76.47, 76.43, 64.33, 55.67, 55.57, 39.94, 39.92, 21.51, 19.11, 18.39, 12.51, 12.49, 12.28.

^{31}P NMR (162 MHz, Acetone-d_6) δ 56.16.

HRMS (ESI-TOF): calc'd for $C_{33}H_{37}N_2O_8PSNa$ [M+Na]+: 675.1906, found: 675.1914.

Compound (S_p)-1.40



Following **General Procedure H** on 1 mmol scale with **1.12a** and 5′-O-(4,4′-dimethoxytrityl) thymidine. Purification by silica gel column chromatography (2% to 5% MeOH in DCM) afforded 574 mg (88%, >20:1 d.r.) of the title compound (S_p)-**1.40**.

Physical State: white foam

R_f = 0.34 (EtOAc)

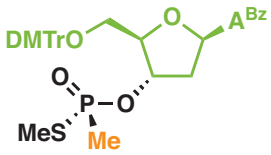
^{1}H NMR (600 MHz, Acetone-d_6) δ 10.13 (s, 1H), 7.61 (d, J = 1.3 Hz, 1H), 7.53 – 7.47 (m, 2H), 7.40 – 7.35 (m, 4H), 7.33 (t, J = 7.8 Hz, 2H), 7.28 – 7.22 (m, 1H), 6.94 – 6.87 (m, 4H), 6.39 (dd, J = 8.3, 6.1 Hz, 1H), 5.38 (ddd, J = 10.0, 5.4, 2.9 Hz, 1H), 4.36 (q, J = 3.0 Hz, 1H), 3.78 (s, 6H), 3.46 (ddd, J = 49.2, 10.6, 3.2 Hz, 2H), 2.63 – 2.53 (m, 2H), 2.31 (d, J = 13.0 Hz, 3H), 1.82 (d, J = 15.7 Hz, 3H), 1.46 (d, J = 1.3 Hz, 3H).

^{13}C NMR (151 MHz, Acetone-d_6) δ 164.19, 159.77, 159.75, 151.29, 145.77, 136.51, 136.34, 136.11, 131.03, 129.02, 128.77, 127.78, 114.05, 111.31, 87.71, 85.72, 85.70, 85.11, 76.74, 76.70, 64.10, 55.54, 39.35, 39.32, 19.09, 18.37, 12.36, 12.34, 12.14.

^{31}P NMR (162 MHz, Acetone-d_6) δ 56.63.

HRMS (ESI-TOF): calc'd for $C_{33}H_{37}N_2O_8PSNa$ [M+Na]+: 675.1906, found: 675.1988.

Compound (R_p)-1.41



Following **General Procedure H** on 1 mmol scale with **1.12b** and N^6-benzoyl-5'-O- (4,4'-dimethoxytrityl)-2'-deoxyadenosine. Purification by silica gel column chromatography (2% to 5% MeOH in DCM) afforded 628 mg (82%, 20:1 d.r.) of the title compound (R_p)-**1.41**.

Physical State: white foam

R_f = 0.23 (DCM/MeOH = 98:2)

^{1}H NMR (600 MHz, Acetone-d_6) δ 9.97 (s, 1H), 8.55 (s, 1H), 8.41 (s, 1H), 8.12 (d, J = 7.6 Hz, 2H), 7.64 (t, J = 7.4 Hz, 1H), 7.56 (dd, J = 8.3, 6.9 Hz, 2H), 7.51 – 7.44 (m, 2H), 7.38 – 7.30 (m, 4H), 7.28 (dd, J = 8.3, 6.6 Hz, 2H), 7.25 – 7.17 (m, 1H), 6.90 – 6.80 (m, 4H), 6.60 (dd, J = 7.7, 6.2 Hz, 1H), 5.48 (ddt, J = 8.8, 5.6, 2.7 Hz, 1H), 4.37 (td, J = 5.3, 2.5 Hz, 1H), 3.77 (d, J = 1.9 Hz, 6H), 3.51 – 3.28 (m, 3H), 2.92 – 2.85 (m, 1H), 2.27 (d, J = 13.0 Hz, 3H), 1.85 (d, J = 15.7 Hz, 3H).

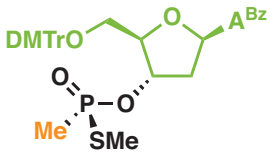
^{13}C NMR (151 MHz, Acetone-d_6) δ 165.93, 159.80, 159.78, 153.02, 152.69, 151.42, 146.06, 143.84, 136.77, 136.75, 135.18, 133.34, 131.11, 131.04, 129.88, 129.54, 129.26,

129.16, 129.10, 128.73, 127.75, 126.46, 126.24, 114.04, 87.40, 85.78, 85.73, 76.98, 76.93, 64.29, 55.65, 38.56, 21.53, 19.21, 18.49, 12.65, 12.63.

^{31}P NMR (162 MHz, Acetone-d_6) δ 55.94.

HRMS (ESI-TOF): calc'd for $C_{40}H_{41}N_5O_7PS$ [M+H]+: 766.2464, found: 766.2474

Compound (S_p)-1.41



Following **General Procedure H** on 1 mmol scale with **1.12a** and N^6-benzoyl-5'-O- (4,4'-dimethoxytrityl)-2'-deoxyadenosine. Purification by silica gel column chromatography (2% to 5% MeOH in DCM) afforded 690 mg (90%, >20:1 d.r.) of the title compound (S_p)-**1.41**.

Physical State: white foam

R_f = 0.38 (EtOAc/acetone = 2:1)

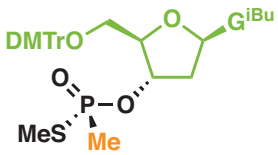
^{1}H NMR (600 MHz, Acetone-d_6) δ 10.06 (s, 1H), 8.54 (s, 1H), 8.41 (s, 1H), 8.11 (d, *J* = 7.7 Hz, 2H), 7.65 – 7.58 (m, 1H), 7.53 (t, *J* = 7.9 Hz, 2H), 7.47 (dd, *J* = 8.4, 1.3 Hz, 2H), 7.34 (d, *J* = 8.6 Hz, 4H), 7.25 (t, *J* = 7.7 Hz, 2H), 7.21 – 7.16 (m, 1H), 6.82 (t, *J* = 9.1 Hz, 4H), 6.59 (dd, *J* = 7.8, 6.2 Hz, 1H), 5.49 (ddd, *J* = 12.3, 5.5, 2.5 Hz, 1H), 4.52 (td, *J* = 5.0, 2.5 Hz, 1H), 3.75 (d, *J* = 2.6 Hz, 6H), 3.51 – 3.41 (m, 2H), 3.41 – 3.33 (m, 1H), 2.77 (ddd, *J* = 14.1, 6.2, 2.7 Hz, 1H), 2.33 (d, *J* = 13.0 Hz, 3H), 1.85 (d, *J* = 15.7 Hz, 3H).

^{13}C NMR (151 MHz, Acetone-d_6) δ 165.90, 159.57, 159.55, 152.86, 152.55, 151.28, 145.98, 143.66, 136.67, 135.01, 133.17, 130.99, 130.93, 129.36, 129.15, 128.99, 128.55, 127.53, 126.26, 113.87, 87.18, 86.17, 86.14, 85.63, 76.94, 76.89, 64.25, 55.50, 38.10, 38.07, 19.21, 18.49, 12.35, 12.33.

^{31}P NMR (162 MHz, Acetone-d_6) δ 56.03.

HRMS (ESI-TOF): calc'd for $C_{40}H_{41}N_5O_7PS$ [M+H]+: 766.2464, found: 766.2480.

Compound (R_p)-1.42



Following **General Procedure H** on 1 mmol scale with **1.12b** and N^2-isobutyryl-5′-O-(4,4′-dimethoxytrityl)-2′-deoxyguanosine. Purification by silica gel column chromatography (2% to 5% MeOH in DCM) afforded 343 mg (46%, >20:1 d.r.) of the title compound (R_p)-**1.42**.

Physical State: white foam

R_f = 0.18 (EtOAc/acetone = 2:1)

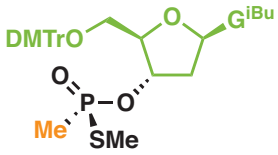
^{1}H NMR (600 MHz, Acetone-d_6) δ 12.02 (s, 1H), 10.52 (s, 1H), 7.96 (s, 1H), 7.47 – 7.42 (m, 2H), 7.35 – 7.17 (m, 7H), 6.89 – 6.82 (m, 4H), 6.33 (dd, J = 7.5, 6.0 Hz, 1H), 5.54 – 5.47 (m, 1H), 4.28 (td, J = 4.6, 3.0 Hz, 1H), 3.81 – 3.78 (m, 6H), 3.43 – 3.37 (m, 1H), 3.12 (ddd, J = 13.6, 7.4, 5.9 Hz, 1H), 2.82 (td, J = 6.3, 5.7, 2.9 Hz, 1H), 2.33 (d, J = 0.7 Hz, 2H), 2.23 (d, J = 13.1 Hz, 3H), 1.90 (d, J = 15.7 Hz, 3H), 1.24 (dd, J = 6.9, 2.7 Hz, 6H).

^{13}C NMR (151 MHz, Acetone-d_6) δ 180.83, 159.80, 159.78, 155.87, 149.35, 149.22, 145.94, 138.12, 136.72, 136.64, 131.10, 131.02, 129.88, 129.16, 129.11, 128.89, 128.40, 127.77, 126.24, 122.35, 114.01, 87.40, 85.40, 85.35, 84.67, 76.55, 76.51, 64.26, 55.63, 39.14, 36.74, 21.53, 19.43, 19.35, 19.21, 18.49, 12.61, 12.58.

^{31}P NMR (162 MHz, Acetone-d_6) δ 57.29.

HRMS (ESI-TOF): calc'd for $C_{37}H_{43}N_5O_8PS$ [M+H]+: 748.2570, found: 748.2568.

Compound (S_p)-1.42



Following **General Procedure H** on 1 mmol scale with **1.12a** and N^2-isobutyryl-5′-O-(4,4′-dimethoxytrityl)-2′-deoxyguanosine. Purification by silica gel column chromatography (2% to 5% MeOH in DCM) afforded 441 mg (59%, >20:1 d.r.) of the title compound (S_p)-**1.42**.

Physical State: white foam

R_f = 0.25 (EtOAc/acetone = 2:1)

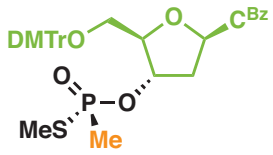
^{1}H NMR (600 MHz, Acetone-d_6) δ 12.04 (s, 1H), 10.84 (s, 1H), 7.92 (s, 1H), 7.41 – 7.37 (m, 2H), 7.30 – 7.15 (m, 7H), 6.79 (dd, J = 9.0, 2.5 Hz, 4H), 6.40 (dd, J = 8.0, 5.8 Hz, 1H), 5.59 (ddt, J = 10.8, 5.6, 2.7 Hz, 1H), 4.62 – 4.55 (m, 1H), 3.75 (d, J = 2.1 Hz, 6H), 3.43 (dd, J = 10.4, 5.0 Hz, 1H), 3.32 (dd, J = 10.4, 3.8 Hz, 1H), 3.06 (ddd, J = 13.9, 8.0, 5.9 Hz, 1H), 2.82 – 2.72 (m, 2H), 2.38 (d, J = 13.4 Hz, 3H), 1.98 (d, J = 15.6 Hz, 3H), 1.15 (dd, J = 34.6, 6.8 Hz, 6H).

^{13}C NMR (151 MHz, Acetone-d_6) δ 180.81, 159.55, 155.79, 149.27, 149.24, 145.80, 137.82, 136.54, 130.88, 130.86, 128.95, 128.54, 127.56, 122.03, 113.83, 87.07, 85.87, 85.85, 84.46, 76.90, 76.85, 64.11, 55.47, 39.14, 39.11, 36.44, 19.35, 19.31, 19.19, 18.60, 12.46, 12.43.

^{31}P NMR (162 MHz, Acetone-d_6) δ 58.75.

HRMS (ESI-TOF): calc'd for $C_{37}H_{43}N_5O_8PS$ [M+H]+: 748.2570, found: 748.2573.

Compound (R_p)-1.43



Following **General Procedure H** on 1 mmol scale with **1.12b** and N^4-benzoyl-5′-*O*- (4,4′-dimethoxytrityl)-2′-deoxycytidine. Purification by silica gel column chromatography (2% to 5% MeOH in DCM) afforded 652 mg (88%, >20:1 d.r.) of the title compound (R_p)-**1.43**.

Physical State: white foam

R_f = 0.21 (DCM/MeOH = 98:2)

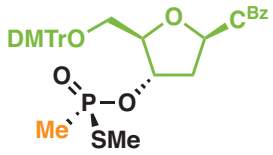
^{1}H NMR (600 MHz, Acetone-d_6) δ 9.79 (s, 1H), 8.25 (d, *J* = 7.4 Hz, 1H), 8.17 (ddt, *J* = 7.5, 6.2, 2.6 Hz, 2H), 7.68 – 7.65 (m, 1H), 7.61 – 7.55 (m, 2H), 7.51 (dt, *J* = 8.8, 2.2 Hz, 2H), 7.42 – 7.34 (m, 5H), 7.31 – 7.17 (m, 3H), 6.96 – 6.92 (m, 4H), 6.29 (t, *J* = 6.4 Hz, 1H), 5.27 (ddt, *J* = 10.4, 7.2, 3.8 Hz, 1H), 4.38 (q, *J* = 3.8 Hz, 1H), 3.82 (s, 6H), 3.54 (d, *J* = 4.0 Hz, 2H), 2.88 (ddd, *J* = 14.4, 6.3, 3.5 Hz, 1H), 2.50 (dt, *J* = 12.3, 5.9 Hz, 1H), 2.22 (d, *J* = 13.0 Hz, 3H), 1.84 (d, *J* = 15.7 Hz, 3H).

^{13}C NMR (151 MHz, Acetone-d_6) δ 159.94, 145.68, 145.16, 138.63, 136.51, 136.45, 133.75, 131.18, 131.16, 129.89, 129.61, 129.24, 129.21, 129.17, 128.90, 127.96, 126.25, 114.20, 87.89, 87.76, 85.94, 85.89, 75.80, 75.76, 63.74, 55.67, 41.31, 21.54, 19.21, 18.48, 12.53, 12.51.

^{31}P NMR (162 MHz, Acetone-d_6) δ 56.15.

HRMS (ESI-TOF): calc'd for $C_{39}H_{41}N_3O_8PS$ [M+H]+: 742.2352, found: 742.2360.

Compound (S_p)-1.43



Following **General Procedure H** on 1 mmol scale with **1.12a** and N^4-benzoyl-5′-*O*- (4,4′-dimethoxytrityl)-2′-deoxycytidine. Purification by silica gel column chromatography (2% to 5% MeOH in DCM) afforded 534 mg (72%, >20:1 d.r.) of the title compound (S_p)-**1.43**.

Physical State: white foam

R_f = 0.33 (EtOAc/acetone = 2:1)

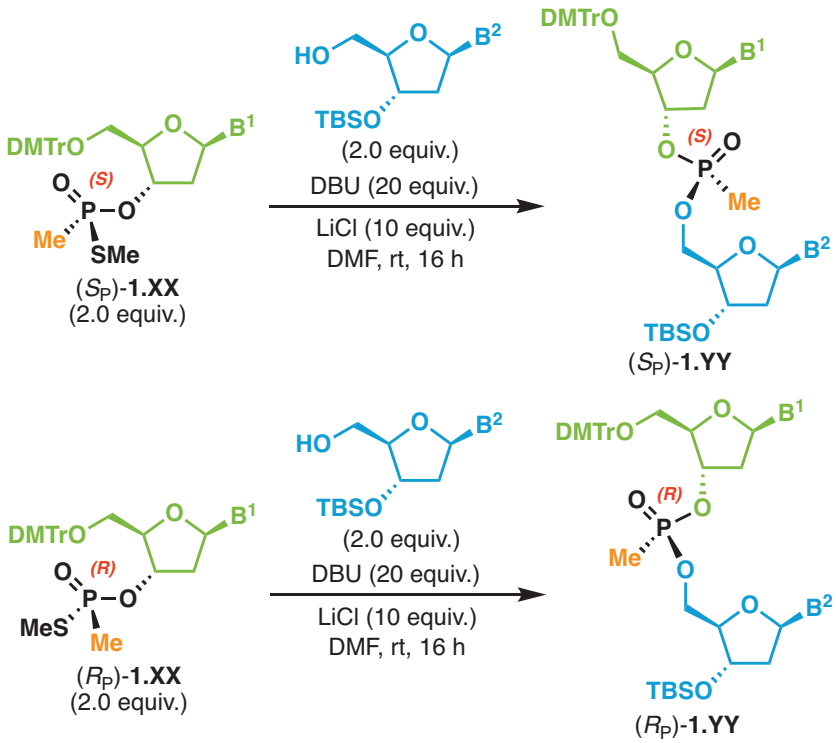
^{1}H NMR (600 MHz, Acetone-d_6) δ 10.07 (s, 1H), 8.25 (d, *J* = 7.5 Hz, 1H), 8.15 (dd, *J* = 8.4, 1.3 Hz, 2H), 7.66 – 7.59 (m, 1H), 7.57 – 7.51 (m, 2H), 7.51 – 7.47 (m, 2H), 7.40 – 7.35 (m, 4H), 7.33 (dd, *J* = 8.4, 7.1 Hz, 2H), 7.29 – 7.21 (m, 2H), 6.93 – 6.88 (m, 4H), 6.25 (t, *J* = 6.4 Hz, 1H), 5.33 (ddt, *J* = 9.7, 6.5, 3.3 Hz, 1H), 4.47 (q, *J* = 3.6 Hz, 1H), 3.78 (d, *J* = 1.3 Hz, 6H), 3.51 (ddd, *J* = 37.0, 10.8, 3.8 Hz, 2H), 2.80 (ddd, *J* = 14.3, 6.2, 3.4 Hz, 1H), 2.50 (dt, *J* = 14.2, 6.5 Hz, 1H), 2.31 (d, *J* = 13.1 Hz, 3H), 1.83 (d, *J* = 15.7 Hz, 3H).

^{13}C NMR (151 MHz, Acetone-d_6) δ 163.77, 159.70, 159.69, 145.60, 145.05, 136.47, 136.33, 134.59, 133.57, 131.05, 130.98, 129.41, 129.13, 129.04, 128.74, 127.72, 114.04, 97.09, 87.70, 86.33, 86.30, 75.76, 75.72, 63.44, 55.51, 40.72, 40.69, 19.10, 18.38, 12.37, 12.35.

^{31}P NMR (162 MHz, Acetone-d_6) δ 56.56.

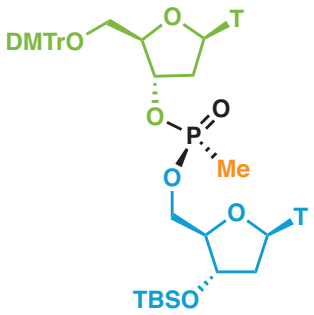
HRMS (ESI-TOF): calc'd for $C_{39}H_{41}N_3O_8PS$ [M+H]+: 742.2352, found: 742.2343.

General Procedure I: MPO Synthesis – Coupling



The coupling step follows a modified version of the reported procedures.[3] A culture tube was charged with LiCl (12.7 mg, 0.3 mmol, 10 equiv.), flame-dried under vacuum, and allowed to cool back to room temperature. The loaded compound (0.06 mmol, 2.0 equiv.) and 3'-TBS-nucleoside (0.03 mmol, 1.0 equiv.) were added to the culture tube, which was then sealed and backfilled with Ar for three times. DMF (0.5 mL) was added, and the reaction was stirred for *circa* 15 min until all LiCl has dissolved. DBU (91.3 mg, 0.09 mL, 0.6 mmol, 20 equiv.) was then introduced *via* syringe, and the resulting mixture was stirred overnight for 16 h. The reaction was quenched with the addition of 1X PBS solution (10 mL) and extracted with DCM (3 x 10 mL). The combined organic layers were washed with water (2 x 10 mL) and brine (10 mL), dried over $MgSO_4$, filtered and concentrated. If needed, residual DMF can be azeotropically removed with toluene. The residue was purified by pTLC to afford the desired compound.

Compound (S_p)-1.44



Following **General Procedure I** on 0.03 mmol scale with (S_p)-**1.40** and **SI-1.31**. Purification by pTLC (EtOAc/DCM:acetone = 5:5:2) afforded 23.9 mg (83%, >20:1 d.r.) of the title compound (S_p)-**1.44**.

Physical State: white amorphous solid

R_f = 0.32 (EtOAc/DCM/acetone = 5:5:2)

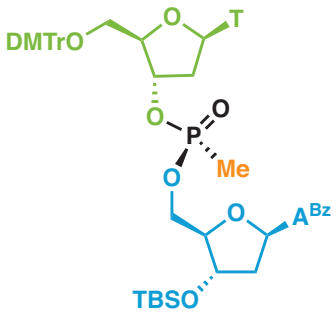
^{1}H NMR (600 MHz, Acetone-d_6) δ 10.12 (s, 1H), 10.06 (s, 1H), 7.58 (q, *J* = 1.2 Hz, 1H), 7.54 (q, *J* = 1.3 Hz, 1H), 7.51 – 7.47 (m, 2H), 7.39 – 7.31 (m, 6H), 7.28 – 7.23 (m, 1H), 6.93 – 6.88 (m, 4H), 6.37 (t, *J* = 7.1 Hz, 1H), 6.30 (dd, *J* = 7.7, 6.1 Hz, 1H), 5.34 (dtd, *J* = 8.3, 4.2, 2.6 Hz, 1H), 4.52 (dt, *J* = 6.1, 3.2 Hz, 1H), 4.27 (q, *J* = 3.0 Hz, 1H), 4.26 – 4.22 (m, 1H), 4.09 (ddd, *J* = 11.4, 7.0, 3.5 Hz, 1H), 4.00 (dt, *J* = 5.2, 3.3 Hz, 1H), 3.79 (s, 6H), 3.48 – 3.39 (m, 2H), 2.61 – 2.55 (m, 2H), 2.31 – 2.16 (m, 2H), 1.81 (d, *J* = 1.3 Hz, 3H), 1.59 (d, *J* = 17.7 Hz, 3H), 1.45 (d, *J* = 1.2 Hz, 3H), 0.91 (s, 9H), 0.12 (d, *J* = 2.0 Hz, 6H).

^{13}C NMR (151 MHz, Acetone-d_6) δ 164.26, 164.19, 159.80, 159.78, 151.29, 151.26, 145.73, 136.55, 136.45, 136.33, 136.17, 131.05, 131.04, 129.05, 128.79, 127.83, 114.07, 111.30, 111.11, 87.74, 86.32, 86.27, 85.74, 85.49, 85.46, 85.07, 76.99, 76.95, 73.06, 65.66, 65.62, 64.22, 55.57, 40.73, 39.57, 39.54, 26.13, 18.49, 12.57, 12.18, 12.13, 11.24, -4.56, -4.65.

^{31}P NMR (162 MHz, Acetone-d_6) δ 33.33.

HRMS (ESI-TOF): calc'd for $C_{48}H_{61}N_4O_{13}PSi$ [M+Na]+: 983.3640, found: 983.3629.

Compound (S_p)-1.45



Following **General Procedure I** on 0.03 mmol scale with (S_p)-**1.40** and **SI-1.32**. Purification by pTLC (EtOAc/DCM/acetone = 5:5:2) afforded 29.3 mg (91%, 20:1 d.r.) of the title compound (S_p)-**1.45**.

Physical State: white amorphous solid

R_f = 0.32 (EtOAc/DC/acetone = 5:5:2)

^{1}H NMR (600 MHz, Acetone-d_6) δ 10.25 (s, 1H), 10.06 (s, 1H), 8.64 (s, 1H), 8.46 (s, 1H), 8.10 (d, *J* = 7.7 Hz, 2H), 7.64 – 7.60 (m, 1H), 7.57 – 7.51 (m, 3H), 7.47 – 7.44 (m, 2H), 7.36 – 7.28 (m, 6H), 7.24 – 7.19 (m, 1H), 6.88 (dd, *J* = 9.0, 1.2 Hz, 4H), 6.56 (t, *J* = 6.5 Hz, 1H), 6.33 (dd, *J* = 8.0, 6.1 Hz, 1H), 5.26 (ddt, *J* = 8.2, 5.5, 2.7 Hz, 1H), 4.88 (dt, *J* = 6.0, 4.0 Hz, 1H), 4.26 – 4.10 (m, 4H), 3.76 (s, 6H), 3.41 – 3.31 (m, 2H), 3.06 (dt, *J* = 13.0, 6.2 Hz, 1H), 2.56 – 2.49 (m, 3H), 1.50 (d, *J* = 17.7 Hz, 3H), 1.42 (d, *J* = 1.2 Hz, 3H), 0.95 (s, 9H), 0.18 (s, 6H).

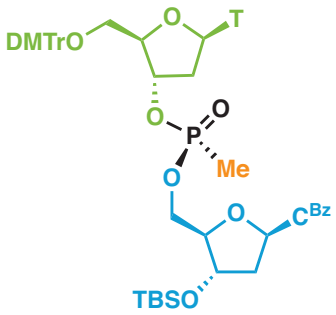
^{13}C NMR (151 MHz, Acetone-d_6) δ 165.88, 164.25, 159.75, 159.73, 152.85, 152.63, 151.33, 151.23, 145.74, 143.57, 136.45, 136.31, 136.22, 135.01, 133.18, 131.03, 131.01, 129.37, 129.21, 129.01, 128.77, 127.77, 126.04, 114.05, 111.26, 87.69, 86.64, 86.60, 85.43,

85.40, 85.36, 85.09, 76.91, 76.87, 73.07, 65.14, 65.10, 64.14, 55.55, 40.44, 39.57, 39.55, 26.18, 18.55, 12.11, 11.16, -4.51, -4.61.

^{31}P NMR (162 MHz, Acetone-d_6) δ 32.99.

HRMS (ESI-TOF): calc'd for $C_{55}H_{64}N_7O_{12}PSi$ [M+H]+: 1074.4198, found: 1074.4181.

Compound (S_p)-1.46



Following **General Procedure I** on 0.03 mmol scale with (S_p)-**1.40** and **SI-1.33**. Purification by pTLC (EtOAc/acetone = 15:1) afforded 25.5 mg (81%, >20:1 d.r.) of the title compound (S_p)-**1.46**.

Physical State: white amorphous solid

R_f = 0.50 (EtOAc/acetone = 10:1)

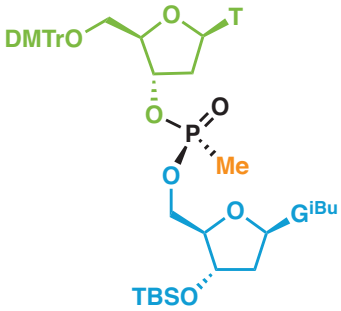
^{1}H NMR (600 MHz, Acetone-d_6) δ 10.09 (s, 1H), 9.95 (s, 1H), 8.22 (d, *J* = 7.6 Hz, 1H), 8.17 – 8.13 (m, 2H), 7.67 – 7.62 (m, 1H), 7.58 (d, *J* = 1.3 Hz, 1H), 7.55 (t, *J* = 7.8 Hz, 2H), 7.50 – 7.46 (m, 2H), 7.39 – 7.29 (m, 7H), 7.26 – 7.21 (m, 1H), 6.89 (d, *J* = 9.0 Hz, 4H), 6.37 (t, *J* = 7.0 Hz, 1H), 6.23 (t, *J* = 6.3 Hz, 1H), 5.35 (dtd, *J* = 8.1, 4.3, 2.5 Hz, 1H), 4.54 (dt, *J* = 6.1, 4.0 Hz, 1H), 4.35 – 4.28 (m, 2H), 4.17 (ddd, *J* = 11.4, 6.8, 3.5 Hz, 1H), 4.12 (q, *J* = 4.1 Hz, 1H), 3.77 (s, 6H), 3.45 (ddd, *J* = 31.5, 10.6, 3.3 Hz, 2H), 2.60 (dd, *J* = 7.1, 4.4 Hz, 2H), 2.46 (ddd, *J* = 13.6, 6.3, 4.1 Hz, 1H), 2.24 (dt, *J* = 13.5, 6.3 Hz, 1H), 1.61 (d, *J* = 17.7 Hz, 3H), 1.45 (d, *J* = 1.3 Hz, 3H), 0.91 (s, 9H), 0.12 (d, *J* = 1.6 Hz, 6H).

^{13}C NMR (151 MHz, Acetone-d_6) δ 164.19, 163.70, 159.77, 159.76, 151.27, 145.73, 145.27, 136.46, 136.32, 136.25, 134.62, 133.59, 131.04, 129.44, 129.16, 129.04, 128.78, 127.81, 114.06, 114.05, 111.24, 97.15, 87.85, 87.72, 86.91, 86.87, 85.48, 85.45, 85.20, 77.05, 77.01, 72.59, 65.27, 65.23, 64.24, 55.55, 42.10, 39.57, 39.55, 26.14, 18.49, 12.22, 12.15, 11.28, -4.53, -4.68.

^{31}P NMR (162 MHz, Acetone-d_6) δ 33.43.

HRMS (ESI-TOF): calc'd for $C_{54}H_{64}N_5O_{13}PSi$ [M+H]+: 1050.4086, found: 1050.4083.

Compound (S_p)-1.47



Following **General Procedure I** on 0.03 mmol scale with (S_p)-**1.40** and **SI-1.34**. Purification by pTLC (EtOAc/acetone = 10:1) afforded 25.0 mg (80%, >20:1 d.r.) of the title compound (S_p)-**1.47**.

Physical State: white amorphous solid

R_f = 0.37 (EtOAc/acetone = 10:1)

^{1}H NMR (600 MHz, Acetone-d_6) δ 12.06 (s, 1H), 11.00 (s, 1H), 10.06 (s, 1H), 7.97 (s, 1H), 7.58 (d, J = 1.3 Hz, 1H), 7.48 (dd, J = 8.4, 1.2 Hz, 2H), 7.38 – 7.29 (m, 6H), 7.26 – 7.20 (m, 1H), 6.91 – 6.86 (m, 4H), 6.38 (dd, J = 7.7, 6.5 Hz, 1H), 6.33 (dd, J = 8.9, 5.7 Hz, 1H), 5.36 (ddt, J = 7.8, 5.8, 3.1 Hz, 1H), 4.63 (dt, J = 5.2, 1.8 Hz, 1H), 4.45 (ddd, J = 11.0, 7.0, 4.9 Hz, 1H), 4.37 – 4.29 (m, 2H), 4.18 (td, J = 5.4, 5.0, 1.6 Hz, 1H), 3.77 (d, J = 1.7

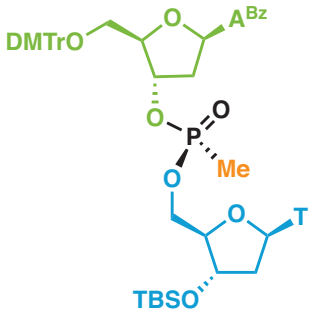
Hz, 6H), 3.45 (qd, *J* = 10.6, 3.4 Hz, 2H), 2.99 – 2.89 (m, 1H), 2.84 – 2.80 (m, 1H), 2.63 – 2.58 (m, 2H), 2.27 (ddd, *J* = 13.3, 5.8, 1.9 Hz, 1H), 1.62 (d, *J* = 17.6 Hz, 3H), 1.45 (d, *J* = 1.1 Hz, 3H), 1.16 (dd, *J* = 16.4, 6.9 Hz, 6H), 0.92 (s, 9H), 0.13 (d, *J* = 3.7 Hz, 6H).

^{13}C NMR (151 MHz, Acetone-d_6) δ 181.00, 164.13, 159.80, 159.78, 155.81, 151.25, 149.07, 148.92, 145.67, 139.55, 136.40, 136.30, 136.22, 131.02, 131.00, 129.04, 128.78, 127.85, 123.14, 114.05, 111.28, 87.74, 87.07, 87.02, 86.90, 85.48, 85.45, 85.25, 77.51, 77.48, 73.92, 66.07, 66.03, 64.26, 55.56, 39.92, 39.47, 39.44, 36.41, 26.17, 19.40, 19.23, 18.56, 12.14, 11.71, 10.78, -4.54, -4.61.

^{31}P NMR (162 MHz, Acetone-d_6) δ 34.75.

HRMS (ESI-TOF): calc'd for $C_{52}H_{66}N_7O_{13}PSi$ [M+Na]+: 1078.4123, found: 1078.4097.

Compound (S_p)-1.48



Following **General Procedure I** on 0.03 mmol scale with (S_p)-**1.41** and **SI-1.31**. Purification by pTLC (EtOAc/acetone = 7:1) afforded 24.2 mg (75%, >20:1 d.r.) of the title compound (S_p)-**1.48**.

Physical State: white amorphous solid

R_f = 0.32 (EtOAc/acetone = 7:1)

^{1}H NMR (600 MHz, Acetone-d_6) δ 10.28 (s, 1H), 10.08 (s, 1H), 8.55 (s, 1H), 8.41 (s, 1H), 8.12 (d, *J* = 7.6 Hz, 2H), 7.63 (t, *J* = 7.4 Hz, 1H), 7.59 (d, *J* = 1.3 Hz, 1H), 7.54 (t, *J* = 7.8

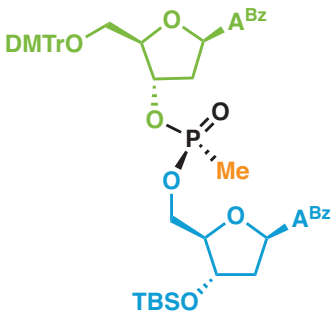
Hz, 2H), 7.45 (dd, *J* = 8.5, 1.3 Hz, 2H), 7.35 – 7.30 (m, 4H), 7.26 (t, *J* = 7.6 Hz, 2H), 7.22 – 7.16 (m, 1H), 6.86 – 6.81 (m, 4H), 6.58 (dd, *J* = 7.7, 6.2 Hz, 1H), 6.34 (dd, *J* = 7.7, 6.1 Hz, 1H), 5.47 (td, *J* = 5.7, 2.9 Hz, 1H), 4.56 (dt, *J* = 6.1, 3.2 Hz, 1H), 4.42 (td, *J* = 5.1, 2.6 Hz, 1H), 4.32 (ddd, *J* = 11.4, 7.7, 5.2 Hz, 1H), 4.19 (ddd, *J* = 11.4, 7.1, 3.5 Hz, 1H), 4.05 (dt, *J* = 5.5, 3.2 Hz, 1H), 3.76 (d, *J* = 2.6 Hz, 6H), 3.51 – 3.41 (m, 2H), 3.37 (ddd, *J* = 13.9, 7.8, 6.1 Hz, 1H), 2.81 (ddd, *J* = 14.1, 6.2, 2.8 Hz, 1H), 2.34 – 2.21 (m, 2H), 1.83 (d, *J* = 1.2 Hz, 3H), 1.63 (d, *J* = 17.7 Hz, 3H), 0.91 (s, 9H), 0.13 (s, 6H).

^{13}C NMR (151 MHz, Acetone-d_6) δ 164.56, 163.02, 158.28, 158.26, 151.54, 151.22, 150.01, 144.58, 142.37, 135.30, 135.26, 133.68, 131.86, 129.65, 129.58, 128.03, 127.87, 127.66, 127.26, 126.27, 124.90, 112.56, 109.82, 85.93, 85.05, 85.01, 84.61, 84.58, 84.42, 84.27, 75.95, 75.91, 71.72, 64.36, 64.32, 62.93, 54.18, 39.46, 36.94, 36.91, 24.81, 17.16, 11.27, 10.92, 9.97, -5.88, -5.96.

^{31}P NMR (162 MHz, Acetone-d_6) δ 33.03.

HRMS (ESI-TOF): calc'd for $C_{55}H_{64}N_7O_{12}PSi$ [M+H]+: 1074.4198, found: 1074.4185.

Compound (S_p)-1.49



Following **General Procedure I** on 0.03 mmol scale with (S_p)-**1.41** and **SI-1.32**. Purification by pTLC (10% MeOH in EtOAc) afforded 27.5 mg (77%, >20:1 d.r.) of the title compound (S_p)-**1.49**.

Physical State: white amorphous solid

R_f = 0.28 (10% MeOH in EtOAc)

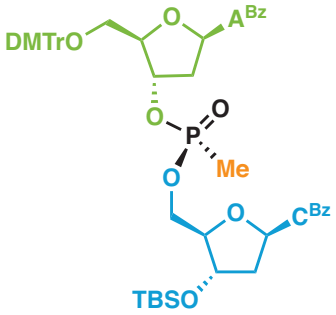
^{1}H NMR (600 MHz, Acetone-d_6) δ 9.99 (d, *J* = 12.5 Hz, 2H), 8.66 (s, 1H), 8.52 (d, *J* = 7.4 Hz, 2H), 8.42 (s, 1H), 8.13 (t, *J* = 6.2 Hz, 4H), 7.65 (dt, *J* = 15.2, 7.4 Hz, 2H), 7.56 (dt, *J* = 15.6, 7.6 Hz, 4H), 7.47 – 7.42 (m, 2H), 7.34 – 7.30 (m, 4H), 7.26 (dd, *J* = 8.5, 7.0 Hz, 2H), 7.21 – 7.16 (m, 1H), 6.85 – 6.80 (m, 4H), 6.61 (t, *J* = 6.5 Hz, 1H), 6.55 (dd, *J* = 7.7, 6.2 Hz, 1H), 5.40 (ddt, *J* = 8.4, 5.8, 2.7 Hz, 1H), 4.93 (dt, *J* = 6.0, 4.0 Hz, 1H), 4.35 (td, *J* = 5.1, 2.5 Hz, 1H), 4.31 (dd, *J* = 7.2, 4.4 Hz, 2H), 4.20 (q, *J* = 4.2 Hz, 1H), 3.76 (d, *J* = 2.0 Hz, 6H), 3.46 – 3.36 (m, 2H), 3.31 (dt, *J* = 14.2, 7.6 Hz, 1H), 3.09 (dt, *J* = 12.9, 6.2 Hz, 1H), 2.76 (ddd, *J* = 14.0, 6.2, 2.8 Hz, 1H), 2.58 (ddd, *J* = 13.4, 6.5, 4.3 Hz, 1H), 1.55 (d, *J* = 17.7 Hz, 3H), 0.97 (s, 9H), 0.21 (s, 6H).

^{13}C NMR (151 MHz, Acetone-d_6) δ 165.92, 165.85, 159.60, 159.58, 152.91, 152.82, 152.65, 152.51, 151.20, 145.95, 143.83, 143.55, 136.66, 136.65, 135.07, 134.99, 133.22, 133.19, 130.98, 130.92, 129.41, 129.39, 129.20, 129.17, 128.99, 128.58, 127.56, 126.48, 126.29, 126.19, 113.89, 87.21, 86.72, 86.68, 85.88, 85.85, 85.64, 85.42, 77.27, 77.24, 73.09, 65.14, 65.10, 64.24, 55.51, 40.64, 38.14, 26.20, 18.57, 12.11, 11.16, -4.50, -4.58.

^{31}P NMR (162 MHz, Acetone-d_6) δ 32.60.

HRMS (ESI-TOF): calc'd for $C_{62}H_{67}N_{10}O_{11}PSi$ [M+H]+: 1187.4576, found: 1187.4561.

Compound (S_p)-1.50



Following **General Procedure I** on 0.03 mmol scale with (S_p)-**1.41** and **SI-1.33**. Purification by pTLC (EtOAc/acetone = 7:1) afforded 26.8 mg (77%, >20:1 d.r.) of the title compound (S_p)-**1.50**.

Physical State: white amorphous solid

R_f = 0.50 (EtOAc/acetone = 5:1)

^{1}H NMR (600 MHz, Acetone-d_6) δ 10.06 (s, 2H), 8.55 (s, 1H), 8.46 (s, 1H), 8.31 (d, *J* = 7.5 Hz, 1H), 8.16 – 8.10 (m, 4H), 7.67 – 7.60 (m, 2H), 7.55 (q, *J* = 8.6, 7.7 Hz, 4H), 7.47 (d, *J* = 7.3 Hz, 2H), 7.41 (s, 1H), 7.35 – 7.31 (m, 4H), 7.26 (t, *J* = 7.7 Hz, 2H), 7.22 – 7.17 (m, 1H), 6.86 – 6.80 (m, 4H), 6.62 (dd, *J* = 7.6, 6.2 Hz, 1H), 6.28 (t, *J* = 6.3 Hz, 1H), 5.50 (ddt, *J* = 8.5, 5.8, 2.6 Hz, 1H), 4.60 (dt, *J* = 6.2, 4.0 Hz, 1H), 4.46 (dt, *J* = 8.0, 3.9 Hz, 1H), 4.40 (ddd, *J* = 11.8, 7.3, 4.8 Hz, 1H), 4.31 (ddt, *J* = 10.3, 6.9, 3.3 Hz, 1H), 4.18 (q, *J* = 4.0 Hz, 1H), 3.76 (dd, *J* = 2.4, 1.5 Hz, 6H), 3.53 – 3.44 (m, 2H), 3.41 (dt, *J* = 13.7, 6.7 Hz, 1H), 2.85 (ddd, *J* = 14.0, 6.2, 2.8 Hz, 1H), 2.50 (ddt, *J* = 11.8, 5.7, 2.8 Hz, 1H), 2.29 (dt, *J* = 13.2, 6.3 Hz, 1H), 1.67 (d, *J* = 17.7 Hz, 3H), 0.93 (s, 9H), 0.15 (s, 6H).

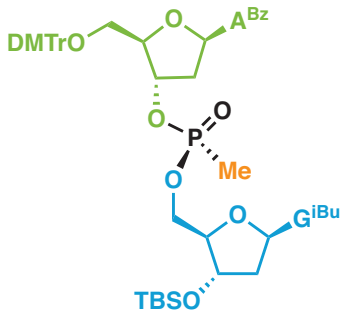
^{13}C NMR (151 MHz, Acetone-d_6) δ 166.11, 163.70, 159.60, 159.58, 152.81, 152.56, 151.17, 145.92, 145.34, 143.93, 136.64, 136.61, 134.96, 134.56, 133.60, 133.27, 130.98, 130.91, 129.44, 129.39, 129.18, 129.14, 128.99, 128.58, 127.59, 126.14, 113.89, 97.10,

87.94, 87.24, 86.98, 86.94, 85.97, 85.94, 85.70, 77.37, 77.33, 72.57, 65.30, 65.26, 64.29, 55.51, 42.21, 38.24, 38.22, 26.15, 18.49, 12.31, 11.36, -4.52, -4.65.

^{31}P NMR (162 MHz, Acetone-d_6) δ 33.17.

HRMS (ESI-TOF): calc'd for $C_{61}H_{67}N_8O_{12}PSi$ [M+H]+: 1163.4464, found: 1163.4448.

Compound (S_p)-1.51



Following **General Procedure I** on 0.03 mmol scale with (S_p)-**1.41** and **SI-1.34**. Purification by pTLC (10% MeOH in EtOAc) afforded 20.0 mg (60%, >20:1 d.r.) of the title compound (S_p)-**1.51**.

Physical State: white amorphous solid

R_f = 0.25 (EtOAc:acetone = 5:1)

^{1}H NMR (600 MHz, Acetone-d_6) δ 12.08 (s, 1H), 11.07 (s, 1H), 10.00 (s, 1H), 8.54 (s, 1H), 8.43 (s, 1H), 8.13 (d, J = 7.6 Hz, 2H), 8.01 (s, 1H), 7.67 – 7.61 (m, 1H), 7.55 (t, J = 7.7 Hz, 2H), 7.47 – 7.40 (m, 2H), 7.34 – 7.27 (m, 4H), 7.23 (dd, J = 8.3, 6.8 Hz, 2H), 7.20 – 7.15 (m, 1H), 6.80 (t, J = 8.7 Hz, 4H), 6.62 (dd, J = 7.6, 6.2 Hz, 1H), 6.36 (dd, J = 8.8, 5.7 Hz, 1H), 5.50 (ddt, J = 8.4, 5.8, 2.7 Hz, 1H), 4.71 – 4.64 (m, 1H), 4.53 (ddd, J = 11.6, 7.1, 4.7 Hz, 1H), 4.47 (td, J = 5.1, 2.5 Hz, 1H), 4.40 (dt, J = 11.1, 6.1 Hz, 1H), 4.22 (t, J = 4.5 Hz, 1H), 3.74 (d, J = 2.7 Hz, 6H), 3.50 – 3.38 (m, 3H), 2.99 (ddd, J = 13.7, 8.8, 5.2 Hz,

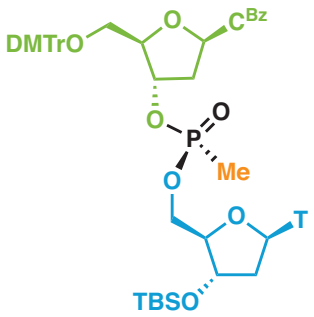
1H), 2.85 – 2.82 (m, 2H), 2.31 (ddd, J = 13.2, 5.8, 1.9 Hz, 1H), 1.65 (d, J = 17.6 Hz, 3H), 1.15 (dd, J = 24.8, 6.8 Hz, 6H), 0.93 (s, 9H), 0.15 (d, J = 1.4 Hz, 6H).

^{13}C NMR (151 MHz, Acetone-d_6) δ 181.01, 165.88, 159.61, 159.58, 155.87, 152.84, 152.51, 151.32, 149.11, 148.97, 145.85, 143.87, 139.57, 136.61, 136.57, 135.03, 133.23, 130.95, 130.88, 129.41, 129.17, 128.99, 128.56, 127.61, 126.31, 123.15, 113.86, 87.20, 87.14, 87.10, 86.92, 86.00, 85.97, 85.71, 77.72, 77.68, 73.91, 66.12, 66.08, 64.35, 55.51, 40.06, 38.10, 38.07, 36.41, 26.18, 19.39, 19.23, 18.56, 11.84, 10.91, -4.50, -4.57.

^{31}P NMR (162 MHz, Acetone-d_6) δ 34.58.

HRMS (ESI-TOF): calc'd for $C_{59}H_{69}N_{10}O_{12}PSi$ [M+H]+: 1169.4682, found: 1169.4675.

Compound (S_p)-1.52



Following **General Procedure I** on 0.03 mmol scale with (S_p)-**1.43** and **SI-1.31**. Purification by pTLC (EtOAc/DCM:acetone = 5:5:3) afforded 14.2 mg (46%, >20:1 d.r.) of the title compound (S_p)-**1.52**.

Physical State: white amorphous solid

R_f = 0.33 (EtOAc/DCM:acetone = 5:5:3)

^{1}H NMR (600 MHz, Acetone-d_6) δ 9.98 (s, 1H), 9.90 (s, 1H), 8.24 (d, J = 7.5 Hz, 1H), 8.18 – 8.12 (m, 2H), 7.68 – 7.63 (m, 1H), 7.58 – 7.53 (m, 3H), 7.50 – 7.47 (m, 2H), 7.39 – 7.32 (m, 6H), 7.28 – 7.19 (m, 2H), 6.95 – 6.88 (m, 4H), 6.31 (dd, J = 7.7, 6.1 Hz, 1H), 6.23

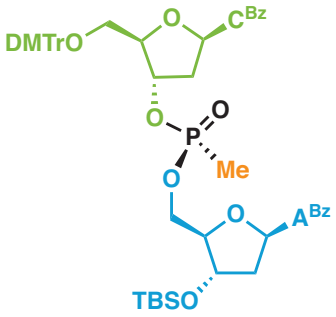
(t, J = 6.2 Hz, 1H), 5.27 (ddt, J = 7.7, 6.2, 3.9 Hz, 1H), 4.54 (dt, J = 6.1, 3.1 Hz, 1H), 4.37 (q, J = 3.8 Hz, 1H), 4.26 (ddd, J = 11.4, 7.7, 5.2 Hz, 1H), 4.10 (ddd, J = 11.4, 7.0, 3.6 Hz, 1H), 4.02 (dt, J = 5.2, 3.3 Hz, 1H), 3.80 (d, J = 1.5 Hz, 6H), 3.55 – 3.46 (m, 2H), 2.82 – 2.77 (m, 1H), 2.52 (dt, J = 14.2, 6.3 Hz, 1H), 2.31 – 2.19 (m, 2H), 1.82 (d, J = 1.2 Hz, 3H), 1.61 (d, J = 17.7 Hz, 3H), 0.91 (s, 9H), 0.12 (d, J = 1.8 Hz, 6H).

^{13}C NMR (151 MHz, Acetone-d_6) δ 164.20, 163.77, 159.77, 151.25, 145.56, 145.05, 136.53, 136.40, 136.34, 134.60, 133.62, 131.05, 131.02, 129.47, 129.13, 129.09, 128.80, 127.81, 114.09, 111.10, 97.08, 87.79, 87.60, 86.33, 86.29, 86.00, 85.97, 85.76, 75.89, 75.85, 73.08, 65.57, 65.53, 63.41, 55.55, 40.85, 40.83, 40.75, 26.14, 18.50, 12.60, 12.20, 11.25, -4.55, -4.64.

^{31}P NMR (162 MHz, Acetone-d_6) δ 33.25.

HRMS (ESI-TOF): calc'd for $C_{54}H_{64}N_5O_{13}PSi$ [M+Na]+: 1072.3905, found: 1072.3926.

Compound (S_p)-1.53



Following **General Procedure I** on 0.03 mmol scale with (S_p)-**1.43** and **SI-1.32**. Purification by pTLC (EtOAc/DCM/acetone = 10:10:7) afforded 27.6 mg (79%, >20:1 d.r.) of the title compound (S_p)-**1.53**.

Physical State: white amorphous solid

R_f = 0.34 (EtOAc/DCM/acetone = 5:5:3)

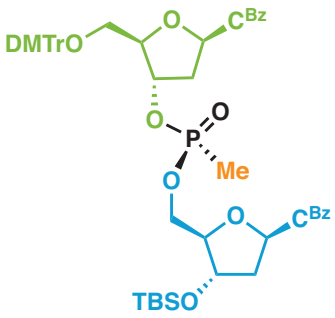
^{1}H NMR (600 MHz, Acetone-d_6) δ 10.03 (s, 2H), 8.64 (s, 1H), 8.47 (s, 1H), 8.22 (d, J = 7.5 Hz, 1H), 8.13 (ddd, J = 8.7, 4.0, 2.6 Hz, 4H), 7.65 – 7.59 (m, 2H), 7.56 – 7.50 (m, 4H), 7.46 – 7.41 (m, 2H), 7.34 – 7.28 (m, 6H), 7.27 – 7.15 (m, 2H), 6.90 – 6.85 (m, 4H), 6.56 (t, J = 6.5 Hz, 1H), 6.18 (t, J = 6.1 Hz, 1H), 5.21 (ddt, J = 8.0, 6.3, 4.2 Hz, 1H), 4.90 (dt, J = 5.9, 4.0 Hz, 1H), 4.28 – 4.17 (m, 3H), 4.14 (q, J = 4.3 Hz, 1H), 3.77 (d, J = 1.7 Hz, 6H), 3.42 (dd, J = 3.6, 1.2 Hz, 2H), 3.06 (dt, J = 13.5, 6.2 Hz, 1H), 2.73 (ddd, J = 14.1, 6.3, 4.4 Hz, 1H), 2.57 – 2.46 (m, 2H), 1.55 (d, J = 17.8 Hz, 3H), 0.95 (s, 9H), 0.17 (s, 6H).

^{13}C NMR (151 MHz, Acetone-d_6) δ 165.90, 163.82, 159.69, 152.86, 152.61, 151.24, 145.50, 145.05, 143.58, 136.40, 136.29, 135.06, 134.59, 133.55, 133.16, 130.99, 130.95, 129.39, 129.22, 129.19, 129.08, 129.04, 128.76, 127.72, 126.18, 114.06, 97.01, 87.71, 87.53, 86.63, 86.59, 85.77, 85.74, 85.34, 75.55, 75.51, 73.10, 65.04, 65.00, 63.17, 55.53, 40.73, 40.71, 40.45, 26.19, 18.56, 12.15, 11.21, -4.51, -4.60.

^{31}P NMR (162 MHz, Acetone-d_6) δ 33.13.

HRMS (ESI-TOF): calc'd for $C_{61}H_{67}N_8O_{12}PSi$ [M+H]+: 1163.4464, found: 1163.4436.

Compound (S_p)-1.54



Following **General Procedure I** on 0.03 mmol scale with (S_p)-**1.43** and **SI-1.33**. Purification by pTLC (DCM/acetone = 2:1) afforded 22.4 mg (66%, >20:1 d.r.) of the title compound (S_p)-**1.54**.

Physical State: white amorphous solid

R_f = 0.31 (DCM/acetone = 2:1)

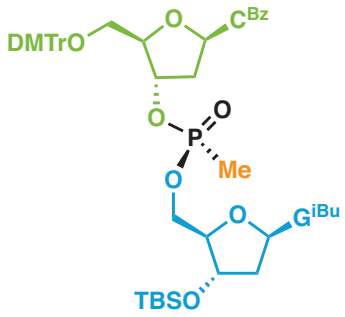
^{1}H NMR (600 MHz, Acetone-d_6) δ 10.02 (s, 2H), 8.24 (dd, *J* = 24.8, 7.5 Hz, 2H), 8.15 (ddd, *J* = 8.6, 2.4, 1.3 Hz, 4H), 7.65 – 7.61 (m, 2H), 7.53 (dd, *J* = 8.2, 7.4 Hz, 4H), 7.47 (dd, *J* = 8.5, 1.3 Hz, 2H), 7.38 – 7.31 (m, 7H), 7.25 – 7.20 (m, 2H), 6.89 (dd, *J* = 9.0, 1.9 Hz, 4H), 6.24 (td, *J* = 6.3, 1.8 Hz, 2H), 5.29 (ddt, *J* = 8.0, 6.3, 4.2 Hz, 1H), 4.57 (dt, *J* = 6.1, 4.0 Hz, 1H), 4.39 (q, *J* = 3.8 Hz, 1H), 4.34 (ddd, *J* = 11.8, 7.3, 4.8 Hz, 1H), 4.20 (ddd, *J* = 11.5, 6.8, 3.6 Hz, 1H), 4.14 (q, *J* = 4.0 Hz, 1H), 3.78 (d, *J* = 1.0 Hz, 6H), 3.51 (t, *J* = 3.4 Hz, 2H), 2.81 (ddd, *J* = 14.1, 6.3, 4.3 Hz, 1H), 2.57 (dt, *J* = 14.2, 6.1 Hz, 1H), 2.47 (ddd, *J* = 13.5, 6.3, 4.1 Hz, 1H), 2.27 (dt, *J* = 13.6, 6.3 Hz, 1H), 1.66 (d, *J* = 17.7 Hz, 3H), 0.91 (s, 9H), 0.12 (s, 6H).

^{13}C NMR (151 MHz, Acetone-d_6) δ 163.84, 163.72, 159.72, 159.70, 145.50, 145.33, 145.14, 136.40, 136.30, 134.56, 133.58, 131.01, 130.98, 129.44, 129.41, 129.16, 129.06, 128.78, 127.78, 114.07, 114.06, 97.10, 87.91, 87.74, 87.68, 86.89, 86.84, 85.91, 85.87, 75.86, 75.82, 72.58, 65.20, 65.16, 63.36, 55.54, 42.09, 40.78, 40.75, 26.14, 18.48, 12.23, 11.29, -4.54, -4.67.

^{31}P NMR (162 MHz, Acetone-d_6) δ 33.53.

HRMS (ESI-TOF): calc'd for $C_{60}H_{67}N_6O_{13}PSi$ [M+H]+: 1139.4351, found: 1139.4324.

Compound (S_p)-1.55



Following **General Procedure I** on 0.03 mmol scale with (S_p)-**1.43** and **SI-1.34**. Purification by pTLC (10% MeOH in EtOAc) afforded 20.3 mg (59%, >20:1 d.r.) of the title compound (S_p)-**1.55**.

Physical State: white amorphous solid

R_f = 0.33 (10% MeOH in EtOAc)

^{1}H NMR (600 MHz, Acetone-d_6) δ 12.08 (s, 1H), 11.07 (s, 1H), 8.26 (d, *J* = 7.5 Hz, 1H), 8.20 – 8.14 (m, 2H), 7.98 (s, 1H), 7.70 – 7.66 (m, 1H), 7.59 (t, *J* = 7.8 Hz, 2H), 7.52 – 7.47 (m, 2H), 7.40 – 7.32 (m, 6H), 7.28 – 7.23 (m, 1H), 6.92 (dd, *J* = 9.0, 2.8 Hz, 4H), 6.36 (dd, *J* = 9.0, 5.7 Hz, 1H), 6.27 (t, *J* = 6.3 Hz, 1H), 5.30 (tt, *J* = 7.0, 3.6 Hz, 1H), 4.67 (d, *J* = 5.2 Hz, 1H), 4.51 – 4.43 (m, 2H), 4.40 (dt, *J* = 11.2, 6.2 Hz, 1H), 4.21 (t, *J* = 5.0 Hz, 1H), 3.79 (d, *J* = 0.8 Hz, 6H), 3.53 (qd, *J* = 10.7, 3.8 Hz, 2H), 3.00 (ddd, *J* = 13.7, 9.0, 5.2 Hz, 1H), 2.91 – 2.84 (m, 2H), 2.54 (dt, *J* = 21.2, 6.9 Hz, 2H), 2.35 – 2.28 (m, 2H), 1.64 (d, *J* = 17.6 Hz, 3H), 1.20 (d, *J* = 6.8 Hz, 3H), 1.16 (d, *J* = 6.9 Hz, 3H), 0.94 (s, 9H), 0.15 (d, *J* = 5.4 Hz, 6H).

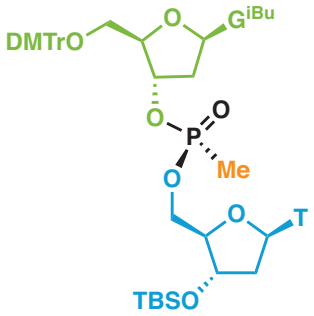
^{13}C NMR (151 MHz, Acetone-d_6) δ 180.96, 159.78, 155.87, 149.12, 148.93, 145.52, 139.61, 136.39, 136.29, 133.67, 131.04, 130.99, 129.51, 129.40, 129.09, 128.79, 127.84, 126.50, 123.23, 114.08, 108.73, 87.79, 87.15, 87.10, 87.02, 86.09, 76.39, 73.95, 66.21,

63.49, 62.77, 55.54, 40.81, 39.99, 36.44, 26.17, 19.41, 19.25, 18.57, 11.68, 10.75, -4.53, -4.60.

^{31}P NMR (162 MHz, Acetone-d_6) δ 34.67.

HRMS (ESI-TOF): calc'd for $C_{58}H_{69}N_8O_{13}PSi$ [M+H]+: 1145.4569, found: 1145.4559.

Compound (S_p)-1.56



Following **General Procedure I** on 0.03 mmol scale with (S_p)-**1.42** and **SI-1.31**. Purification by pTLC (EtOAc/DCM/acetone = 5:5:3) afforded 13.3 mg (42%, >20:1 d.r.) of the title compound (S_p)-**1.56**.

Physical State: white amorphous solid

R_f = 0.19 (EtOAc/DCM/acetone = 5:5:3)

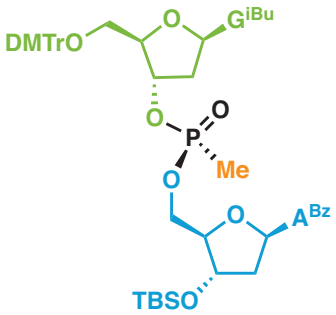
^{1}H NMR (600 MHz, Acetone-d_6) δ 12.03 (s, 1H), 10.51 (s, 1H), 10.17 (s, 1H), 7.92 (s, 1H), 7.59 (d, *J* = 1.3 Hz, 1H), 7.44 – 7.41 (m, 2H), 7.32 – 7.29 (m, 4H), 7.28 – 7.25 (m, 2H), 7.23 – 7.18 (m, 1H), 6.86 – 6.80 (m, 4H), 6.34 (t, *J* = 6.8 Hz, 1H), 6.25 (dd, *J* = 7.9, 5.8 Hz, 1H), 5.50 (ddt, *J* = 8.4, 5.6, 2.8 Hz, 1H), 4.58 (dt, *J* = 6.3, 3.8 Hz, 1H), 4.33 (td, *J* = 4.7, 2.7 Hz, 1H), 4.24 – 4.15 (m, 2H), 3.98 (qd, *J* = 3.6, 1.1 Hz, 1H), 3.77 (s, 6H), 3.38 (ddd, *J* = 47.0, 10.3, 4.7 Hz, 2H), 3.03 (ddd, *J* = 13.9, 8.0, 5.9 Hz, 1H), 2.89 (p, *J* = 6.9 Hz, 1H), 2.70 (ddd, *J* = 13.9, 5.9, 2.9 Hz, 1H), 2.37 – 2.22 (m, 2H), 1.92 (d, *J* = 1.2 Hz, 3H), 1.66 (d, *J* = 17.7 Hz, 3H), 1.23 (dd, *J* = 6.9, 0.8 Hz, 6H), 0.91 (s, 9H), 0.12 (s, 6H).

^{13}C NMR (151 MHz, Acetone-d_6) δ 179.49, 163.52, 158.30, 158.29, 154.41, 149.87, 147.98, 147.86, 144.50, 136.52, 135.63, 135.25, 135.18, 129.66, 129.60, 127.68, 127.25, 126.29, 120.77, 112.54, 109.65, 85.97, 84.70, 84.66, 84.35, 84.32, 84.16, 82.89, 75.87, 75.83, 71.18, 63.65, 63.60, 63.00, 54.15, 39.60, 37.65, 35.19, 24.76, 18.02, 17.90, 17.13, 11.46, 11.14, 10.18, -5.91, -6.04.

^{31}P NMR (162 MHz, Acetone-d_6) δ 33.50.

HRMS (ESI-TOF): calc'd for $C_{52}H_{66}N_7O_{13}PSi$ [M+H]+: 1056.4304, found: 1056.4304.

Compound (S_p)-1.57



Following **General Procedure I** on 0.03 mmol scale with (S_p)-**1.42** and **SI-1.32**. Purification by pTLC (EtOAc/DCM/acetone = 1:1:1) afforded 25.0 mg (71%, >20:1 d.r.) of the title compound (S_p)-**1.57**.

Physical State: white amorphous solid

R_f = 0.26 (EtOAc/DCM/acetone = 1:1:1)

^{1}H NMR (600 MHz, Acetone-d_6) δ 11.97 (s, 1H), 10.73 (s, 1H), 10.03 (s, 1H), 8.69 (s, 1H), 8.51 (s, 1H), 8.07 (d, J = 7.6 Hz, 2H), 7.90 (s, 1H), 7.63 (t, J = 7.4 Hz, 1H), 7.55 – 7.49 (m, 2H), 7.41 – 7.36 (m, 2H), 7.28 – 7.20 (m, 6H), 7.19 – 7.14 (m, 1H), 6.79 (dd, J = 9.0, 2.9 Hz, 4H), 6.57 (t, J = 6.4 Hz, 1H), 6.16 (dd, J = 7.5, 6.0 Hz, 1H), 5.35 (ddt, J = 8.8, 6.1, 3.2 Hz, 1H), 4.95 (q, J = 4.9 Hz, 1H), 4.28 – 4.09 (m, 4H), 3.74 (d, J = 1.7 Hz, 6H),

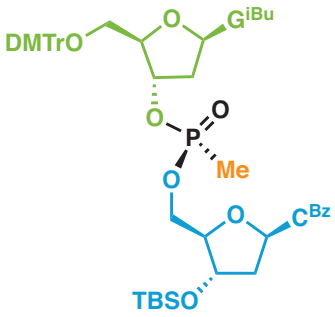
3.36 – 3.25 (m, 2H), 3.12 (dt, *J* = 12.8, 6.1 Hz, 1H), 2.96 (ddd, *J* = 13.6, 7.6, 6.0 Hz, 1H), 2.84 – 2.81 (m, 1H), 2.64 – 2.53 (m, 2H), 1.53 (d, *J* = 17.7 Hz, 3H), 1.19 (dd, *J* = 19.1, 6.9 Hz, 6H), 0.95 (s, 9H), 0.18 (d, *J* = 3.5 Hz, 6H).

^{13}C NMR (151 MHz, Acetone-d_6) δ 180.76, 166.01, 159.59, 155.79, 152.91, 152.68, 151.19, 149.27, 149.09, 145.87, 143.90, 138.06, 136.61, 136.56, 134.78, 133.31, 130.95, 130.91, 129.41, 129.16, 129.00, 128.57, 127.57, 126.20, 122.22, 113.86, 87.20, 86.55, 86.51, 85.51, 85.47, 84.38, 76.87, 76.83, 72.83, 64.96, 64.92, 64.20, 55.49, 40.42, 38.68, 38.65, 36.53, 26.18, 19.38, 19.23, 18.55, 12.21, 11.26, -4.49, -4.61.

^{31}P NMR (162 MHz, Acetone-d_6) δ 33.01.

HRMS (ESI-TOF): calc'd for $C_{59}H_{69}N_{10}O_{12}PSi$ [M+H]+: 1169.4682, found: 1169.4667.

Compound (S_p)-1.58



Following **General Procedure I** on 0.03 mmol scale with (S_p)-**1.42** and **SI-1.33**. Purification by pTLC (EtOAc/acetone = 5:1) afforded 17.4 mg (51%, >20:1 d.r.) of the title compound (S_p)-**1.58**.

Physical State: white amorphous solid

R_f = 0.51 (EtOAc/acetone = 5:1)

^{1}H NMR (600 MHz, Acetone-d_6) δ 12.04 (s, 1H), 10.68 (s, 1H), 10.00 (s, 1H), 8.28 (d, *J* = 7.5 Hz, 1H), 8.10 – 8.03 (m, 2H), 7.94 (s, 1H), 7.66 – 7.60 (m, 1H), 7.53 (dd, *J* = 8.3, 7.3

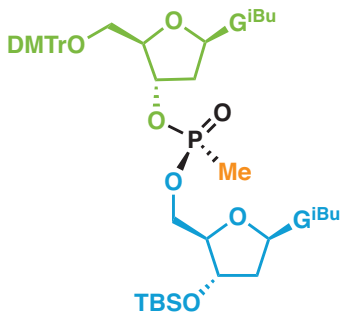
Hz, 2H), 7.46 – 7.38 (m, 3H), 7.30 – 7.26 (m, 4H), 7.26 – 7.21 (m, 2H), 7.20 – 7.15 (m, 1H), 6.84 – 6.76 (m, 4H), 6.30 – 6.24 (m, 2H), 5.46 (dp, J = 8.6, 3.0 Hz, 1H), 4.58 (dt, J = 6.2, 4.3 Hz, 1H), 4.39 – 4.34 (m, 1H), 4.34 – 4.24 (m, 2H), 4.14 (dt, J = 4.7, 3.6 Hz, 1H), 3.75 (d, J = 0.8 Hz, 6H), 3.46 – 3.33 (m, 2H), 3.08 (dt, J = 13.7, 6.7 Hz, 1H), 2.73 (ddd, J = 13.8, 6.1, 3.2 Hz, 1H), 2.52 (ddd, J = 13.5, 6.5, 4.6 Hz, 1H), 2.30 (dt, J = 13.6, 6.1 Hz, 1H), 1.67 (d, J = 17.6 Hz, 3H), 1.38 (s, 1H), 1.22 (dd, J = 6.9, 0.8 Hz, 6H), 0.91 (s, 9H), 0.12 (d, J = 0.9 Hz, 6H).

^{13}C NMR (151 MHz, Acetone-d_6) δ 180.72, 163.78, 159.61, 159.60, 155.87, 149.33, 149.10, 145.85, 145.44, 138.09, 136.60, 136.53, 134.50, 133.64, 130.98, 130.92, 129.46, 129.09, 129.01, 128.58, 127.60, 122.17, 113.87, 97.20, 87.91, 87.24, 86.77, 86.72, 85.76, 85.73, 84.39, 77.25, 77.22, 72.27, 65.00, 64.96, 64.37, 55.49, 42.23, 38.89, 38.86, 36.54, 26.13, 19.35, 19.31, 18.49, 12.29, 11.35, -4.54, -4.69.

^{31}P NMR (162 MHz, Acetone-d_6) δ 33.52.

HRMS (ESI-TOF): calc'd for $C_{58}H_{69}N_8O_{13}PSi$ [M+H]+: 1145.4569, found: 1145.4556.

Compound (S_p)-1.59



Following **General Procedure I** on 0.03 mmol scale with (S_p)-**1.42** and **SI-1.34**. Purification by pTLC (EtOAc/acetone/MeOH = 5:5:1) afforded 13.4 mg (39%, >20:1 d.r.) of the title compound (S_p)-**1.59**.

Physical State: white amorphous solid

R_f = 0.21 (EtOAc/acetone/MeOH = 5:5:1)

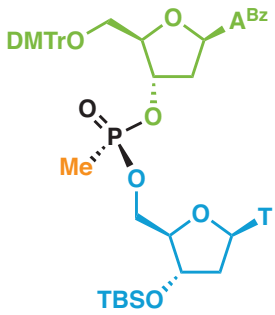
^{1}H NMR (600 MHz, Acetone-d_6) δ 12.10 (s, 2H), 10.82 (s, 1H), 10.72 (s, 1H), 8.06 (s, 1H), 7.92 (s, 1H), 7.47 – 7.42 (m, 2H), 7.34 – 7.25 (m, 6H), 7.24 – 7.19 (m, 1H), 6.87 – 6.81 (m, 4H), 6.34 (t, *J* = 6.6 Hz, 1H), 6.22 (dd, *J* = 8.3, 5.7 Hz, 1H), 5.37 (ddt, *J* = 8.1, 5.3, 2.5 Hz, 1H), 4.75 (dt, *J* = 6.1, 3.3 Hz, 1H), 4.37 – 4.23 (m, 3H), 4.15 (q, *J* = 3.9 Hz, 1H), 3.78 (s, 6H), 3.44 – 3.33 (m, 2H), 3.05 – 2.87 (m, 3H), 2.84 – 2.82 (m, 1H), 2.68 (ddd, *J* = 14.0, 5.7, 2.5 Hz, 1H), 2.44 (ddd, *J* = 13.4, 6.2, 3.7 Hz, 1H), 1.59 (d, *J* = 17.8 Hz, 3H), 1.25 (dd, *J* = 6.8, 1.7 Hz, 6H), 1.17 (d, *J* = 6.8 Hz, 3H), 1.10 (d, *J* = 6.9 Hz, 3H), 0.95 (s, 9H), 0.18 (d, *J* = 2.9 Hz, 6H).

^{13}C NMR (151 MHz, Acetone-d_6) δ 180.92, 180.78, 159.67, 156.16, 155.78, 149.55, 149.46, 149.23, 149.09, 145.84, 138.86, 137.65, 136.60, 136.50, 131.00, 130.95, 129.01, 128.62, 127.67, 122.57, 122.10, 113.91, 87.31, 86.89, 86.85, 85.72, 85.66, 85.63, 84.16, 77.35, 77.31, 73.15, 65.31, 65.27, 64.46, 55.51, 40.40, 38.94, 38.92, 36.64, 36.43, 26.16, 19.37, 19.26, 19.15, 18.54, 12.08, 11.13, -4.51, -4.65.

^{31}P NMR (162 MHz, Acetone-d_6) δ 34.00.

HRMS (ESI-TOF): calc'd for $C_{56}H_{71}N_{10}O_{13}PSi$ [M+H]+: 1151.4787, found: 1151.4779.

Compound (R_p)-1.48



Following **General Procedure I** on 0.03 mmol scale with (R_p)-**1.41** and **SI-1.31**. Purification by pTLC (EtOAc/acetone = 7:1) afforded 22.1 mg (69%, >20:1 d.r.) of the title compound (R_p)-**1.48**.

Physical State: white amorphous solid

R_f = 0.31 (EtOAc/DCM/acetone = 5:5:2)

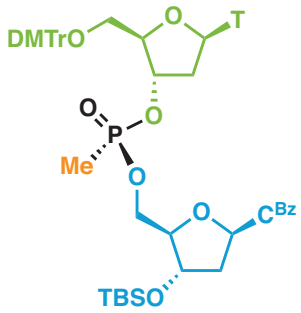
^{1}H NMR (600 MHz, Acetone-d_6) δ 10.01 (s, 1H), 9.95 (s, 1H), 8.57 (s, 1H), 8.38 (s, 1H), 8.14 (d, *J* = 7.7 Hz, 2H), 7.69 – 7.64 (m, 1H), 7.63 (q, *J* = 1.2 Hz, 1H), 7.58 (t, *J* = 7.6 Hz, 2H), 7.49 – 7.44 (m, 2H), 7.36 – 7.32 (m, 3H), 7.32– 7.12 (m, 4H), 6.89 – 6.80 (m, 4H), 6.60 (dd, *J* = 7.6, 6.2 Hz, 1H), 6.29 (dd, *J* = 7.7, 6.1 Hz, 1H), 5.44 (ddt, *J* = 8.5, 5.8, 2.9 Hz, 1H), 4.60 (dt, *J* = 6.2, 3.2 Hz, 1H), 4.41 (td, *J* = 4.9, 2.6 Hz, 1H), 4.37 – 4.28 (m, 1H), 4.26 – 4.19 (m, 1H), 4.09 (q, *J* = 4.0 Hz, 1H), 3.79 (s, 6H), 3.49 – 3.44 (m, 2H), 3.38 – 3.32 (m, 1H), 2.82 – 2.78 (m, 1H), 2.37 – 2.30 (m, 1H), 2.25 (ddd, *J* = 13.4, 6.2, 3.3 Hz, 1H), 1.81 (d, *J* = 1.2 Hz, 3H), 1.61 (d, *J* = 17.6 Hz, 3H), 0.92 (s, 9H), 0.14 (d, *J* = 2.7 Hz, 6H).

^{13}C NMR (151 MHz, Acetone-d_6) δ 165.94, 164.32, 159.78, 159.76, 153.02, 152.76, 151.41, 151.35, 146.06, 143.61, 136.76, 136.69, 135.21, 133.35, 132.16, 131.12, 131.05, 129.90, 129.78, 129.56, 129.30, 129.18, 129.13, 128.74, 127.74, 126.38, 126.26, 114.05, 113.97, 111.27, 87.39, 86.40, 86.35, 86.14, 86.10, 85.94, 85.61, 77.24, 77.20, 73.24, 68.46, 65.79, 65.75, 64.49, 55.65, 40.81, 39.81, 38.61, 31.32, 26.26, 24.64, 23.78, 18.64, 14.46, 12.63, 12.30, 11.45, 11.35, -4.41, -4.52.

^{31}P NMR (162 MHz, Acetone-d_6) δ 32.39.

HRMS (ESI-TOF): calc'd for $C_{55}H_{64}N_7O_{12}PSi$ [M+H]+: 1074.4198, found: 1074.4189.

Compound (R_p)-1.46



Following **General Procedure I** on 0.03 mmol scale with (R_p)-**1.40** and **SI-1.33**. Purification by pTLC (EtOAc/acetone = 15:1) afforded 22.0 mg (70%, >20:1 d.r.) of the title compound (R_p)-**1.46**.

Physical State: white amorphous solid

R_f = 0.63 (EtOAc/acetone = 7:1)

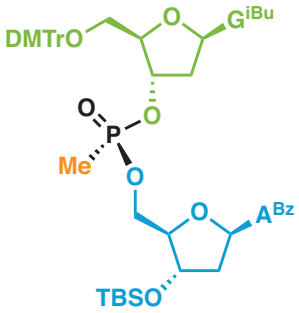
^{1}H NMR (600 MHz, Acetone-d_6) δ 10.08 (s, 1H), 8.30 (d, *J* = 7.5 Hz, 1H), 8.16 – 8.12 (m, 2H), 7.66 – 7.62 (m, 1H), 7.58 (d, *J* = 1.3 Hz, 1H), 7.57 – 7.52 (m, 2H), 7.49 – 7.45 (m, 2H), 7.41 – 7.30 (m, 7H), 7.26 – 7.21 (m, 1H), 6.89 (dd, *J* = 8.9, 1.7 Hz, 3H), 6.37 (dd, *J* = 8.1, 6.1 Hz, 1H), 6.22 (t, *J* = 6.3 Hz, 1H), 5.35 (ddt, *J* = 8.4, 5.6, 2.7 Hz, 1H), 4.57 (dt, *J* = 6.2, 4.1 Hz, 1H), 4.38 – 4.25 (m, 3H), 4.18 (q, *J* = 4.2 Hz, 1H), 3.77 (s, 6H), 3.43 (qd, *J* = 10.6, 3.4 Hz, 2H), 2.65 – 2.54 (m, 2H), 2.48 (ddd, *J* = 13.5, 6.3, 4.2 Hz, 1H), 2.29 (dt, *J* = 13.6, 6.3 Hz, 1H), 1.55 (d, *J* = 17.7 Hz, 3H), 1.43 (d, *J* = 1.2 Hz, 3H), 0.92 (s, 9H), 0.13 (d, *J* = 1.5 Hz, 6H).

^{13}C NMR (151 MHz, Acetone-d_6) δ 164.17, 163.70, 159.78, 159.76, 151.28, 145.70, 145.42, 136.44, 136.32, 136.21, 133.57, 131.03, 131.00, 129.42, 129.17, 129.03, 128.77, 127.81, 114.05, 111.29, 88.05, 87.71, 86.86, 86.82, 85.39, 85.35, 85.06, 77.07, 77.04, 72.72, 65.43, 65.39, 64.24, 55.55, 42.01, 39.61, 39.58, 26.14, 18.51, 12.18, 12.14, 11.23, -4.51, -4.66.

^{31}P NMR (162 MHz, Acetone-d_6) δ 32.91.

HRMS (ESI-TOF): calc'd for $C_{54}H_{64}N_5O_{13}PSi$ [M+H]+: 1050.4086, found: 1050.4081.

Compound (R_p)-1.57



Following **General Procedure I** on 0.03 mmol scale with (R_p)-**1.42** and **SI-1.32**. Purification by pTLC (EtOAc/acetone = 9:2) afforded 22.1 mg (63%, >20:1 d.r.) of the title compound (R_p)-**1.57**.

Physical State: white amorphous solid

R_f = 0.29 (EtOAc/acetone = 5:1)

^{1}H NMR (600 MHz, Acetone-d_6) δ 11.96 (s, 1H), 10.82 (s, 1H), 10.01 (s, 1H), 8.67 (s, 1H), 8.55 (s, 1H), 8.12 (d, J = 7.6 Hz, 2H), 7.90 (s, 1H), 7.63 (t, J = 7.4 Hz, 1H), 7.53 (t, J = 7.8 Hz, 2H), 7.38 – 7.33 (m, 2H), 7.26 – 7.19 (m, 6H), 7.18 – 7.13 (m, 1H), 6.81 – 6.76 (m, 4H), 6.57 (t, J = 6.5 Hz, 1H), 6.17 (t, J = 6.3 Hz, 1H), 5.56 (dq, J = 9.1, 5.1 Hz, 1H), 4.95 (dt, J = 6.2, 4.5 Hz, 1H), 4.38 (ddd, J = 11.0, 7.0, 3.9 Hz, 1H), 4.31 (dt, J = 11.2, 6.2 Hz, 1H), 4.15 (dq, J = 16.6, 4.1 Hz, 2H), 3.74 (d, J = 0.9 Hz, 6H), 3.29 (d, J = 4.3 Hz, 2H), 3.16 (dt, J = 12.9, 6.2 Hz, 1H), 2.93 – 2.89 (m, 1H), 2.83 – 2.79 (m, 1H), 2.59 – 2.50 (m, 2H), 1.43 (d, J = 17.7 Hz, 3H), 1.14 (dd, J = 8.5, 6.8 Hz, 6H), 0.93 (s, 9H), 0.16 (d, J = 2.5 Hz, 6H).

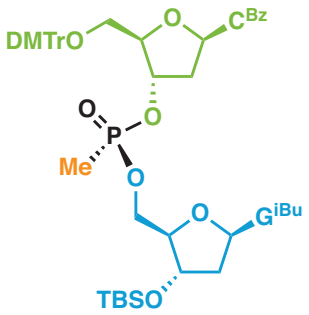
^{13}C NMR (151 MHz, Acetone-d_6) δ 180.76, 166.10, 159.57, 159.56, 156.00, 152.71, 151.02, 148.97, 145.81, 144.13, 138.61, 136.65, 136.55, 134.69, 133.36, 130.97, 130.92,

130.85, 129.43, 129.21, 128.97, 128.54, 128.52, 127.56, 125.99, 122.25, 113.84, 87.06, 86.62, 86.58, 85.48, 84.93, 84.89, 84.33, 75.86, 75.82, 73.04, 65.84, 65.79, 63.63, 55.48, 40.15, 38.51, 36.57, 26.15, 19.39, 19.17, 18.53, 12.07, 11.11, -4.49, -4.64.

^{31}P NMR (162 MHz, Acetone-d_6) δ 33.13.

HRMS (ESI-TOF): calc'd for $C_{59}H_{69}N_{10}O_{12}PSi$ [M+H]+: 1169.4682, found: 1169.4670.

Compound (R_p)-1.55



Following **General Procedure I** on 0.03 mmol scale with (R_p)-**1.43** and **SI-1.34**. Purification by pTLC (10% MeOH in EtOAc) afforded 16.1 mg (48%, >20:1 d.r.) of the title compound (R_p)-**1.55**.

Physical State: white amorphous solid

R_f = 0.30 (10% MeOH in EtOAc)

^{1}H NMR (600 MHz, Acetone-d_6) δ 12.02 (s, 1H), 10.86 (s, 1H), 8.20 – 8.16 (m, 2H), 8.14 (d, J = 7.6 Hz, 1H), 7.93 (s, 1H), 7.69 – 7.63 (m, 1H), 7.56 (t, J = 7.8 Hz, 2H), 7.46 – 7.41 (m, 2H), 7.35 – 7.28 (m, 5H), 7.22 (ddt, J = 7.8, 6.8, 1.3 Hz, 1H), 6.94 – 6.87 (m, 4H), 6.33 (dd, J = 8.5, 6.0 Hz, 1H), 6.15 (t, J = 6.3 Hz, 1H), 5.25 – 5.18 (m, 1H), 4.79 – 4.72 (m, 2H), 4.36 – 4.29 (m, 1H), 4.29 – 4.18 (m, 3H), 3.79 (d, J = 3.0 Hz, 6H), 3.41 (m, 2H), 3.00 (ddd, J = 13.6, 8.6, 5.4 Hz, 1H), 2.80 – 2.74 (m, 3H), 2.44 (dt, J = 13.8, 6.3 Hz, 1H), 2.34 (ddd,

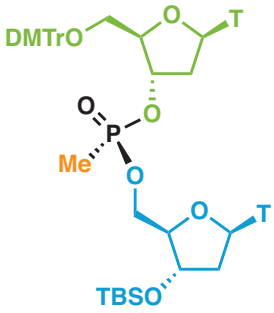
J = 13.4, 6.1, 2.0 Hz, 1H), 1.62 (d, *J* = 17.7 Hz, 3H), 1.49 – 1.36 (m, 1H), 1.18 (d, *J* = 6.9 Hz, 3H), 1.08 (d, *J* = 6.8 Hz, 3H), 0.97 – 0.86 (m, 9H), 0.18 (d, *J* = 6.5 Hz, 6H).

^{13}C NMR (151 MHz, Acetone-d_6) δ 181.04, 168.14, 159.91, 159.88, 156.08, 149.03, 148.95, 145.62, 139.61, 136.55, 136.33, 133.74, 133.61, 132.17, 131.17, 131.04, 129.90, 129.78, 129.62, 129.18, 129.14, 128.90, 127.90, 126.26, 123.35, 114.21, 88.08, 87.91, 87.20, 87.15, 87.08, 86.05, 86.01, 76.62, 74.18, 68.46, 65.91, 65.87, 63.73, 55.68, 40.98, 40.07, 39.81, 36.46, 32.76, 31.32, 27.91, 26.32, 24.64, 23.78, 19.60, 19.35, 18.73, 14.46, 11.96, 11.45, 11.01, -4.40, -4.51.

^{31}P NMR (162 MHz, Acetone-d_6) δ 33.24.

HRMS (ESI-TOF): calc'd for $C_{58}H_{69}N_8O_{13}PSi$ [M+H]+: 1145.4569, found: 1145.4553.

Compound (R_p)-1.44



Following **General Procedure I** on 1.5 mmol scale with (R_p)-**1.40** and **SI-1.31**. Purification by silica gel column chromatography (DCM/MeOH = 95:5) afforded 1.1 g (75%, >20:1 d.r.) of the title compound (R_p)-**1.44**.

Physical State: white amorphous solid

R_f = 0.38 (EtOAc/DCM:acetone = 5:5:2)

^{1}H NMR (600 MHz, Acetone-d_6) δ 10.02 (s, 1H), 9.96 (s, 1H), 7.63 (q, *J* = 1.2 Hz, 1H), 7.58 (q, *J* = 1.2 Hz, 1H), 7.52 – 7.47 (m, 2H), 7.40 – 7.32 (m, 6H), 7.30 – 7.24 (m, 1H),

6.95 – 6.90 (m, 4H), 6.39 (dd, *J* = 8.3, 5.9 Hz, 1H), 6.30 (dd, *J* = 7.6, 6.1 Hz, 1H), 5.33 (ddt, *J* = 8.2, 5.4, 2.6 Hz, 1H), 4.60 (dt, *J* = 6.2, 3.2 Hz, 1H), 4.33 – 4.27 (m, 3H), 4.24 (ddd, *J* = 11.4, 6.7, 4.7 Hz, 1H), 4.11 – 4.05 (m, 1H), 3.81 (s, 6H), 3.47 – 3.43 (m, 2H), 2.65 – 2.53 (m, 2H), 2.33 (ddd, *J* = 13.6, 7.6, 6.1 Hz, 1H), 2.25 (ddd, *J* = 13.4, 6.2, 3.3 Hz, 1H), 1.83 (d, *J* = 1.2 Hz, 3H), 1.55 (d, *J* = 17.6 Hz, 3H), 1.45 (d, *J* = 1.2 Hz, 3H), 0.93 (s, 9H), 0.15 (d, *J* = 1.5 Hz, 6H).

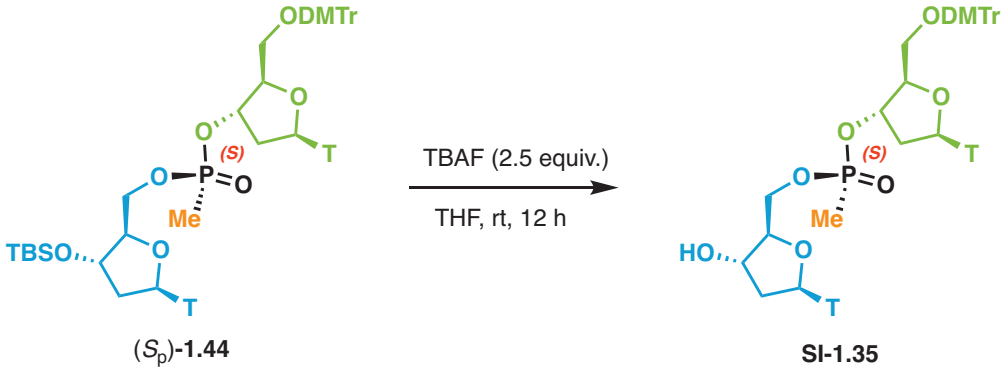
^{13}C NMR (151 MHz, Acetone-d_6) δ 164.32, 164.20, 159.95, 159.93, 151.39, 151.35, 145.80, 136.70, 136.59, 136.43, 136.25, 131.16, 129.18, 128.92, 127.97, 114.20, 111.44, 111.23, 87.88, 86.37, 86.33, 85.95, 85.55, 85.51, 85.15, 77.24, 77.20, 73.26, 65.71, 65.67, 64.40, 55.68, 40.83, 39.65, 39.63, 26.26, 18.64, 12.61, 12.24, 11.29, -4.41, -4.52.

^{31}P NMR (162 MHz, Acetone-d_6) δ 32.53.

HRMS (ESI-TOF): calc'd for $C_{48}H_{61}N_4O_{13}PSi$ [M+Na]+: 983.3640, found: 983.3632.

Ψ Activation of MPO Dimers

Step 1: TBS Deprotection to afford SI-1.35



(S_p)-**1.44** **SI-1.35**

A mixture of dinucleotide (S_p)-**1.44** (290 mg, 0.3 mmol, 1.0 equiv.) and TBAF (1.0 M in THF, 0.75 mL, 0.75 mmol, 2.5 equiv.) in THF (5 mL) was stirred at rt for 12 h, upon which the mixture was concentrated to dryness under reduced pressure and co-evaporated with toluene (2 x 3 mL). Purification by silica gel column chromatography (DCM/MeOH = 9:1) afforded 223 mg (75%, >20:1 d.r.) of the title compound **SI-1.35**.

Physical State: white amorphous solid

R_f = 0.43 (DCM/MeOH = 85:15)

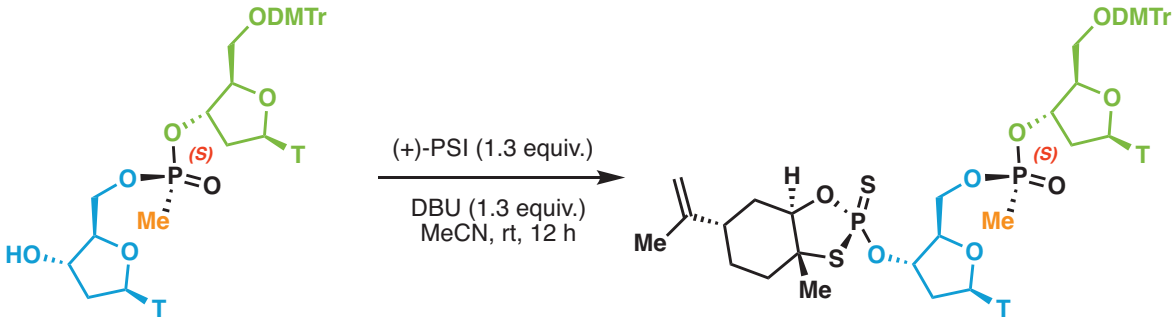
^{1}H NMR (600 MHz, Acetone-d_6) δ 10.05 (d, J = 15.0 Hz, 1H), 9.98 (d, J = 14.4 Hz, 1H), 7.57 (dq, J = 13.1, 1.2 Hz, 2H), 7.51 – 7.46 (m, 2H), 7.39 – 7.33 (m, 4H), 7.33 – 7.31 (m, 2H), 7.28 – 7.23 (m, 1H), 6.94 – 6.88 (m, 4H), 6.36 (t, J = 7.1 Hz, 1H), 6.31 (dd, J = 7.7, 6.2 Hz, 1H), 5.32 (dtt, J = 10.4, 4.2, 2.0 Hz, 1H), 4.59 (s, 1H), 4.44 – 4.40 (m, 1H), 4.27 (q, J = 3.2 Hz, 1H), 4.26 – 4.18 (m, 1H), 4.08 (ddd, J = 11.1, 7.3, 3.3 Hz, 1H), 4.01 (dt, J = 6.2, 3.3 Hz, 1H), 3.79 (s, 6H), 3.46 (dd, J = 10.6, 3.5 Hz, 1H), 3.42 (dd, J = 10.6, 3.3 Hz, 1H), 2, 2.60 – 2.55 (m, 2H), 2.25 (ddd, J = 13.6, 6.2, 3.4 Hz, 1H), 2.19 (dddd, J = 13.9, 7.6, 6.2, 1.2 Hz, 1H), 1.82 (d, J = 1.2 Hz, 3H), 1.58 (d, J = 17.7 Hz, 3H), 1.46 (d, J = 1.2 Hz, 3H).

^{13}C NMR (151 MHz, Acetone-d_6) δ 164.34, 164.26, 164.19, 159.92, 159.90, 151.39, 151.32, 145.87, 136.61, 136.55, 136.49, 136.32, 131.18, 131.15, 129.17, 128.91, 127.95, 114.19, 111.40, 111.22, 87.84, 86.18, 86.14, 85.68, 85.57, 85.53, 85.23, 76.91, 76.87, 71.89, 71.78, 66.26, 66.22, 64.33, 55.68, 40.52, 40.47, 39.67, 39.64, 12.66, 12.25, 12.19, 11.24.

^{31}P NMR (162 MHz, Acetone-d_6) δ 33.29.

HRMS (ESI-TOF): calc'd for $C_{42}H_{47}N_4O_{13}P$ $[M+Na]^+$: 869.2775, found: 869.2766.

Step 2: Loading of (+)-Ψ to afford 1.60



SI-1.35 1.60

SI-1.35 (170 mg, 0.2 mmol, 1.0 equiv.) and (+)-PSI (120 mg, 0.26 mmol, 1.3 equiv.) were dissolved in anhydrous acetonitrile (2 mL, 0.1 M) in a flame-dried round-bottom flask. DBU (39 µL, 0.26 mmol, 1.3 equiv.) was added dropwise to the reaction mixture while stirring. After 30 minutes, the crude reaction mixture was quenched with the addition of 1X PBS solution (10 mL) and extracted with DCM (10 mL x 3). The combined organic layers were washed with water (10 mL x 2) and brine (10 mL), dried over $MgSO_4$, filtered and concentrated. The residue crude product was purified by silica gel column chromatography (DCM:MeOH = 98:2) afforded 168 mg (77%, >20:1 d.r.) of the title compound **1.60**.

Physical State: pale yellow amorphous solid

R_f = 0.48 (DCM:MeOH = 95:5)

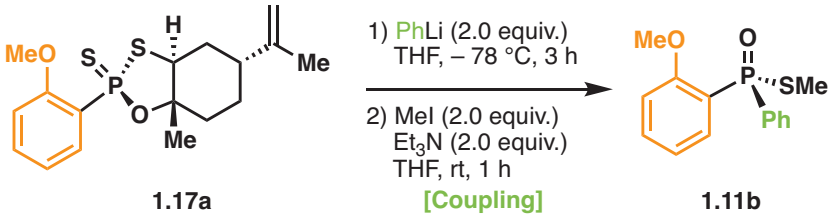
^{1}H NMR (600 MHz, Acetone-d_6) δ 7.60 (t, *J* = 1.2 Hz, 1H), 7.55 (q, *J* = 1.3 Hz, 1H), 7.54 – 7.48 (m, 2H), 7.41 – 7.33 (m, 4H), 7.31 – 7.22 (m, 2H), 7.21 – 7.12 (m, 1H), 6.96 – 6.90 (m, 4H), 6.39 (t, *J* = 7.1 Hz, 1H), 6.29 (dd, *J* = 7.9, 6.4 Hz, 1H), 5.34 (dddt, *J* = 19.3, 11.2, 5.6, 2.7 Hz, 2H), 5.02 (t, *J* = 1.5 Hz, 1H), 4.98 – 4.94 (m, 1H), 4.54 (dt, *J* = 12.8, 3.3 Hz, 1H), 4.36 – 4.27 (m, 3H), 4.18 (ddd, *J* = 9.7, 7.1, 2.6 Hz, 1H), 4.02 – 3.97 (m, 1H), 3.81 (s, 6H), 3.52 – 3.42 (m, 2H), 3.29 – 3.23 (m, 1H), 2.67 (s, 1H), 2.60 (dd, *J* = 7.2, 4.3 Hz, 2H), 2.51 – 2.44 (m, 1H), 2.39 – 2.34 (m, 1H), 2.16 – 2.09 (m, 1H), 2.03 – 1.86 (m, 3H), 1.84 (d, *J* = 1.2 Hz, 3H), 1.82 – 1.79 (m, 3H), 1.71 (s, 3H), 1.63 (d, *J* = 17.7 Hz, 3H), 1.47 (d, *J* = 1.2 Hz, 3H).

^{13}C NMR (151 MHz, Acetone-d_6) δ 164.16, 159.91, 159.89, 151.31, 151.26, 146.54, 145.83, 138.60, 136.58, 136.56, 136.45, 136.26, 131.16, 131.14, 129.86, 129.18, 129.14, 128.92, 127.96, 126.22, 114.20, 112.24, 111.52, 111.40, 87.87, 87.18, 86.01, 85.57, 85.54, 85.16, 84.33, 84.30, 84.26, 79.38, 79.33, 77.13, 77.09, 67.11, 65.53, 65.49, 64.41, 64.38, 59.48, 55.70, 54.92, 49.38, 46.32, 44.03, 39.89, 39.72, 39.69, 38.45, 38.41, 34.62, 34.56, 32.77, 28.36, 28.26, 27.36, 27.32, 24.71, 24.52, 24.06, 22.92, 22.15, 21.51, 20.48, 20.23, 13.94, 12.64, 12.28, 12.22, 11.33.

^{31}P NMR (162 MHz, Acetone-d_6) δ 101.46, 33.22.

HRMS (ESI-TOF): calc'd for $C_{52}H_{62}N_4O_{14}P_2S_2Na$ [M+Na]+: 1115.3077, found: 1115.3088.

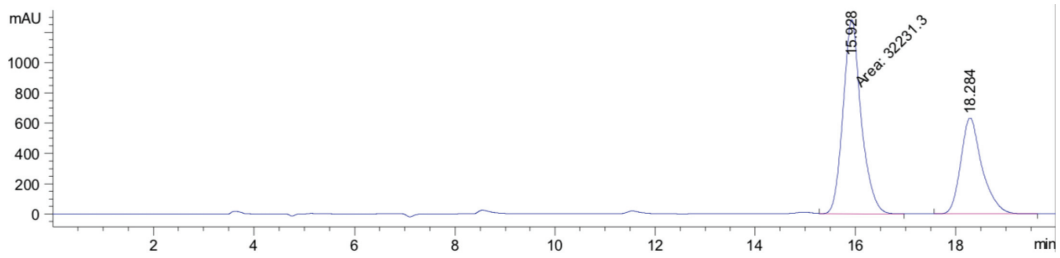
P-Chiral Phosphine: Inversed-Order Loading and Coupling Experiment



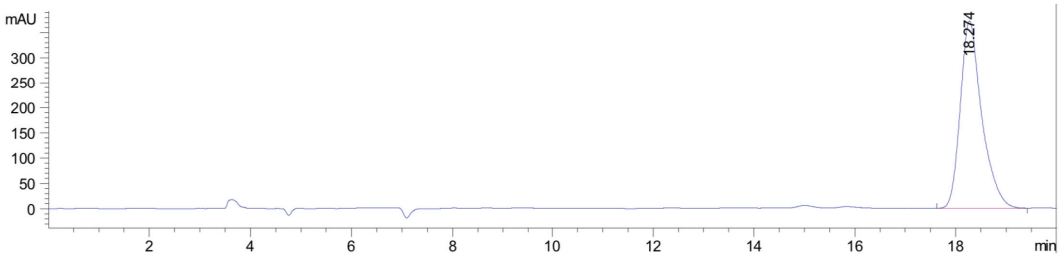
1.17a **1.11b**

Following **General Procedure C**, compound **1.11b** was prepared on 0.05 mmol scale from **1.17a** in 35% yield and >98:2 e.r. All physical and spectroscopic data matches with **1.11b** synthesized from **1.8b**. Stereochemical outcome was determined bychiral HPLC analysis (Chiralpak AD-H, isopropanol/hexane = 15:85, 0.8 mL/min, 280 nm) of the reaction product and a standard sample of **1.11b** derived from **1.8b**, as is shown below:

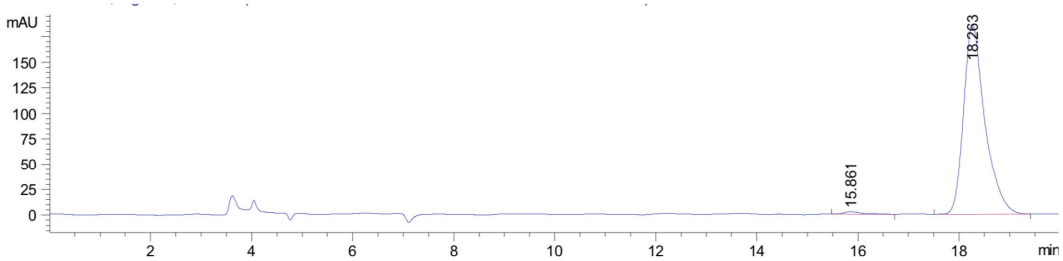
Racemic:



*Standard of **1.11b**:*

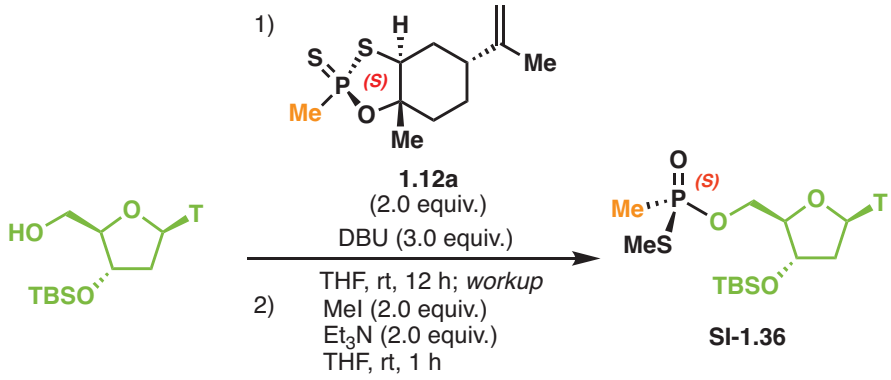


Reaction product:



MPO: Inversed-Order Loading and Coupling Experiment

Loading of Nucleoside-5'-OH:



To a flame-dried 50 mL round bottom flask under argon was charged nucleoside (1.0 mmol, 1.0 equiv.), **1.12a** (524.6 mg, 2.0 mmol, 2.0 equiv.), and THF (10 mL). DBU (3.0 mmol, 3.0 equiv.) was added dropwise, and the resulting solution was stirred for 12 h at rt. The reaction was then quenched with 20 mL of 1X PBS solution and extracted with DCM (3 x 30 mL). The combined organic layers were washed with saturated aqueous $NaHCO_3$ solution (10 mL), brine (10 mL), dried over Na_2SO_4, filtered and concentrated. The residue was re-dissolved in THF (5 mL). Et_3N (2 equiv.) and MeI (2 equiv.) were added, and the heterogeneous mixture was stirred vigorously for 1 h. The reaction was quenched with 10 mL of water and extracted with EtOAc (3 x 20 mL). The combined organic layers were dried over Na_2SO_4, filtered and concentrated. The residue was purified by silica gel chromatography to afford the desired product **SI-1.36**.

Physical State: white amorphous solid

$\mathbf{R_f}$ = 0.3 (EtOAc)

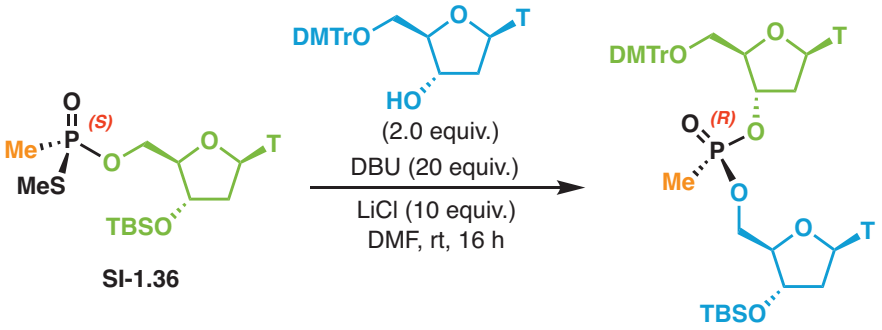
^{1}H NMR (600 MHz, Acetone-d_6) δ 10.00 (s, 1H), 7.54 (q, J = 1.3 Hz, 1H), 6.39 – 6.31 (m, 1H), 4.66 (dt, J = 6.4, 3.3 Hz, 1H), 4.36 – 4.17 (m, 2H), 4.15 – 4.07 (m, 1H), 2.40 – 2.22 (m, 5H), 1.90 – 1.79 (m, 6H), 0.94 (s, 9H), 0.17 (d, J = 3.3 Hz, 6H).

^{13}C NMR (151 MHz, Acetone-d_6) δ 164.29, 164.21, 151.37, 136.64, 136.55, 132.16, 129.77, 111.18, 86.37, 86.32, 85.89, 85.72, 73.66, 73.35, 68.45, 65.08, 64.85, 64.81, 40.86, 40.73, 39.80, 31.31, 27.29, 26.26, 24.64, 23.77, 18.83, 18.63, 18.11, 14.46, 12.68, 12.58, 12.29, 12.27, 11.45, -4.43, -4.45, -4.55.

^{31}P NMR (162 MHz, Acetone-d_6) δ 55.99

HRMS (ESI-TOF): calc'd for $C_{18}H_{33}N_2O_6P_2SSi$ [M+H]+: 465.1644, found: 465.1645.

Coupling of Nucleoside 3'-OH:



Following **General Procedure I**, the coupling reaction of 5'-DMTr-dT-3'-OH to **SI-1.36** afforded the desired dT-dT dimer product. Its ^{31}P NMR δ 32.57 corresponds to the reported ^{31}P shift of (R_p) dT-dT dimers (see above). The stereochemistry at phosphorus of the reaction product was thus assigned to be R_p.

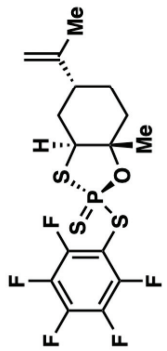
Chapter 1 Experimental References

1. Knouse, K. W.; deGruyter, J. N.; Schmidt, M. A.; Zheng, B.; Vantourout, J. C.; Kingston, C.; Mercer, S. E.; McDonald, I. M.; Olson, R. E.; Zhu, Y.; Hang, C.; Zhu, J.; Yuan, C.; Wang, Q.; Park, P.; Eastgate, M. D.; Baran, P. S., Unlocking P(V): Reagents for chiral phosphorothioate synthesis. *Science* **2018,** *361*, 1234.
2. Steiner, D.; Ivison, L.; Goralski, C. T.; Appell, R. B.; Gojkovic, J. R.; Singaram, B., A facile and efficient method for the kinetic separation of commercially available cis- and trans-limonene epoxide. *Tetrahedron: Asymmetry* **2002,** *13*, 2359–2363.
3. Woźniak, L. A.; Wieczorek, M.; Pyzowski, J.; Majzner, W.; Stec, W. J., Stereochemistry of the DBU/LiCl-Assisted Nucleophilic Substitution at Phosphorus in Nucleoside-3‘-O-(Se-methyl Methanephosphonoselenolate). *J. Org. Chem.* **1998,** *63*, 5395–5402.
4. Krasovskiy, A.; Knochel, P., Convenient Titration Method for Organometallic Zinc, Magnesium, and Lanthanide- Reagents. *Synthesis* **2006,** *2006*, 890–891.
5. Han, Z. S.; Goyal, N.; Herbage, M. A.; Sieber, J. D.; Qu, B.; Xu, Y.; Li, Z.; Reeves, J. T.; Desrosiers, J.-N.; Ma, S.; Grinberg, N.; Lee, H.; Mangunuru, H. P. R.; Zhang, Y.; Krishnamurthy, D.; Lu, B. Z.; Song, J. J.; Wang, G.; Senanayake, C. H., Efficient Asymmetric Synthesis of P-Chiral Phosphine Oxides via Properly Designed and Activated Benzoxazaphosphinine-2-oxide Agents. *J. Am. Chem. Soc.* **2013,** *135*, 2474–2477.
6. Rajendran, K. V.; Gilheany, D. G., Simple unprecedented conversion of phosphine oxides and sulfides to phosphine boranes using sodium borohydride. *Chem. Comm.* **2012,** *48*, 817–819.

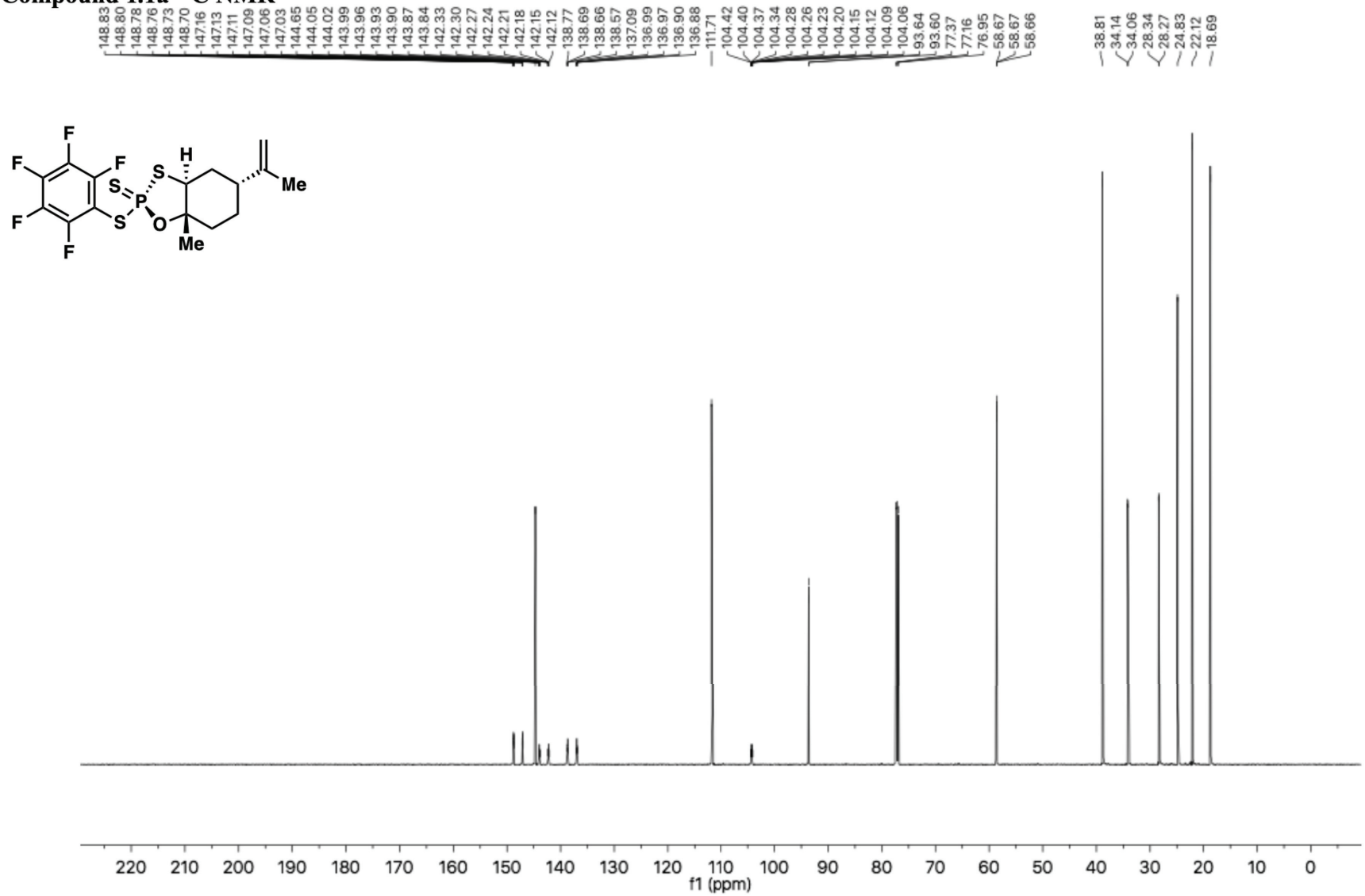
7. Paul, S.; Roy, S.; Monfregola, L.; Shang, S.; Shoemaker, R.; Caruthers, M. H., Oxidative Substitution of Boranephosphonate Diesters as a Route to Post-synthetically Modified DNA. *J. Am. Chem. Soc.* **2015,** *137*, 3253–3264.
8. Huang, H.-S.; Kong, R.; Zheng, X.-A.; Chen, W.-J.; Han, S.-B.; Zeng, D.-Y.; Gong, S.-S.; Sun, Q., A Practical Method for Regioselective 5′-O-tert-Butyldimethylsilyl Deprotection of Persilylated Nucleosides by Methanolic Phosphomolybdic Acid. *Synlett* **2018,** *29*, 2437–2443.
9. Molina, A.G.; Kungurtsev, V.; Virta, P.; Lönnberg, H. Acetylated and Methylated β-Cyclodextrins as Viable Soluble Supports for the Synthesis of Short 2′-Oligodeoxyribo-nucleotides in Solution. *Molecules* **2012**, *17*, 12102–12120.

NMR Spectra

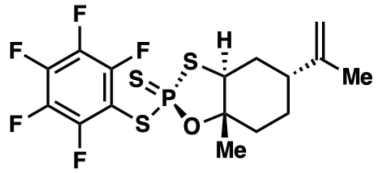
Compound 1.1a ^{1}H NMR



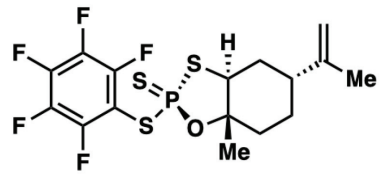
Compound 1.1a ^{13}C NMR



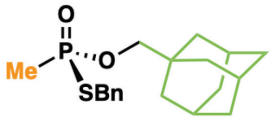
Compound 1.1a ^{19}F NMR

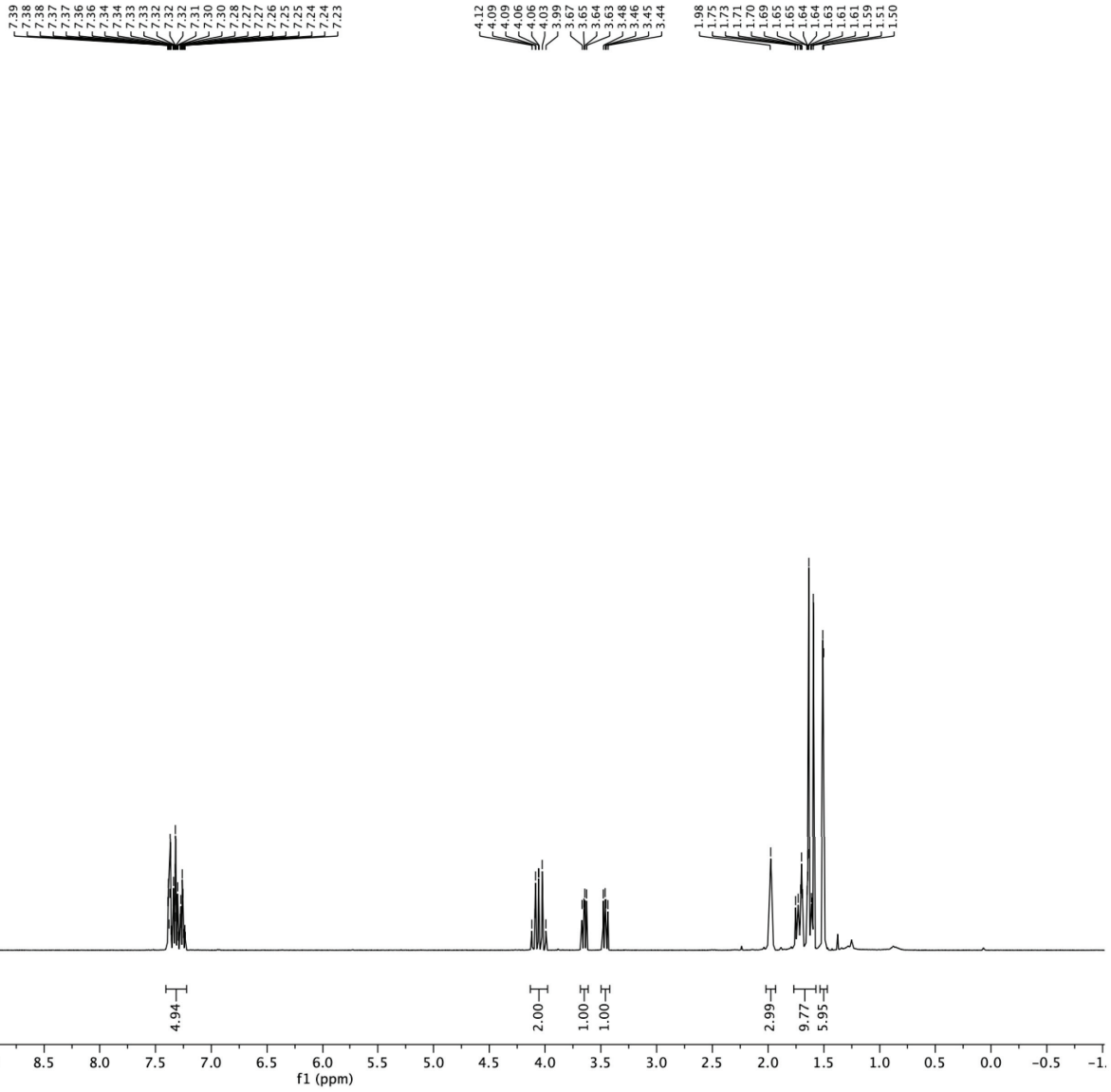


Compound 1.1a ^{31}P NMR

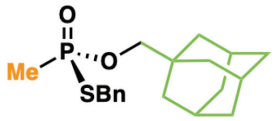


Compound SI-1.3 ^{1}H NMR

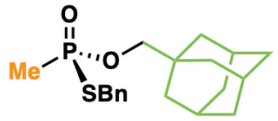




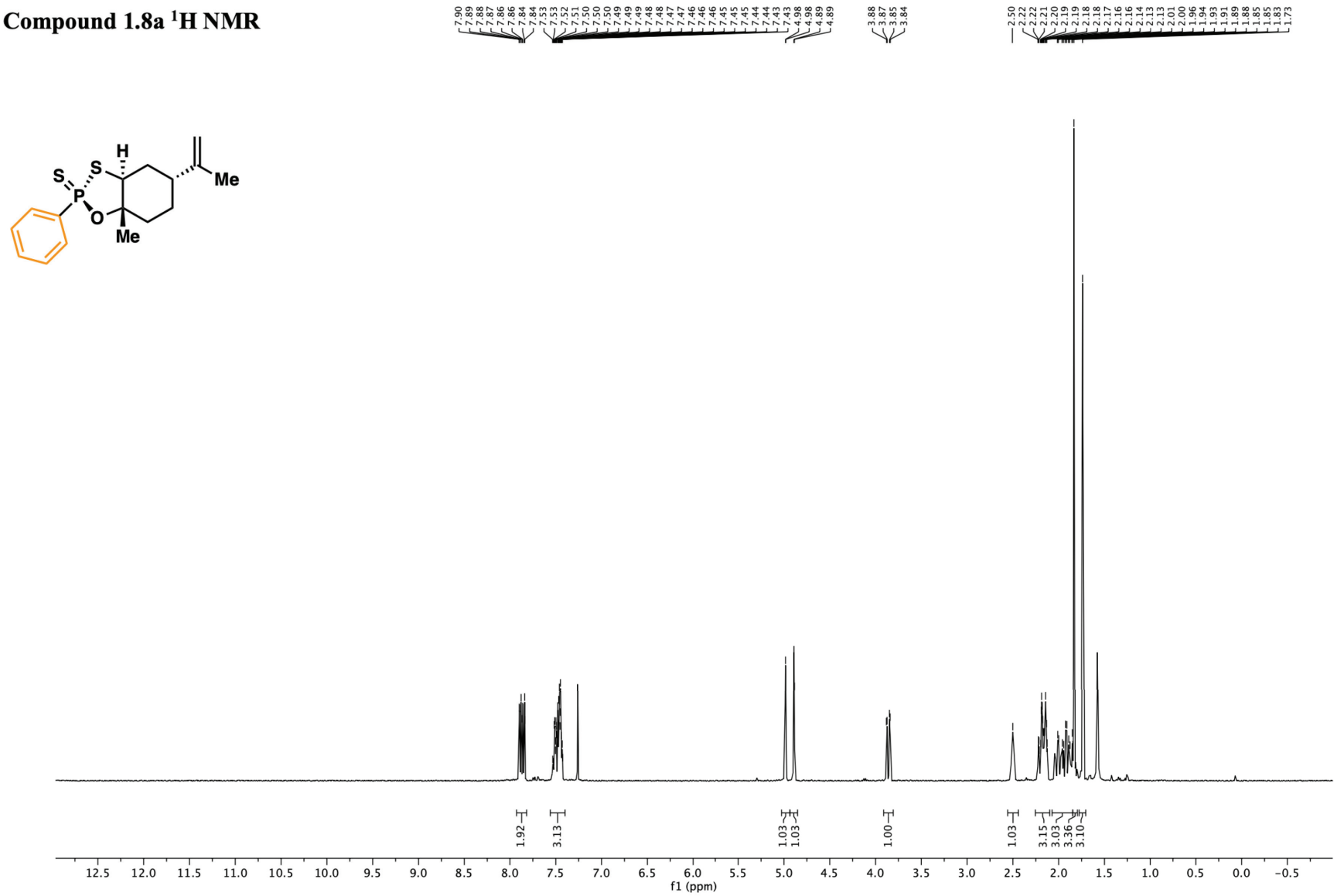
Compound SI-1.3 ^{13}C NMR



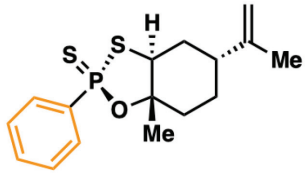
Compound SI-1.3 ^{31}P NMR



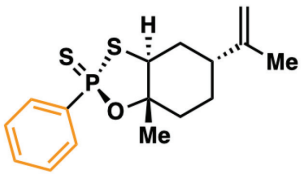
Compound 1.8a ^{1}H NMR



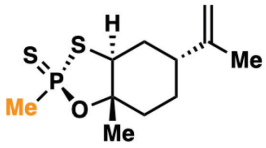
Compound 1.8a ^{13}C NMR



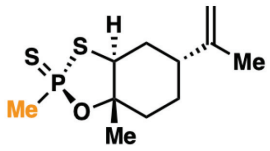
Compound 1.8a ^{31}P NMR



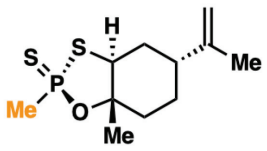
Compound 1.12a ^{1}H NMR



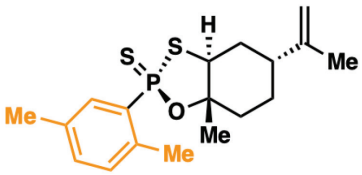
Compound 1.12a ^{13}C NMR



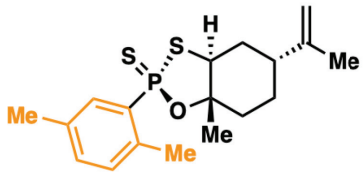
Compound 1.12a ^{31}P NMR



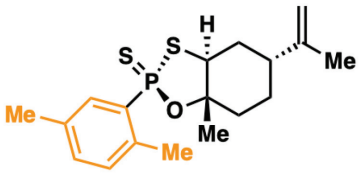
Compound 1.13a ^{1}H NMR



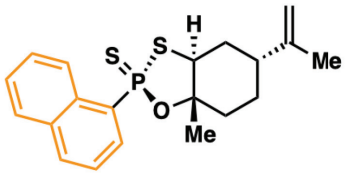
Compound 1.13a ^{13}C NMR



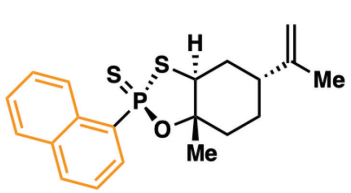
Compound 1.13a ^{31}P NMR



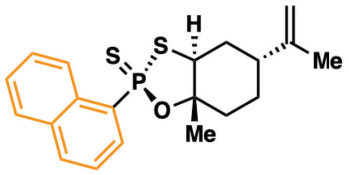
Compound 1.14a ^{1}H NMR



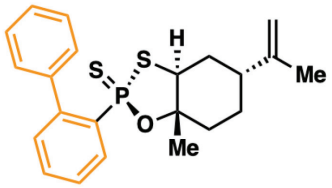
Compound 1.14a ^{13}C NMR

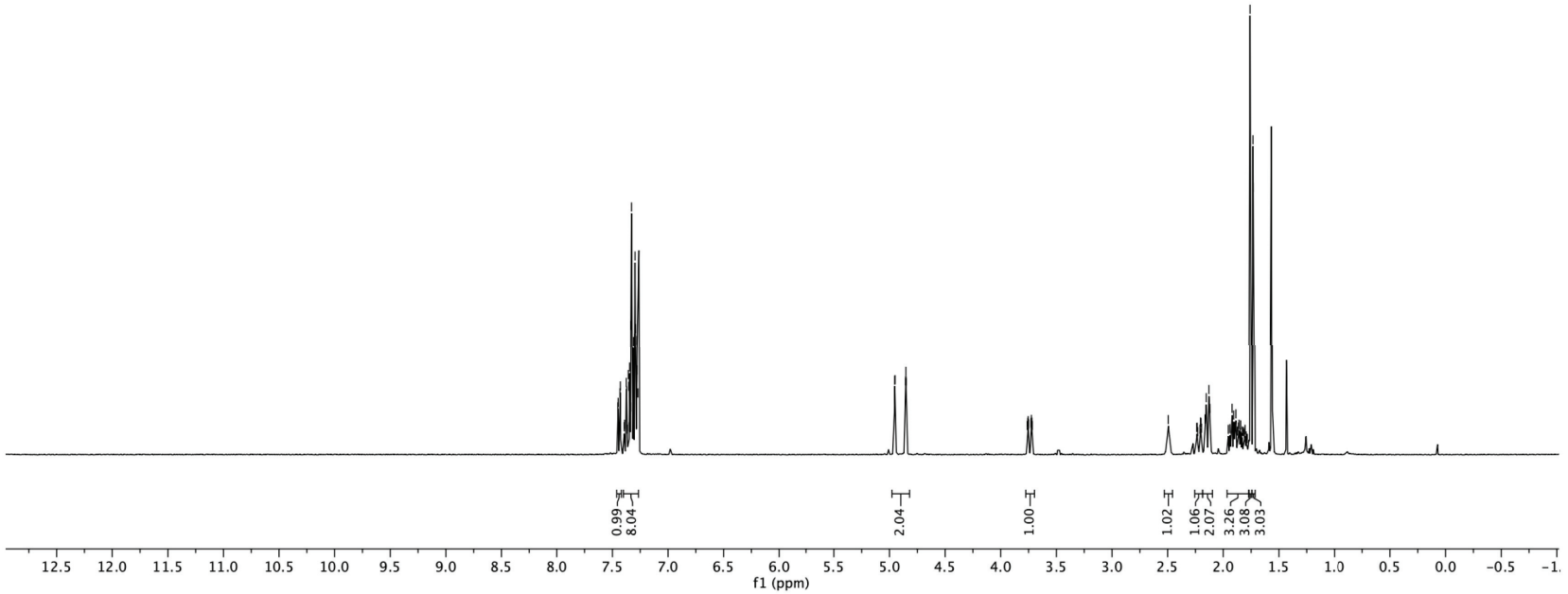


Compound 1.14a ^{31}P NMR

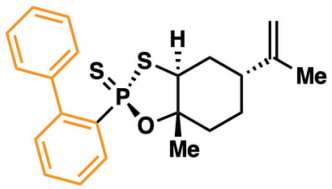


Compound 1.15a ^{1}H NMR

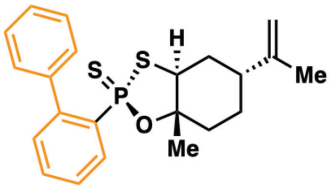




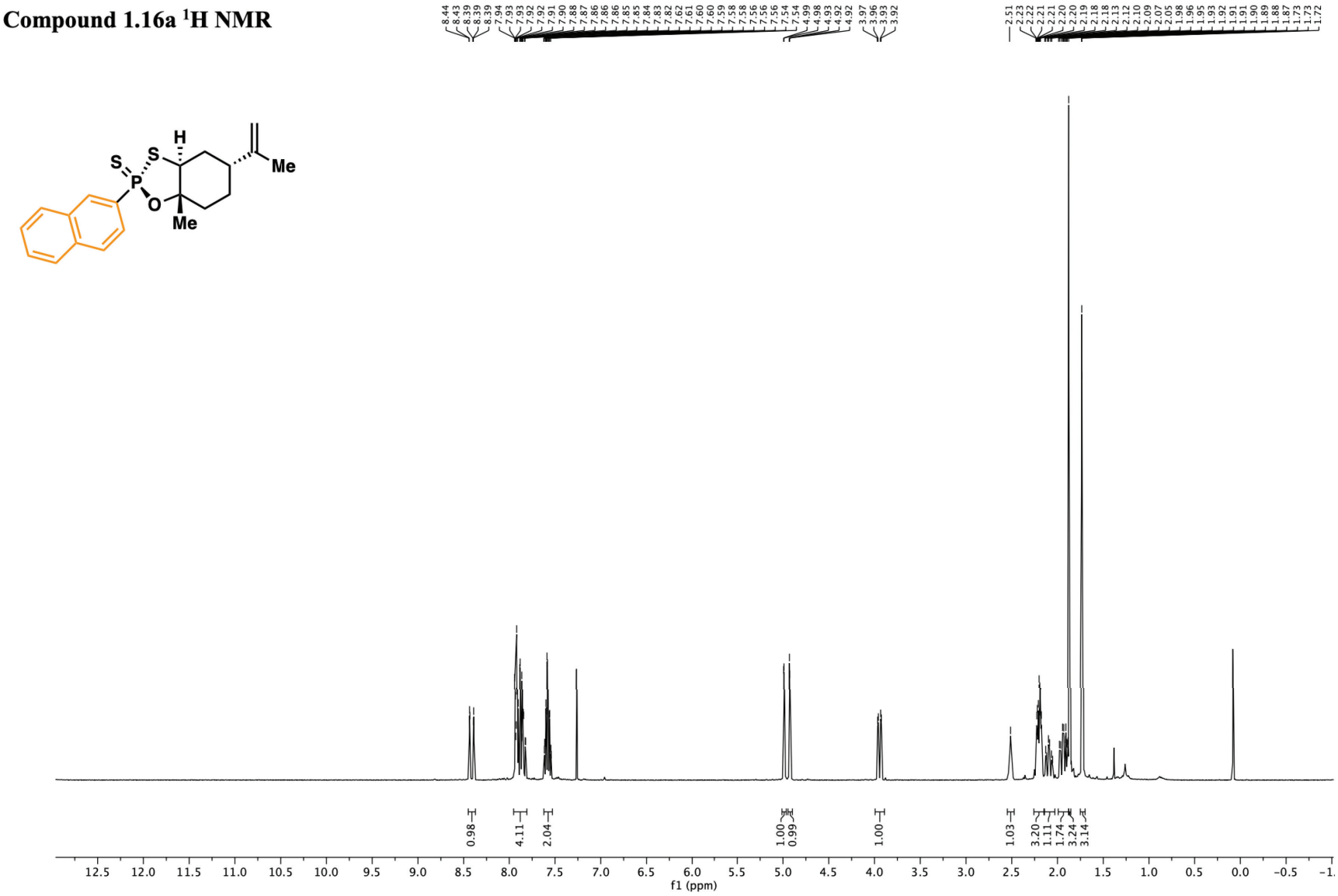
Compound 1.15a ^{13}C NMR



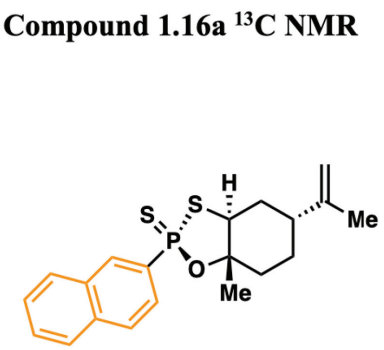
Compound 1.15a ^{31}P NMR



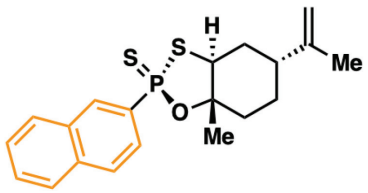
Compound 1.16a ^{1}H NMR



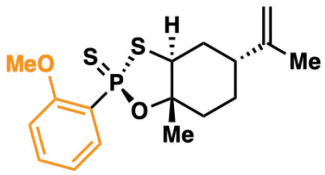
Compound 1.16a ^{13}C NMR



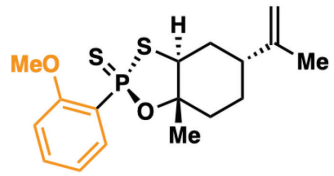
Compound 1.16a ^{31}P NMR



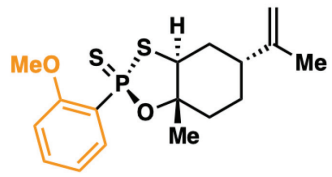
Compound 1.17a ^{1}H NMR



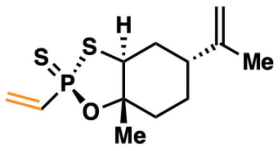
Compound 1.17a ^{13}C NMR



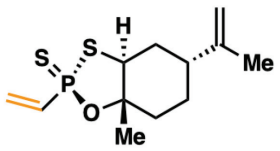
Compound 1.17a ^{31}P NMR



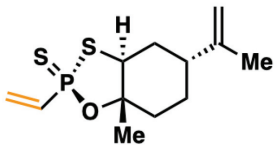
Compound 1.18a ^{1}H NMR



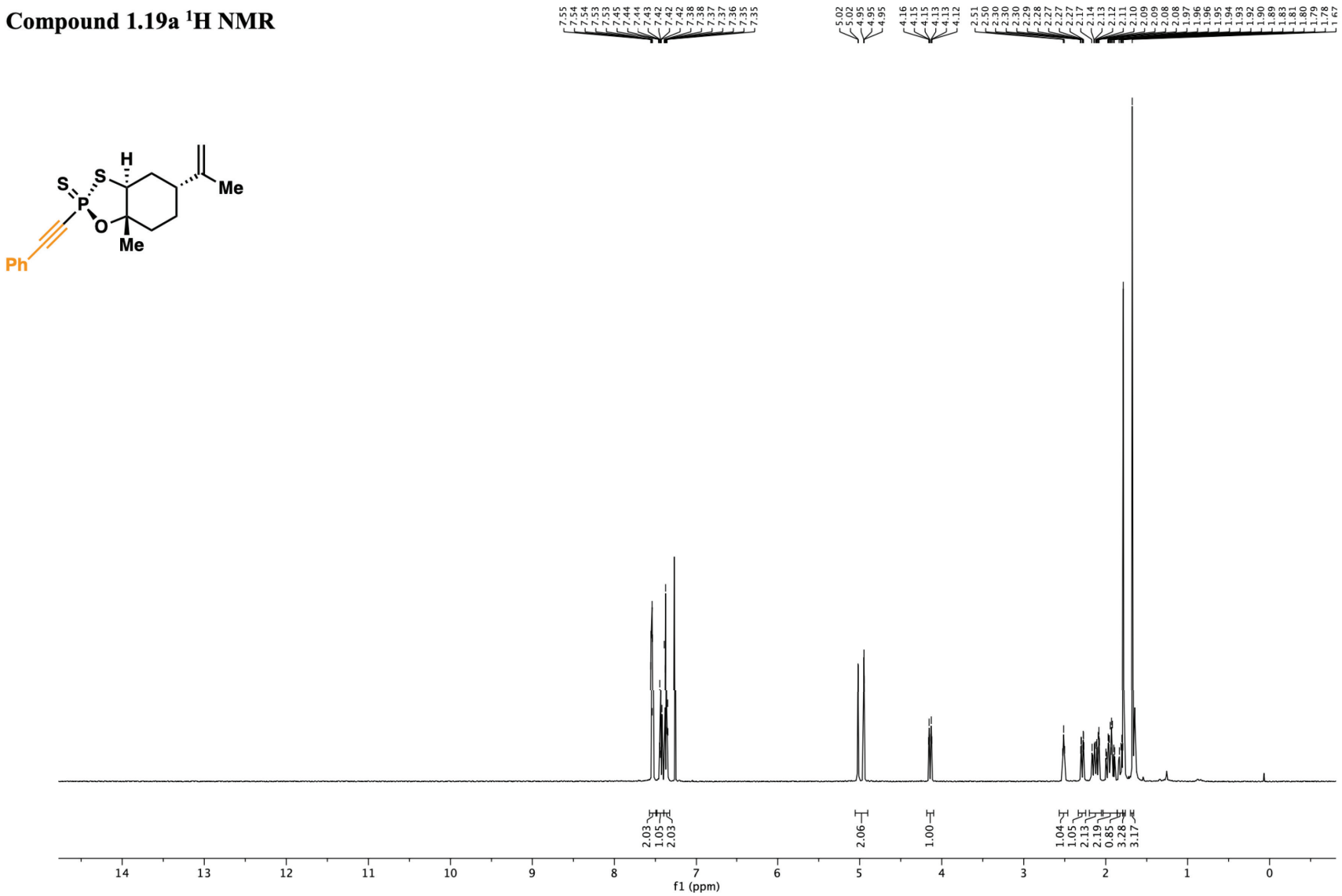
Compound 1.18a ^{13}C NMR



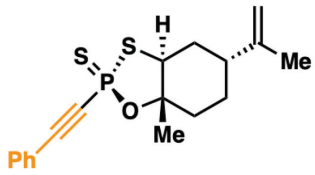
Compound 1.18a ^{31}P NMR



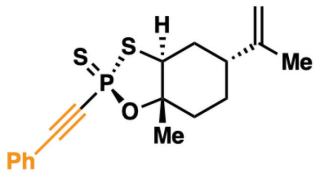
Compound 1.19a ^{1}H NMR

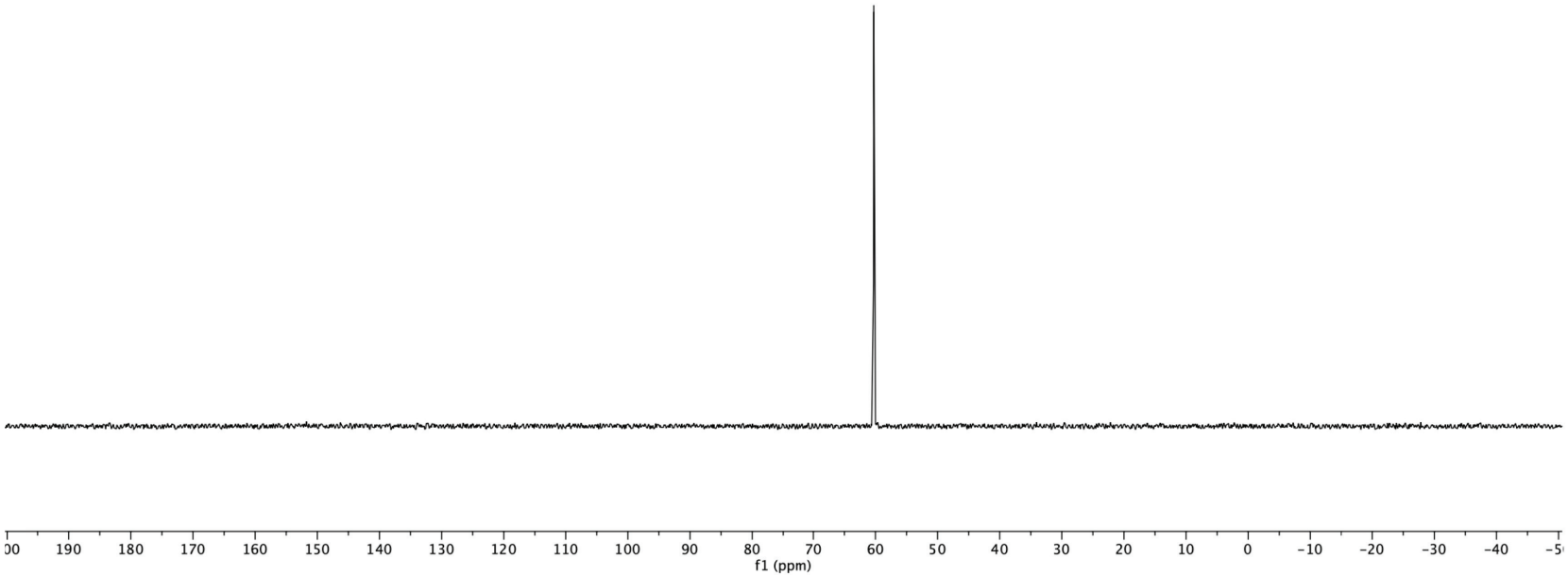


Compound 1.19a ^{13}C NMR

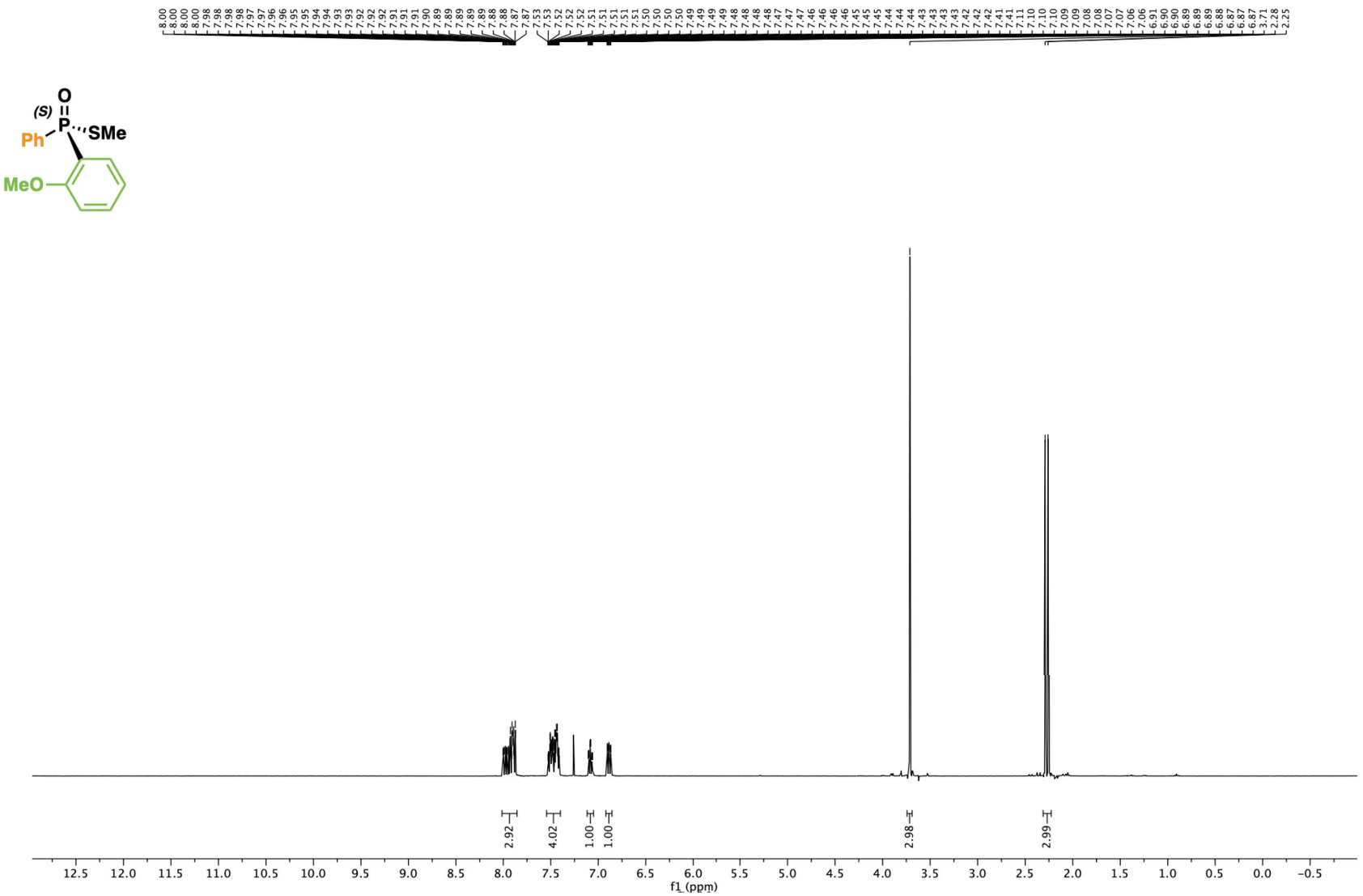


Compound 1.19a ^{31}P NMR

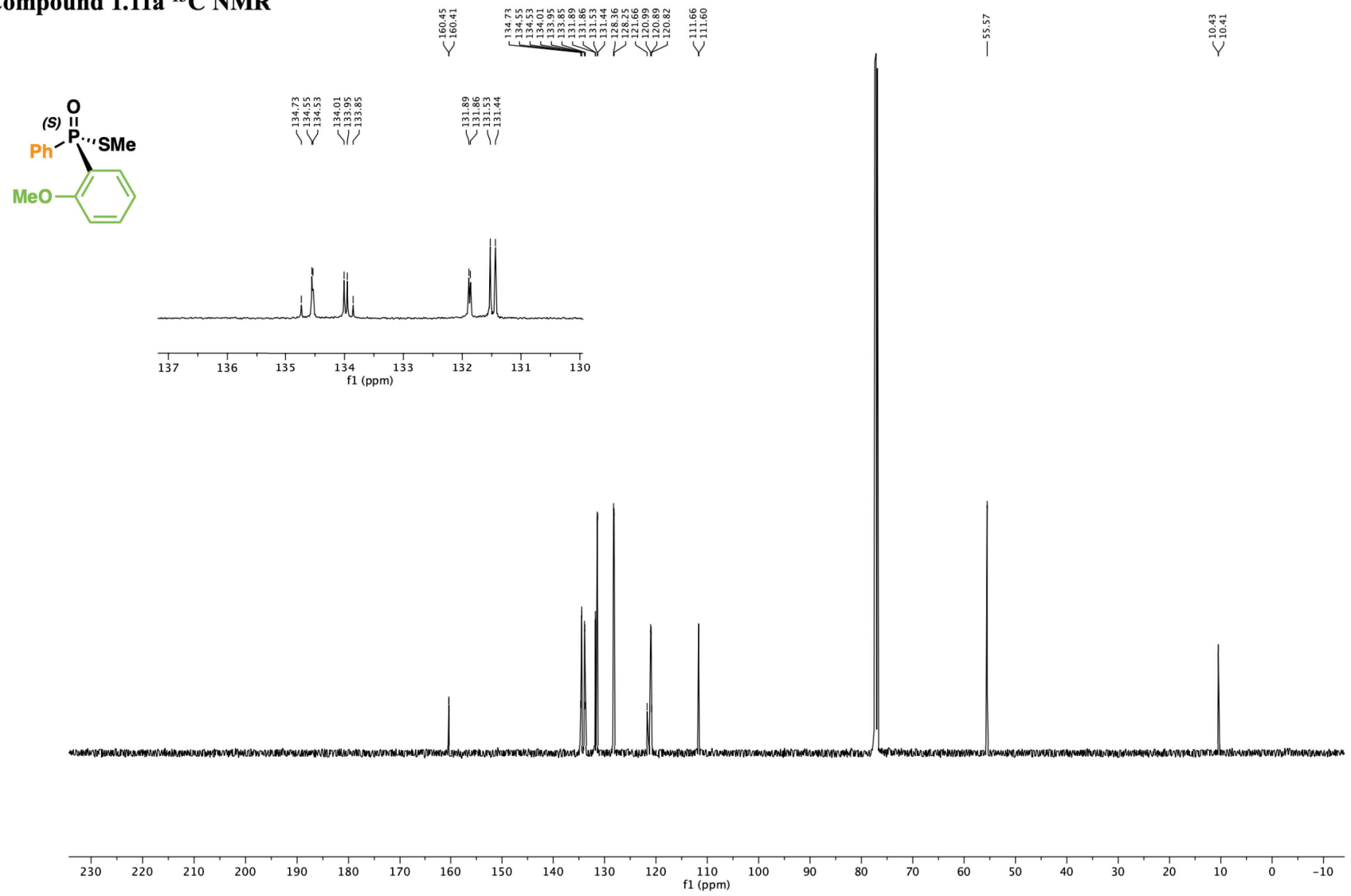




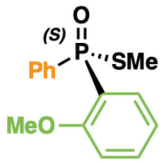
Compound 1.11a ^{1}H NMR



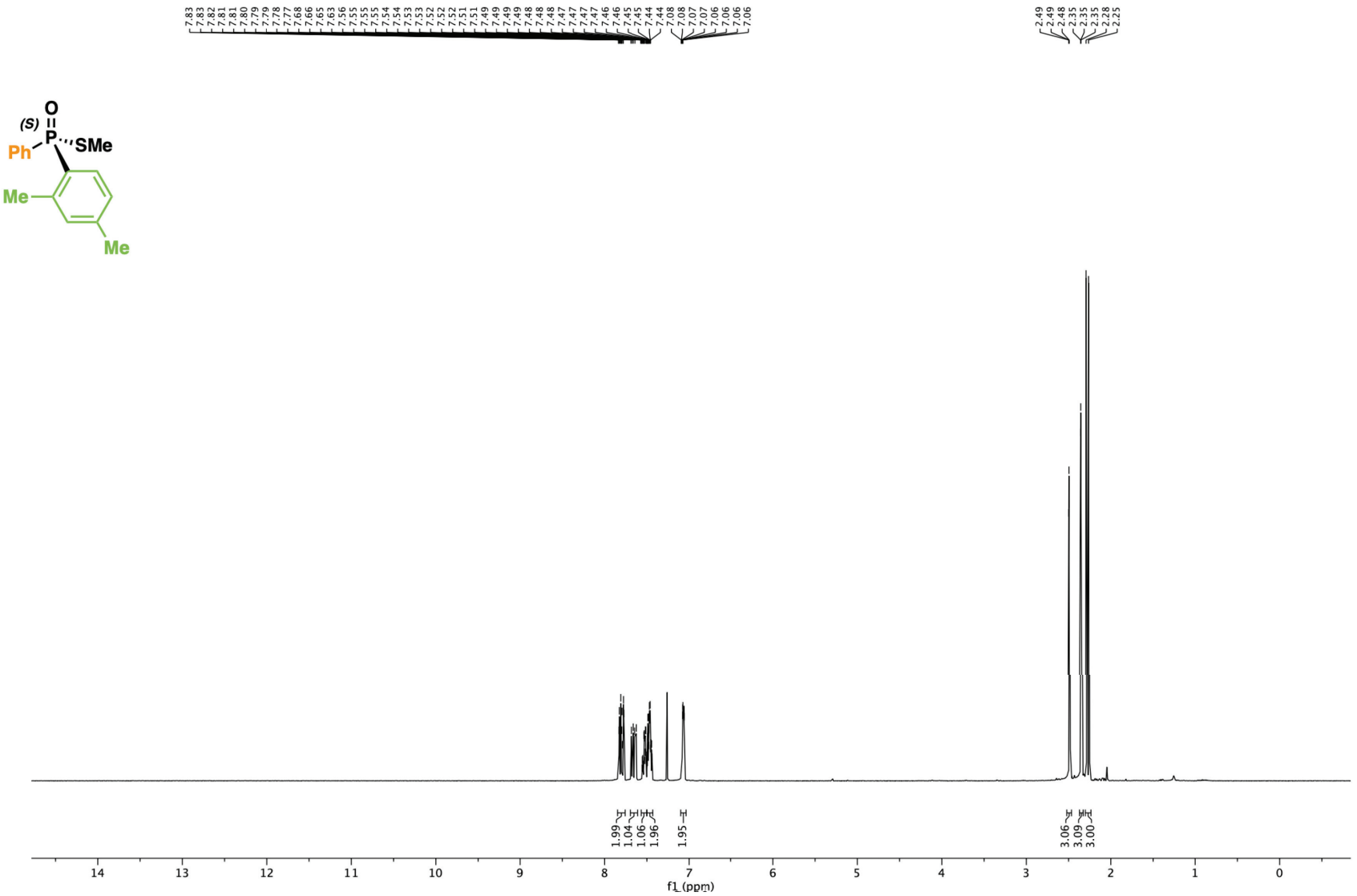
Compound 1.11a ^{13}C NMR



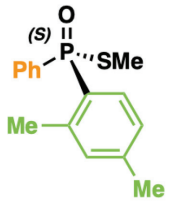
Compound 1.11a ^{31}P NMR



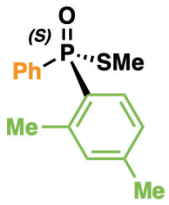
Compound 1.20a ^{1}H NMR



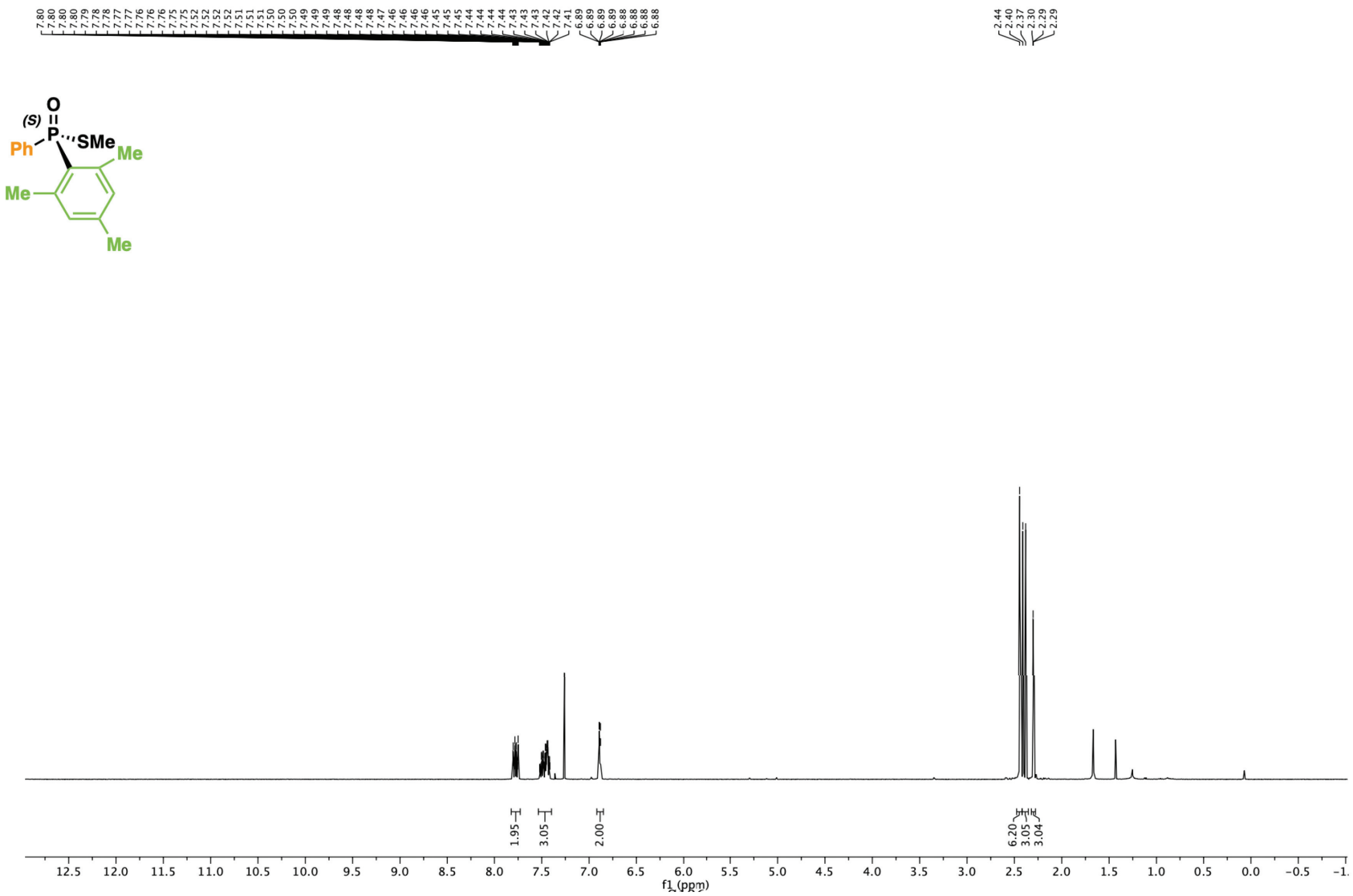
Compound 1.20a ^{13}C NMR



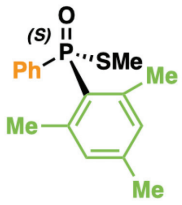
Compound 1.20a ^{31}P NMR



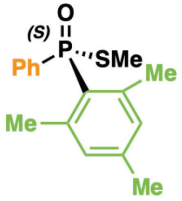
Compound 1.21a ^{1}H NMR



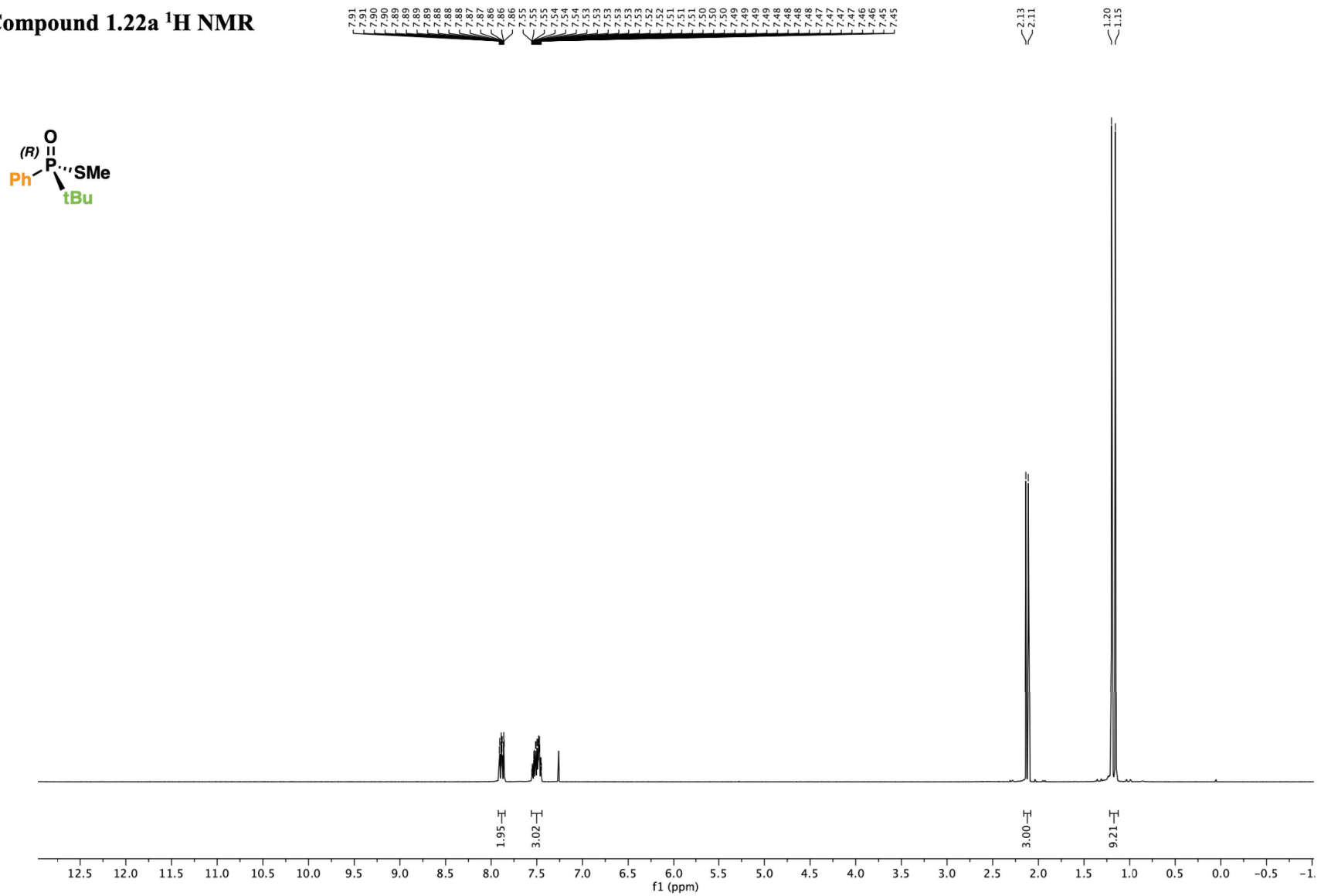
Compound 1.21a ^{13}C NMR



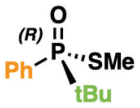
Compound 1.21a ^{31}P NMR



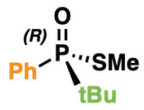
Compound 1.22a ^{1}H NMR



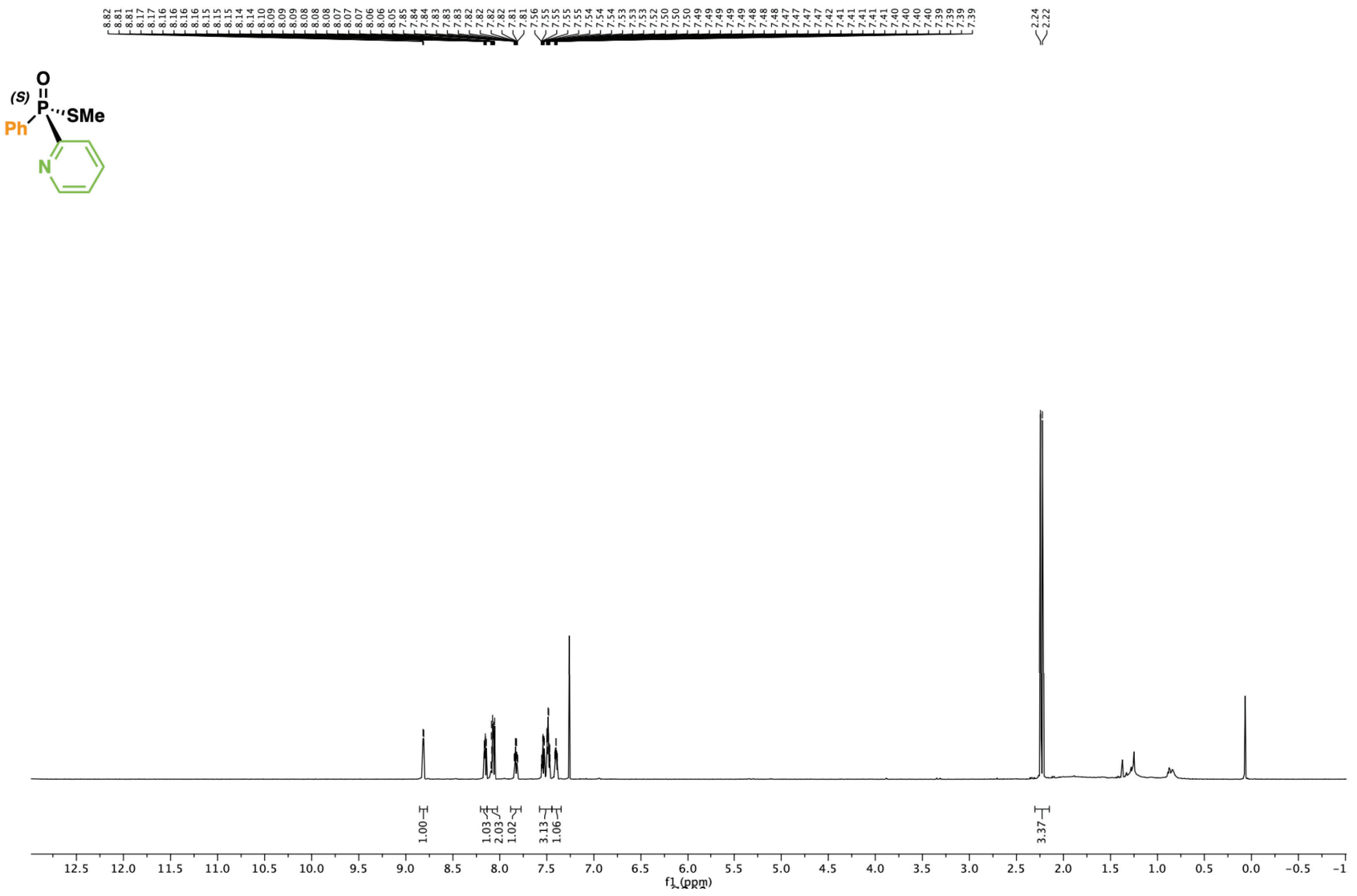
Compound 1.22a ^{13}C NMR



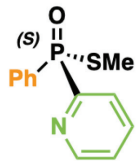
Compound 1.22a ^{31}P NMR



Compound 1.23a ^{1}H NMR



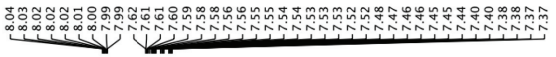
Compound 1.23a ^{13}C NMR

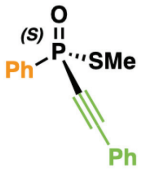


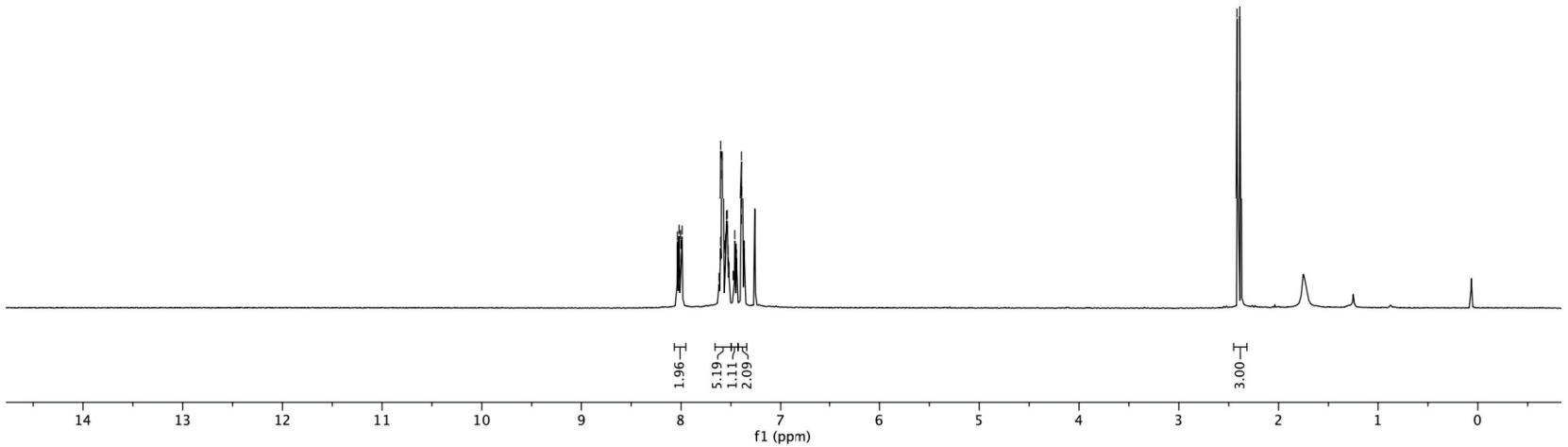
Compound 1.23a ^{31}P NMR



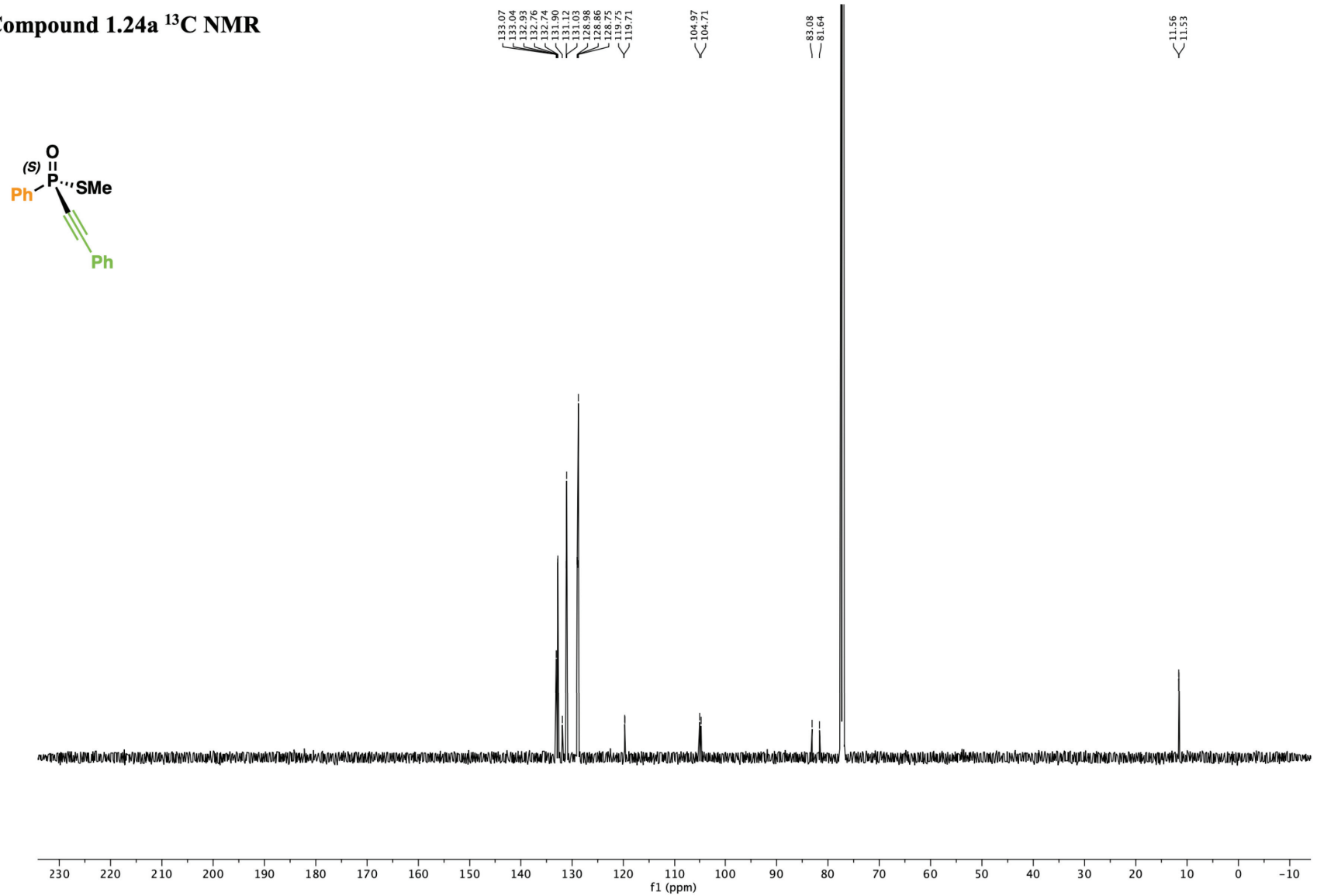
Compound 1.24a ^{1}H NMR



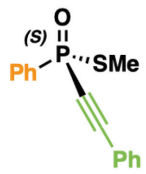




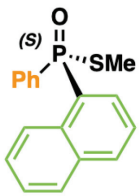
Compound 1.24a ^{13}C NMR

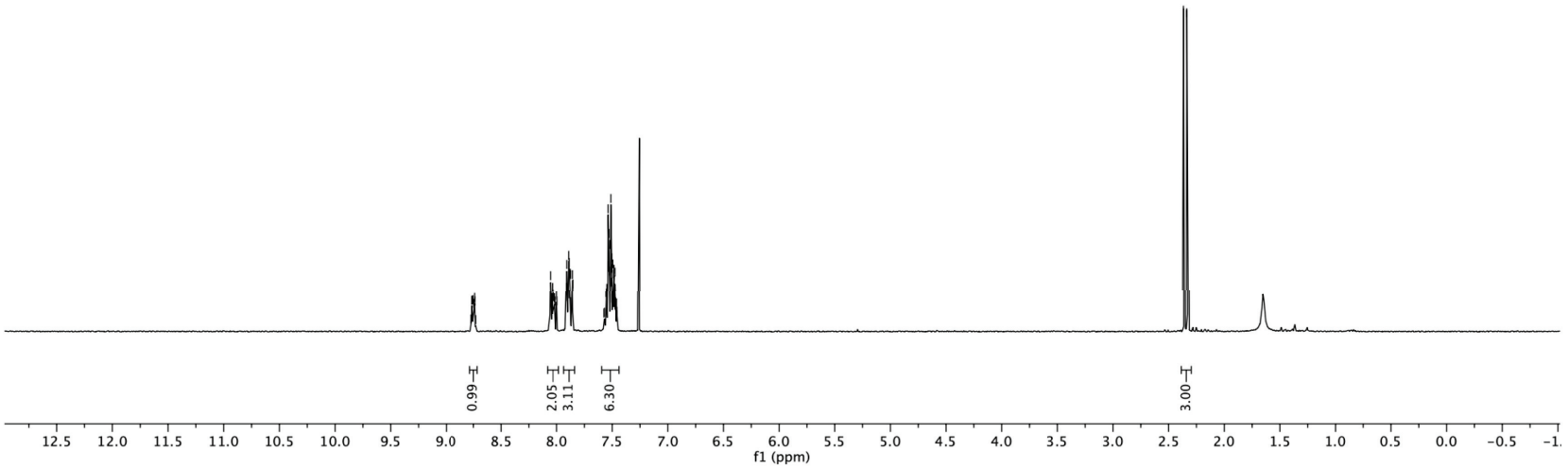


Compound 1.24a ^{31}P NMR

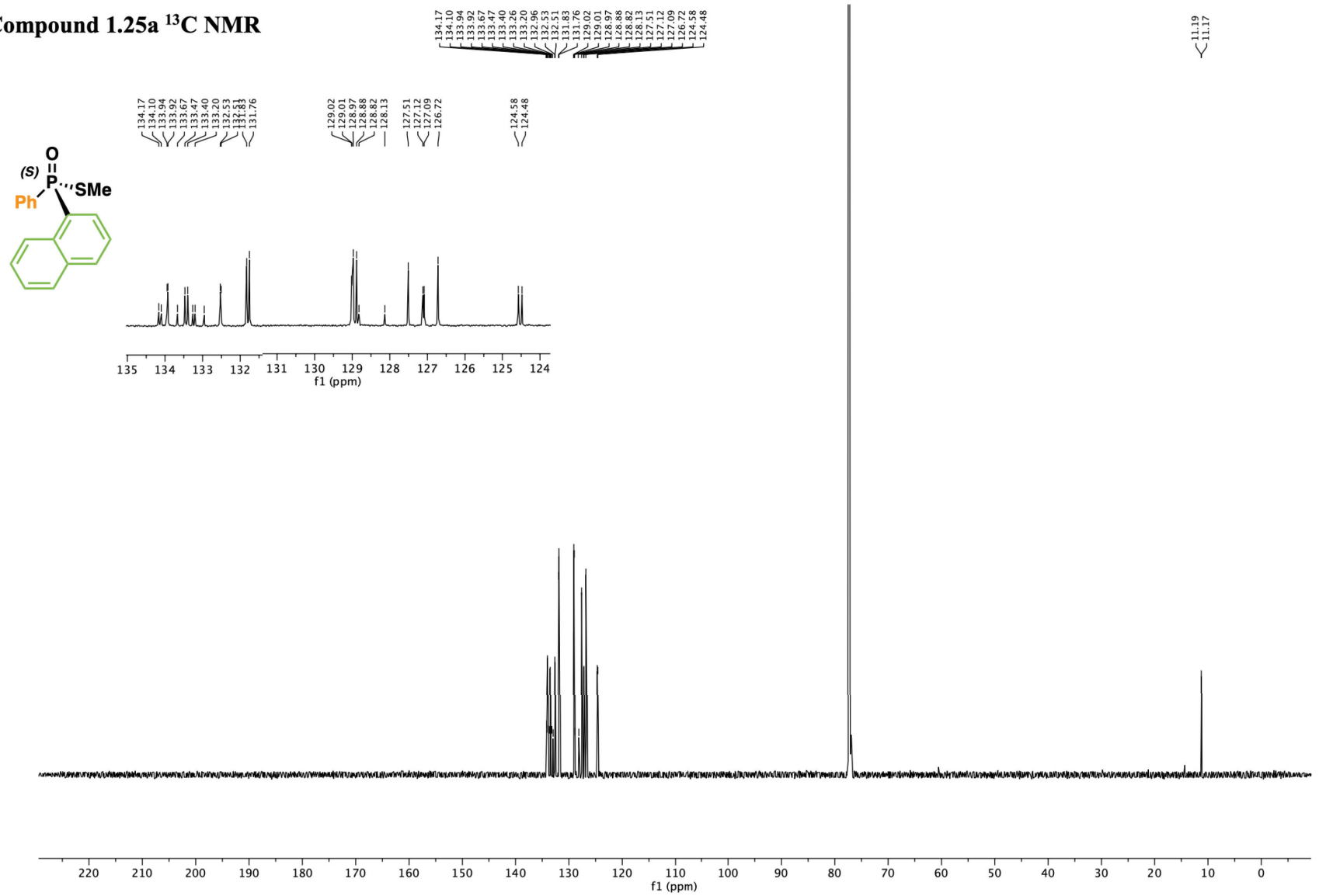


Compound 1.25a ^{1}H NMR

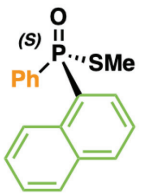


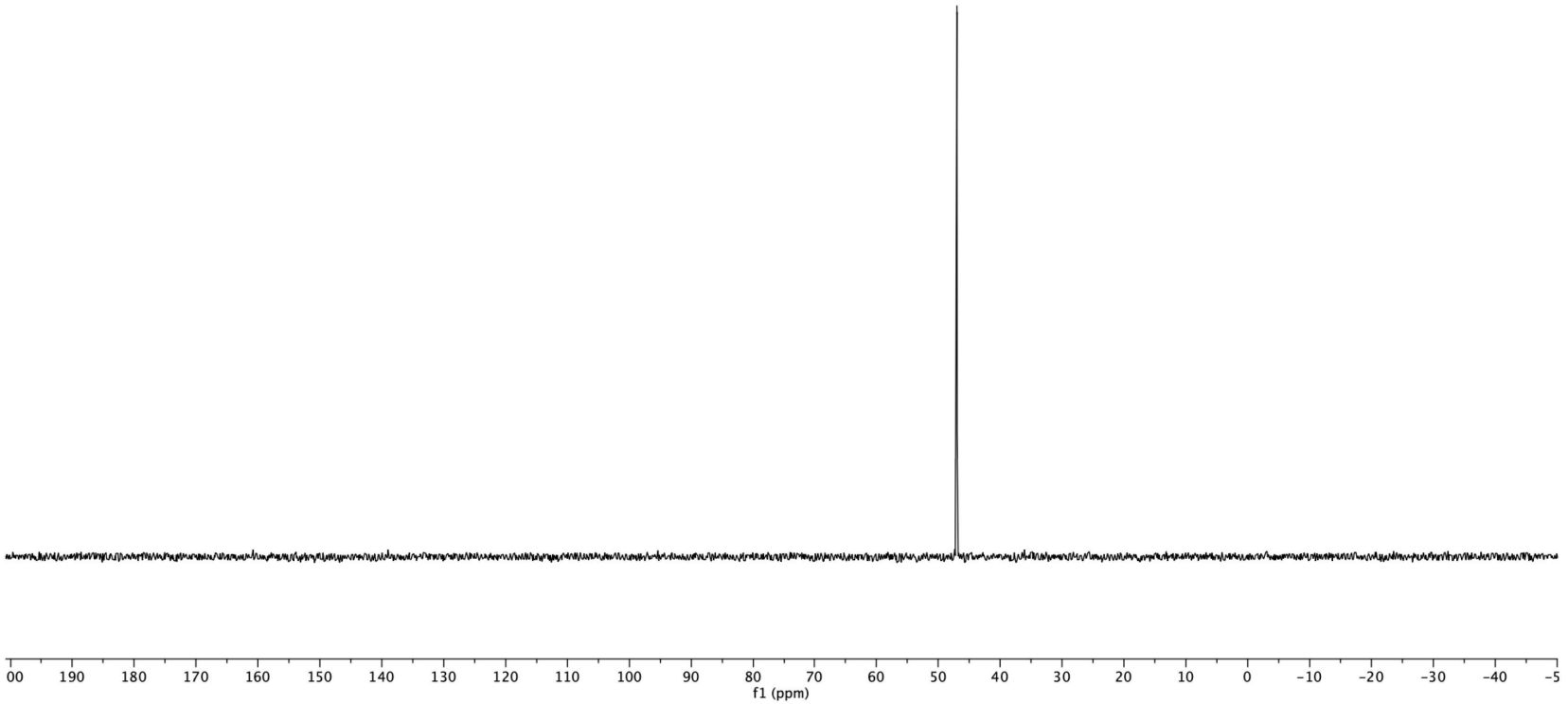


Compound 1.25a ^{13}C NMR

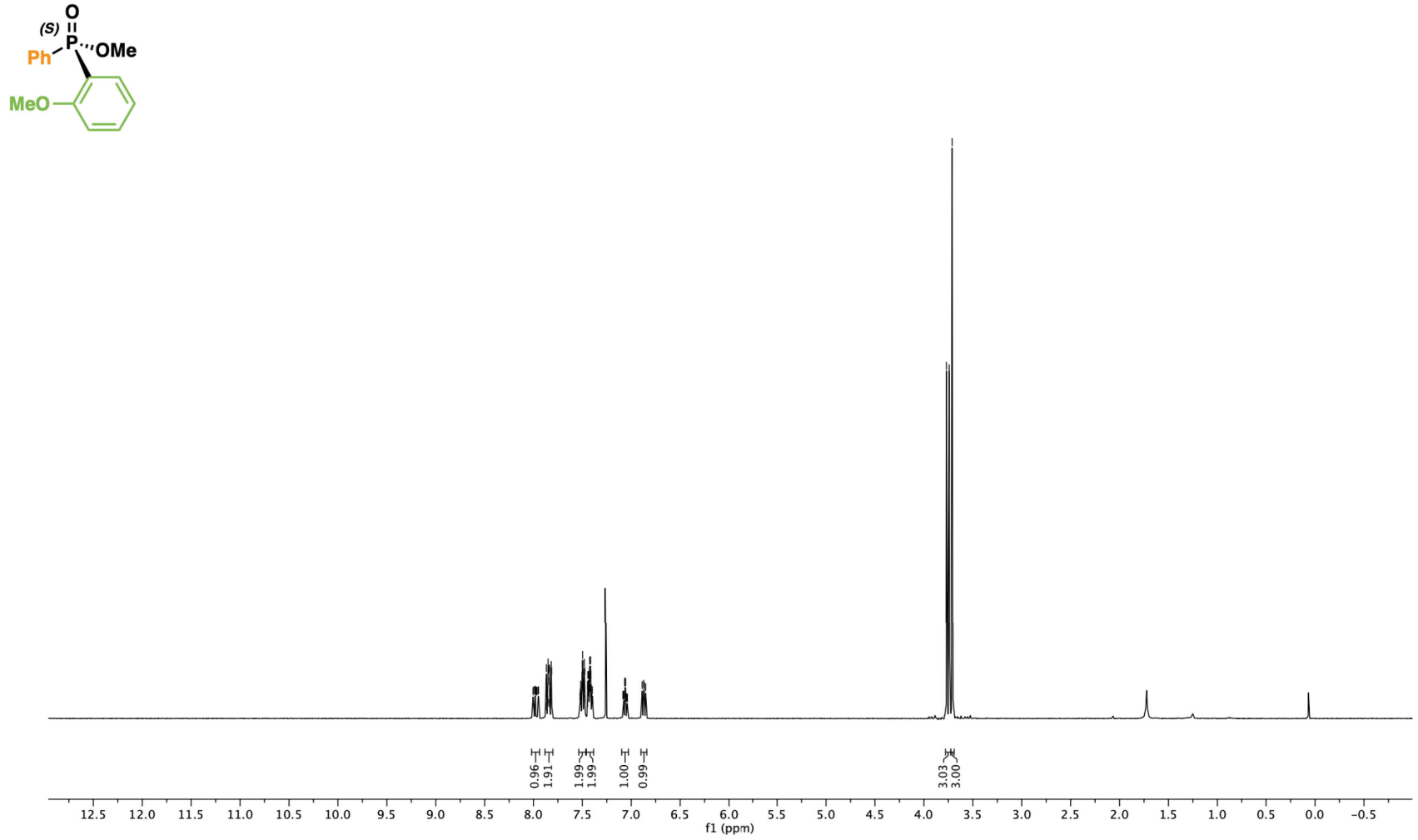


Compound 1.25a ^{31}P NMR

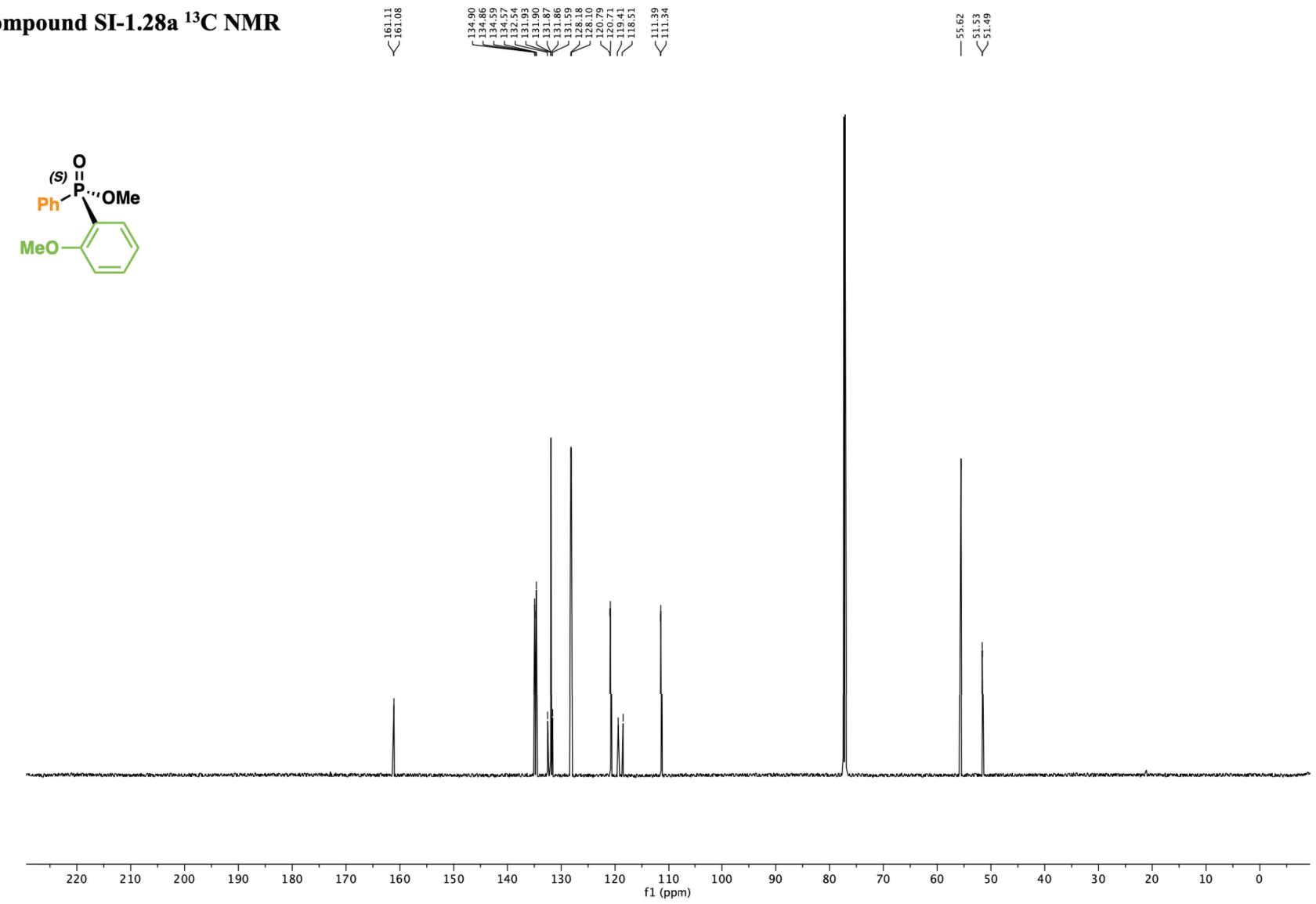




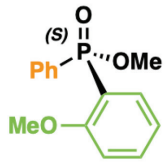
Compound SI-1.28a ^{1}H NMR



Compound SI-1.28a ^{13}C NMR

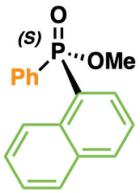


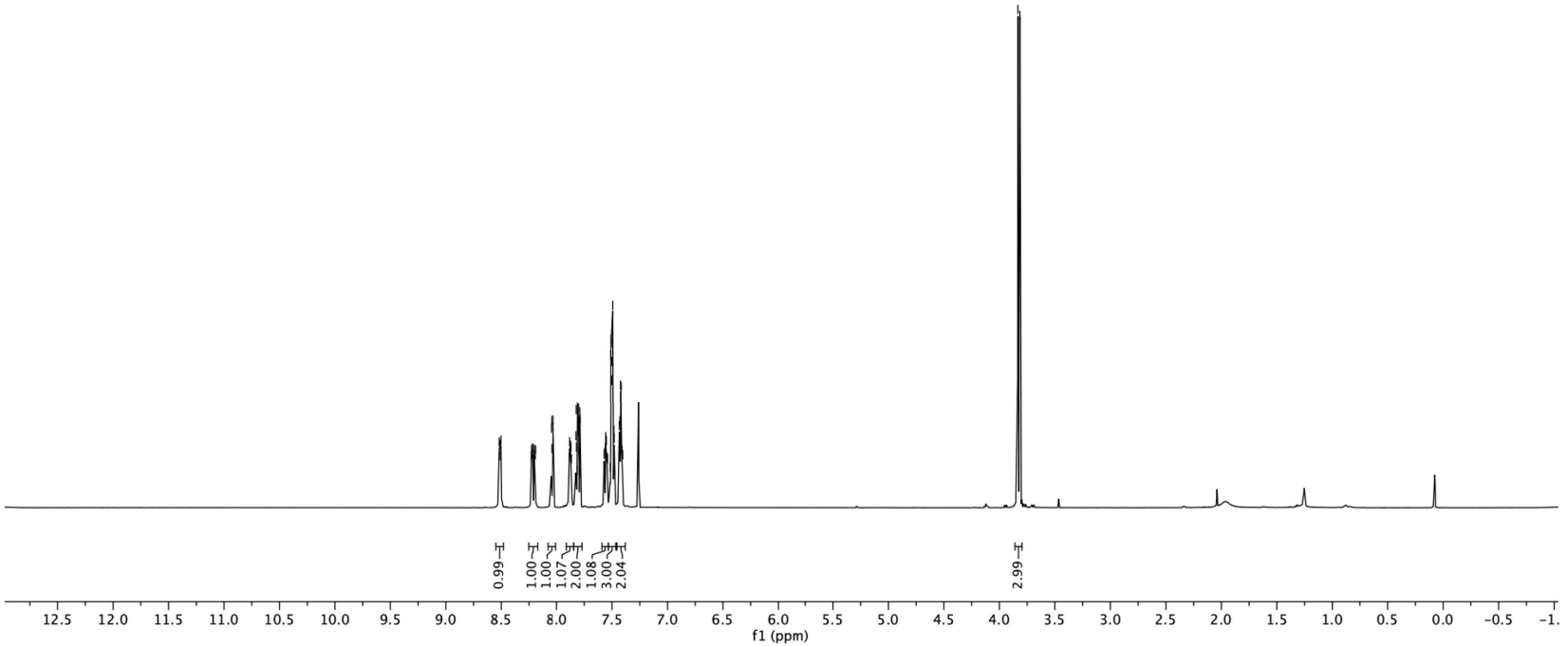
Compound SI-1.28a ^{31}P NMR



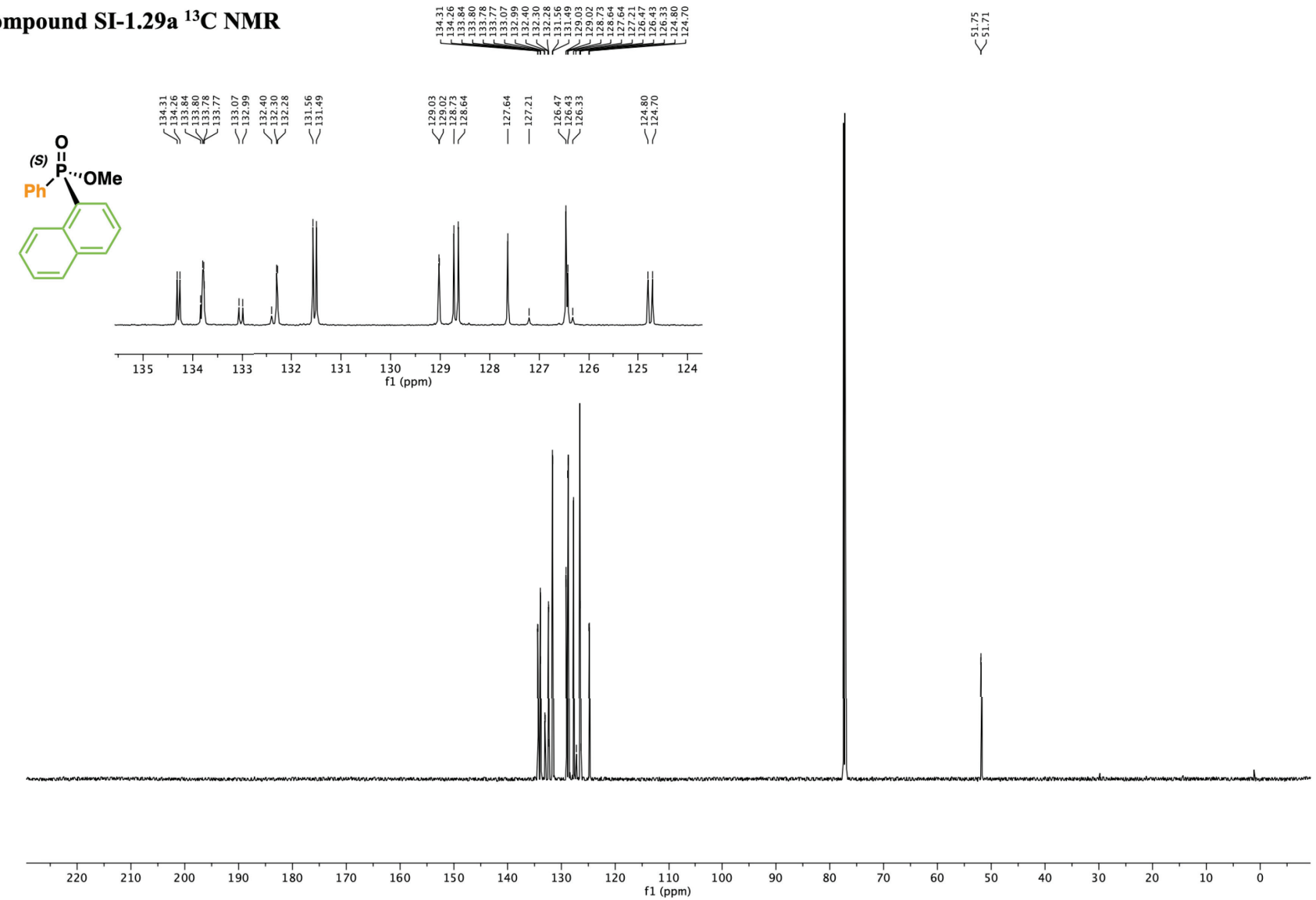
Compound SI-1.29a ^{1}H NMR



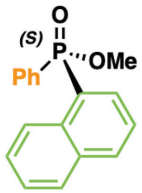




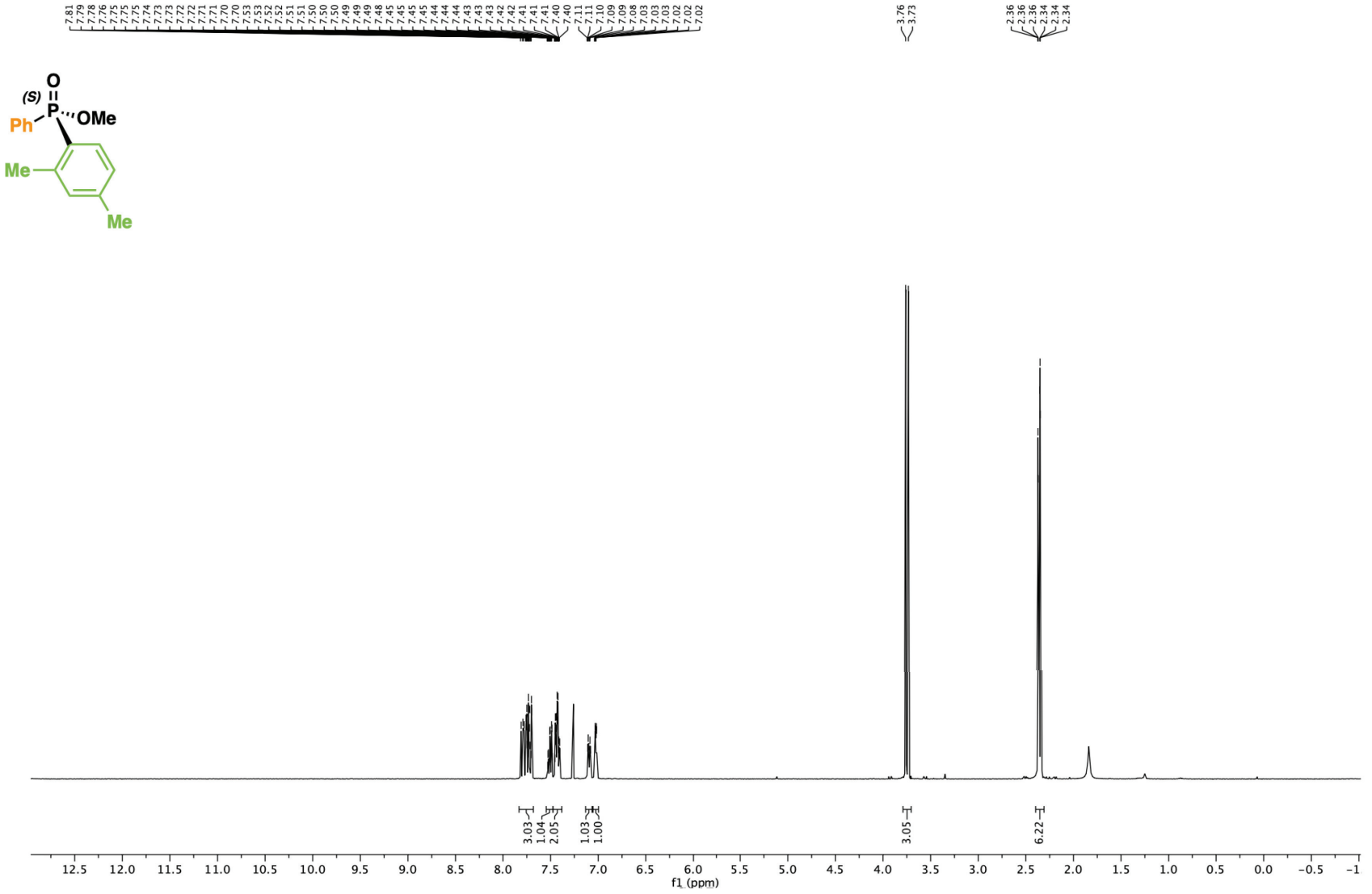
Compound SI-1.29a ^{13}C NMR



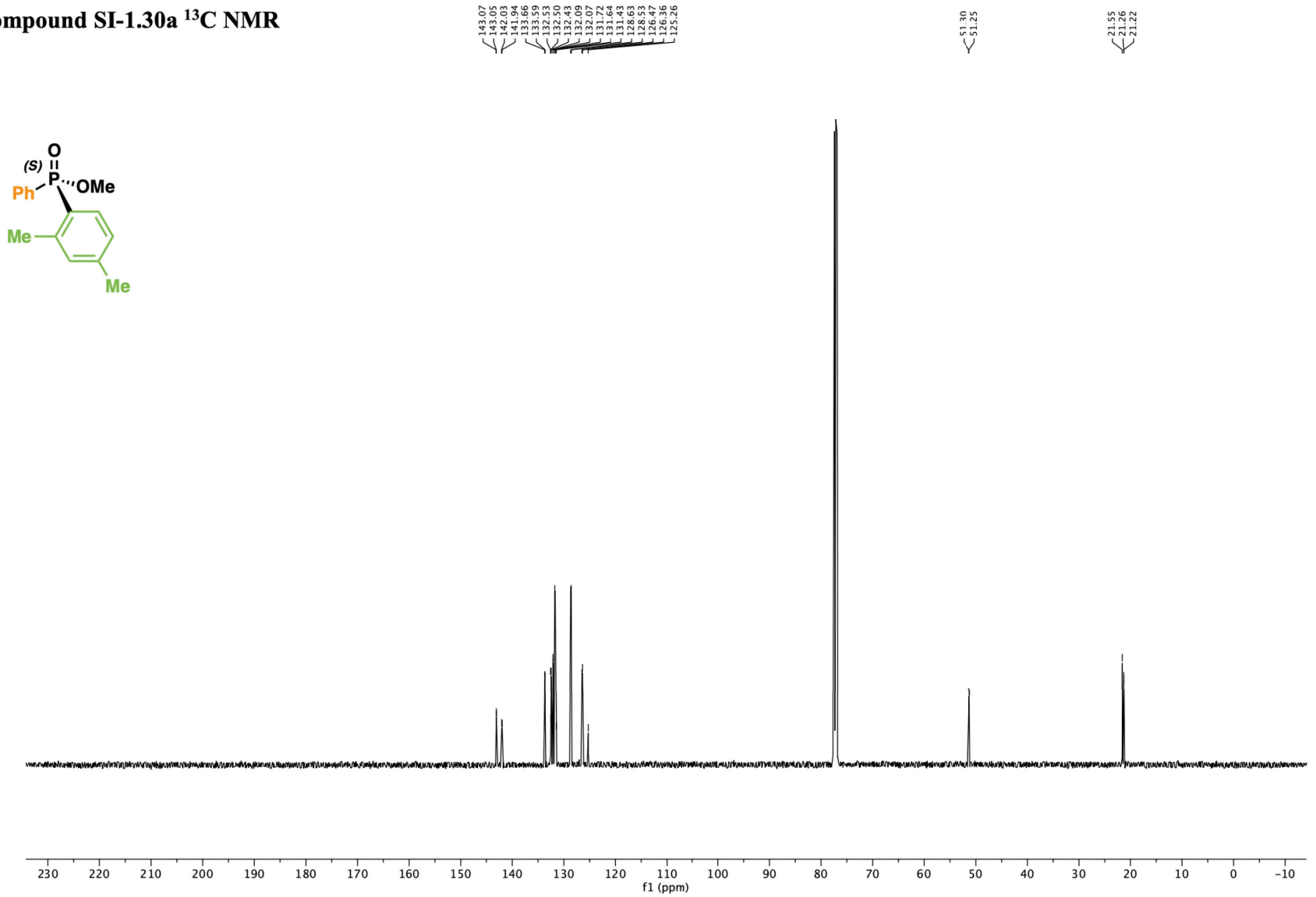
Compound SI-1.29a ^{31}P NMR



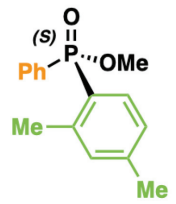
Compound SI-1.30a ^{1}H NMR



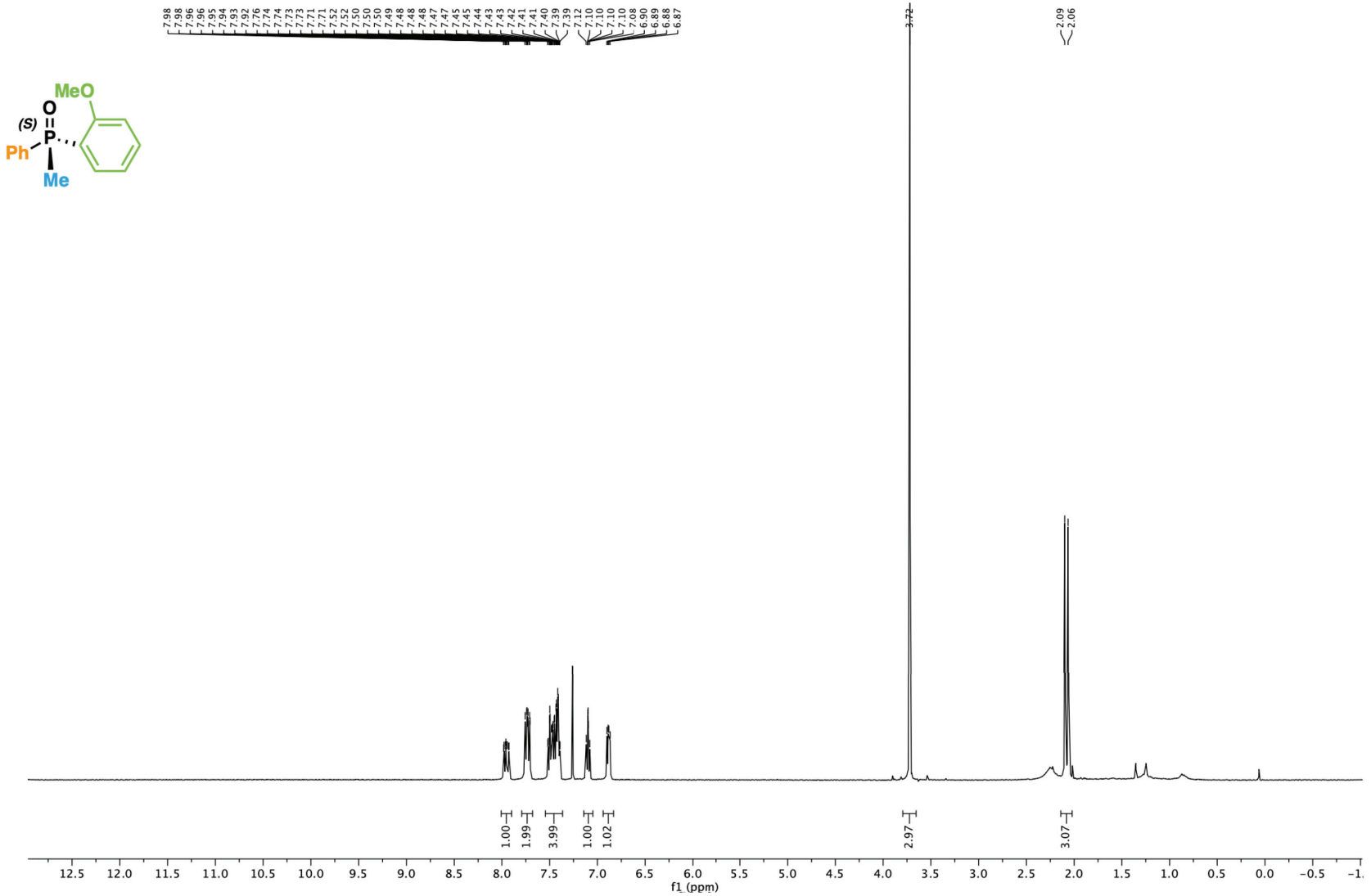
Compound SI-1.30a ^{13}C NMR



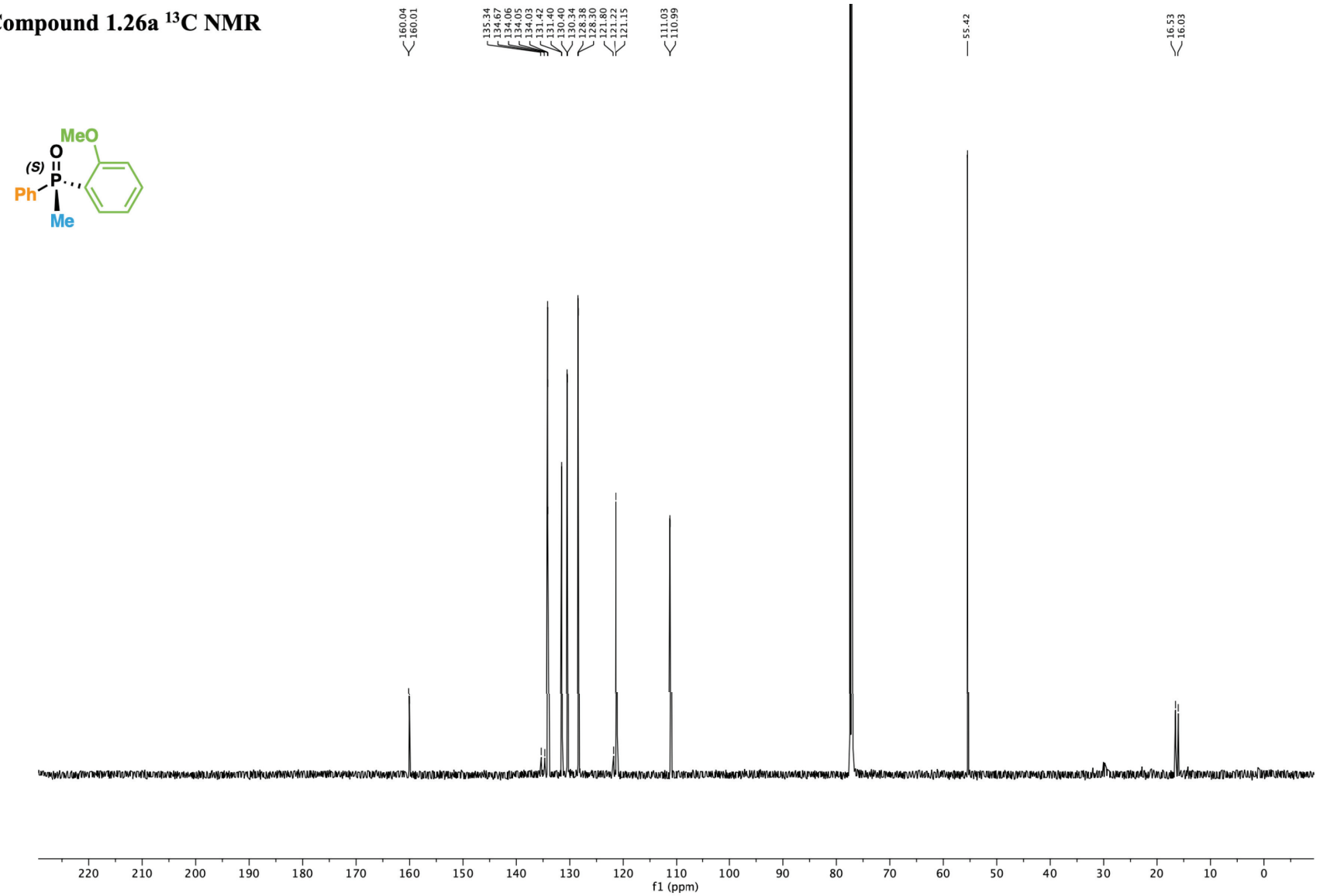
Compound SI-1.30a ^{31}P NMR



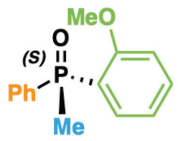
Compound 1.26a ^{1}H NMR



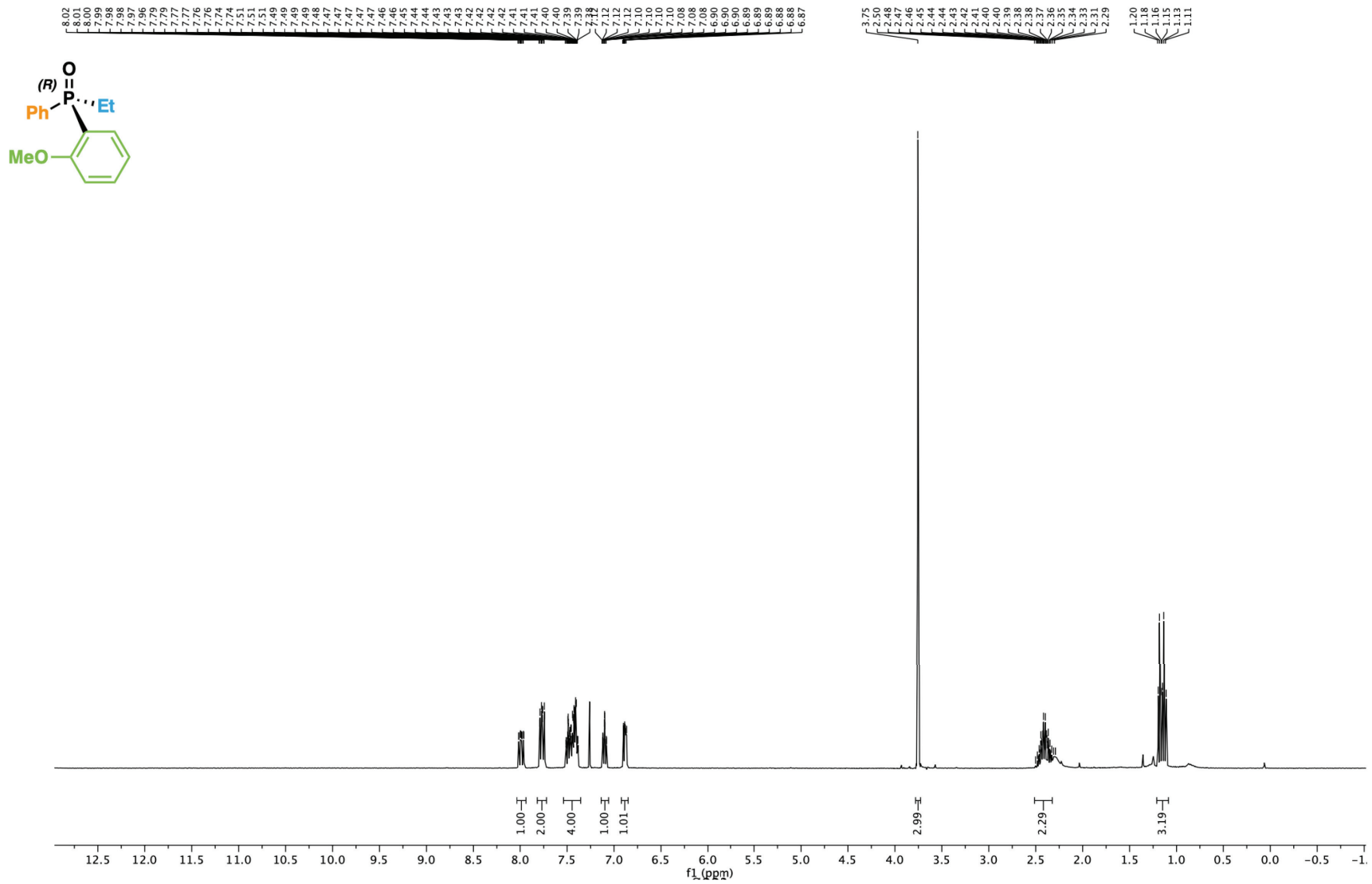
Compound 1.26a ^{13}C NMR



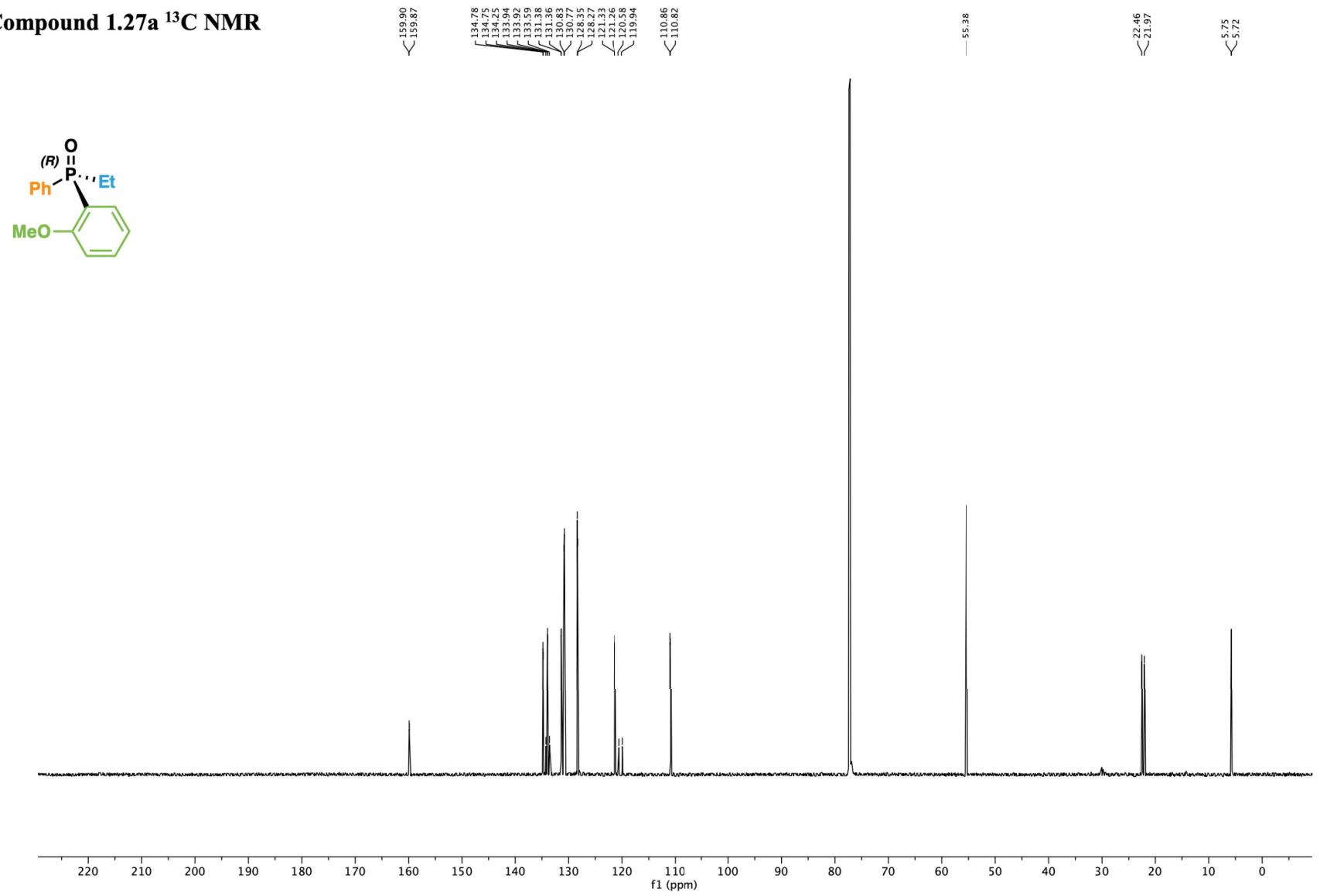
Compound 1.26a ^{31}P NMR



Compound 1.27a ^{1}H NMR



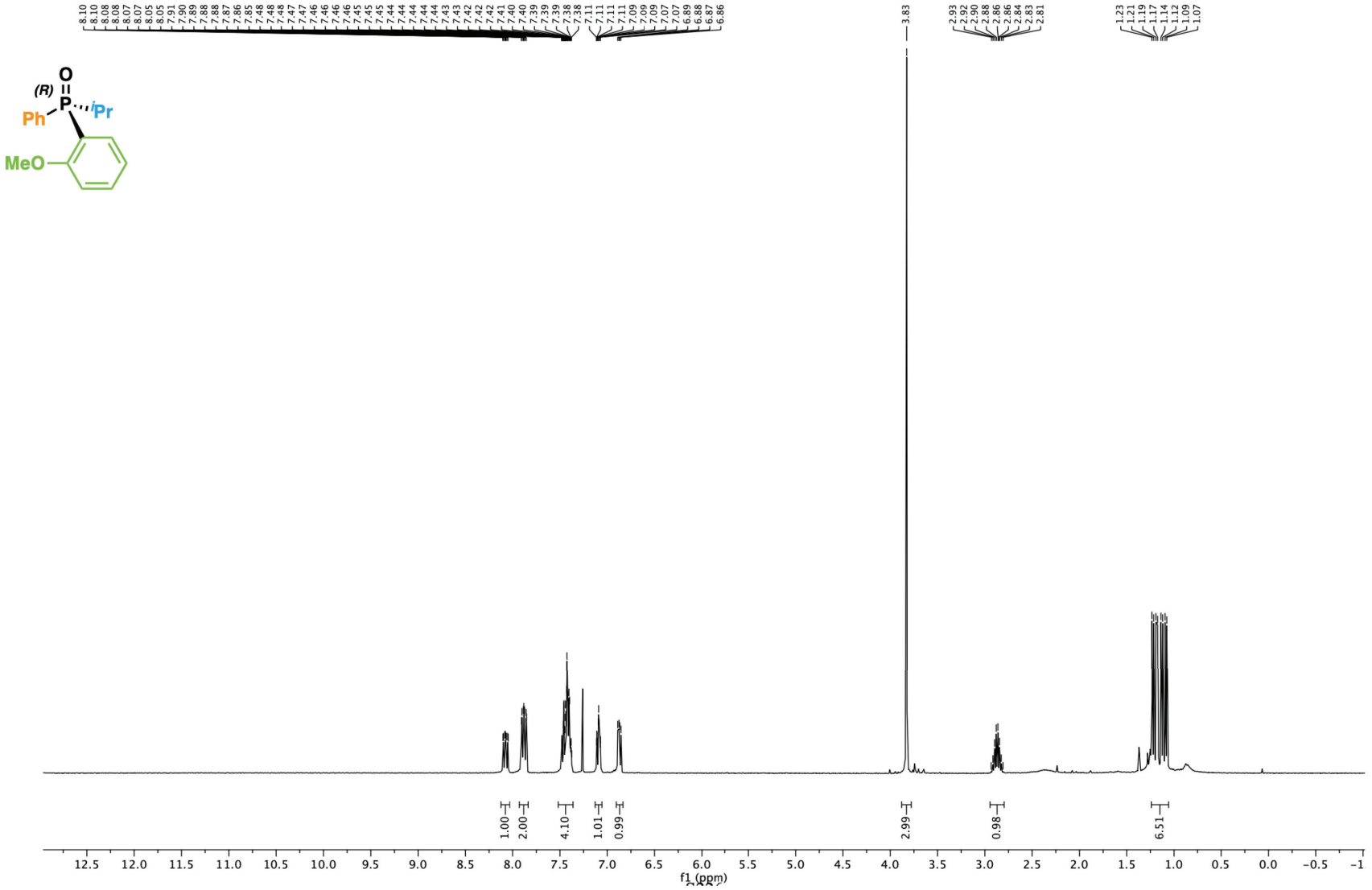
Compound 1.27a ^{13}C NMR



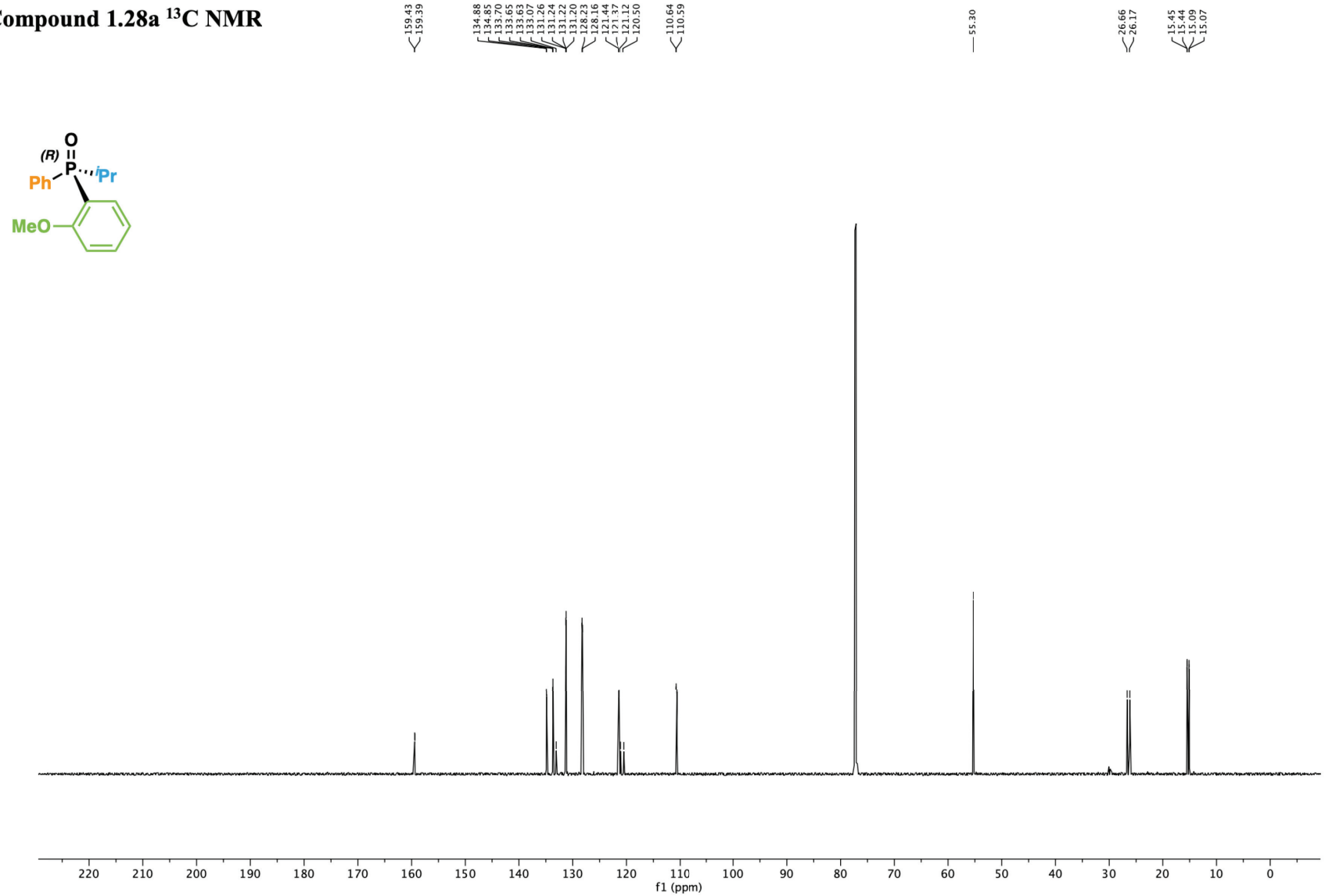
Compound 1.27a ^{31}P NMR



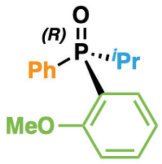
Compound 1.28a ^{1}H NMR



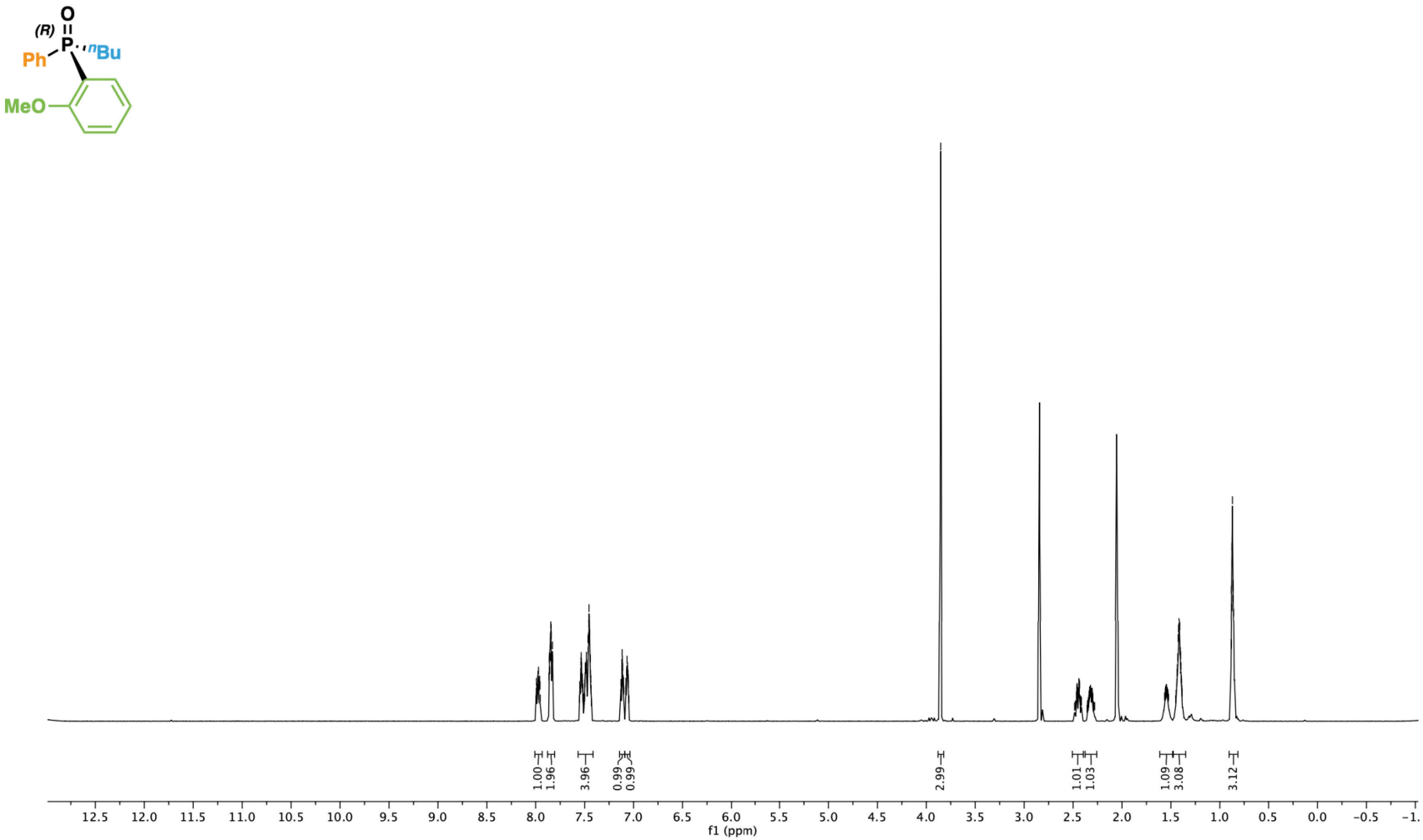
Compound 1.28a ^{13}C NMR



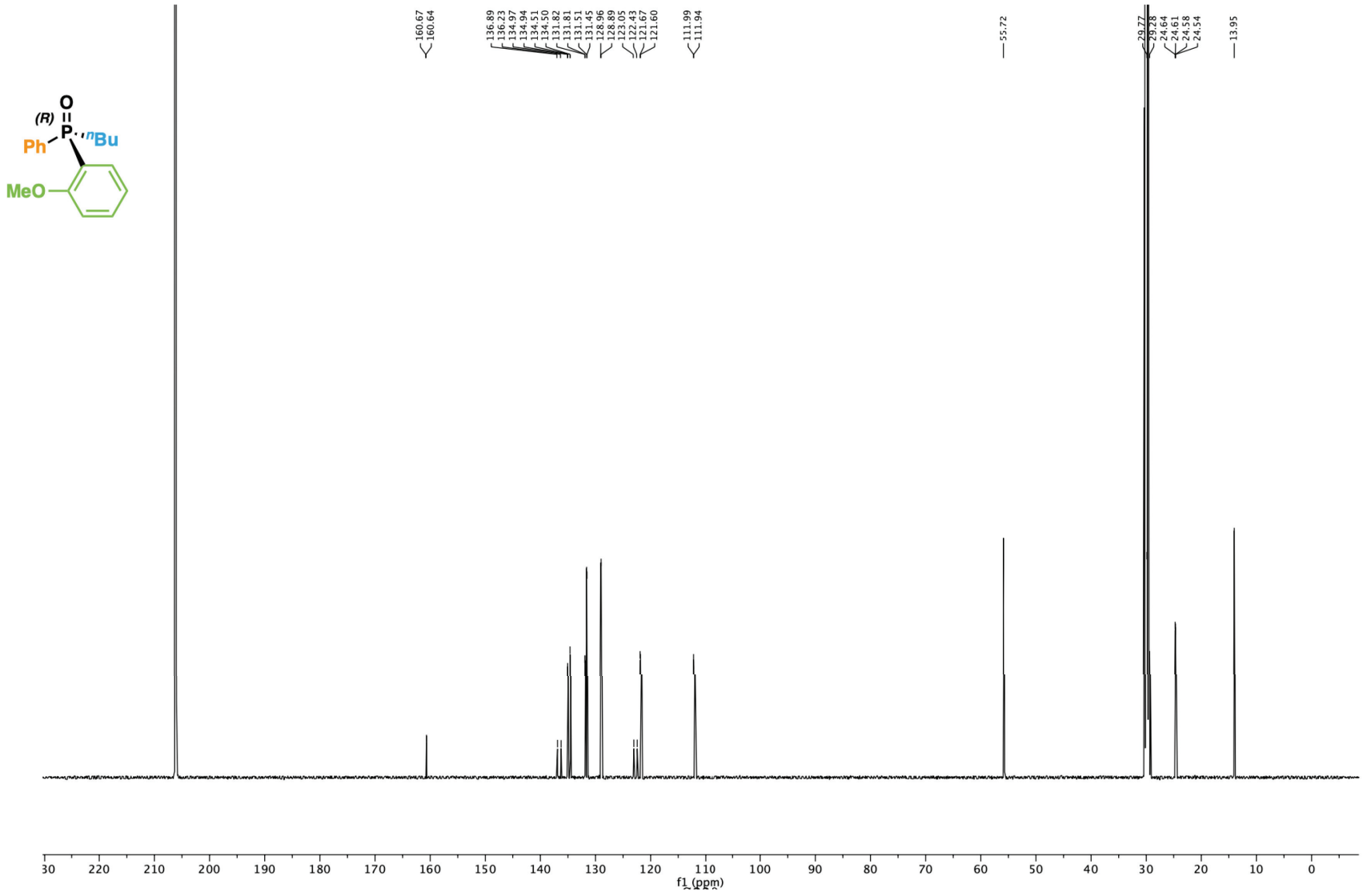
Compound 1.28a ^{31}P NMR



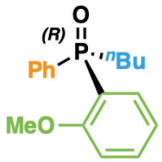
Compound 1.29a ^{1}H NMR



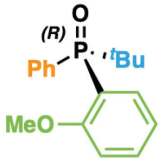
Compound 1.29a ^{13}C NMR



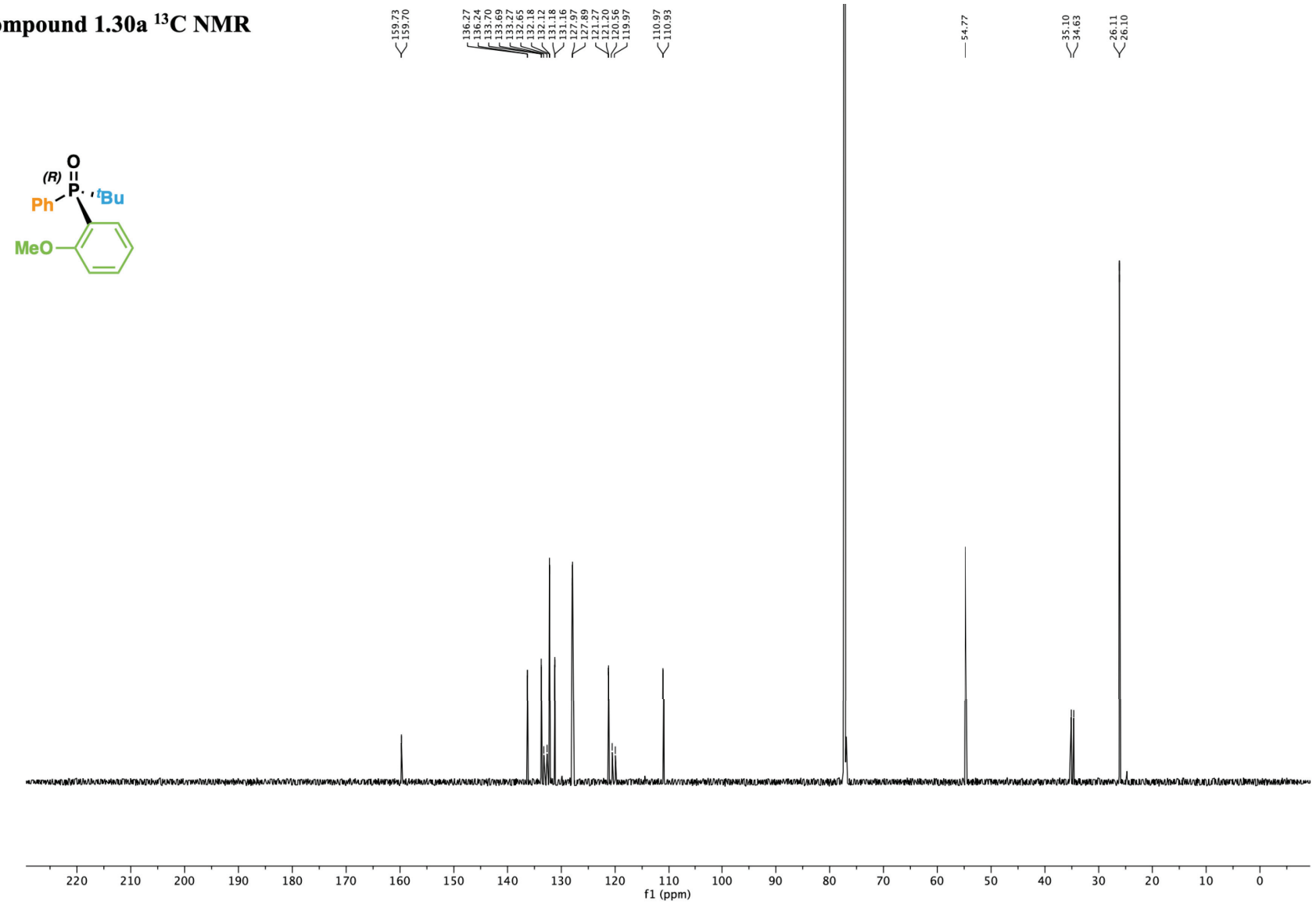
Compound 1.29a ^{31}P NMR



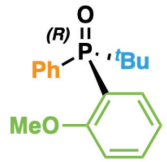
Compound 1.30a ^{1}H NMR



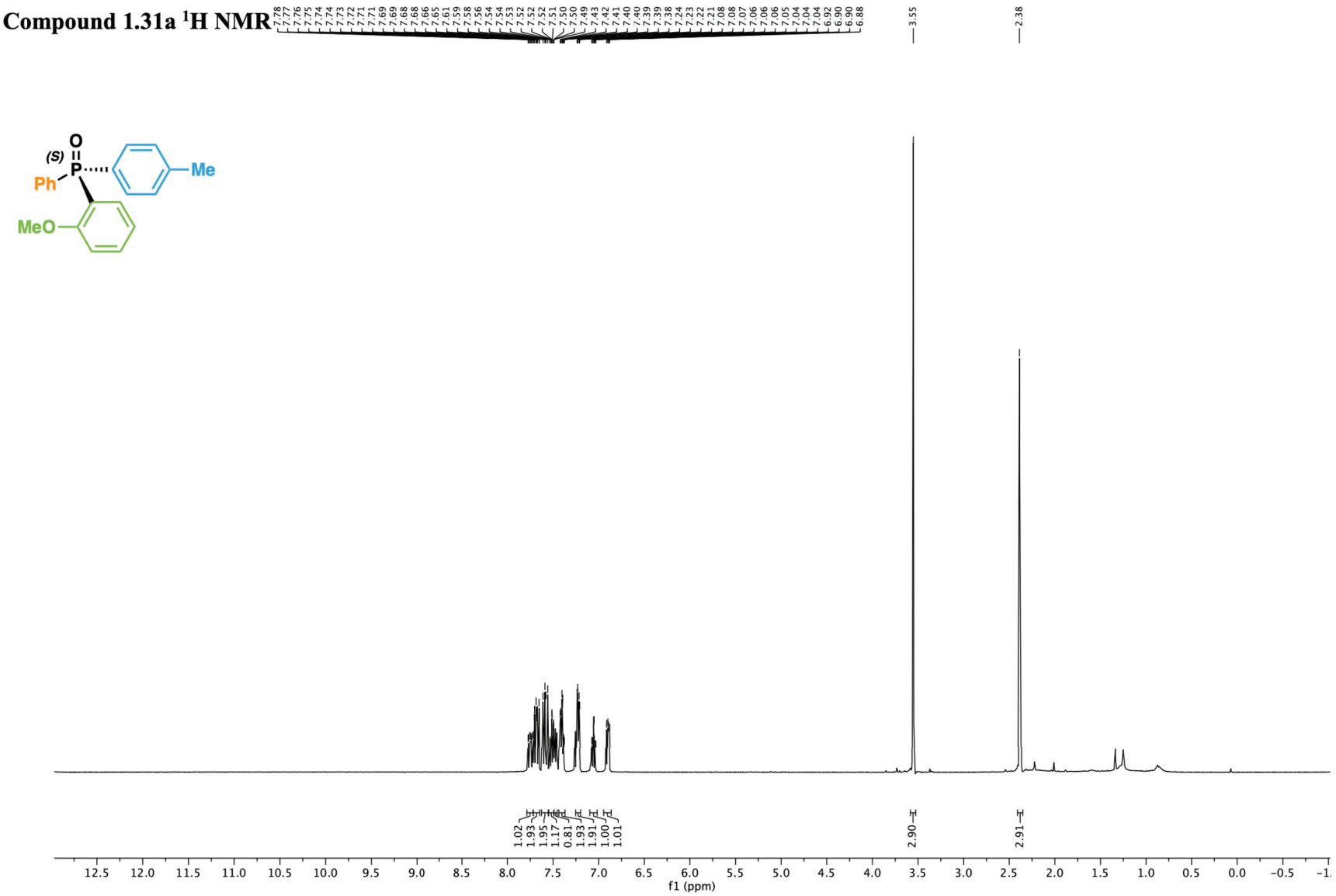
Compound 1.30a ^{13}C NMR



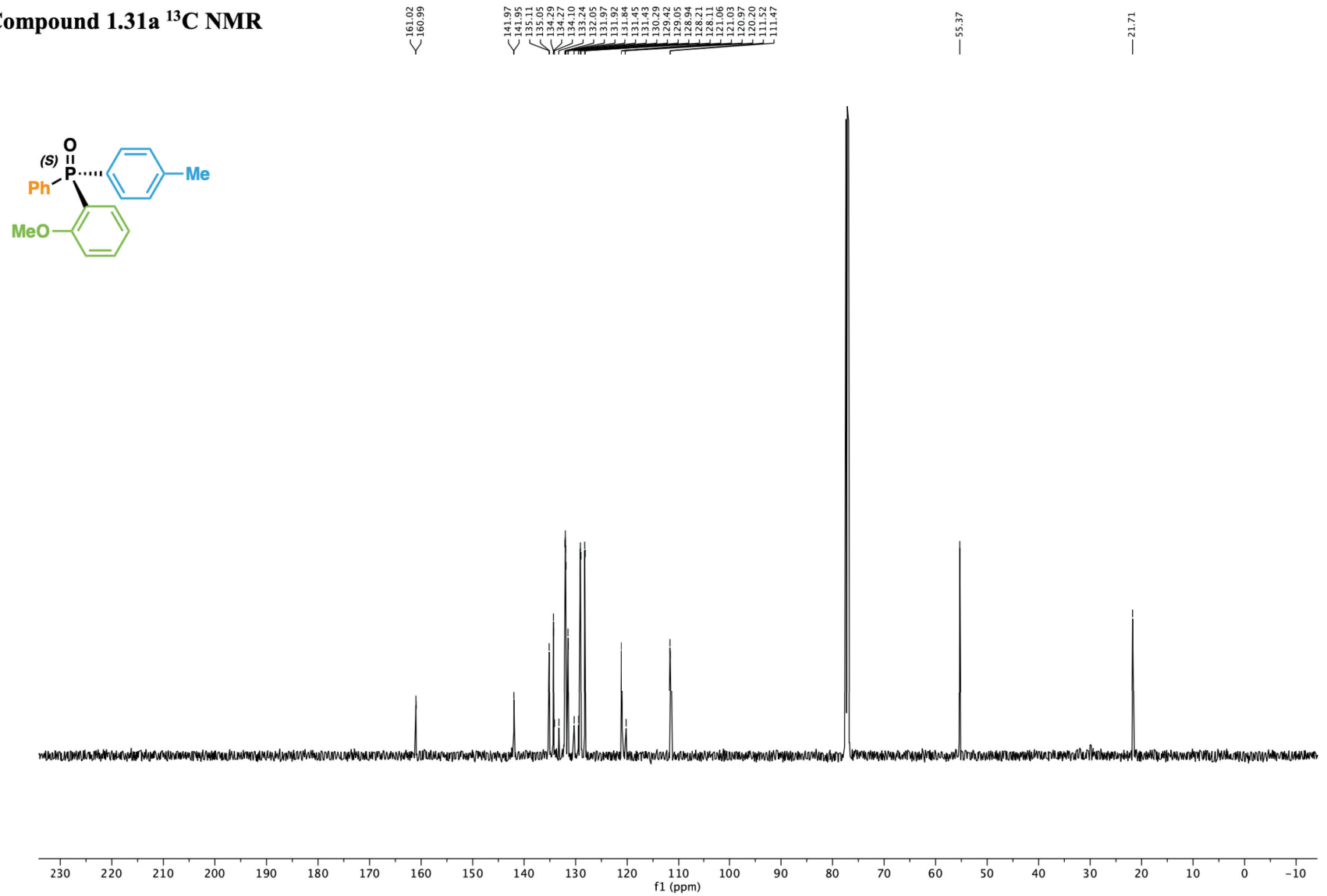
Compound 1.30a ^{31}P NMR



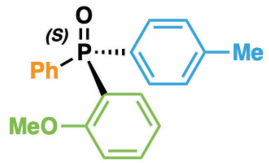
Compound 1.31a ^{1}H NMR



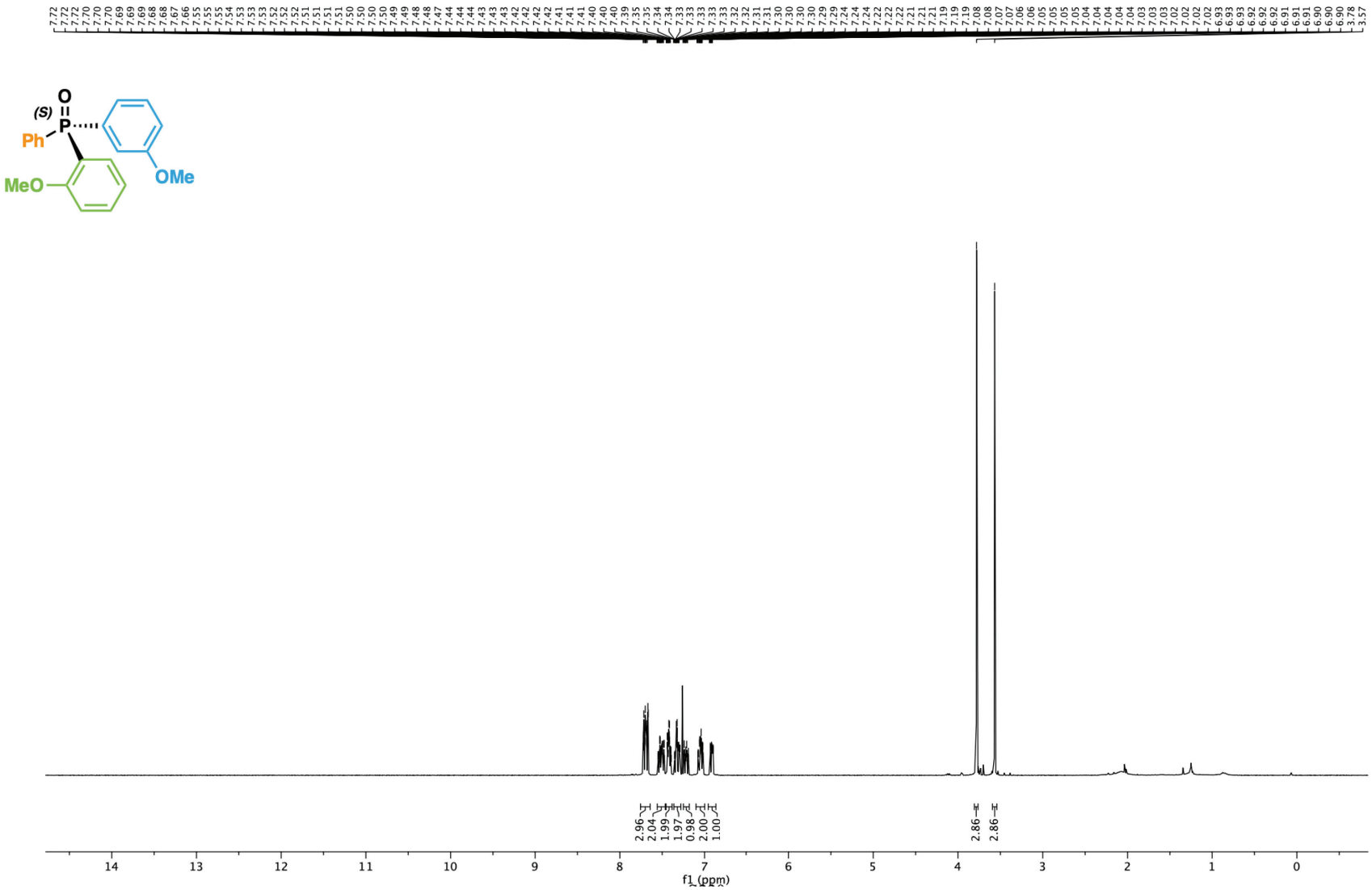
Compound 1.31a ^{13}C NMR



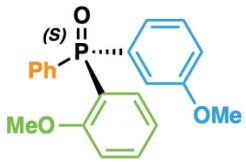
Compound 1.31a ^{31}P NMR



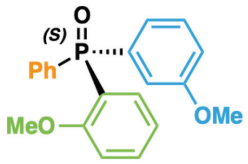
Compound 1.32a ^{1}H NMR



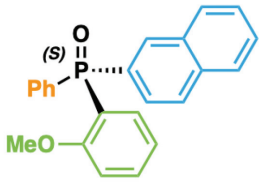
Compound 1.32a ^{13}C NMR

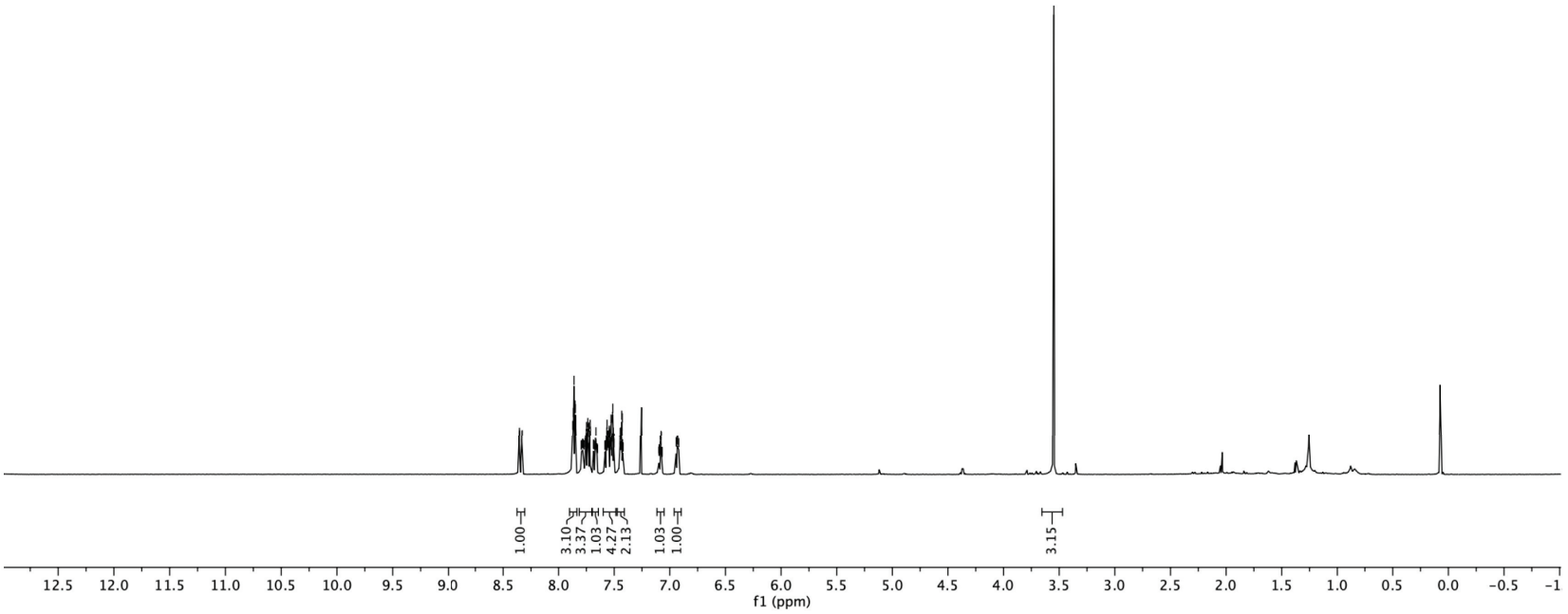


Compound 1.32a ^{31}P NMR

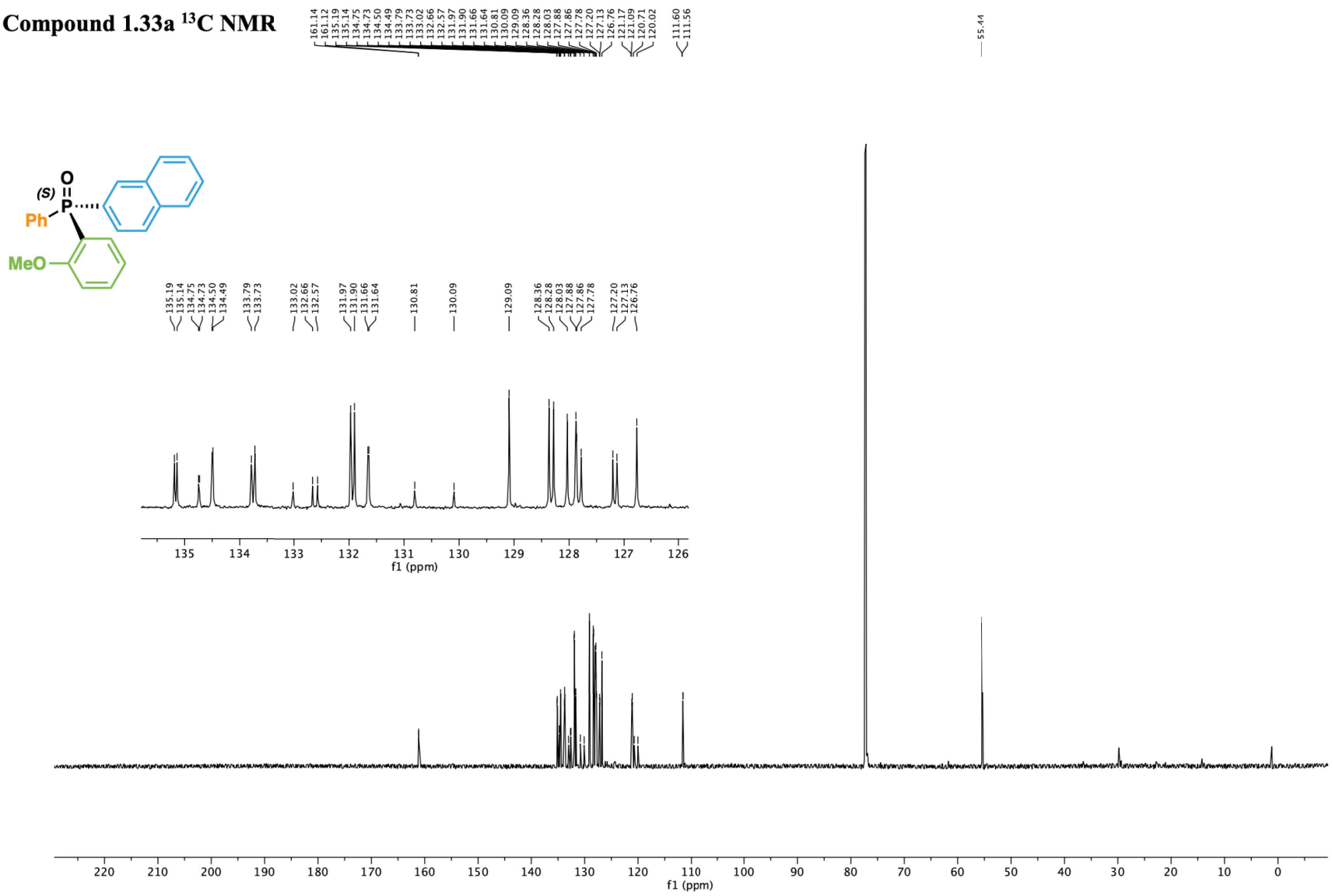


Compound 1.33a ^{1}H NMR

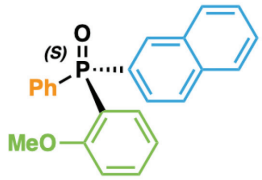




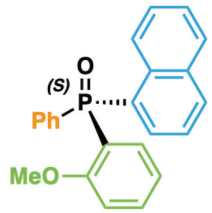
Compound 1.33a ^{13}C NMR



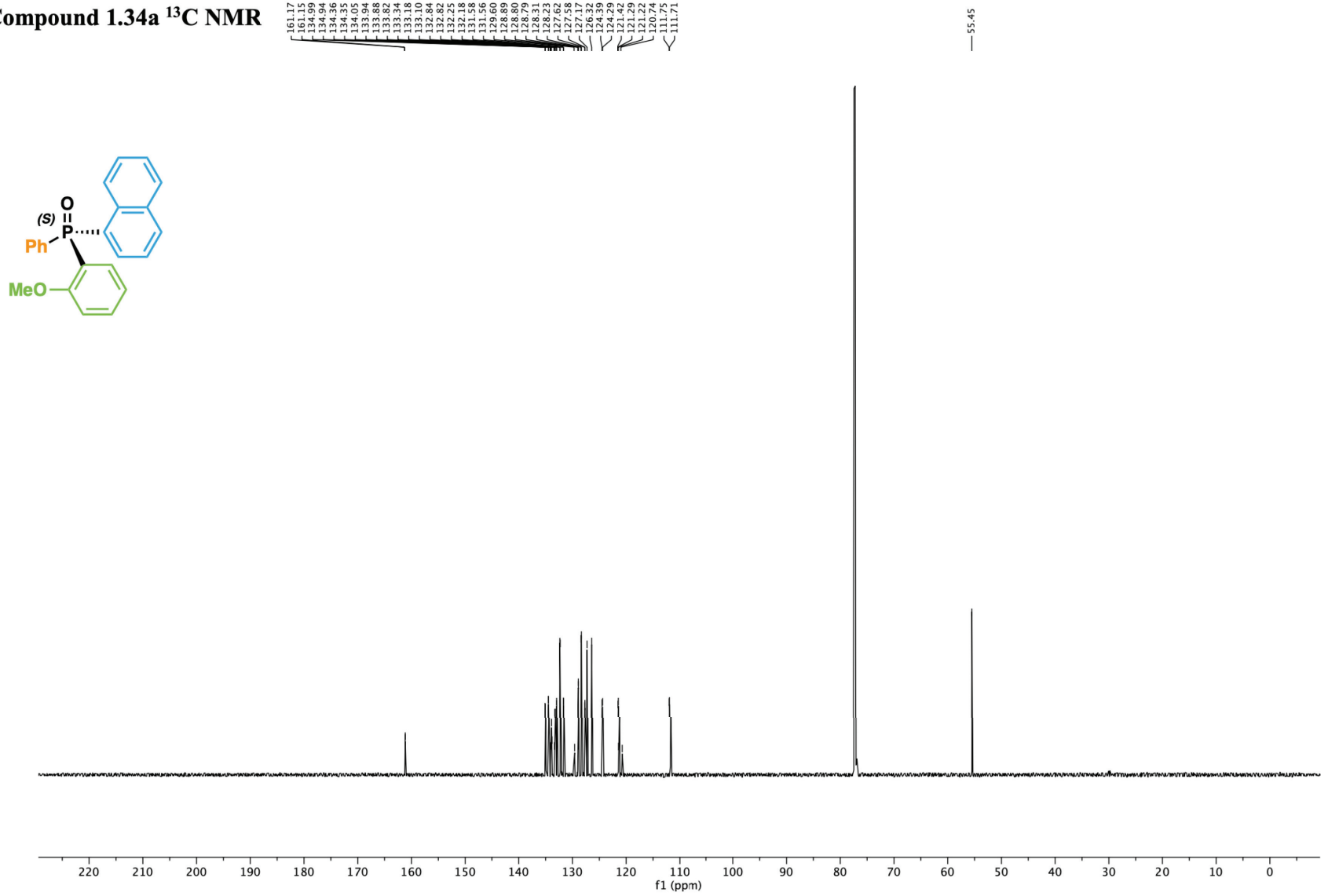
Compound 1.33a ^{31}P NMR



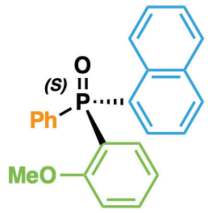
Compound 1.34a ^{1}H NMR



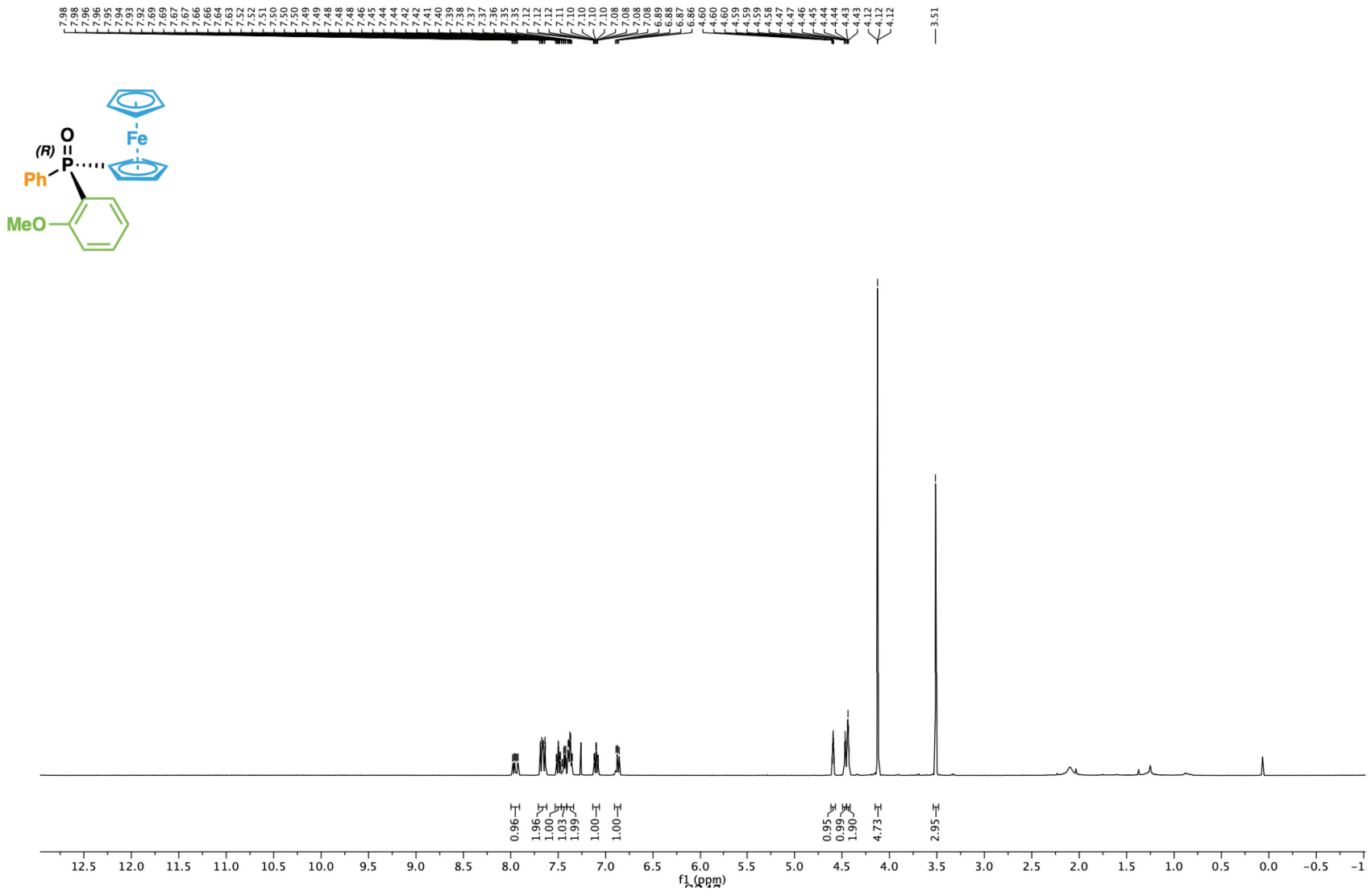
Compound 1.34a ^{13}C NMR



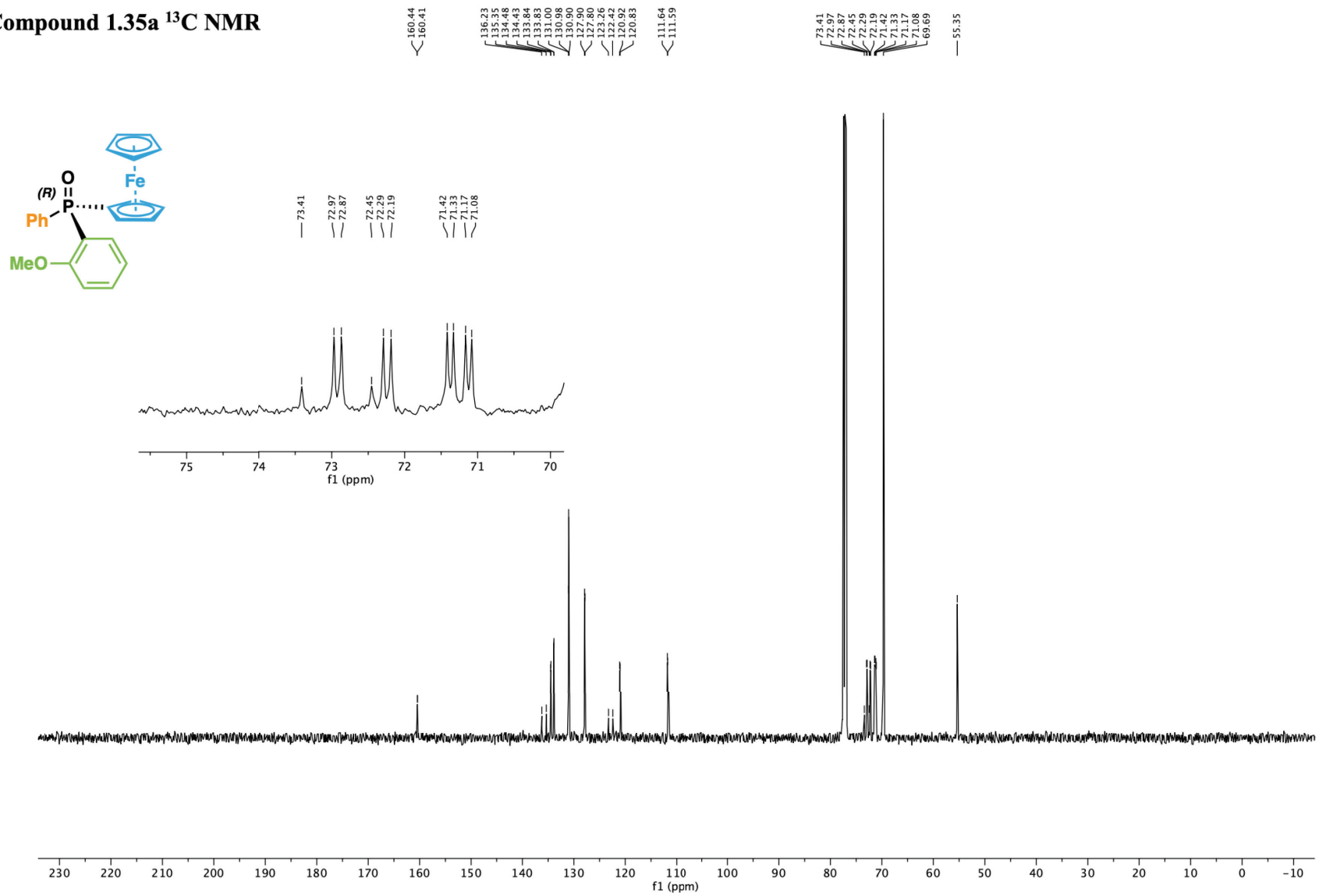
Compound 1.34a ^{31}P NMR



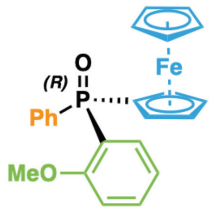
Compound 1.35a ^{1}H NMR



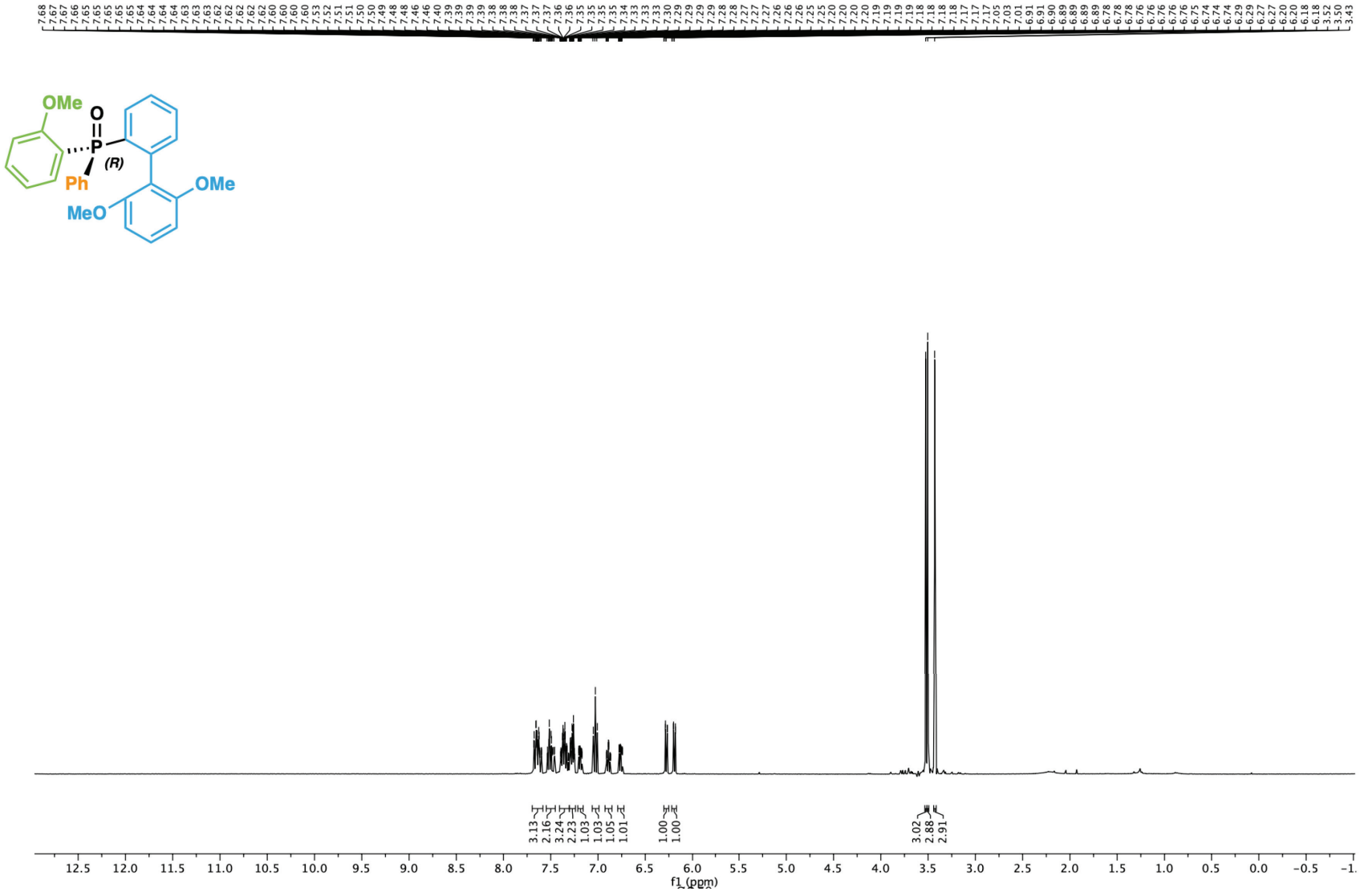
Compound 1.35a ^{13}C NMR



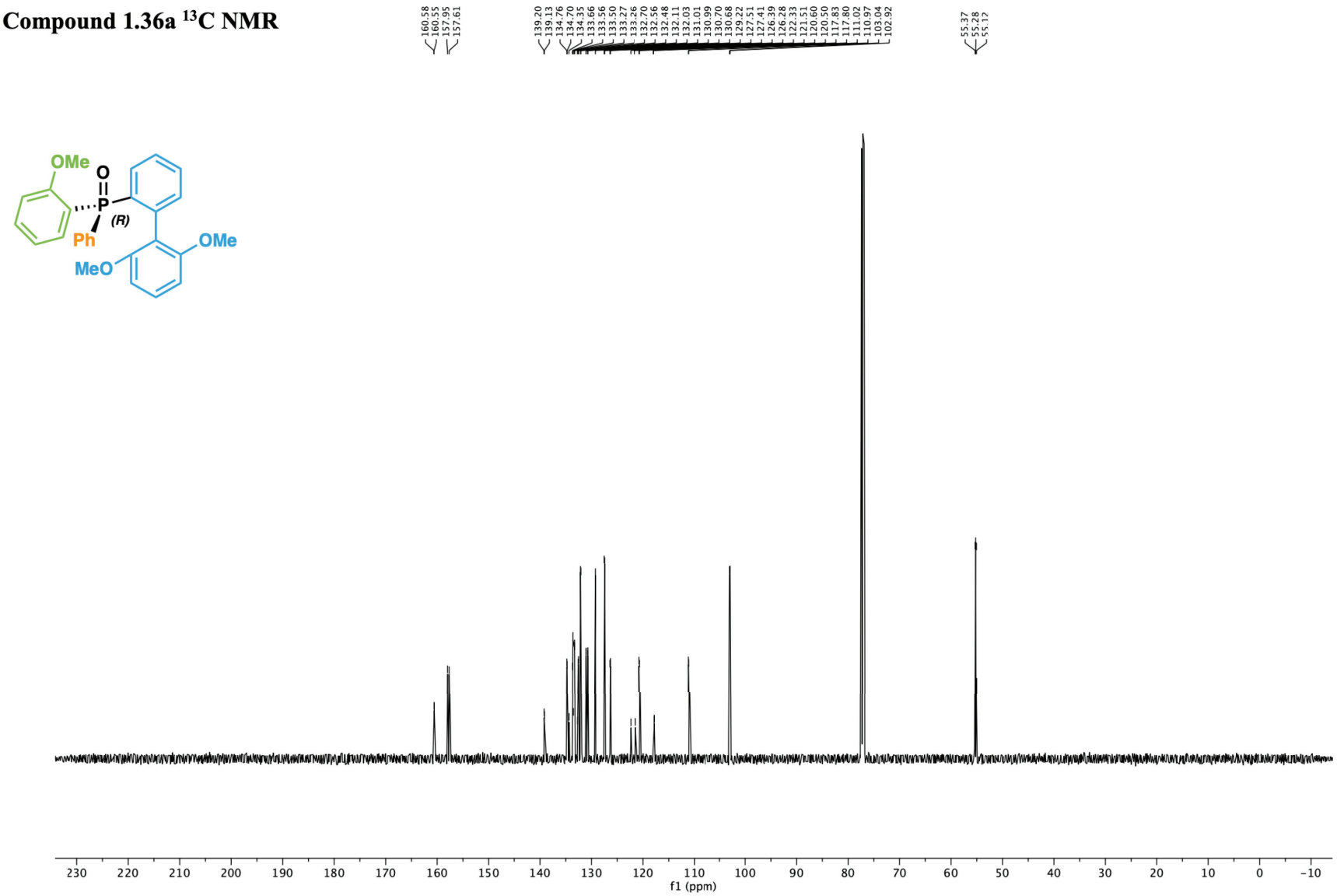
Compound 1.35a ^{31}P NMR



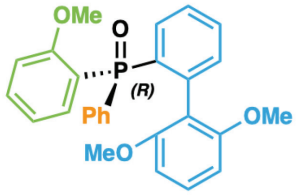
Compound 1.36a ^{1}H NMR



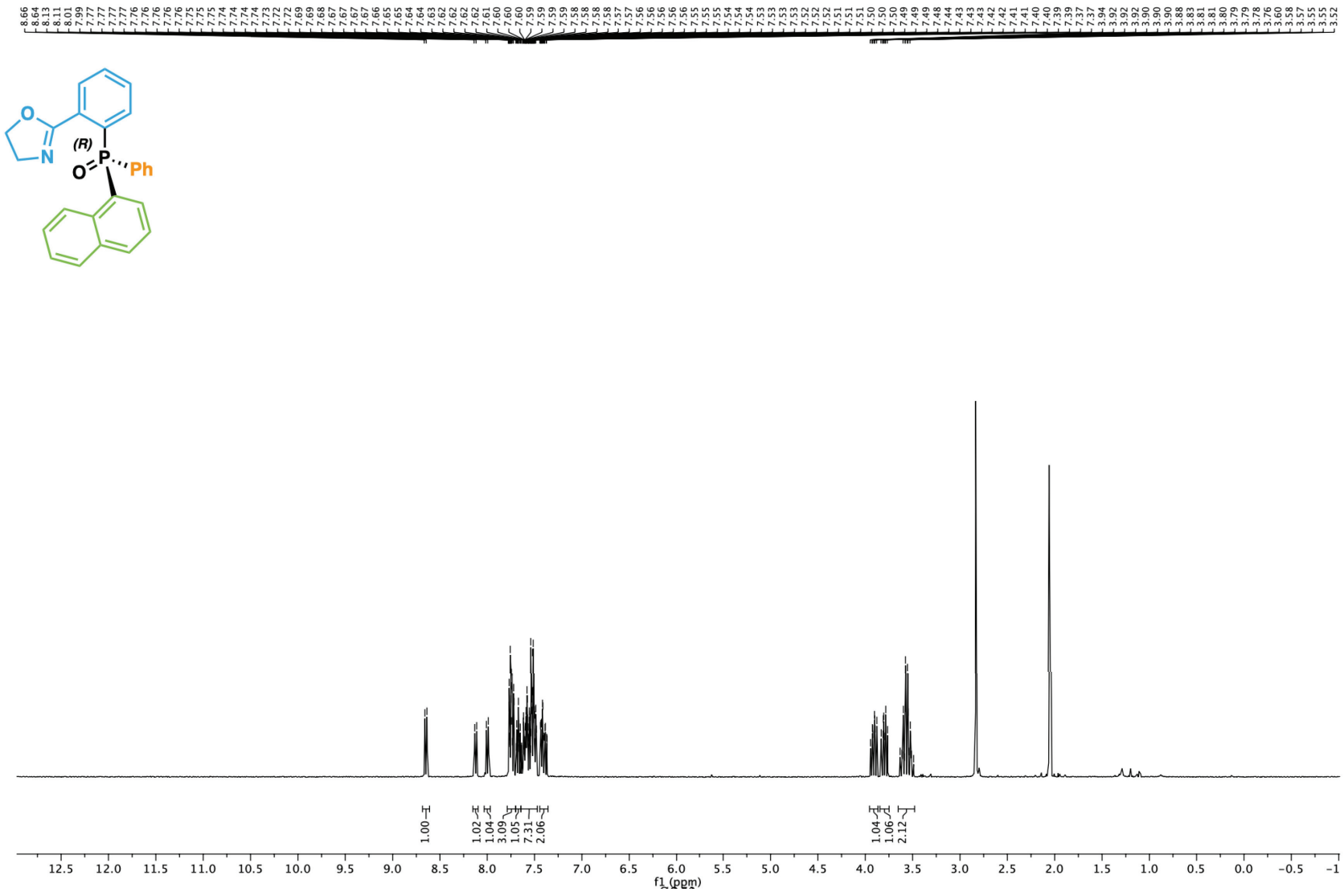
Compound 1.36a ^{13}C NMR



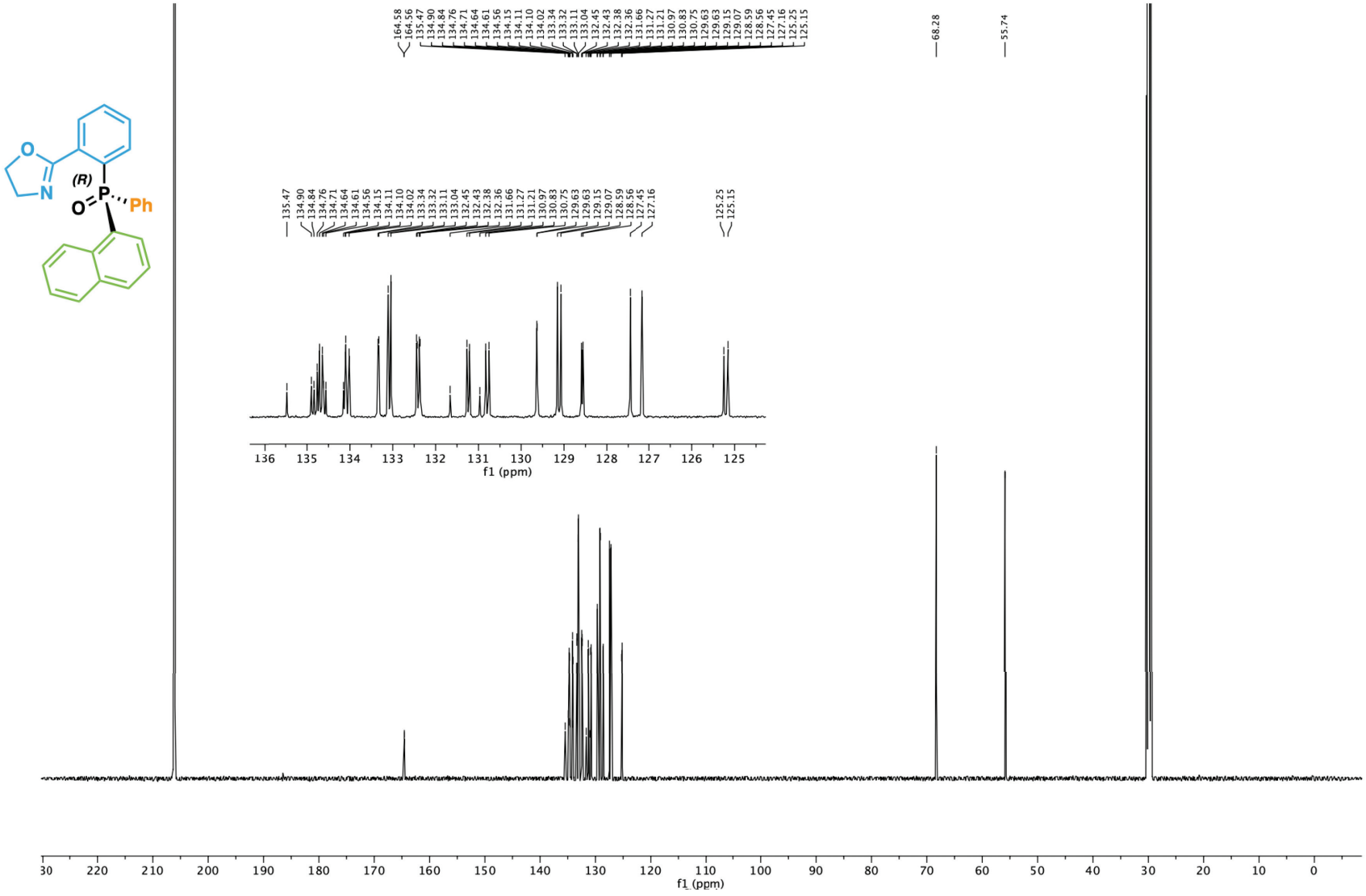
Compound 1.36a ^{31}P NMR



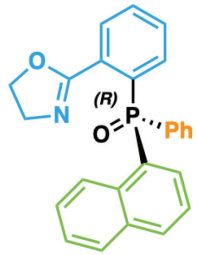
Compound 1.37a ^{1}H NMR



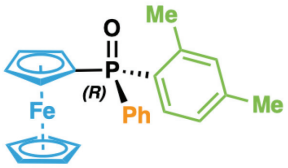
Compound 1.37a ^{13}C NMR

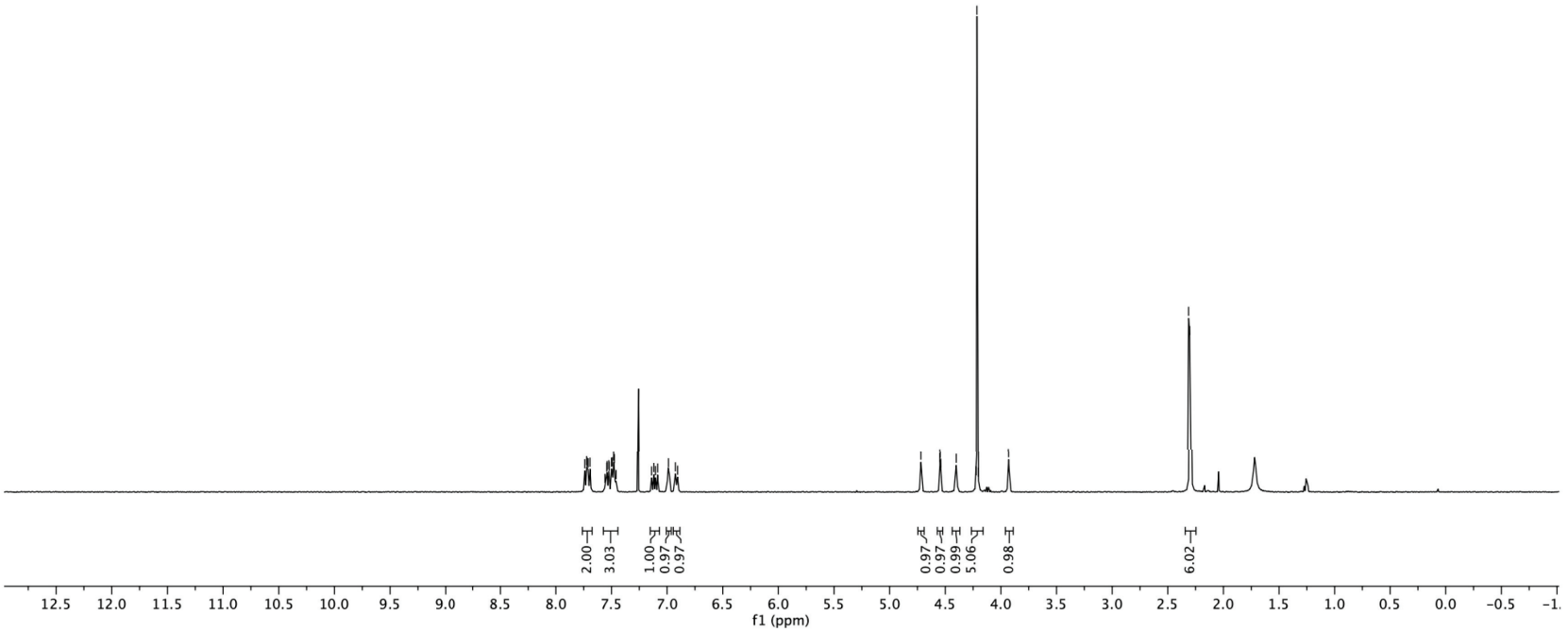


Compound 1.37a ^{31}P NMR

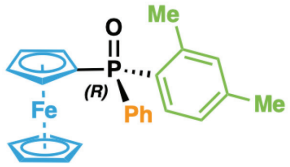


Compound 1.38a ^{1}H NMR

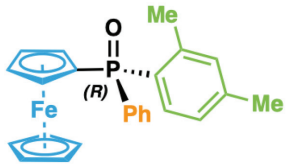




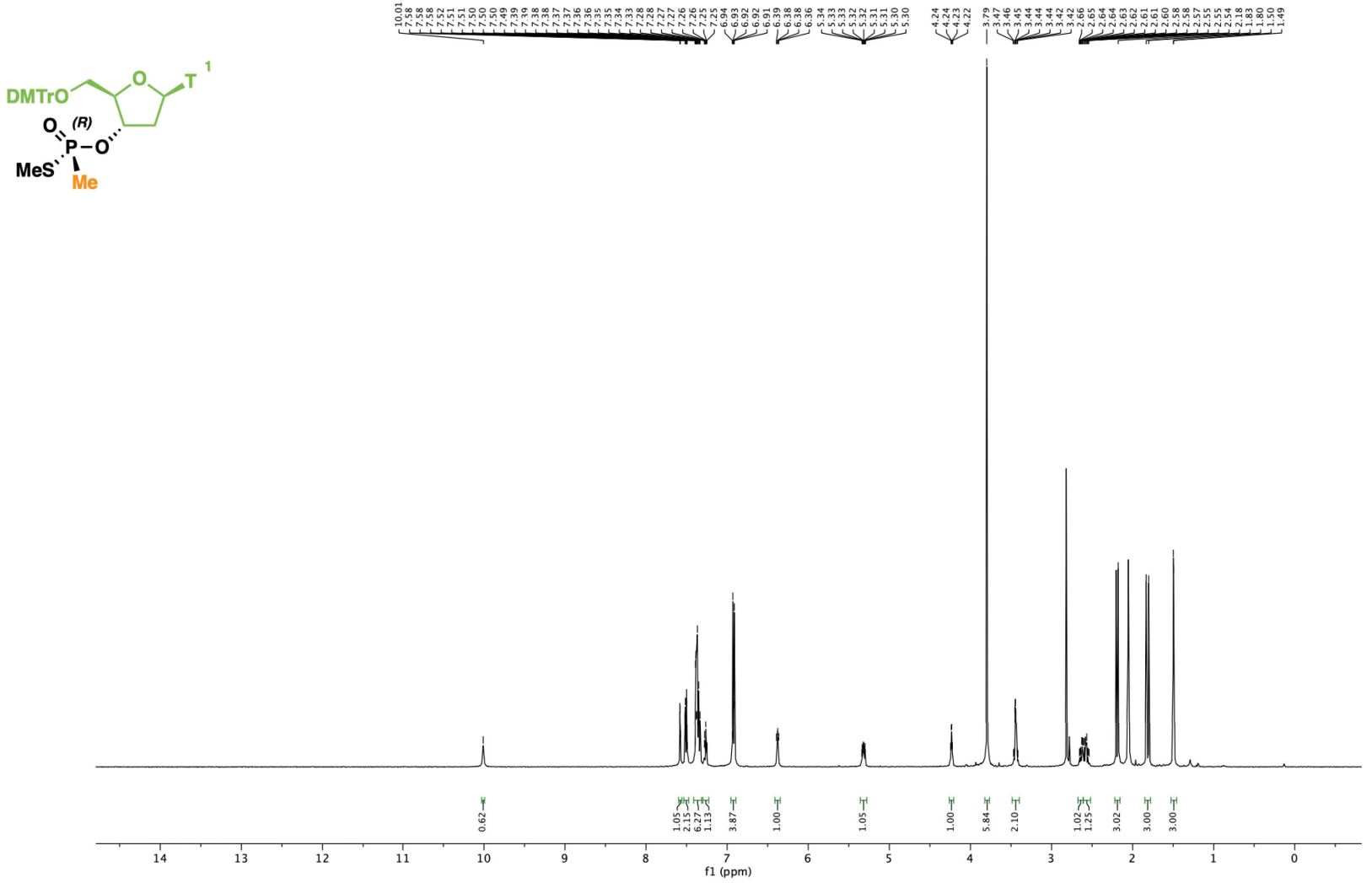
Compound 1.38a ^{13}C NMR



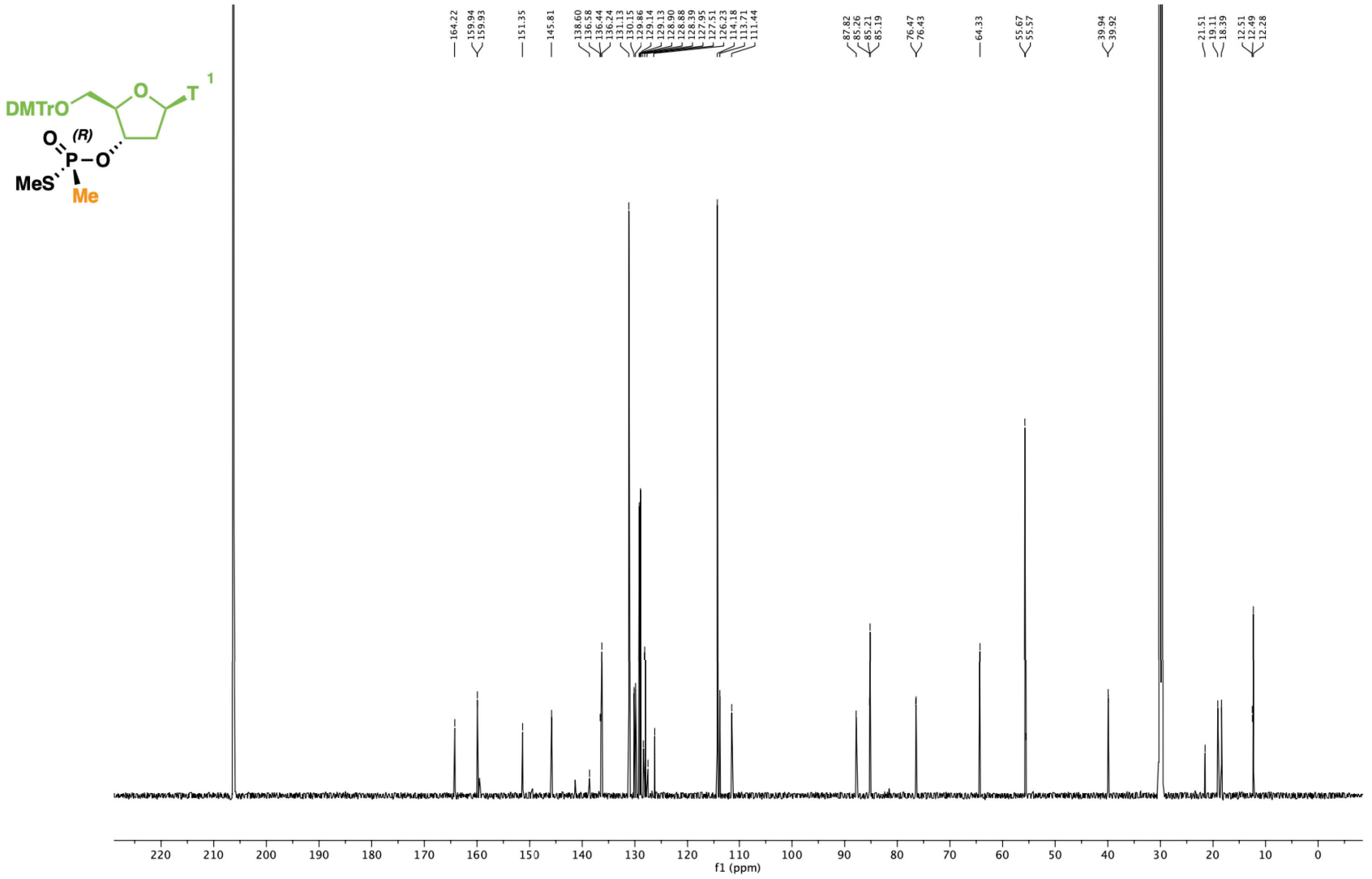
Compound 1.38a ^{31}P NMR



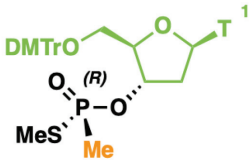
Compound (R_p)-1.40 ^{1}H NMR



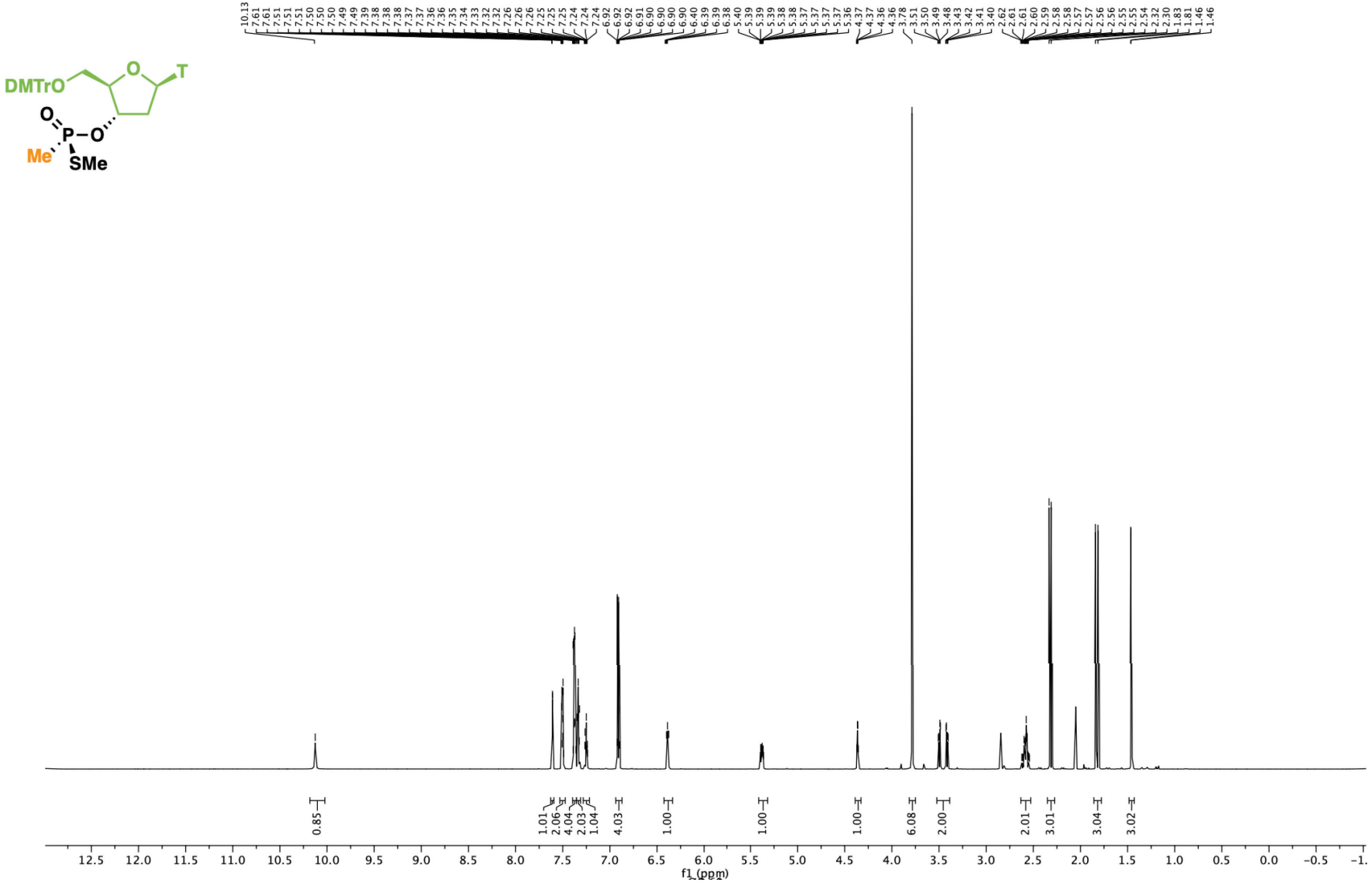
Compound (R_p)-1.40 ^{13}C NMR



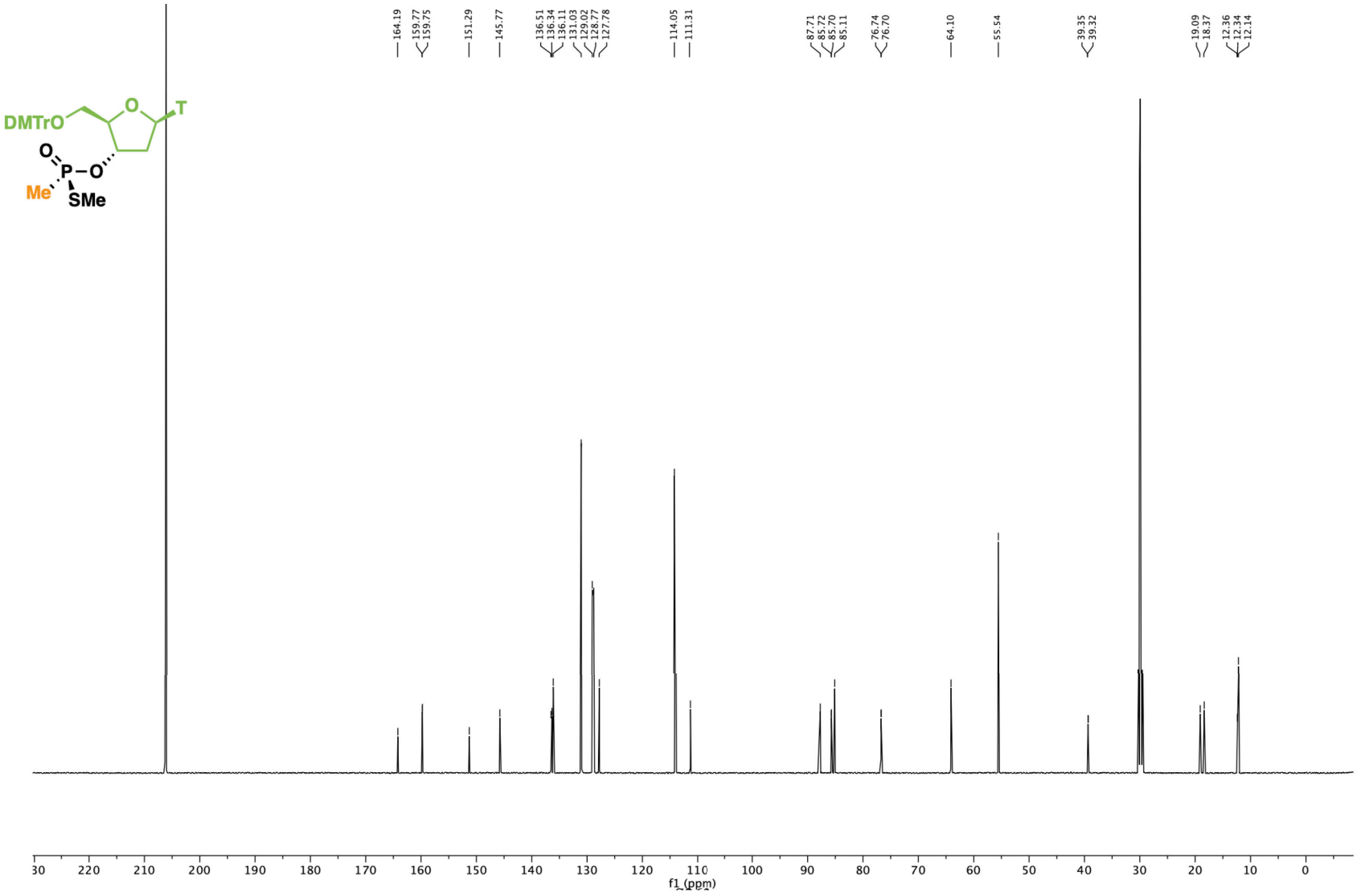
Compound (R_p)-1.40 ^{31}P NMR



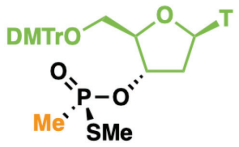
Compound (S_p)-1.40 ^{1}H NMR



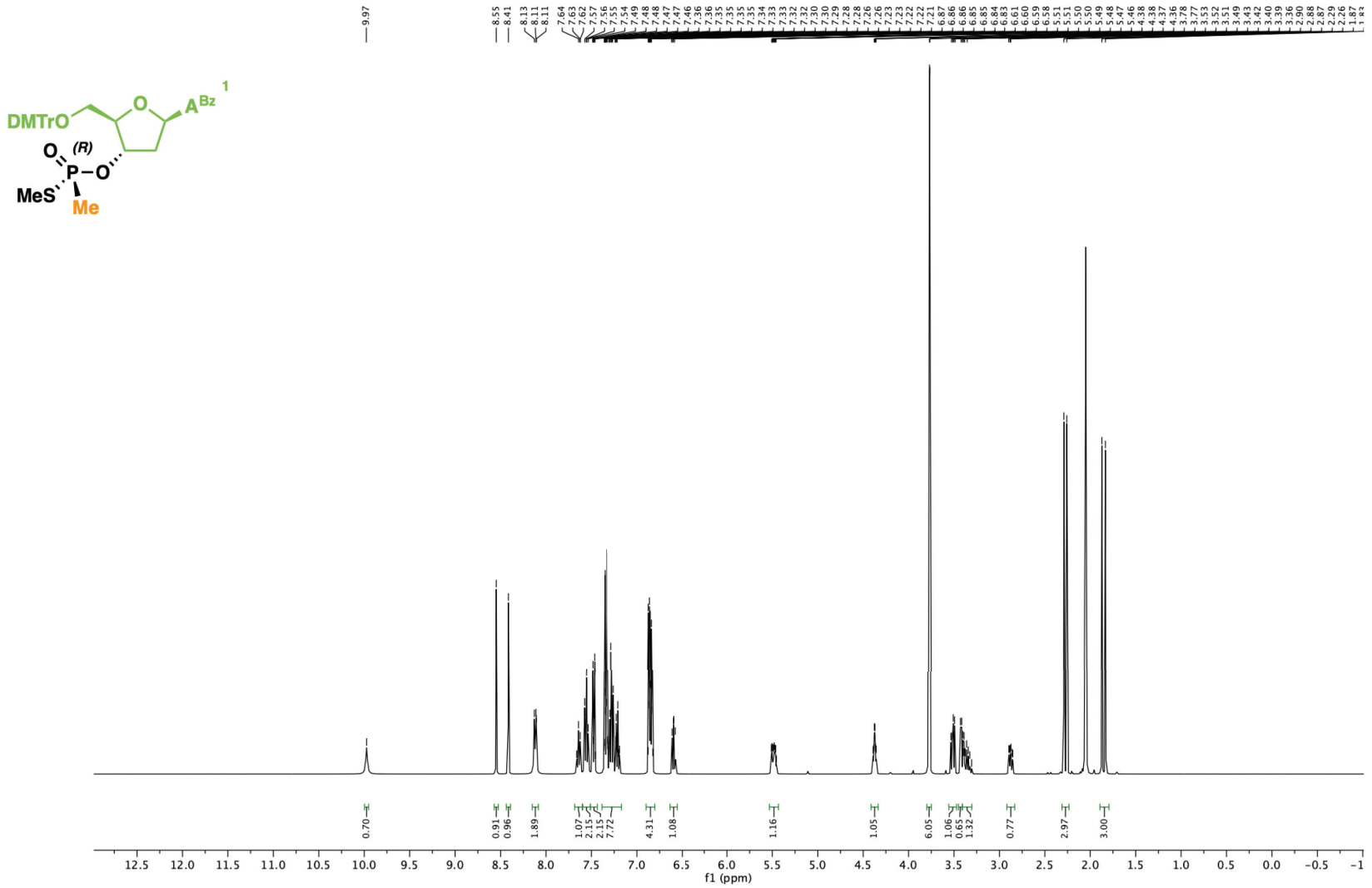
Compound (S_p)-1.40 ^{13}C NMR



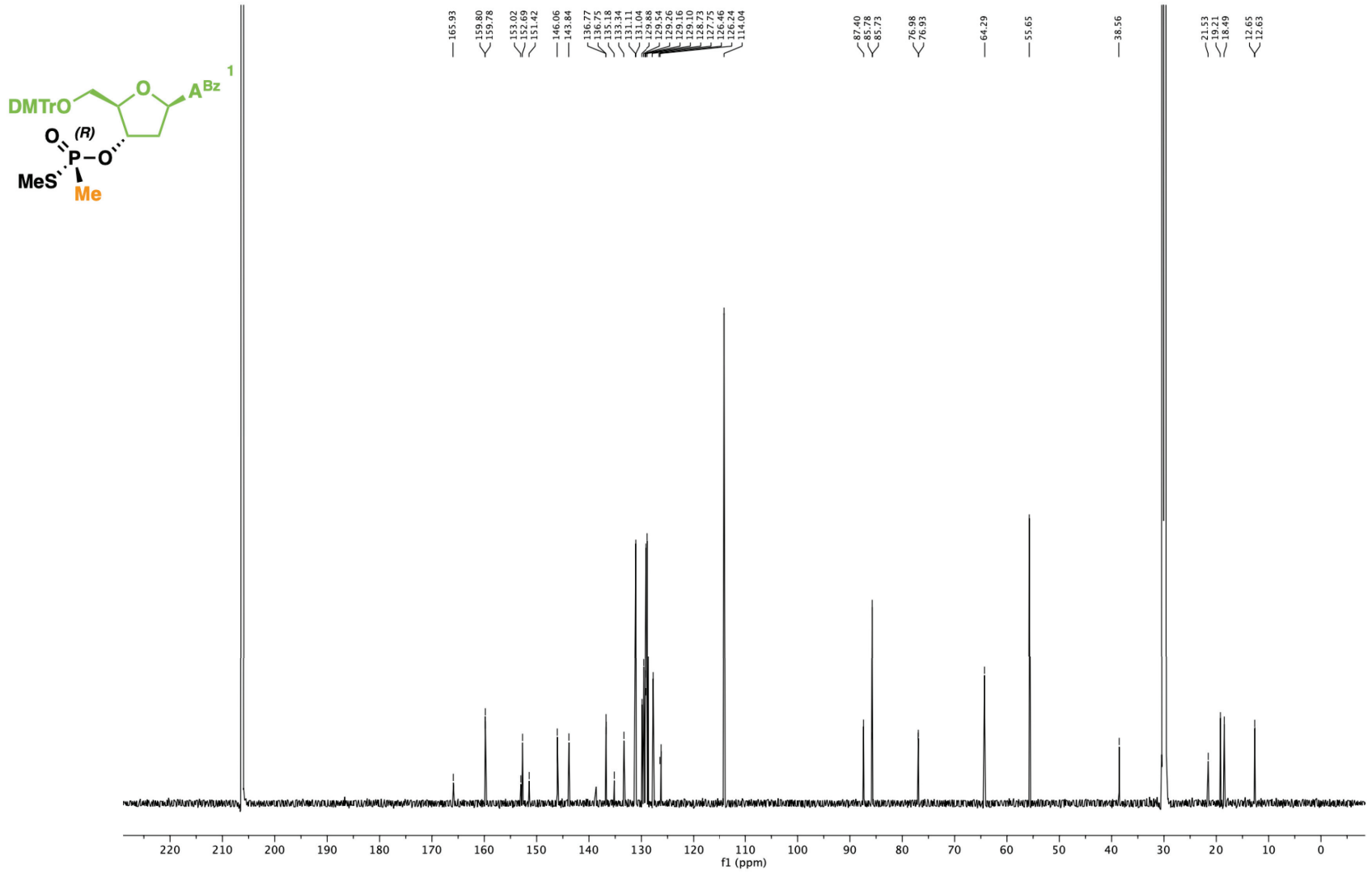
Compound (S_p)-1.40 ^{31}P NMR



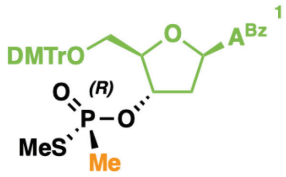
Compound (R_p)-1.41 ^{1}H NMR



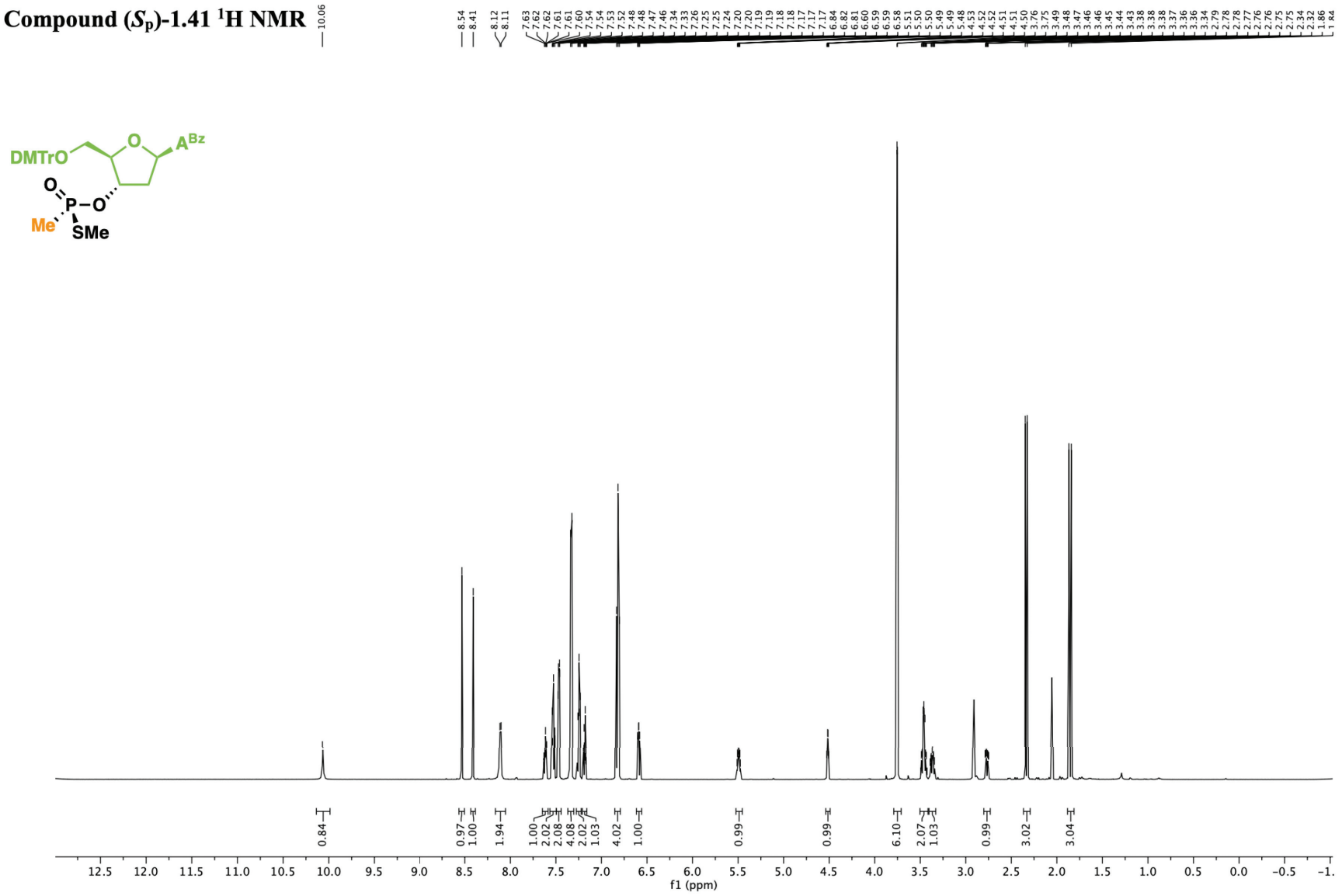
Compound (R_p)-1.41 ^{13}C NMR



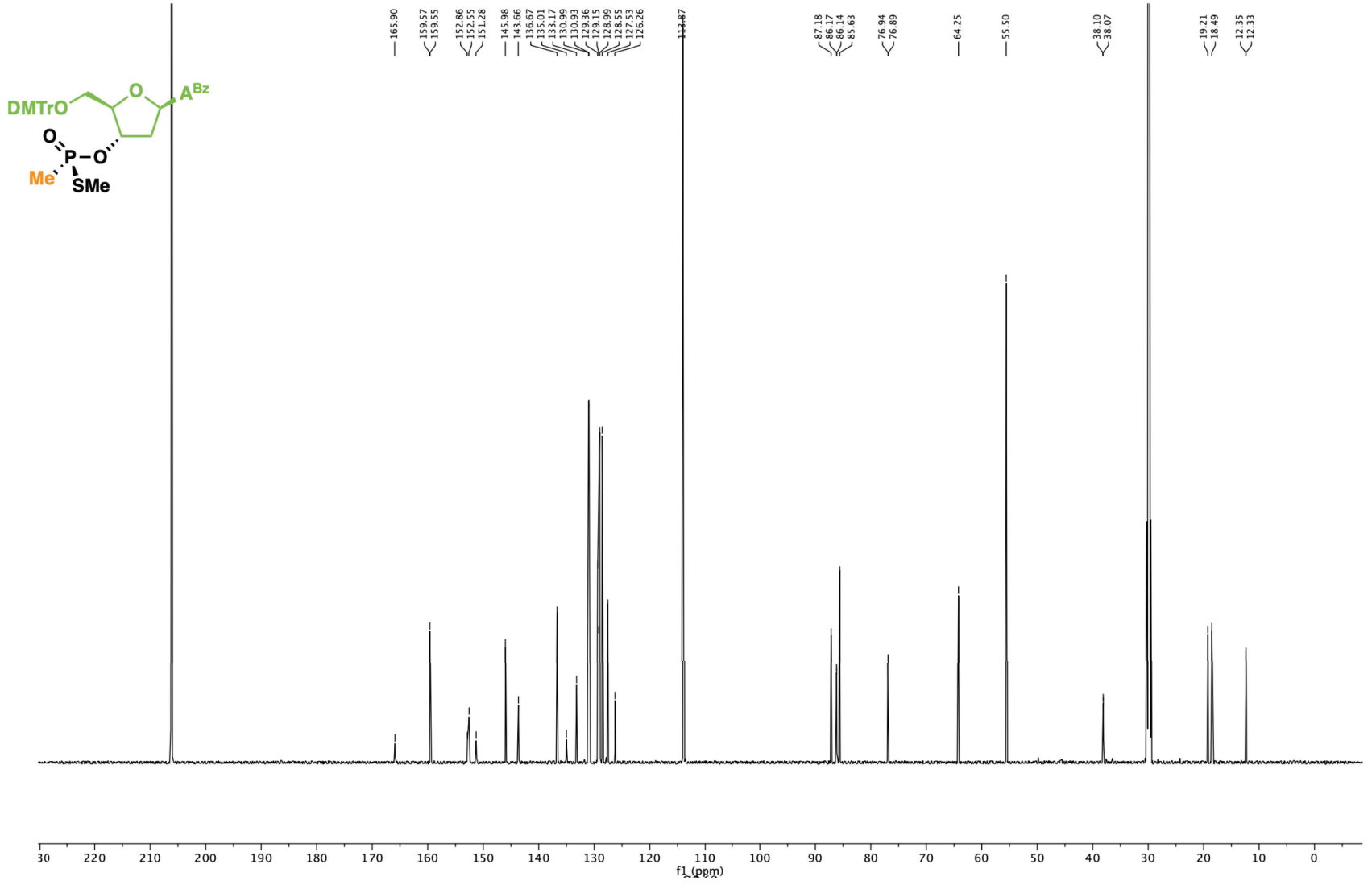
Compound (R_p)-1.41 ^{31}P NMR



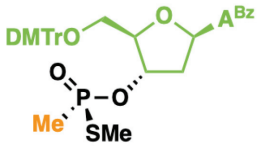
Compound (S_p)-1.41 ^{1}H NMR



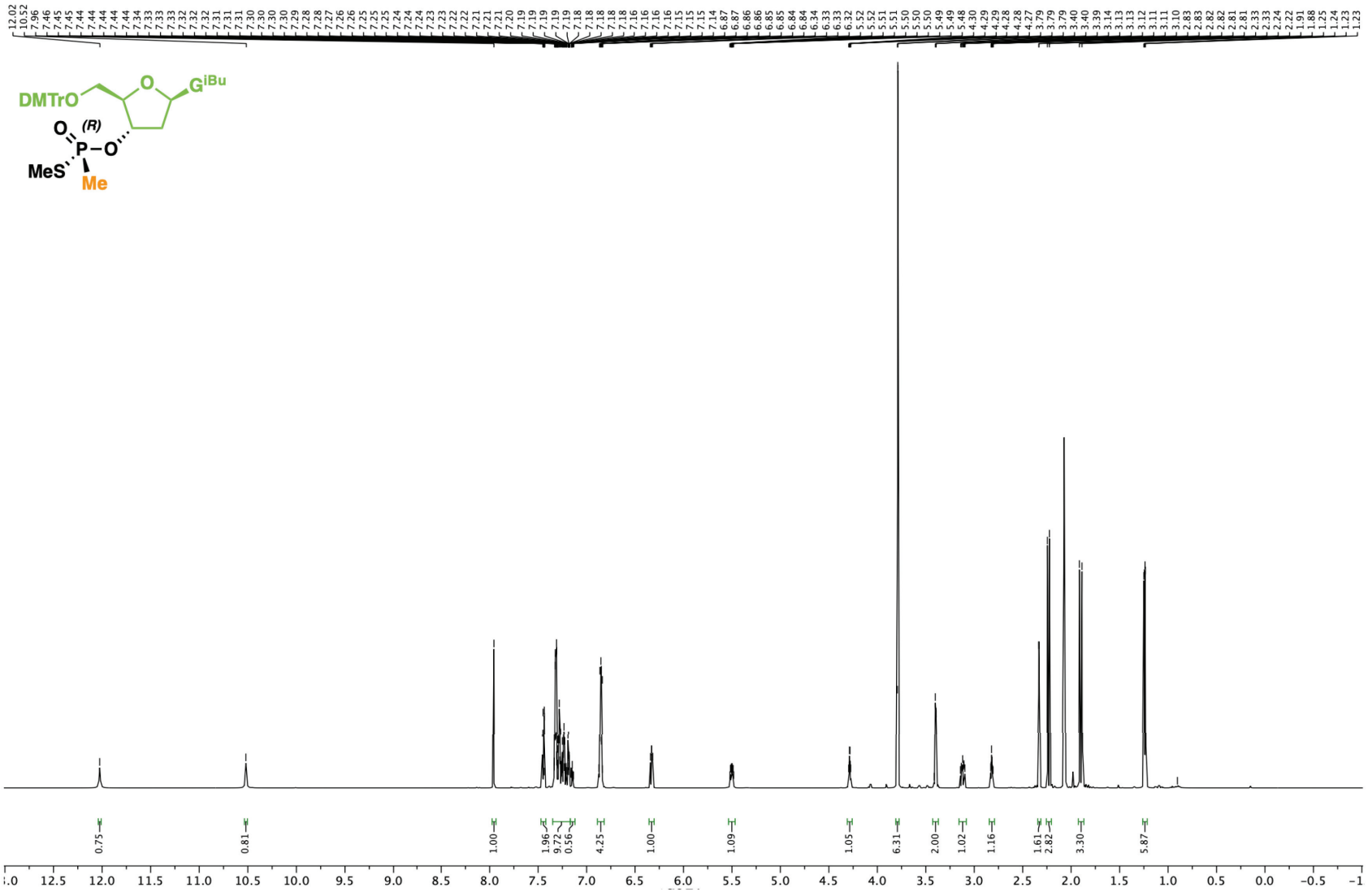
Compound (S_p)-1.41 ^{13}C NMR



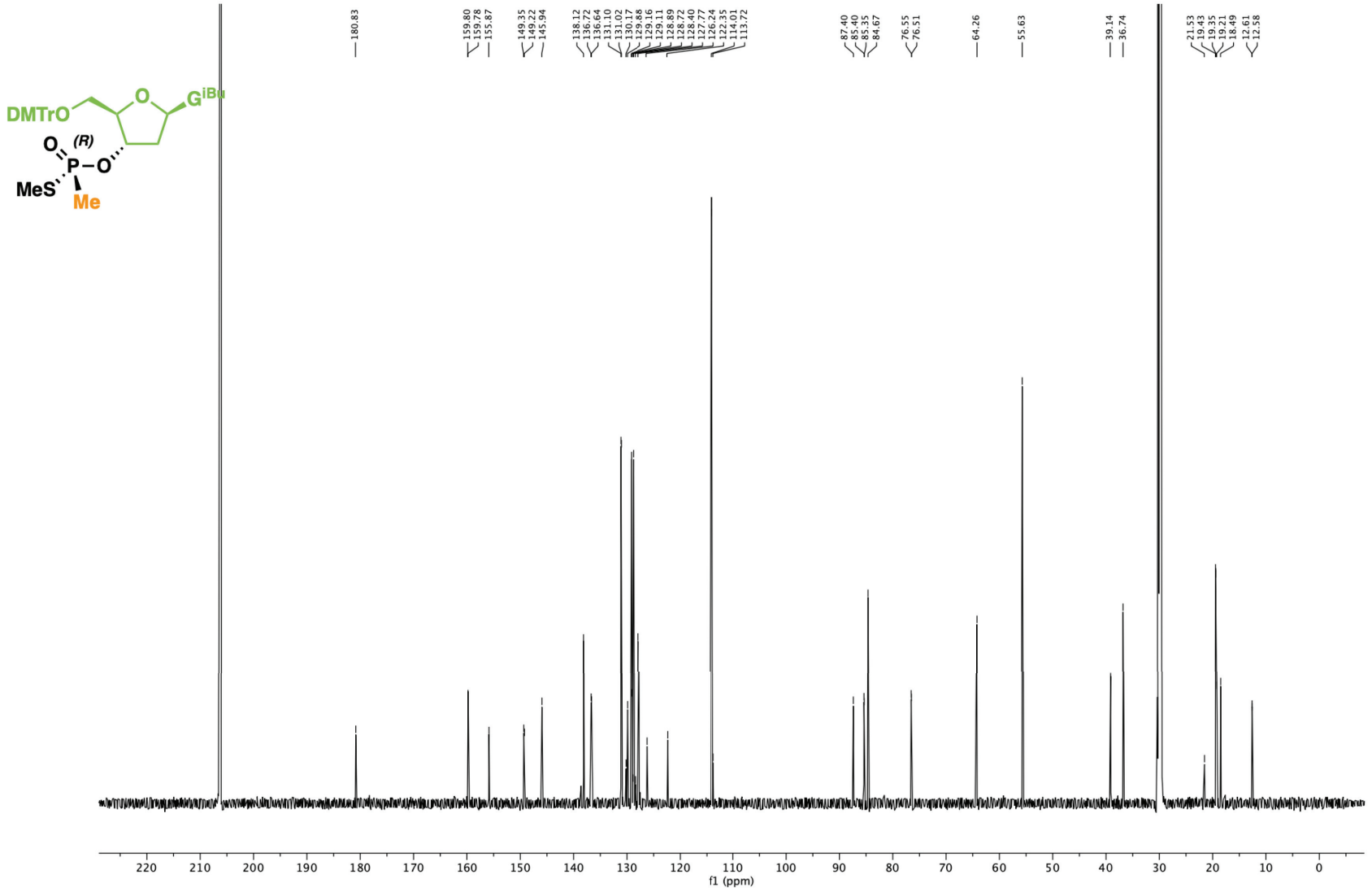
Compound (S_p)-1.41 ^{31}P NMR



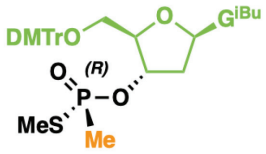
Compound (R_p)-1.42 ^{1}H NMR



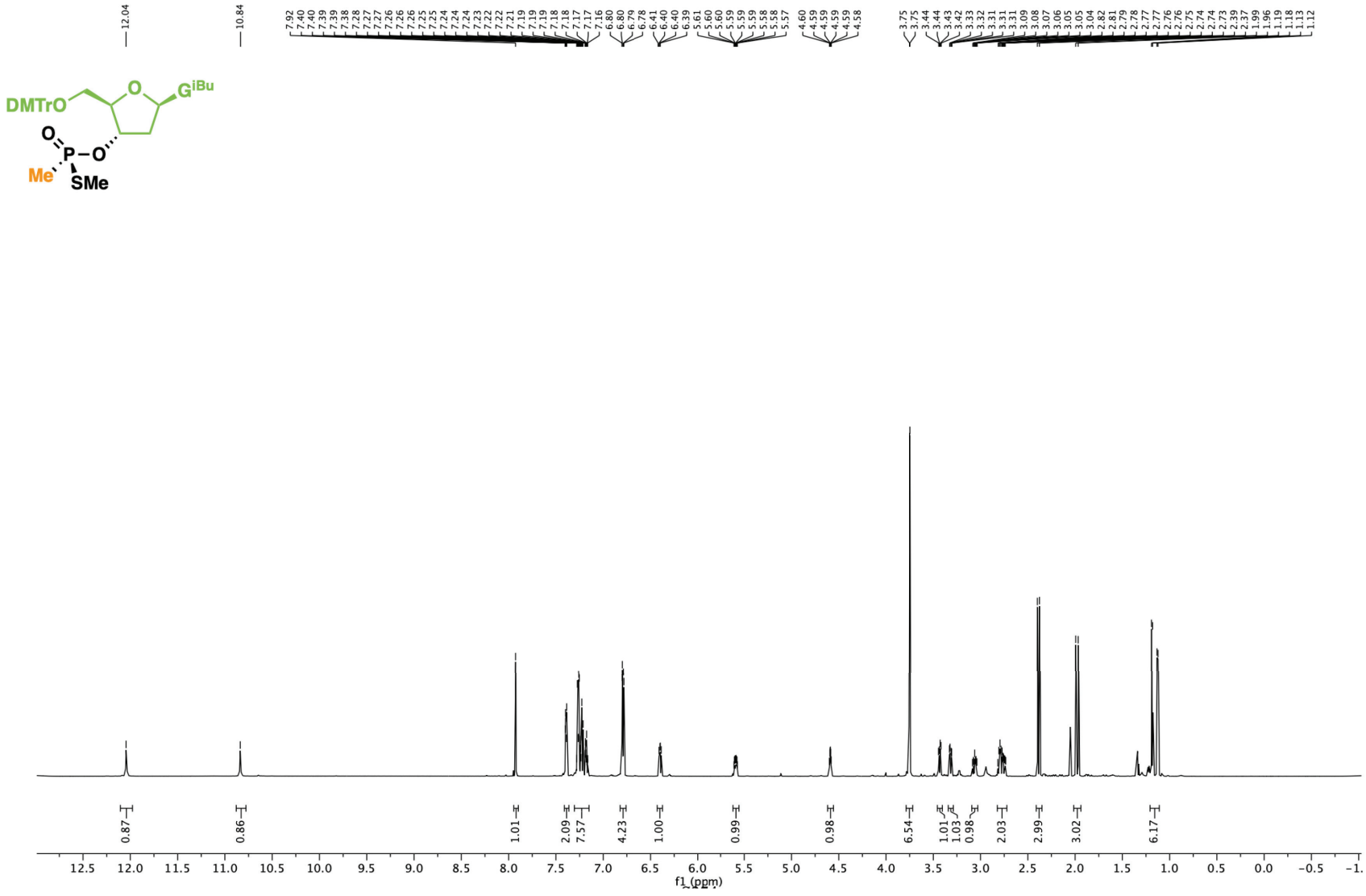
Compound (R_p)-1.42 ^{13}C NMR



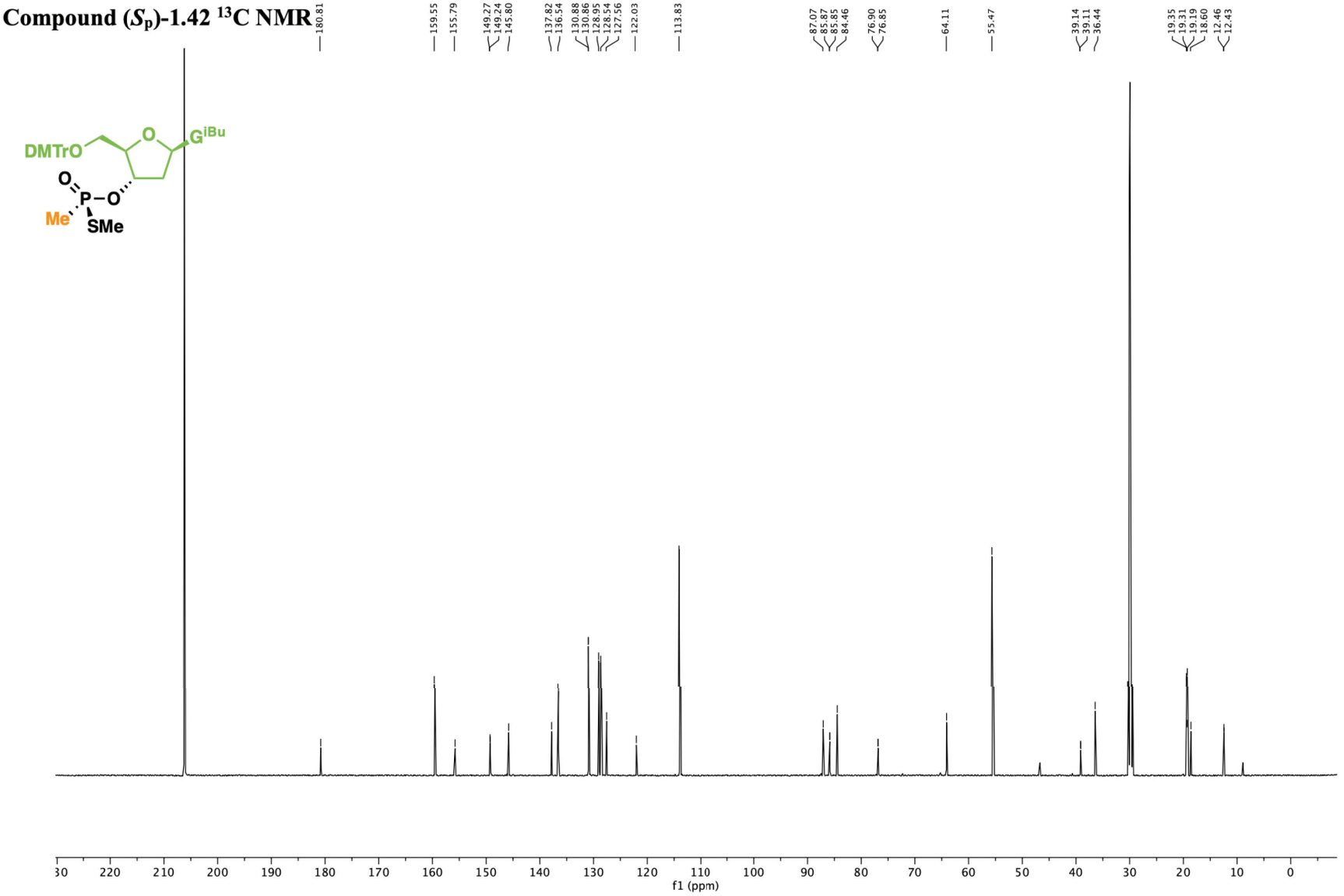
Compound (R_p)-1.42 ^{31}P NMR



Compound (S_p)-1.42 ^{1}H NMR



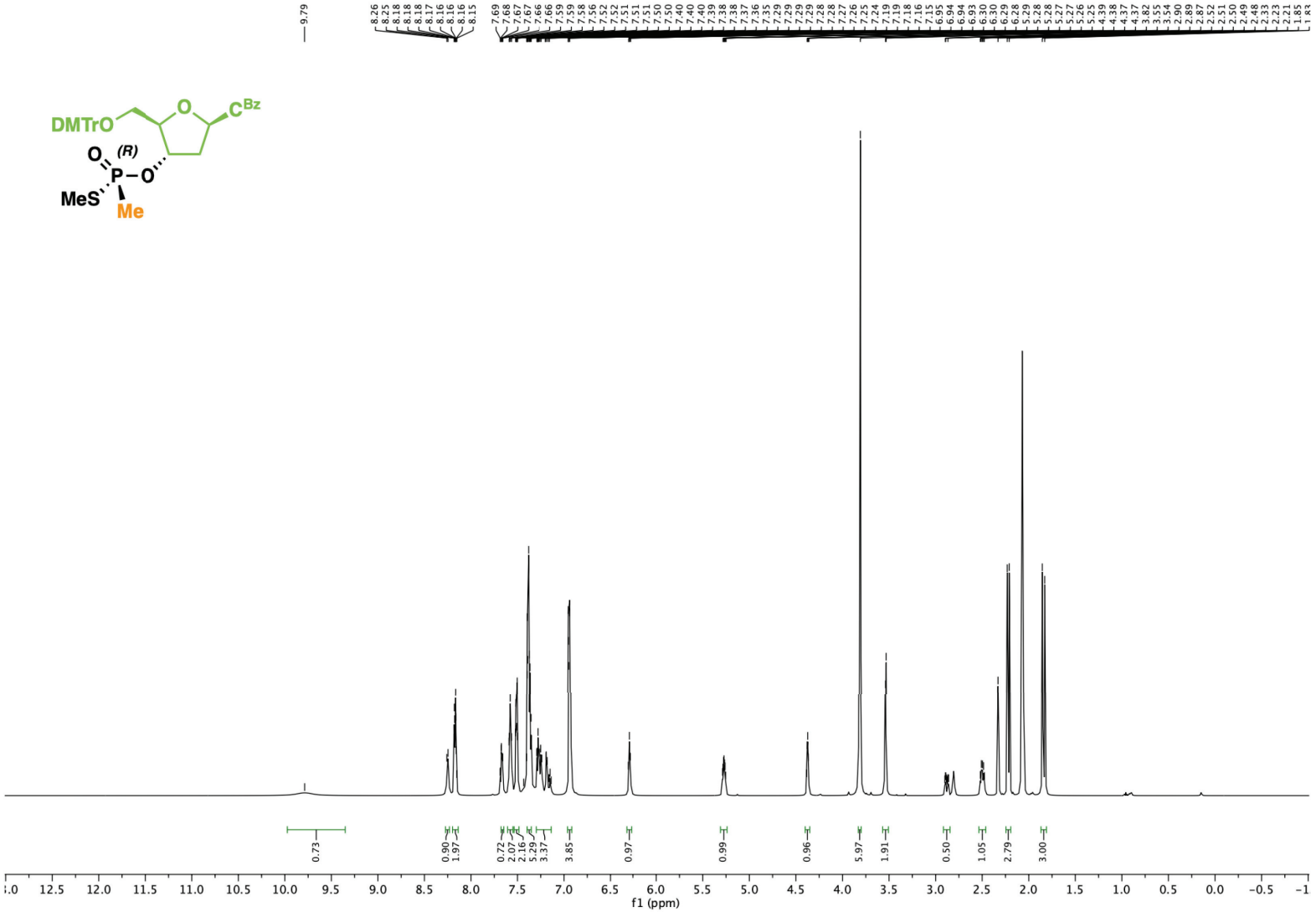
Compound (S_p)-1.42 ^{13}C NMR



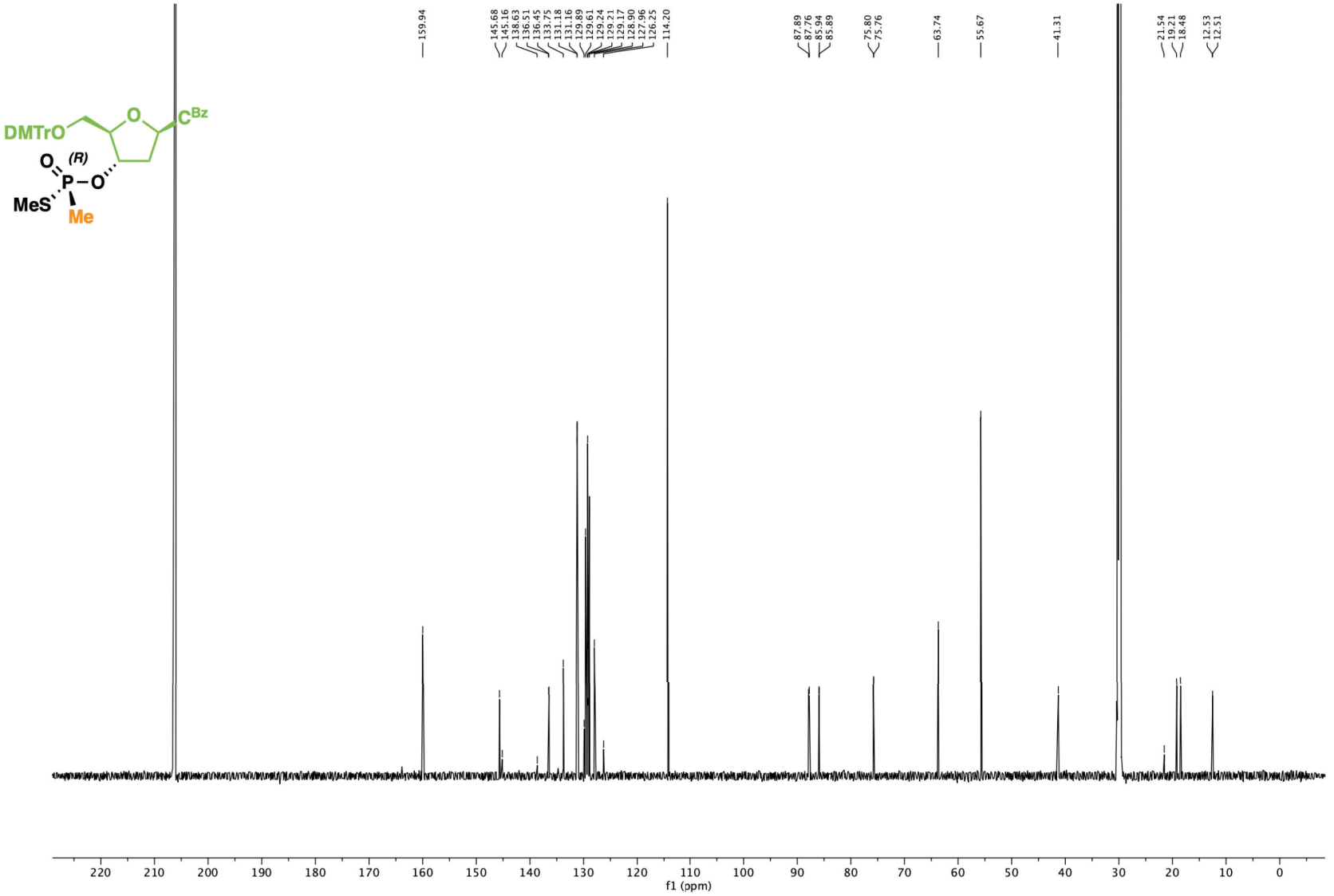
Compound (S_p)-1.42 ^{31}P NMR



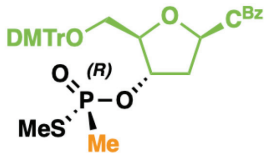
Compound (R_P)-1.43 ^{1}H NMR



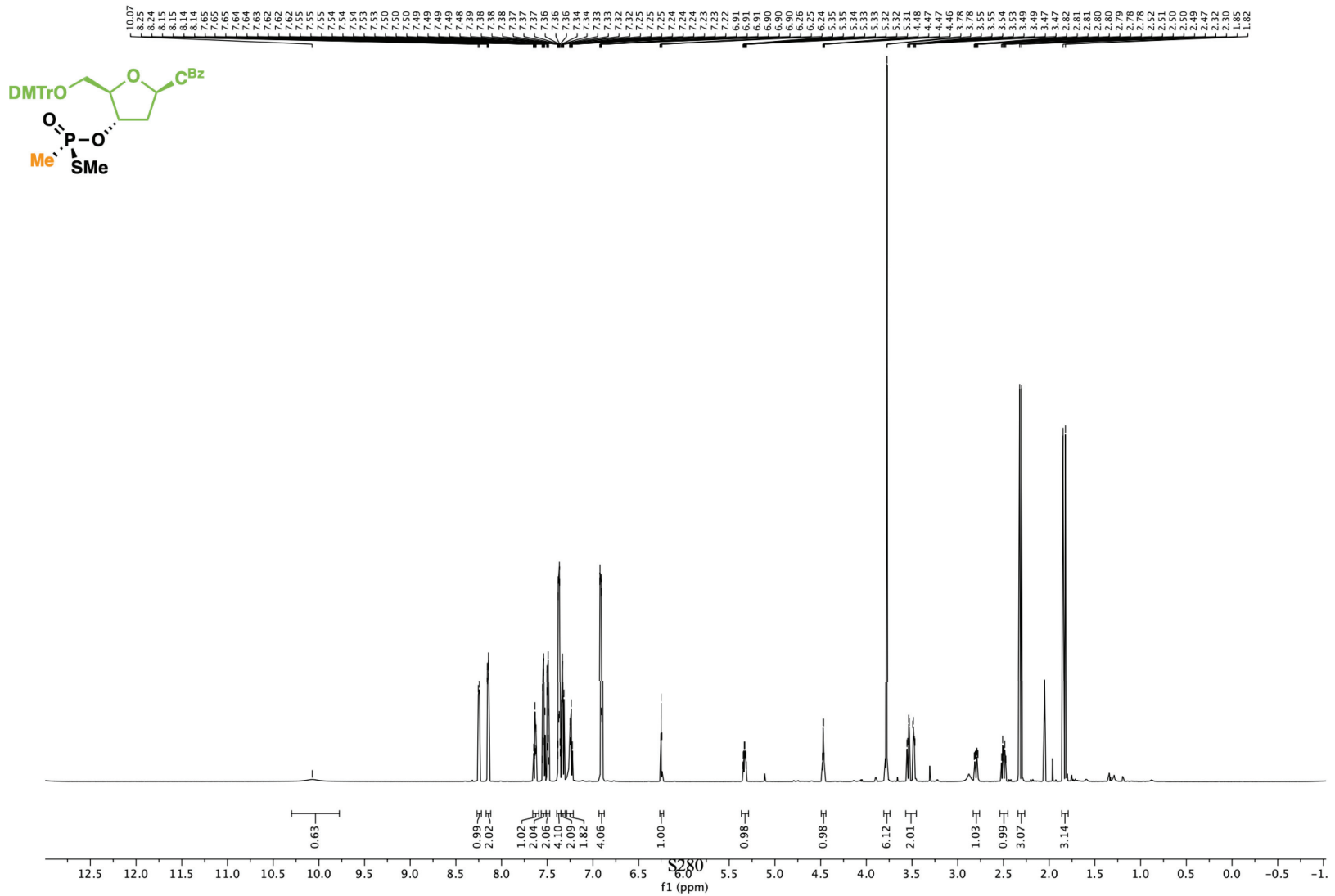
Compound (R_p)-1.43 ^{13}C NMR



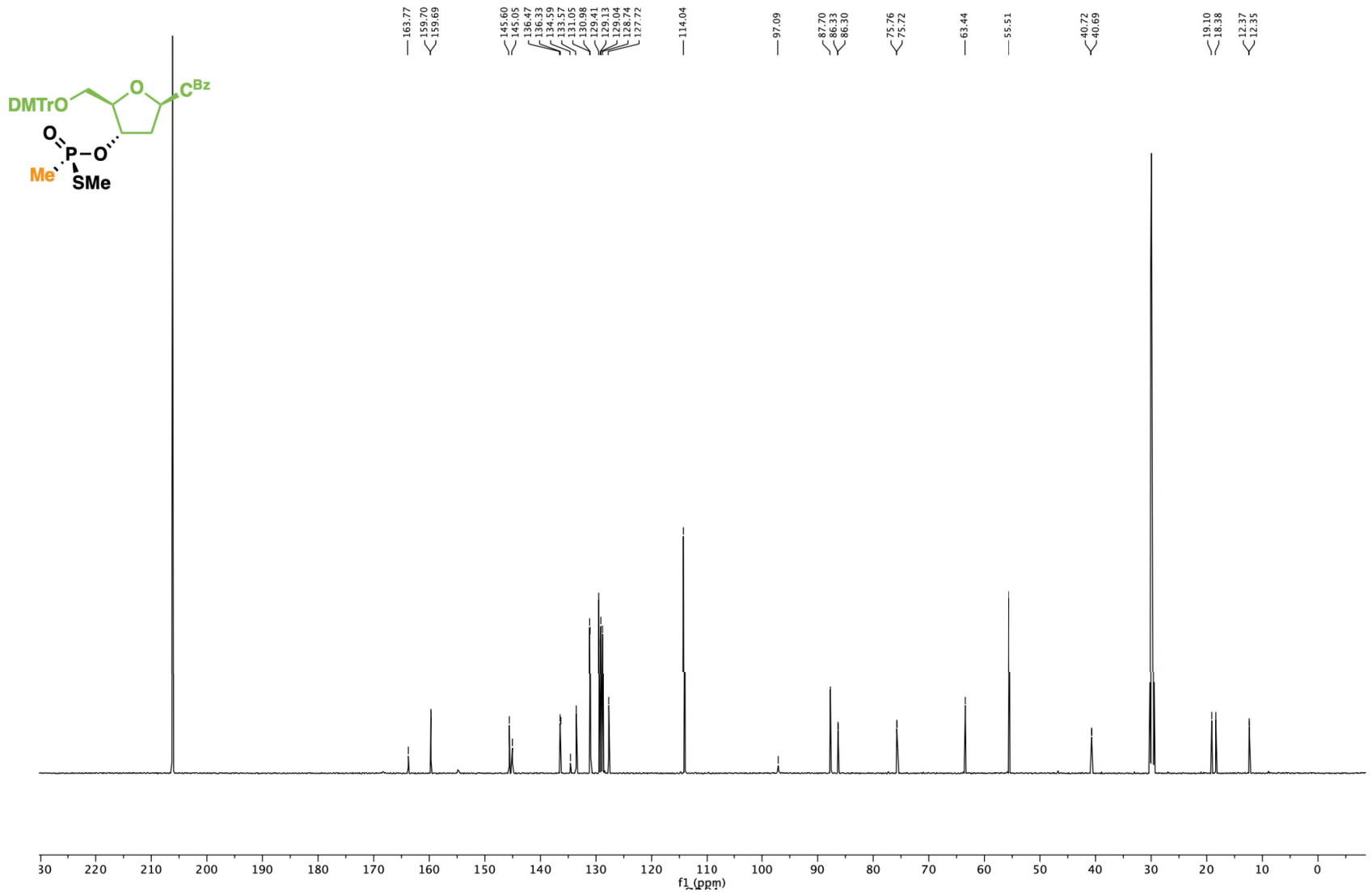
Compound (R_p)-1.43 ^{31}P NMR



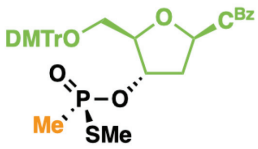
Compound (S_p)-1.43 ^{1}H NMR

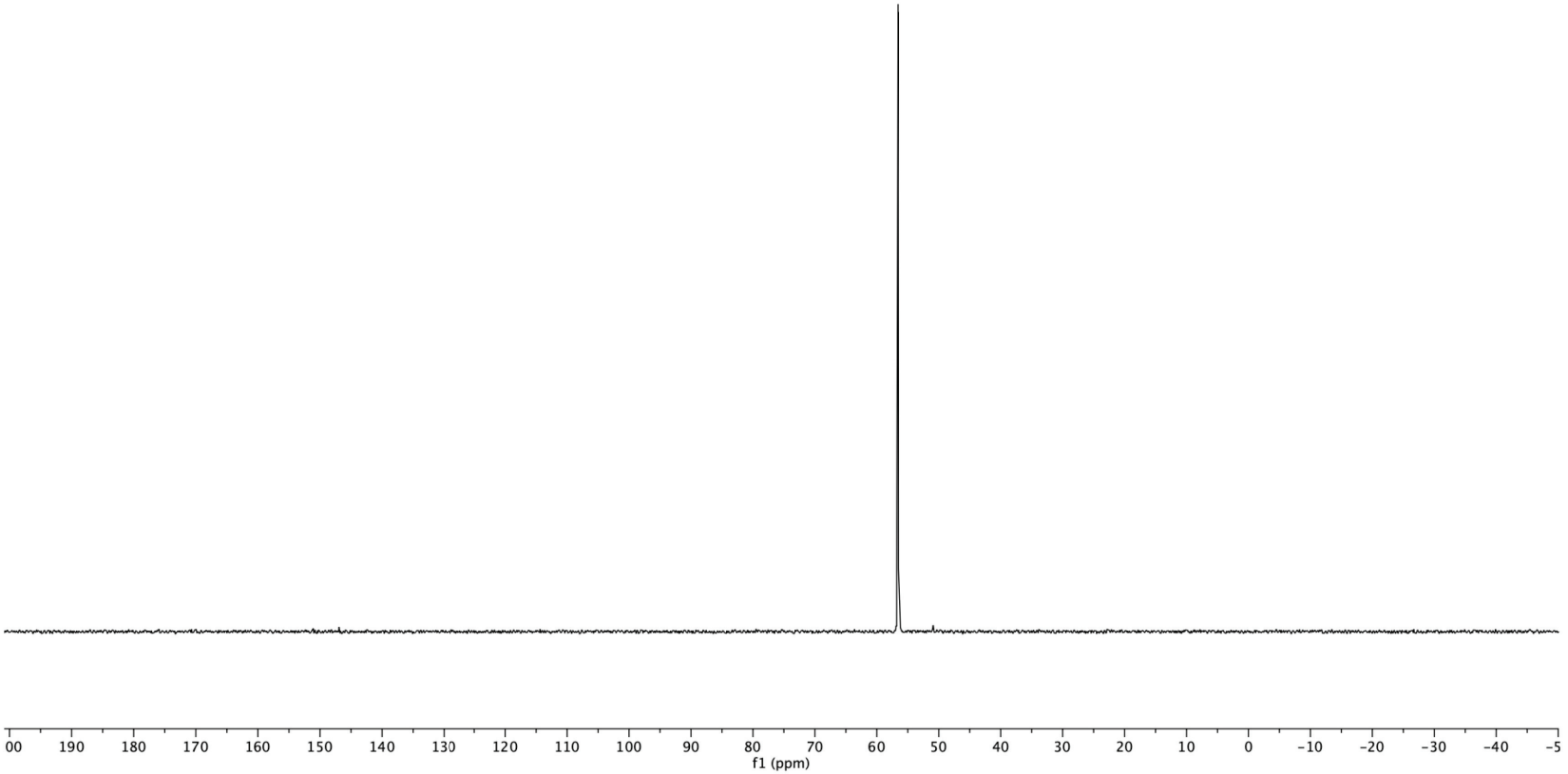


Compound (S_p)-1.43 ^{13}C NMR

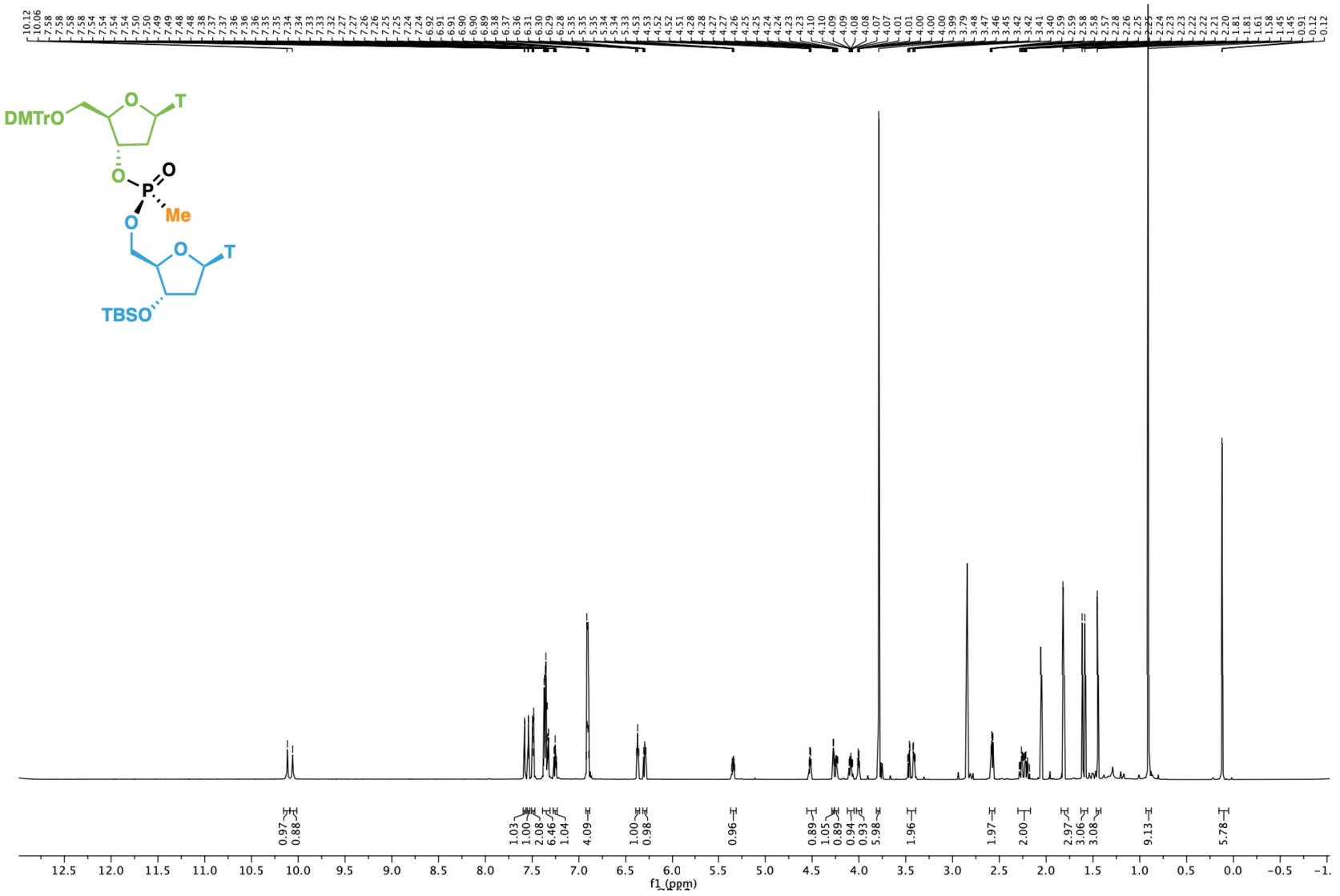


Compound (S_p)-1.43 ^{31}P NMR

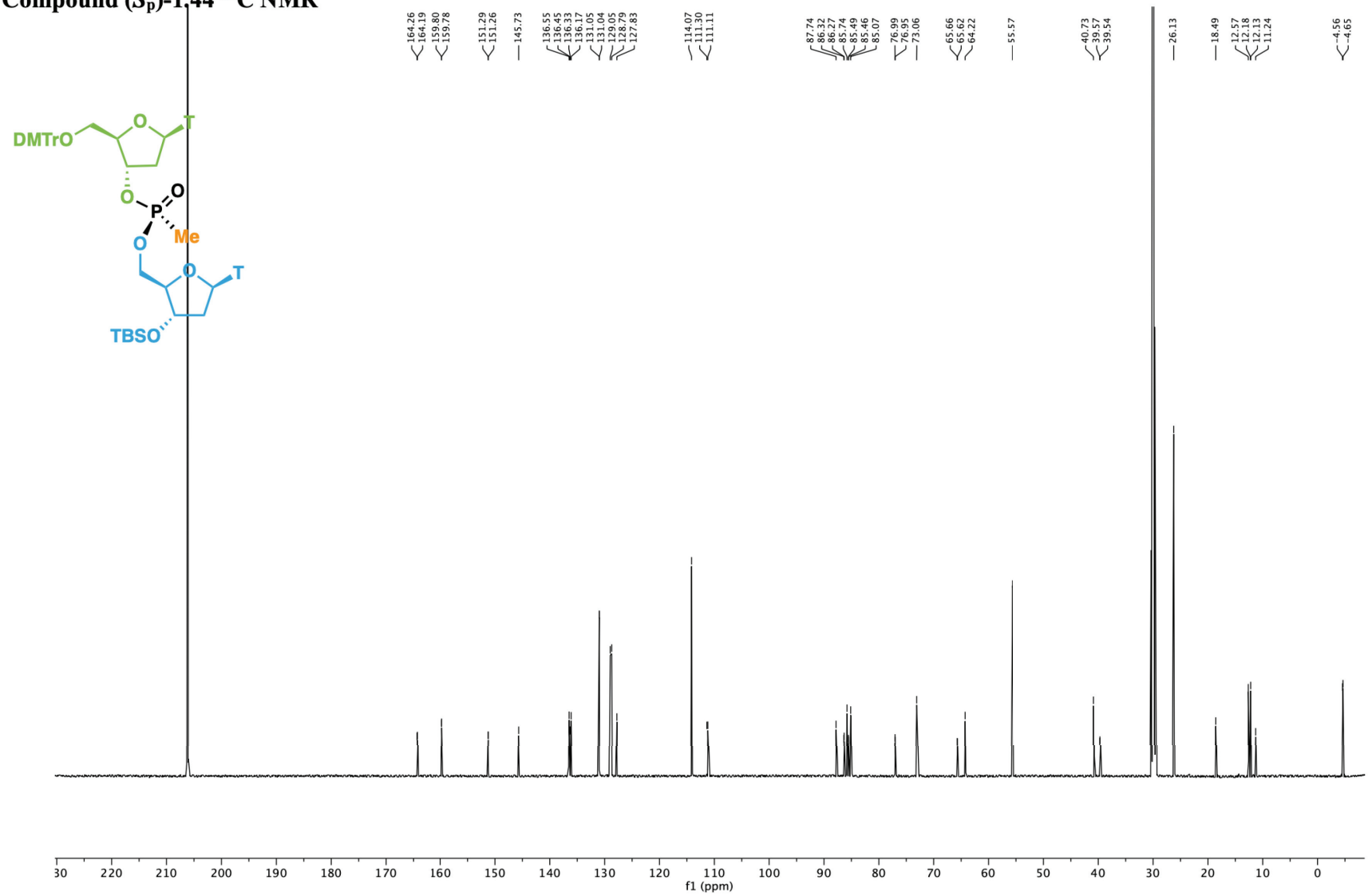




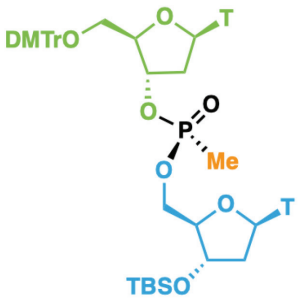
Compound (S_p)-1.44 ^{1}H NMR



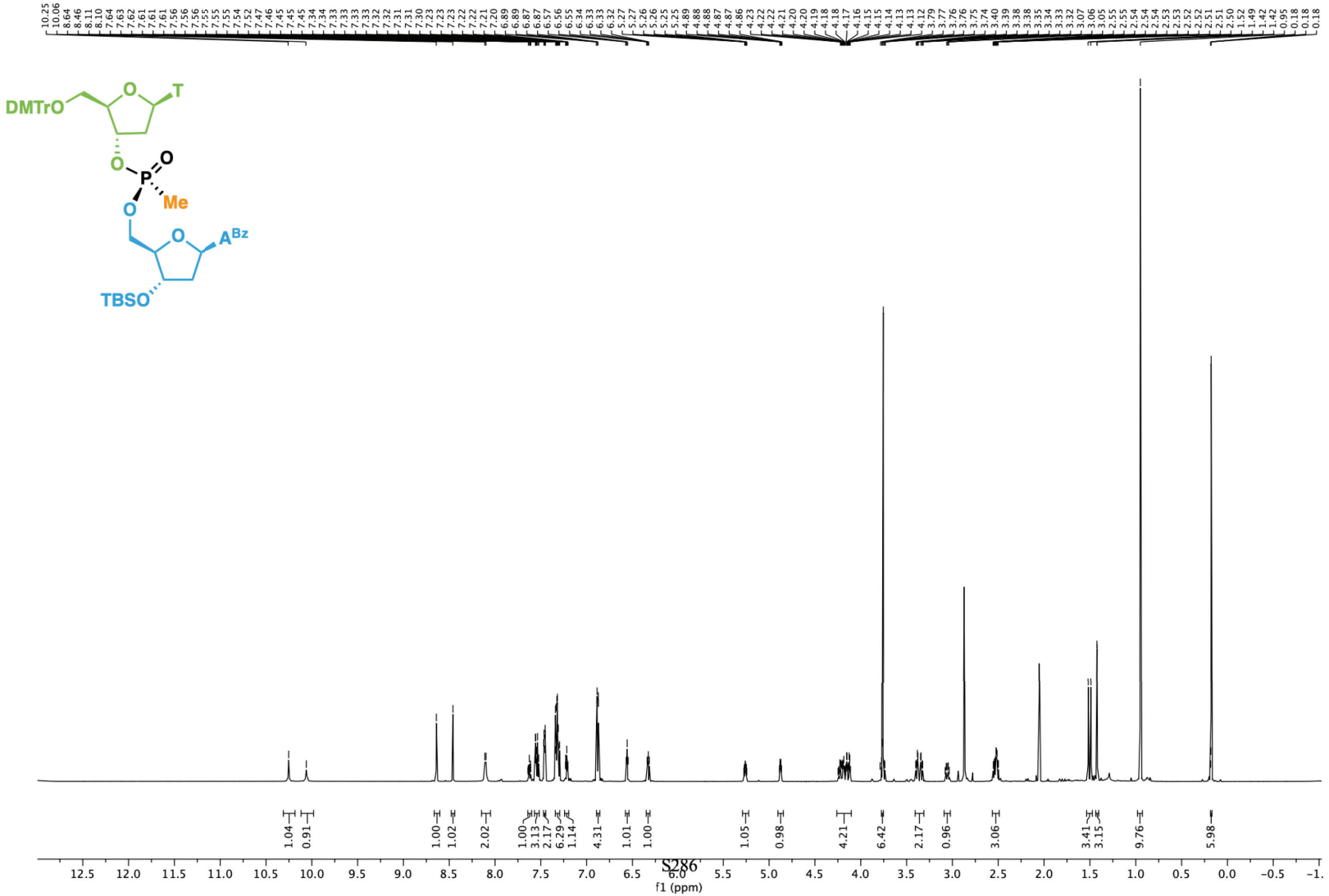
Compound (S_p)-1.44 ^{13}C NMR



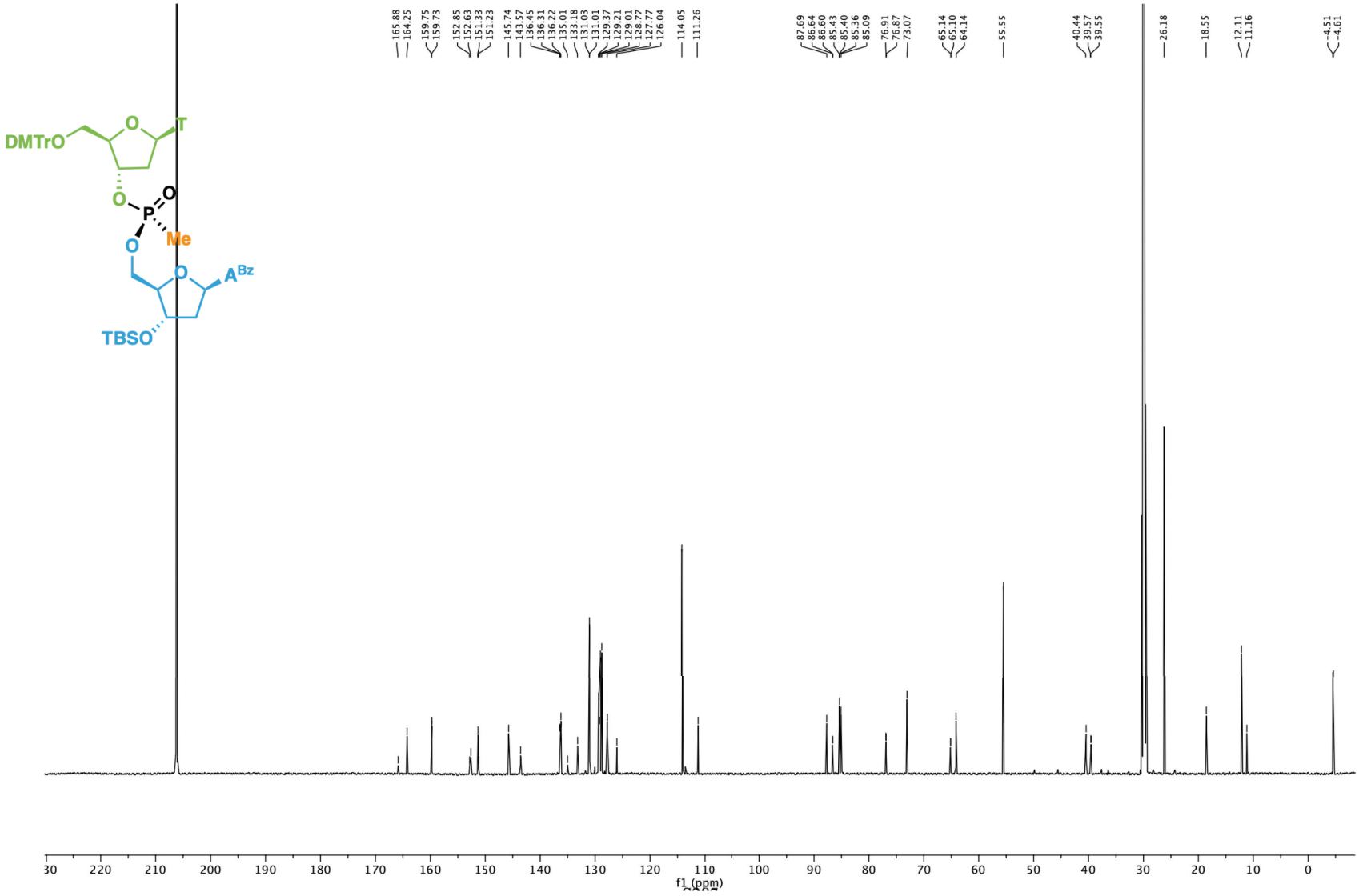
Compound (S_p)-1.44 ^{31}P NMR



Compound (S_p)-1.45 ^{1}H NMR



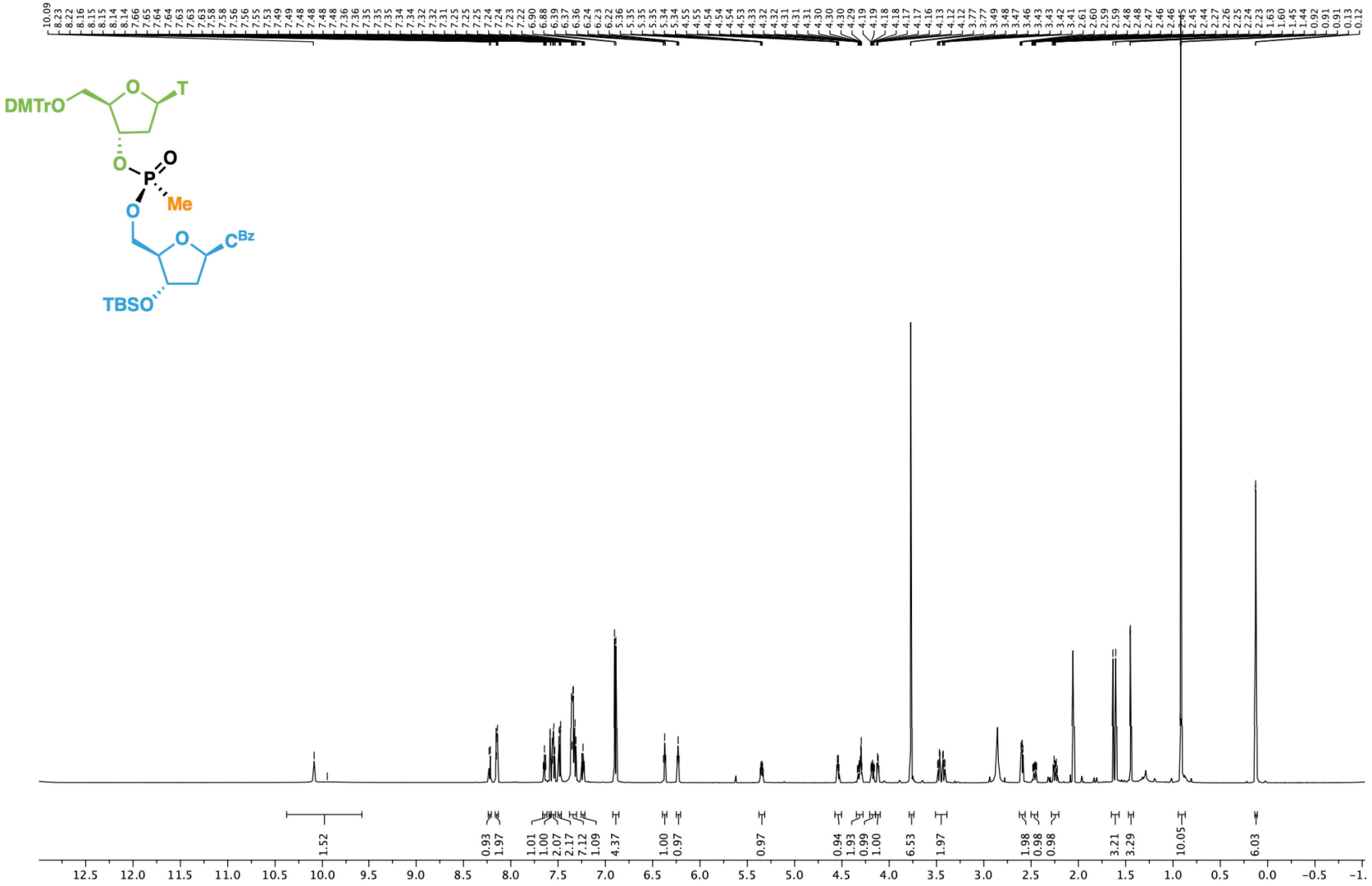
Compound (S_p)-1.45 ^{13}C NMR



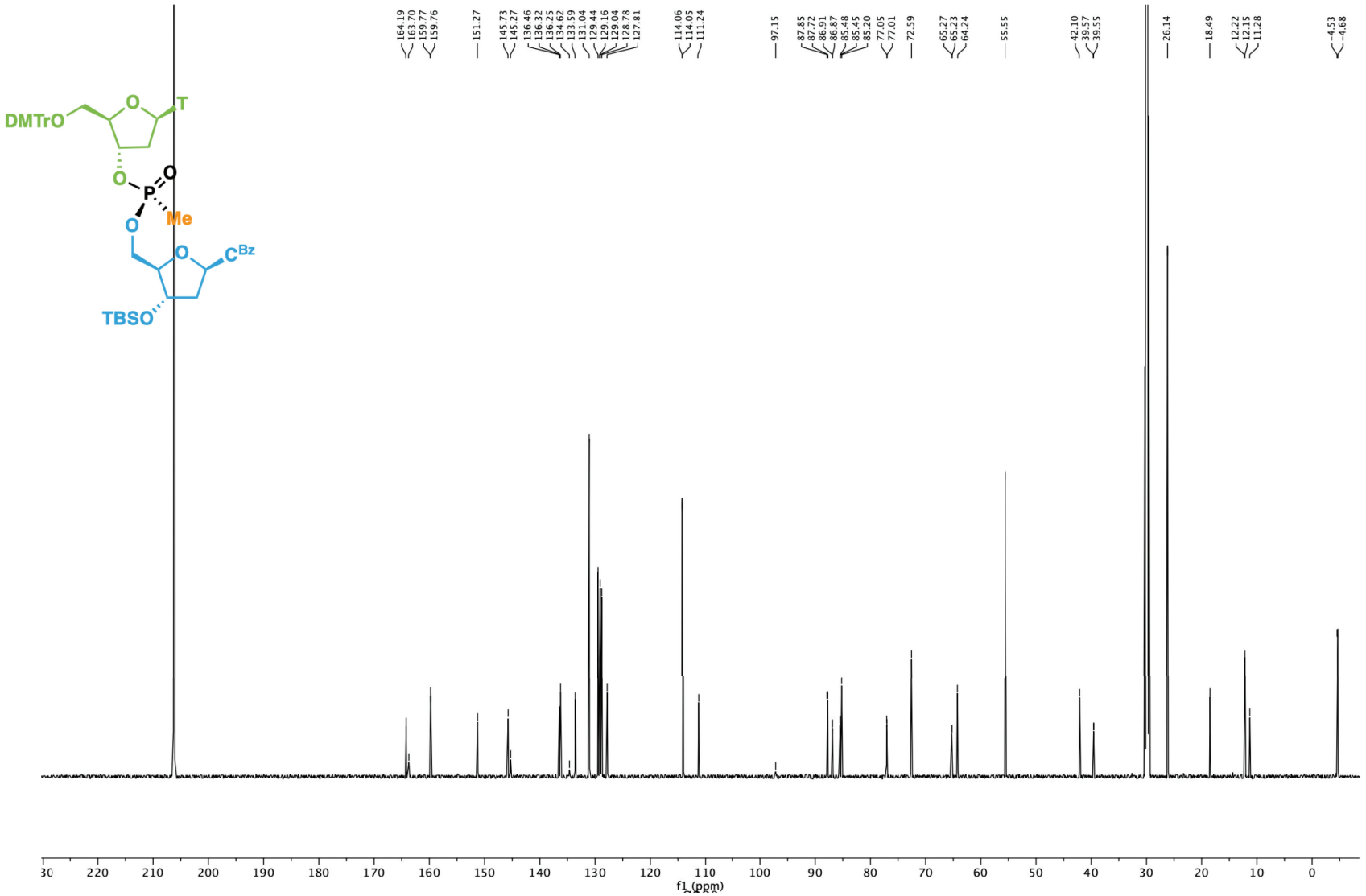
Compound (S_p)-1.45 ^{31}P NMR



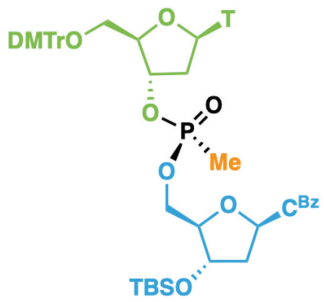
Compound (S_p)-1.46 ^{1}H NMR



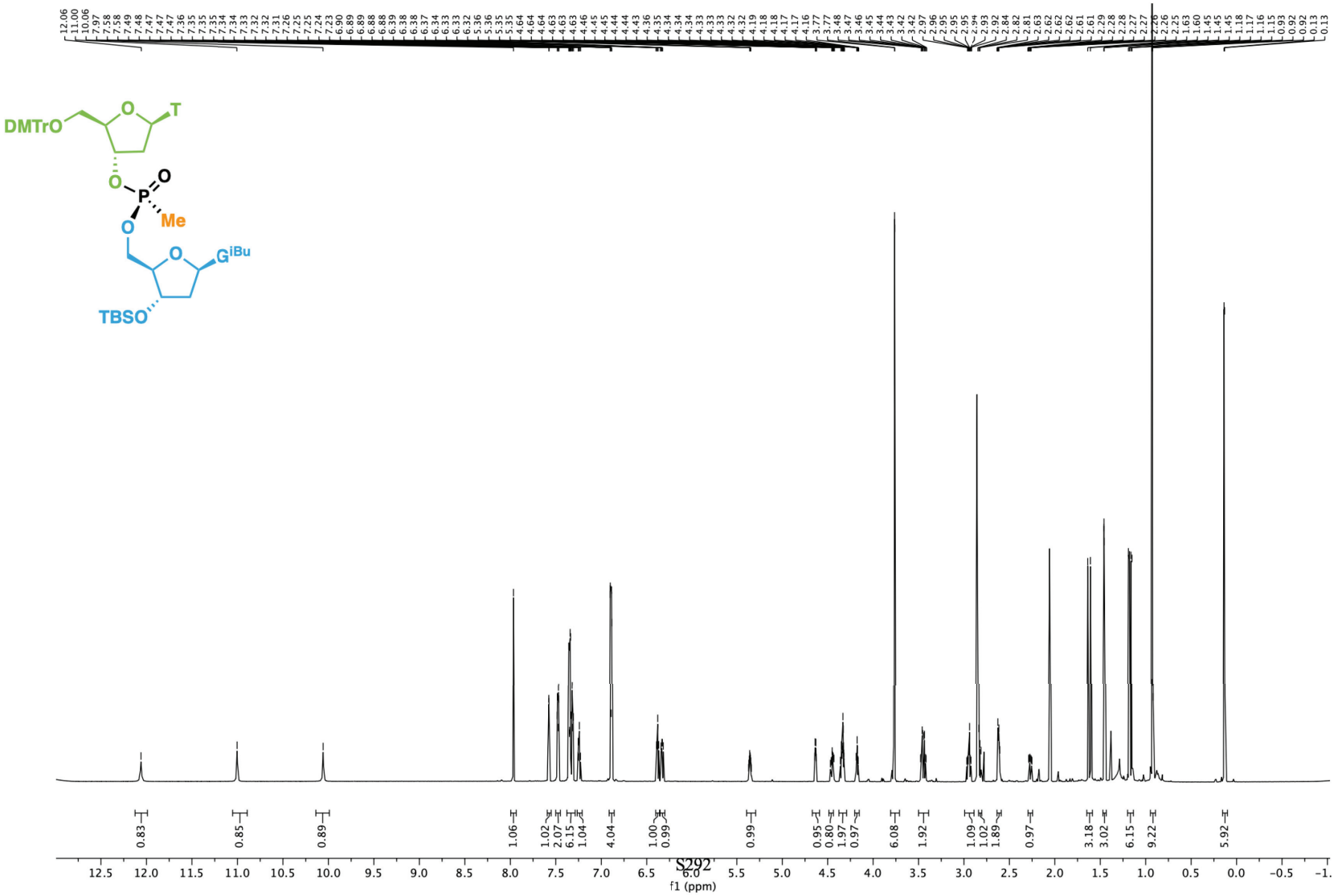
Compound (S_p)-1.46 ^{13}C NMR



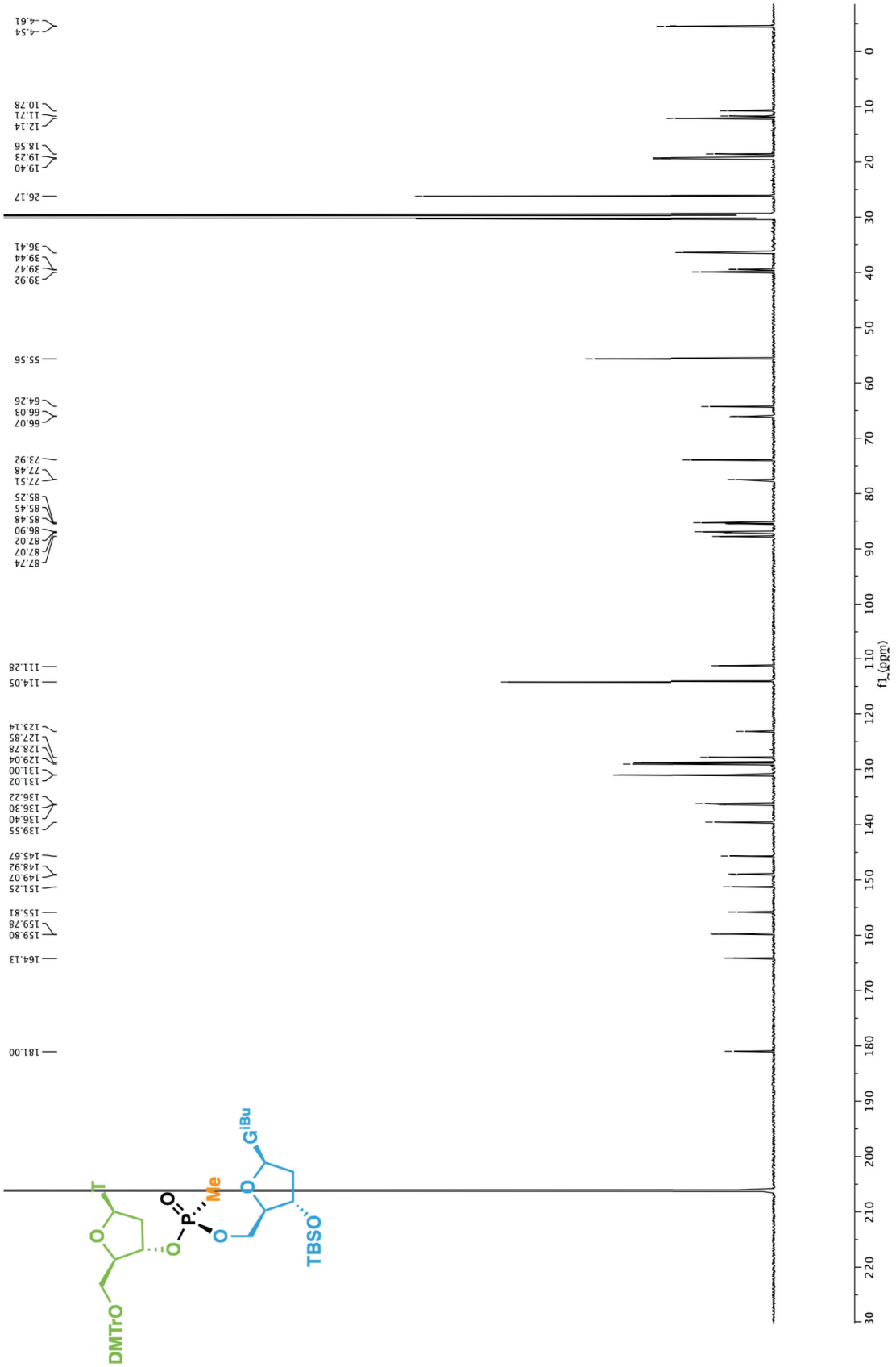
Compound (S_p)-1.46 ^{31}P NMR



Compound (S_p)-1.47 ^{1}H NMR



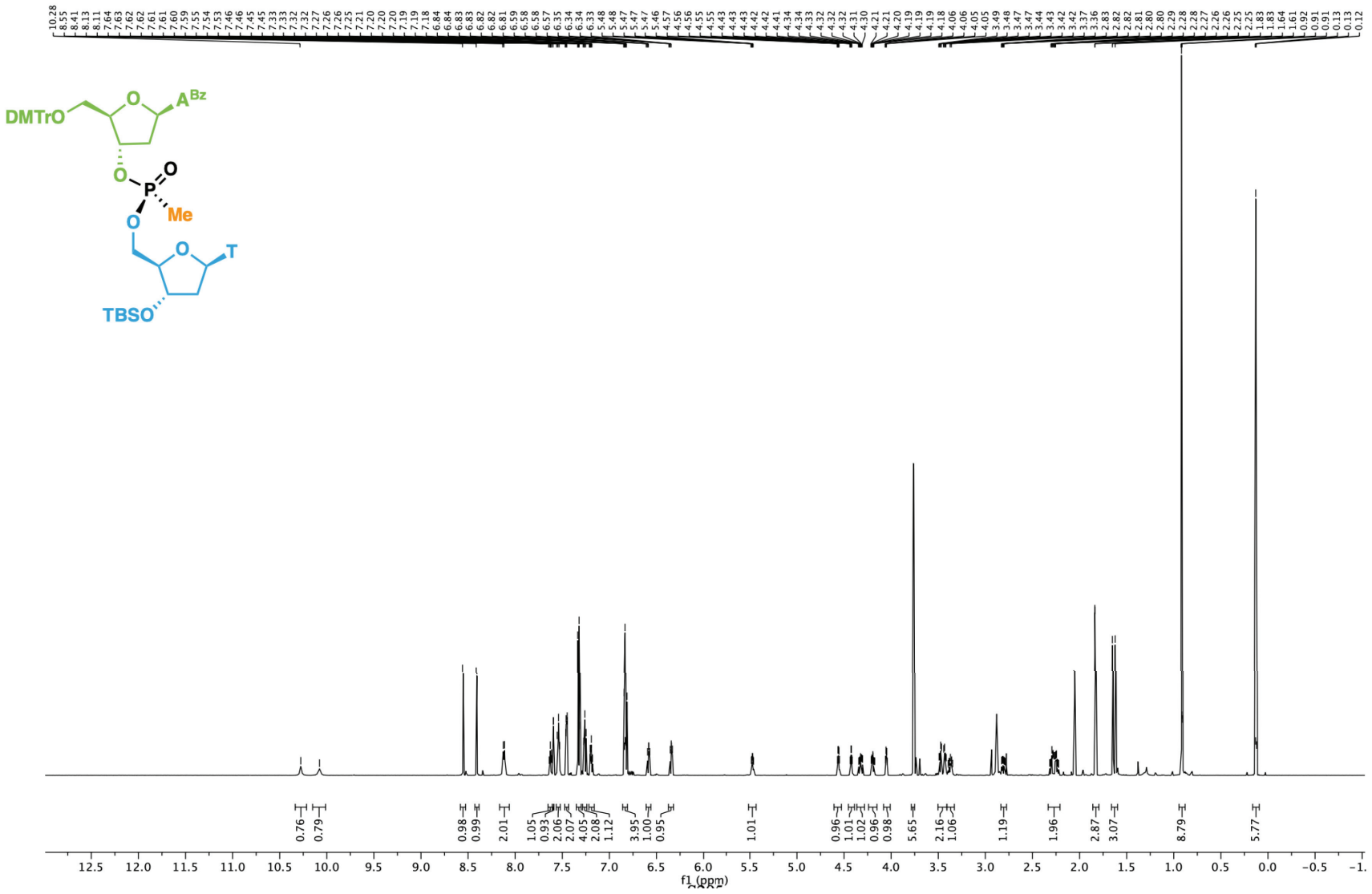
Compound (S_p)-1.47 ^{13}C NMR



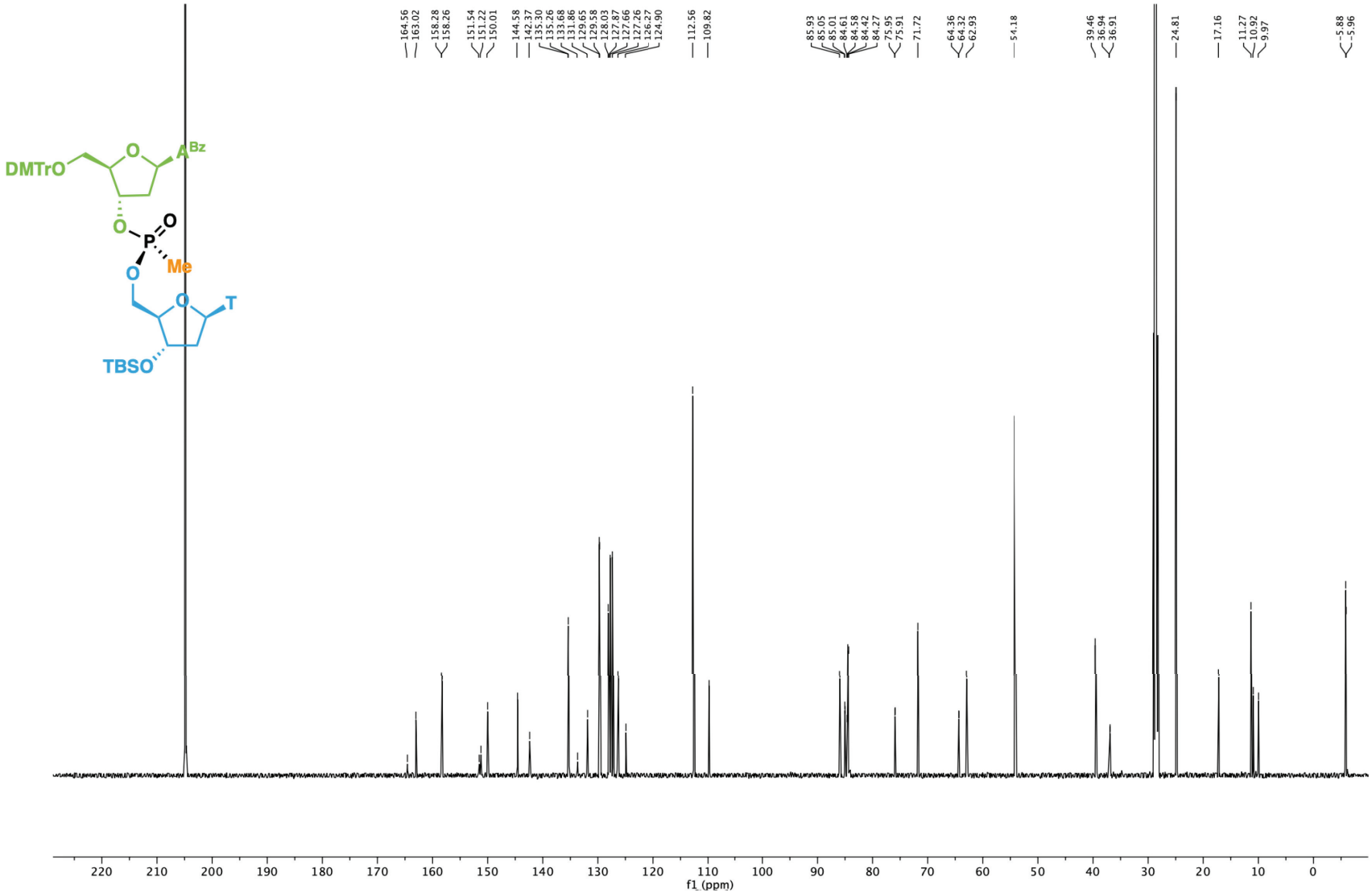
Compound (S_p)-1.47 ^{31}P NMR



Compound (S_p)-1.48 ^{1}H NMR



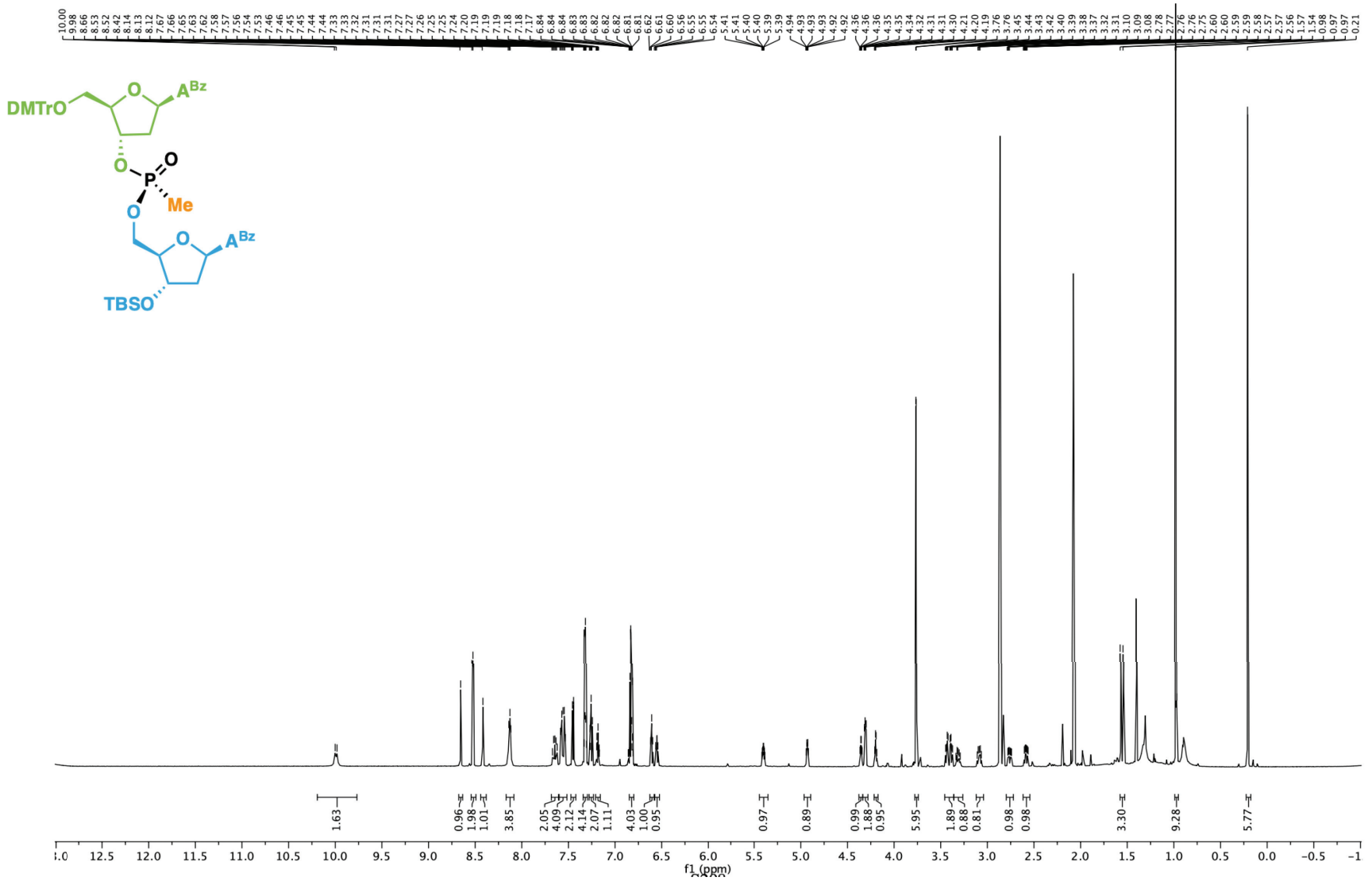
Compound (S_p)-1.48 ^{13}C NMR



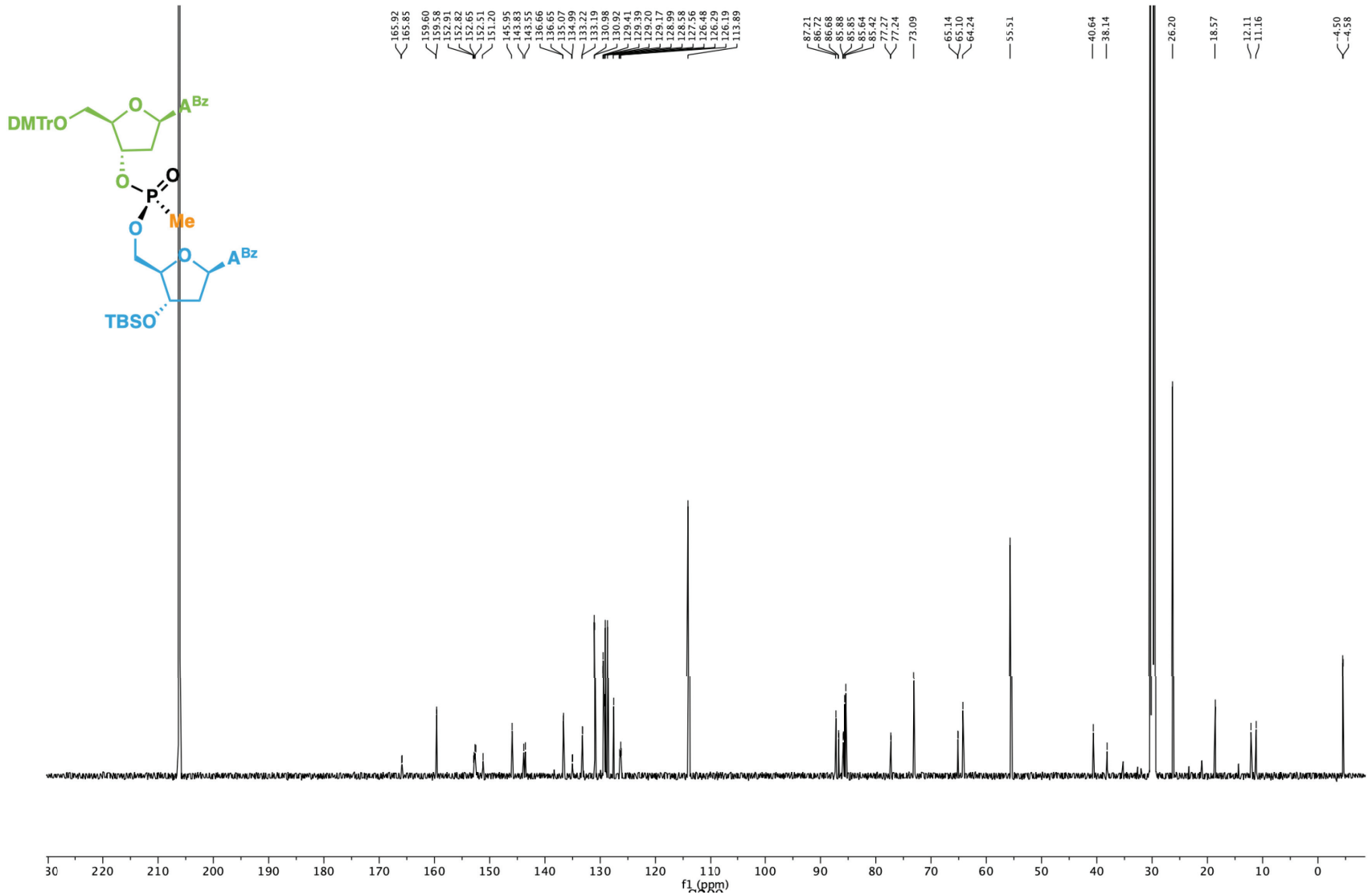
Compound (S_p)-1.48 ^{31}P NMR



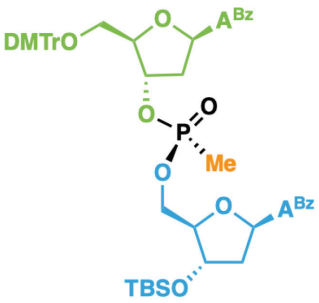
Compound (S_p)-1.49 ^{1}H NMR

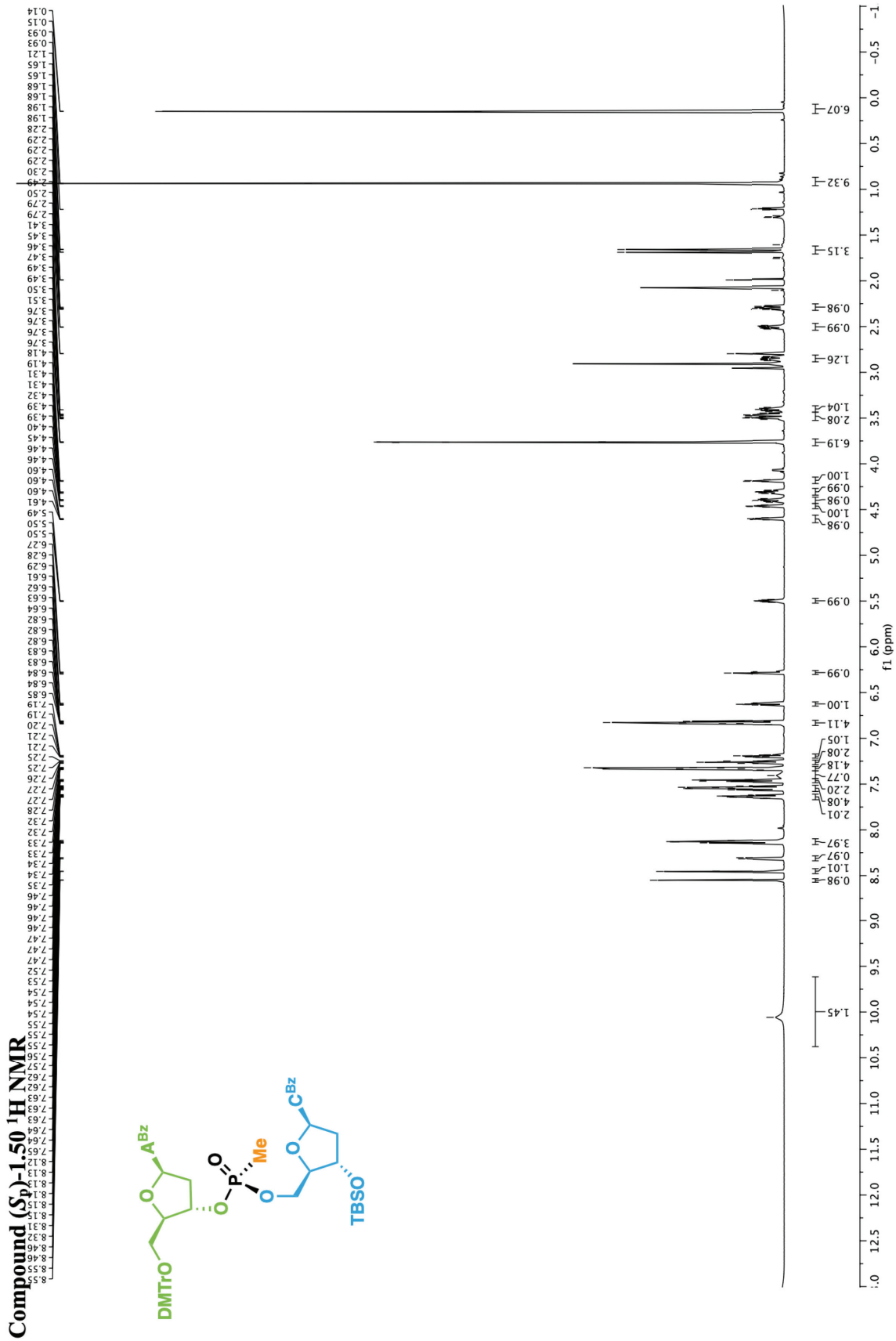


Compound (S_p)-1.49 ^{13}C NMR

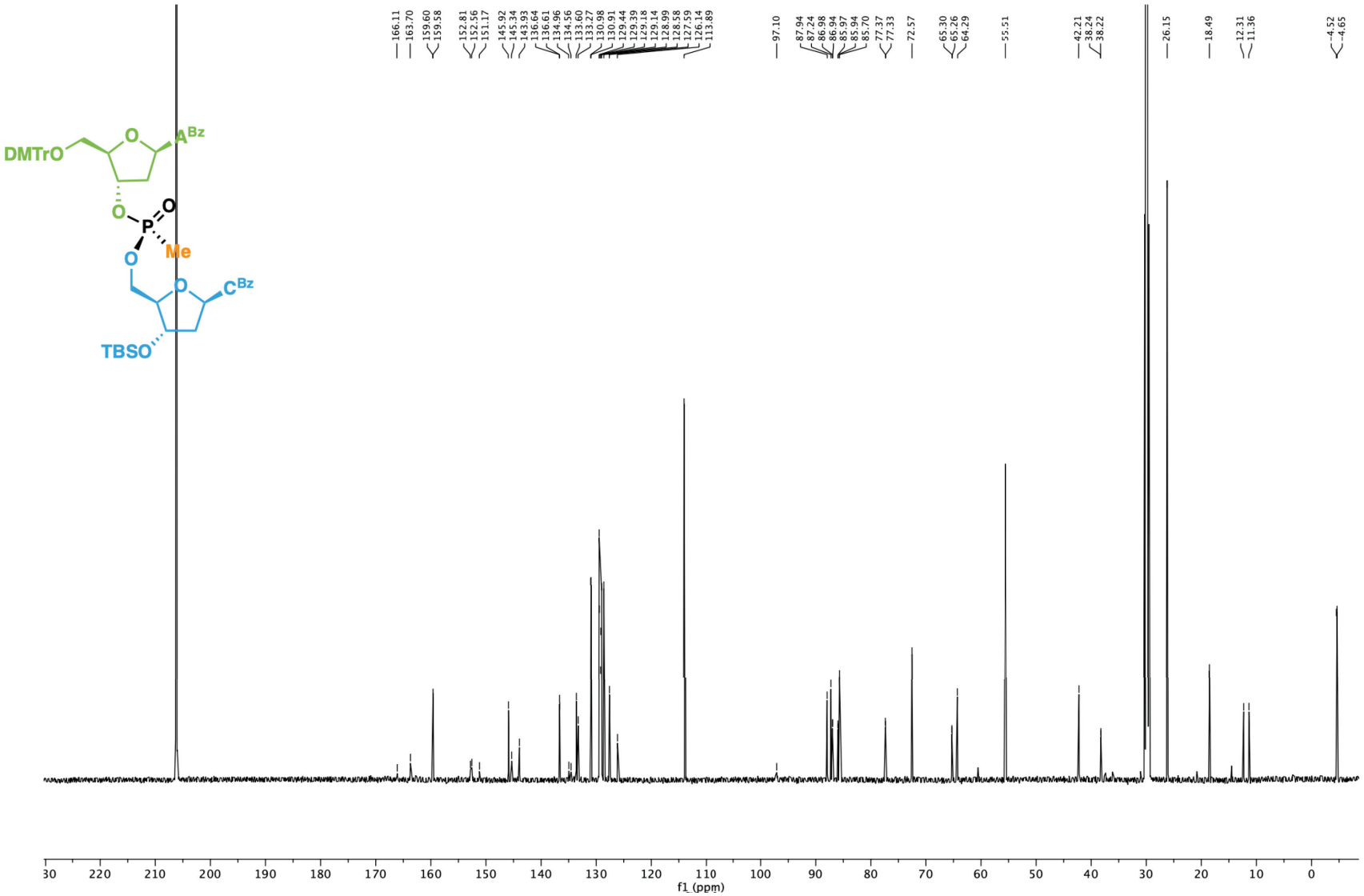


Compound (S_p)-1.49 ^{31}P NMR

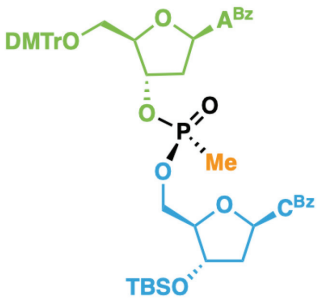



Compound (Sp)-1.50 1H NMR
DMTrO
ABz
Me
CBz
TBSO
f1 (ppm)

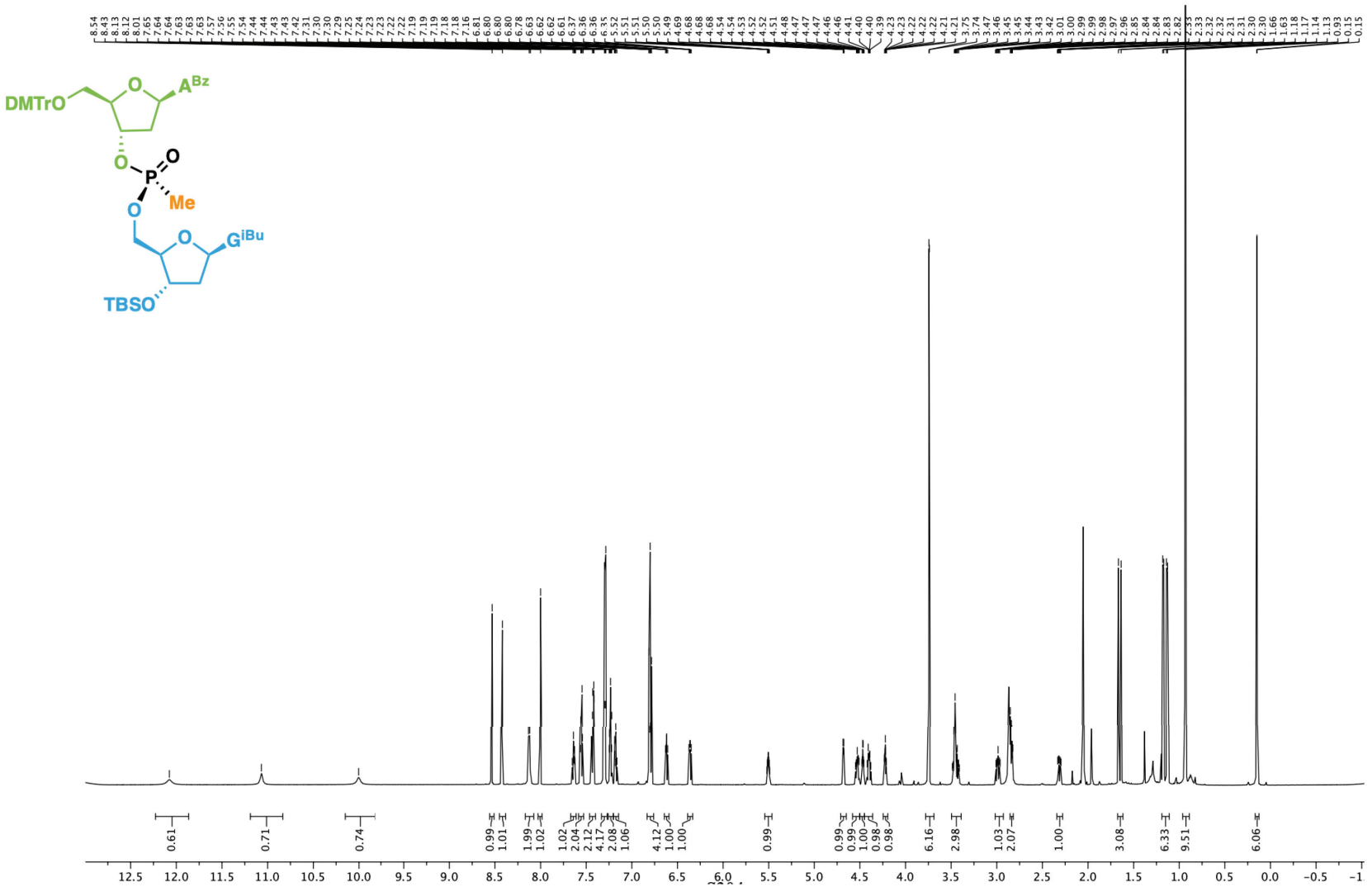
Compound (S_p)-1.50 ^{13}C NMR



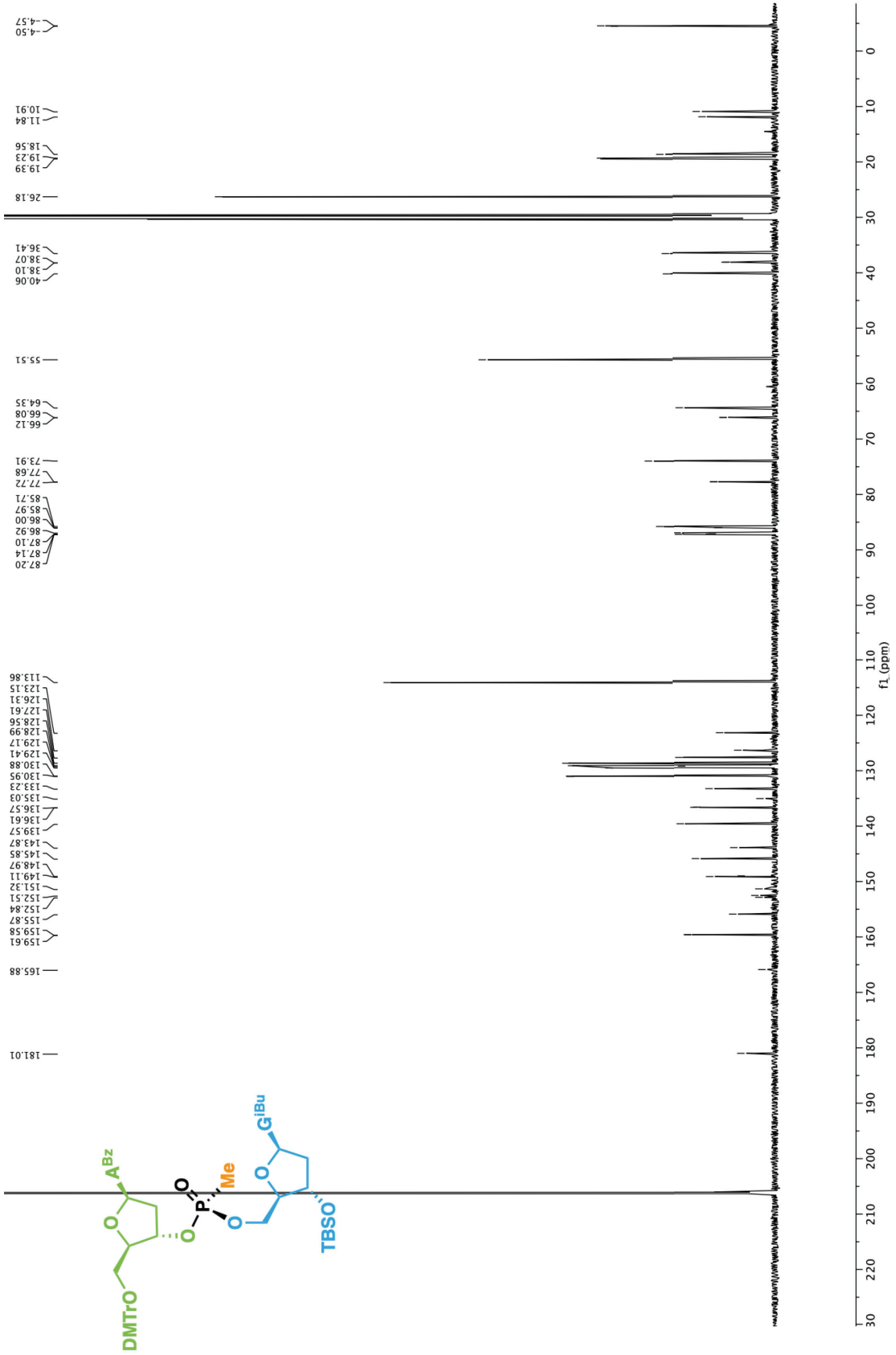
Compound (S_p)-1.50 ^{31}P NMR



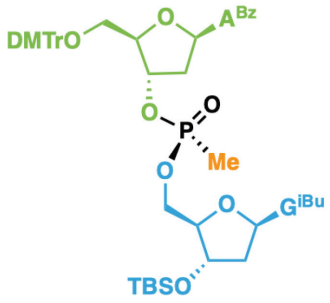
Compound (S_p)-1.51 ^{1}H NMR



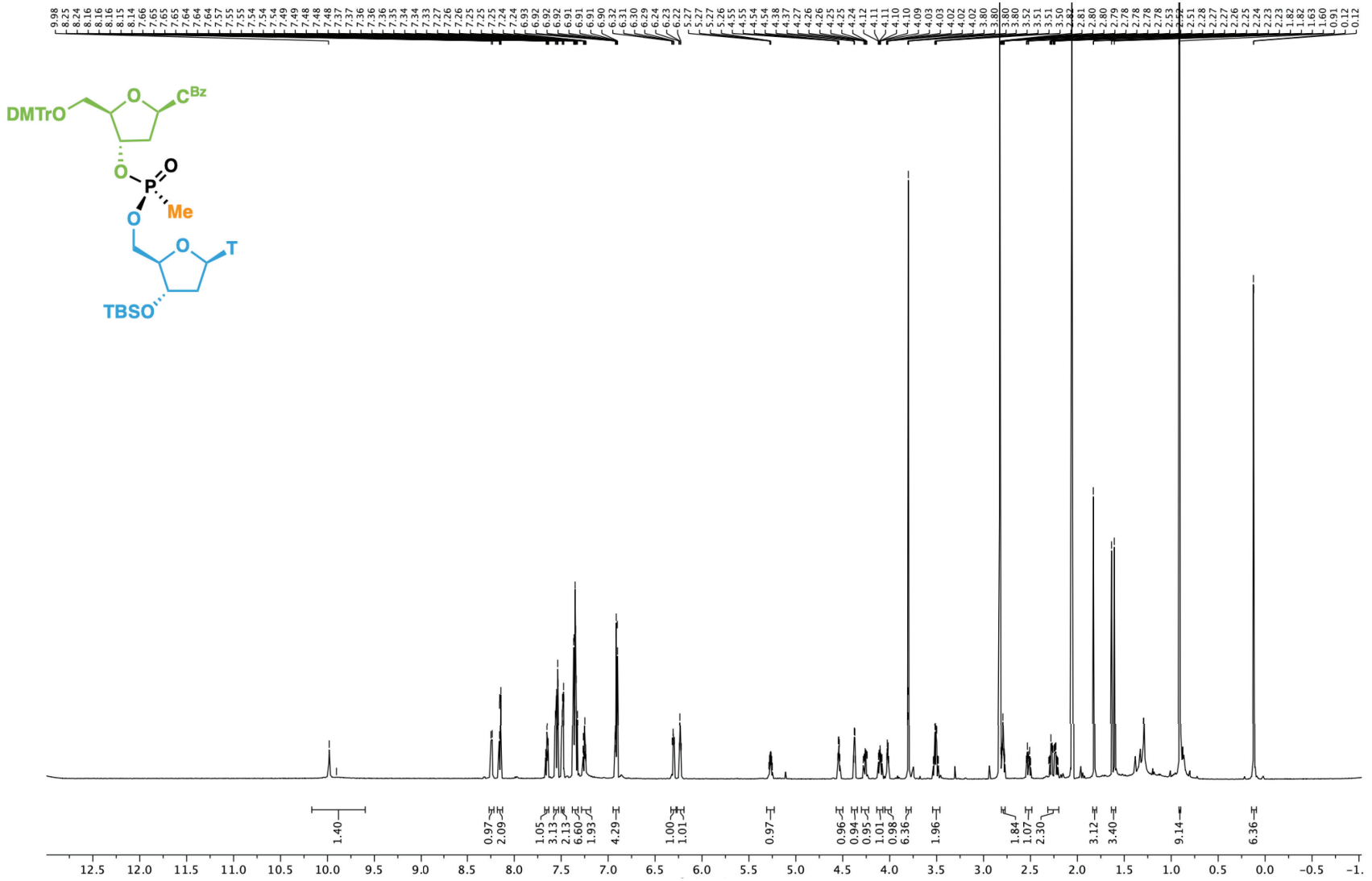
Compound (S_p)-1.51 ^{13}C NMR



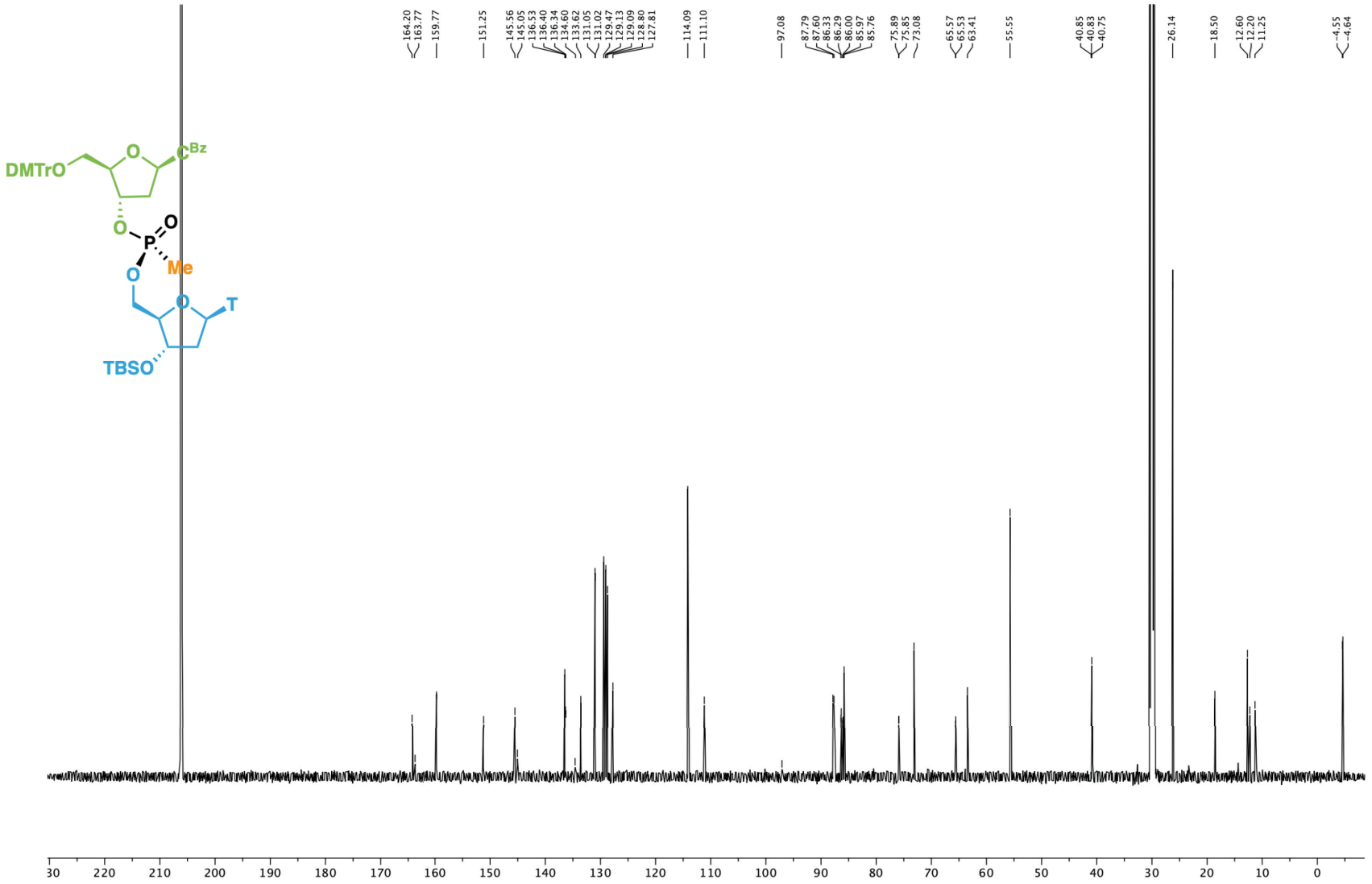
Compound (S_p)-1.51 ^{31}P NMR



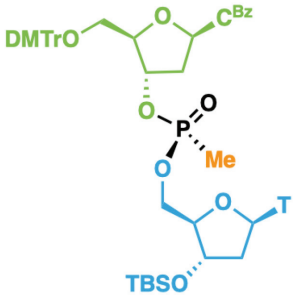
Compound (S_p)-1.52 ^{1}H NMR



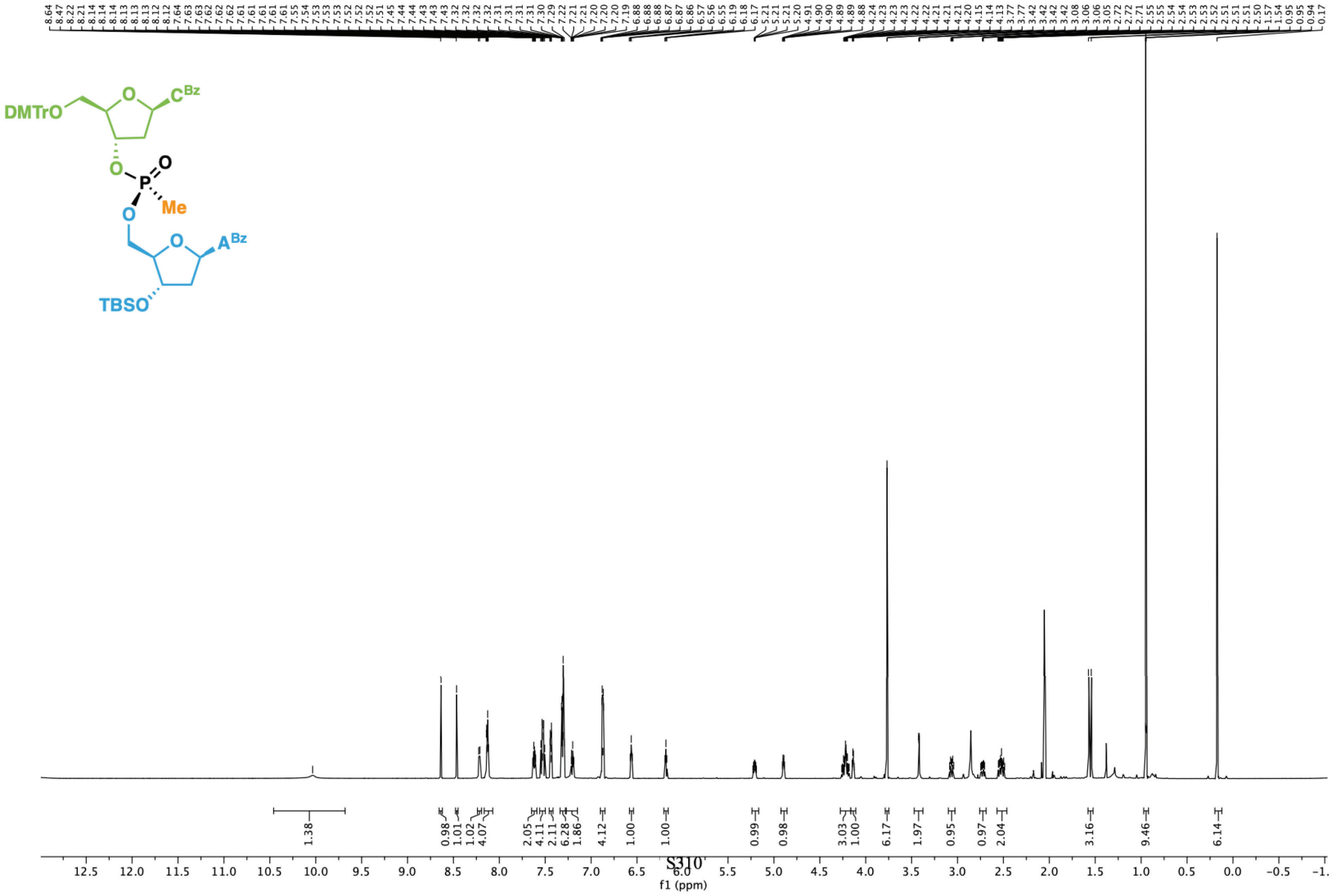
Compound (S_p)-1.52 ^{13}C NMR



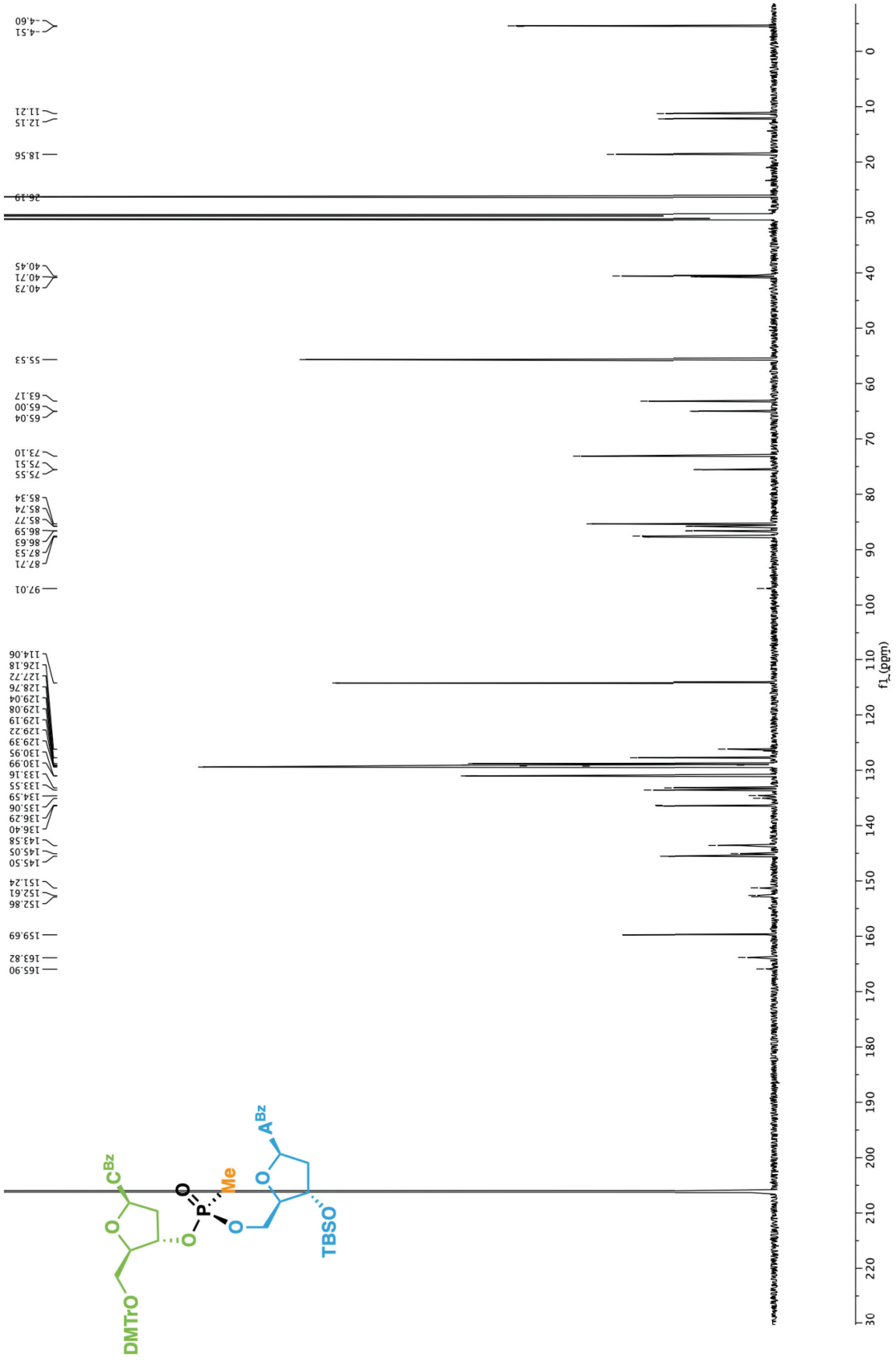
Compound (S_p)-1.52 ^{31}P NMR



Compound (S_p)-1.53 ^{1}H NMR



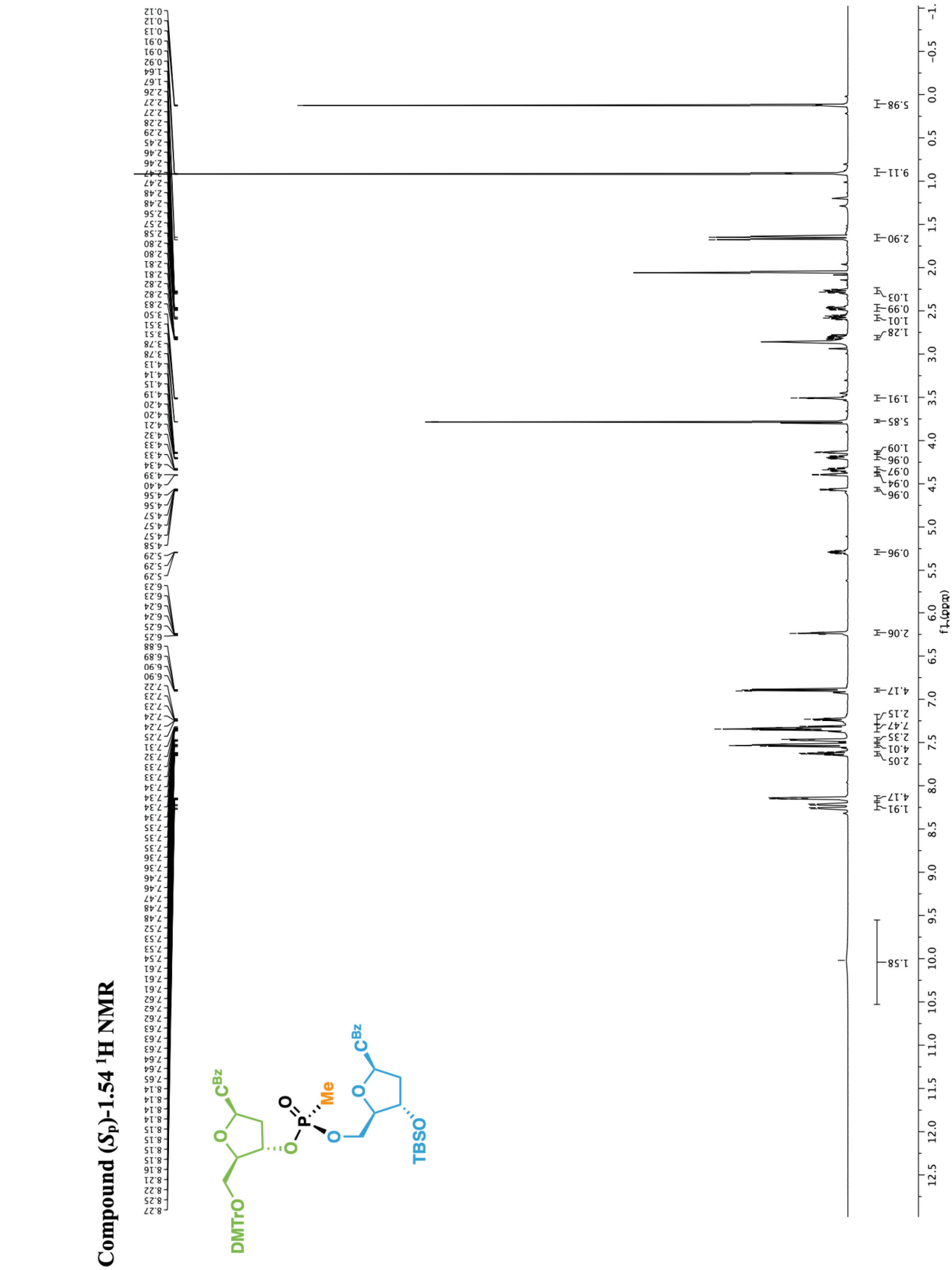
Compound (S_P)-1.53 ^{13}C NMR



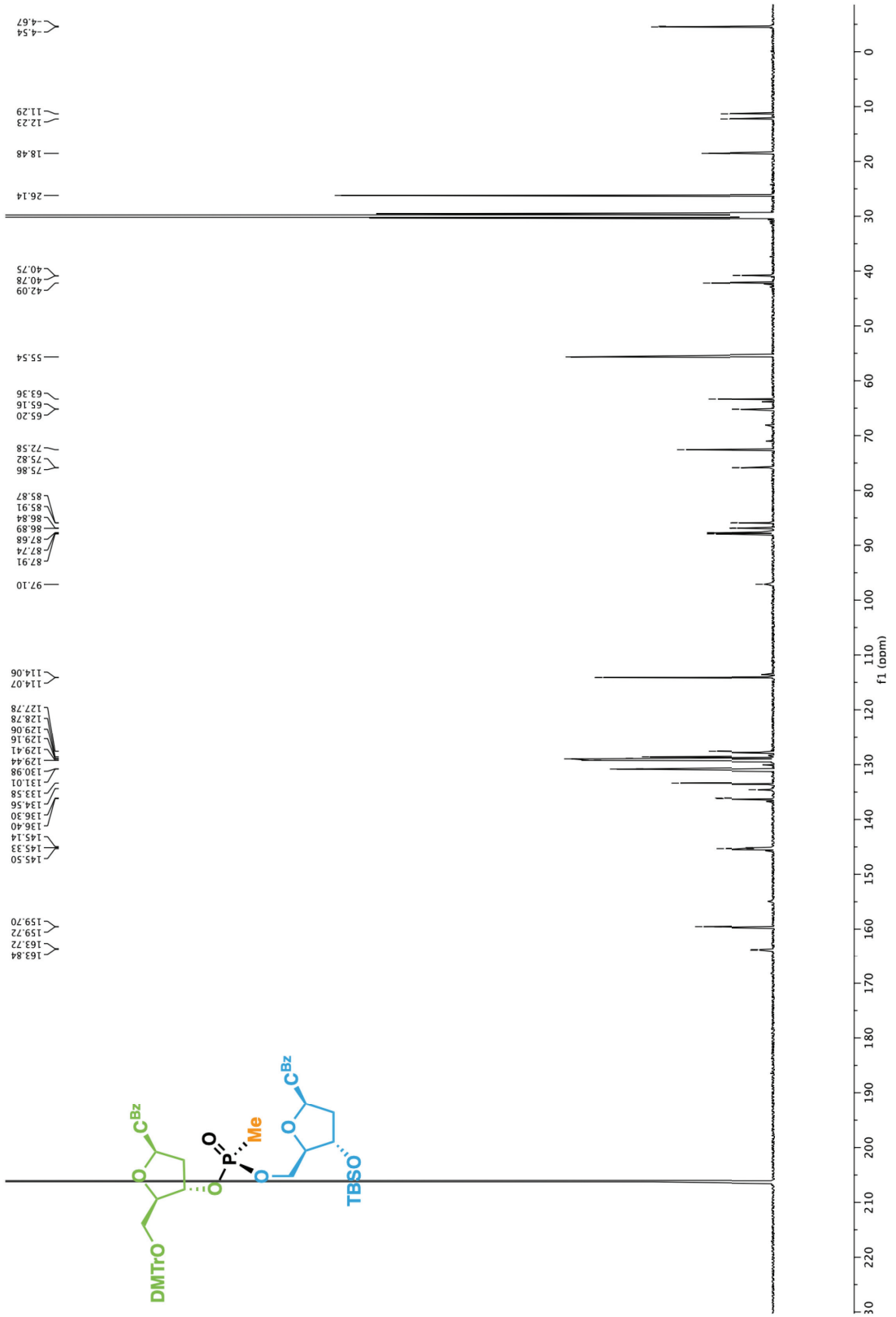
Compound (S_p)-1.53 ^{31}P NMR



Compound (S_P)-1.54 ^{1}H NMR



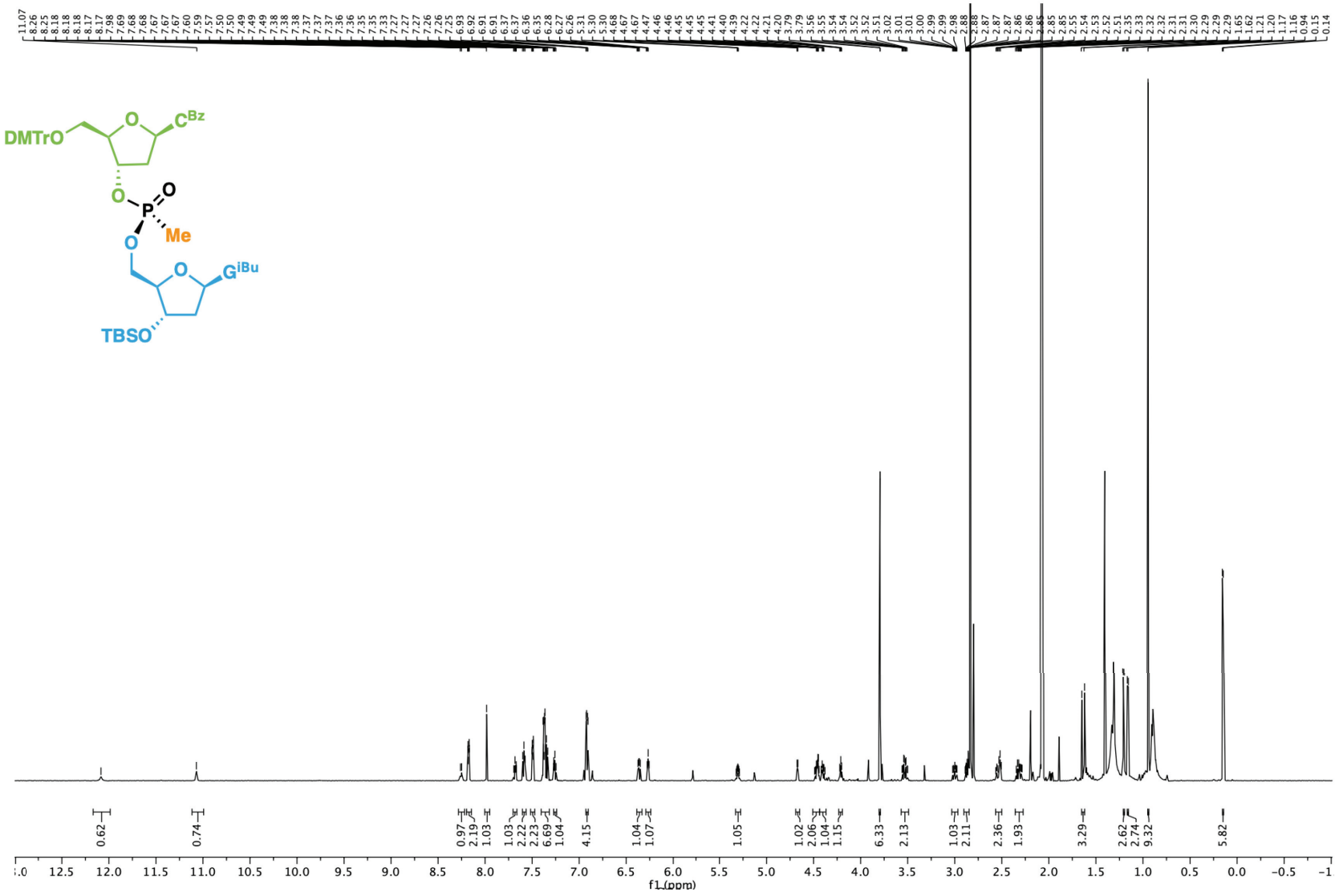
Compound (S_p)-1.54 ^{13}C NMR



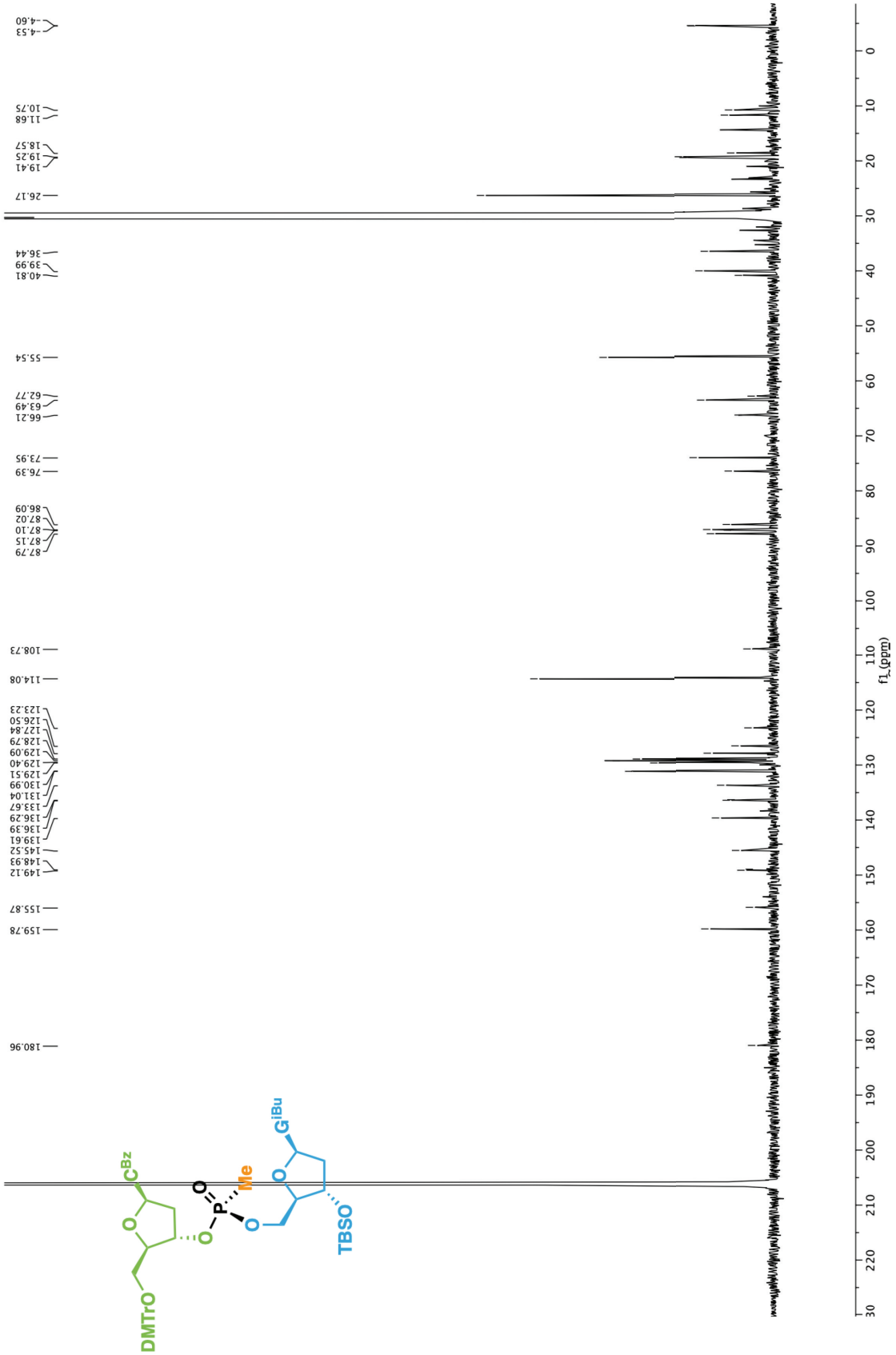
Compound (S_p)-1.54 ^{31}P NMR



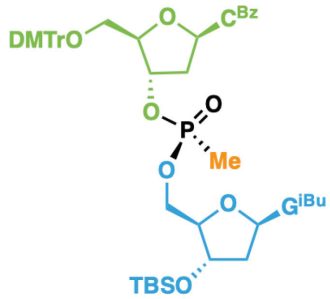
Compound (S_p)-1.55 ^{1}H NMR



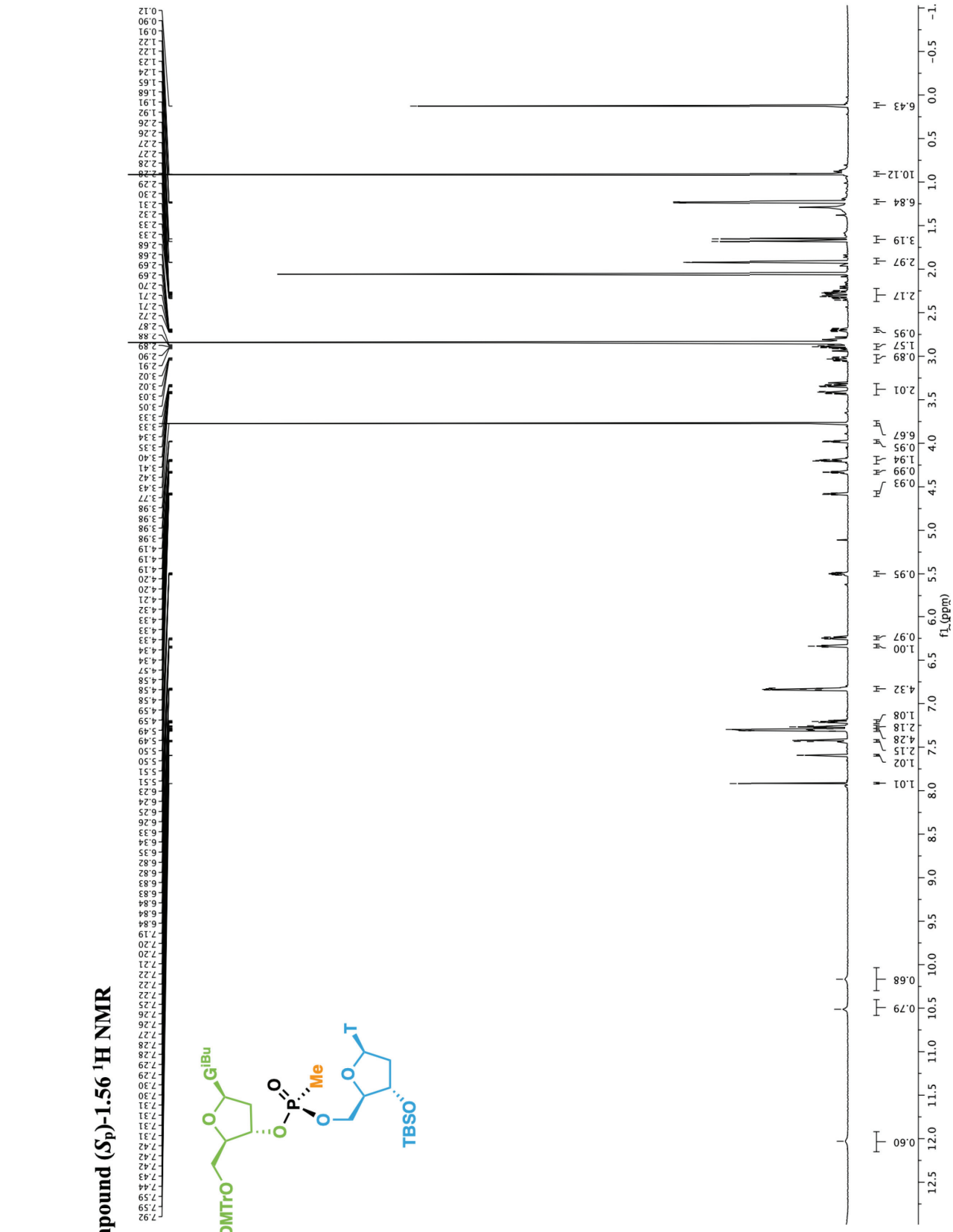
Compound (S_p)-1.55 ^{13}C NMR



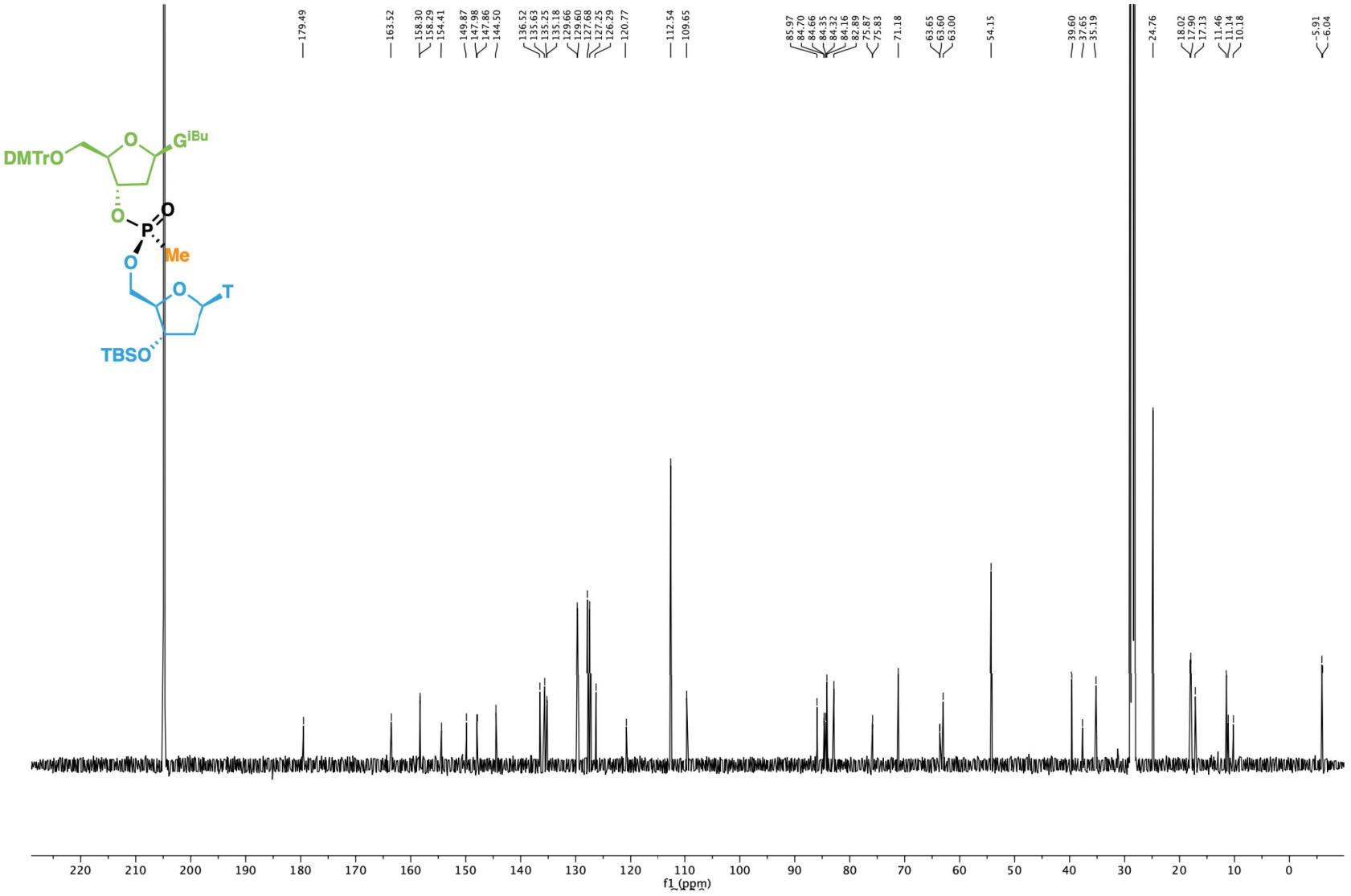
Compound (S_p)-1.55 ^{31}P NMR



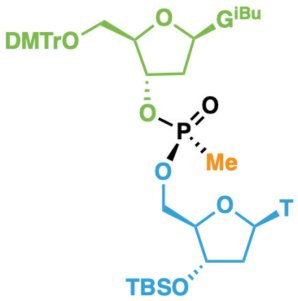
Compound (S_p)-1.56 ^{1}H NMR



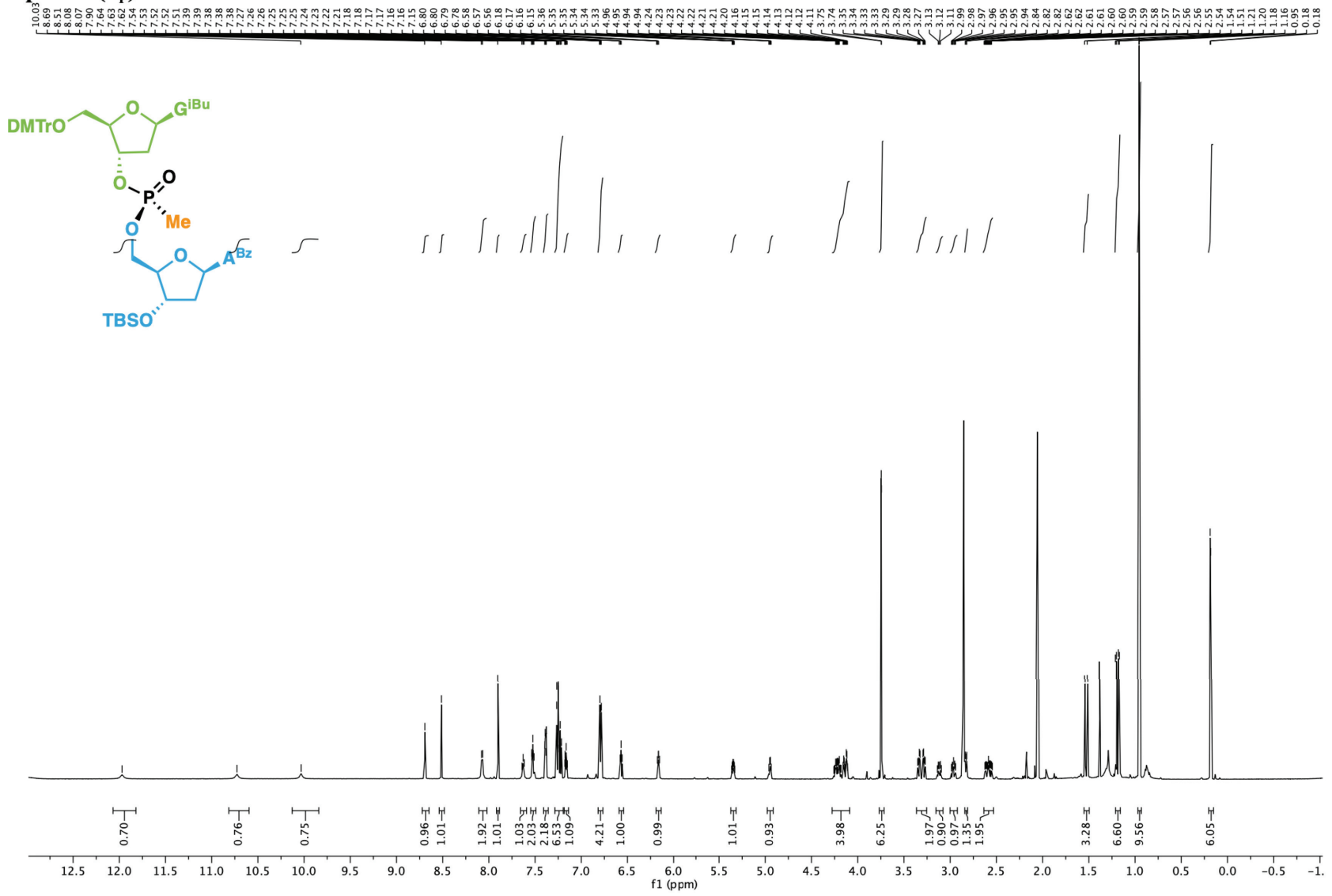
Compound (S_p)-1.56 ^{13}C NMR



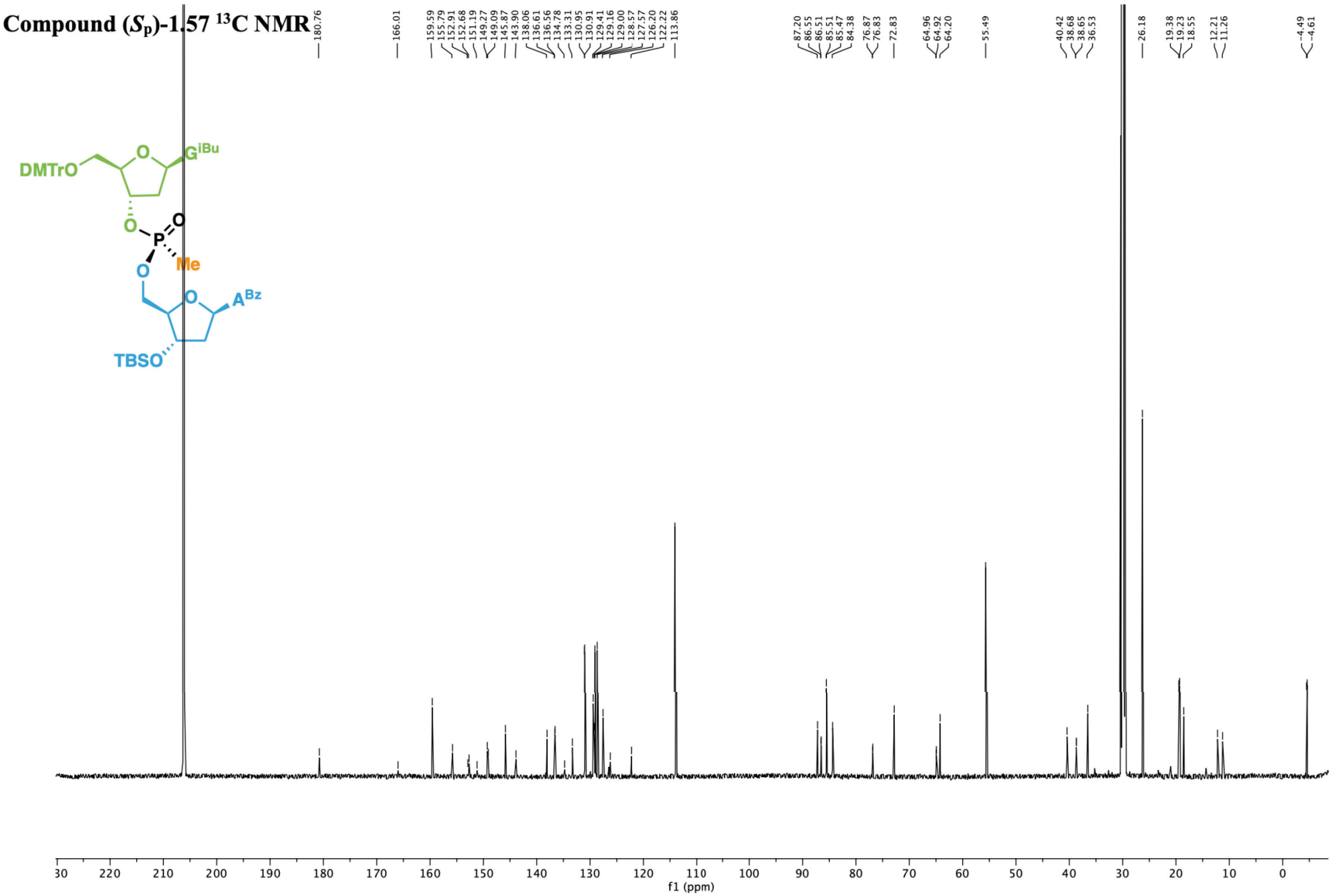
Compound (S_p)-1.56 ^{31}P NMR



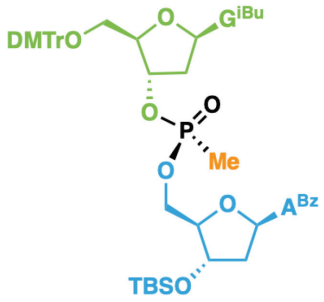
Compound (S_p)-1.57 ^{1}H NMR



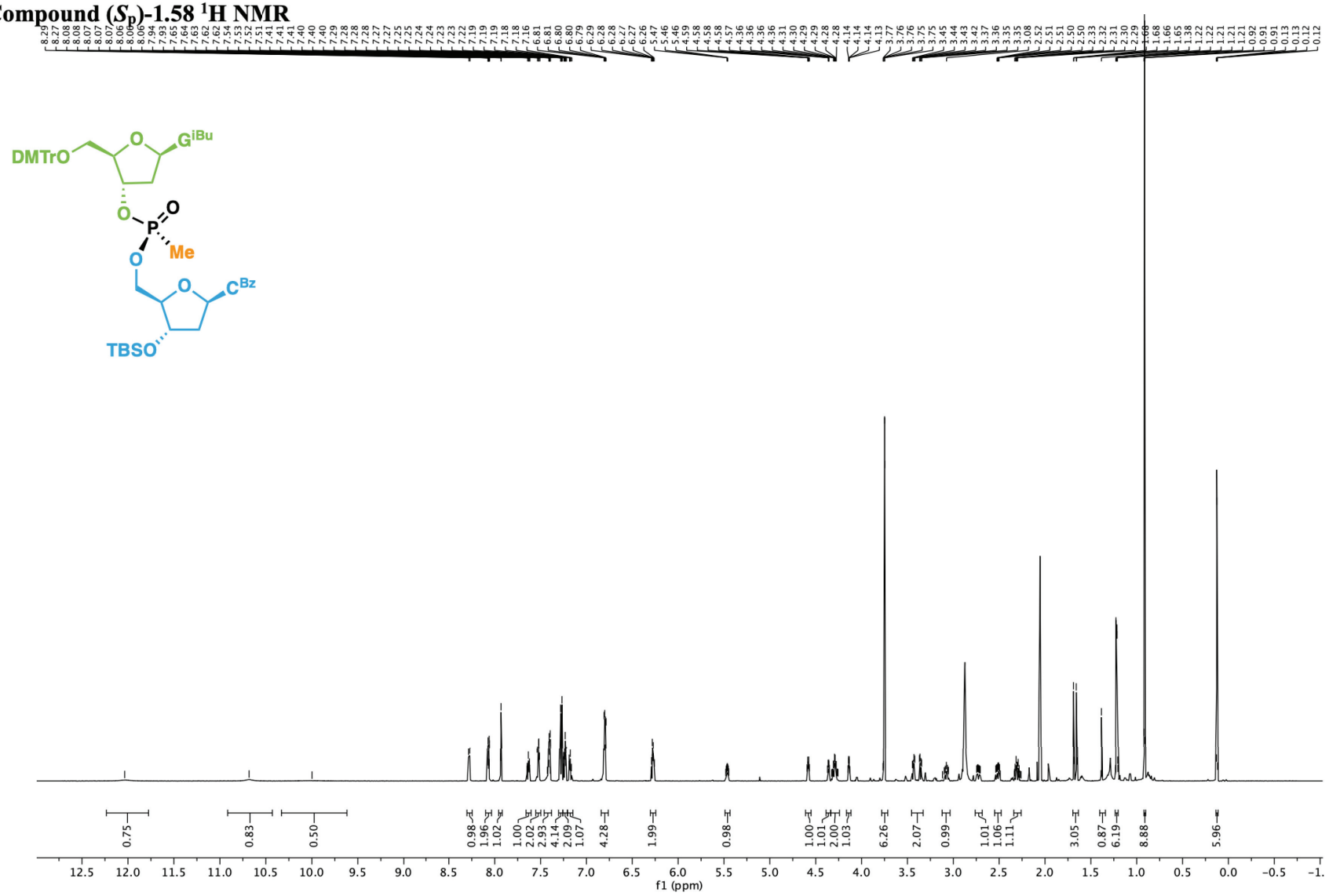
Compound (S_p)-1.57 ^{13}C NMR



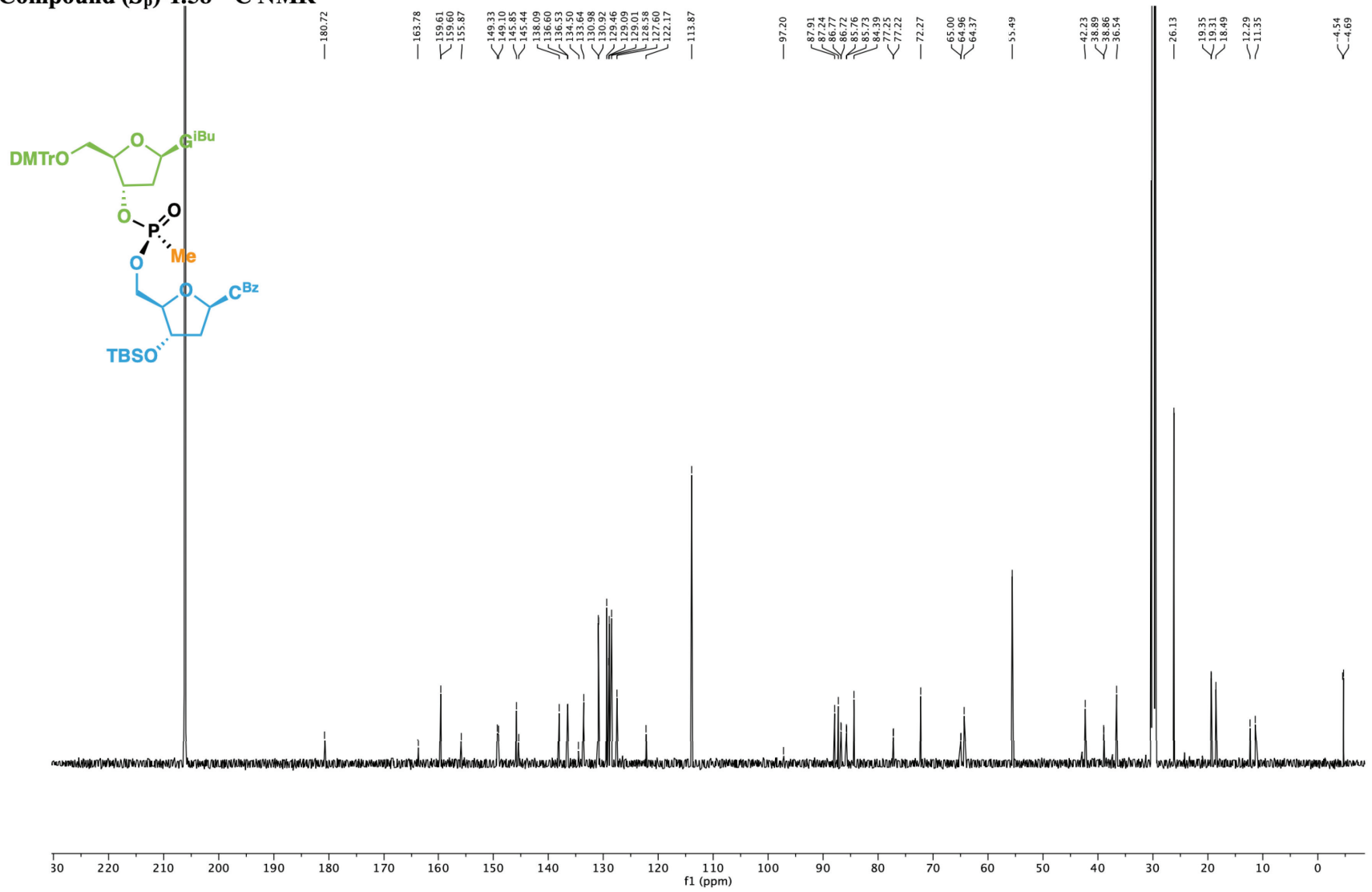
Compound (S_p)-1.57 ^{31}P NMR



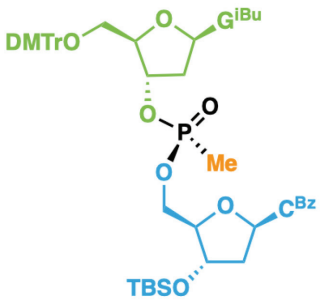
Compound (S_p)-1.58 ^{1}H NMR

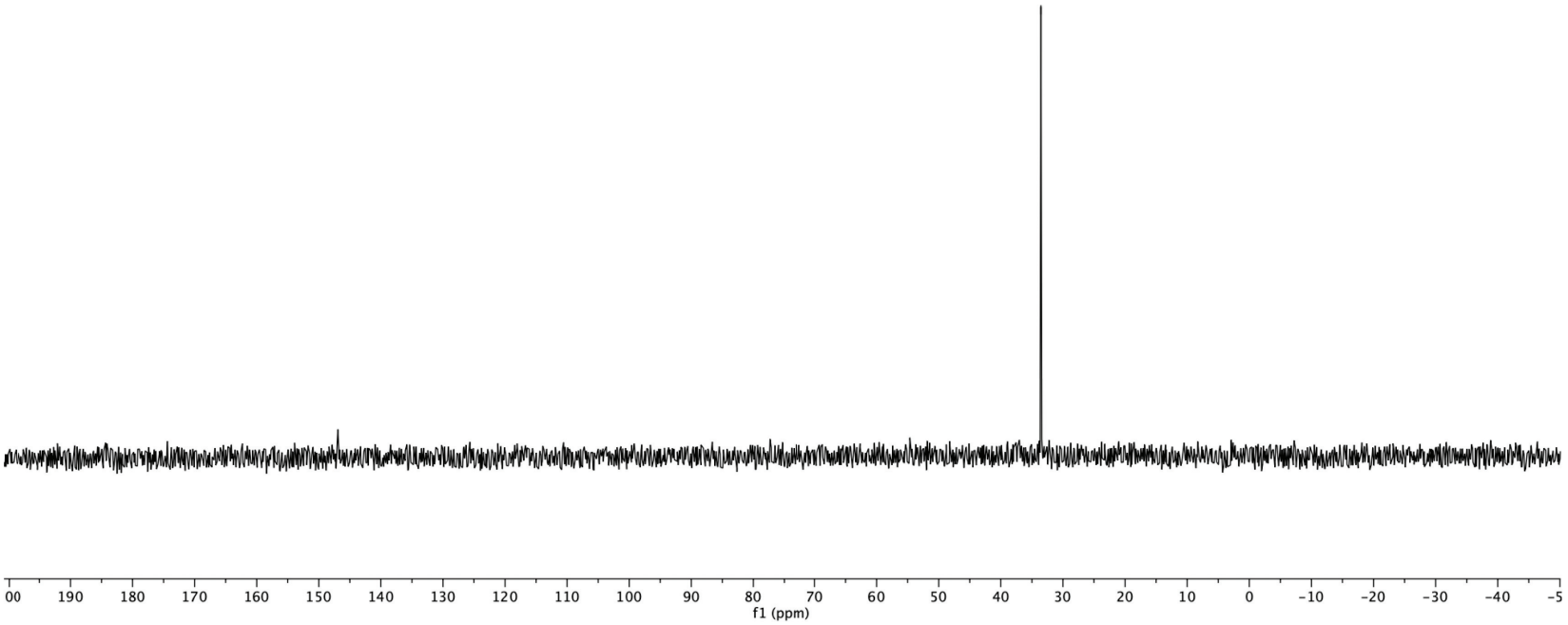


Compound (S_p)-1.58 ^{13}C NMR

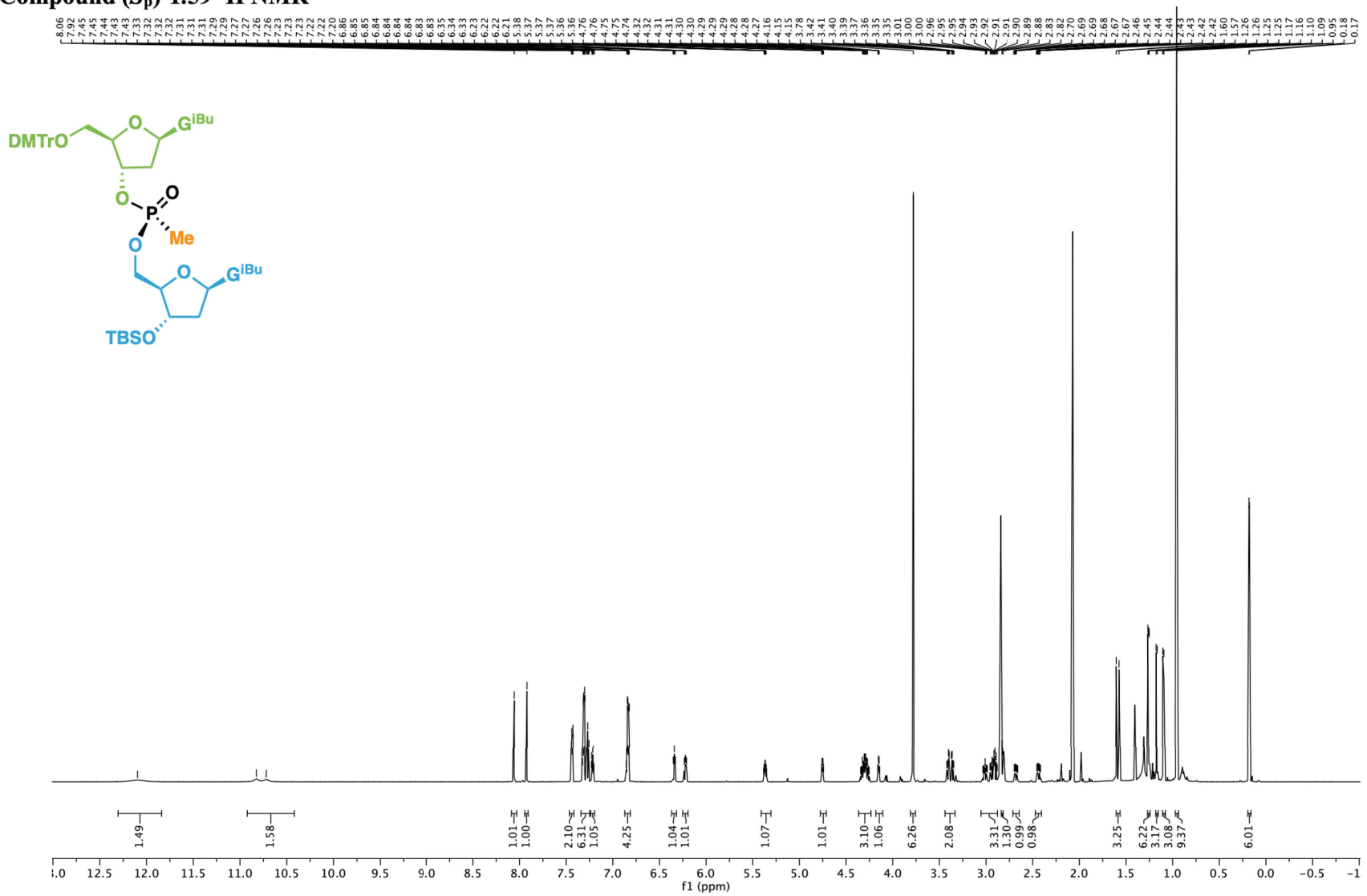


Compound (S_p)-1.58 ^{31}P NMR

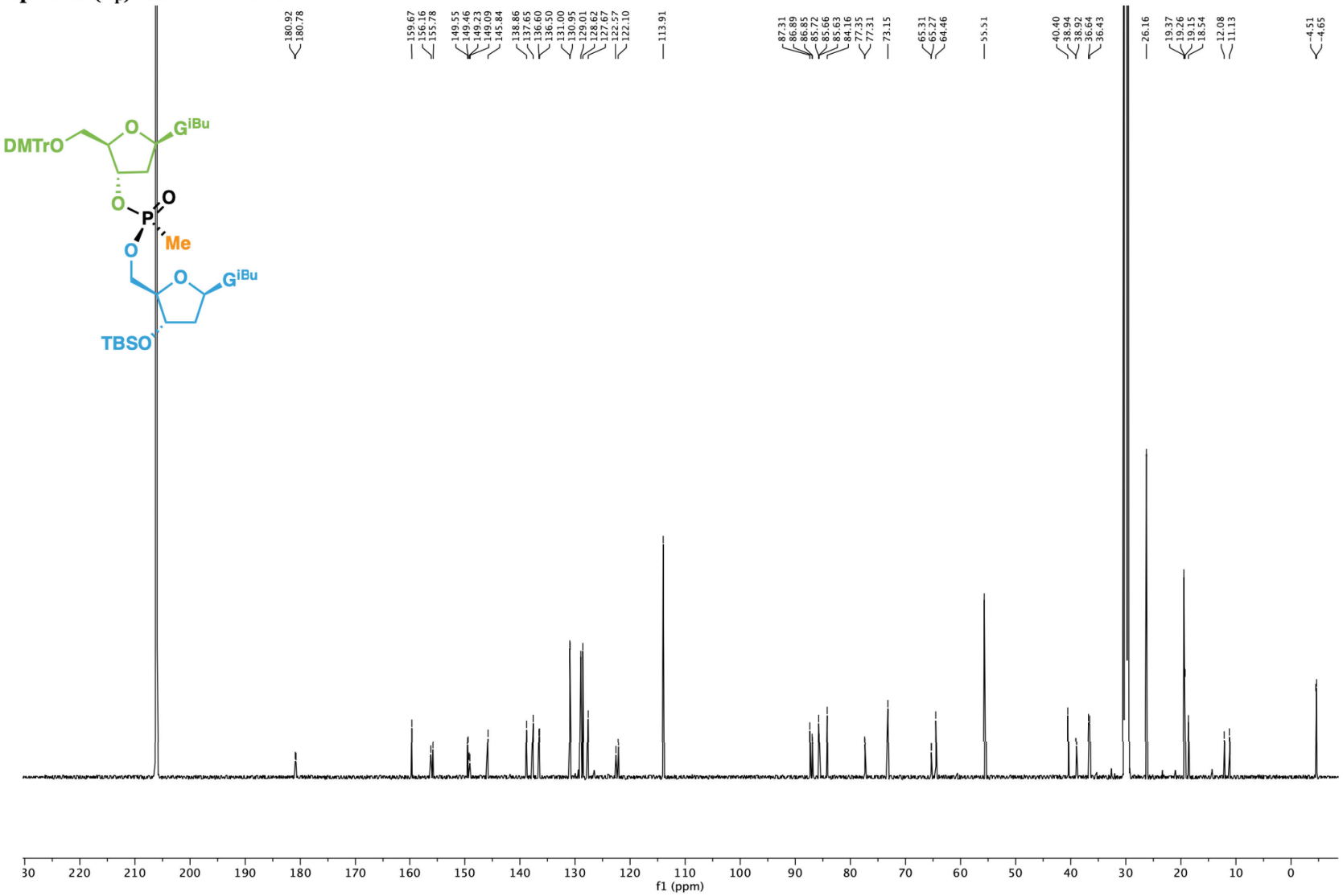




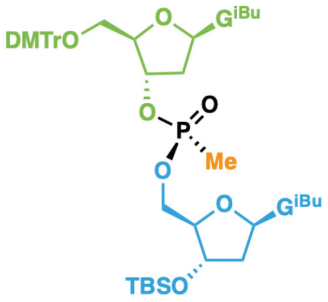
Compound (S_p)-1.59 ^{1}H NMR

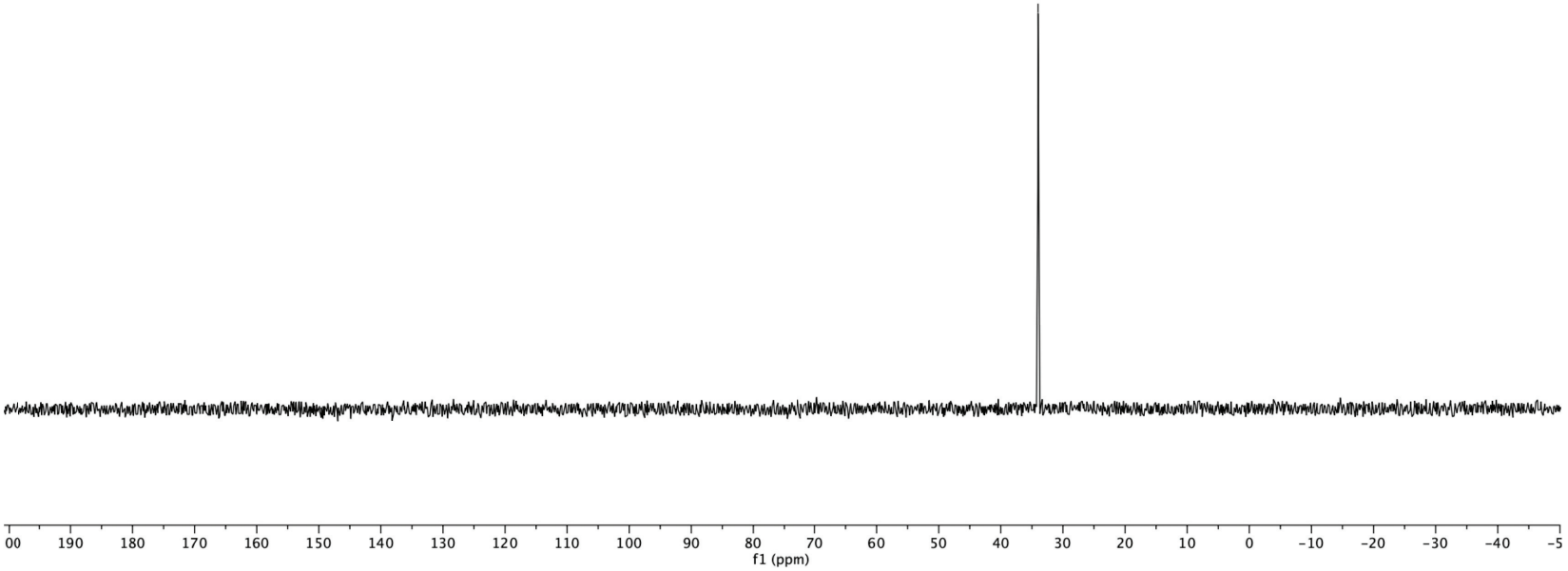


Compound (S_p)-1.59 ^{13}C NMR

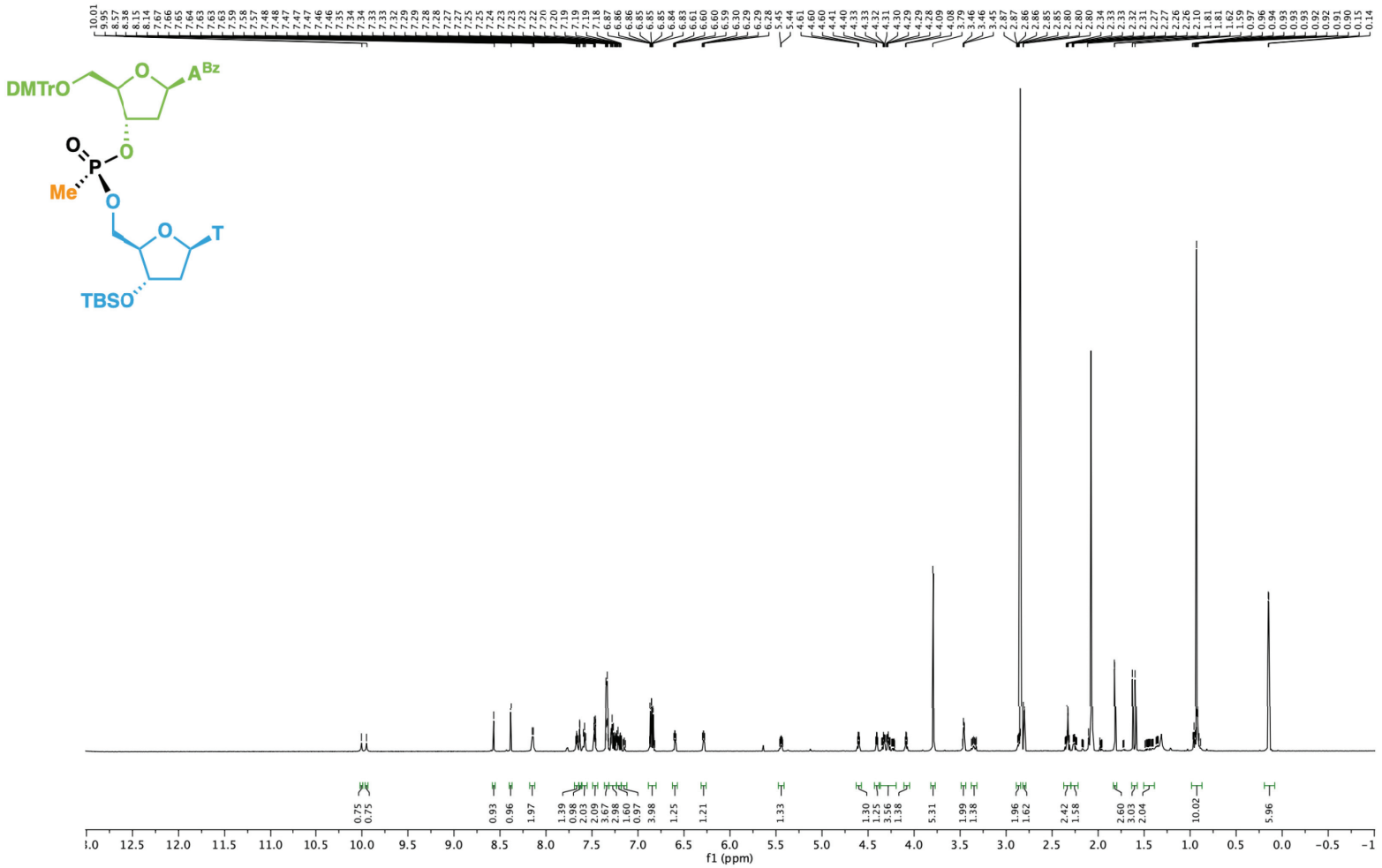


Compound (S_p)-1.59 ^{31}P NMR

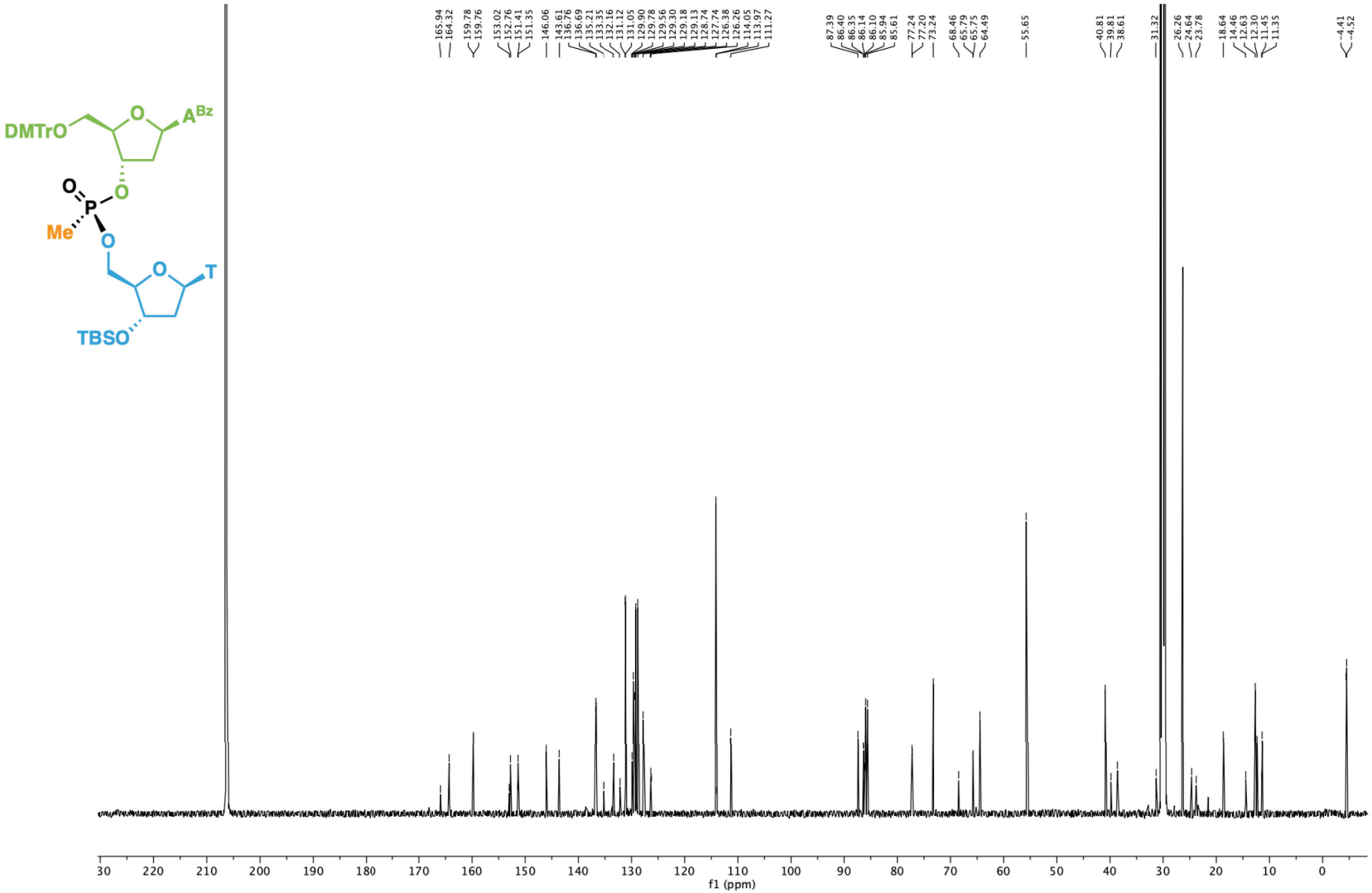




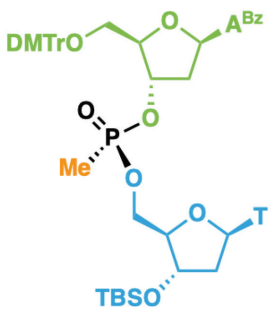
Compound (R_p)-1.48 ^{1}H NMR



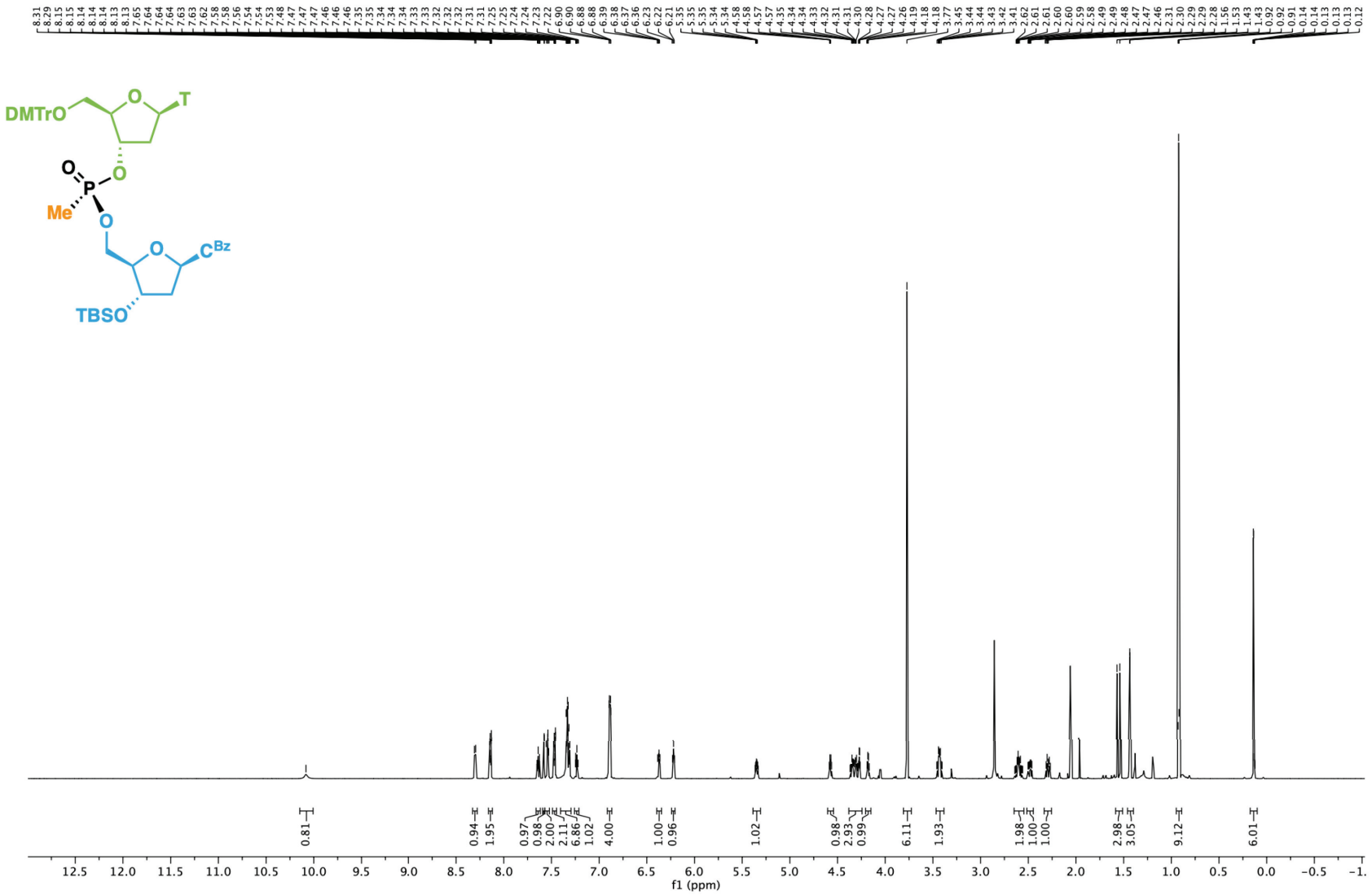
Compound (R_p)-1.48 ^{13}C NMR



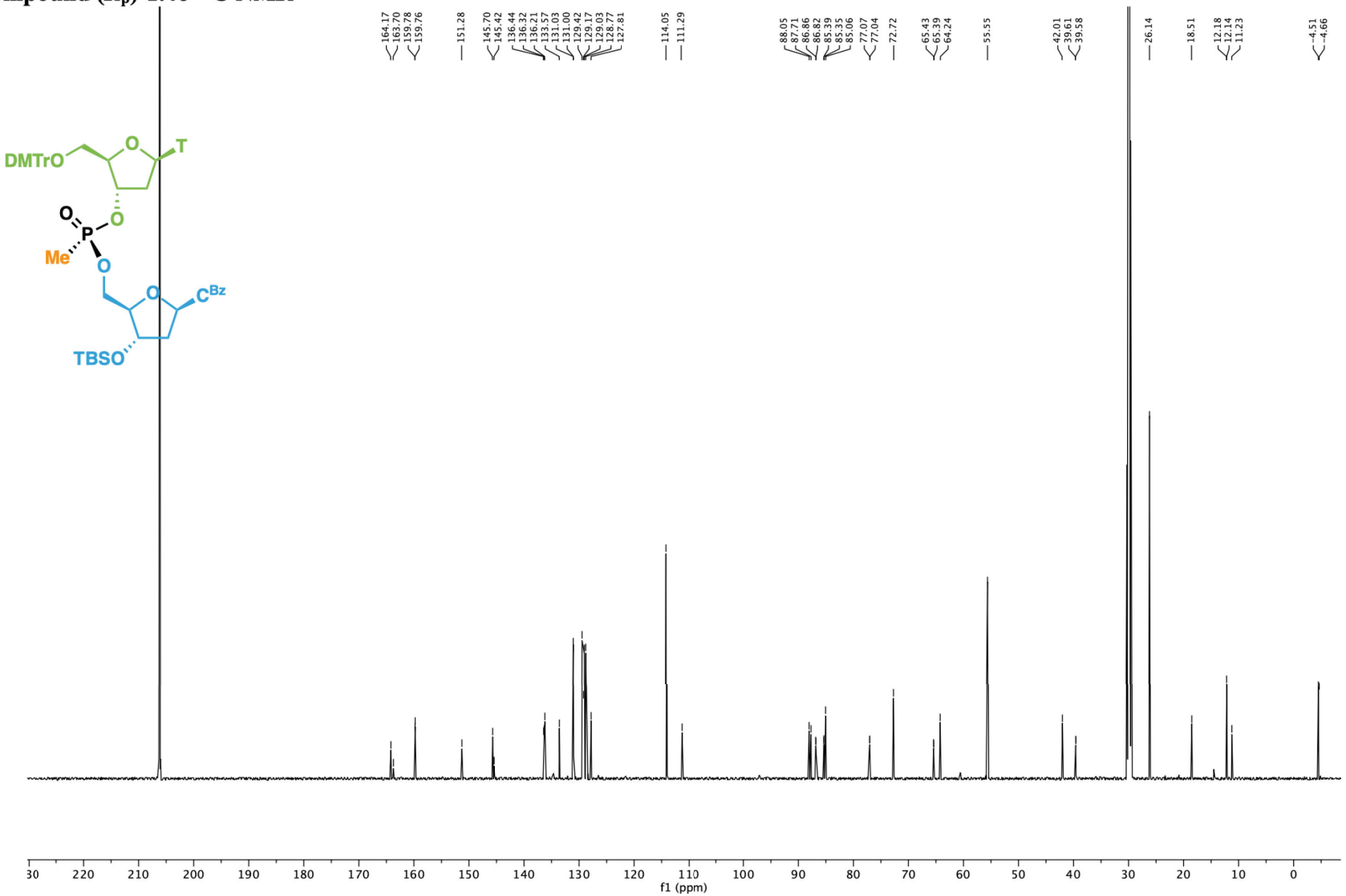
Compound (R_p)-1.48 ^{31}P NMR



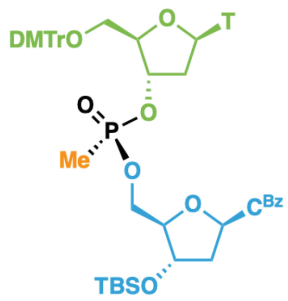
Compound (R_p)-1.46 ^{1}H NMR



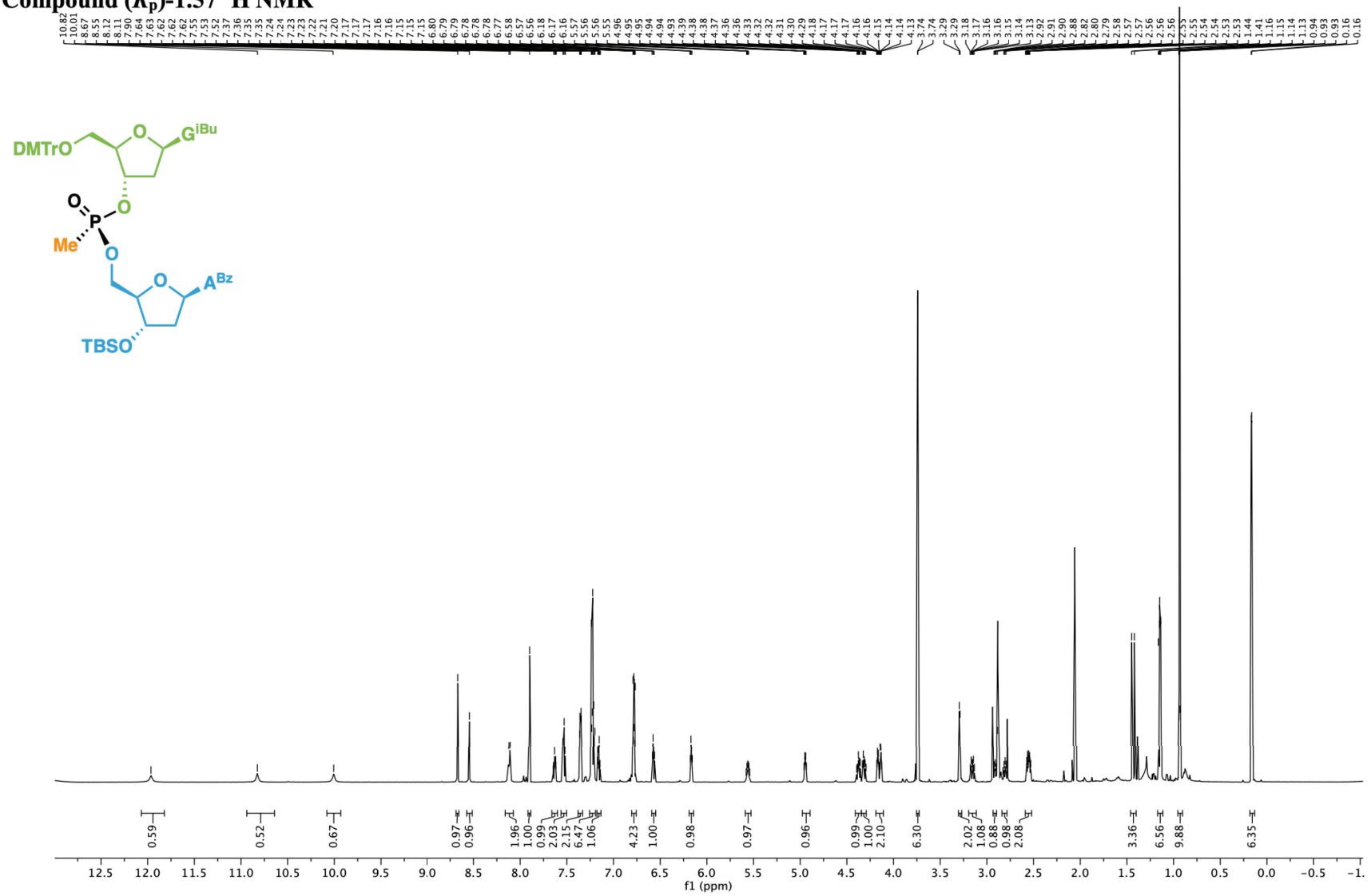
Compound (R_p)-1.46 ^{13}C NMR



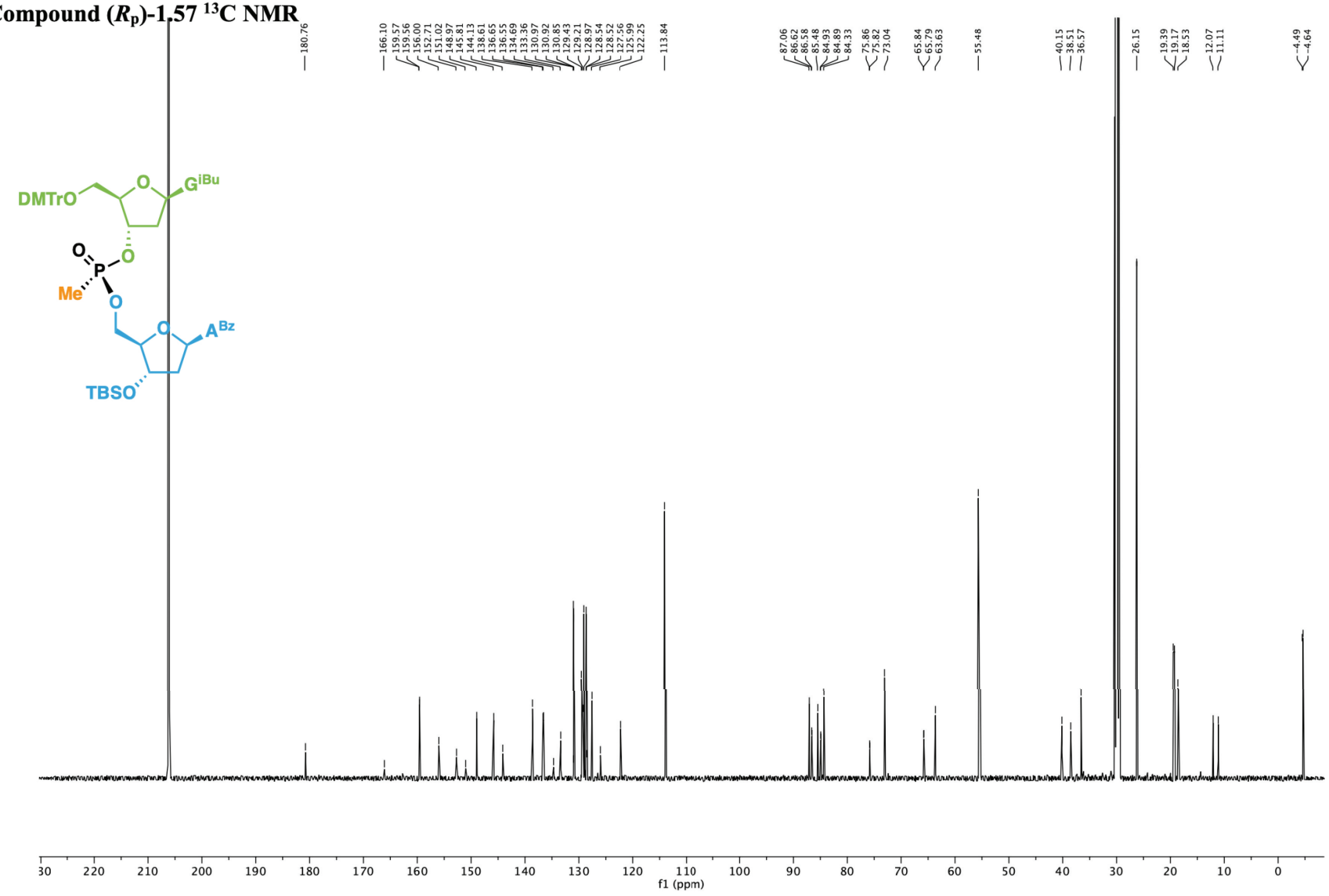
Compound (R_p)-1.46 ^{31}P NMR



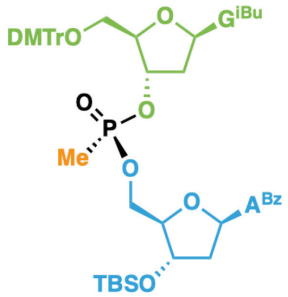
Compound (R_p)-1.57 ^{1}H NMR



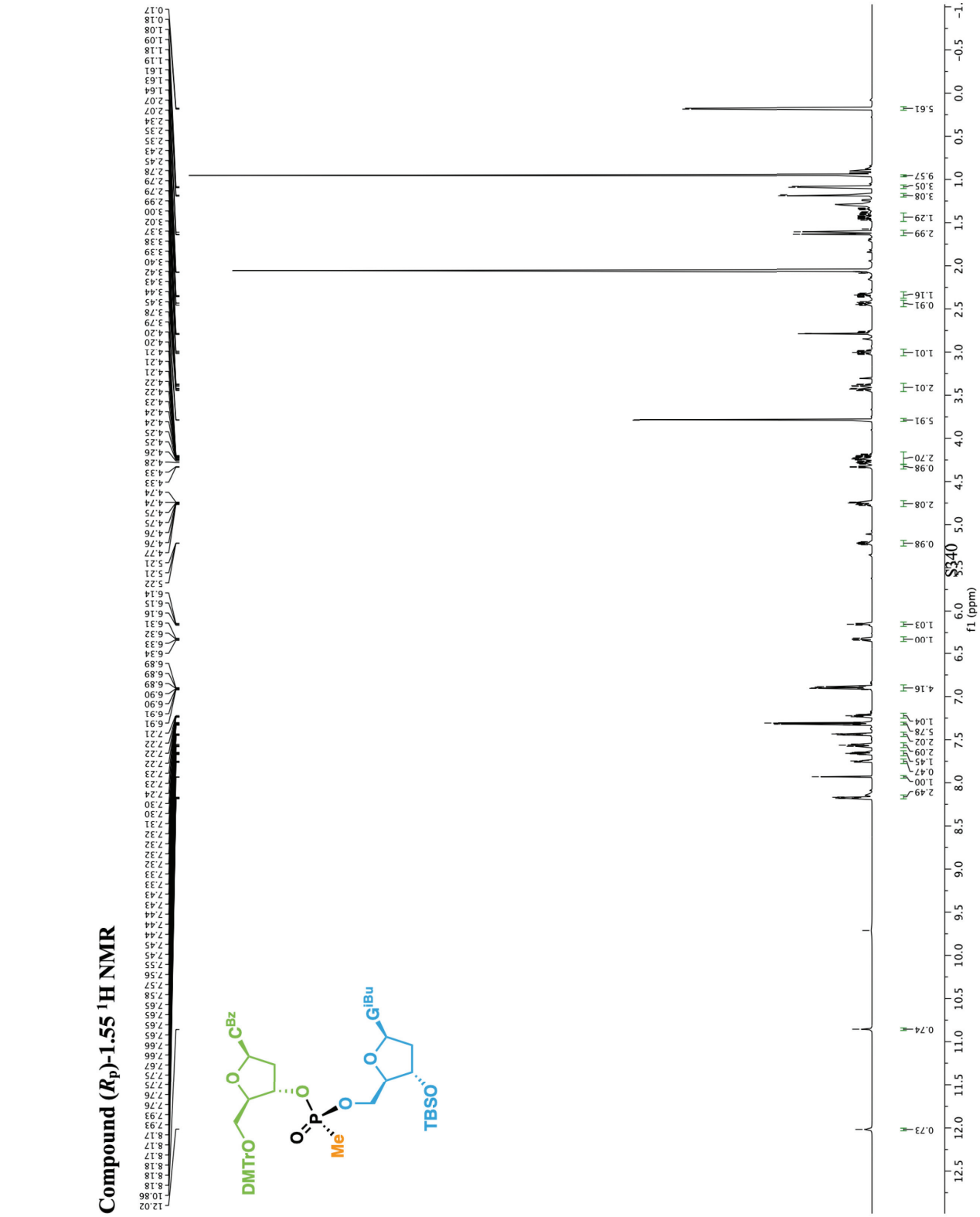
Compound (R_p)-1.57 ^{13}C NMR



Compound (R_p)-1.57 ^{31}P NMR

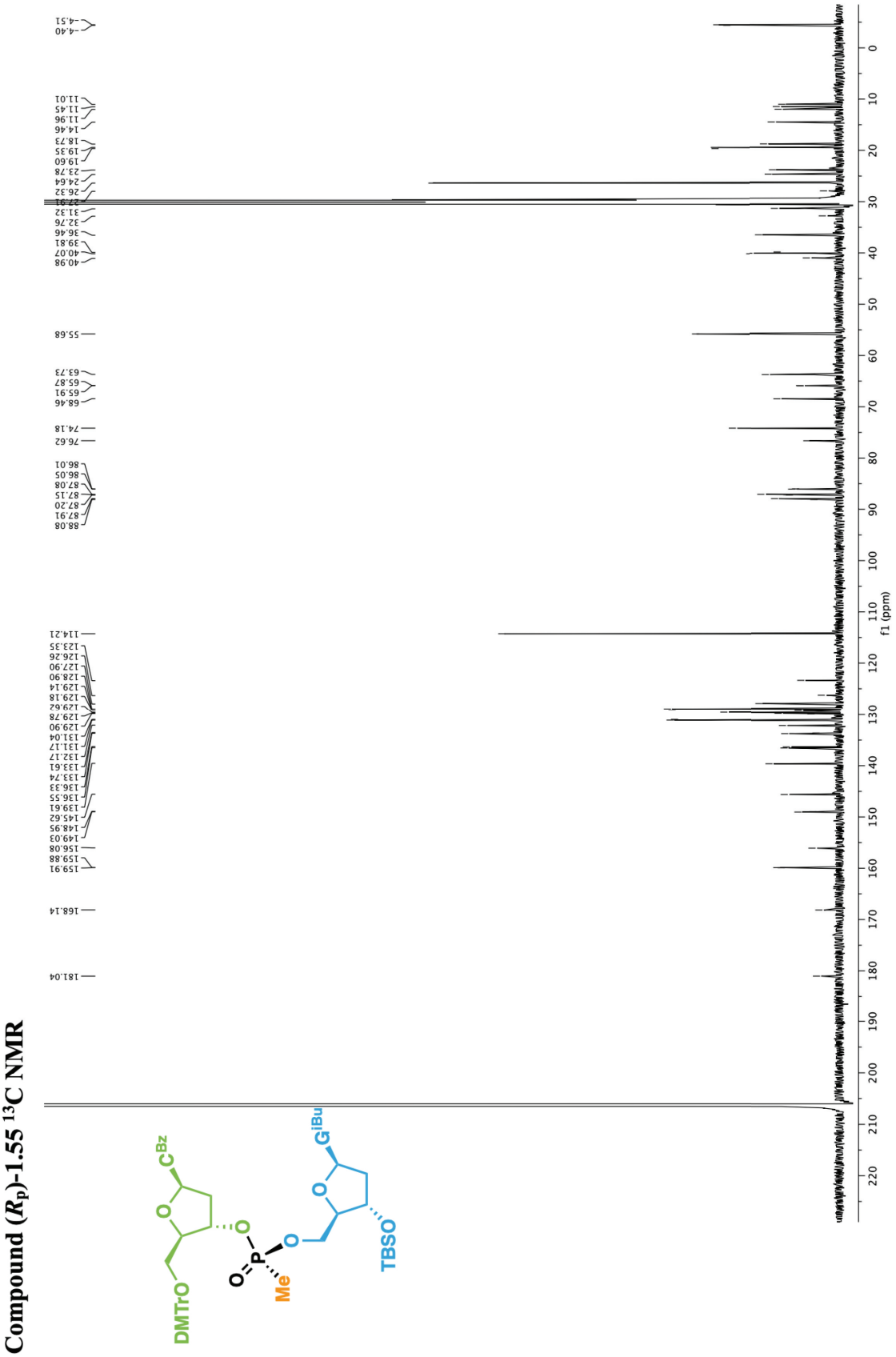


Compound (R_p)-1.55 ^{1}H NMR

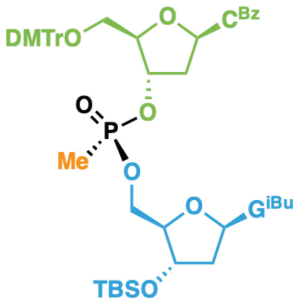


S340

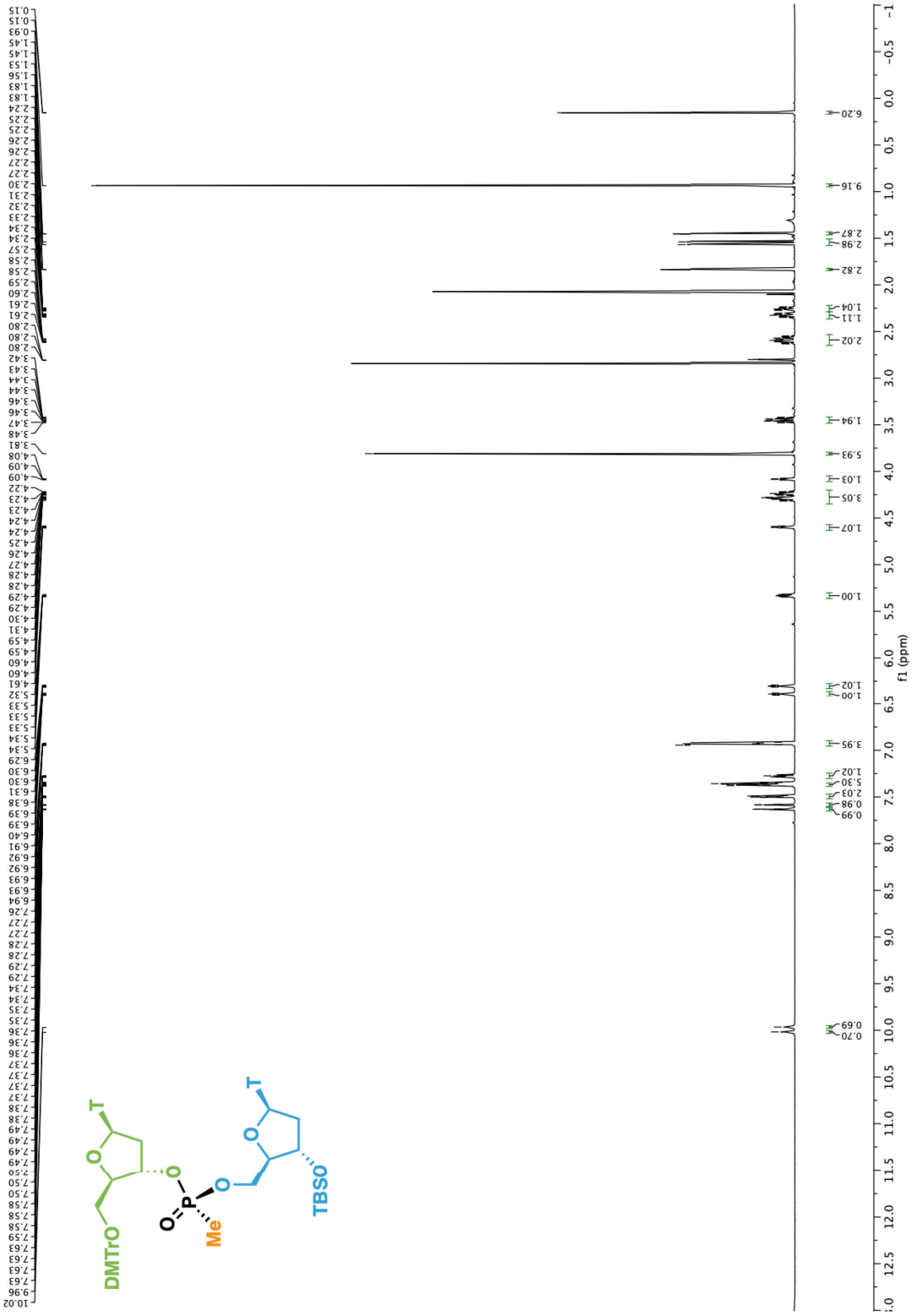
Compound (R_p)-1.55 ^{13}C NMR



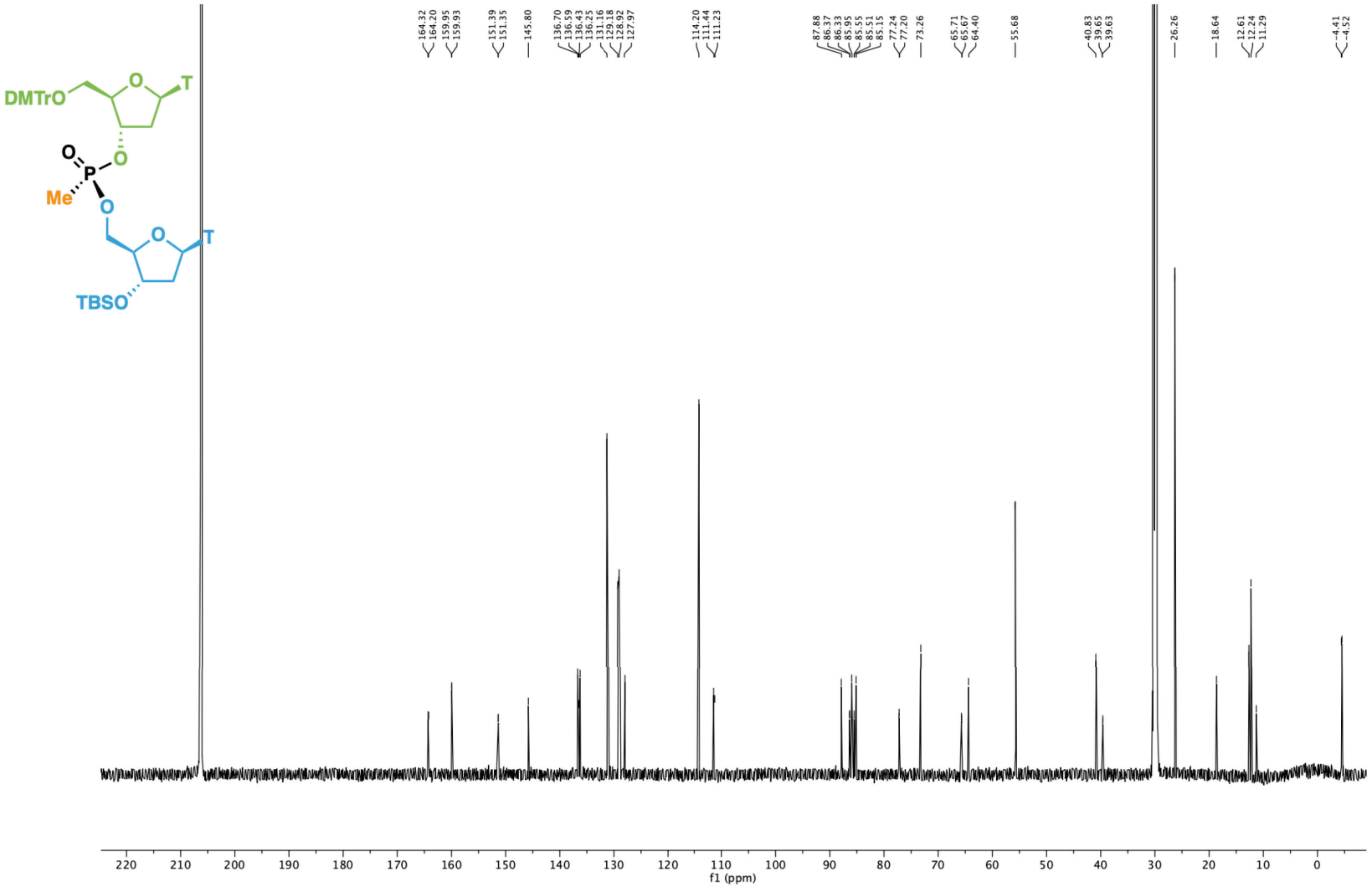
Compound (R_p)-1.55 ^{31}P NMR



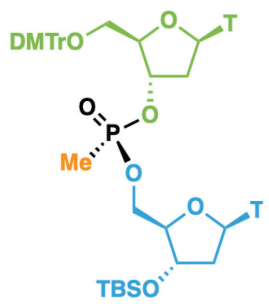
Compound (R_p)-1.44 ^{1}H NMR



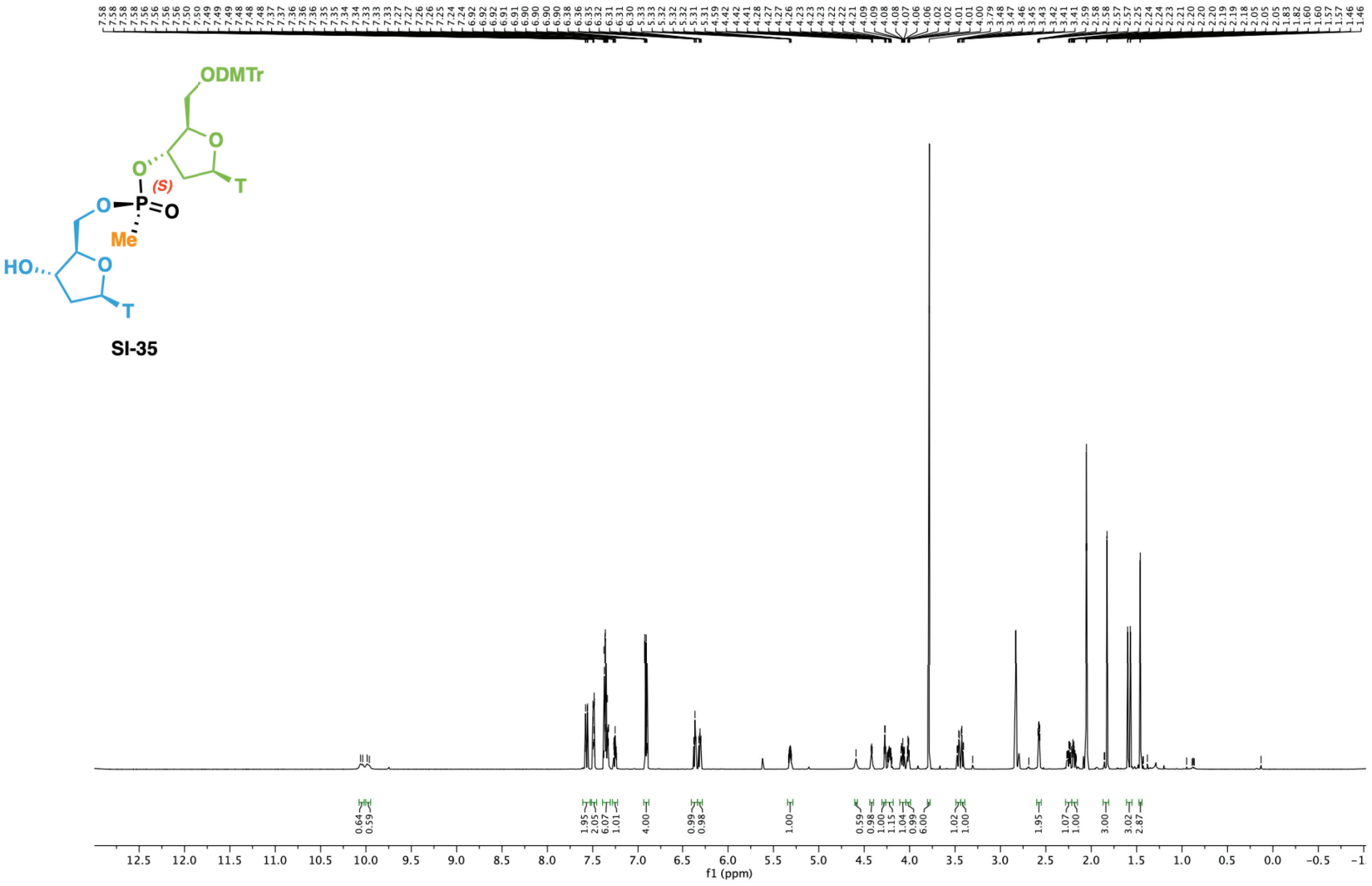
Compound (R_p)-1.44 ^{13}C NMR



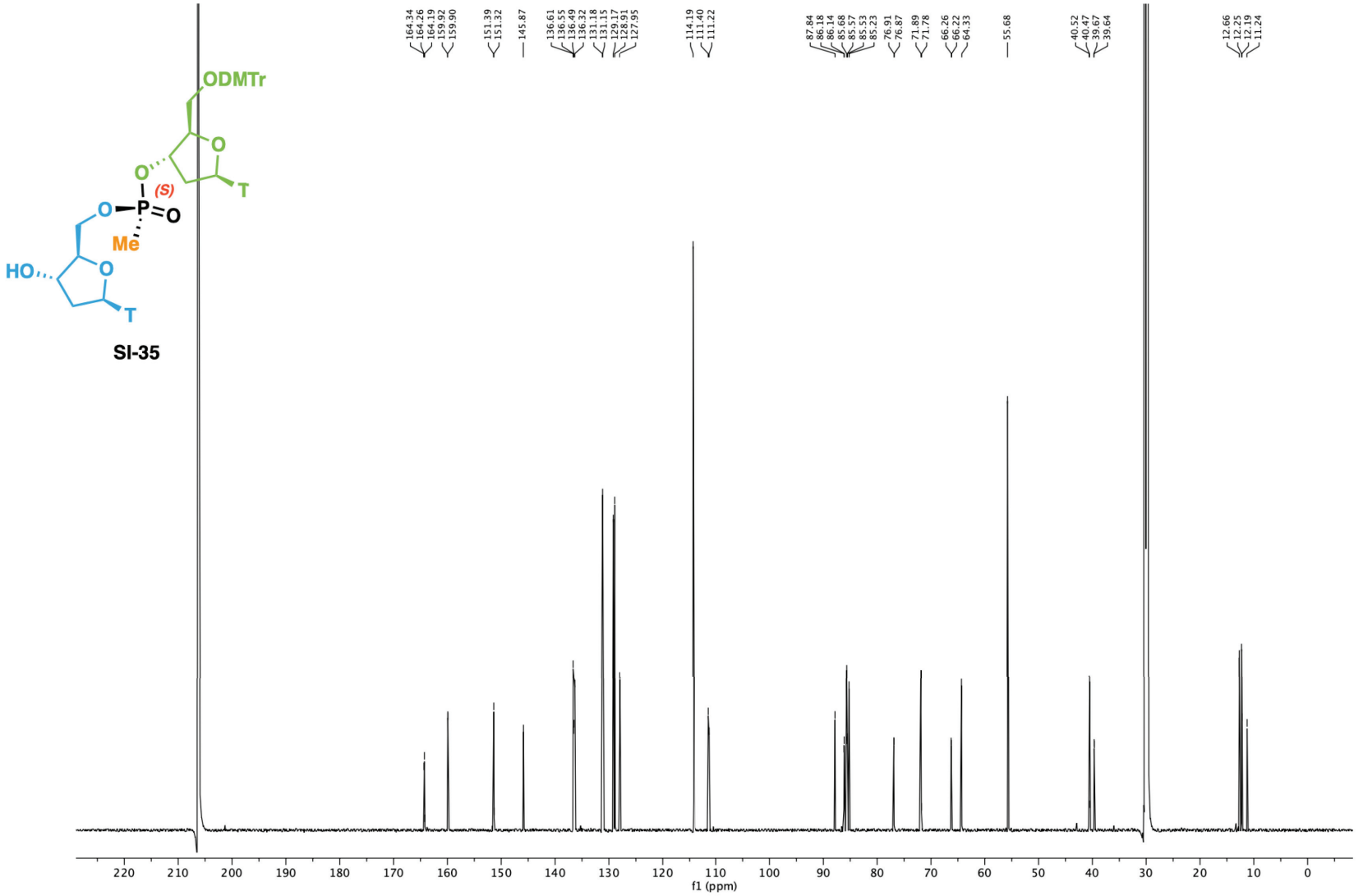
Compound (R_p)-1.44 ^{31}P NMR



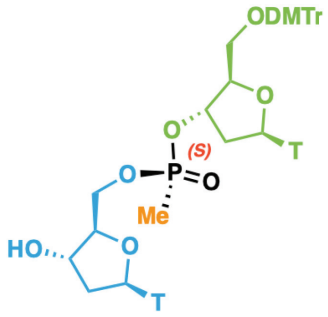
Compound SI-1.35 ^{1}H NMR



Compound SI-1.35 ^{13}C NMR

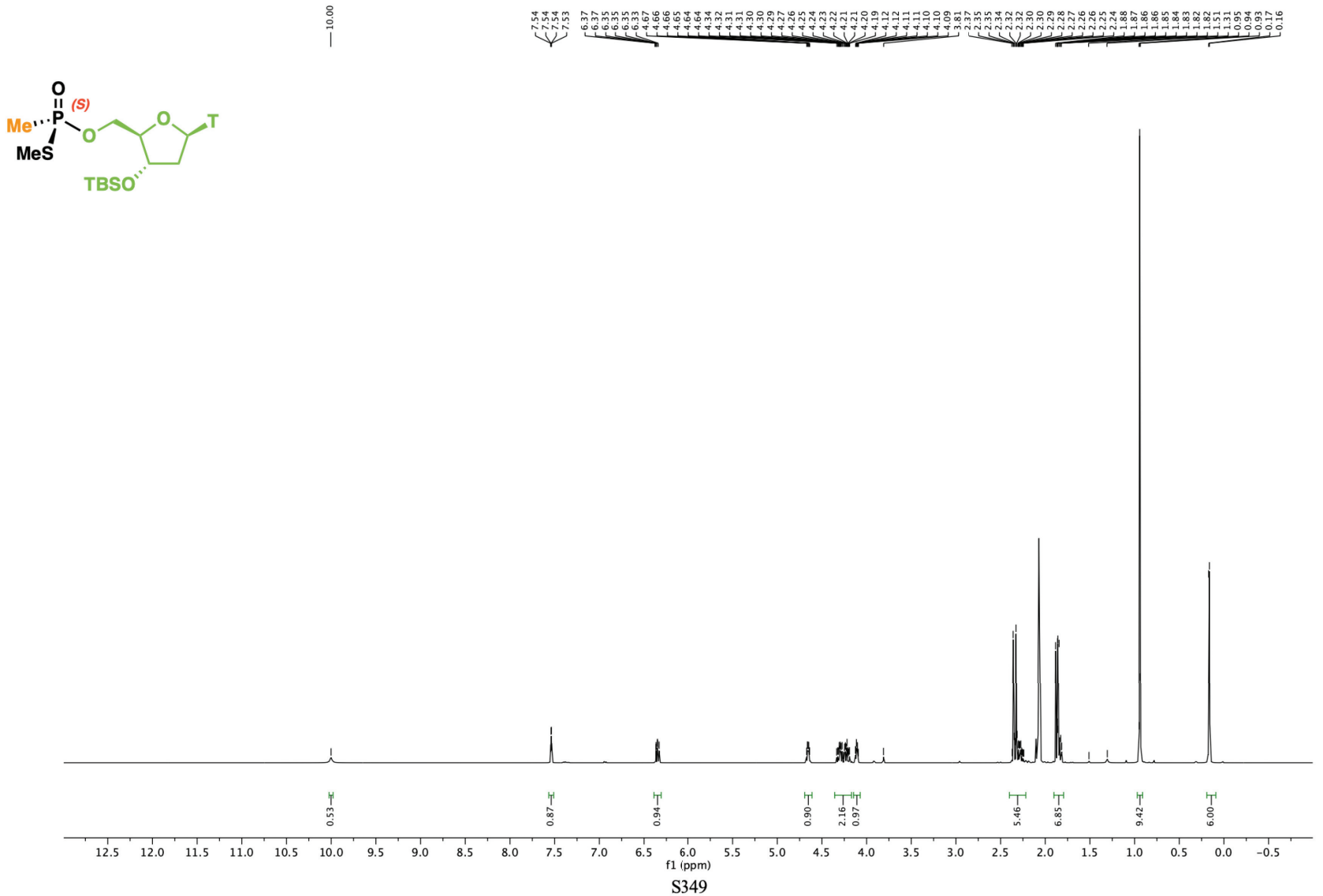


Compound SI-1.35 ^{31}P NMR

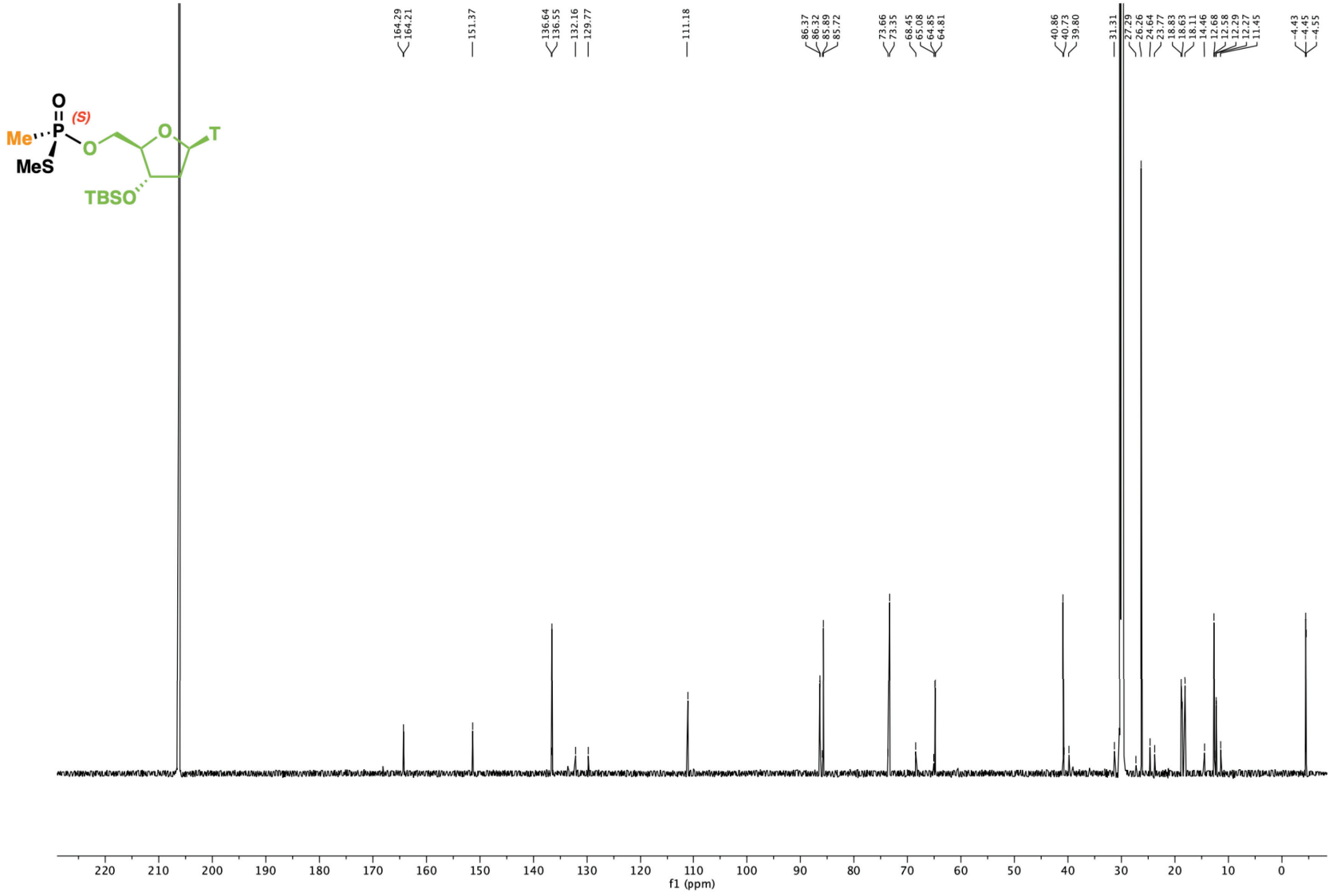


SI-35

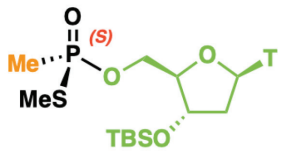
Compound SI-1.36 ^{1}H NMR



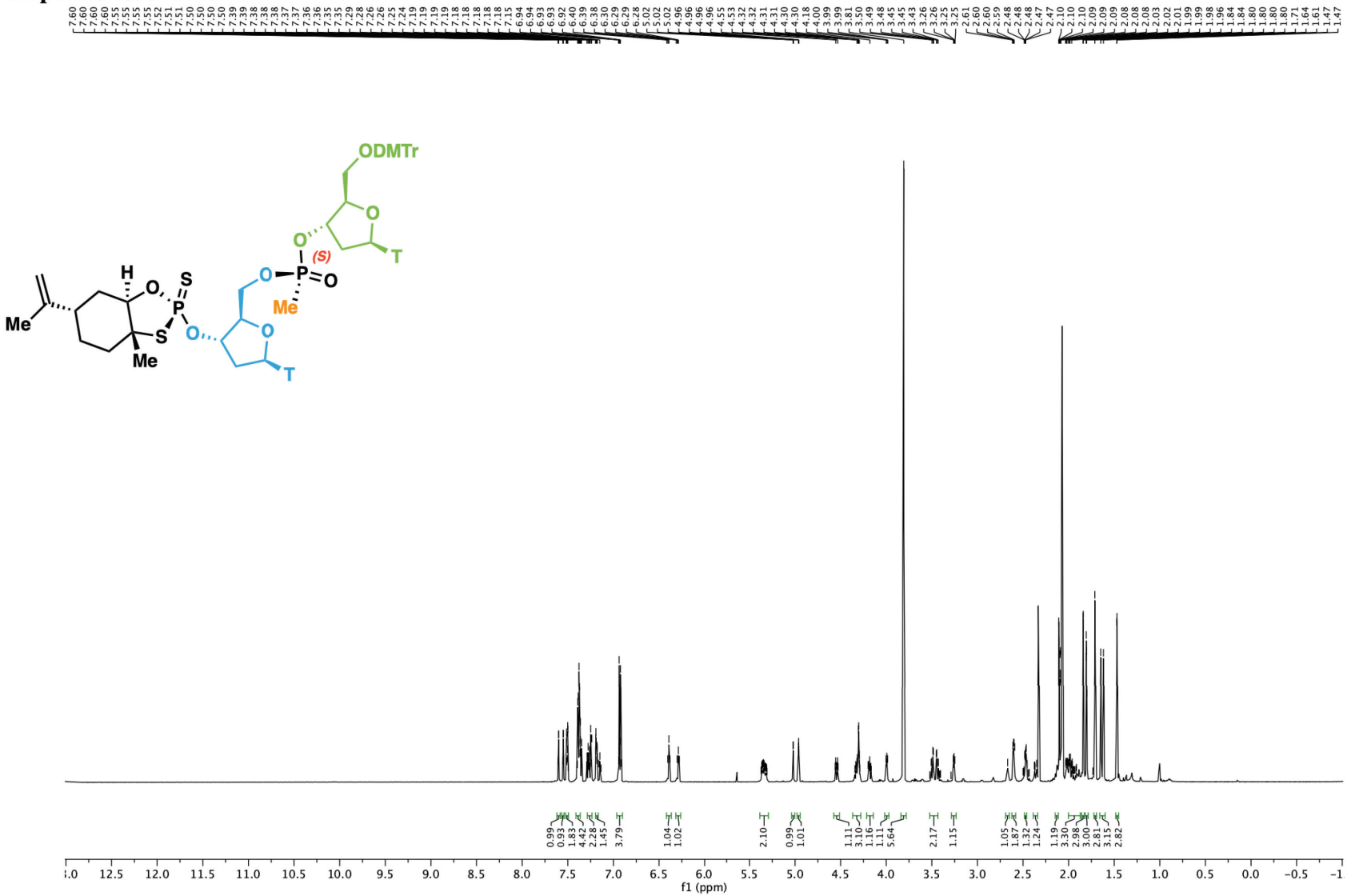
Compound SI-1.36 ^{13}C NMR



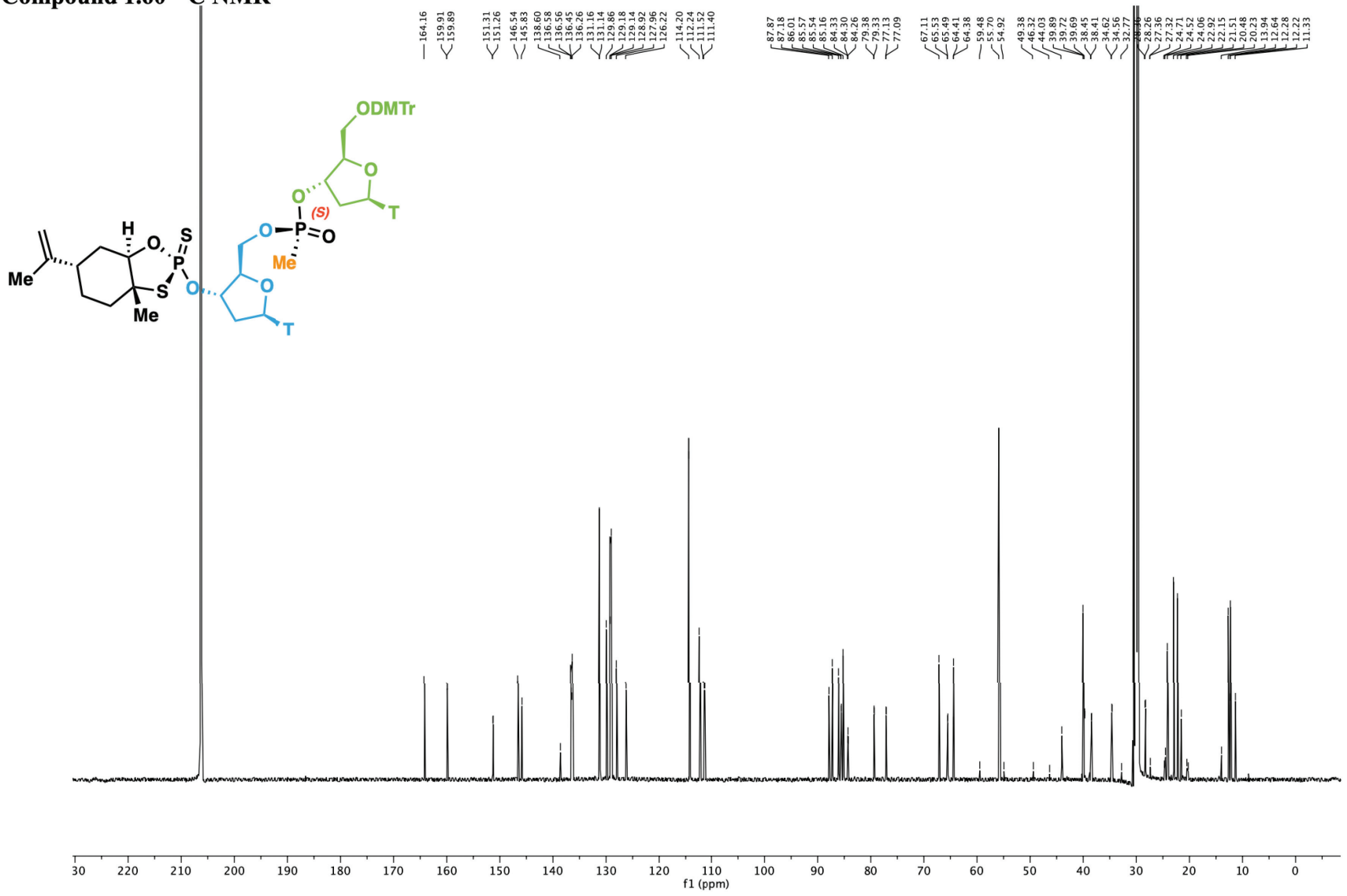
Compound SI-1.36 ^{31}P NMR



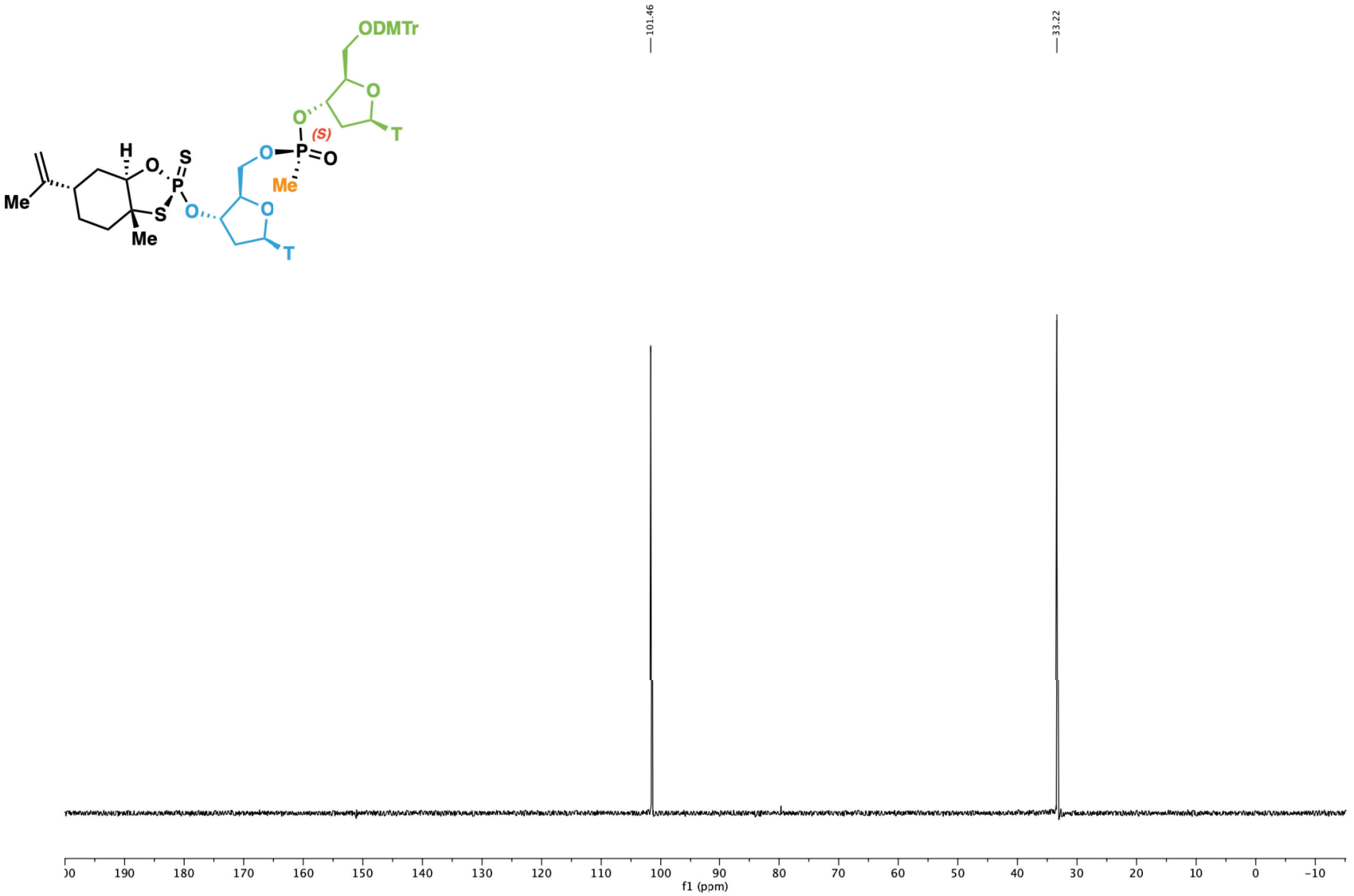
Compound 1.60 ^{1}H NMR



Compound 1.60 ^{13}C NMR



Compound 1.60 ^{31}P NMR



Distribution of Credit

I am immensely grateful to my collaborators on this project: Dr. Nazaret Rivas-Bascón (N.R.B.), Dr. Natalia Munoz-Padial (N.M.P.), Dr. Kyle W. Knouse (K.W.K.), and Dr. Julien C. Vantourout (J.C.V.). I would also like to thank our industry collaborators at Bristol-Myers Squibb: Dr. Martin D. Eastgate (M.D.E.) and Dr. Michael A. Schmidt (M.A.S.). Finally, none of this would be possible without my supervisor Prof. Phil S. Baran (P.S.B.).

The credit for this project is distributed as follow: the project was conceived by P.S.B., M.D.E., M.A.S., J.C.V., and K.W.K. I was responsible for the initial exploration of Ψ and Π reagents with help and valuable inputs from K.W.K. The P-chiral phosphine scope was explored by me and N.M.P. The MPO scope was explored by me, N.R.B. and N.M.P. The phosphine reduction reaction and the enantiodivergent design section were carried out by N.M.P. and me. N.M.P. was responsible for Ψ activation of the MPO dimer. The manuscript was written by P.S.B., me, K.W.K., N.M.P., and J.C.V.

Chapter 2. Convergent Total Synthesis of (–)-Cyclopamine

Background

Cyclopamine (**2.1**), first isolated from *Veratrum californicum* (California corn lily),[1] is a notable member of the *Veratrum* alkaloid family that possesses a complex polycyclic structure and intriguing biological activities (Figure 2.1A).[2] The story of cyclopamine's discovery dates back to 1957, when sheep shepherds in Idaho reported multiple cases of unsettling birth defects in their sheep herds: the affected new-born lambs were found with distorted facial features and only one eye in the middle.[3] Anatomical evidence suggested that this phenotype, which was termed *cyclopia* due to its resemblance to cyclops in Greek mythology, was a result of the brain failing to split into two hemispheres (holoprosencephaly).[3b] In response, the United States Department of Agriculture (USDA) launched a decade-long investigation that eventually established a connection between ingestion of corn lily by the pregnant sheep and occurrence of cyclopia in its offspring.[3a] Subsequent isolation efforts from Keeler and coworkers led to the discovery of cyclopamine, which was shown to be responsible for the teratogenic effects of the corn lily plants.[1]

The mechanism of action (MOA) of cyclopamine was revealed in a seminal study by Beachy *et al.*, whose team discovered that cyclopamine is a potent inhibitor of the hedgehog (hh) signaling pathway.[4] To be exact, cyclopamine binds to and attenuates the activity of the Smoothened (Smo) protein, which is an important component in the hh pathway that normally triggers downstream responses by translocation from cytosolic space to the cell membrane.[5] Since the hh pathway was known to be critically important to symmetry development of embryos and correct differentiation of embryonic cells,

disruption of the hh pathway leads to abnormalities in the fetus and hence the one-eyed sheep observed in Idaho.[2d]

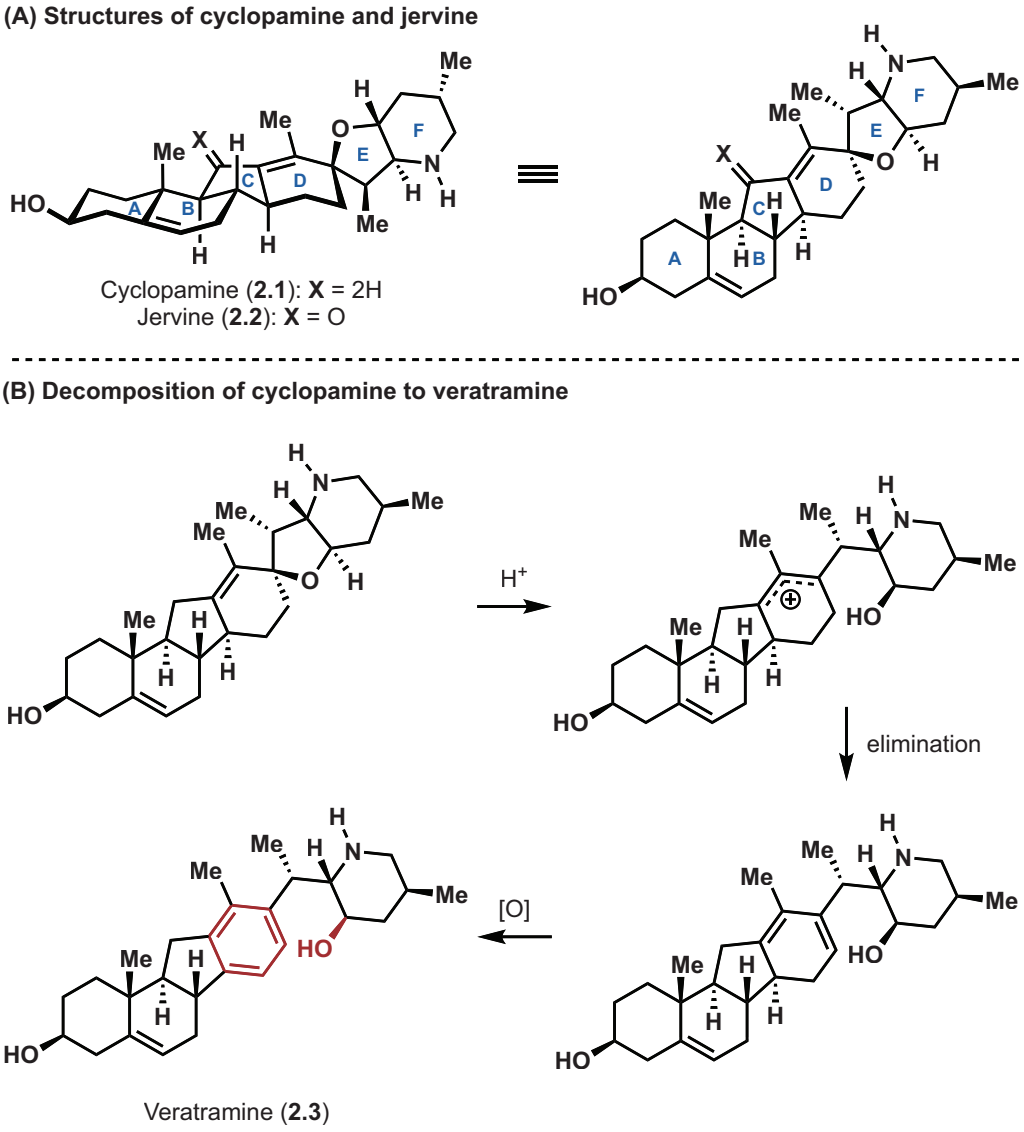


Figure 2.1 Cyclopamine and Related Natural Products

(A) Structures of cyclopamine and jervine. (B) Decomposition pathway of cyclopamine to veratramine under acidic conditions.

The hh pathway inhibition capabilities of cyclopamine have also attracted attention to its potential as an anti-cancer agent. It has been demonstrated in several cancer models

that overactivation of the hh pathway is essential for the uncontrolled proliferation of cancer cells, and that inhibition of the hh pathway can often lead to tumor reduction.[5] However, cyclopamine itself was deemed unsuitable as a drug candidate due to its known decomposition pathway under acidic conditions (Figure 2.1B).[6] The presumed mechanism is that the strained spirocyclic THF ring first opens up to form a stabilized allylic tertiary carbocation, which then undergoes an E1 elimination and subsequent auto-oxidation of the diene to form veratramine (**2.3**) with a fully aromatic D ring.[6a] For this reason, numerous medicinal analogs of cyclopamine have been reported to date, most notably saridegib (**2.4**, codenamed IPI-926 by Infinity Pharmaceuticals) which was prepared semi-synthetically from cyclopamine through a cyclopropanation/ring-expansion sequence (Figure 2.2).[7] Intended for treatment of pancreatic cancer, saridegib is essentially an acid-stable D-*homo* cyclopamine analog, where the extra methylene in the D ring renders ring-opening unfavorable due to the resulting carbocation being less stabilized and the lack of aromatization driving force.[7a]

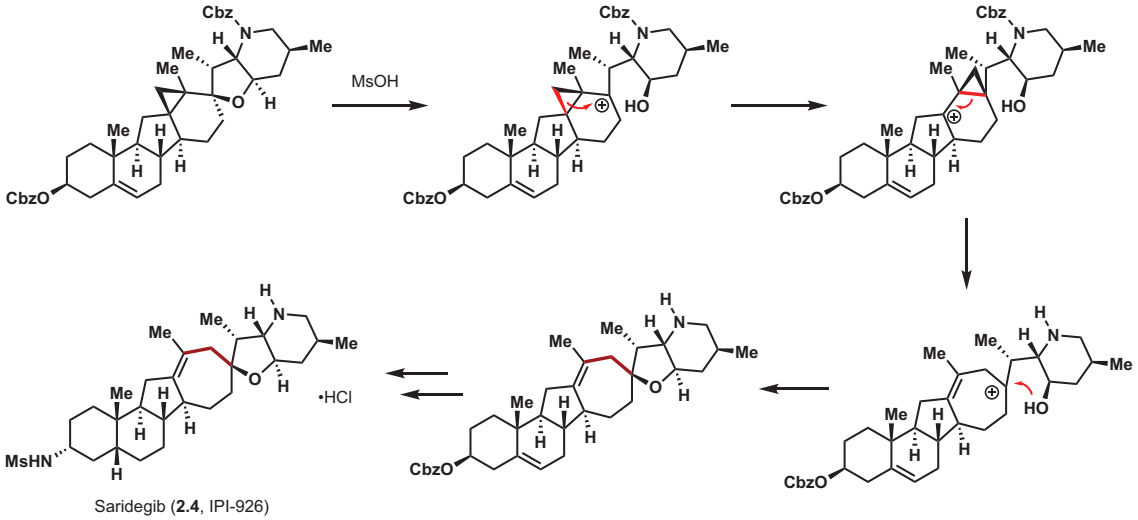


Figure 2.2. Cyclopropanation/Ring-Expansion *En Route* to Saridegib (IPI-926)

Previous Syntheses and Progress-Towards Studies

The intricate structures of *Veratrum* alkaloids have piqued the interest of synthetic chemists for years. With respect to cyclopamine, the rare C-*nor*-D-*homo* steroid skeleton is further complicated by the fully substituted, spirocyclic THF motif, the unique *trans*-6,5 EF ring system, and the central tetrasubstituted olefin, all of which posed unique challenges to its synthesis. A pioneering synthesis of the closely related jervine (**2.2**) by the Masamune group involves an 18-step sequence starting from the advanced intermediate **2.6**, which in turn must be prepared in 25 steps from Hagemann's ester (**2.5**) or obtained from degradation of hecogenin (Figure 2.3).[8] Key features of this synthesis include 1) a fragment coupling step between the bromo derivative of **2.6** and the enamine **2.7** to afford the veratramine derivative **2.8**, 2) a birch reduction/Pt hydrogenation sequence followed by epoxidation to afford **2.9**, and 3) a THF formation step enabled by epoxide opening of **2.9**.

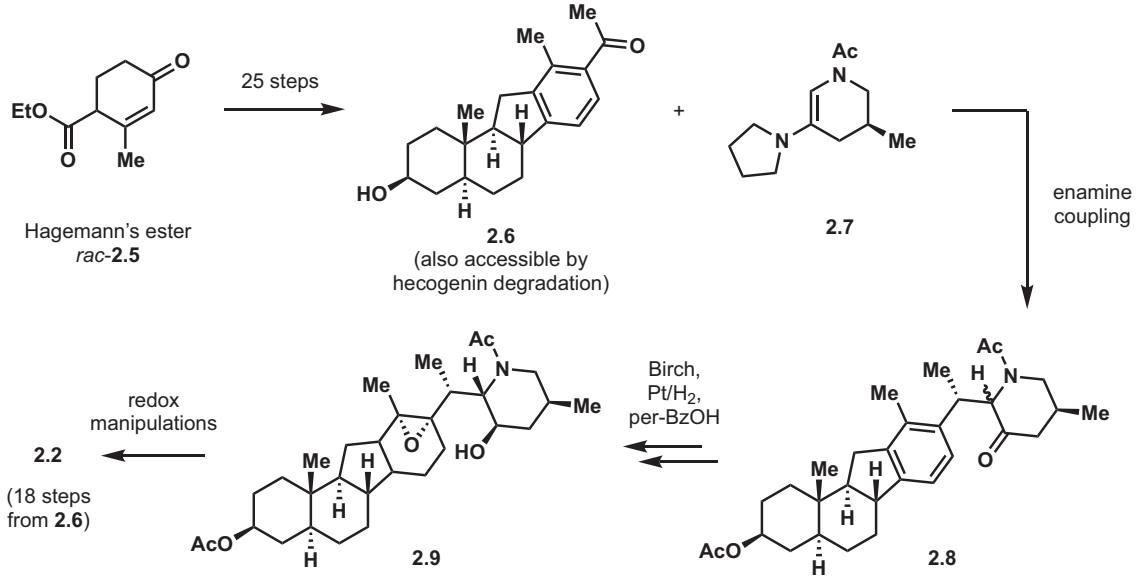


Figure 2.3 Masamune's Synthesis of Jervine

It is worth mentioning that Kutney *et al.* also formally achieved the synthesis of cyclopamine by intercepting an advanced intermediate (prior to Birch) in Masamune's route.[9] They were able to improve the key fragment coupling step by enlisting a lithiated picoline fragment as the coupling partner, resulting in a more streamlined synthetic sequence.

More recently in 2009, Giannis *et al.* disclosed an elegant semi-synthesis of cyclopamine in 20 steps from dehydroepiandrosterone (**2.10**, DHEA), featuring a biomimetic 1,2-rearrangement reaction to construct the C-*nor*-D-*homo* steroid scaffold of cyclopamine.[10] This synthesis commenced with the strategic C12 oxidation of DHEA with Schoenecker's protocol followed by lactone formation to afford **2.11**. Subsequent skeletal rearrangement to **2.12**, which was studied in depth in a separate publication,[11] utilized the C12 hydroxyl group for a 1,2-rearrangement to establish the core scaffold of cyclopamine and set the stage for the F ring construction sequence, which entailed azidation followed by tandem HWE/Michael. Finally, the resulting compound **2.13** underwent olefin isomerization and deprotection to afford cyclopamine (**2.1**).

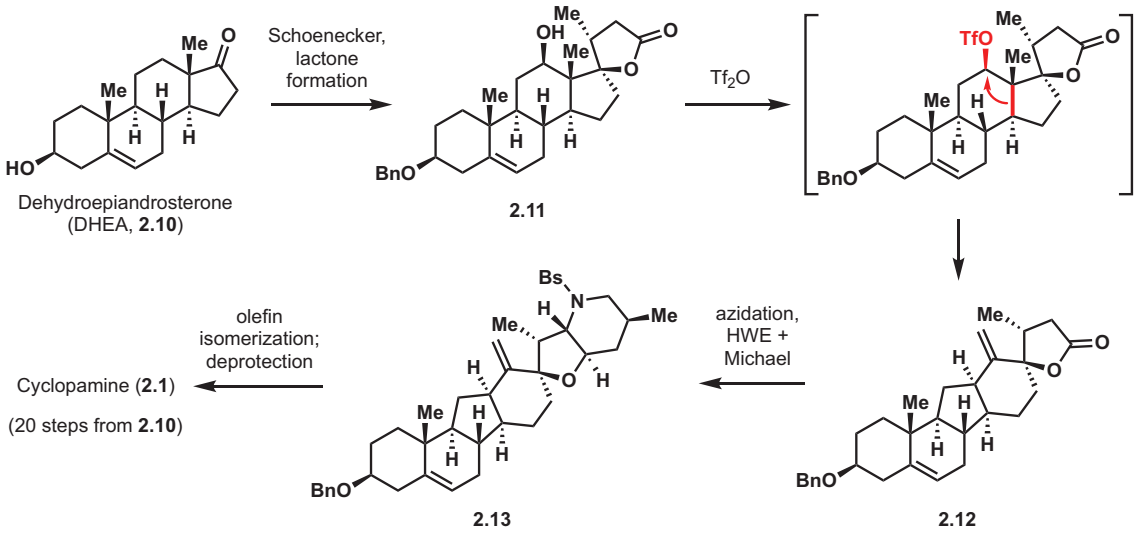


Figure 2.4 Giannis's Semisynthesis of Cyclopamine

Besides the finished syntheses mentioned above, a large number of progress-towards studies and fragment/analog syntheses of cyclopamine or jervine have been reported to date. [12] To name a few, Giannis *et al.* reported a chiral-pool based synthesis of cyclopamine's EF ring system starting from (*S*)-citronellic acid,[12c] a precedent that was further improved in subsequent reports from Taber and coworkers.[12g] Wright *et al.* reported a creative tandem metathesis approach towards constructing the spirocyclic core structure of cyclopamine.[12d] With respect to cyclopamine's ABC ring system, there are reports of an aldol-based approach by Brown *et al.*,[12a] a carbene C-H insertion approach by Taber and coworkers,[12h] and a Nazarov cyclization-enabled strategy from Giannis and his team.[12i] Winkler *et al.* have multiple reports on the synthesis and biological evaluation of numerous cyclopamine analogs, some of which exhibited enhanced potency in *in vitro* assays compared to cyclopamine.[12b, e-f] Finally, Johnson *et al.* has two recent progress-towards reports regarding the synthesis of jervine, with one of them detailing a streamlined synthesis of cyclopamine's DEF ring system with an oxidative dearomatization strategy,[12k] and the other describing their overall progress towards jervine (**2.2**) with a concise synthesis of the AB ring system and a diastereoselective selenium-mediated cyclization to forge the spirocyclic THF ring.[12j]

The seminal studies outlined above showcase the immense and long-lasting interest of the synthetic community towards cyclopamine and related natural products. We feel extremely fortunate to be able to learn valuable lessons and draw inspirations from these prior works when coming up with our own synthetic strategies, the details of which will be described in the following sections.

1st Generation Route

Our retrosynthetic plan for the 1st generation route (Figure 2.5) invoked the same 1,2-rearrangement strategy described by Giannis *et al*,[10-11] which we believe was an extremely efficient method for establishing cyclopamine's C-*nor*-D-*homo* steroid scaffold. The main area that we wanted to improve upon Giannis's synthesis was the formation of the EF ring system to arrive at **2.13**: our ambition was to build the EF system by forging both the C-O and C-N bond in the same step *via* a double cyclization sequence. The precursor **2.14** can in turn be synthesized from olefin-cross metathesis between a simple olefin fragment and a crotylated DHEA derivative **2.15**.

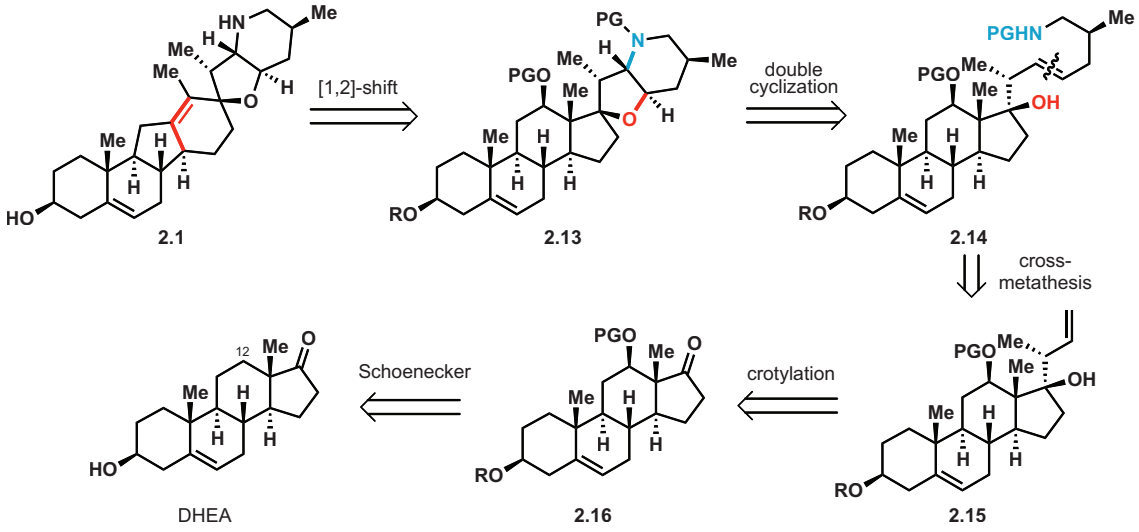


Figure 2.5 Retrosynthetic Plan for the 1st Generation Route

While the C-12 oxidation state in **2.16** is essential for the 1,2-rearrangement step, we decided to test out our ambitious double-cyclization strategy on the DHEA scaffold (i.e. no C-12 OH) first. While crotylation of TBS-protected DHEA proceeded smoothly to afford **2.17** in 70% yield, albeit as a 1:1 mixture of diastereomers at the methyl group, the subsequent olefin cross-metathesis was extremely sluggish even with 5 equivalents of

partner **2.19** and 10 mol% of either Grubbs second-generation catalyst (G-II) or Hoveyda-Grubbs second-generation (HG-II) catalyst at rt or 40 °C (Figure 2.6A). We observed no conversion of **2.17** and only dimerization of **2.19** across the board. We hypothesized that the free homoallylic alcohol in **2.17** could form stable chelates with the ruthenium catalyst and hamper reaction progress. However, the TMS protected **2.18** turned out to be equally unsuitable as a cross-metathesis partner, providing no noticeable conversion with the same conditions that were employed for **2.17**.

This setback prompted us to opt for a slightly less risky strategy to access the double cyclization precursor **2.14**, which was to add an enolate nucleophile to DHEA first and then extend the side chain. While addition of *tert*-butyl propionate enolates proceeded smoothly to afford the aldol adduct **2.21** in decent yields, no diastereoselectivity was observed at the

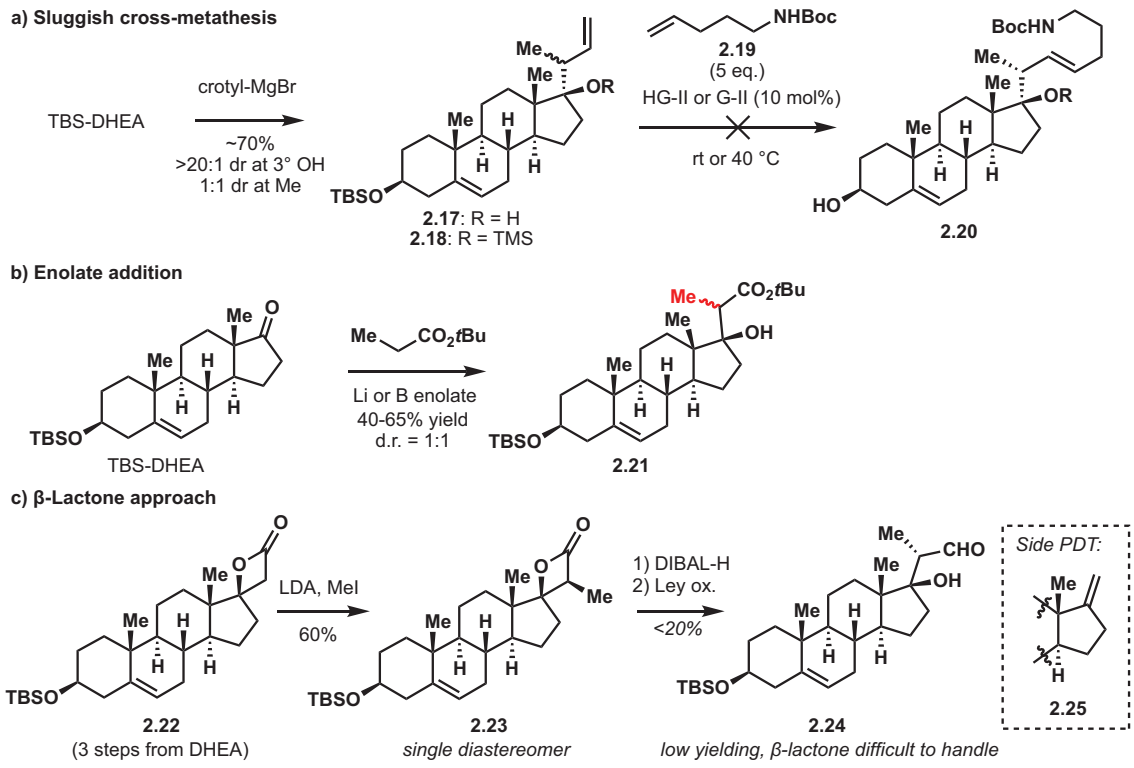


Figure 2.6 Early-Stage Explorations for the 1st Generation Route.

methyl group (Figure 2.6B). To combat this stereoselectivity problem, we decided to utilize an unconventional β-lactone intermediate **2.22**, the preparation of which from DHEA was described in a report by Giannis and coworkers (Figure 2.6C).[13] We were delighted to see that methylation of **2.22** proceeded stereoselectively to afford **2.23** as a single diastereomer favoring the desired methyl group stereochemistry. However, subsequent manipulations of **2.23** to synthesize aldehyde **2.24** turned out to problematic, with both the DIBAL-H and oxidation steps being extremely low yielding. Besides, we consistently observed side product olefin **2.25** from our reactions, suggesting that the β-lactone had stability issues where it readily underwent retro [2+2] with loss of CO_2.

Given that none of the alkyl or enolate nucleophiles outlined above gave satisfactory results, we shifted our focus to the use of alkenyl nucleophiles. Addition of

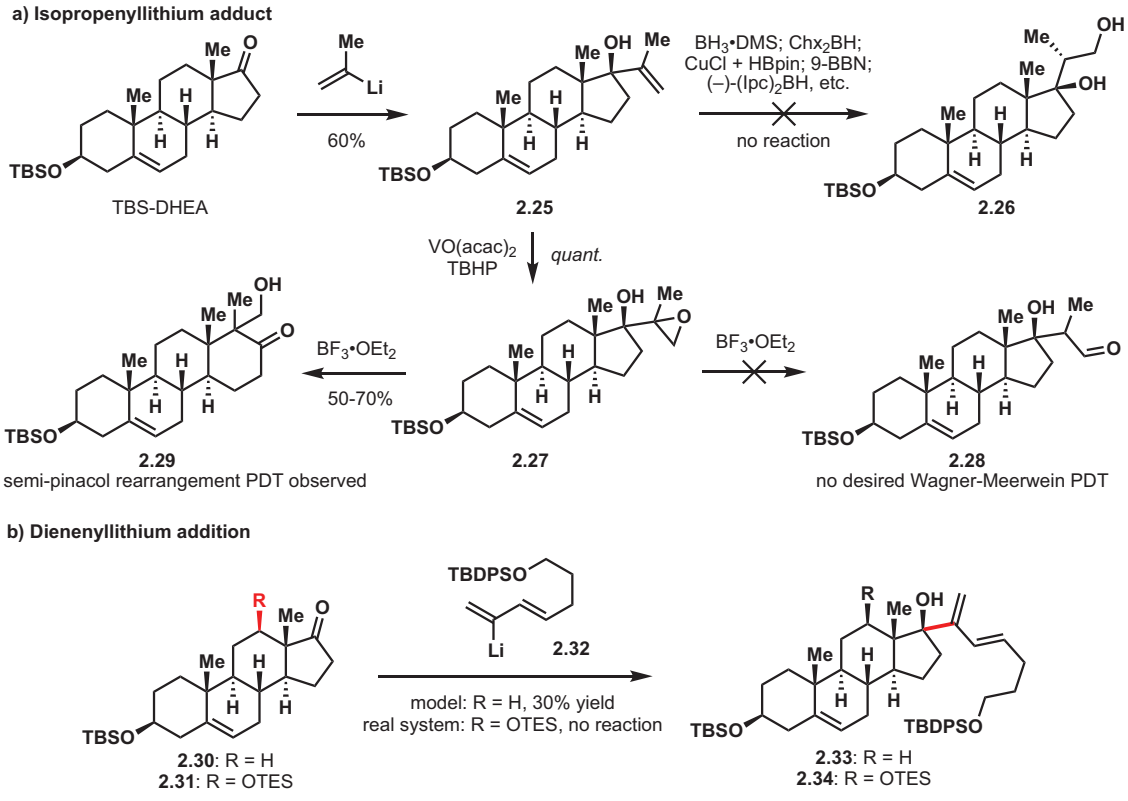


Figure 2.7 Addition of Alkenyl Nucleophiles to the DHEA Scaffold.

isopropenyllithium to TBS-protected DHEA (Figure 2.7A) proceeded smoothly to afford adduct **2.25** as a single diastereomer. While we were unable to transform **2.25** to primary alcohol **2.26** with various hydroboration/oxidation conditions, treatment of **2.25** with $VO(acac)_2$ cleanly delivered epoxide **2.27** in nearly quantitative yield as a potential Wagner-Meerwein rearrangement precursor. Unfortunately, we observed no Wagner-Meerwein product after treating **2.27** with $BF_3 \bullet OEt_2$. Instead, the only isolated compound from this reaction was the ring expansion product **2.29**, which resulted from a competing semi-pinacol rearrangement pathway. Alternatively, another strategy that we explored involved installing the entire sidechain in one sitting by addition of the dienenyllithium species **2.32** (Figure 2.7B). While the addition worked decently well on the DHEA scaffold to deliver **2.33** in 30% yield, the Schoenecker intermediate **2.31** with a C12 siloxy group failed to give any conversion when treated with **2.32**, crippling our original plan for downstream functionalization and the eventual 1,2-rearrangement reaction.

As the final effort towards a semisynthetic strategy, we chose to re-evaluate the efficacy of enolate chemistry for addition to DHEA, this time with non-ester-based enolate nucleophiles. We first investigated aza-enolates and deprotonated pyridines (Figure 2.8A): the aza-enolates **2.35** and **2.36** tentatively formed 1,2-addition products in the reaction vessel, but rapid retro-aldol was observed upon workup and only the TBS-DHEA starting material could be isolated after purification. On the other hand, addition of benzylic deprotonated 2-ethylpyridine (**2.37**) afforded a stable 1,2 adduct based on crude NMR. However, it was deemed too challenging to access the desired EF ring system from a pyridine motif (possibly *via* a structure such as **2.38**, but it won't be trivial to synthesize), not to mention the potential stereochemical maze one must navigate through (for example,

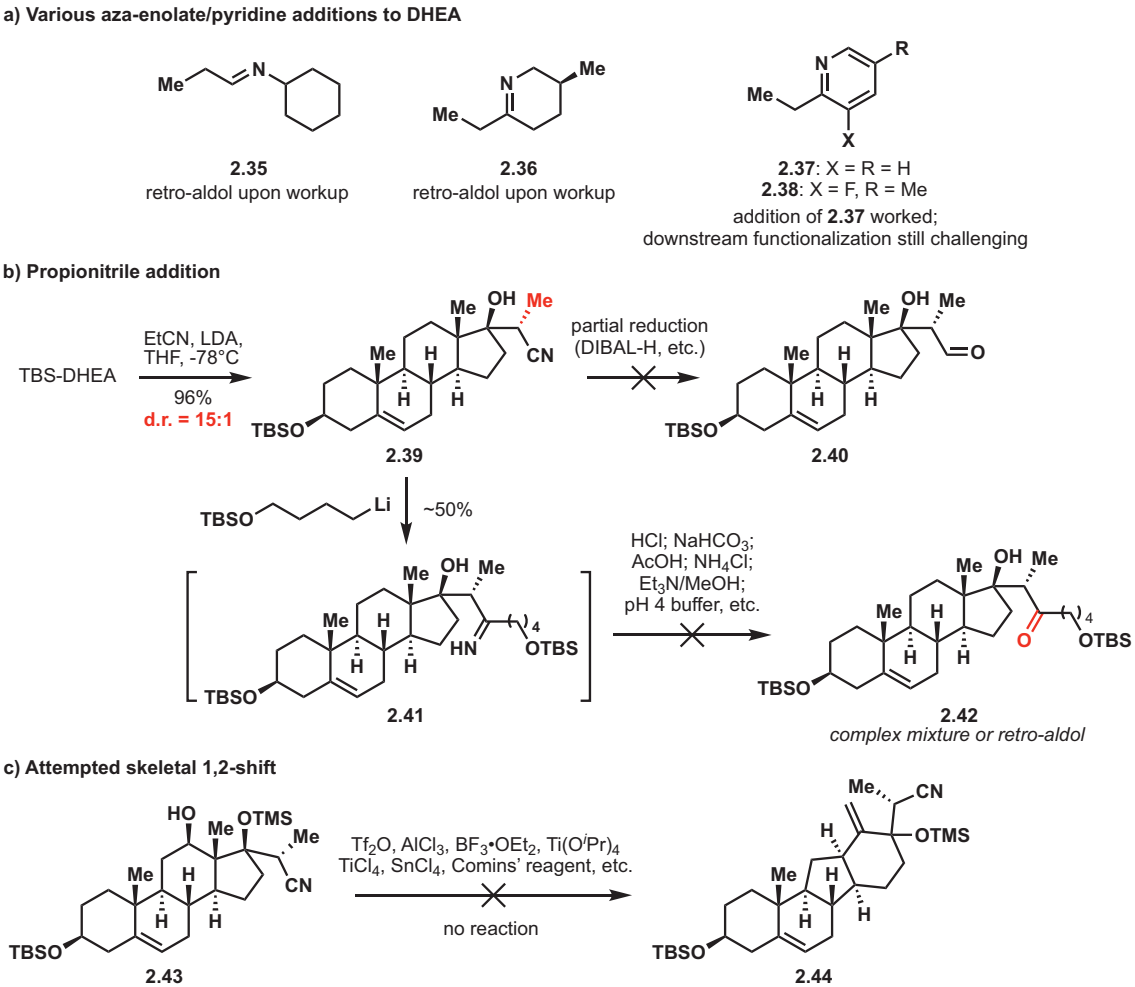


Figure 2.8 Final Efforts Towards the 1st Generation Route

pyridine hydrogenation would give the wrong relative stereochemistry across the F ring). We then moved on to investigate the addition of nitrile enolates to DHEA (Figure 2.8B). To our delight, addition of propionitrile enolate to TBS protected DHEA cleanly afforded the 1,2-adduct **2.39** as a 15:1 mixture of diastereomers, favoring the desired stereochemistry at the methyl group. Despite our unsuccessful attempts toward a partial reduction of the nitrile moiety to the aldehyde **2.40**, we discovered that addition of an alkyllithium species to **2.39** cleanly yielded the imine adduct **2.41**. Unfortunately, hydrolysis of **2.41** to the corresponding ketone **2.42** proved to be problematic, with most

conditions we tried resulting in either complete decomposition or again facile retro-aldol reactions. To make matters worse, a parallel proof-of-concept reaction for the 1,2-rearrangement of the C-12 oxidized, DHEA propionitrile adduct **2.43** also turned out to be unfruitful (Figure 2.8C): we were never able to detect any trace of the desired product **2.44**, and no reaction was observed across a number of conditions we screened, including Giannis's conditions with Comins' reagent.[11]

In summary, our 1st generation route was an effort to develop a more concise semisynthetic route towards cyclopamine. During the ideation phase, such an approach was deemed desirable due to the need to only construct the EF ring system on top of the existing steroid scaffold. However, our plan was eventually thwarted because 1) 1,2-addition into the DHEA ketone was challenging and the products had a propensity for retro-aldol processes, 2) controlling the methyl stereocenter was not trivial, and 3) the most promising propionitrile adduct turned out to be unsuitable for the skeletal 1,2-rearrangement. As such, we decided to recalibrate our synthetic strategy and shifted our focus to a 2nd generation, total synthetic approach towards cyclopamine.

2nd Generation Route

Unlike the linear approach that was largely adopted in the 1st generation route, our retrosynthetic plan for the 2nd generation total synthetic route (Figure 2.9A) entailed a convergent design, where the western fragment containing the ABC ring system (**2.45**, the "ABC fragment") would be coupled to the eastern EF ring system (**2.46**, the "EF fragment") through a number of late-stage operations such as ketone alkylation and ring-closing metathesis (RCM). We believed that the D ring is the most strategic position for such a disconnection due to its central position in the molecule and the relative abundance of functional group handles that can be leveraged for the late-stage union of the two fragments. Although it is typically non-ideal to form a tetrasubstituted olefin from an RCM reaction due to the sheer amount of steric hindrance, we were encouraged by literature reports of six-membered ring-closures of similar systems,[14] as well as evidence suggesting that the presence of allylic heteroatoms could facilitate reaction progress.[15] In terms of synthesizing the fragments, the ABC fragment progenitor **2.47** (Figure 2.9B) could originate from the intramolecular hydrogen-atom transfer (HAT) cyclization of the precursor **2.48**,[16] which in turn could be accessed *via* **2.50** by an aldol reaction between ketone **2.51** (commercially available) and aldehyde **2.52** (accessed in 6 steps from norbornadiene in a literature report).[17] On the other hand, the EF fragment (Figure 2.9C) could be accessed by 1,4-addition of an alkenyl cuprate species into the α,β-unsaturated ester **2.54**, which in turn could be obtained from olefination of the lactone **2.55**. It was envisioned that the lactone motif could be formed by addition of an enolate species into the epoxide **2.56**, the preparation of which from the chiral-pool feedstock material (*S*)-citronellic acid was reported by Taber *et al*.[12g]

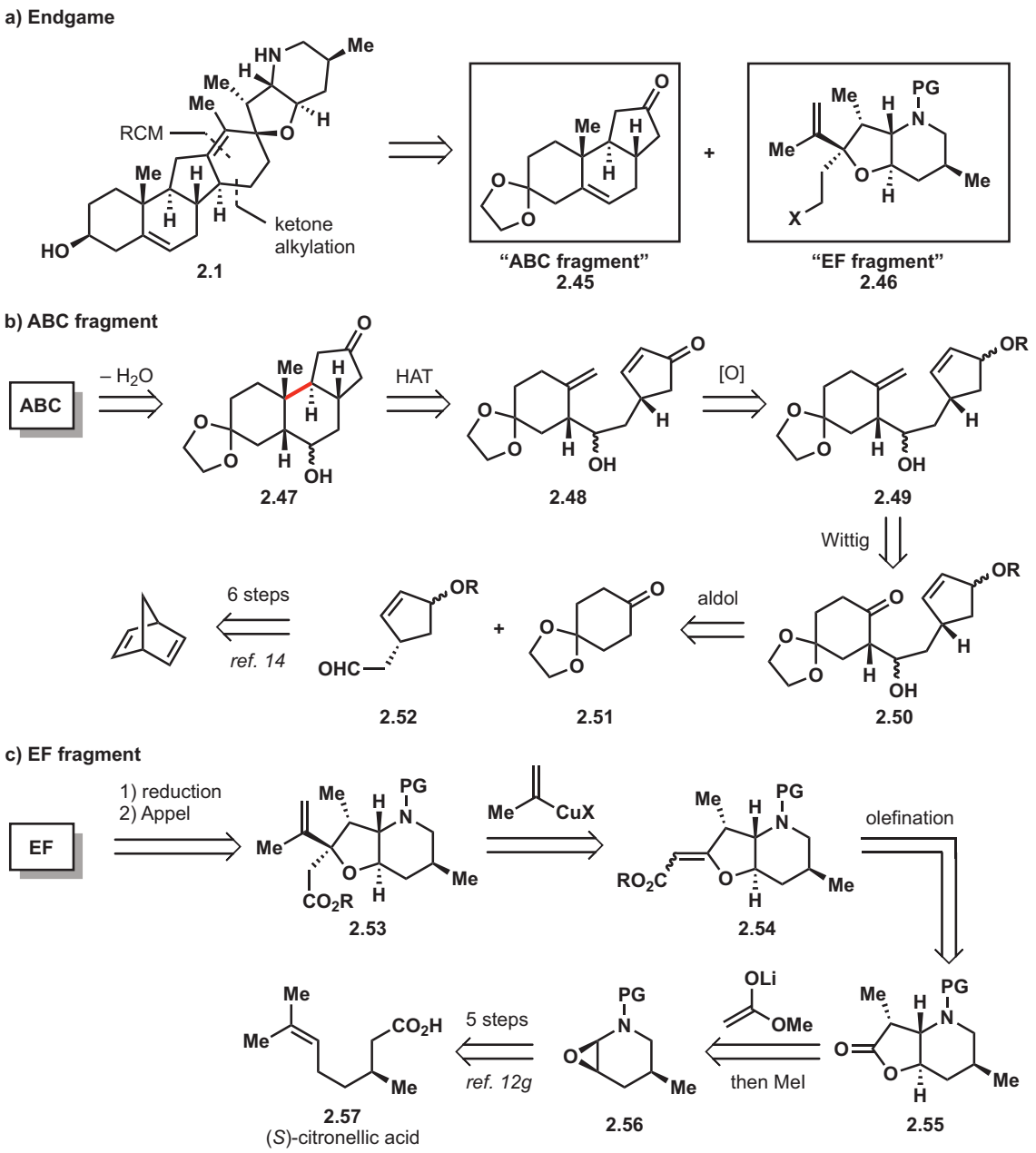


Figure 2.9 Retrosynthetic Plan for the 2nd Generation Route

Our initial efforts were directed towards the ABC fragment in hopes of quickly de-risking the intramolecular HAT cyclization (Figure 2.10). The required cyclopentene motif **2.58** could be enantioselectively prepared from norbornadiene according to a report from Nicolaou *et al.*,[17] which set the stage for a cross-aldol reaction between **2.58** and

cyclohexanone **2.59** to yield the product **2.60** as a roughly equal mixture of four inseparable diastereomers. In hopes of obtaining a proof of concept for this route, we decided to carry this diastereomeric mixture forward: MOM protection of **2.60**, followed by Wittig olefination, TBS deprotection and MnO_2 oxidation yielded the HAT cyclization precursor **2.63**. Treatment of **2.63** with conventional HAT conditions [iron (III) catalyst + phenylsilane][16] cleanly yielded cyclized product **2.64** in 41% yield. Unfortunately, NOESY correlations revealed that the major diastereomer of **2.64** possessed the wrong geometry at the 6,5-ring junction – formation of the less-strained *cis* ring junction was favored over the desired *trans* ring junction required for downstream operations. However, we were aware that the HAT precursor **2.63** was a mixture of four diastereomers, and it was reasoned that stereochemistry at the ketone α position of compound **2.60**, which was set during the aldol reaction, could dictate the stereochemical outcome of the HAT cyclization. For this reason, we decided to explore ways to synthesize **2.63** in an enantioselective manner. Unfortunately, both the NHK (Figure 2.11A) and the Weinreb amide approaches (Figure 2.11B) were unsuccessful due to the facile isomerization and/or decomposition of the β,γ-unsaturated

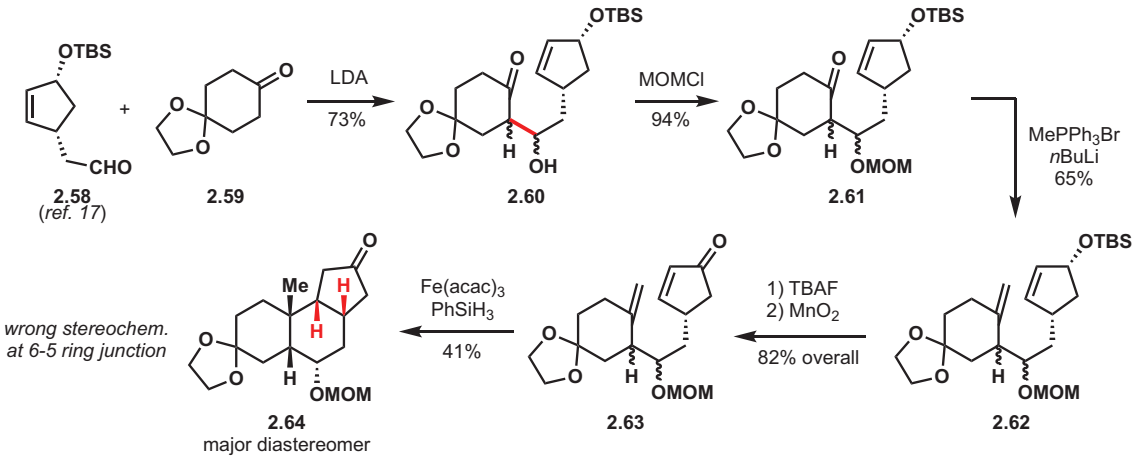


Figure 2.10 Unsuccessful HAT Cyclization *En Route* to the ABC Fragment

carbonyl motif in starting materials **2.65** and **2.68**. On the other hand, a slightly different strategy involving an intermolecular HAT reaction (Figure 2.11C) between Giese acceptor **2.72** and donor **2.73** was able to deliver the cross-coupling product **2.74** in 31% yield, but unfortunately without any stereocontrol (1:1 d.r.).

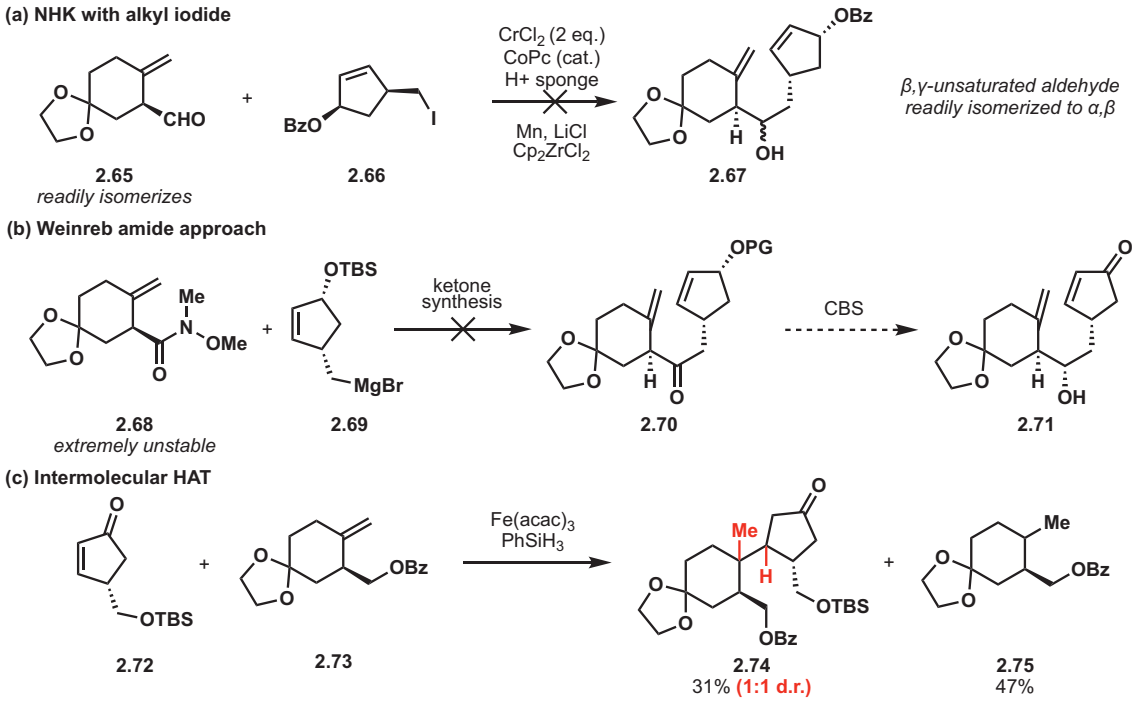


Figure 2.11 Synthetic Strategies Towards Enantiopure 2.63

While we were exploring these enantioselective strategies towards **2.63**, we also noticed literature reports detailing the preparation of **2.79** (Figure 2.12A), an ABC fragment precursor bearing a cyclopentenone motif in the C ring.[18] The key feature of this report was a cyclopentenone annulation sequence employing the enol ether phosphonate reagent **2.77**: it first served as the alkylating agent for the enolate of **2.76**, which afforded **2.78** as a 1:1 mixture of epimers after acid hydrolysis of the enol ether motif; subsequent treatment of **2.78** with Cs_2CO_3 triggered an intramolecular HWE reaction to forge the

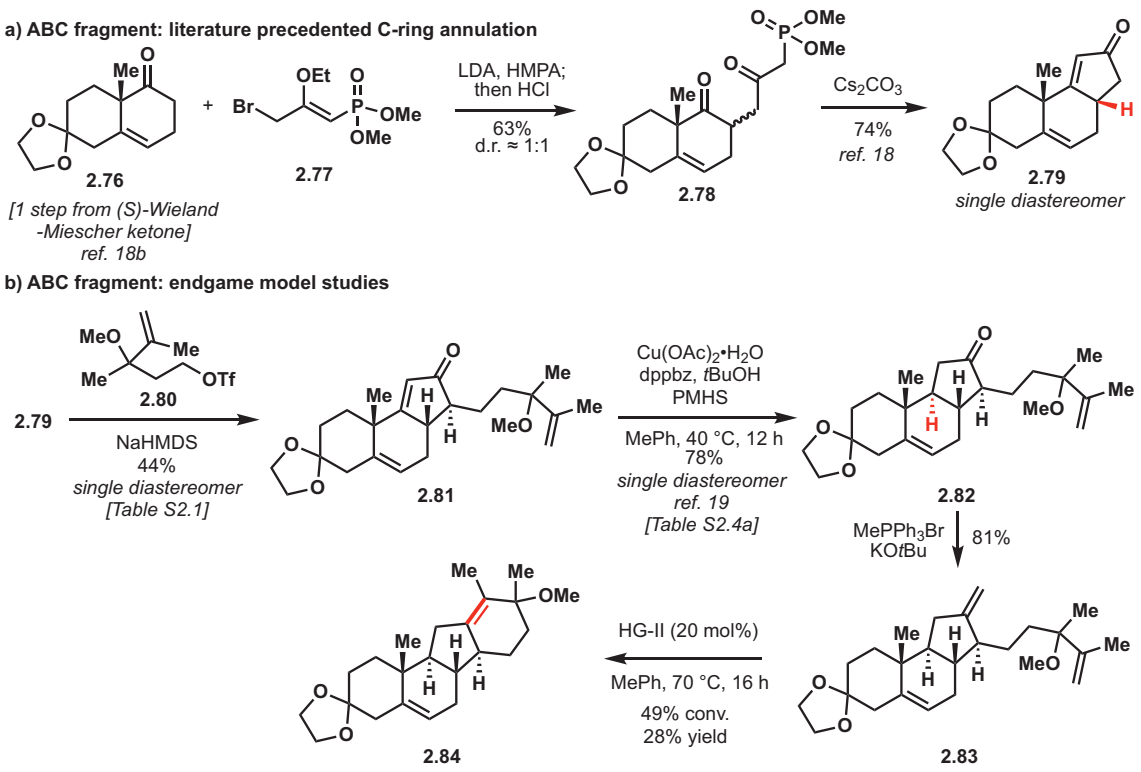


Figure 2.12 Synthesis of the ABC Fragment and Endgame Model Studies

cyclopentenone motif, and in the meantime allowed the epimers to re-equilibrate and eventually yield **2.79** as a single diastereomer. However, there were some concerns about the downstream functionalization of the cyclopentenone motif – for example, the β position of the enone was quite hindered and would likely cause issues in the event of a 1,4-reduction. We were thus faced with a tough decision: whether to keep pursuing the HAT strategy that would be quite challenging to render stereoselective, or pivot to this cyclopentenone annulation strategy while taking the risk of functionalizing the hindered enone in **2.91**. In the end, we decided to go with the latter due to the possibility of quickly de-risking the endgame sequence with this route. After successfully reproducing the reported sequence outlined in Figure 2.12A, we decided to use a model substrate **2.80** in lieu of the fully formed EF fragment to test out our plan for the endgame sequence (Figure

2.12B), the first step of which is the α-alkylation of the enone **2.79**. After extensive screening (see Table S2.1), we discovered that the combination of an alkyl triflate with NaHMDS offered the best reactivity, regioselectivity (α- vs. γ-alkylation), and diastereoselectivity. Just as we expected, the aforementioned 1,4-reduction of the enone turned out to be quite challenging and required substantial screening (Table S2.4a); fortunately, an *in situ* formed reactive CuH species reported by Lipshutz *et. al.* proved to be the singularly successful condition for this transformation, furnishing the 1,4-reduction product **2.82** as a single diastereomer favoring the desired stereochemistry.[19] The facial selectivity of the hydride delivery could be rationalized as the axial methyl group blocking hydride approach from the top face of the molecule. Methylenation of **2.82** with Wittig afforded diene **2.83**, which set the stage for a pilot reaction for the RCM cyclization. To our delight, treatment of **2.83** with 20 mol% of Hoveyda-Grubbs 2nd generation (HG-II) catalyst at 70 °C for 16 h resulted in 49% conversion of the starting material and 28% isolated yield of the RCM product **2.84**. Despite the sluggish reactivity observed, this RCM result provided an invaluable proof-of-concept for our endgame strategy and greatly motivated us to proceed with this route.

However, there was one small issue we needed to address before moving on to the EF fragment: due to cyclopamine's known acid sensitivity, we realized that it was quite risky to mask the A ring secondary alcohol as an acetal and attempt to perform deprotection and reduction on a late-stage intermediate. Instead, a superior tactic would be an early installation of the secondary alcohol during fragment synthesis and protecting it as a benzyl ether. The advantage would be three-fold: 1) deprotection of benzyl groups could be achieved in neutral conditions (hydrogenation or single electron reduction), 2) the

possibility of a global deprotection with an appropriate protecting group for the F-ring piperidine, and 3) the possibility of intercepting the *O*-benzyl-*N*-benzenesulfonyl-protected cyclopamine intermediate in Giannis's synthesis,[10] thus simplifying the structural elucidation process. For the above reasons, we envisioned that **2.91**, the *O*-benzyl variant of the ABC fragment, could arise from a similar cyclopentenone annulation sequence with the benzyl-protected decalin **2.90** (Figure 2.13). While a literature report exists for the preparation of the TBS variant **2.89** in 4 steps,[12j] our attempt to directly adapt this procedure for **2.90** turned out to be unsuccessful due to the non-selective benzylation of diol **2.86**. We were thus forced to prepared **2.89** first through the known 4 step sequence (where the mono TBS protection proceeded selectively) followed by a 2-step protecting group exchange. While serviceable at the moment, we eventually developed a shorter sequence to access **2.91** in 3 steps instead (*vide infra*). Finally, the cyclopentenone annulation sequence with **2.90** proceeded smoothly to yield **2.91** in 71% yield, albeit in a diminished 9:1 d.r. Luckily, this issue could be easily resolved by a single round of recrystallization of **2.91**, which restored its d.r. to >20:1.

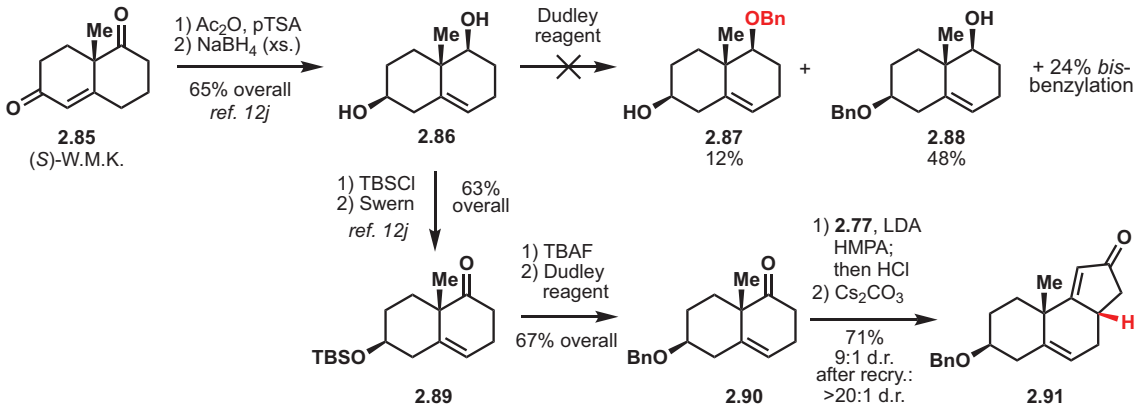


Figure 2.13 Preparation of the *O*-Benzyl Variant of the ABC Fragment

With gram quantities of the optimal ABC fragment in hand and a proof-of-concept for the endgame sequence putting our mind at ease, we proceeded to synthesize the EF fragment required for completing the synthesis. Synthesis of the lactone **2.99** was relatively straightforward due to the existence of literature reports mentioned above,[12g] albeit requiring slight modifications to the procedures for decagram scale (Figure 2.14). This sequence commenced with the chiral pool feedstock (*S*)-citronellic acid (**2.93**), which can be easily prepared from (*S*)-citronellal (**2.92**) with a Tollens oxidation. Treatment of **2.93** with DPPA effected a Curtius rearrangement, the resulting isocyanate from which was subjected to benzyl alcohol to furnish the Cbz protected primary amine **2.94**. From there, oxidative cleavage of the isopropylidene motif under Lemieux-Johnson conditions yielded an hemiaminal, which was subsequently dehydrated with TFA to yield the enecarbamate **2.95**. This slightly unstable intermediate was quickly subjected to NBS/H_2O to afford the bromohydrin **2.96** (as a single diastereomer due to Fürst-Plattner control), setting the stage for a key allylation reaction in this sequence: upon treatment with base, the bromohydrin collapsed to form an epoxide *in situ*, which was then opened with allylmagnesium chloride

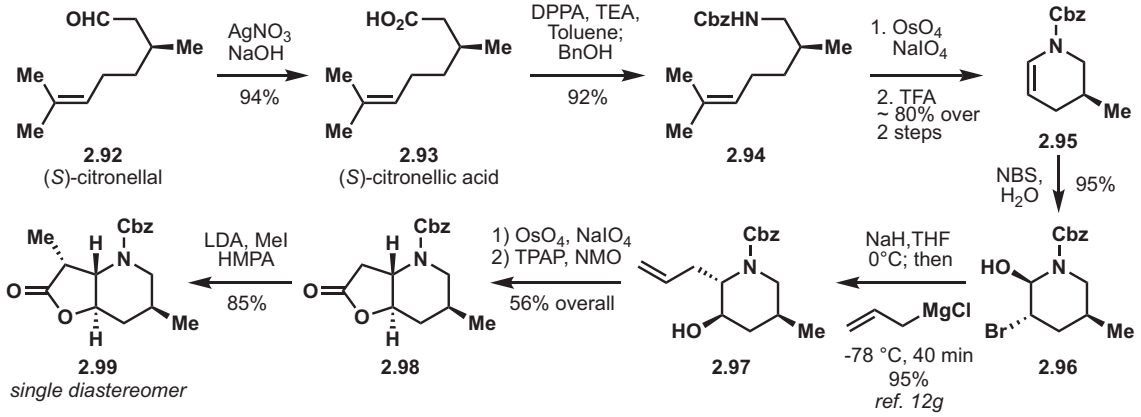


Figure 2.14 Synthesis of the Lactone Intermediate *En Route* to the EF Fragment

to afford the allylated product **2.97** as a single diastereomer. The neighboring carbamate nitrogen caused sufficient electronic bias in the transient epoxide and was likely responsible for the exclusive regioselectivity observed in this reaction. **2.97** underwent a second Lemieux-Johnson cleavage, this time yielding a hemiacetal that was subsequently oxidized with TPAP/NMO to afford the lactone **2.98**. Finally, methylation of the lactone enolate proceeded stereoselectively to deliver the key lactone intermediate **2.99** as a single diastereomer, a result that was in line with observations from the Taber *et al.* report.[12g]

With 4 out of 5 stereocenters in the full-fledged EF fragment already set correctly in lactone **2.99**, we turned our attention to the formation of the last and most challenging stereocenter – the fully-substituted carbon center on the THF ring (**Figure 2.15**). Our original plan quickly derailed when we realized that the Cbz group in **2.99** was incompatible with alkenyllithium or enolate nucleophiles that we were attempting to add to the lactone, giving rise to complex mixtures in both cases. We were thus forced to enlist a two-step sequence to exchange the protecting group from Cbz in **2.99** to benzenesulfonyl (Bs) in **2.100**. It was rationalized that a sulfonamide protecting group will be more resistant to nucleophilic attacks, plus with the added benefit of being able to intercept one of Giannis's late-stage intermediates carrying the same protecting groups (*vide supra*).[10] And just as we expected, addition of enolates to **2.100** now proceeded smoothly to yield the α,β-unsaturated ester **2.101** after dehydration with the Burgess reagent. Unfortunately, addition of isopropenyl cuprate reagents to **2.101** proved unfruitful, which was probably a result of unfavorable electronics posed by the β-alkoxy substituent. We also attempted to change the order of operation by adding in isopropenyllithium first, which furnished the lactol **2.103** in excellent yield; however, addition of a second nucleophile to this system turned

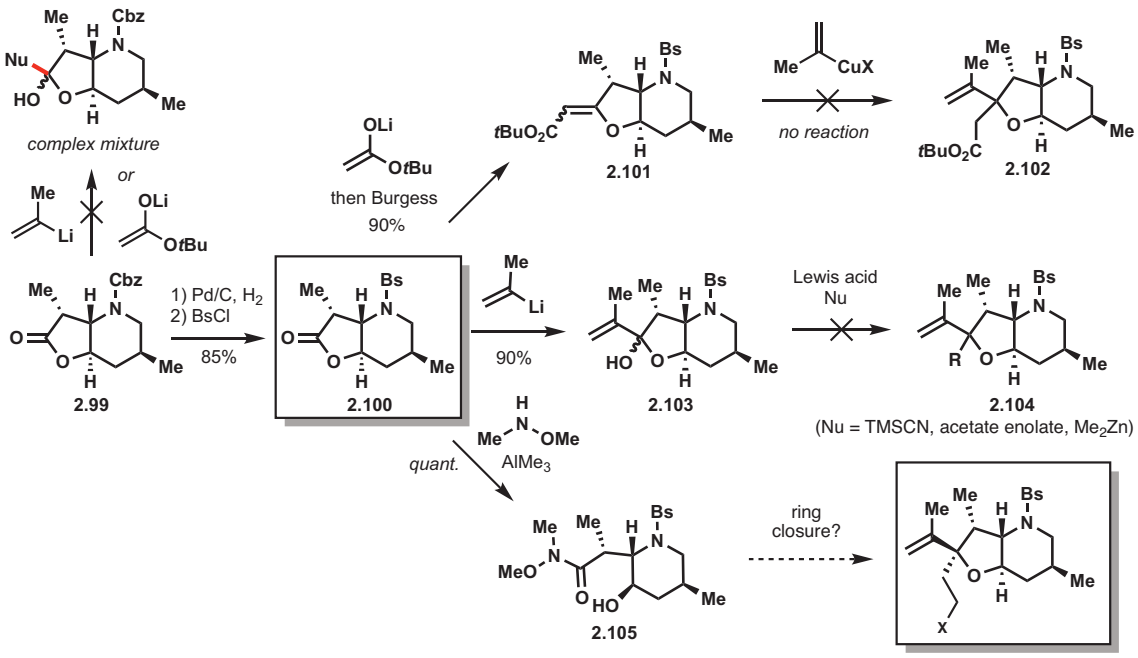


Figure 2.15 Attempts to Elaborate the Lactone to the EF Fragment

out to be challenging as well, with a number of nucleophiles and/or Lewis acids resulting in complex mixtures. A common side product was actually a seven-membered ring ketone, which arose from ring-chain tautomerization of the lactol, followed by an intramolecular oxa-Michael addition of the secondary alcohol to the newly revealed enone system. There was still one silver lining though – addition of Weinreb amine aluminate to **2.100** cleanly yielded the hydroxy Weinreb amide **2.105** in nearly quantitative yield. Although it is sub-optimal that the lactone was opened in this reaction, we decided to move forward with this result since it was the only thing that worked. Perhaps there would be a way to re-cyclize the THF ring later?

With that question in mind we set out to explore what we could do with the Weinreb amide. Amongst a few things that we tried, the most promising strategy was to first install both the isopropenyl and the ethylene groups *via* sequential addition to the Weinreb amide,

followed by a Tsuji-Trost ring closure to re-form the THF ring. The details of this route was shown in Figure 2.16, where **2.105** first underwent PMB protection and sequential addition of isopropenyllithium and *tert*-butyl acetate enolate, furnishing the tertiary alcohol **2.108** as a single diastereomer. The stereochemistry at the tertiary alcohol was unclear to us at the moment but will be later revealed in the 4th generation route (*vide infra*). **2.108** subsequently underwent a number of functional group interconversions: LAH reduction of the ester to the primary alcohol **2.109**, TBDPS protection, ethyl carbonate formation, and finally PMB deprotection with DDQ to arrive at the Tsuji-Trost precursor **2.112**. The Tsuji-

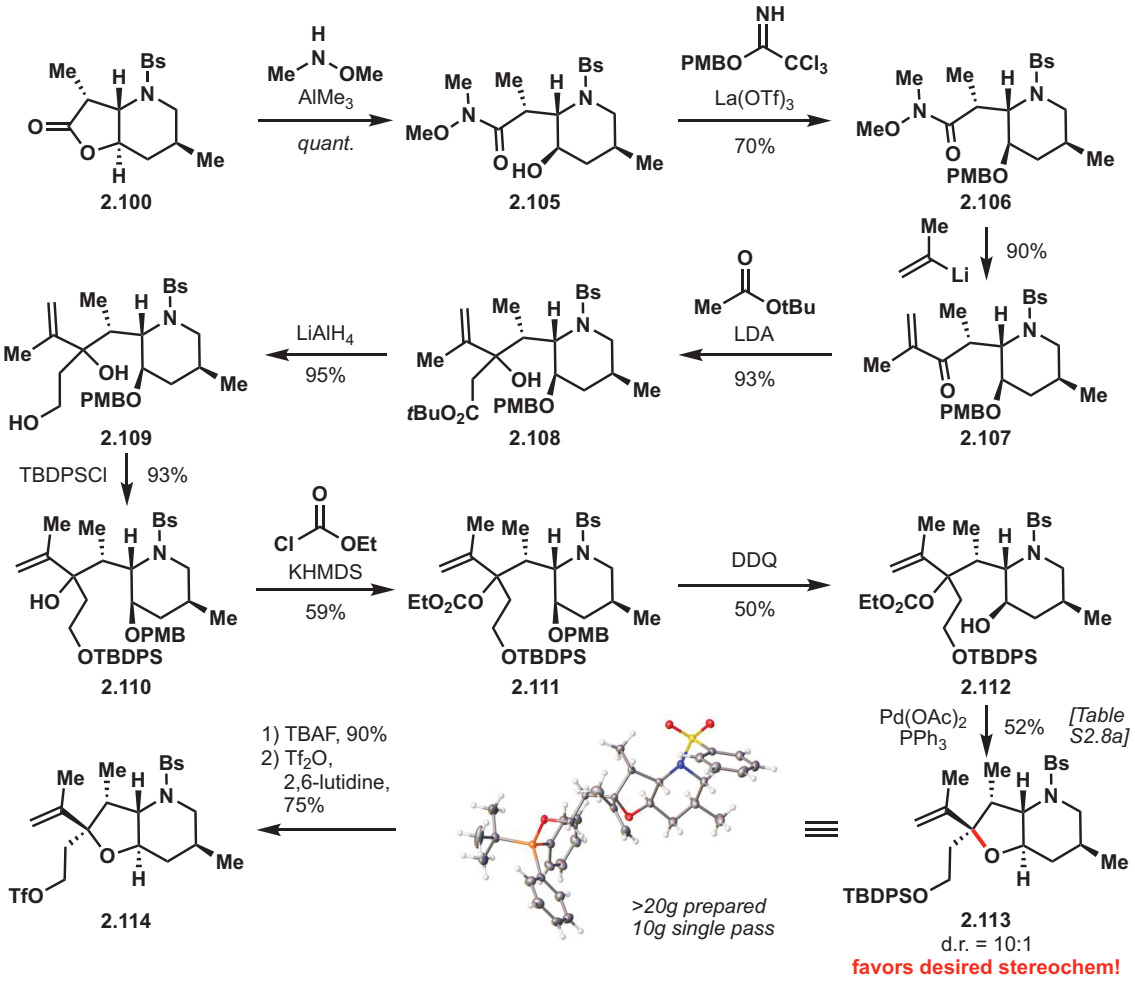


Figure 2.16. Synthesis of the EF Fragment *via* Tsuji-Trost Cyclization

Trost cyclization required some optimization (Table S2.8a) to eventually deliver the cyclized product **2.113** in 52% yield. We were delighted to find that the product was a separable 10:1 mixture of diastereomers favoring the desired stereochemistry at the fully substituted carbon center (confirmed by X-ray analysis). We subsequently scaled up this entire route to prepare decagrams of **2.113** in a single pass. Finally, **2.113** underwent TBDPS deprotection with TBAF and triflation with Tf_2O to yield **2.114**, the required alkyl triflate EF fragment for the endgame sequence.

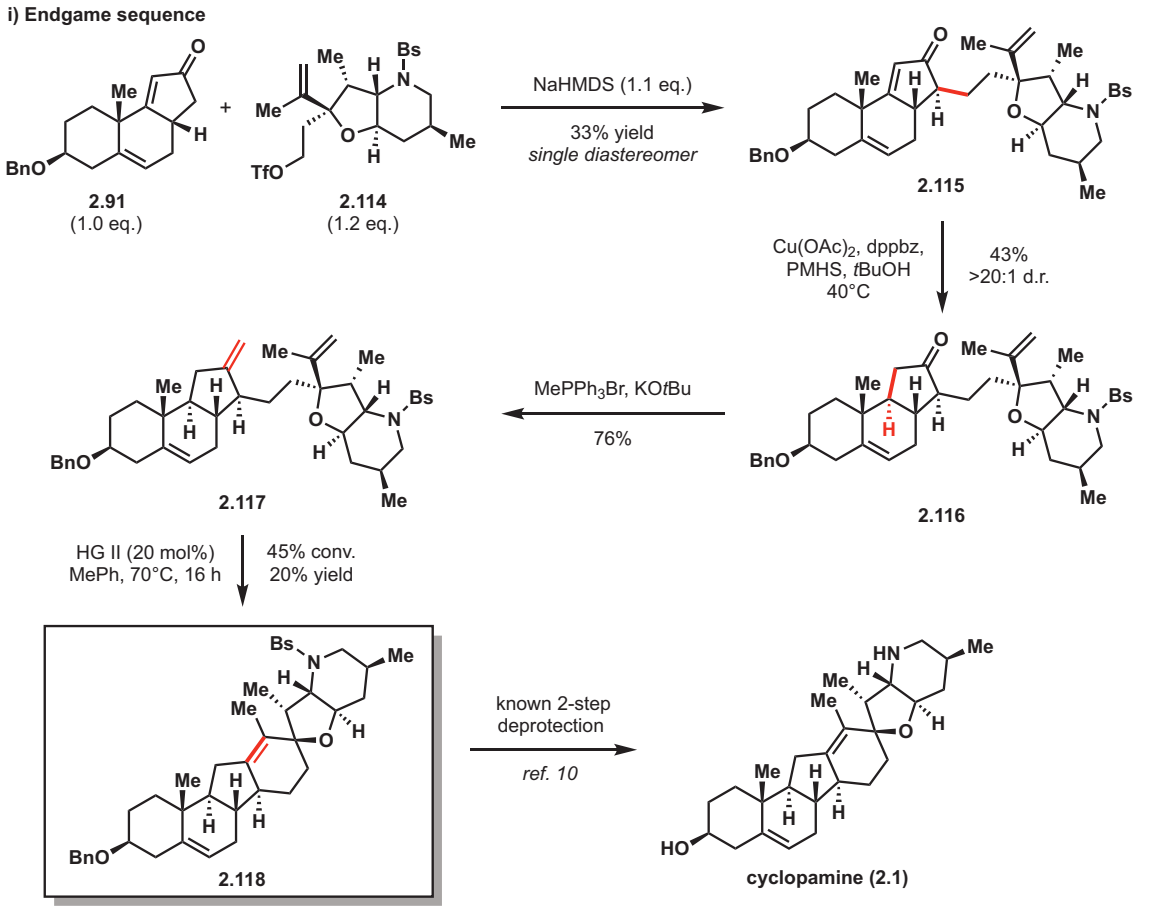


Figure 2.17. Endgame Sequence of the 2nd Generation Route

With sufficient quantities of both the ABC and the EF fragments in hand, and with the knowledge from our endgame model studies, we proceeded to carry out the endgame sequence on the real system (Figure 2.17). We were extremely lucky in the sense that everything worked as it was: the alkylation of **2.91** with **2.114** proceeded smoothly to deliver **2.115** in 33% yield as a single diastereomer; enone 1,4-reduction with Lipshutz's CuH conditions gave slight decomposition and hence only 43% yield of **2.116**, albeit still as a single diastereomer. Wittig olefination proceeded uneventfully to deliver the RCM precursor **2.117**, which was treated with HG-II and underwent a successful RCM cyclization to deliver *bis*-protected cyclopamine **2.118** in 20% yield. At this point, we have intercepted the same intermediate from the Giannis synthesis, which enlisted a two-step sequence to remove the benzyl and the benzenesulfonyl groups and reveal the natural product cyclopamine (**2.1**). We have thus formally achieved the total synthesis of (–)-cyclopamine.

In summary, the 2nd generation route achieved formal total synthesis of cyclopamine and offered invaluable lessons and proof of concepts along the way. Some of the transformations enabled powerful disconnections that would be revisited in later routes (*vide infra*). However, this was far being a definitive final route – the overall route was plagued with low yielding steps, multiple protecting group /redox manipulations, and the sheer number of steps (28 steps LLS). Our efforts to further improve this synthesis are disclosed in the following sections.

3rd Generation Routes

The two strategies outlined in this section were both aiming to develop a more convergent endgame sequence vs. the 2nd generation route. We were inspired by the development of a doubly decarboxylative cross coupling (DDCC) methodology in our own lab,[20] which allowed us to make an unconventional C-C bond disconnection in RCM precursor **2.117** (Figure 2.18A) and greatly increase the convergency of the endgame. Unfortunately, after extensive screening of reaction conditions (Table S2.2), the best yield of **2.117** we could obtain from fragments **2.121** and **2.122** was only 16% (Fiure 2.18B). A major reason for the diminished yield across the board was the consistent presence of the diene side product **2.123** (~30% yield in most cases), which likely arose from β-O elimination of the nickel complex accompanied by release of ring strain. We tested a

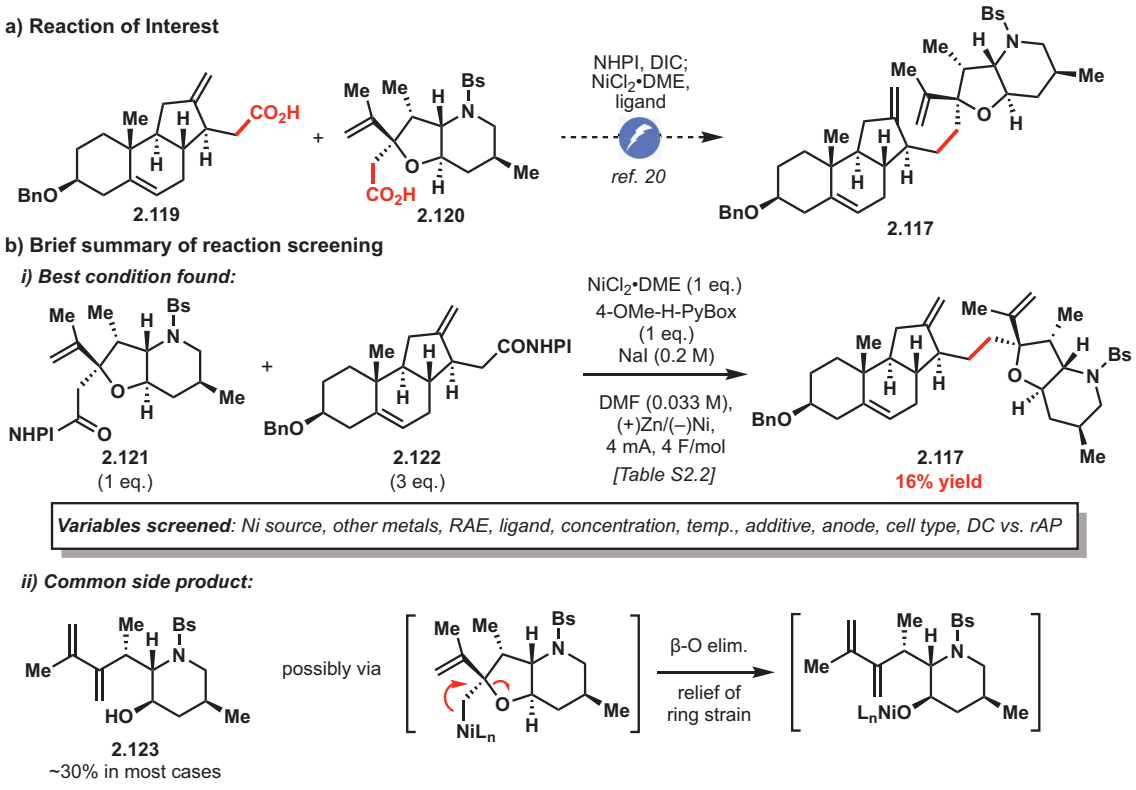


Figure 2.18 Doubly Decarboxylative Cross Coupling (DDCC) Strategy

number of alternative substrates **2.124**-**127** (Figure 2.19A) but ultimately to no avail: all of them gave either worse or similar reactivities. We attempted to remedy the ring opening situation by using the homologated EF fragment **2.128**, the free acid of which was prepared from an Arndt-Eistert reaction of the regular EF fragment, and it smoothly underwent cross coupling with a cyclohexyl model substrate to deliver **2.129** in 25% yield without generating any ring opening product (Figure 2.19B). However, the corresponding des-methylene ABC fragment now became an incompatible cross coupling partner (which was a reported limitation in the original publication: allylic substrates did not work well). Out of curiosity, we conducted some control experiments with different metal catalysts in order to pinpoint when the ring opening took place (Figure 2.19C). When **2.121** was subjected to iron-catalyzed decarboxylative Kumada coupling conditions, no product was observed

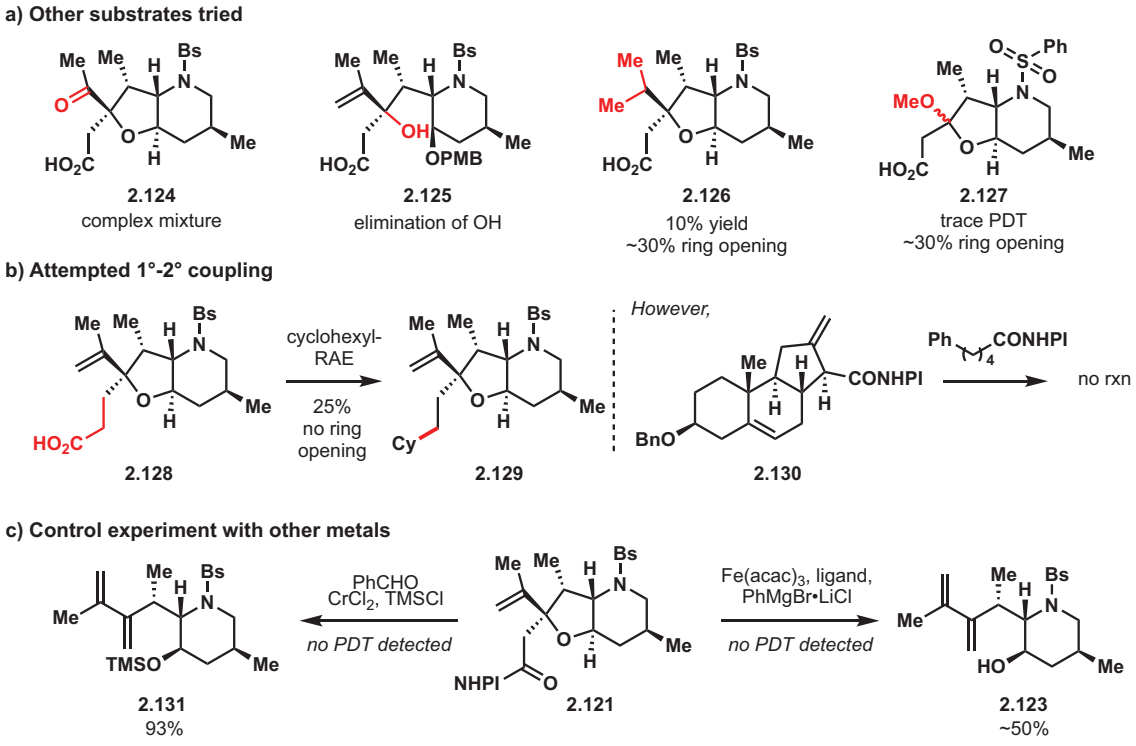


Figure 2.19 Alternative DDCC Substrates and Control Experiments

and the same ring opening product **2.123** could be isolated in an increased 50% yield. Furthermore, when **2.121** was subjected to decarboxylative NHK conditions, no product was observed but the ring-opening product (TMS protected) could now be isolated in near quantitative yield. The fact that different metals led to drastically different yields of the ring opening product (and very crudely, more electron positive metal = higher yield) suggested that ring opening happened while the EF fragment was bound to nickel, supporting our hypothesis of a nickel mediated ring-opening pathway.

Another strategy that we pursued involved a slightly different disconnection from the 2nd generation route – namely a Prins reaction to forge the central D ring (Figure 2.20A). It was deemed desirable mainly because the corresponding EF fragment would be much easier to prepare compared to previous ones, only requiring minimal manipulation from the lactone intermediate **2.100**. We originally envisioned that the Prins precursor **2.118** could arise from a similar enolate alkylation reaction between the same ABC fragment **2.91** and the slightly modified EF fragment **2.133** (Figure 2.20B). However, unlike the previous EF fragment **2.114**, the alkyl triflate **2.133** proved to be extremely unstable and readily decomposed under various reaction conditions, leaving **2.91** untouched. We were thus forced to alter our approach by bringing in a more functionalized ABC fragment **2.134** (prepared from **2.91** following a sequence similar to the endgame of the 2nd generation route: alkylation with *tert*-butyl bromoacetate, CuH reduction with Lipshutz's protocol, Wittig olefination with $EtPPh_3Br$, reduction of ester to alcohol, and finally Appel; preparation of an analogous methylenated fragment can be found in the 4th generation route) as a 4:1 mixture of *Z* and *E* isomers at the olefin. After lithium-halogen exchange of the primary iodide **2.134** with *t*BuLi, the resulting alkyllithium species underwent an 1,2-

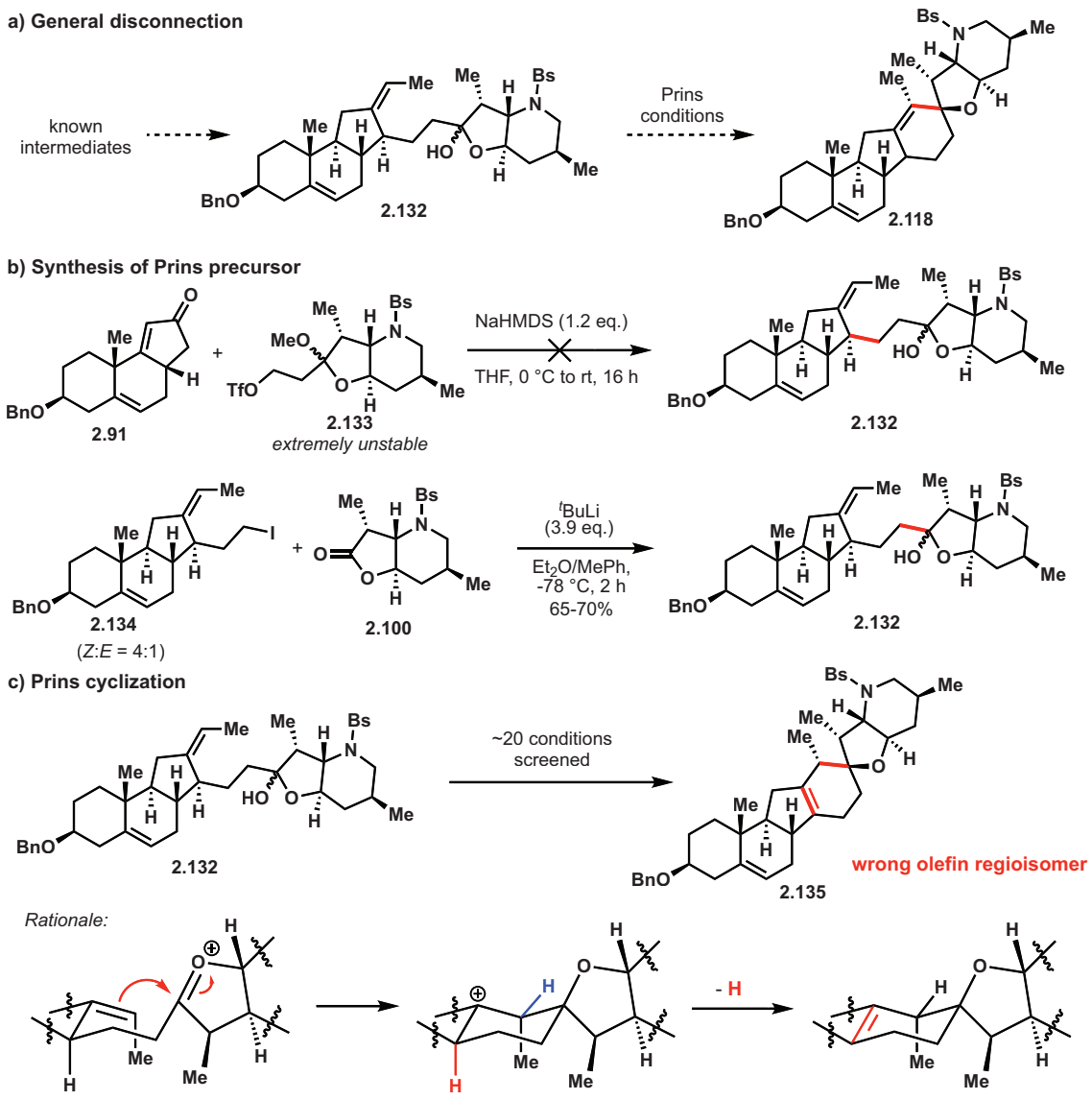


Figure 2.20. A Prins Approach Towards the Endgame Sequence

addition with the known lactone **2.100** to afford the Prins precursor **2.132** in 65% yield. To our delight, Prins cyclization of the hemiacetal **2.132** (Figure 2.20C) readily took place when it was treated with a number of Bronsted or Lewis acids that we screened (Table S2.3), cleanly yielding a single compound with nearly full conversion of **2.132**. However, our initial excitement was quenched by NMR evidence suggesting that the product is not

the desired *bis*-protected cyclopamine **2.118**, but instead the wrong olefin regioisomer **2.135**. In hindsight, this outcome could be easily rationalized with a 3D model of the Prins transition state: when the olefin attacks the oxonium and forms a carbocation, it would prefer to undergo E1 elimination with the axial proton (in red) to form the wrong regioisomer instead of eliminating the equatorial proton (in blue) required to form the desired product. In other words, the current Prins strategy was fundamentally flawed and unlikely to give rise to the desired cyclization product.

After this initial setback, the most logical next step was seemingly to synthesize the *E* olefin isomer of the ABC fragment **2.134** and render both β protons axial. However, we were concerned about the fact that not even a trace of the product was observed, despite the starting material being a 4:1 *Z:E* mixture. We speculated that the Prins cyclization might have proceeded with some degree of concertedness – in other words, it could be challenging to eliminate the correct proton even if it was axial, since doing so would require a perfectly stepwise mechanism. It was also possible that there might be an interconversion pathway between the two olefin isomers, with the wrong olefin regioisomer being more stable under acidic conditions and thus remaining as the only final product. For the reasons above, we chose to instead look at alternative substrates for the Prins cyclization (Figure 2.21). Despite compelling precedents of Prins cyclization with alkenyl-silanes,[21] as well as a promising report of ketone *gem*-silylborylation,[22] we were unable to apply this reaction to the ABC ketone and thus failed to make the silyl Prins precursor **2.136**. Another strategy involving allene Prins was met with similar fate – we quickly realized that intermediates bearing the terminal allene were difficult to handle over multiple steps and readily isomerized to their propargyl isomers, rendering the sequence unrealistic in terms of

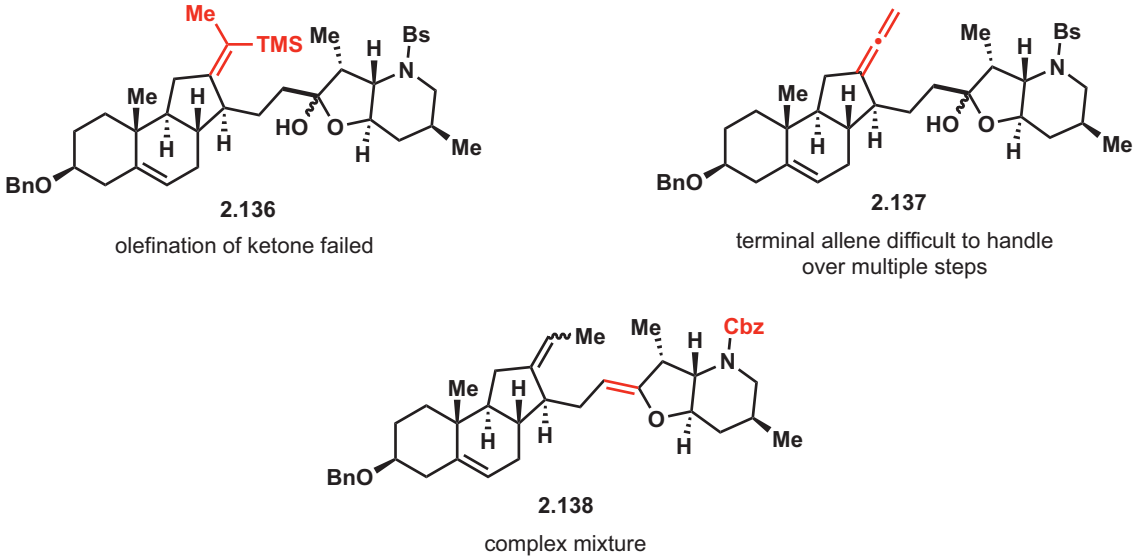


Figure 2.21. Other Potential Prins Substrates

material throughput. Finally, we prepared the Cbz analog **2.138** in hopes that changing the protecting group could affect the reaction outcome. Unfortunately, subjecting **2.138** to a number of acidic conditions only resulted in formation of complex mixtures.

To sum up, our DDCC strategy was defeated by the spring-loaded nature of the EF system that led to our eventual failure to suppress the ring-opening side reaction. The fact that different metals gave variable yields of the ring-opening product suggested that ring-opening happens while the substrate is bound to the metal catalyst, instead of it being a free radical or anion process. On the other hand, the Prins cyclization would have been an excellent solution to the endgame sequence because the required EF fragment would be much easier to access compared to previous routes. However, wrong regioselectivity of the E1 elimination and difficulty of making other related substrates led to this route being eventually abandoned. These setbacks have prompted us to go back to the drawing board

and develop a new design that utilized our existing knowledge about the 2nd generation route, yet with the order of operation scrambled to improve conciseness.

4th Generation/Final Route

It was fair to say that we felt rather defeated when the Prins strategy did not work out. To quote one of Phil's favorite sayings, we "went down a rabbit hole" in pursuit of improving the 2nd generation route by proposing these novel and creative 3rd generation disconnections, our vision clouded by the sole need to reduce the step count so that we eventually lost sight of what key information could be extracted from the 2nd generation route. When we took a step back instead and looked at the 2nd generation route with a pair of fresh eyes, it became obvious that there were a lot of useful transformations in this route despite its length: the cyclopentenone annulation sequence provided easy entry into the ABC scaffold, the Tsuji-Trost cyclization to forge the THF ring with stereocontrol was extremely powerful, and the final RCM reaction to form the D ring was clean and likely could be optimized. It seemed only logical that we should stick to the same set of key bond formation reactions, which took months to discover and optimize, yet rearranging the order of operation to improve the conciseness and convergency of the route.

After taking a deep breath, we set out once again. Our 4th generation disconnection (Figure 2.22) took inspiration from both the 2nd and 3rd generation routes but also made several key modifications. After the same RCM disconnection to break open the D ring, we invoked a late-stage Tsuji-Trost cyclization where the E ring would now be formed with the entirety of the ABC ring system appended. This adjustment allowed us to disconnect the Tsuji-Trost precursor with a 1,2-addition reaction that was rather reminiscent of our

synthesis of the Prins precursor **2.132**. The resulting ABC fragment **2.139** could be prepared similarly to **2.134** *via* a concise sequence (*vide infra*), and the required enone EF fragment **2.140** could arise from 1,2-addition of isopropenyllithium to **2.100** followed by TES protection. Synthesis of the lactone **2.100** could also be improved with a novel sequence involving an asymmetric allylation reaction of siloxyfurans.

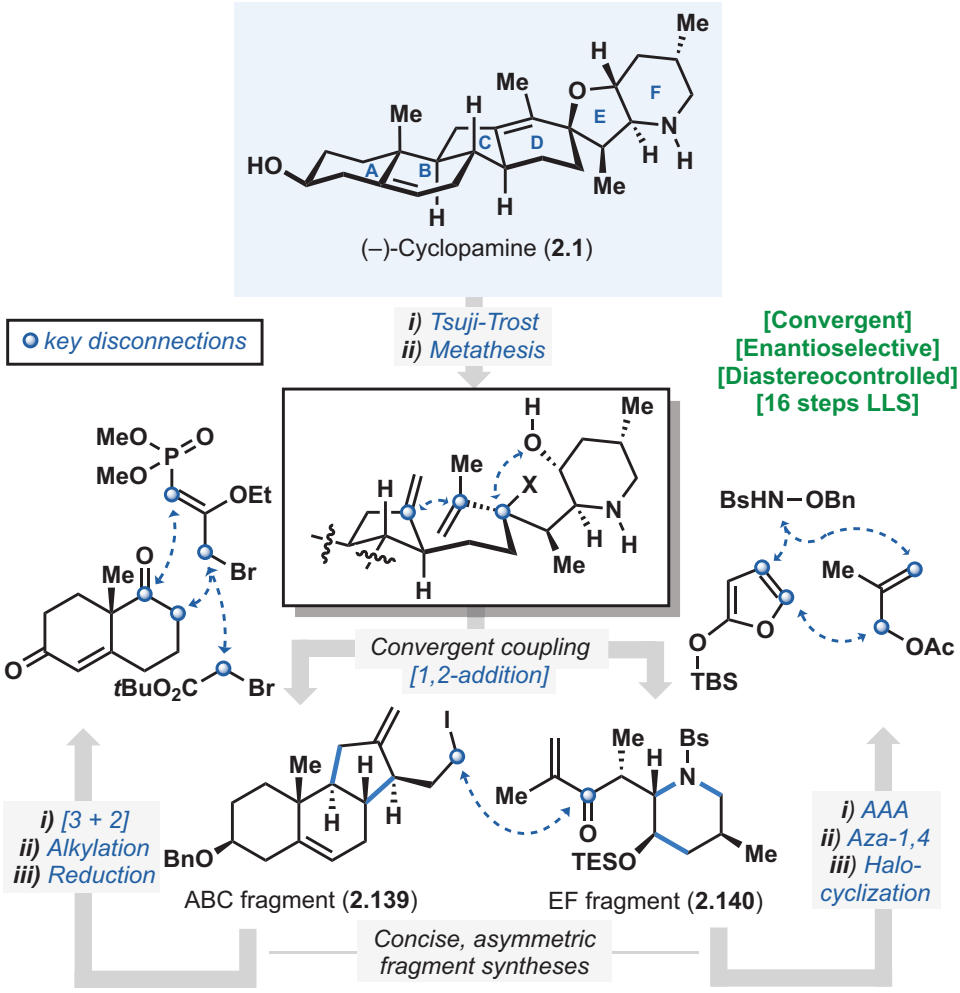


Figure 2.22. Retrosynthetic Analysis of the 4th Generation Route

---

Our synthesis of the ABC fragment (Figure 2.23) commenced with decalin **2.142**, the TBS variant of which was previously prepared in 4 steps from (*S*)-Wieland-Miescher

ketone (**2.141**).[12j] Unfortunately, our attempts to directly adapt this procedure for the preparation of Bn-protected **2.142** were unsuccessful (*vide supra*) and eventually required 2 additional steps to exchange the protecting group, resulting in a non-ideal 6 step sequence. An alternative 3-step protocol amenable to gram scale operations was thus developed involving enone isomerization/reduction of acetal protected **2.141** (see Experimental section for details). A cyclopentenone annulation sequence was subsequently carried out using the known phosphonate reagent **2.143**:[18] the lithium enolate of **2.142** was first alkylated with **2.143** to afford intermediate **2.144** as a 1:1 mixture of C9 epimers (after hydrolysis of the enol ether), which upon treatment with Cs_2CO_3 underwent an intramolecular Horner-Wadsworth-Emmons reaction to forge the cyclopentenone motif with concomitant equilibration to a 9:1 mixture of C9 epimers favoring the desired diastereomer, as confirmed by X-ray crystallographic analysis. Further enrichment of **2.145** to >20:1 dr was achieved after a single round of recrystallization from hexanes/DCM (*ca.* 10:1). With gram quantities of **2.145** at hand, a second enolate alkylation at C13 with *tert*-butyl bromoacetate proceeded smoothly to yield **2.146** as a single diastereomer.

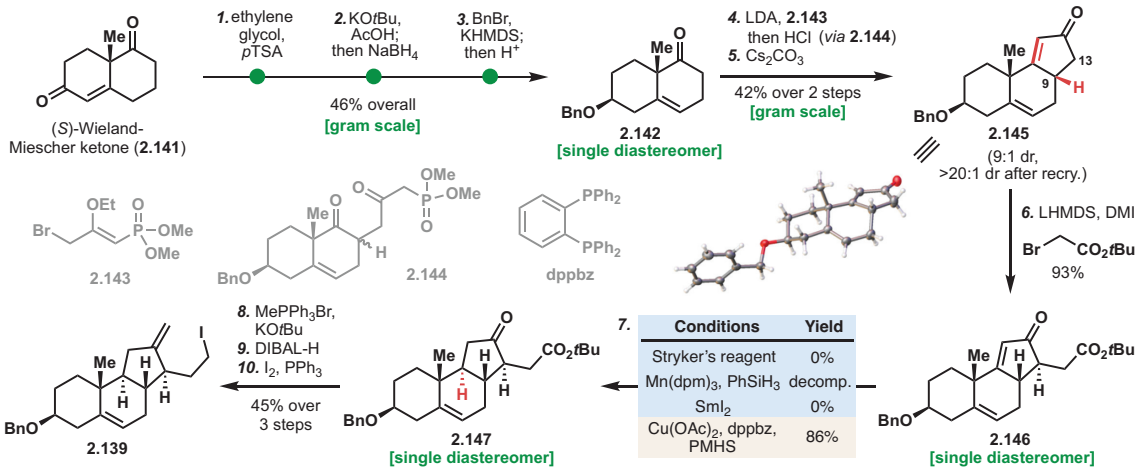


Figure 2.23 Synthesis of the ABC Fragment

The conjugate reduction of enone **2.146** required judicious choice of reagents (Table S2.4). Whereas Stryker's reagent and SmI_2 gave no reaction and Shenvi's HAT reduction conditions[23] resulted in decomposition, a reactive CuH species reported by Lipshutz and coworkers[19] proved to be the optimal choice, furnishing the desired 1,4-reduction product **2.147** in 86% yield as a single diastereomer without any undesired 1,2-reduction. The excellent diastereoselectivity observed could be rationalized by the angular methyl group blocking CuH approach from the top face of **2.146**. Ketone **2.147** was ultimately transformed to the 1,2-addition precursor **2.139** by Wittig olefination, DIBAL-H reduction of the *t*Bu ester, and finally an Appel reaction to convert the primary alcohol to iodide.

Multiple strategies to access the EF fragment (**2.140**) were evaluated *via* a structure such as lactone **2.152** (Figure 2.24). Similar molecules have been prepared in the past through labor-intensive chiral pool strategies. For instance, a derivative of **2.152** bearing a Cbz instead of a benzenesulfonyl (Bs) group was previously accessed in either 9 steps[12c] or 6 steps[12g] from (*S*)-citronellal, with 2 additional steps required for protecting group exchange as the Bs group has proven to be essential for late-stage manipulations (*vide supra*). A concise 4-step route to **2.152** was thus developed through an unusual sequence

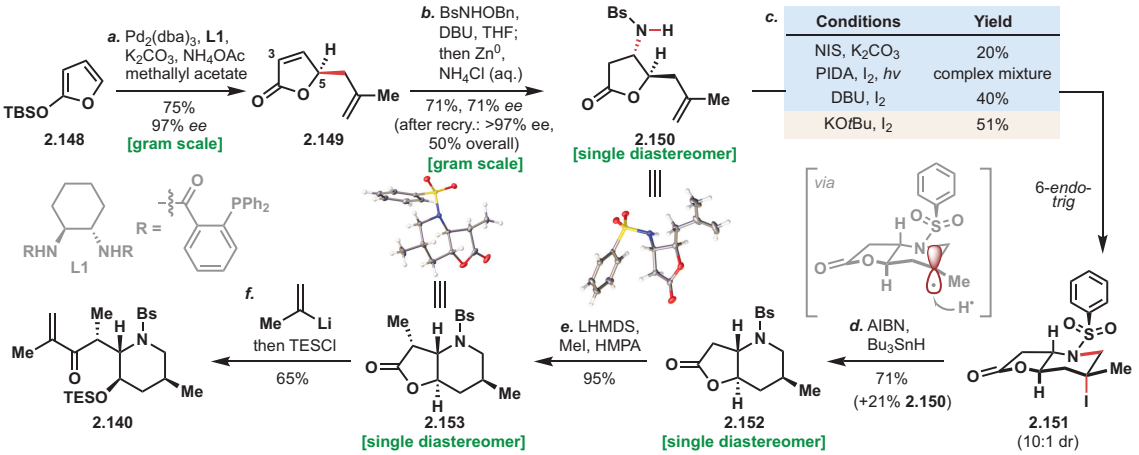


Figure 2.24 Synthesis of the EF Fragment

relying on the C5-selective asymmetric allylic alkylation (AAA) of siloxyfuran **2.148** as reported by Arseniyadis *et al.*[24] This key precedent was improved for the synthesis of γ-butenolide **2.149** through the addition of NH_4OAc (suggested by the Arseniyadis group in our correspondence), which further boosted reaction efficiency and regioselectivity (favoring C5 allylation over C3), delivering **2.149** in 75% isolated yield and 97% *ee.* Subsequent aza-Michael addition to **2.149** required substantial screening (Table S2.5) that eventually led to the identification of BsNHOBn (*N*-benzenesulfonyl-*O*-benzylhydroxylamine) as the optimal nucleophile. X-ray analysis confirmed that addition occurred exclusively *trans* to the existing γ substituent on the butenolide. In its fully optimized form, this reaction involved directly treating the aza-Michael adduct with Zn^0/NH_4Cl in the same reaction vessel to effect N-O bond cleavage and furnish the sulfonamide **2.150** as a single diastereomer in 71% isolated yield. Racemization of **2.150** (71% *ee*) was observed but could be rectified by a single round of recrystallization from DCM/Et_2O (1:1), which restored its enantiopurity (>97% *ee*, 50% yield overall). With gram quantities of **2.150** at hand, the key halocyclization step to construct the strained *trans*-6,5 EF bicycle was investigated. Due to the extreme strain that would be incurred through a 5-*exo*-*trig* cyclization to deliver a *trans*-5,5 ring system, it was rationalized that an unusual 6-*endo*-*trig* cyclization would be preferred. After the initial hit with NIS/K_2CO_3 verified this hypothesis, further screening was performed (Table S2.6) that eventually led to the most reproducible and scalable protocol with KO*t*Bu/I_2. In its fully optimized form, the halocyclization step furnished the tertiary iodide **2.151** in 51% yield as an inconsequential 10:1 mixture of diastereomers favoring the axial iodide, which was then subjected to a tin hydride-mediated dehalogenation reaction to afford the desired lactone **2.152** in 71% yield

as a single diastereomer. This stereochemical outcome could be rationalized as a combination of stereoelectronics (axial iodide is more susceptible to abstraction), thermodynamic preference (methyl group prefers to be equatorial), and steric bulk of the benzenesulfonyl group (which disfavors hydride approach from top face of the tertiary radical). It is worth noting that the ring-opening side product **2.150** was consistently observed on larger scale (>100 mg) and could be isolated in 21% yield. Attempts to suppress this process by running the reaction at ambient temperature instead of 100 °C surprisingly exacerbated ring-opening (**2.152** : **2.150** = 1:1, vs. 3:1 with AIBN at 100 °C). Besides this piece of evidence, we also observed that 1) the halocyclization reaction exhibited certain degrees of reversibility over prolonged reaction times, and 2) addition of TEMPO to the halocyclization reaction inhibited product formation. These clues led us to speculate that the halocylization might proceed through a one-electron pathway involving formation and homolysis of an N-I species (see Experimental section). Methylation of **2.152** by enolate alkylation proceeded smoothly to deliver the key lactone **2.153** as a single diastereomer, the structure of which was confirmed by X-ray analysis. The diastereoselectivity observed was in line with Taber's report[8h] on a similar scaffold and could be attributed to the axial β-H at the ring junction blocking electrophile approach from the top face of **2.152**. Finally, addition of isopropenyllithium to lactone **2.153** yielded a hemiketal that was in equilibrium with the open chain hydroxyketone, the secondary alcohol of which could be TES protected in the same pot to furnish enone **2.140** in 65% yield.

With both fragments (**2.139** and **2.140**) in hand, the endgame sequence (Figure 2.25) commenced with union of the two fragments by 1,2-addition, wherein the primary iodide

2.139 first underwent lithium halogen exchange with *t*BuLi, and then the resulting alkyllithium species added into enone **2.140**. Addition of $LaCl_3$•2LiCl proved to be crucial for the exclusive 1,2-regioselectivity observed in this reaction (see Table S2.7),[25] yielding tertiary alcohol **2.154** as a single diastereomer (confirmed by X-ray) possibly due to Felkin-Anh selectivity. This success set the stage for the final D/E ring double cyclization sequence, which entailed formation of the E ring through an alkoxide Tsuji-Trost cyclization followed by formation of the D ring by ring-closing metathesis (RCM). The challenging Tsuji-Trost cyclization turned out to be an immense undertaking that required considerable optimization (Table S2.8b). To our delight, Boc carbonate **2.155** (prepared from **2.154** in two steps) emerged as the singularly successful substrate, delivering the desired THF-containing RCM precursor **2.117** in 73% yield with perfect net stereoretention from tertiary alcohol **2.154**. This diastereochemical outcome was in line with previous observations in similar THF-forming Tsuji-Trost cyclizations.[26] The RCM reaction to form the tetrasubstituted olefin, which was the final hurdle in this synthesis, was initially met

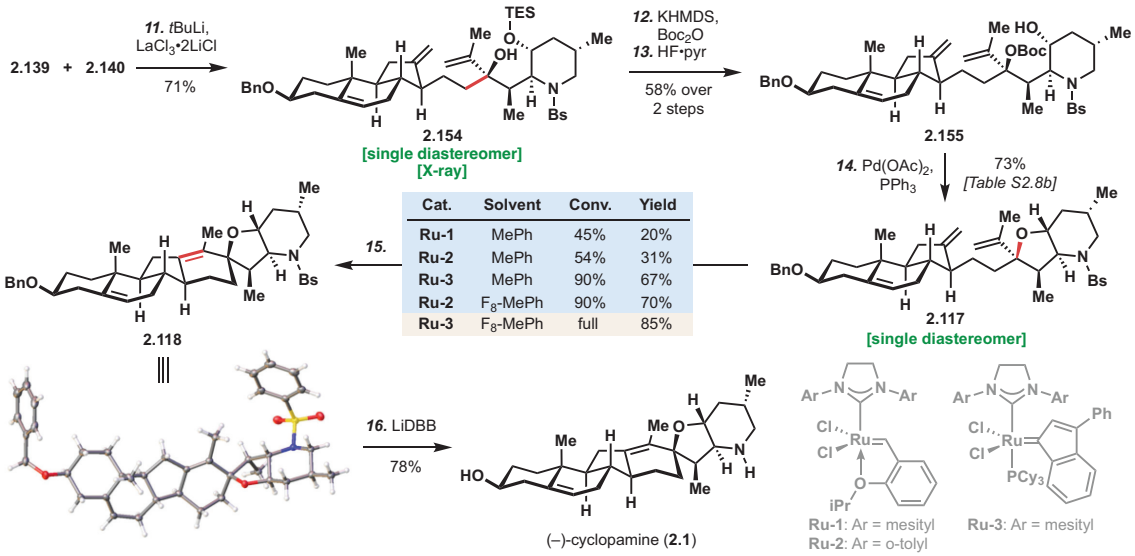


Figure 2.25 Completion of the Total Synthesis of (–)-Cyclopamine

with expected difficulties (see Table S2.9): conventional metathesis catalysts such as Hoveyda-Grubbs 2nd generation catalyst (**Ru-1**) gave low conversions even at elevated temperatures, and the less sterically encumbering *o*-tolyl variant **Ru-2** only led to slightly improved results. Fortunately, the indenylidene catalyst **Ru-3** was reported to be an extremely effective metathesis catalyst for sterically demanding substrates.[27] Indeed, a significant improvement in yield was observed with **Ru-3**, which, when combined with perfluorotoluene as solvent, [27b] led to the optimal condition that afforded *bis*-protected cyclopamine **2.118** in 85% yield, the structure of which was confirmed by X-ray analysis. The prior approach of Giannis necessitated two distinct reductive deprotection conditions to excise Bn and sulfonamide groups in 79% overall yield.[10] Instead, removal of both groups could be accomplished with freshly prepared LiDBB,[28] yielding (–)-cyclopamine in 78% yield. It is worth noting that when acquiring NMR data for cyclopamine in CD_2Cl_2, a solvent that was used in multiple previous reports, we observed that concentration of the sample had a significant impact on the chemical shifts of cyclopamine's ^1H and ^{13}C spectra (see Experimental section).

To conclude, a convergent total synthesis of (–)-cyclopamine (**2.1**) was achieved with a 16-step LLS (1.4% overall yield, 61% ideality,[29] calculation *vide infra*) from (*S*)-Wieland-Miescher ketone. Unlike the semi-synthetic routes which predate this disclosure, the strategy outlined herein should be amenable to exploring deep-seated structural modifications for further SAR studies of this promising class of natural products. Key areas for improvement for which there are methodological gaps include a more direct conversion of **2.150** to **2.152** and a more concise fragment coupling that can minimize protecting group manipulations. That said, notable features of this synthesis include rapid stereocontrolled

access to similarly sized coupling fragments, namely the streamlined ABC-ring synthesis through annulation/CuH reduction and an unusually concise furan-based access to the key EF ring system via AAA/aza-Michael/halocyclization. Furthermore, the exquisite stereocontrol exhibited in the fragment coupling/strained THF ring formation prior to the high-yielding RCM cyclization represents a bold yet effective means of accessing **2.1**.

References

1) Keeler, R. F., Teratogenic compounds of veratrum californicum (durand)—IV. First isolation of veratramine and alkaloid Q and A reliable method for isolation of cyclopamine. *Phytochemistry* **1968,** *7*, 303-306.

2) For reviews of cyclopamine and/or other *Veratrum* alkaloids, see: (a) Li, H.-J.; Jiang, Y.; Li, P., Chemistry, bioactivity and geographical diversity of steroidal alkaloids from the Liliaceae family. *Nat. Prod. Rep.* **2006,** *23*, 735-752. (b) Heretsch, P.; Giannis, A. The Veratrum and Solanum Alkaloids. In *The Alkaloids: Chemistry and Biology*; Elsevier, 2015; Vol. 74, pp 201−232. (c) Dirks, M. L.; Seale, J. T.; Collins, J. M.; McDougal, O. M. Review: *Veratrum californicum* Alkaloids. *Molecules* **2021**, *26*, 5934. (d) Heretsch, P.; Tzagkaroulaki, L.; Giannis, A., Cyclopamine and Hedgehog Signaling: Chemistry, Biology, Medical Perspectives. *Angew. Chem. Int. Ed.* **2010,** *49*, 3418-3427. (e) Lee, S. T.; Welch, K. D.; Panter, K. E.; Gardner, D. R.; Garrossian, M.; Chang, C.-W. T., Cyclopamine: From Cyclops Lambs to Cancer Treatment. *J. Agric. Food Chem.* **2014,** *62*, 7355-7362. (f) Chen, J. K., I only have eye for ewe: the discovery of cyclopamine and development of Hedgehog pathway-targeting drugs. *Nat. Prod. Rep.* **2016,** *33*, 595-601.

3) (a) Binns, W.; James, L. F.; Shupe, J. L.; Everett, G, A Congenital Cyclopian-Type Malformation in Lambs Induced by Maternal Ingestion of a Range Plant, *Veratrum Californicum*. *Am. J. Vet. Res.* **1963**, *24*, 1164-1175. (b) Keeler, R. F., Toxic and teratogenic alkaloids of western range plants. *J. Agric. Food Chem.* **1969,** *17*, 473-482. (c) James, L. F.; Panter, K. E.; Gaffield, W.; Molyneux, R. J., Biomedical

Applications of Poisonous Plant Research. *J. Agric. Food Chem.* **2004,** *52*, 3211-3230.

4) Cooper, M. K.; Porter, J. A.; Young, K. E.; Beachy, P. A., Teratogen-Mediated Inhibition of Target Tissue Response to Shh Signaling. *Science* **1998,** *280*, 1603-1607.

5) See review: S. J. Scales, F. J. de Sauvage, Mechanisms of Hedgehog pathway activation in cancer and implications for therapy. *Trends Pharmacol. Sci.* **2009**, *30*, 303-312.

6) There are disagreements in literature regarding the exact acid decomposition products of cyclopamine. See: (a) Keeler, R. F., Teratogenic compounds of veratrum californicum (durand) - VI: The structure of cyclopamine. *Phytochemistry* **1969,** *8*, 223-225. (b) Wilson, S. R.; Strand, M. F.; Krapp, A.; Rise, F.; Petersen, D.; Krauss, S., Hedgehog antagonist cyclopamine isomerizes to less potent forms when acidified. *J. Pharm. Biomed. Anal.* **2010,** *52*, 707-713.

7) (a) Tremblay, M. R.; Nevalainen, M.; Nair, S. J.; Porter, J. R.; Castro, A. C.; Behnke, M. L.; Yu, L.-C.; Hagel, M.; White, K.; Faia, K.; Grenier, L.; Campbell, M. J.; Cushing, J.; Woodward, C. N.; Hoyt, J.; Foley, M. A.; Read, M. A.; Sydor, J. R.; Tong, J. K.; Palombella, V. J.; McGovern, K.; Adams, J., Semisynthetic Cyclopamine Analogues as Potent and Orally Bioavailable Hedgehog Pathway Antagonists. *J. Med. Chem.* **2008,** *51*, 6646-6649. (b) Tremblay, M. R.; Lescarbeau, A.; Grogan, M. J.; Tan, E.; Lin, G.; Austad, B. C.; Yu, L.-C.; Behnke, M. L.; Nair, S. J.; Hagel, M.; White, K.; Conley, J.; Manna, J. D.; Alvarez-Diez, T. M.; Hoyt, J.; Woodward, C. N.; Sydor, J. R.; Pink, M.; MacDougall, J.; Campbell, M. J.; Cushing,

J.; Ferguson, J.; Curtis, M. S.; McGovern, K.; Read, M. A.; Palombella, V. J.; Adams, J.; Castro, A. C., Discovery of a Potent and Orally Active Hedgehog Pathway Antagonist (IPI-926). *J. Med. Chem.* **2009,** *52*, 4400-4418. (c) Martinot, T. A.; Austad, B. C.; Côté, A.; Depew, K. M.; Genov, D.; Grenier, L.; Helble, J.; Lescarbeau, A.; Nair, S.; Trudeau, M.; White, P.; Yu, L.-C., A Design of Experiments Approach to a Robust Final Deprotection and Reactive Crystallization of IPI-926, A Novel Hedgehog Pathway Inhibitor. *Org. Process Res. Dev.* **2015,** *19*, 1693-1702. (d) Austad, B. C.; Hague, A. B.; White, P.; Peluso, S.; Nair, S. J.; Depew, K. M.; Grogan, M. J.; Charette, A. B.; Yu, L.-C.; Lory, C. D.; Grenier, L.; Lescarbeau, A.; Lane, B. S.; Lombardy, R.; Behnke, M. L.; Koney, N.; Porter, J. R.; Campbell, M. J.; Shaffer, J.; Xiong, J.; Helble, J. C.; Foley, M. A.; Adams, J.; Castro, A. C.; Tremblay, M. R., Development of a Multi Kilogram-Scale, Tandem Cyclopropanation Ring-Expansion Reaction en Route to Hedgehog Antagonist IPI-926. *Org. Process Res. Dev.* **2016,** *20*, 786-798.

8) Masamune, T.; Takasugi, M.; Murai, A.; Kobayashi, K. C-*nor*-D-*homo* steroids and related alkaloids. IX. Synthesis of jervine and related alkaloids. *J. Am. Chem. Soc.* **1967**, *89*, 4521−4523.

9) (a) Kutney, J. P.; Cable, J.; Gladstone, W. A. F.; Hanssen, H. W.; Torupka, E. J.; Warnock, W. D. C. Total synthesis of steroidal derivatives. V. The total synthesis of veratrum alkaloids. 1. Verarine. *J. Am. Chem. Soc.* **1968**, *90*, 5332−5334. (b) Kutney, J. P.; By, A.; Cable, J.; Gladstone, W. A. F.; Inaba, T.; Leong, S. Y.; Roller, P.; Torupka, E. J.; Warnock, W. D. C. Synthetic Studies in the Veratrum Alkaloid Series. I. Introduction and the Total Synthesis of Appropriate C-*nor*-D-*homo* Steroid

Derivatives. *Can. J. Chem.* **1975**, *53*, 1775−1795. (c) Kutney, J. P.; Cable, J.; Gladstone, W. A. F.; Hanssen, H. W.; Nair, G. V.; Torupka, E. J.; Warnock, W. D. C. Synthetic Studies in the Veratrum Alkaloid Series. II. The Total Synthesis of Verarine, Veratramine, Jervine, and Veratrobasine. *Can. J. Chem.* **1975**, *53*, 1796−1817. (d) Kutney, J. P.; Fortes, C. C.; Honda, T.; Murakami, Y.; Preston, A.; Ueda, Y. Synthetic Studies in the Veratrum Alkaloid Series. The Total Synthesis of Verticine. *J. Am. Chem. Soc.* **1977**, *99*, 964−966. (e) Kutney, J. P.; Brookes, R. W.; Fortes, C. C.; Murakami, Y.; Preston, A.; Ueda, Y. Synthetic Studies in the Veratrum Alkaloid Series. The Total Synthesis of C_{18}-functionalized C-*nor*-D-*homo* Steroid Derivatives – Valuable Intermediates in the Total Synthesis of Veratrum Alkaloids. *J. Am. Chem. Soc.* **1977**, *99*, 963−964.

10) Giannis, A.; Heretsch, P.; Sarli, V.; Stößel, A., Synthesis of Cyclopamine Using a Biomimetic and Diastereoselective Approach. *Angew. Chem. Int. Ed.* **2009,** *48*, 7911-7914.

11) Heretsch, P.; Rabe, S.; Giannis, A. A Biomimetic Approach to C-*nor*-D-*homo* Steroids. *J. Am. Chem. Soc.* **2010**, *132*, 9968−9969.

12) (a) Brown, E.; Lebreton, J. A total synthesis of C-*nor*-D-*homo* steroids of the A→B→ C→D type, involving a reductive alkylation step for construction of the d-ring. *Tetrahedron Lett.* **1986**, *27*, 2595−2598. (b) Winkler, J. D.; Isaacs, A.; Holderbaum, L.; Tatard, V.; Dahmane, N., Design and Synthesis of Inhibitors of Hedgehog Signaling Based on the Alkaloid Cyclopamine. *Org. Lett.* **2009,** *11*, 2824-2827. (c) Heretsch, P.; Rabe, S.; Giannis, A. Synthesis of All Diastereomers of the Piperidine−Alkaloid Substructure of Cyclopamine. *Org. Lett.* **2009**, *11*,

5410−5412. (d) Oblak, E. Z.; G-Dayanandan, N.; Wright, D. L. Tandem Metathesis Reactions of Oxabicyclo[2.2.1]heptenes: Studies on the Spirocyclic Core of Cyclopamine. *Org. Lett.* **2011**, *13*, 2433−2435. (e) Zhang, Z.; Baubet, V.; Ventocilla, C.; Xiang, C.; Dahmane, N.; Winkler, J. D., Stereoselective Synthesis of F-Ring Saturated Estrone-Derived Inhibitors of Hedgehog Signaling Based on Cyclopamine. *Org. Lett.* **2011,** *13*, 4786-4789. (f) Isaacs, A. K.; Xiang, C.; Baubet, V.; Dahmane, N.; Winkler, J. D., Studies Directed toward the Elucidation of the Pharmacophore of Steroid-Based Sonic Hedgehog Signaling Inhibitors. *Org. Lett.* **2011,** *13*, 5140-5143. (g) Taber, D. F.; DeMatteo, P. W. A Piperidine Chiron for the Veratrum Alkaloids. *J. Org. Chem.* **2012**, *77*, 4235−4241. (h) Taber, D. F.; Berry, J. F. Construction of the Tricyclic A-B-C Core of the Veratrum Alkaloids. *J. Org. Chem.* **2013**, *78*, 8437−8441. (i) Krieger, J.; Smeilus, T.; Schackow, O.; Giannis, A. Lewis Acid Mediated Nazarov Cyclization as a Convergent and Enantioselective Entry to C-*nor*-D-*homo*-Steroids. *Chem. Eur. J.* **2017**, *23*, 5000−5004. (j) Zavesky, B. P.; De Jesus Cruz, P.; Johnson, J. S. Progress toward a Convergent, Asymmetric Synthesis of Jervine. *Org. Lett.* **2020**, *22*, 3537−3541. (k) Horwitz, M. A.; Robins, J. G.; Johnson, J. S. *De Novo* Synthesis of the DEF-Ring Stereotriad Core of the Veratrum Alkaloids. *J. Org. Chem.* **2020**, *85*, 6808−6814.

13) Thiele, M.; Rabe, S.; Hessenkemper, W.; Roell, D.; Bartsch, S.; Kraft, F.; Abraham, T. E.; Houtsmuller, A. B.; van Royen, M. E.; Giannis, A.; Baniahmad, A., Novel nor-homo-and spiro-oxetan-steroids target the human androgen receptor and act as antiandrogens. *Curr. Med. Chem.* **2015**, *22*, 1156-1167.

14) For examples, see: (a) Paek, S.-M. Synthesis of Tetrasubstituted Alkenes via Metathesis *Molecules* [Online], 2012, p. 3348-3358. (b) Heinrich, C. F.; Durand, D.; Starck, J.; Michelet, V., Ruthenium Metathesis: A Key Step To Access a New Cyclic Tetrasubstituted Olefin Platform. *Org. Lett.* **2020,** *22*, 7064-7067.

15) Xu, C.; Liu, Z.; Torker, S.; Shen, X.; Xu, D.; Hoveyda, A. H., Synthesis of Z- or E-Trisubstituted Allylic Alcohols and Ethers by Kinetically Controlled Cross-Metathesis with a Ru Catechothiolate Complex. *J. Am. Chem. Soc.* **2017,** *139*, 15640-15643.

16) (a) Lo, J. C.; Gui, J.; Yabe, Y.; Pan, C.-M.; Baran, P. S., Functionalized olefin cross-coupling to construct carbon–carbon bonds. *Nature* **2014,** *516*, 343-348. (b) Lo, J. C.; Yabe, Y.; Baran, P. S., A Practical and Catalytic Reductive Olefin Coupling. *J. Am. Chem. Soc.* **2014,** *136*, 1304-1307.

17) Nicolaou, K. C.; Pulukuri, K. K.; Yu, R.; Rigol, S.; Heretsch, P.; Grove, C. I.; Hale, C. R. H.; ElMarrouni, A., Total Synthesis of Δ12-Prostaglandin J3: Evolution of Synthetic Strategies to a Streamlined Process. *Chem. Eur. J.* **2016,** *22*, 8559-8570.

18) (a) Piers, E.; Abeysekera, B., Alkylation of enolate anions with dimethyl 3-bromo-2-ethoxypropenylphosphonate. A convergent cyclopentenone annulation method. *Can. J. Chem.* **1982,** *60*, 1114-1121. (b) Enomoto, M.; Morita, A.; Kuwahara, S., Total Synthesis of the Tremorgenic Indole Diterpene Paspalinine. *Angew. Chem. Int. Ed.* **2012,** *51*, 12833-12836.

19) (a) Baker, B. A.; Bošković, Ž. V.; Lipshutz, B. H., (BDP)CuH: A “Hot” Stryker's Reagent for Use in Achiral Conjugate Reductions. *Org. Lett.* **2008,** *10*, 289-292. (b)

Gao, A. X.; Hamada, T.; Snyder, S. A., The Enantioselective Total Synthesis of Exochomine. *Angew. Chem. Int. Ed.* **2016,** *55*, 10301-10306.

20) Zhang, B.; Gao, Y.; Hioki, Y.; Oderinde, M. S.; Qiao, J. X.; Rodriguez, K. X.; Zhang, H.-J.; Kawamata, Y.; Baran, P. S., Ni-electrocatalytic Csp3–Csp3 doubly decarboxylative coupling. *Nature* **2022,** *606*, 313-318.

21) (a) Dobbs, A. P.; Guesné, S. J. J.; Martinović, S.; Coles, S. J.; Hursthouse, M. B., A Versatile Indium Trichloride Mediated Prins-Type Reaction to Unsaturated Heterocycles. *J. Org. Chem.* **2003,** *68*, 7880-7883. (b) Dobbs, A. P.; Martinović, S., The silyl–Prins reaction: a novel method for the synthesis of dihydropyrans. *Tetrahedron Lett.* **2002,** *43*, 7055-7057.

22) La Cascia, E.; Cuenca, A. B.; Fernández, E., Opportune gem-Silylborylation of Carbonyl Compounds: A Modular and Stereocontrolled Entry to Tetrasubstituted Olefins. *Chem. Eur. J.* **2016,** *22*, 18737-18741.

23) Iwasaki, K.; Wan, K. K.; Oppedisano, A.; Crossley, S. W. M.; Shenvi, R. A., Simple, Chemoselective Hydrogenation with Thermodynamic Stereocontrol. *J. Am. Chem. Soc.* **2014,** *136*, 1300-1303.

24) Richard, F.; Aubert, S.; Katsina, T.; Reinalda, L.; Palomas, D.; Crespo-Otero, R.; Huang, J.; Leitch, D. C.; Mateos, C.; Arseniyadis, S., Enantioselective synthesis of γ-butenolides through Pd-catalysed C5-selective allylation of siloxyfurans. *Nat. Synth.* **2022,** *1*, 641-648.

25) Krasovskiy, A.; Kopp, F.; Knochel, P., Soluble Lanthanide Salts ($LnCl_3 \cdot 2LiCl$) for the Improved Addition of Organomagnesium Reagents to Carbonyl Compounds. *Angew. Chem. Int. Ed.* **2006,** *45*, 497-500.

26) (a) He, A.; Sutivisedsak, N.; Spilling, C. D., Stereoselective Synthesis of Cyclic Ethers via the Palladium-Catalyzed Intramolecular Addition of Alcohols to Phosphono Allylic Carbonates. *Org. Lett.* **2009,** *11*, 3124-3127. For an excellent review on fully substituted carbon center formation with Tsuji-Trost reactions, see: (b) Trost, B. M.; Schultz, J. E., Palladium-catalyzed asymmetric allylic alkylation strategies for the synthesis of acyclic tetrasubstituted stereocenters. *Synthesis* **2019,** *51*, 1-30.

27) (a) Clavier, H.; Nolan, S. P., N-Heterocyclic Carbene and Phosphine Ruthenium Indenylidene Precatalysts: A Comparative Study in Olefin Metathesis. *Chem. Eur. J.* **2007,** *13*, 8029-8036. For an example of its application in total synthesis, see: (b) Wang, Y.; Nagai, T.; Watanabe, I.; Hagiwara, K.; Inoue, M., Total Synthesis of Euonymine and Euonyminol Octaacetate. *J. Am. Chem. Soc.* **2021,** *143*, 21037-21047.

28) Hill, R. R.; Rychnovsky, S. D., Generation, Stability, and Utility of Lithium 4,4′-Di-tert-butylbiphenylide (LiDBB). *J. Org. Chem.* **2016,** *81*, 10707-10714.

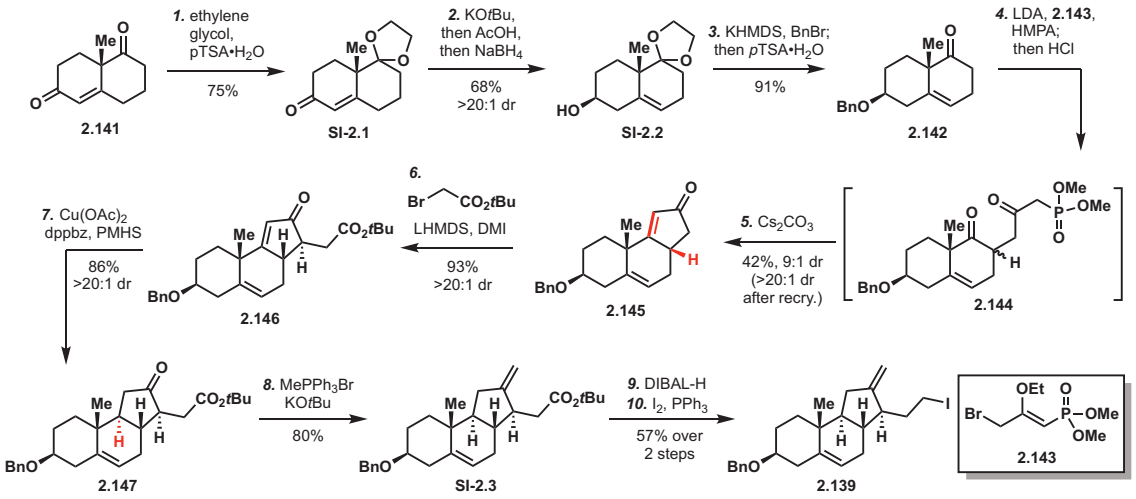
29) (a) Hendrickson, J. B. Systematic synthesis design. IV. Numerical codification of construction reactions. *J. Am. Chem. Soc.* **1975**, *97*, 5784-5800. (b) Gaich, T.; Baran, P. S., Aiming for the Ideal Synthesis. *J. Org. Chem.* **2010,** *75*, 4657-4673. (c) Peters, D. S.; Pitts, C. R.; McClymont, K. S.; Stratton, T. P.; Bi, C.; Baran, P. S., Ideality in Context: Motivations for Total Synthesis. *Acc. Chem. Res.* **2021,** *54*, 605-617.

Experimental

Tetrahydrofuran (THF), *N,N*-dimethylformamide (DMF), dicloromethane (DCM), acetonitrile (MeCN) and methanol (MeOH) were obtained by passing the previously degassed solvents through an activated alumina column. Commercial samples of natural cyclopamine were purchased from AdipoGen Life Sciences and Cayman Chemical Company. All reagents were purchased at the highest commercial quality and used without further purification unless otherwise stated. Yields refer to chromatographically and spectroscopically (^{1}H NMR) homogeneous material, unless otherwise stated. Reactions were monitored by thin layer chromatography (TLC), GC/MS, GC/FID, or LC/MS. TLC was performed using 0.25 mm E. Merck silica plates (60F-254), using short-wave UV light as the visualizing agent, and $KMnO_4$ and heat, or Seeback's magic stain as developing agents. NMR spectra were recorded on Bruker DRX-600, DRX-500, and AMX-400 instruments and are calibrated using residual undeuterated solvent ($CHCl_3$, CH_2Cl_2 at 7.26, 5.32 ppm for ^{1}H NMR, respectively, and 77.16, 53.84 ppm for ^{13}C NMR, respectively). The following abbreviations were used to explain multiplicities: s = singlet, d = doublet, t = triplet, q = quartet, m = multiplet, br = broad. Column chromatography was performed using E. Merck silica gel (60, particle size 0.043–0.063 mm), and preparative TLC (pTLC) was performed on Merck silica plates (60F-254). High-resolution mass spectra (HRMS) were recorded on an Agilent LC/MSD TOF mass spectrometer by electrospray ionization time of flight reflectron experiments. Melting points were recorded on a Fisher-Johns 12-144 melting point apparatus and are uncorrected. The enantiomeric ratios were determined with Waters UPC2 SFC equipped with a photodiode array detector or an Agilent Technologies 1220 Infinity II LC HPLC. Optical rotation data was recorded on an Anton Paar 100 Modular Circular Polarimeter.

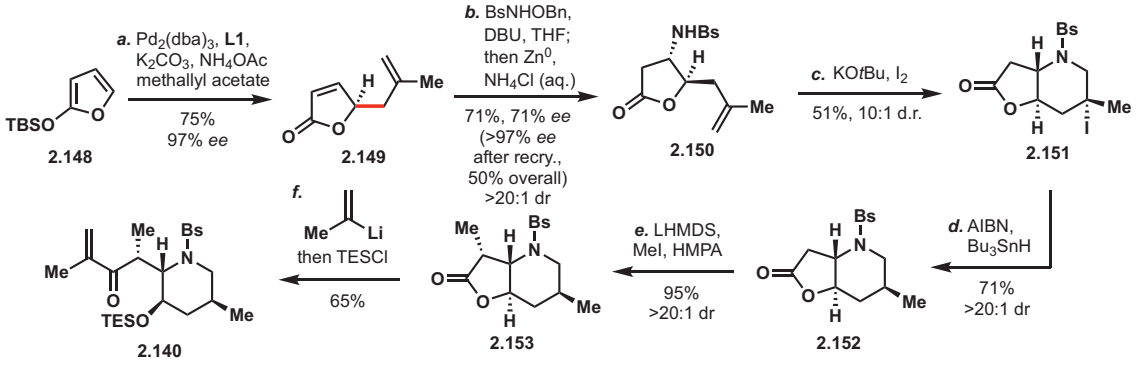
Route Details and Optimization Tables

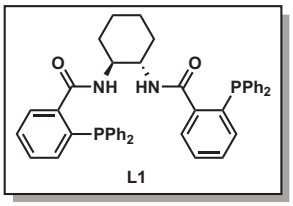
Detailed Synthesis of the ABC Fragment



Reagents and conditions: 1) *p*TSA•H_2O (1 eq.), ethylene glycol, rt, 30 min. **2)** KO*t*Bu (2 eq.), THF, 0 °C to rt, 2 h; then AcOH (3 eq.), rt, 2 min; then $NaBH_4$ (4 eq.), EtOH/THF (2:3 v/v), 0 °C, 1 h. **3)** BnBr (2.5 eq.), KHMDS (1.2 eq.), THF, 0 °C to rt, 8 h; then *p*TSA•H_2O (3 eq.), acetone/H_2O/THF (1:1:2 v/v/v), rt 16 h. **4)** LDA (1.2 eq.), **2.143** (1.2 eq.), HMPA (2.6 eq.), THF, –78 °C to rt, 16 h; then 1 M aq. HCl (5 eq.), acetone/THF (1:2 v/v), rt, 8 h. **5)** Cs_2CO_3 (5 eq.), THF, 50 °C, 16 h. **6)** LHMDS (1.2 eq.), *tert*-butyl bromoacetate (4 eq.), DMI (4 eq.), THF, -78 °C to rt, 6 h. **7)** $Cu(OAc)_2$•H_2O (20 mol %), dppbz (10 mol %), *t*BuOH (4 eq.), PMHS (4 eq.), MePh, 40 °C, 16 h. **8)** $MePPh_3Br$ (4 eq.), KO*t*Bu (3 eq.), THF, 0 °C to rt, 2 h. **9)** DIBAL-H (4 eq.), DCM, 0 °C, 2 h. **10)** I_2 (1.2 eq.), PPh_3 (1.2 eq.), imidazole (1.3 eq.), DCM, 0 °C, 2 h.

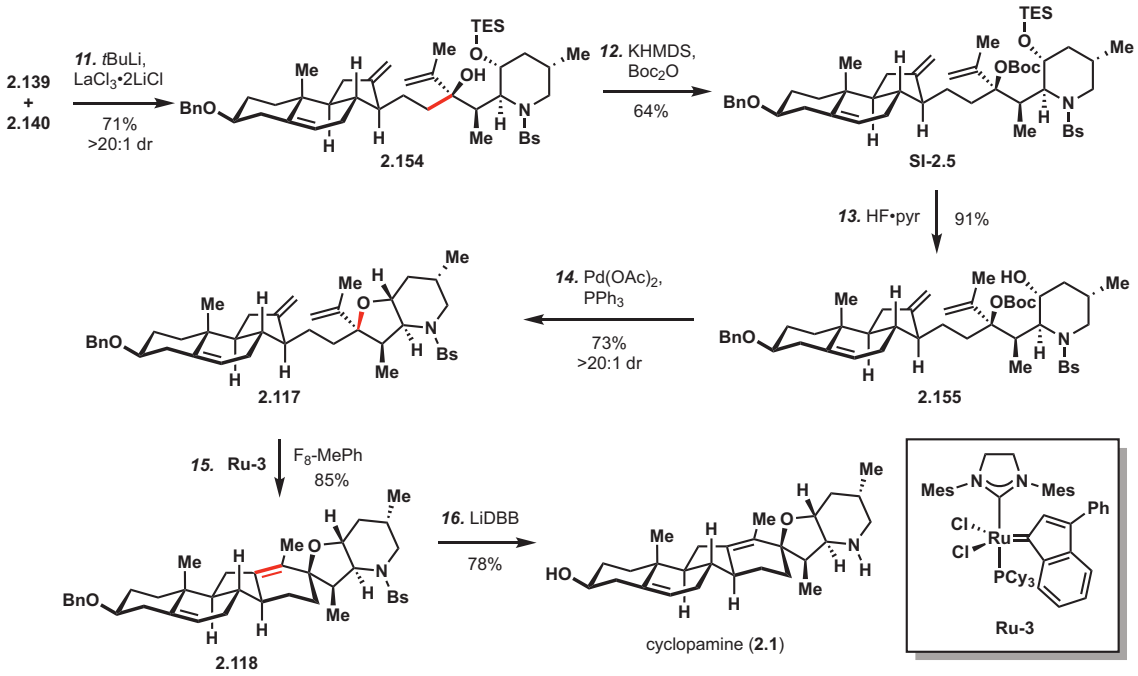
Detailed Synthesis of the EF Fragment





Reagents and conditions: a) $Pd_2(dba)_3$ (5 mol %), **L1** (12 mol %), NH_4OAc (20 mol %), K_2CO_3 (2 eq.), methallyl acetate (2 eq.), THF, -20 °C, 10 h. **b)** BsNHOBn (2 eq.), DBU (0.5 eq.), THF, -20 °C, 24 h; then Zn^0 (40 eq.), sat. aq. NH_4Cl, reflux, 16 h. **c)** KO*t*Bu (1.5 eq.), I_2 (3 eq.), MePh, 0 °C to rt, 9 h. **d)** AIBN (0.2 eq.), Bu_3SnH (2 eq.), MePh, 100 °C, 1 h. **e)** LHMDS (1.2 eq.), MeI (1.2 eq.), HMPA (1.2 eq.), THF, -78 °C, 1 h. **f)** 2-lithiopropene (2.0 eq.), THF, -78 °C; then TESCl (5.0 eq.), THF/pyr (2:3 v/v), rt, 6 h.

Detailed Endgame Sequence



Reagents and conditions: 11) 2.139 (2 eq.), **2.140** (1 eq.), *t*BuLi (3.9 eq.), $LaCl_3$•2LiCl (2 eq.), THF/Et_2O (1:2 v/v), -78 to -40 to -78 °C, 3 h. **12)** KHMDS (2 eq.), Boc_2O (2 eq.), THF, -78 °C, 1 h. **13)** HF•pyr (ca. 120 eq.), pyr (ca. 120 eq.), THF, rt, 3 d. **14)** $Pd(OAc)_2$ (1 eq.), PPh_3 (4 eq.), DMF, 120 °C, 2 h. **15) Ru-3** (60 mol %), F_8-MePh, 70 °C, 16 h. **16)** LiDBB (12 eq.), THF, -78 °C, 2 h.

Calculation of Ideality Percentage

By definition,[1] ideality is described by the following formula:

$$Ideality\% = \frac{(\#\ of\ construction\ rxns) + (\#\ of\ strategic\ redox\ rxns)}{(total\ \#\ of\ steps)} \times 100\%$$

The idealness of each step in this synthesis (ideal = **green**, non-ideal = **red**) is outlined in the following table:

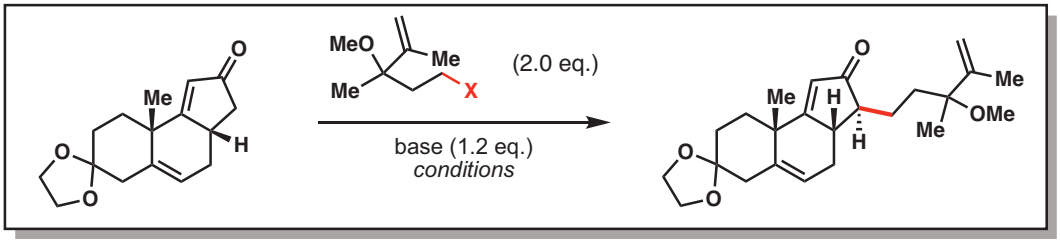
Step	Ideal/Non-Ideal
1	**Concession step** (protection)
2	**Strategic redox reaction** (olefin isomerized to the correct position; stereocenter formation)
3	**Concession step** (protection; deprotection)
4	**Construction reaction** (C-C bond formation)
5	**Construction reaction** (C-C bond formation; stereocenter formation)
6	**Construction reaction** (C-C bond formation; stereocenter formation)
7	**Strategic redox reaction** (stereocenter formation)
8	**Construction reaction** (C-C bond formation)
9	**Concession step** (non-strategic redox manipulation)
10	**Concession step** (functional group interconversion)
a_0 *	**Concession step** (protection)
a	**Construction reaction** (C-C bond formation; stereocenter formation)
b	**Construction reaction** (C-N bond formation; stereocenter formation)
c	**Construction reaction** (C-N bond formation; stereocenter formation)
d	**Concession step** (functional group interconversion)
e	**Construction reaction** (C-C bond formation; stereocenter formation)
f	**Construction reaction** (C-C bond formation)
11	**Construction reaction** (C-C bond formation; stereocenter formation)
12	**Concession step** (functional group interconversion)
13	**Concession step** (deprotection)
14	**Construction reaction** (ring construction; stereocenter formation)
15	**Construction reaction** (ring construction)
16	**Concession step** (deprotection)

* a_0 refers to the TBS protection step to synthesis compound **2.148**.

Therefore,

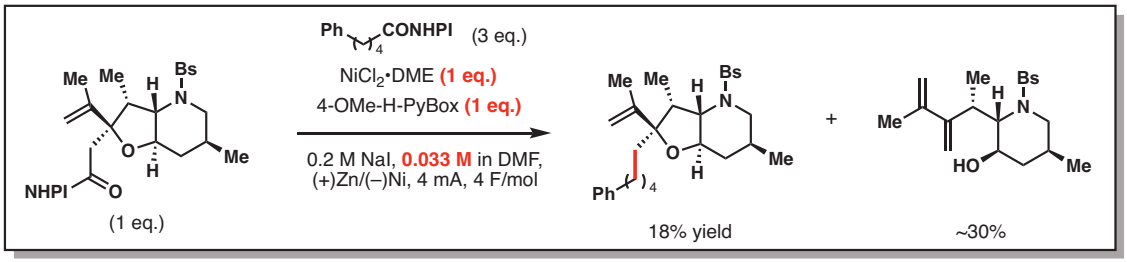
$$Ideality\% = \frac{12 + 2}{23} \times 100\% = 61\%$$

Table S2.1 Optimization of Enone Alkylation

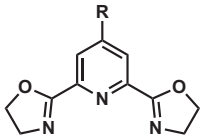


X	base	conditions	results
I	LDA	HMPA (2 eq.), THF, -78 °C to rt, 12 h	no rxn
I	LHMDS	HMPA (2 eq.), THF, -78 °C to rt, 12 h	no rxn
I	NaH	THF, 0 °C to rt, 12 h	no rxn
I	NaHMDS	THF, 0 °C to rt, 12 h	no rxn
I	KO^{t}Bu	THF, 0 °C to rt, 12 h	enone γ-alkylation only (18%)
I	KHMDS	THF, 0 °C to rt, 12 h	enone γ-alkylation only (10%)
OTf	LDA	HMPA (2 eq.), THF, -78 °C to rt, 12 h	40% conv., complex mixture
OTf	LHMDS	HMPA (2 eq.), THF, -78 °C to rt, 12 h	~30 % conv., clean, trace PDT
OTf	NaH	THF, 0 °C to rt, 12 h	no rxn
OTf	**NaHMDS**	**THF, 0 °C to rt, 12 h**	**65% conv., 47% yield, 27% SM recovered**
OTf	KO^{t}Bu	THF, 0 °C to rt, 12 h	full conv., complex mixture
OTf	KHMDS	THF, 0 °C to rt, 12 h	full conv., complex mixture

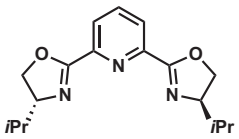
Table S2.2 Optimization of the Doubly Decarboxylative Cross Coupling



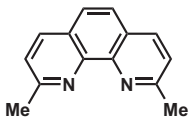
Entries	Deviation from above	Results
1	0.0067 M	10% yield
2	0.067 M	17% yield
3	2 eq. AcOH as additive	17% yield
4	2 eq. acac as additive	trace PDT, mostly hydrolysis to acid
5	2 mA current	11% yield (NMR)
6	4 eq. Ni and ligand	16% yield (NMR)
7	Ag NP conditions	only hydrolysis to acid
8	Mg anode	5% yield (NMR)
9	Ni anode	no reaction
10	Al anode	only hydrolysis to acid
11	terpy as ligand	only hydrolysis to acid
12	PyBox as ligand (no 4-OMe)	8% yield (NMR)
13	4-NMe_2-H-PyBox as ligand	11% yield (NMR)
14	4-Cl-H-PyBox as ligand	trace PDT, mostly hydrolysis to acid
15	Ni(BPhen)Cl_2•2DMF	only hydrolysis to acid
16	Ni(dppp)Cl_2	messy rxn, no PDT
17	Ni(dppe)Cl_2	messy rxn, no PDT
18	neocuproine as ligand	only hydrolysis to acid
19	4,4'-OMe-bipy as ligand	trace PDT, mostly hydrolysis to acid
20	(R,R)-iPr-PyBox as ligand	5% yield (NMR)
21	4,4',4''-tri-tBu-terpy as ligand	trace PDT, mostly hydrolysis to acid
22	0 °C, 16 F/mol	11% yield, ~30% ring opening



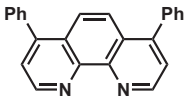
4-R-H-PyBox
(R = OMe, Cl, NMe_2, etc.)



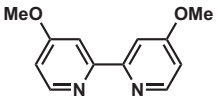
(*R,R*)-*i*Pr-PyBox



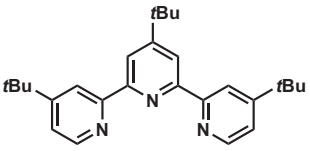
neocuproine



BPhen (bathophenanthroline)

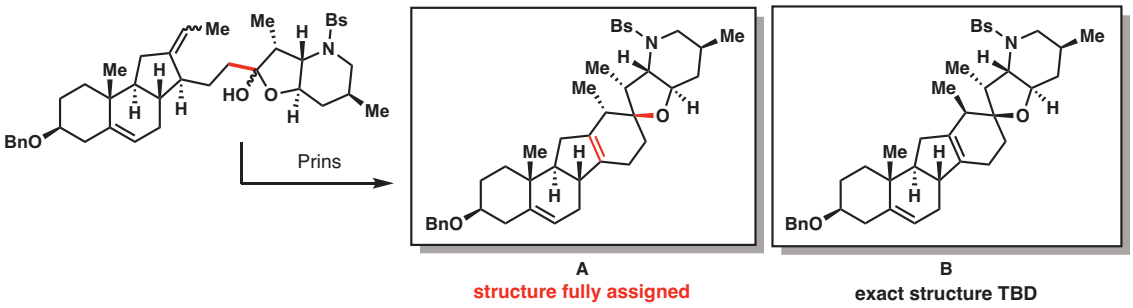


4,4'-OMe-bipy



4,4',4''-tri-tBu-terpy

Table S2.3 Optimization of Prins Cyclization



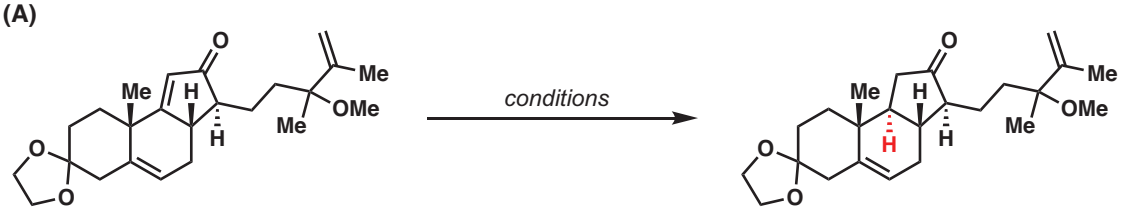
A
structure fully assigned

B
exact structure TBD

Conditions	Results
pTSA (0.1 eq.), MePh, rt, 1 h	full conv., predominantly **A** (40% isolated yield), traces of **B**
pTSA (0.1 eq.), MePh, 40 °C, 16 h	full conv., predominantly **A**, traces of **B**
TFA (1 eq.), DCM, 0 °C, 30 min	full conv., predominantly **A**, traces of **B**
$Bi(OTf)_3$ (1 eq.), DCM, rt, 30 min	full conv., predominantly **A**, traces of **B**
BF_3•Et_2O (1 eq.), AcOH (10 eq.), DCM, 0 °C, 30 min	full conv., predominantly **A**, traces of **B**
Amberlyst 15, DCM, rt, 2 h	full conv., predominantly **A**, traces of **B**
$FeBr_3$, -78 °C, 1 h	exclusive formation of **B**
$BiBr_3$, -78 to -50 °C, 2 h	formation of a new, unidentified side PDT
$InBr_3$, -78 °C to rt, 16 h	sluggish reaction, mixture of **A** and **B**
HFIP, 80 °C, 16 h	mixture of **A** and **B**
H_2O, 80 °C, 4 d	extremely slow reaction
neat, 80 °C, 4 d	extremely slow reaction

Table S2.4 Optimization of Enone 1,4-Reduction

(A)



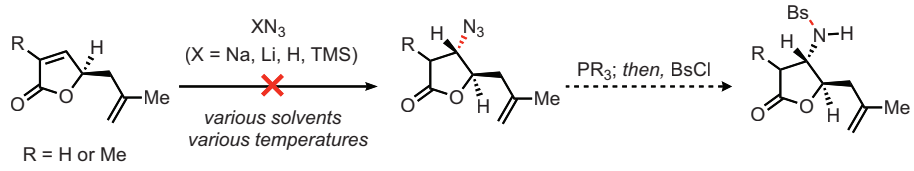
conditions	results
L-selectride, THF, -78 °C to rt, 4 h	only 1,2-reduction
$[Cu(PPh_3)H]_6$ (1 eq.), PhH, 80 °C, 12 h	no reaction
$[Cu(PPh_3)H]_6$ (1 eq.), MePh, 130 °C, 12 h	no reaction
$Mn(dpm)_3$ (20 mol %), $PhSiH_3$ (1.5 eq.), THF, rt, 12 h	no reaction
$Mn(dpm)_3$ (20 mol %), $PhSiH_3$ (1.5 eq.), THF, 60 °C, 12 h	complex mixture
$Mn(dpm)_3$ (20 mol %), $PhSiH_3$ (1.5 eq.), TBHP (2 eq.), THF, rt, 2 h	non-selective reduction of all olefins
SmI_2 (2 eq.), ^{i}PrOH (10 eq.), THF, rt, 12 h	no reaction
$Cu(OAc)_2•H_2O$ (1 eq.), dppBz (0.5 eq.), PMHS (3 eq.), MePh, rt, 12 h	53% yield, 34% SM recovered

(B)

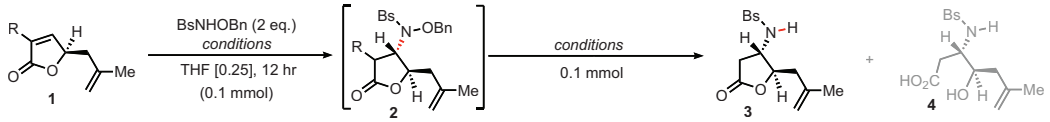


conditions	results
$Cu(OAc)_2•H_2O$ (1 eq.), dppBz (0.5 eq.), PMHS (3 eq.), MePh, rt, 2 d	47% yield, 40% SM recovered
$Cu(OAc)_2•H_2O$ (1 eq.), dppBz (0.5 eq.), PMHS (3 eq.), MePh, 40 °C, 16 h	81% yield
$Cu(OAc)_2•H_2O$ (0.2 eq.), dppBz (0.1 eq.), PMHS (4 eq.), MePh, 40 °C, 16 h	86% yield

Table S2.5 Optimization of Aza-Michael/Zn Reduction



· *significant effort was directed towards 1,4-azidation of our key butenolide fragment, which at the onset seemed feasible given the plethora of literature examples (with varying γ-substitution) on known butenolides. However, in our hands none of these reported methods ever yielded any desired product - which, we hypothesized may have been due to our γ-substituant lacking electron withdrawing character.*



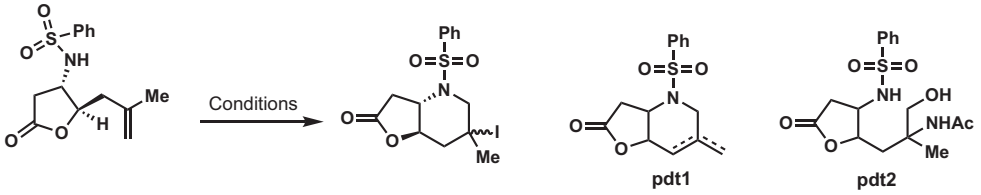
entry	R	*conditions*	*results*
1	Me	BEMP (10 mol%), RT	NAR
2		DBU (10 mol%), RT	NAR
3	H	TEA (10 mol%), RT	NAR
4		BEMP (10 mol%), RT	80% yield, 1% e.e.
5		DBU (10 mol%), RT	80% yield, 42% e.e.
6[a]		DBU (10 mol%), -20 °C	20% yield, 99% e.e.
7		DBU (1 eq), -20 °C	80% yield, 82% e.e.
8		DBU (50 mol%), -20 °C	80% yield, 70-75% e.e.
9[a]		DBU (25 mol%), -20 °C	57% yield, 89% e.e.
10[b]		DBU (50 mol%), -20 °C	80% yield, 70-75% e.e.

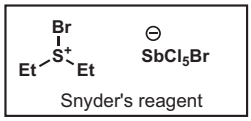
[a] *prolonged reaction times, to achieve higher conversion/yield, resulted in significant enantio-erosion*
[b] *>1g scale(s), slow addition of DBU (on scale, these conditions were the most robust - and, recrystallization allowed access to enantiopure material)*

entry	*pot*	*conditions*	*results*
1	two-pot	Zn^o, AcOH:H_2O:DCM, RT	NAR
2	two-pot	Zn^o, HCl (10%), THF, RT	NAR
3	two-pot	SmI_2, THF, RT	trace **3**
4[c,d]	two-pot	Zn^o (20 eq), sat'd NH_4Cl [0.1], 100 °C, overnight	full conversion, 22% **3**, 52% **4**
5[c,d]	two-pot	Zn^o (20 eq), sat'd NH_4Cl [0.1], 75 °C, overnight	50% conversion, 20% **3**, 17% **4**
6[c,d]	two-pot	Zn^o (20 eq), sat'd NH_4Cl [0.05], 75 °C, overnight	full conversion, 50% **3**, 30% **4**
7[c,d]	one-pot	BsNHOBn (1.2 eq); Zn^o (40 eq), sat'd NH_4Cl [0.05], 75 °C, overnight	variable conversion, 30-40% yield **3**
8[c,d]	one-pot	BsNHOBn (1.2 eq); Zn^o (40 eq), sat'd NH_4Cl [0.05], 100 °C, overnight	full conversion, 40% **3**, 24% **4**
9[c,d]	one-pot	BsNHOBn (2 eq); Zn^o (40 eq), sat'd NH_4Cl [0.05], 100 °C, overnight	full conversion, 55% **3**, 25% **4**
10[e,f]	one-pot	BsNHOBn (2 eq); Zn^o (40 eq), sat'd NH_4Cl [0.05], 100 °C, overnight	full conversion, 71% **3**, 0% **4**

[c] ***4*** *could be quantitatively lactonized to* ***3*** *using EDCI (1.5 eq), HOAt (1.5 eq), and DMF [0.01] (rt, overnight)*
[d] ***3*** *maintains the enantiopurity determined for* ***2****, Zn^o reduction does not racemize*
[e] *1g scale(s); although stalling was sometimes observed on scale, the reaction could be cooled to RT and be re-acidified with 6M HCl along with additional NH_4Cl (s) (40 eq) and taken back to reflux - also re-lactonizes any* ***4*** *that is present*

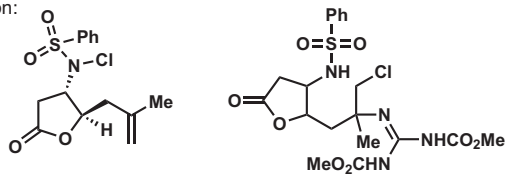
Table S2.6 Optimization of Halocyclization



Entry	Reagent	Result	Notes
1.	I_2, $NaHCO_3$, MeCN	No desired pdt	
2.	I_2, Chloramine-T, MeCN	Traces of pdt	
3.	NIS, DCM: HFIP	Traces of pdt, messy	
4.	NIS, pTSA, DCM	Complex mixture	
5.	NIS, K_2CO_3, DCM	~20% yield, low conv.	
6.	NIS(xs), K_2CO_3(xs), DCM	Complex mixture	First hit!
7.	PIDA, I_2, DCM, *hv* (125W, whiite LEDs)	Complex mixture	N-centered radical
8.	Snyder's reagent, $MeNO_2$, 0°C, 1h	No reaction	
9.	Snyder's reagent, $MeNO_2$, rt, 2h	pdt1	 Snyder's reagent
10.	Snyder's reagent, DCM, 0°C, 1h	No reaction	
11.	Snyder's reagent, DCM, rt, 1h	Complex mixture	
12.	Snyder's reagent, MeCN, 0°C, 1h	No reaction	
13.	Snyder's reagent, MeCN, rt, 1h	pdt2	
14.	LHMDS, Toluene -78°C; I_2, -78°C to rt	SM recovered	
15.	NaHMDS, Toluene -78°C; I_2, -78°C to rt	SM recovered	
16.	KHMDS, Toluene -78°C; I_2, -78°C to rt	Elimination pdt	
17.	TMG, 10'; then I_2, MePh, rt, 2h	60% conv., 30% isolated yield	
18.	TMG, 10'; then I_2, MePh/THF, rt, 4h	Low conv. in 6h, pdt observed; Full conv. in 24h, no pdt observed	
19.	TMG, 10'; then I_2, DCM, rt, 2h	Low conv. in 6h, pdt observed; Full conv. in 24h, no pdt observed	
20.	Barton's base, 10'; then I_2, MePh, rt, 2h	Low conversion, byproduct observed	
21.	NIS, K_2CO_3, DCE	Low conversion	
22.	**KO*t*Bu, 0 °C, 30 min; then I_2, MePh, rt, 9 h**	**51% pdt, 47% recovered SM (note 1)**	**Clean profile**
23.	DBU, rt, 10'; then I_2, DCM, rt, 16h	~90 conv., ~40% yield	Not reproducible on large scale
24.	Et_3N, rt, 10'; then I_2, DCM, 35 °C, 16h	no conversion	
25.	DBU, rt; then NIS, DCM, rt	25% yield	
26.	DBU, rt; then NIS, MeCN, rt	Low conversion	
27.	NIS, K_2CO_3, DMF	Complex mixture	
28.	Palau'Chlor, $CHCl_3$	no pdt **(note 2)**	
29.	same as entry 22, with 3 eq. TEMPO	no reaction	
30.	same as entry 22, under ambient light	full conv. in 15 min, messy reaction	

Note 1: If left for another 16 h, the reaction resulted in 15% isolated yield and ca. 80% recovered SM.

Note 2: Byproducts isolated from the Palau'Chlor reaction:



Mechanistic hypothesis:

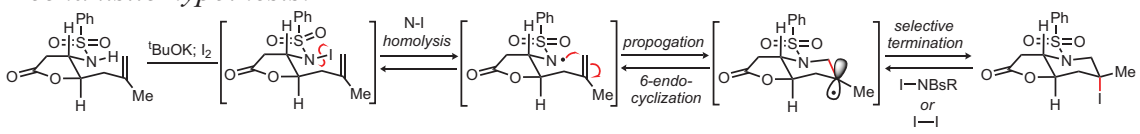
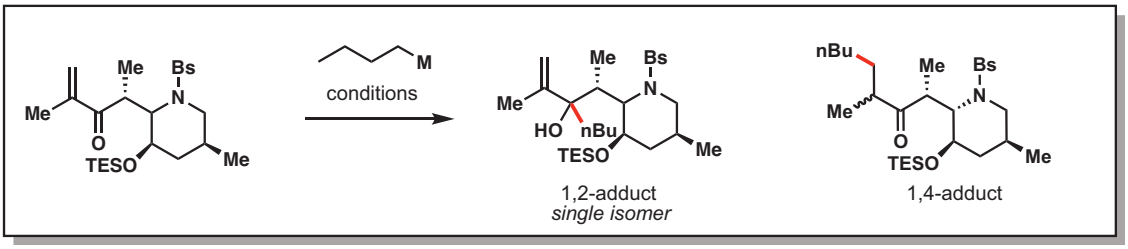


Table S2.7 Model Studies of the 1,2-Addition to the EF Enone



Entry	Conditions	Ratio of 1,2 vs. 1,4
1	nBuLi (1.1 eq.), Et_2O, –78 °C, 1 h	1 : 3
2	nBuLi (1.1 eq.), $ZnCl_2$ (1.1 eq.), Et_2O, –78 °C, 1 h	only 1,4
3	nBuLi (1.1 eq.), THF, –78 °C, 1 h	1.2 : 1
4	nBuLi (1.1 eq.), inverse addn, THF, –78 °C, 1 h	3 : 1
5	nBuMgCl (1.1 eq.), inverse addn, THF, –78 °C to 0 °C, 1 h	~1:1, sluggish reaction
6	nBuLi (1.1 eq.), $CeCl_3$ (1.1 eq.), inverse addn, THF, –78 °C, 1 h	only 1,2, incomplete conv.
7	**nBuLi (1.1 eq.), $LaCl_3$•2LiCl (1.1 eq.), inverse addn, THF, –78 °C, 1 h**	**only 1,2, full conv.**

Comments:

- Full conversion was observed unless otherwise specified
- For entries 1-3, nBuLi was added to a solution of SM;
  For entries 4-7, SM was added to the organometallic reagent (i.e. inverse addition)

Table S2.8 Optimization of Tsuji-Trost Cyclization

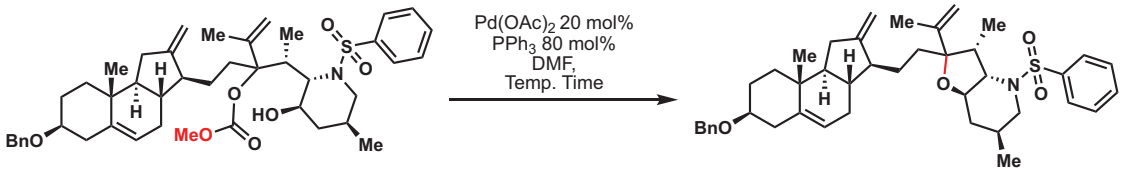
(A)



Metal	Ligand	Solvent	Temp.	Time	Outcome
$Pd(OAc)_2$ 10%mol	PPh_3 40%mol	THF	rt	12h	No reaction
$Pd(OAc)_2$ 10%mol	PPh_3 40%mol	THF	65°C	12h	No reaction
$Pd(OAc)_2$ 10%mol	PPh_3 40%mol	DCM	rt	12h	No reaction
$Pd(OAc)_2$ 10%mol	PPh_3 40%mol	DCM	45°C	12h	No reaction
$Pd(OAc)_2$ 10%mol	PPh_3 40%mol	DMF	rt	12h	No reaction
$Pd(OAc)_2$ 10%mol	PPh_3 40%mol	DMF	70°C	12h	No reaction
$Pd(OAc)_2$ 10%mol	**PPh_3 40%mol**	**DMF**	**100°C**	**36h**	**100% conv. ~60%yield dr=2:1**

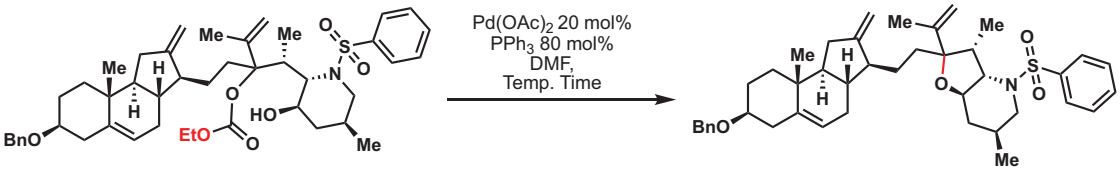
(B)

Methyl carbonate:



Temp.	Time	Results
rt	4h	NR
50 °C	4h	NR
110 °C	12h	<10% conversion

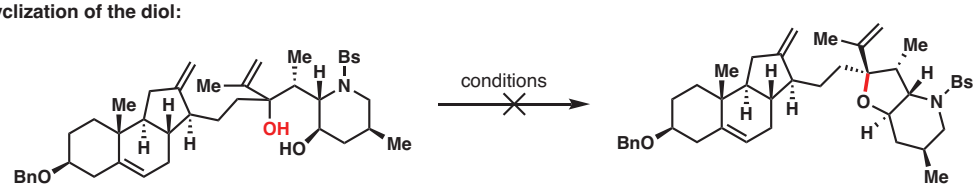
Ethyl carbonate:



Temp.	Time	Results
rt	2h	NR
50 °C	2h	NR
80 °C	2h	NR
85 °C	2h	NR
90 °C	2h	NR
95 °C	2h	NR
100 °C	2h	NR
105 °C	2h	NR
110 °C	2h	<10% conv., no desired PDT
115 °C	30 min	<10% conv., no desired PDT
110 °C	24h	<10% conv., no desired PDT

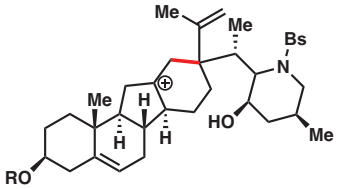
Table S2.8 Optimization of Tsuji-Trost Cyclization (Continued)

Acid cyclization of the diol:

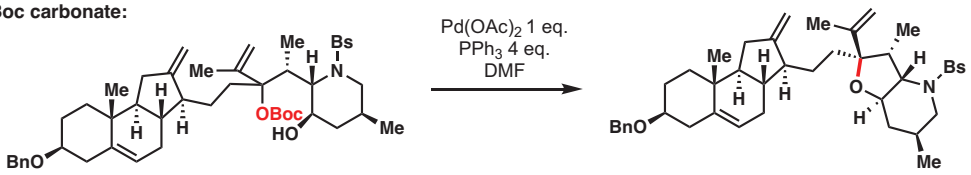


Conditions	Results
aq. HCl (30 eq.), THF/H_2O (9:1), rt, 2 h	no rxn
HCl in dioxane (30 eq.), THF, 0 °C, 16 h	<10% conv., multiple byproducts
HCl in dioxane (30 eq.), DCM, 0 °C, 2 h	multiple byproducts
HCl in dioxane (30 eq.), Et_2O, 0 °C, 2 h	no rxn
trace HCl, HFIP, rt, 30 min	full conv., multiple byproducts
DCM/HFIP (9:1 to 3:1 to 0:1), rt, 2 h each	no rxn
PPTS (30 eq.), HFIP, rt, 16 h	single byproduct, no PDT
pTSA•H_2O (30 eq.), HFIP, 0 °C, 1 h	decomp.
$BiCl_3$ (10 eq.), DCM, 0 °C, 2 h	single byproduct, no PDT

byproducts via:

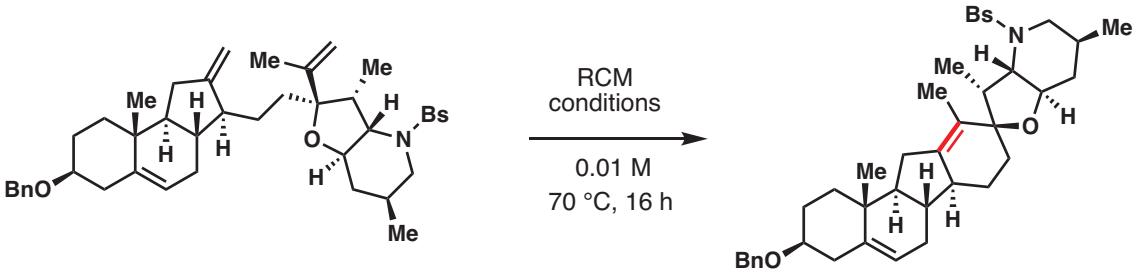


Boc carbonate:

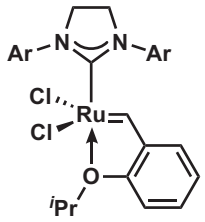


Temp.	Time	Results
100 °C	2h	12%
120 °C	**2h**	**73%**

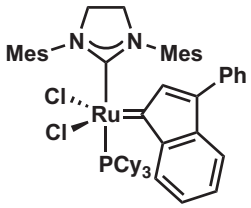
Table S2.9 Optimization of RCM



Entry	Conditions	Results
1	HG-II (60 mol%), MePh	20% yield, 45% conv.
2	*o*-tolyl (60 mol%), MePh	31% yield, 54% conv.
3	indenylidene cat. (60 mol%), MePh	67% yield, 90% conv.
4	HG-II (60 mol%), F_8-MePh	56% yield, 76% conv.
5	*o*-tolyl (60 mol%), F_8-MePh	70% yield, 90% conv.
6	**indenylidene cat. (60 mol%), F_8-MePh**	**85% yield, full conv.**
7	indenylidene cat. (20 mol%), F_8-MePh	<10% conv.



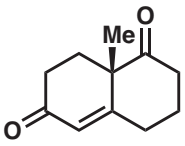
HG-II: Ar = mesityl
o-tolyl: Ar = o-tolyl



"indenylidene cat."

Reaction Protocols and Characterization Data

Compound 2.141 [(*S*)-Wieland Miescher Ketone]

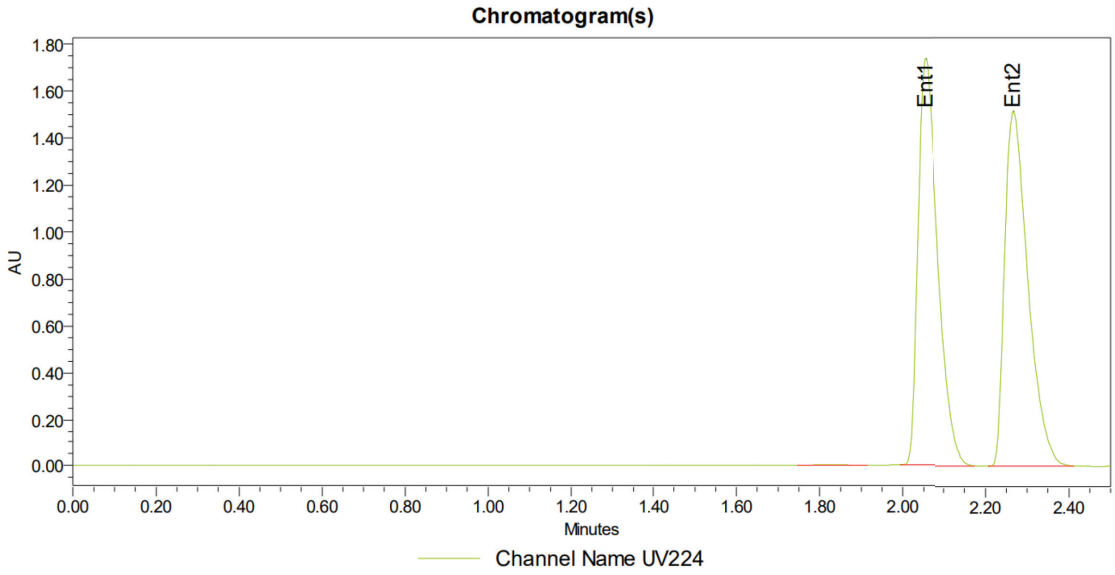


Compound **2.141** was prepared according to a literature reported procedure.[2] All characterization data matched the literature report. The *ee* was determined to be 95% by chiral SFC analysis.

Chiral HPLC Traces:

The analysis was performed on a Waters UPC2 SFC with a Diacel IA column (3 μm, 4.6x250 mm) under isocratic conditions (3.3 mL/min, 15% MeOH / CO_2, 1600 psi backpressure) at 30 °C. The enantiomers were detected by UV light (224 nm).

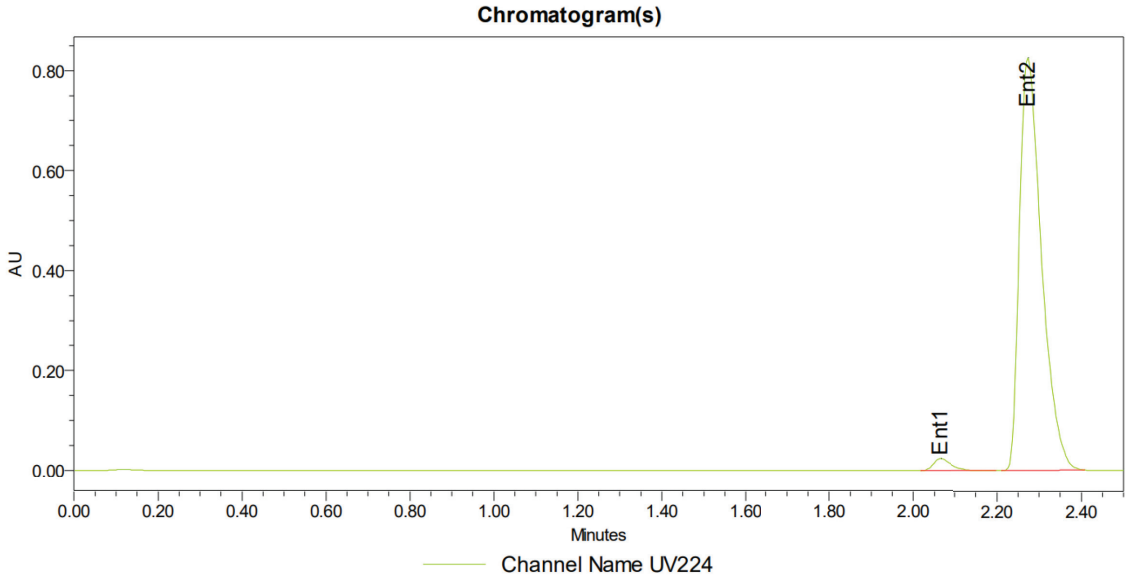
Racemic:



Peak Info

	Channel Name	Name	RT	Area	Height (μV)	ent1	ent2	ee
1	UV224		1.80	9581	2172	49.91	50.09	-0.18
2	UV224	Ent1	2.06	5819702	1738586	49.91	50.09	-0.18
3	UV224	Ent2	2.27	5840913	1512714	49.91	50.09	-0.18

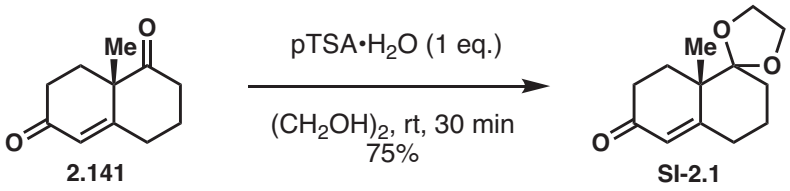
Enantiopure:



Peak Info

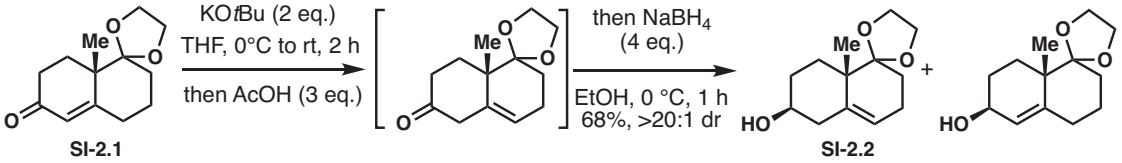
	Channel Name	Name	RT	Area	Height (μV)	ent1	ent2	ee
1	UV224	Ent1	2.06	72222	24320	2.36	97.64	-95.28
2	UV224	Ent2	2.27	2987470	825970	2.36	97.64	-95.28

Compound SI-2.1



Compound SI-2.1 was prepared according to a literature reported procedure.[3] All characterization data matched the literature report.

Compound SI-2.2



A flame-dried 1 L round-bottom flask was charged with compound **SI-2.1** (10.0 g, 45 mmol, 1.0 eq.) and backfilled with Ar. THF (360 mL) was introduced and the resulting solution was cooled to 0 °C. KO^{t}Bu (1.0 M in THF, 90 mL, 90 mmol, 2 eq.) was added dropwise, and the reaction was allowed to warm to rt. After 2 h, aq. AcOH (10% v/v, 77 mL, 135 mmol, 3 eq.) was added. The reaction was allowed to stir for 2 min at rt and then cooled to 0 °C. After 30 min, a solution of $NaBH_4$ (6.9 g, 180 mmol, 4 eq.) in EtOH (250 mL) [sonication was usually needed to uniformly dissolve/suspend all solids] was added dropwise via an addition funnel over 30 min, and the reaction was stirred for another 30 min after addition was complete. The reaction was carefully quenched at 0 °C by dropwise addition of sat. aq. NH_4Cl (100 mL), and the resulting mixture was concentrated *in vacuo* to about 1/3 of its original volume to remove most of the THF and EtOH. The residue was diluted with 300 mL of H_2O and extracted with EtOAc (500 mL x3). The combined organic layers were washed with brine (300 mL), dried over Na_2SO_4, filtered, and concentrated *in vacuo*. The crude material was purified by silica gel flash column chromatography (hexanes:EtOAc 3:1 to 1:1 gradient) to afford compound **SI-2.2** (6.9 g, 68%, single diastereomer) and the allylic alcohol byproduct (1.5 g, 15%).

Physical state: white solid

TLC: R_f = 0.4 (hexanes:EtOAc 1:2, $KMnO_4$)

Melting point: 81-85 °C

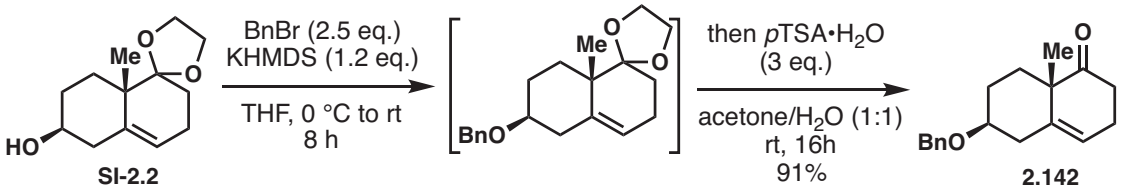
$[\alpha]_{25}^{D}$: -88.6 (c = 0.83 in $CHCl_3$)

^{1}H NMR (600 MHz, $CDCl_3$): δ 5.41 – 5.33 (m, 1H), 4.03 – 3.86 (m, 4H), 3.57 (tt, *J* = 11.1, 4.4 Hz, 1H), 2.38 (ddd, *J* = 13.0, 4.9, 2.4 Hz, 1H), 2.26 – 2.16 (m, 2H), 2.11 – 2.02 (m, 1H), 1.93 – 1.83 (m, 2H), 1.73 (td, *J* = 13.4, 3.5 Hz, 1H), 1.65 – 1.60 (m, 1H), 1.54 – 1.50 (m, 1H), 1.48 (dt, *J* = 13.0, 3.2 Hz, 1H), 1.23 (s, 3H).

^{13}C NMR (151 MHz, $CDCl_3$): δ 139.7, 121.0, 112.2, 71.3, 65.3, 64.8, 42.4, 41.7, 31.2, 27.9, 27.1, 24.0, 22.0.

HRMS (ESI-TOF): Molecular ion peak not observed due to poor ionization.

Compound 2.142



A flamed-dried 1 L round-bottom flask was charged with compound **SI-2.2** (6.8 g, 30 mmol, 1 eq.) and backfilled with Ar. THF (300 mL) was introduced and the resulting solution was cooled to 0 °C. KHMDS (1.0 M in THF, 36 mmol, 1.2 eq.) was added dropwise. After 30 min, BnBr (8.9 mL, 75 mmol, 2.5 eq.) was added dropwise and the reaction was allowed to warm to rt and stirred for 8 h. *p*TSA•H_2O (17.1 g, 90 mmol, 3 eq.) was added, followed by 200 mL of acetone and 100 mL of H_2O, and the reaction was allowed to stir at rt for 16 h. The reaction was quenched by sat. aq. $NaHCO_3$ (200 mL), and the resulting mixture was concentrated *in vacuo* to about 1/3 of its original volume to remove most of the THF and acetone. The aqueous residue was extracted with EtOAc (300 mL x3), and the combined organic layers washed with brine (300 mL), dried over Na_2SO_4, filtered, and concentrated *in vacuo*. The crude material was purified by silica gel flash column chromatography (hexanes:EtOAc 20:1 to 10:1) to afford compound **2.142** (8.06 g, 91%).

Physical state: colorless oil

TLC: R_f = 0.5 (hexanes:EtOAc 5:1, UV and $KMnO_4$)

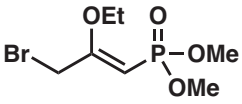
$[\alpha]_{25}^{D}$: +9.4 (c = 0.47 in $CHCl_3$)

^{1}H NMR (500 MHz, $CDCl_3$): δ 7.41 – 7.18 (m, 5H), 5.59 – 5.52 (m, 1H), 4.57 (s, 2H), 3.30 (tt, *J* = 11.1, 4.6 Hz, 1H), 2.70 – 2.62 (m, 1H), 2.57 (ddd, *J* = 12.9, 4.7, 2.2 Hz, 1H), 2.44 – 2.26 (m, 4H), 2.10 – 2.04 (m, 1H), 1.86 (dt, *J* = 13.8, 3.5 Hz, 1H), 1.67 – 1.56 (m, 1H), 1.40 (td, *J* = 13.9, 4.1 Hz, 1H), 1.30 (s, 3H).

^{13}C NMR (126 MHz, $CDCl_3$): δ 215.1, 140.1, 138.8, 128.5, 127.6, 127.6, 121.1, 78.1, 70.2, 47.2, 38.1, 35.7, 32.2, 27.9, 25.3, 22.1.

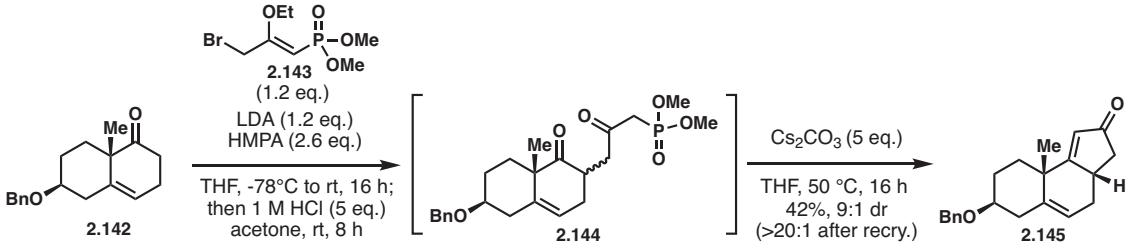
HRMS (ESI-TOF): calc'd for $C_{18}H_{22}O_2$ $[M+H]^+$: 271.1698, found: 271.1709.

Compound 2.143



Compound **2.143** was prepared according to a literature reported procedure.[4] All characterization data matched the literature report.

Compound 2.145



The following procedure was adapted from a literature report.[5] LDA was freshly prepared in a flame-dried 1 L round-bottom flask under Ar by adding *n*BuLi (2.5 M in hexanes, 6.9 mL, 17.3 mmol, 1.2 eq.) to a solution of iPr_2NH (2.7 mL, 18.8 mmol, 1.3 eq.) in THF (100 mL) at 0 °C and stirring for 30 min. The solution was cooled to -78 °C, and a solution of compound **2.142** (3.9 g, 14.4 mmol, 1 eq.) in THF (20 mL) was added dropwise. After 1 h, a solution of **2.143** (4.73 g, 17.3 mmol, 1.2 eq.) in THF (20 mL) was added, followed by dry HMPA (6.5 mL, 37.5 mmol, 2.6 eq.), and the reaction was allowed to warm to rt and stirred for 16 h. 1 M HCl (75 mL, 75 mmol, ca. 5 eq.) and acetone (75 mL) was added, and the resulting mixture was stirred vigorously at rt for 8 h. Upon complete hydrolysis of the enol ether by TLC analysis, the reaction was quenched by addition of solid $NaHCO_3$ (8.4 g, 100 mmol, 6.7 eq.) in small batches. The resulting mixture was directly concentrated *in vacuo* to about 1/4 of its original volume to remove most of the THF and acetone. The aqueous residue was diluted with H_2O (150 mL) and extracted with EtOAc (200 mL x3). The combined organic layers were washed with brine (200 mL), dried over Na_2SO_4, filtered and concentrated. The resulting crude **2.144** was redissolved in THF (300 mL), to which Cs_2CO_3 (23.5 g, 72 mmol, 5 eq.) was added. The resulting suspension was heated to 50 °C and stirred vigorously for 16 h. The reaction was allowed to cool back to rt and concentrated *in vacuo* to half of its original volume. H_2O (300 mL) was added, and the mixture was extracted with EtOAc (300 mL x3). The combined organic layers were

washed with brine (300 mL), dried over Na_2SO_4, filtered, and concentrated *in vacuo*. The crude material was purified by silica gel flash column chromatography (hexanes:EtOAc 5:1 to 3:1) to afford compound **2.145** (2.3 g, 52%, 9:1 d.r.). Recrystallization from hot hexanes/DCM afforded diastereomerically enriched **2.145** (1.87 g, >20:1 d.r., 81% recovery, 42% overall).

Physical state: yellow solid

TLC: R_f = 0.4 (hexanes:EtOAc 2:1, UV and $KMnO_4$)

Melting point: 101-103 °C

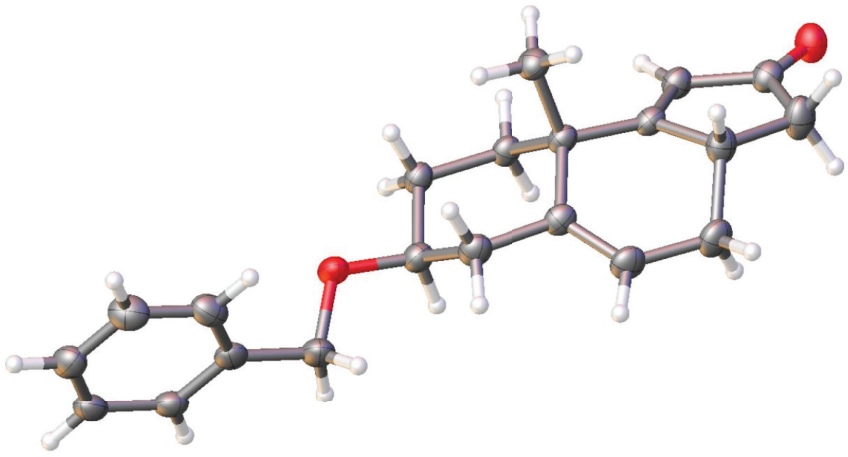
$[\alpha]_{25}^{D}$: -160.2 (c = 0.43 in $CHCl_3$)

^{1}H NMR (600 MHz, $CDCl_3$): δ 7.38 – 7.23 (m, 5H), 5.86 (d, *J* = 1.6 Hz, 1H), 5.45 (dt, *J* = 5.6, 2.0 Hz, 1H), 4.57 (s, 2H), 3.29 (tt, *J* = 11.2, 4.6 Hz, 1H), 3.12 – 3.04 (m, 1H), 2.62 (dd, *J* = 18.7, 6.4 Hz, 1H), 2.59 – 2.50 (m, 2H), 2.37 – 2.30 (m, 1H), 2.10 (dq, *J* = 12.9, 3.5, 3.0 Hz, 1H), 2.03 (dd, *J* = 18.8, 1.8 Hz, 1H), 1.97 (dt, *J* = 13.3, 3.5 Hz, 1H), 1.82 (dddd, *J* = 16.8, 10.9, 3.5, 2.0 Hz, 1H), 1.71 (dddd, *J* = 14.8, 13.1, 11.1, 3.8 Hz, 1H), 1.51 (td, *J* = 13.7, 3.9 Hz, 1H), 1.34 (s, 3H).

^{13}C NMR (151 MHz, $CDCl_3$): δ 209.3, 190.5, 138.7, 138.4, 128.5, 127.6, 127.6, 124.7, 121.1, 78.1, 70.3, 42.1, 39.3, 38.2, 35.7, 34.4, 34.3, 28.0, 25.3.

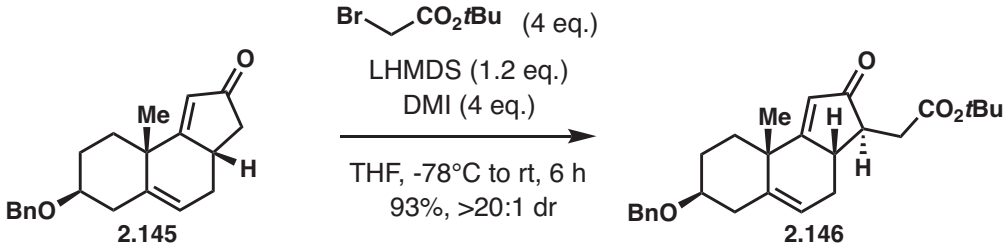
HRMS (ESI-TOF): calc'd for $C_{21}H_{24}O_2$ $[M+H]^+$: 309.1849, found: 309.1844.

X-ray crystallography structure:



(See **X-Ray Crystallography Data** for full report)

Compound 2.146



A flame-dried 25 mL round-bottom flask under Ar was charged with LHMDS (1.0 M in THF, 1.4 mL, 1.4 mmol, 1.2 eq.) and THF (6 mL) and cooled to -78 °C. A solution of compound **2.145** (356.9 mg, 1.16 mmol, 1 eq.) in THF (4 mL) was slowly added dropwise. After 2 h, *tert*-butyl bromoacetate (0.69 mL, 4.63 mmol, 4 eq.) and DMI (0.50 mL, 4.63 mmol, 4 eq.) were added and the reaction was allowed to warm to rt and stirred for 4 h. The reaction was quenched with sat. aq. NH_4Cl (20 mL), diluted with H_2O (20 mL), and extracted with EtOAc (50 mL x3). The combined organic layers were washed with brine (20 mL), dried over Na_2SO_4, filtered, and concentrated *in vacuo*. The crude material was purified by silica gel flash column chromatography (hexanes:EtOAc 8:1 to 6:1) to afford compound **2.146** (479.9 mg, 93%, single diastereomer).

Physical state: light yellow oil

TLC: R_f = 0.4 (hexanes:EtOAc 3:1, UV and $KMnO_4$)

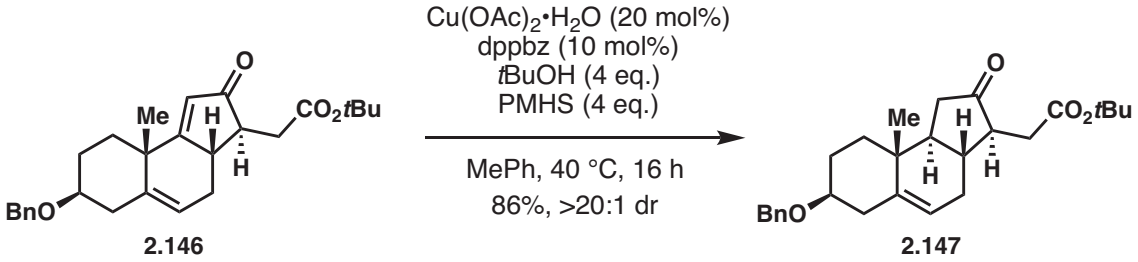
$[\alpha]_{25}^{D}$: -40.4 (c = 0.78 in $CHCl_3$)

^{1}H NMR (600 MHz, $CDCl_3$): δ 7.37 – 7.23 (m, 5H), 5.89 (d, *J* = 1.5 Hz, 1H), 5.49 – 5.43 (m, 1H), 4.57 (s, 2H), 3.29 (tt, *J* = 11.2, 4.5 Hz, 1H), 2.81 – 2.74 (m, 2H), 2.70 (dddd, *J* = 17.3, 7.8, 5.5, 2.5 Hz, 1H), 2.55 (ddd, *J* = 13.0, 4.7, 2.3 Hz, 1H), 2.36 – 2.27 (m, 3H), 2.10 (dq, *J* = 13.4, 3.4 Hz, 1H), 1.99 (dt, *J* = 13.3, 3.5 Hz, 1H), 1.89 (dddd, *J* = 16.6, 10.7, 3.4, 2.1 Hz, 1H), 1.76 – 1.66 (m, 1H), 1.51 (td, *J* = 13.7, 3.9 Hz, 1H), 1.44 (s, 9H), 1.33 (s, 3H).

^{13}C NMR (151 MHz, $CDCl_3$): δ 209.2, 189.0, 171.4, 138.8, 138.0, 128.5, 127.7, 127.7, 123.9, 121.2, 81.0, 78.1, 70.3, 49.7, 42.6, 39.3, 38.2, 36.6, 34.4, 33.7, 28.2, 28.1, 25.6.

HRMS (ESI-TOF): calc'd for $C_{27}H_{34}O_4$ $[M+Na]^+$: 445.2349, found: 445.2359.

Compound 2.147



The following procedure was adapted from literature reports.[6] A flame-dried 25 mL round-bottom flask was charged with $Cu(OAc)_2•H_2O$ (45.3 mg, 0.23 mmol, 20 mol%) and dppbz (50.7 mg, 0.11 mmol, 10 mol%). The flask was backfilled with Ar three times to ensure an oxygen-free environment. Freshly degassed MePh (5 mL, sonication + Ar bubbling for 1 h) and *t*BuOH (4.54 mmol, 4 eq.) were added, and the resulting suspension was vigorously stirred for 30 min. PMHS (0.27 mL, 4.54 mmol, 4 eq.) was added and vigorous stirring was continued for 2 h. The blue-green suspension slowly became a red/orange solution during this period, indicating successful formation of CuH. To this solution was added a solution of compound **2.146** (479.9 mg, 1.14 mmol, 1 eq.) in degassed MePh (5 mL). The resulting solution was heated to 40 °C for 16 h. The reaction was diluted with Et_2O (20 mL) and passed through a silica gel plug. The plug was washed with additional Et_2O (20 mL x3), and the combined fractions were directly concentrated *in vacuo*. The resulting crude material was purified by silica gel flash column chromatography (hexanes:EtOAc 10:1 to 8:1) to afford compound **2.147** (428.3 mg, 86%, single diastereomer), plus recovered starting material **15** (48.2 mg, 10%).

Physical state: white solid

TLC: R_f = 0.5 (hexanes:EtOAc 3:1, UV and $KMnO_4$)

Melting point: 53-58 °C

$[\alpha]_{25}^{D}$: +23.8 (c = 0.53 in $CHCl_3$)

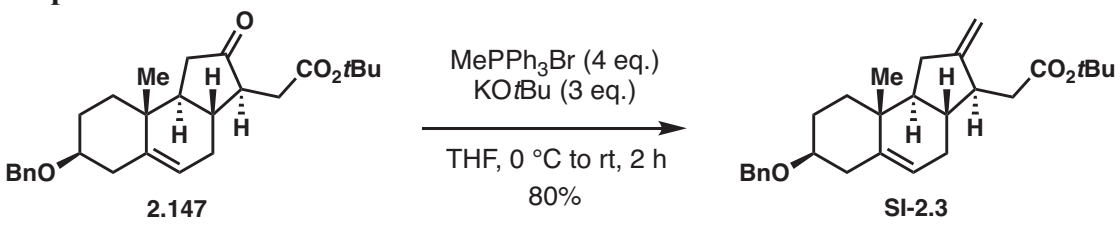
^{1}H NMR (600 MHz, $CDCl_3$): δ 7.38 – 7.26 (m, 5H), 5.42 (dt, *J* = 5.7, 2.0 Hz, 1H), 4.57 (s, 2H), 3.32 (tt, *J* = 11.2, 4.5 Hz, 1H), 2.61 (dd, *J* = 16.5, 4.5 Hz, 1H), 2.52 (ddd, *J* = 13.2, 4.7, 2.3 Hz, 1H), 2.44 (dd, *J* = 16.5, 6.6 Hz, 1H), 2.36 – 2.26 (m, 3H), 2.17 – 2.06 (m, 2H), 2.03 – 1.95 (m, 1H), 1.93 – 1.84 (m, 2H), 1.73 – 1.65 (m, 2H), 1.63 – 1.53 (m, 1H), 1.44 (s, 9H), 1.20 (td, *J* = 13.6, 3.7 Hz, 1H), 1.04 (s, 3H).

^{13}C NMR (151 MHz, $CDCl_3$): δ 217.5, 171.3, 141.5, 139.0, 128.5, 127.7, 127.6, 121.3,

81.0, 78.4, 70.2, 53.0, 49.2, 39.0, 38.9, 38.3, 37.9, 36.6, 34.2, 31.8, 28.2, 28.1, 18.7.

HRMS (ESI-TOF): calc'd for $C_{27}H_{36}O_4$ $[M+H]^+$: 425.2692, found: 425.2689.

Compound SI-2.3



A flame-dried 25 mL round-bottom flask was charged with $MePPh_3Br$ (1.43 g, 4 mmol, 4 eq.) and backfilled with Ar. THF (4 mL) was introduced, and the resulting suspension was cooled to 0 °C. KO*t*Bu (1.0 M in THF, 3 mL, 3 mmol, 3 eq.) was added dropwise, and the suspension was stirred for 30 min at 0 °C. A solution of compound **2.147** (418.0 mg, 1 mmol, 1 eq.) in THF (3 mL) was added, and the reaction was allowed to warm to rt and stir for 1.5 h. The reaction was quenched with sat. aq. NH_4Cl (10 mL), diluted with H_2O (5 mL), and extracted with EtOAc (30 mL x3). The combined organic layers were washed with brine (20 mL), dried over Na_2SO_4, filtered and concentrated *in vacuo*. The crude material was purified by silica gel flash column chromatography (hexanes:EtOAc 40:1 to 20:1) to afford compound **SI-2.3** (338.5 mg, 80%).

Physical state: white solid

TLC: R_f = 0.7 (hexanes:EtOAc 4:1, UV and $KMnO_4$)

Melting point: 87-90 °C

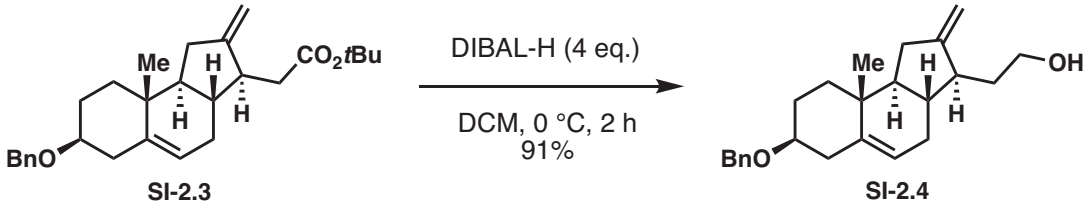
$[\alpha]_{25}^{D}$: -10.7 (c = 1.0 in $CHCl_3$)

^{1}H NMR (600 MHz, $CDCl_3$): δ 7.37 – 7.25 (m, 5H), 5.36 (dt, *J* = 4.5, 2.0 Hz, 1H), 4.93 (d, *J* = 2.1 Hz, 1H), 4.81 (d, *J* = 2.4 Hz, 1H), 4.57 (s, 2H), 3.29 (tt, *J* = 11.2, 4.5 Hz, 1H), 2.53 – 2.41 (m, 3H), 2.38 (dd, *J* = 16.1, 7.5 Hz, 1H), 2.35 – 2.30 (m, 1H), 2.30 – 2.16 (m, 3H), 1.99 – 1.93 (m, 1H), 1.79 (dddd, *J* = 17.2, 10.5, 3.4, 2.1 Hz, 1H), 1.72 (dt, *J* = 13.4, 3.5 Hz, 1H), 1.62 – 1.49 (m, 2H), 1.46 (s, 9H), 1.42 (td, *J* = 12.1, 7.5 Hz, 1H), 1.15 (td, *J* = 13.8, 3.8 Hz, 1H), 0.98 (s, 3H).

^{13}C NMR (151 MHz, $CDCl_3$): δ 172.6, 154.5, 141.6, 139.1, 128.5, 127.7, 127.6, 121.9, 105.6, 80.4, 78.7, 70.1, 52.2, 46.9, 42.2, 39.3, 38.8, 38.2, 37.1, 32.3, 31.8, 28.3, 28.3, 18.7.

HRMS (ESI-TOF): calc'd for $C_{28}H_{38}O_3$ $[M+H]^+$: 423.2899, found: 423.2904.

Compound SI-2.4



A flamed-dried 25 mL round-bottom flask was charged with compound **SI-2.3** (211.0 mg, 0.5 mmol, 1 eq.) and backfilled with Ar. DCM (3 mL) was introduced and the resulting solution was cooled to 0 °C. DIBAL-H (1.0 M in DCM, 2 mL, 2 mmol, 4 eq.) was added dropwise, and the reaction was allowed to stir at 0 °C for 2 h. Sat. aq. Rochelle's salt (10 mL) was slowly added at 0 °C to quench the reaction, followed by dilution with EtOAc (10 mL). The resulting suspension was allowed to warm to rt, transferred to a 125 mL Erlenmeyer, and stirred vigorously for 2 h (or until a clear phase separation was achieved). The layers were separated and the aqueous phase was extracted with EtOAc (20 mL x3). The combined organic phases were washed with brine (20 mL), dried over Na_2SO_4, filtered, and concentrated *in vacuo*. The crude material was purified by silica gel column chromatography (hexanes:EtOAc 4:1 to 2:1) to afford compound **SI-2.4** (160.8 mg, 91%).

Physical state: white solid

TLC: R_f = 0.3 (hexanes:EtOAc 3:1, UV and $KMnO_4$)

Melting point: 70-74 °C

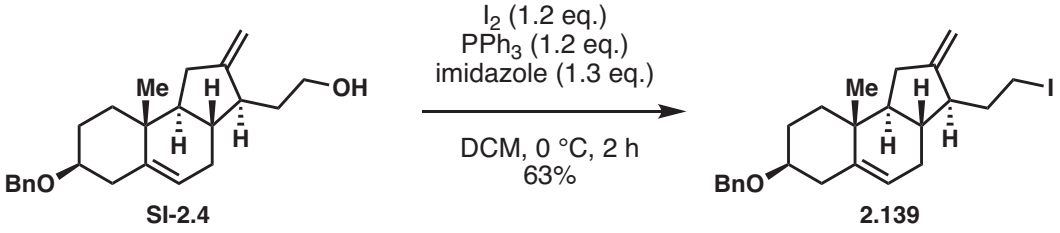
$[\alpha]_{25}^{D}$: -15.3 (c = 1.03 in $CHCl_3$)

^{1}H NMR (600 MHz, $CDCl_3$): δ 7.37 – 7.25 (m, 5H), 5.39 – 5.34 (m, 1H), 4.95 (s, 1H), 4.86 – 4.82 (m, 1H), 4.57 (s, 2H), 3.75 (dq, *J* = 25.2, 10.4, 8.7 Hz, 2H), 3.29 (tt, *J* = 11.3, 4.5 Hz, 1H), 2.50 (ddd, *J* = 13.2, 4.8, 2.3 Hz, 1H), 2.36 (dd, *J* = 15.7, 7.1 Hz, 1H), 2.31 – 2.23 (m, 2H), 2.18 (ddd, *J* = 15.5, 12.5, 2.7 Hz, 1H), 2.15 – 2.09 (m, 1H), 2.00 – 1.89 (m, 2H), 1.83 – 1.69 (m, 3H), 1.63 – 1.49 (m, 2H), 1.37 (td, *J* = 12.2, 7.1 Hz, 1H), 1.14 (td, *J* = 13.7, 3.8 Hz, 1H), 0.99 (s, 3H).

^{13}C NMR (151 MHz, $CDCl_3$): δ 155.6, 141.8, 139.1, 128.5, 127.7, 127.6, 121.9, 105.5, 78.7, 70.1, 61.4, 52.7, 47.0, 41.8, 38.7, 38.3, 37.0, 36.4, 33.0, 32.6, 28.3, 18.7.

HRMS (ESI-TOF): calc'd for $C_{24}H_{32}O_2$ $[M+H]^+$: 353.2475, found: 353.2468.

ABC Fragment (2.139)



A flame-dried 10 mL round-bottom flask was charged with PPh_3 (94.4 mg, 0.36 mmol, 1.2 eq.) and imidazole (27.2 mg, 0.4 mmol, 1.3 eq.) and backfilled with Ar. DCM (2 mL) was introduced and the resulting solution was cooled to 0 °C. I_2 (91.4 mg, 0.36 mmol, 1.2 eq.) was added and the solution was stirred at 0 °C for 30 min. A solution of compound **SI-2.4** (105.8 mg, 0.3 mmol) in DCM (1 mL) was added dropwise, and the reaction was stirred at 0 °C for 1.5 h. The reaction was quenched H_2O (5 mL) and extracted with DCM (10 mL x3). The combined organic layers were washed with brine (5 mL), dried over Na_2SO_4, filtered, and concentrated *in vacuo*. The crude material was purified by silica gel flash column chromatography (hexanes:EtOAc 40:1 to 20:1) to afford compound **2.139** (87.6 mg, 63%).

Physical state: white solid

TLC: R_f = 0.7 (hexanes:EtOAc 6:1, UV and $KMnO_4$)

Melting point: 60-63 °C

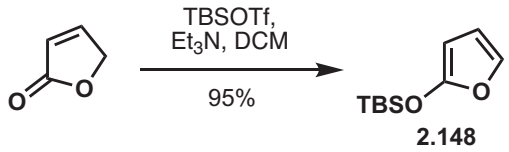
$[\alpha]_{25}^{D}$: +0.7 (c = 1.05 in $CHCl_3$)

^{1}H NMR (600 MHz, $CDCl_3$): δ 7.38 – 7.25 (m, 5H), 5.39 – 5.32 (m, 1H), 4.96 (d, *J* = 0.9 Hz, 1H), 4.81 (s, 1H), 4.57 (s, 2H), 3.35 – 3.26 (m, 2H), 3.22 (td, *J* = 9.2, 6.7 Hz, 1H), 2.51 (ddd, *J* = 13.0, 4.8, 2.3 Hz, 1H), 2.34 (dd, *J* = 15.9, 7.0 Hz, 1H), 2.31 – 2.23 (m, 2H), 2.23 – 2.11 (m, 3H), 2.05 (dddd, *J* = 13.9, 9.0, 6.9, 5.4 Hz, 1H), 2.01 – 1.92 (m, 1H), 1.91 – 1.82 (m, 1H), 1.72 (dt, *J* = 13.4, 3.5 Hz, 1H), 1.62 – 1.56 (m, 1H), 1.55 – 1.47 (m, 1H), 1.38 (td, *J* = 12.3, 7.0 Hz, 1H), 1.14 (td, *J* = 13.7, 3.7 Hz, 1H), 0.98 (s, 3H).

^{13}C NMR (126 MHz, $CDCl_3$): δ 154.2, 141.8, 139.1, 128.5, 127.7, 127.6, 121.8, 106.0, 78.7, 70.1, 52.7, 50.8, 41.6, 38.7, 38.5, 38.2, 37.0, 33.1, 32.7, 28.3, 18.7, 4.7.

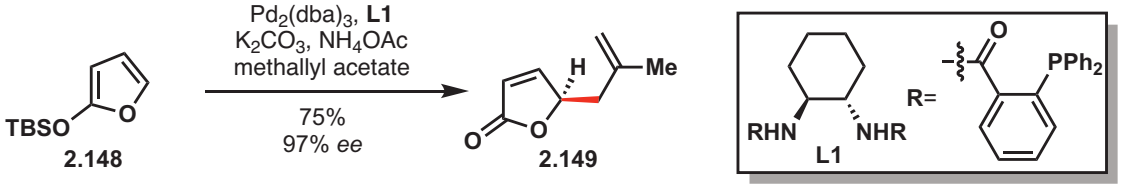
HRMS (ESI-TOF): molecular ion peak not observed due to extensive fragmentation. Major fragment peaks: m/z = 262.1792, 293.1746, 368.4235.

Compound 2.148



Compound **2.148** was prepared according to a reported procedure.[7] It was purified by silica gel flash column chromatography (neutralized by Et_3N, hexanes: EtOAc = 50:1 to 25:1). Spectra data matches those reported previously in the literature.[6]

Compound 2.149



Compound **2.149** was prepared according to a reported procedure with the following modifications detailed below.[8]

Recrystallization of $Pd_2(dba)_3$

Following a literature procedure,[9] $Pd_2(dba)_3$ (250 mg) was dissolved in ca. 15 mL of neutralized $CHCl_3$ (passed through basic Al_2O_3) and filtered through Celite® to remove the undissolved palladium black. The plug was rinsed with additional neutralized $CHCl_3$ until the Celite underneath returned to its original beige color [to ensure maximum recovery of $Pd_2(dba)_3$]. The volatiles were removed *in vacuo* (<30 °C water bath temperature*)* and the black residue was dissolved in 5 mL $CHCl_3$ (*Note: all solids should be fully dissolved*). Acetone (20 mL, ACS reagent grade) was slowly added, and the flask was stored at -20 °C for ca. 10 h. The precipitate was collected by a quick filtration and washed with cold acetone (2 x 2 mL), care being taken to minimize air exposure. The resulting slurry of $Pd_2(dba)_3$ was poured on top of multiple layers of filter paper (to remove remaining acetone and water) and then transferred to a flask and placed on high vacuum (1 torr) at rt. The solid was finely grounded every 5 min using a spatula and placed back on vacuum, a process that was repeated three times. The purity was determined by NMR ($CDCl_3$, neutralized over K_2CO_3).[8] Typically a black to brown solid of ca. 90% purity was obtained, which was stored at -20 °C.

Preparation of Pd/ligand stock solution

To a flame dried flask, $Pd_2(dba)_3$ (0.5 mmol, 5 mol%) was added and the flask was placed on high vacuum and backfilled with Ar (3x). THF (20 mL, 0.025 M) was added, and the suspension was stirred for 10 minutes at rt. A solution of the ligand (1.2 mmol, 12 mol%) in THF (15 mL, 0.08 M) was added and the reaction mixture was vigorously stirred for 30 min at rt. A deep red color developed after ~5 minutes (see below). *Note: A slight excess of ligand was required, as any Pd:L ratio lower than 1:1.2 gave irreproducible results in our hands.*

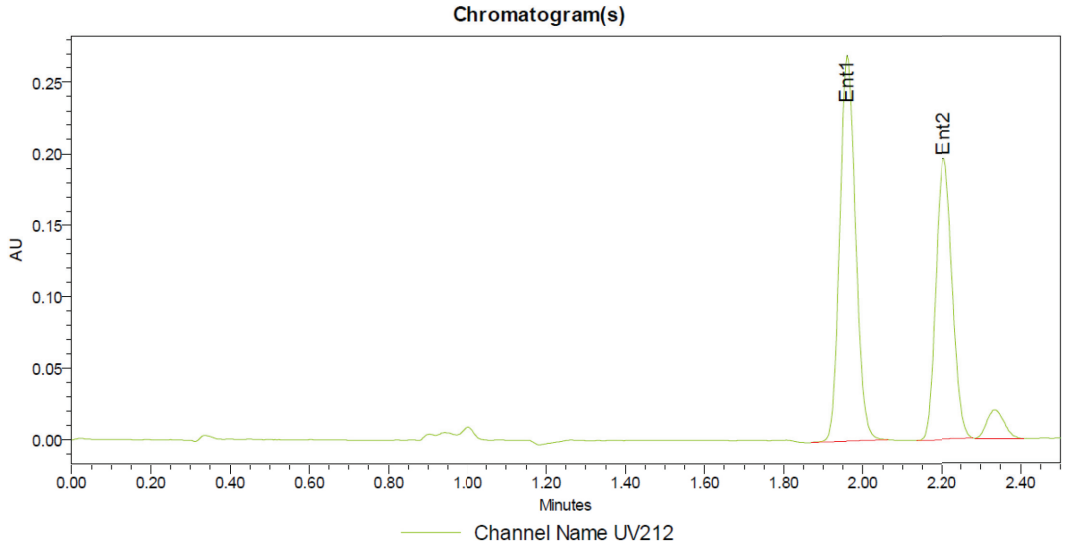
Set up of AAA

To a flame dried flask, K_2CO_3 (20 mmol, 2 equiv., finely grounded using mortar and pestle and kept on high vacuum for at least 1 hour at 40 °C) and NH_4OAc (2 mmol, 0.2 equiv., dried at 100 °C on high vacuum for 2 hours. Using a big flask is recommended due to sublimation) were added, followed by anhydrous and degassed THF (0.3 M with respect to K_2CO_3, degassed by Ar bubbling under sonication for 45 min) and the suspension was stirred for 10 min at rt. Then, it was cooled down to –20 °C and methallyl acetate (neat, 20 mmol, 2 equiv.) was added followed by a solution of **10** (10 mmol, 1.98 g) in THF (0.3 M). Then, a stock solution of palladium and ligand (*vide supra*) was added, and the reaction (yellow-red suspension) was left at –20 °C for 10 h. An aliquot of the reaction mixture was filtered through Celite® and the volatiles were carefully removed *in vacuo* (200 mbar, 25 °C). NMR analysis showed full consumption of siloxyfuran **10**. Cold Et_2O was added to the reaction mixture which was subsequently filtered through Celite®. After removing the volatiles *in vacuo* (200 mbar, 25 °C) the compound was purified by silica gel flash column chromatography (pentanes: Et_2O = 25:1 to 5:1) to afford **17** (1.03 g, 75%, 97% *ee*). All characterization data matched those reported in literature.[7]

Chiral SFC traces

The analysis was performed on a Waters UPC2 SFC with a Diacel IK column (3 μm, 4.6x250 mm) under isocratic conditions (3.3 mL/min, 15% IPA / CO_2, 1600 psi backpressure) at 30 °C. The enantiomers were detected by UV light (212 nm).

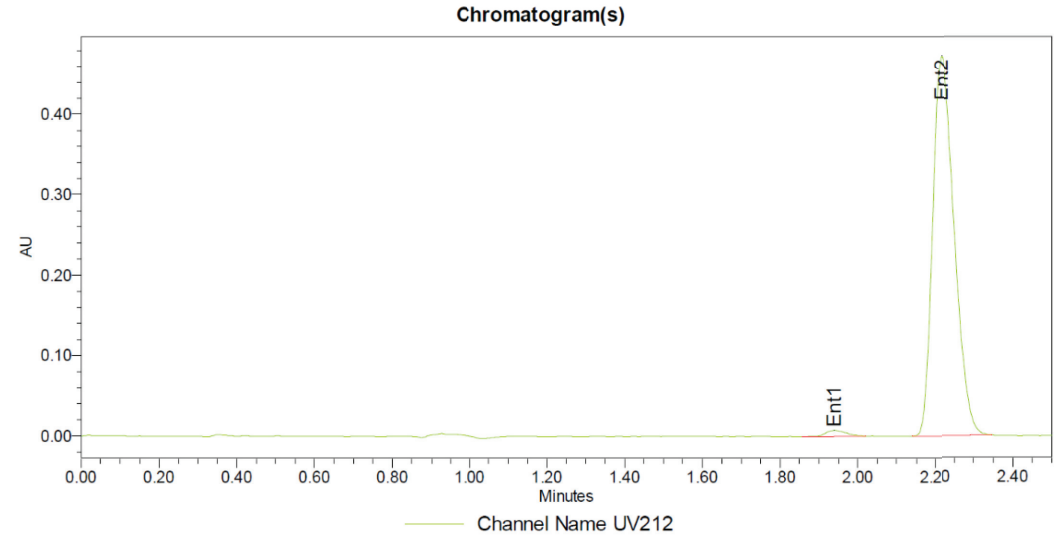
Mixture of two enantiomers:



Peak Info

	Channel Name	Name	RT	Area	Height (μV)	ent1	ent2	ee
1	UV212	Ent1	1.96	750037	269894	56.37	43.63	12.74
2	UV212	Ent2	2.20	580570	197112	56.37	43.63	12.74
3	UV212		2.34	59932	20068	56.37	43.63	12.74

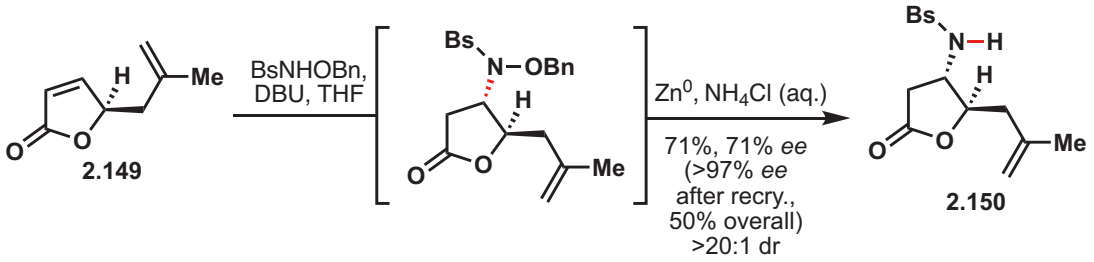
Enantiopure:



Peak Info

	Channel Name	Name	RT	Area	Height (μV)	ent1	ent2	ee
1	UV212	Ent1	1.94	27487	7402	1.44	98.56	-97.11
2	UV212	Ent2	2.22	1876621	473696	1.44	98.56	-97.11

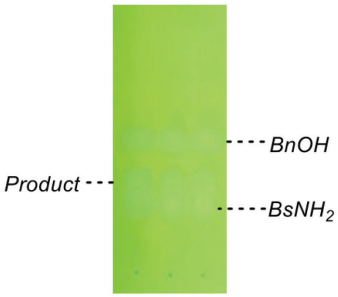
Compound 2.150



To a 500 mL flamed-dried flask, BsNHOBn (3.81 g, 14.5 mmol, 2 equiv.)[10] was added to a solution of **2.149** (1.0 g, 7.25 mmol, 1.0 equiv.) in THF (anhydrous, 0.25 M) at -20 °C followed by dropwise addition of DBU (3.63 mmol, 0.5 equiv.). The solution was left at this temperature for 12-24 h under stirring. At approximately 80% conversion, as was judged by LCMS analysis, a freshly prepared solution of sat. NH_4Cl (aq.) (0.05 M with respect to **2.149**) was added at -20 °C and the temperature was slowly raised to rt. Freshly activated Zn powder (40 equiv.)[11] was added, and the flask was fitted with a chilled reflux condenser. The reaction was brought to reflux and stirred vigorously for 16 hours. *[Note: Full conversion was typically observed by TLC analysis after 16 h, but in some instances the reaction prematurely reached pH 7 and stalled. In this case, the neutral solution was re-acidified to pH 3-4 by dropwise addition of 6 M HCl (aq.), charged with additional 40 eq. of solid NH_4Cl, and then brought back to reflux for an additional 5 hours.]* After full consumption of the aza-Michael adduct the reaction was cooled down to room temperature. All solids and residual Zn powder were filtered off and washed with ethyl acetate. The resulting biphasic mixture was extracted with ethyl acetate (100 mL x3) and the combined organics were washed with sat. $NaHCO_3$ (aq.) and dried over Na_2SO_4 (s). After concentration *in vacuo*, the solid crude material was dissolved in a minimal amount of hot DCM and placed in a -20 °C freezer for 2 hours. The precipitated benzenesulfonamide byproduct was filtered off and the flask and crystals were washed with hexanes *[This typically removes 90+% of the benzenesulfonamide from the mixture]*. The filtrate was concentrated and purified by silica gel flash column chromatography (hexanes:EtOAc = 3:1) to afford the desired product **2.150** (1.5 g, 71%, 71% *ee*), which was recrystallized from DCM/Et_2O (1:1, dissolved at rt and stored at 4 °C for 2 days) to yield enantiopure **2.150** (1.06 g, 72% recovery, 50% yield overall) for the downstream sequence.

Physical state: off-white solid

TLC: R_f = 0.5 (hexanes:EtOAc = 1:1, UV and $KMnO_4$)



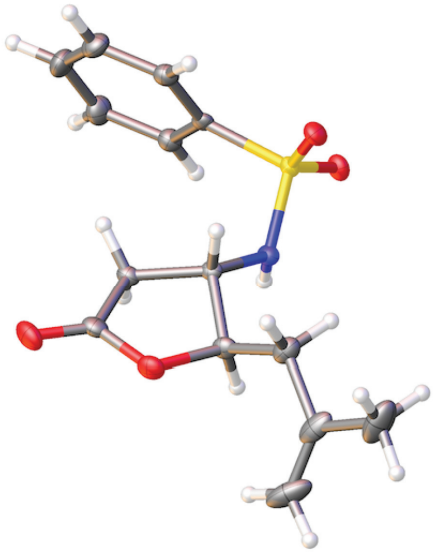
$[\alpha]_{25}^{D}$: +25.8° (c = 0.5 in $CHCl_3$)

^{1}H NMR (600 MHz, $CDCl_3$): δ 7.87 – 7.85 (m, 2H), 7.64 (tt, *J* = 7.5, 2.0 Hz, 1H), 7.56 – 7.54 (m, 2H), 5.33 (d, *J* = 7.9 Hz, 1H), 4.83 (br, 1H), 4.68 (br, 1H), 4.40 (m, 1H), 3.82 (m, 1H), 2.70 (dd, *J* = 18.1, 8.2 Hz, 1H), 2.34 (dd, *J* = 18.1, 6.0 Hz, 1H), 2.29 (d, *J* = 6.5 Hz, 2H), 1.69 (s, 3H).

^{13}C NMR (151 MHz, $CDCl_3$): δ 175.6, 139.6, 133.4, 129.5, 127.0, 114.7, 83.4, 53.8, 41.0, 35.3, 22.6.

HRMS (ESI-TOF): calc'd for $C_{14}H_{18}NO_4S$ $[M+H]^+$: 296.0951, found: 296.0956.

X-ray crystallography structure:

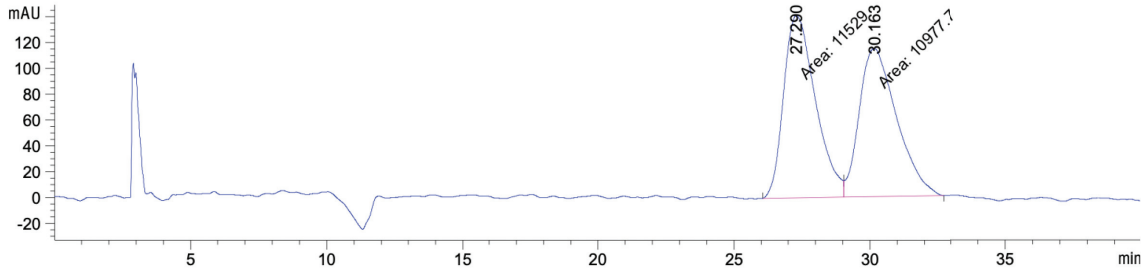


(See **X-Ray Crystallography Data** for the full report)

Chiral HPLC traces:

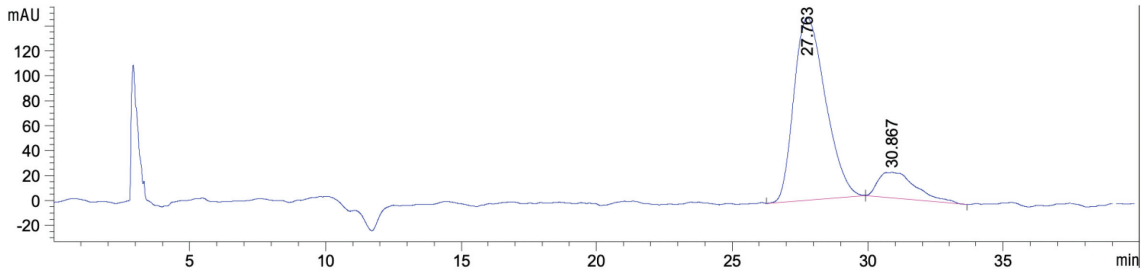
The analysis was performed on an Agilent Technologies 1220 Infinity II LC HPLC with a CHIRALCEL® OD-H column (5 µm particle size, 4.6x250 mm) under isocratic conditions (1 mL/min, 10% IPA / hexanes) at 23 °C. The enantiomers were detected by UV light (212 nm).

Racemic:



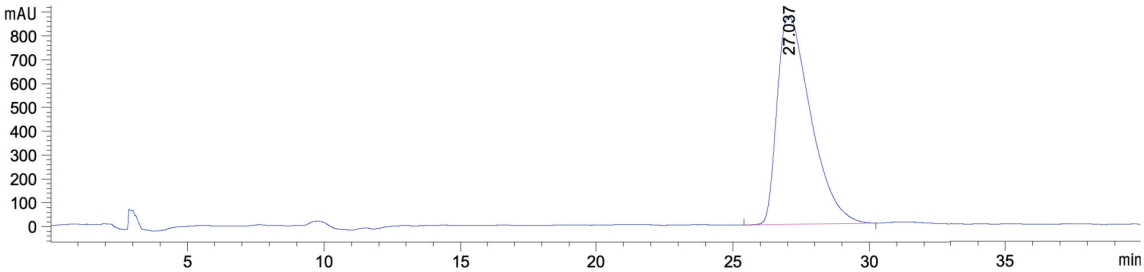
Peak #	RetTime [min]	Type	Width [min]	Area [mAU*s]	Height [mAU]	Area %
1	27.290	MF	1.3574	1.15290e4	141.55455	51.2248
2	30.163	FM	1.5965	1.09777e4	114.60438	48.7752

Before recrystallization:



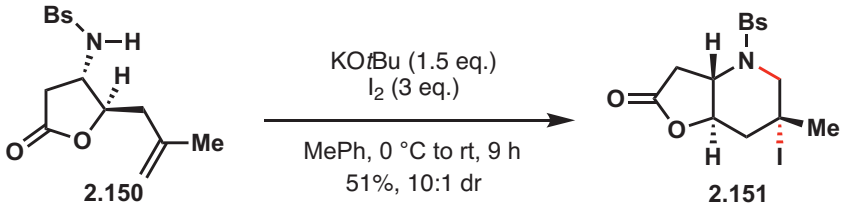
Peak #	RetTime [min]	Type	Width [min]	Area [mAU*s]	Height [mAU]	Area %
1	27.763	BB	1.2238	1.18156e4	146.67654	85.5600
2	30.867	BB	1.1617	1994.12463	20.27089	14.4400

Enantiopure (after recrystallization):



Peak #	RetTime [min]	Type	Width [min]	Area [mAU*s]	Height [mAU]	Area %
1	27.037	BB	1.2412	7.47727e4	874.80670	100.0000

Compound 2.151



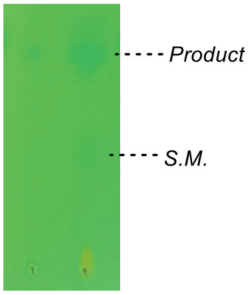
In a flamed-dried flask backfilled with Ar, KO*t*Bu (1 M in THF, 1.5 mL, 1.5 mmol, 1.5 equiv.) was added to a solution of **2.150** (300 mg, 1.0 mmol, 1.0 equiv.) in dry toluene (20 mL, 0.05 M) at 0 °C and the suspension was stirred for 30 min (solution should slowly take on a yellow color and become homogenous overtime). I_2 (761 mg, 3 mmol, 3 equiv.) was added in one portion and the reaction mixture was protected from light (flask covered with aluminum foil) and stirred at ambient temperature for 9 h. At this point, an aliquot was taken for a crude NMR which would typically indicate ca. 50% conversion of starting material. *[Note: Longer reaction times were detrimental to the conversion. See discussion on page 26.]* The reaction was quenched by slow addition of freshly prepared sat. aq. $Na_2S_2O_3$ (20 mL). The phases were separated, and the organic layer was washed with additional sat. aq. $Na_2S_2O_3$ (20 mL x3). The combined aqueous phases were back extracted with EtOAc (50 mL, x3) and the combined organic phases were washed with brine (50 mL) and dried over Na_2SO_4. The volatiles were removed *in vacuo* in a 27 °C water bath (protected from light) and the compound was purified by silica gel column chromatography (hexanes:EtOAc = 4:1) to afford **2.151** (215 mg, 51%) as an inconsequential 10:1 mixture of two diastereomers, as well as recovered **2.150** (140 mg, 47%). Stereochemistry of the major diastereomer was determined by NOESY analysis (*vide infra*).

Physical state: off-white foam

TLC: R_f = 0.7 (hexanes:EtOAc = 1:1, UV and Seebach's magic)

$[\alpha]_{25}^{D}$: +81.8° (c = 0.3 in $CHCl_3$)

^{1}H NMR (major diastereomer, 600 MHz, $CDCl_3$): δ 7.82 (d, *J* = 7.6 Hz, 2H), 7.63 (m, 1H), 7.55 (t, *J* = 7.9 Hz, 2H), 3.95 (m, 1H), 3.94 (d, *J* = 10.0 Hz, 1H), 3.58 (d, *J* = 9.9 Hz, 1H), 3.54 (m, 1H), 2.81 (dd, *J* = 15.5, 5.7 Hz, 1H), 2.40 (m, 2H), 2.30 (t, *J* = 11.6 Hz, 1H), 1.89 (s, 3H).



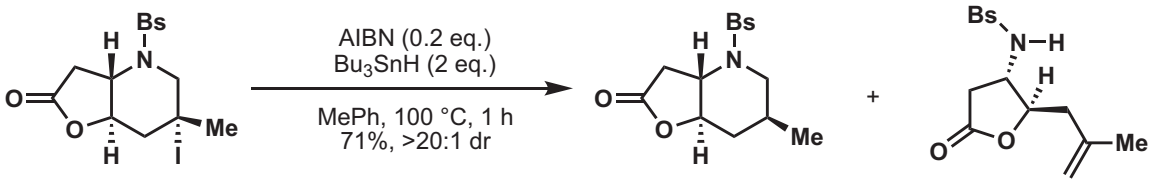
Conditions: 40% EtOAc:Hexanes

^{13}C NMR (major diastereomer, 151 MHz, $CDCl_3$): δ 174.6,

140.8, 133.5, 129.6, 127.4, 80.0, 74.3, 63.2, 44.1, 38.4, 27.8, 15.6.

HRMS (ESI-TOF): molecular ion peak not observed due to extensive fragmentation. Major fragment peaks: m/z = 147.0849, 215.0539, 288.1012.

Compound 2.152



2.151 (10:1 d.r.) **2.152** **2.150**

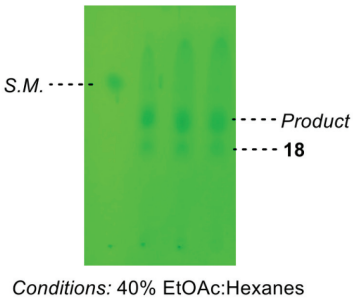
To a flamed-dried 100 mL round-bottom flask containing the iodide **2.151** (mixture of two diastereomers, 300 mg, 0.713 mmol, 1.0 equiv.) in degassed toluene (7.13 mL, 0.1 M) was added freshly recrystallized AIBN (0.143 mmol, 0.2 equiv.) at ambient temperature. Bu_3SnH (neat, 0.38 mL, 1.43 mmol, 2 equiv.) was added and the reaction mixture was placed directly into a 100 °C oil bath for 1 hour. Subsequently, the reaction mixture was cooled down to ambient temperature, diluted with EtOAc (~7 mL) and passed through KF impregnated SiO_2 (10% wt); the reaction flask was rinsed twice more with ~7 mL EtOAc. The volatiles were removed *in vacuo* and the compound was purified by silica gel flash column chromatography (hexanes:EtOAc = 7.5 to 5:1) to afford **2.152** (150 mg, 0.51 mmol, 71%, single diastereomer). Ring opening by-product **2.150** was also recovered (43 mg, 0.15 mmol, 21%) and could be recycled *via* subsequent halocyclization reactions.

*Note: Smaller scale reactions (<10 mg) led solely to the desired product and no ring-opening was observed. However, on larger scales (>100 mg) this process began to consistently occur. Efforts to suppress this undesired byproduct formation included lower reaction temperature with AIBN (80 °C) and running the reaction at rt with V70 (room temperature radical initiator). Unfortunately, neither attempt was successful and the latter actually led to more significant ring-opening (**20**:**18** = 1:1).*

Physical state: off-white solid

TLC: R_f = 0.45 (hexanes:EtOAc = 3:2, UV and Seebach's magic)

$[\alpha]_{25}^{D}$: +192.1 (c = 0.75 in $CHCl_3$)

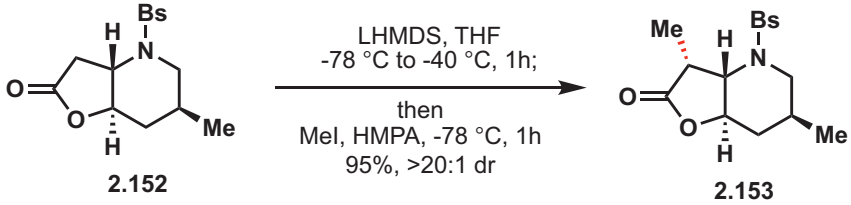


^{1}H NMR (600 MHz, $CDCl_3$): δ 7.75 – 7.73 (m, 2H), 7.68 (tt, *J* = 6.6, 1.3 Hz, 1H), 7.62 – 7.59 (m, 2H), 4.01 (td, *J* = 9.3, 3.9 Hz, 1H), 3.81 (dd, *J* = 11.7, 3.7 Hz, 1H), 3.18 (dd, *J* = 16.8, 12.5 Hz, 1H), 2.96 (dd, *J* = 16.8, 6.4 Hz, 1H), 2.38 (ddd, *J* = 12.6, 7.8, 6.5 Hz, 1H), 2.27 (dt, *J* = 12.2, 4.0 Hz, 1H), 2.04 (m, 1H), 1.89 (t, *J* = 11.4 Hz, 1H), 1.13 (q, *J* = 11.9 Hz, 1H), 1.01 (d, *J* = 6.7 Hz, 3H).

^{13}C NMR (151 MHz, $CDCl_3$): δ 173.1, 134.6, 133.6, 129.5, 127.8, 81.0, 60.5, 55.5, 36.9, 35.9, 29.4, 18.5.

HRMS (ESI-TOF): molecular ion peak not observed due to poor ionization.

Compound 2.153



To a flamed-dried flask, LHMDS (4.8 mL, 4.8 mmol, 1.2 equiv. 1.0 M in THF) was added dropwise to a solution of lactone **20** (1.18 g, 4.0 mmol, 1.0 equiv.) in THF (anhydrous, 20 mL, 0.2 M) at -78 °C. The temperature was raised to -40 °C and the reaction mixture was stirred for 1h at this temperature and then it was dropped to -78 °C again. MeI (0.3 mL, 1.2 equiv.) and HMPA (anhydrous, 0.84 mL, 1.2 equiv.) subsequently dropwise added to the reaction mixture, and it was stirred for 1 h at this temperature. Upon completion, the reaction mixture was quenched by sat. NH_4Cl (aq.) and the biphasic suspension was left to reach ambient temperature. EtOAc (20 mL) was added, and the phases were separated. The aqueous phase was extracted with EtOAc (3 x 20 mL) and the combined organic phases were washed with brine (1 x 10 mL) and dried over $MgSO_4$. The volatiles were removed *in vacuo* and the compound was purified by silica gel flash column chromatography (hexanes: EtOAc = 7.5:1 to 5:1) to afford **21** (1.1 g, 95%, single diastereomer).

Physical state: off-white solid

TLC: R_f = 0.5 (hexanes:EtOAc = 3:2, UV and Seebach's magic)

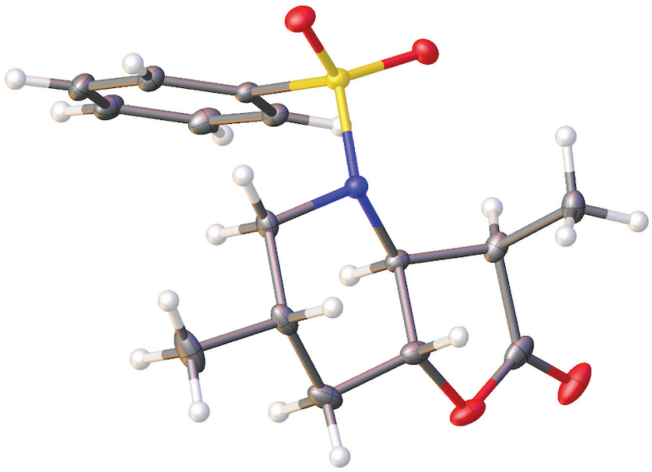
$[\alpha]_{25}^{D}$: +236.6 (c = 0.93 in $CHCl_3$)

^{1}H NMR (600 MHz, $CDCl_3$): δ 7.76 – 7.73 (m, 2H), 7.70 (tt, *J* = 6.7, 1.3 Hz, 1H), 7.63 – 7.60 (m, 2H), 4.24 (td, *J* = 11.8, 9.7, 4.0 Hz, 1H), 3.66 (ddd, *J* = 11.3, 4.0, 1.1 Hz, 1H), 3.21 (qui, *J* = 9.7, 6.2 Hz, 1H),

^{13}C NMR (151 MHz, $CDCl_3$): δ 176.7, 133.8, 132.9, 129.4, 128.5, 63.3, 56.0, 41.7, 35.5, 28.6, 18.6, 9.8.

HRMS (ESI-TOF): calc'd for $C_{15}H_{20}NO_4S$ $[M+H]^+$: 310.1107, found: 310.1090.

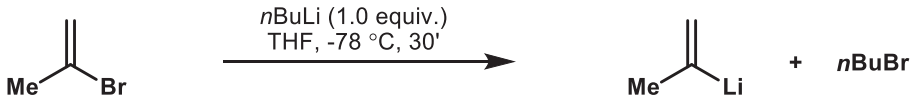
X-ray crystallography structure:



(See **X-Ray Crystallography Data** for the full report)

The EF Fragment (2.140)

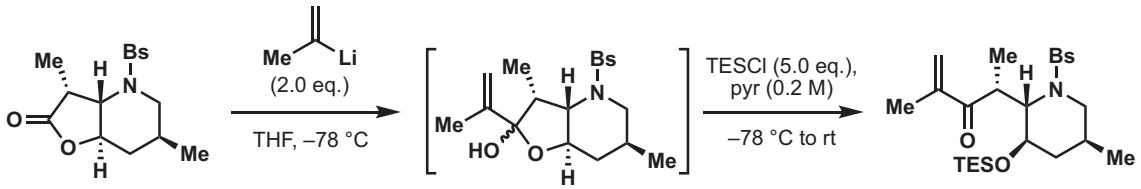
1) Preparation of 2-lithiopropene solution



To a flamed-dried flask, *n*BuLi (2.4 mL, 6 mmol, 1.0 equiv.) was added dropwise to a solution of 2-bromopropene (0.53 mL, 6 mmol, 1.0 equiv.) in THF (anhydrous, 8.5 mL, 0.7 M) at -78 °C and stirred for 30 min.

[Note: 2-lithiopropene is stable at -78°C but reacts with nBuBr at higher temperatures.]

2) Reaction setup:



To a flamed-dried flask, a -78 °C cold solution of 2-lithiopropene (*vide supra*, 6 mmol, 2.0 equiv.) was cannulated to a solution of lactone **2.153** (927 mg, 3.0 mmol, 1.0 equiv.) in THF (anhydrous, 10 mL, 0.2 M) at -78 °C and the resulting solution was left at this temperature until full consumption of the starting material by TLC. Upon full conversion, TESCl (2.5 mL, 5.0 equiv.) and pyridine (anhydrous, 15 mL, 0.2 M) were added at -78 °C and the reaction was left to reach ambient temperature and stirred for 6 h. The reaction was quenched by sat. NH_4Cl (aq.) and the aqueous phase was extracted with EtOAc (3 x 30 mL). The combined organic phases were washed with brine (10 mL) and dried over $MgSO_4$, volatiles removed *in vacuo* and the compound was purified by silica gel flash column chromatography (hexanes: EtOAc = 15:1 to 10:1) to afford **2.140** (0.9 g, 65%).

[Note: the addition of 2-lithiopropene must be slow (~1 drop/second) to avoid over-addition.]

Physical state: off-white solid

TLC: R_f = 0.85 (hexanes:EtOAc = 3:1, UV and Seebach's magic)

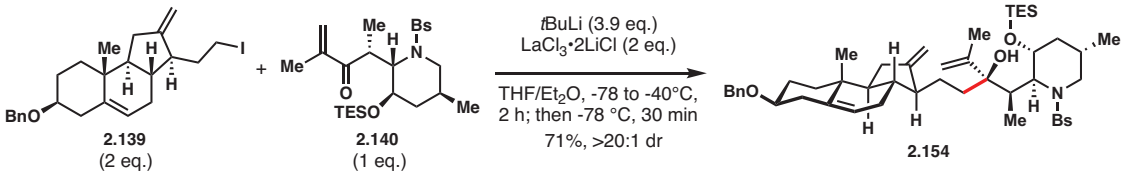
$[\alpha]_{25}^{D}$: -12.0 (c = 0.83 in $CHCl_3$)

^{1}H NMR (600 MHz, $CDCl_3$): δ 7.81 – 7.80 (m, 2H), 7.51 (tt, *J* = 6.7, 1.2 Hz, 1H), 7.45 – 7.42 (m, 2H), 6.22 (s, 1H), 5.87 (q, *J* = 1.4 Hz, 1H), 4.10 (dd, *J* = 7.1, 2.1 Hz, 1H), 3.89 (qui, *J* = 7.0 Hz, 1H), 3.86 (m, 1H), 3.42 (dd, *J* = 12.3, 4.9 Hz, 1H), 3.07 (dd, *J* = 12.3, 7.0 Hz, 1H), 1.90 – 1.84 (m, 4H), 1.82 – 1.78 (m, 1H), 1.14 (d, *J* = 7.0 Hz, 3H), 1.07 (m, 1H), 0.84 (m, 12H), 0.42 (q, *J* = 7.9 Hz, 6H).

^{13}C NMR (151 MHz, $CDCl_3$): δ 203.3, 144.3, 139.5, 132.1, 128.5, 127.8, 125.3, 66.7, 62.2, 47.2, 42.4, 34.6, 26.3, 20.7, 17.2, 13.7, 6.8, 4.6.

HRMS (ESI-TOF): calc'd for $C_{24}H_{40}NO_4SSi$ $[M+H]^+$: 466.2442, found: 466.2411.

Compound 2.154



A flame-dried 20x125 mm culture tube under Ar was charged with a solution of compound **2.139** (73.2 mg, 0.16 mmol, 2 eq.) in Et_2O (1.6 mL). The reaction was cooled to -78 °C, and *t*BuLi (1.7 M in pentane, 0.18 mL, 3.9 eq.) was slowly added dropwise with a syringe (with needle pressed against the tube wall to maintain a constant reaction temperature). After 15 min, the reaction was allowed to slowly warm to -40 °C in a dry ice-acetonitrile bath and stirred for another 45 min. $LaCl_3$•2LiCl (0.6 M in THF, 0.28 mL, 0.16 mmol, 2 eq.) was added dropwise, and vigorous stirring was continued for another 1 h at -40 °C. The reaction was cooled back down to -78 °C, and a solution of compound **2.140** (37.2 mg, 0.08 mmol, 2 eq.) in Et_2O/THF (1.2 mL, 1:1 *v*/*v*) was slowly added dropwise. A milk-white suspension formed upon complete addition. After 30 min, the reaction was quenched with addition of sat. aq. NH_4Cl (3 mL), diluted with H_2O (3 mL), and extracted with EtOAc (5 mL x5). The combined organic layers were washed with brine (5 mL), dried over Na_2SO_4, filtered, and concentrated *in vacuo*. The crude material was purified by pTLC (hexanes:EtOAc 7:1) to afford compound **2.154** (45.6 mg, 71%, single diastereomer).

Physical state: white solid

TLC: R_f = 0.45 (hexanes:EtOAc 6:1, UV and Seebach's magic stain)

Melting point: 157-160 °C

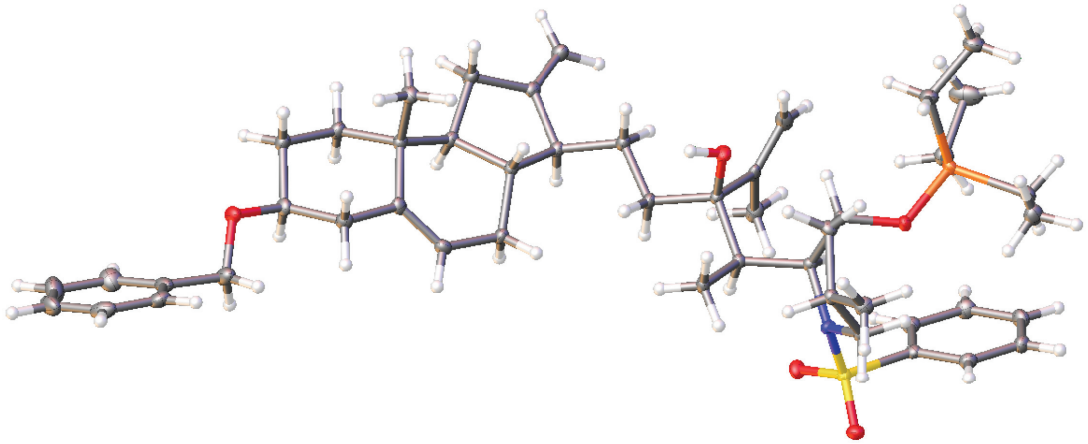
$[\alpha]_{25}^{D}$: +0.3 (c = 1.07 in $CHCl_3$)

^{1}H NMR (600 MHz, $CDCl_3$): δ 7.81 – 7.76 (m, 2H), 7.55 – 7.50 (m, 1H), 7.49 – 7.43 (m, 2H), 7.37 – 7.31 (m, 4H), 7.29 – 7.25 (m, 1H), 5.37 (dt, *J* = 4.5, 2.0 Hz, 1H), 4.99 (s, 1H), 4.96 (s, 1H), 4.90 (s, 1H), 4.74 (s, 1H), 4.57 (s, 2H), 4.23 (td, *J* = 6.1, 4.2 Hz, 1H), 3.69 (dd, *J* = 12.2, 5.2 Hz, 1H), 3.51 (dd, *J* = 5.9, 3.3 Hz, 1H), 3.29 (tt, *J* = 11.2, 4.4 Hz, 1H), 2.81 (s, 1H), 2.69 (t, *J* = 11.4 Hz, 1H), 2.50 (ddd, *J* = 13.2, 4.7, 2.2 Hz, 1H), 2.41 (qd, *J* = 7.2, 3.3 Hz, 1H), 2.34 – 2.27 (m, 2H), 2.27 – 2.19 (m, 1H), 2.12 (ddq, *J* = 15.3, 12.3, 2.6 Hz, 1H), 2.06 – 1.91 (m, 4H), 1.77 – 1.69 (m, 2H), 1.68 – 1.64 (m, 1H), 1.63 (s, 3H), 1.60 – 1.54 (m, 2H), 1.46 (dtd, *J* = 11.8, 10.3, 5.4 Hz, 1H), 1.40 – 1.25 (m, 3H), 1.20 (d, *J* = 7.2 Hz, 3H), 1.13 (td, *J* = 13.6, 3.7 Hz, 1H), 0.98 (s, 3H), 0.97 – 0.91 (m, 1H), 0.88 (d, *J* = 6.5 Hz, 3H), 0.86 (t, *J* = 7.9 Hz, 9H), 0.47 (q, *J* = 7.9 Hz, 6H).

^{13}C NMR (151 MHz, $CDCl_3$): δ 155.4, 148.1, 141.7, 140.5, 139.2, 132.3, 128.9, 128.5, 127.7, 127.6, 127.5, 122.1, 112.7, 105.2, 79.6, 78.7, 70.1, 68.5, 64.1, 52.7, 51.8, 50.1, 42.3, 41.2, 39.3, 38.8, 38.3, 37.0, 34.0, 33.2, 32.7, 28.4, 28.3, 26.1, 20.3, 19.8, 18.7, 9.7, 7.0, 5.2.

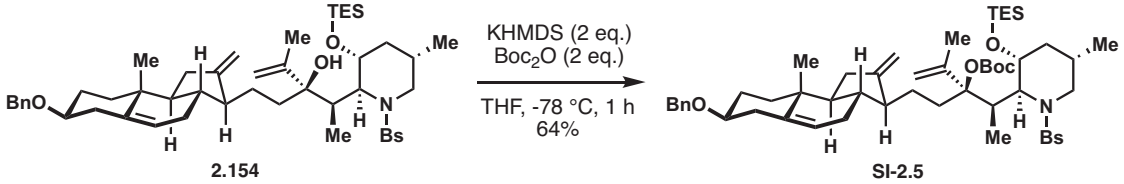
HRMS (ESI-TOF): calc'd for $C_{48}H_{71}NO_5SSi$ $[M+H]^+$: 802.4895, found: 802.4896.

X-ray crystallography structure:



(See **X-Ray Crystallography Data** for full report)

Compound SI-2.5



A flame-dried 13x100 mm culture tube under Ar was charged with a solution of compound **2.154** (40.8 mg, 0.05 mmol, 1 eq.) in THF (0.5 mL) and cooled to -78 °C. KHMDS (1.0 M in THF, 0.1 mL, 0.1 mmol, 2 eq.) was added dropwise, and the reaction was allowed to stir for 30 min. A solution of Boc_2O (21.8 mg, 0.1 mmol, 2 eq.) in THF (0.5 mL) was then added, and the reaction was stirred for 1.5 h at -78 °C. The reaction was quenched with sat. aq. NH_4Cl (2 mL), diluted with H_2O (1 mL), and extracted with EtOAc (5 mL x3). The combined organic layers were washed with brine (3 mL), dried over Na_2SO_4, filtered, and concentrated *in vacuo*. The crude material was purified by pTLC (pentane:Et_2O 4:1) to afford compound **SI-2.5** (31.7 mg, 64%).

Physical state: white foam

TLC: R_f = 0.5 (hexanes:EtOAc 6:1, UV and Seebach's magic stain)

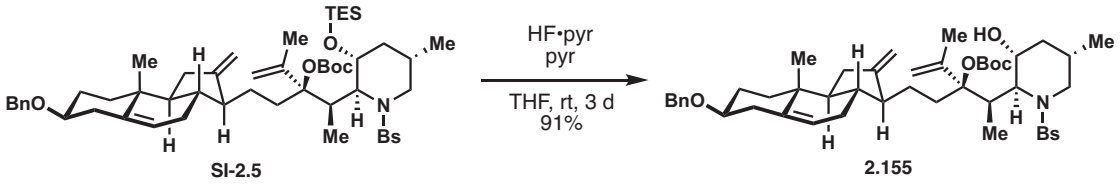
$[\alpha]_{25}^{D}$: +2.8 (c = 0.47 in $CHCl_3$)

^{1}H NMR (600 MHz, $CDCl_3$): δ 7.79 – 7.74 (m, 2H), 7.57 – 7.51 (m, 1H), 7.49 – 7.44 (m, 2H), 7.38 – 7.31 (m, 4H), 7.29 – 7.25 (m, 1H), 5.39 – 5.34 (m, 1H), 5.12 (s, 1H), 5.04 (s, 1H), 4.92 (s, 1H), 4.81 (s, 1H), 4.57 (s, 2H), 4.39 (dt, *J* = 4.6, 2.1 Hz, 1H), 3.71 – 3.65 (m, 1H), 3.56 (dd, *J* = 10.1, 5.0 Hz, 1H), 3.29 (tt, *J* = 11.3, 4.5 Hz, 1H), 2.99 – 2.89 (m, 1H), 2.84 (dd, *J* = 12.0, 10.1 Hz, 1H), 2.81 – 2.73 (m, 1H), 2.50 (ddd, *J* = 13.2, 4.7, 2.2 Hz, 1H), 2.34 – 2.23 (m, 3H), 2.19 – 2.08 (m, 2H), 2.00 – 1.97 (m, 3H), 1.97 – 1.93 (m, 2H), 1.83 (ddd, *J* = 14.4, 9.5, 4.5 Hz, 1H), 1.80 – 1.67 (m, 3H), 1.62 – 1.56 (m, 1H), 1.55 – 1.45 (m, 2H), 1.43 (s, 9H), 1.41 – 1.31 (m, 2H), 1.27 (d, *J* = 7.6 Hz, 3H), 1.13 (td, *J* = 13.9, 3.7 Hz, 1H), 1.02 (dd, *J* = 15.7, 7.8 Hz, 1H), 0.98 (s, 3H), 0.89 (d, *J* = 6.7 Hz, 3H), 0.75 (t, *J* = 7.9 Hz, 9H), 0.28 (q, *J* = 8.1 Hz, 6H).

^{13}C NMR (151 MHz, $CDCl_3$): δ 155.7, 151.7, 144.0, 141.5, 139.2, 137.5, 132.2, 128.7, 128.5, 128.1, 127.7, 127.6, 122.2, 113.6, 105.5, 91.3, 80.6, 78.8, 70.1, 67.5, 61.3, 52.8, 50.3, 47.7, 44.5, 41.8, 38.7, 38.3, 37.0, 35.3, 33.2, 32.8, 31.4, 28.3, 27.9, 27.7, 25.8, 21.7, 20.1, 18.6, 10.4, 7.1, 5.0.

HRMS (ESI-TOF): calc'd for $C_{53}H_{79}NO_7SSi$ $[M+Na]^+$: 924.5239, found: 924.5243.

Compound 2.155



A 1.5-mL Eppendorf tube was charged with a solution of compound **SI-2.5** (28.4 mg, 0.029 mmol, 1 eq.) in THF (0.3 mL) and set aside. A separate, flame-dried 13x100 mm culture tube was charged with pyridine (0.57 mL) and THF (1 mL) and cooled to 0 °C. Commercial HF•pyr (0.19 mL, HF:pyr = 70/30 *w*/*w*) was slowly added dropwise, and 0.88 mL of the resulting stock solution was withdrawn with a syringe and added to the Eppendorf tube. Effectively, about 0.095 mL of HF•pyr (3.6 mmol, 120 eq.) and 0.29 mL of pyridine (3.6 mmol, 120 eq.) were added. The reaction was stirred at rt for 3 d, after which it was quenched by slow addition of the reaction mixture to a stirring sat. aq. $NaHCO_3$ solution (5 mL) at 0 °C. The resulting mixture was extracted with EtOAc (10 mL x3). The combined organic layers were wash with brine (5 mL), dried over Na_2SO_4, filtered, and concentrated *in vacuo*. The crude material was purified by pTLC (hexanes:EtOAc 3:1) to afford compound **2.155** (22.8 mg, 91%). *[Note: Carbonate migration was observed with TBAF]*

Physical state: white foam

TLC: R_f = 0.25 (hexanes:EtOAc 4:1, UV and Seebach's magic stain)

$[\alpha]_{25}^{D}$: +5.1 (c = 0.80 in $CHCl_3$)

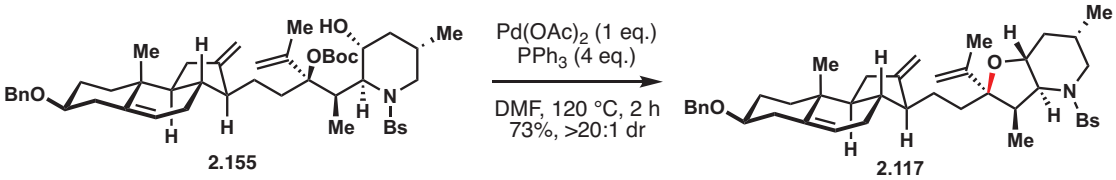
^{1}H NMR (600 MHz, $CDCl_3$): δ 7.84 – 7.79 (m, 2H), 7.57 – 7.53 (m, 1H), 7.52 – 7.47 (m, 2H), 7.38 – 7.31 (m, 4H), 7.29 – 7.25 (m, 1H), 5.38 – 5.34 (m, 1H), 5.19 – 5.15 (m, 1H), 5.07 – 5.03 (m, 1H), 4.93 (t, *J* = 1.3 Hz, 1H), 4.79 (dd, *J* = 2.8, 1.4 Hz, 1H), 4.57 (s, 2H), 4.10 (dd, *J* = 4.2, 2.8 Hz, 1H), 3.87 (dt, *J* = 8.7, 4.0 Hz, 1H), 3.53 (dd, *J* = 13.0, 6.7 Hz, 1H), 3.29 (tt, *J* = 11.1, 4.4 Hz, 1H), 2.99 (dd, *J* = 13.0, 8.6 Hz, 1H), 2.75 (ddd, *J* = 14.3, 12.2, 4.5 Hz, 1H), 2.68 (s, 1H), 2.57 – 2.47 (m, 2H), 2.35 – 2.24 (m, 3H), 2.18 – 2.10 (m, 1H), 2.02 – 1.93 (m, 2H), 1.91 (s, 3H), 1.76 (dddd, *J* = 39.8, 16.7, 9.6, 3.7 Hz, 4H), 1.66 (dt, *J* = 13.2, 4.8 Hz, 1H), 1.61 – 1.54 (m, 1H), 1.54 – 1.46 (m, 3H), 1.44 (s, 9H), 1.34 (td, *J* = 12.2, 6.9 Hz, 1H), 1.23 (d, *J* = 7.3 Hz, 3H), 1.13 (td, *J* = 13.8, 3.7 Hz, 1H), 0.98 (s, 3H), 0.83 (d, *J* = 6.7 Hz, 3H), 0.58 (ddd, *J* = 13.1, 11.2, 9.2 Hz, 1H).

^{13}C NMR (151 MHz, $CDCl_3$): δ 155.5, 151.3, 145.1, 141.6, 139.7, 139.2, 132.6, 129.0,

128.5, 127.7, 127.6, 127.5, 122.1, 113.8, 105.5, 91.8, 81.8, 78.7, 70.1, 67.3, 62.9, 52.8, 50.3, 49.8, 46.3, 41.7, 38.7, 38.3, 37.0, 35.8, 33.2, 32.9, 30.8, 28.3, 27.8, 27.6, 26.7, 20.8, 20.4, 18.6, 11.5.

HRMS (ESI-TOF): calc'd for $C_{47}H_{65}NO_7S$ $[M+Na]^+$: 810.4373, found: 810.4379.

Compound 2.117



A flame-dried 13x100 mm culture tube was charged with $Pd(OAc)_2$ (5.9 mg, 0.026 mmol, 1 eq.) and PPh_3 (27.6 mg, 0.105 mmol, 4 eq.) and backfilled with Ar. Freshly degassed DMF (1.6 mL, sonication + Ar bubbling for 1 h) was introduced and the mixture was vigorously stirred for 15 min until all solids dissolved. A solution of compound **2.155** (22.8 mg, 0.026 mmol, 1 eq.) in degassed DMF (1 mL) was added, and the resulting solution was heated to 120 °C for 2 h. Upon complete consumption of starting material by TLC analysis, the reaction was allowed to cool back to rt, diluted with H_2O (20 mL), and extracted with EtOAc (30 mL x3). The combined organic phases were washed with brine (20 mL), dried over Na_2SO_4, filtered, and concentrated *in vacuo*. The crude material was purified by pTLC (hexanes:EtOAc 4:1) to afford compound **2.117** (12.7 mg, 73%, single diastereomer).

Physical state: white foam

TLC: R_f = 0.4 (hexanes:EtOAc 4:1, UV and Seebach's magic stain)

$[\alpha]_{25}^{D}$: +66.5 (c = 0.19 in $CHCl_3$)

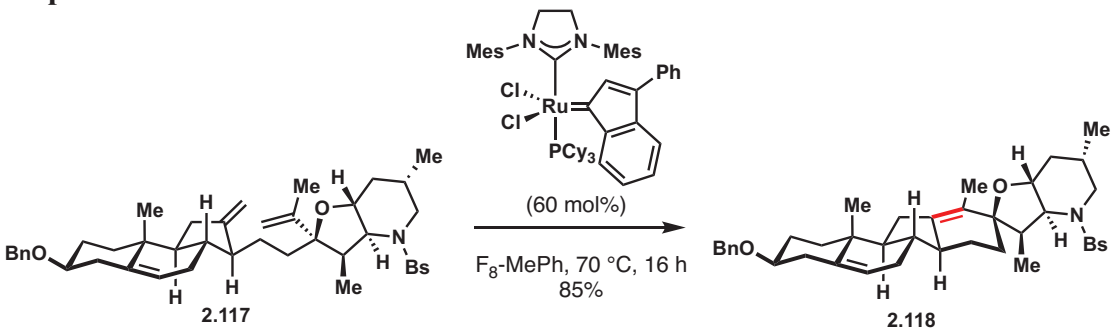
^{1}H NMR (600 MHz, $CDCl_3$): δ 7.71 – 7.68 (m, 2H), 7.65 – 7.61 (m, 1H), 7.54 (t, *J* = 7.8 Hz, 2H), 7.37 – 7.31 (m, 4H), 7.28 – 7.25 (m, 1H), 5.40 – 5.35 (m, 1H), 4.94 – 4.88 (m, 2H), 4.82 (s, 1H), 4.77 (s, 1H), 4.57 (s, 2H), 3.79 (ddd, *J* = 11.4, 9.7, 4.0 Hz, 1H), 3.56 (dd, *J* = 11.1, 3.6 Hz, 1H), 3.29 (tt, *J* = 11.1, 4.5 Hz, 1H), 2.87 (p, *J* = 6.6 Hz, 1H), 2.50 (ddd, *J* = 13.1, 4.8, 2.2 Hz, 1H), 2.35 – 2.23 (m, 4H), 2.13 (ddq, *J* = 15.3, 12.5, 2.8 Hz, 1H), 2.06 (dt, *J* = 11.8, 3.8 Hz, 1H), 2.02 – 1.93 (m, 2H), 1.81 – 1.75 (m, 2H), 1.74 (s, 3H), 1.73 – 1.68 (m, 2H), 1.65 – 1.46 (m, 5H), 1.40 (dt, *J* = 12.8, 4.4 Hz, 1H), 1.35 (dd, *J* = 12.3, 7.1

Hz, 1H), 1.32 (d, J = 6.9 Hz, 3H), 1.13 (td, J = 13.5, 3.8 Hz, 1H), 0.98 (s, 3H), 0.89 (d, J = 6.6 Hz, 3H), 0.80 (q, J = 11.6 Hz, 1H).

^{13}C NMR (151 MHz, $CDCl_3$): δ 155.3, 148.6, 141.8, 139.1, 133.5, 133.3, 129.0, 128.7, 128.5, 127.7, 127.6, 122.1, 111.7, 105.3, 89.6, 78.7, 75.8, 70.1, 63.1, 56.3, 52.8, 50.2, 41.8, 41.4, 38.8, 38.3, 37.8, 37.1, 33.2, 32.9, 31.2, 29.0, 28.3, 27.1, 20.4, 18.8, 18.7, 10.2.

HRMS (ESI-TOF): calc'd for $C_{42}H_{55}NO_4S$ $[M+H]^+$: 670.3925, found: 670.3922.

Compound 2.118



A flame-dried 13x100 mm culture tube was backfilled with Ar three times and charged with compound **2.117** (12.7 mg, 0.019 mmol, 1 eq.), followed by a fine suspension (sonicate if needed) of the Ru catalyst (10.8 mg, 0.011 mmol, 60 mol %) in freshly degassed perfluorotoluene (2 mL, sonication + Ar bubbling for 1 h). The mixture was heated to 70 °C for 16 h under vigorous stirring. Upon complete consumption of starting material by TLC analysis, the reaction was cooled down to rt and quenched by addition of ethyl vinyl ether (1 mL). The resulting solution was directly concentrated *in vacuo*, and the crude material was purified by pTLC (hexanes:EtOAc = 5:1) to afford compound **2.118** (10.4 mg, 85%). All NMR data matched Giannis's report of the same intermediate.[12]

Physical state: white solid

TLC: R_f = 0.3 (hexanes:EtOAc 5:1, UV and Seebach's magic stain)

Melting point: 152-155 °C

$[\alpha]_{25}^{D}$: +83.1 (c = 0.42 in $CHCl_3$)

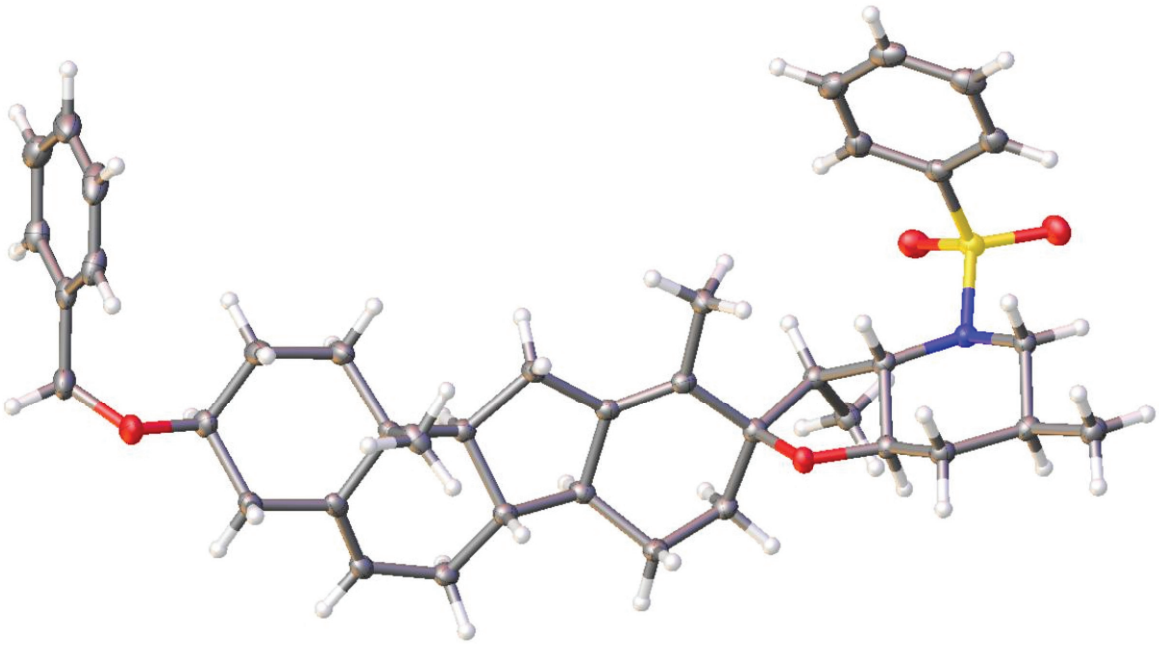
^{1}H NMR (600 MHz, $CDCl_3$): δ 7.84 – 7.79 (m, 2H), 7.69 – 7.64 (m, 1H), 7.58 (t, J = 7.8 Hz, 2H), 7.37 – 7.31 (m, 4H), 7.29 – 7.25 (m, 1H), 5.39 – 5.34 (m, 1H), 4.57 (s, 2H), 3.60 – 3.52 (m, 2H), 3.30 (tt, J = 11.2, 4.5 Hz, 1H), 2.87 (p, J = 6.9 Hz, 1H), 2.53 – 2.44 (m,

2H), 2.31 – 2.21 (m, 3H), 2.14 (dd, J = 17.3, 11.3 Hz, 1H), 2.03 – 1.90 (m, 3H), 1.81 (dq, J = 12.0, 4.0 Hz, 1H), 1.78 – 1.67 (m, 5H), 1.61 (d, J = 2.4 Hz, 3H), 1.64 – 1.53 (m, 2H), 1.40 (td, J = 11.5, 8.6 Hz, 1H), 1.36 (d, J = 7.0 Hz, 3H), 1.35 – 1.22 (m, 2H), 1.17 (td, J = 13.7, 3.7 Hz, 1H), 0.94 (s, 3H), 0.91 (d, J = 5.8 Hz, 3H), 0.80 (q, J = 11.5 Hz, 1H).

^{13}C NMR (151 MHz, $CDCl_3$): δ 144.1, 141.9, 139.1, 133.8, 133.5, 129.1, 129.1, 128.5, 127.7, 127.6, 126.3, 121.9, 84.7, 78.7, 74.1, 70.1, 64.9, 56.6, 52.2, 49.4, 42.6, 41.7, 38.8, 38.3, 37.1, 37.0, 33.6, 31.2, 29.3, 28.9, 28.3, 24.8, 18.9, 18.8, 13.9, 11.5.

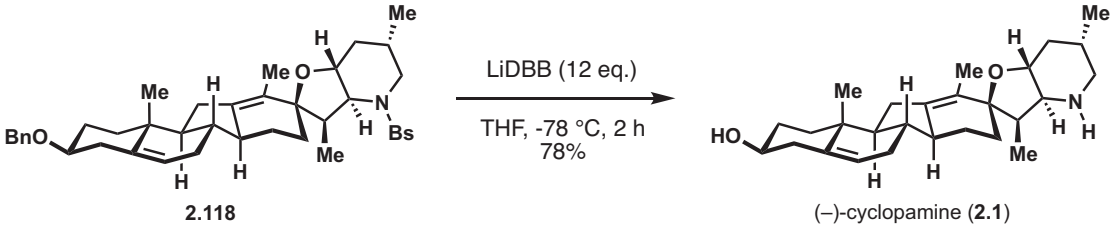
HRMS (ESI-TOF): calc'd for $C_{40}H_{51}NO_4S$ $[M+H]^+$: 642.3612, found: 642.3616.

X-ray crystallography structure:



(See **X-Ray Crystallography Data** for full report)

(–)-Cyclopamine (2.1)



A flame-dried 13x100 mm culture tube was backfilled with Ar three times and charged with a solution of compound **2.118** (5.0 mg, 7.8 μmol, 1 eq.) in THF (0.7 mL). The reaction was cooled to -78 °C, and freshly prepared LiDBB solution[13] (ca. 0.17 M in THF, 0.23 mL, 39 μmol, 5 eq.) was slowly added dropwise. Upon complete addition, a dark-green color developed in the reaction mixture but faded after ca. 3 min. At this point, small portions of additional LiDBB solution were added every 5 min, adding up to a total of 0.32 mL (54.4 μmol, 7 eq.) over 45 min. Upon complete addition the dark-green color persisted in the reaction. The resulting mixture was allowed to stir for 1 h at -78 °C, and then quenched with addition of sat. aq. $NaHCO_3$ (2 mL). The mixture was extracted with DCM (3 mL x5), and the combined organic layers were dried over Na_2SO_4, filtered, and concentrated *in vacuo*. The crude material was purified by pTLC (DCM:MeOH:Et_3N 10:1:0.05) to afford (–)-cyclopamine (**2.1**) (2.5 mg, 78%).

[Note: In most cases we observed rapid Bs deprotection (<10 min) but much slower Bn deprotection, which was why additional LiDBB was used to drive the reaction to completion. Care was also taken to maintain the temperature at -78 °C. No allylic ether cleavage was observed under these conditions.]

Physical state: white solid

TLC: R_f = 0.3 (DCM:MeOH:Et_3N 10:1:0.05, Seebach's magic stain)

Melting point: 228-232 °C

$[\alpha]_{25}^{D}$: -79.0 (c = 0.2 in $CHCl_3$)

^{1}H NMR (600 MHz, CD_2Cl_2): δ 5.37 (dt, *J* = 4.6, 2.0 Hz, 1H), 3.47 (tt, *J* = 11.1, 4.6 Hz, 1H), 3.19 (td, *J* = 10.3, 3.8 Hz, 1H), 3.04 (dd, *J* = 12.6, 3.8 Hz, 1H), 2.62 (t, *J* = 9.2 Hz, 1H), 2.41 (p, *J* = 7.7 Hz, 1H), 2.34 (ddd, *J* = 13.1, 4.8, 2.3 Hz, 1H), 2.31 – 2.20 (m, 3H), 2.20 – 2.07 (m, 3H), 1.85 (ddd, *J* = 13.7, 4.1, 2.4 Hz, 1H), 1.82 – 1.75 (m, 2H), 1.75 – 1.65

(m, 3H), 1.61 (s, 3H), 1.60 – 1.55 (m, 1H), 1.54 – 1.44 (m, 2H), 1.41 (td, *J* = 11.4, 8.7 Hz, 1H), 1.31 – 1.27 (m, 1H), 1.26 – 1.15 (m, 2H), 1.11 (q, *J* = 11.4 Hz, 1H), 0.96 (s, 3H), 0.92 (d, *J* = 6.7 Hz, 3H), 0.91 (d, *J* = 7.6 Hz, 3H).

^{13}C NMR (151 MHz, CD_2Cl_2): δ 142.7, 142.2, 127.3, 122.1, 85.5, 75.7, 72.1, 66.6, 54.9, 52.5, 49.5, 42.3, 42.3, 40.1, 39.4, 38.6, 36.9, 32.2, 31.9, 31.8, 31.5, 29.2, 25.0, 19.0, 18.8, 13.2, 10.9.

^{1}H NMR (600 MHz, $CDCl_3$): δ 5.41 – 5.34 (m, 1H), 3.53 (tt, *J* = 11.2, 4.6 Hz, 1H), 3.25 (td, *J* = 10.3, 3.8 Hz, 1H), 3.09 (dd, *J* = 12.8, 4.2 Hz, 1H), 2.67 (t, *J* = 9.2 Hz, 1H), 2.47 (p, *J* = 7.7 Hz, 1H), 2.37 (ddd, *J* = 13.9, 5.3, 2.7 Hz, 1H), 2.33 (t, *J* = 12.2 Hz, 1H), 2.28 – 2.12 (m, 5H), 1.90 (ddd, *J* = 13.7, 4.0, 2.3 Hz, 1H), 1.87 – 1.77 (m, 2H), 1.77 – 1.66 (m, 3H), 1.64 (s, 3H), 1.63 – 1.58 (m, 1H), 1.57 – 1.46 (m, 2H), 1.43 – 1.36 (m, 1H), 1.36 – 1.27 (m, 2H), 1.23 – 1.15 (m, 2H), 0.96 (d, *J* = 7.5 Hz, 3H), 0.95 – 0.92 (m, 6H).

^{13}C NMR (151 MHz, $CDCl_3$): δ 143.1, 141.8, 126.7, 122.0, 85.6, 75.4, 71.9, 66.2, 54.6, 52.2, 49.4, 41.9, 41.7, 39.7, 39.2, 38.3, 36.7, 32.1, 31.6, 31.5, 31.3, 29.1, 24.7, 19.0, 18.8, 13.3, 10.9.

HRMS (ESI-TOF): calc'd for $C_{27}H_{41}NO_2$ $[M+H]^+$: 412.3216, found: 412.3225.

Spectra Comparison Between Synthetic and Natural Cyclopamine

^{1}H Spectra Comparison in CD_2Cl_2

^{1}H NMR (δ) Literature report[12] (400 MHz, CD_2Cl_2)	**^{1}H NMR (δ)** Authentic sample* (600 MHz, CD_2Cl_2)	**^{1}H NMR (δ)** Synthetic sample (600 MHz, CD_2Cl_2)	**Deviation (ppm)**†
5.40 (m, 1H)	5.37 (dt, *J* = 4.6, 2.0 Hz, 1H)	5.37 (dt, *J* = 4.6, 2.0 Hz, 1H)	0
3.50 (tt, *J* = 11.2, 4.0 Hz, 1H)	3.47 (tt, *J* = 11.2, 4.6 Hz, 1H)	3.47 (tt, *J* = 11.1, 4.6 Hz, 1H)	0
3.18 (ddd, *J* = 10.8, 9.7, 3.9 Hz, 1H)	3.15 (td, *J* = 10.4, 3.9 Hz, 1H)	3.19 (td, *J* = 10.3, 3.8 Hz, 1H)	+0.04
3.03 (ddd, *J* = 12.4, 4.2, 1.1 Hz, 1H)	3.00 (dd, *J* = 12.5, 3.9 Hz, 1H)	3.04 (dd, *J* = 12.6, 3.8 Hz, 1H)	+0.04
2.62 (t, *J* = 8.8 Hz, 1H)	2.59 (t, *J* = 9.2 Hz, 1H)	2.62 (t, *J* = 9.2 Hz, 1H)	+0.03
2.41 (p, *J* = 7.6 Hz, 1H)	2.38 (p, *J* = 7.9 Hz, 1H)	2.41 (p, *J* = 7.7 Hz, 1H)	+0.03
2.37 (ddd, *J* = 10.8, 4.8, 2.2 Hz, 1H	2.34 (ddd, *J* = 13.0, 4.9, 2.3 Hz, 1H)	2.34 (ddd, *J* = 13.1, 4.8, 2.3 Hz, 1H)	0
2.27 (m, 3H)	2.28 – 2.20 (m, 3H)	2.31 – 2.20 (m, 3H)	+0.02 (center)
2.23 (m, 1H)	2.20 – 2.06 (m, 3H)	2.20 – 2.07 (m, 3H)	+0.01 (center)
2.18 (m, 1H)			
2.11 (m, 1H)			
1.89 (m, 1H)	1.84 (ddd, *J* = 13.6, 4.1, 2.4 Hz, 1H)	1.85 (ddd, *J* = 13.7, 4.1, 2.4 Hz, 1H)	+0.01 (center)
1.83 (m, 1H)	1.82 – 1.75 (m, 2H)	1.82 – 1.75 (m, 2H)	0
1.81 (m, 1H)			
1.78 (m, 1H)	1.75 – 1.65 (m, 3H)	1.75 – 1.65 (m, 3H)	0
1.76 (m, 1H)			
1.72 (m, 1H)			
1.64 (s, 3H)	1.61 (s, 3H)	1.61 (s, 3H)	0
1.58 (m, 1H)	1.57 – 1.44 (m, 3H)	1.60 – 1.44 (m, 3H)	+0.02 (center)
1.55 (m, 1H)			
1.51 (m, 1H)			
1.44 (m, 1H)	1.41 (td, *J* = 11.5, 8.7 Hz, 1H)	1.41 (td, *J* = 11.4, 8.7 Hz, 1H)	0
1.31 (m, 1H)	1.30 – 1.25 (m, 1H)	1.31 – 1.27 (m, 1H)	+0.02 (center)
1.25 (m, 1H)	1.25 – 1.16 (m, 2H)	1.26 – 1.15 (m, 2H)	+0.01 (center)
1.23 (m, 1H)			
1.13 (m, 1H)	1.10 (q, *J* = 11.4 Hz, 1H)	1.11 (q, *J* = 11.4 Hz, 1H)	+0.01
1.00 (s, 3H)	0.96 (s, 3H)	0.96 (s, 3H)	0
0.94 (d, *J* = 5.2 Hz, 3H)	0.91 (d, J = 7.0 Hz, 3H)	0.92 (d, *J* = 6.7 Hz, 3H)	+0.01
0.92 (d, *J* = 5.6 Hz, 3H)	0.89 (d, J = 7.8 Hz, 3H)	0.91 (d, *J* = 7.6 Hz, 3H)	+0.02

* Natural cyclopamine was purchased from AdipoGen Life Sciences or Cayman Chemical Company.

† Between authentic and synthetic samples.

^{13}C Spectra Comparison in CD_2Cl_2

^{13}C NMR (δ) Literature report[12] (400 MHz, CD_2Cl_2)	**^{13}C NMR (δ)** Authentic sample* (600 MHz, CD_2Cl_2)	**^{13}C NMR (δ)** Synthetic sample (600 MHz, CD_2Cl_2)	**Deviation (ppm)**†
142.2	142.6	142.7	+0.1
141.9	142.3	142.2	–0.1
127.0	127.4	127.3	–0.1
121.7	122.1	122.2	+0.1
85.0	85.4	85.5	+0.1
75.6	75.9	75.7	–0.2
71.7	72.1	72.1	0
66.5	66.9	66.6	–0.3
54.9	55.2	54.9	–0.3
52.1	52.5	52.5	0
49.1	49.5	49.5	0
41.9	42.3	42.3	0
41.9	42.3	42.3	0
39.9	40.3	40.1	–0.2
39.2	39.5	39.4	–0.1
38.2	38.6	38.6	0
36.5	36.9	36.9	0
31.9	32.2	32.2	0
31.7	32.0	31.9	–0.1
31.5	31.9	31.8	–0.1
31.1	31.5	31.5	0
28.8	29.2	29.2	0
24.7	25.1	25.0	–0.1
18.7	19.1	19.0	–0.1
18.4	18.8	18.8	0
12.8	13.2	13.2	0
10.4	10.8	10.9	+0.1

* Natural cyclopamine was purchased from AdipoGen Life Sciences and Cayman Chemical Company.

† Between authentic and synthetic samples.

^{1}H Spectra Comparison in $CDCl_3$

^{1}H NMR (δ) Authentic sample* (600 MHz, $CDCl_3$)	**^{1}H NMR (δ)** Synthetic sample (600 MHz, $CDCl_3$)	**Deviation (ppm)**
5.40 – 5.33 (m, 1H)	5.41 – 5.34 (m, 1H)	+0.01 (center)
3.53 (tt, *J* = 11.2, 4.6 Hz, 1H)	3.53 (tt, *J* = 11.2, 4.6 Hz, 1H)	0
3.24 (td, *J* = 10.4, 3.9 Hz, 1H)	3.25 (td, *J* = 10.3, 3.8 Hz, 1H)	+0.01
3.09 (dd, *J* = 12.7, 3.8 Hz, 1H)	3.09 (dd, *J* = 12.8, 4.2 Hz, 1H)	0
2.67 (t, *J* = 9.2 Hz, 1H)	2.67 (t, *J* = 9.2 Hz, 1H)	0
2.46 (p, *J* = 7.7 Hz, 1H)	2.47 (p, *J* = 7.7 Hz, 1H)	+0.01
2.37 (ddd, *J* = 13.1, 4.9, 2.3 Hz, 1H)	2.37 (ddd, *J* = 13.9, 5.3, 2.7 Hz, 1H)	0
2.33 (t, *J* = 12.0 Hz, 1H)	2.33 (t, *J* = 12.2 Hz, 1H)	0
2.28 – 2.12 (m, 5H)	2.28 – 2.12 (m, 5H)	0
1.90 (ddd, *J* = 13.7, 4.0, 2.3 Hz, 1H)	1.90 (ddd, *J* = 13.7, 4.0, 2.3 Hz, 1H)	0
1.86 – 1.77 (m, 2H)	1.87 – 1.77 (m, 2H)	+0.01 (center)
1.77 – 1.66 (m, 3H)	1.77 – 1.66 (m, 3H)	0
1.64 (s, 3H)	1.64 (s, 3H)	0
1.63 – 1.58 (m, 1H)	1.63 – 1.58 (m, 1H)	0
1.58 – 1.46 (m, 2H)	1.57 – 1.46 (m, 2H)	–0.01 (center)
1.39 (ddd, *J* = 12.1, 10.8, 8.5 Hz, 1H)	1.43 – 1.36 (m, 1H)	0
1.36 – 1.25 (m, 2H)	1.36 – 1.27 (m, 2H)	+0.01 (center)
1.23 – 1.14 (m, 2H)	1.23 – 1.15 (m, 2H)	+0.01 (center)
0.96 (d, *J* = 7.5 Hz, 3H)	0.96 (d, *J* = 7.5 Hz, 3H)	0
0.94 (d, *J* = 6.5 Hz, 3H)	0.95 – 0.92 (m, 6H)	0 (center)
0.93 (s, 3H)		

* Natural cyclopamine was purchased from AdipoGen Life Sciences and Cayman Chemical Company.

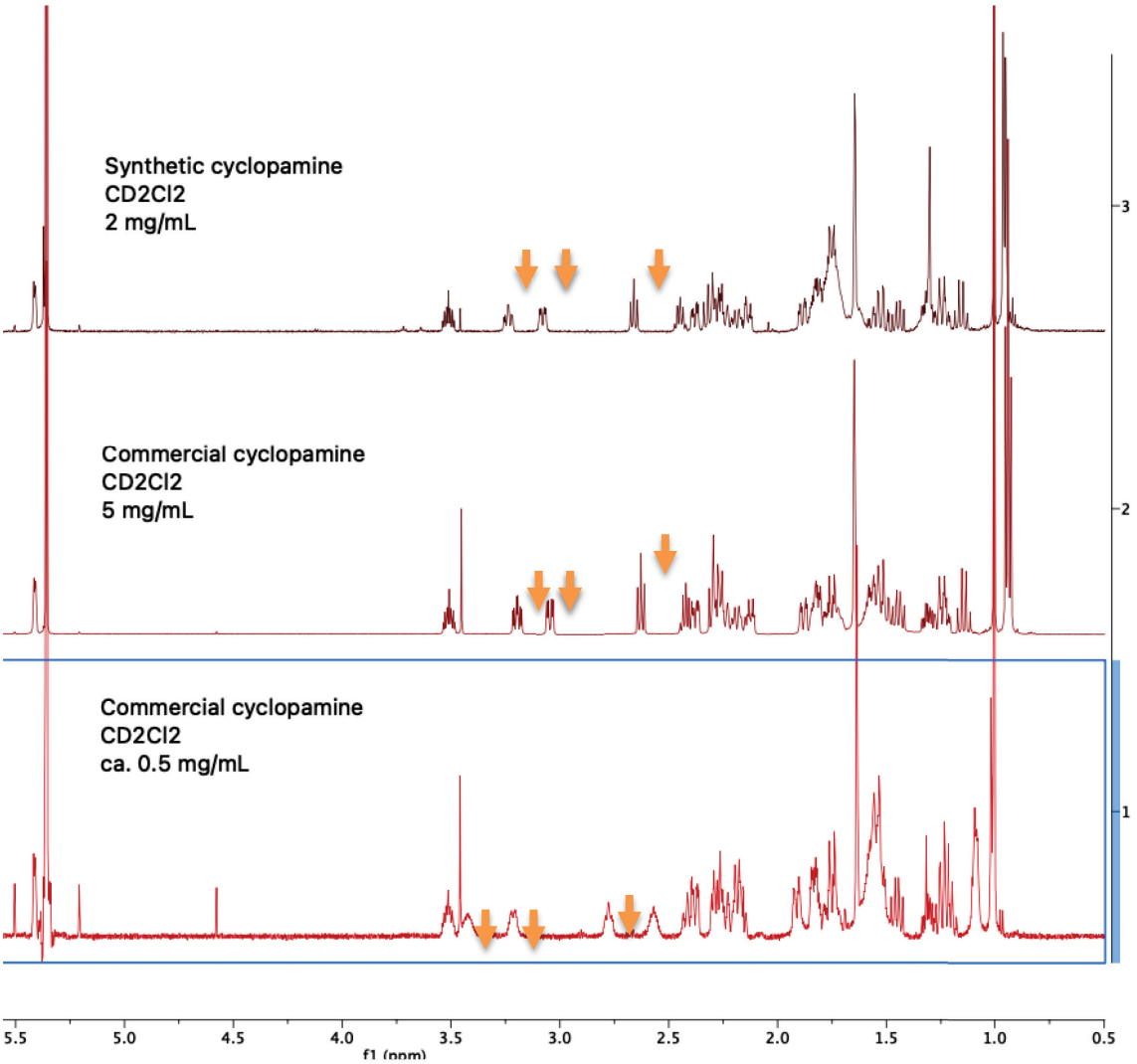
^{13}C Spectra Comparison in $CDCl_3$

^{13}C NMR (δ) Authentic sample* (600 MHz, $CDCl_3$)	**^{13}C NMR (δ)** Synthetic sample (600 MHz, $CDCl_3$)	**Deviation (ppm)**
143.1	143.1	0
141.8	141.8	0
126.8	126.7	–0.1
122.0	122.0	0
85.6	85.6	0
75.5	75.4	–0.1
72.0	71.9	–0.1
66.3	66.2	–0.1
54.8	54.6	–0.2
52.2	52.2	0
49.4	49.4	0
42.0	41.9	–0.1
41.7	41.7	0
39.8	39.7	–0.1
39.2	39.2	0
38.3	38.3	0
36.7	36.7	0
32.1	32.1	0
31.7	31.6	–0.1
31.5	31.5	0
31.3	31.3	0
29.1	29.1	0
24.7	24.7	0
19.0	19.0	0
18.8	18.8	0
13.3	13.3	0
10.9	10.9	0

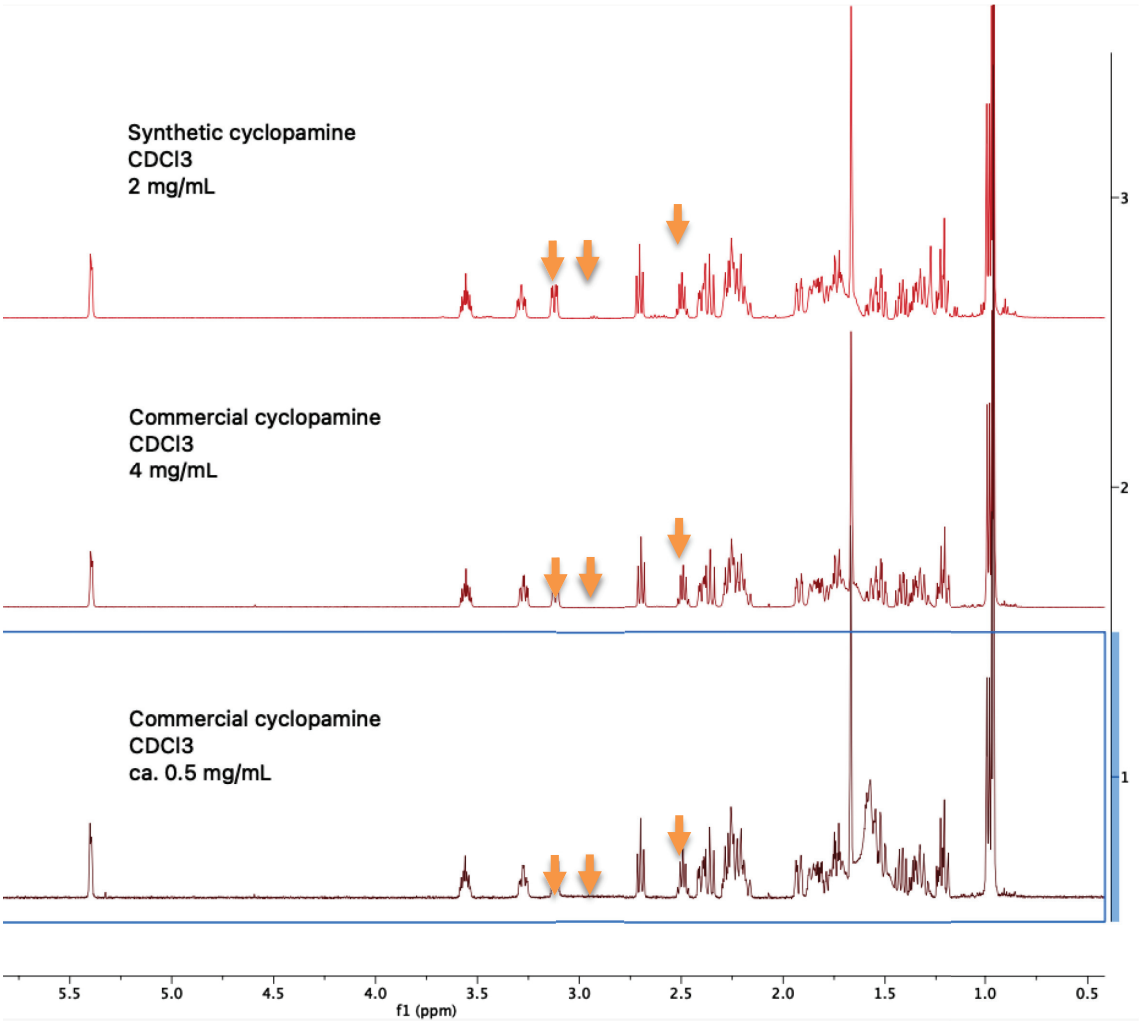
* Natural cyclopamine was purchased from AdipoGen Life Sciences and Cayman Chemical Company.

Discussion of Concentration Effect

Significant concentration dependence was observed in the NMR spectra of cyclopamine in CD_2Cl_2 (see below). This was likely caused by the poor CD_2Cl_2 solubility of cyclopamine, which started crashing out at concentrations above 4 mg/mL.

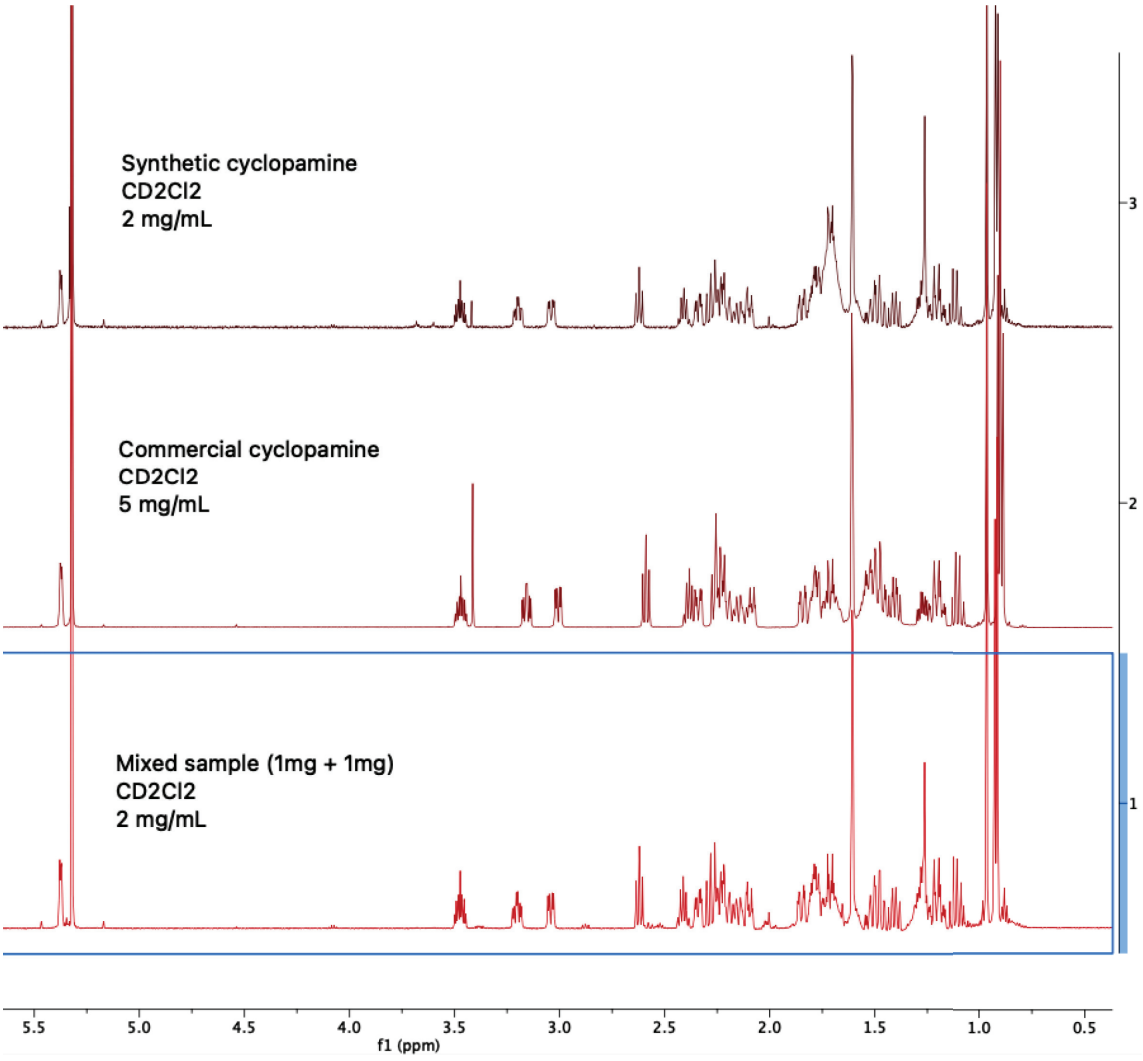


However, such concentration effect was negligible in $CDCl_3$ (see below), which was a better solvent for cyclopamine and formed uniform solutions up to ca. 10 mg/mL.



Mixed Sample (Authentic + Synthetic) Spectra in CD_2Cl_2

A mixed sample containing both synthetic and commercial cyclopamine (1 mg + 1 mg) in CD_2Cl_2 was prepared and its ^1H NMR spectrum measured (see below, 3rd row). The mixed sample produced a single set of peaks.



Chapter 2 Experimental References

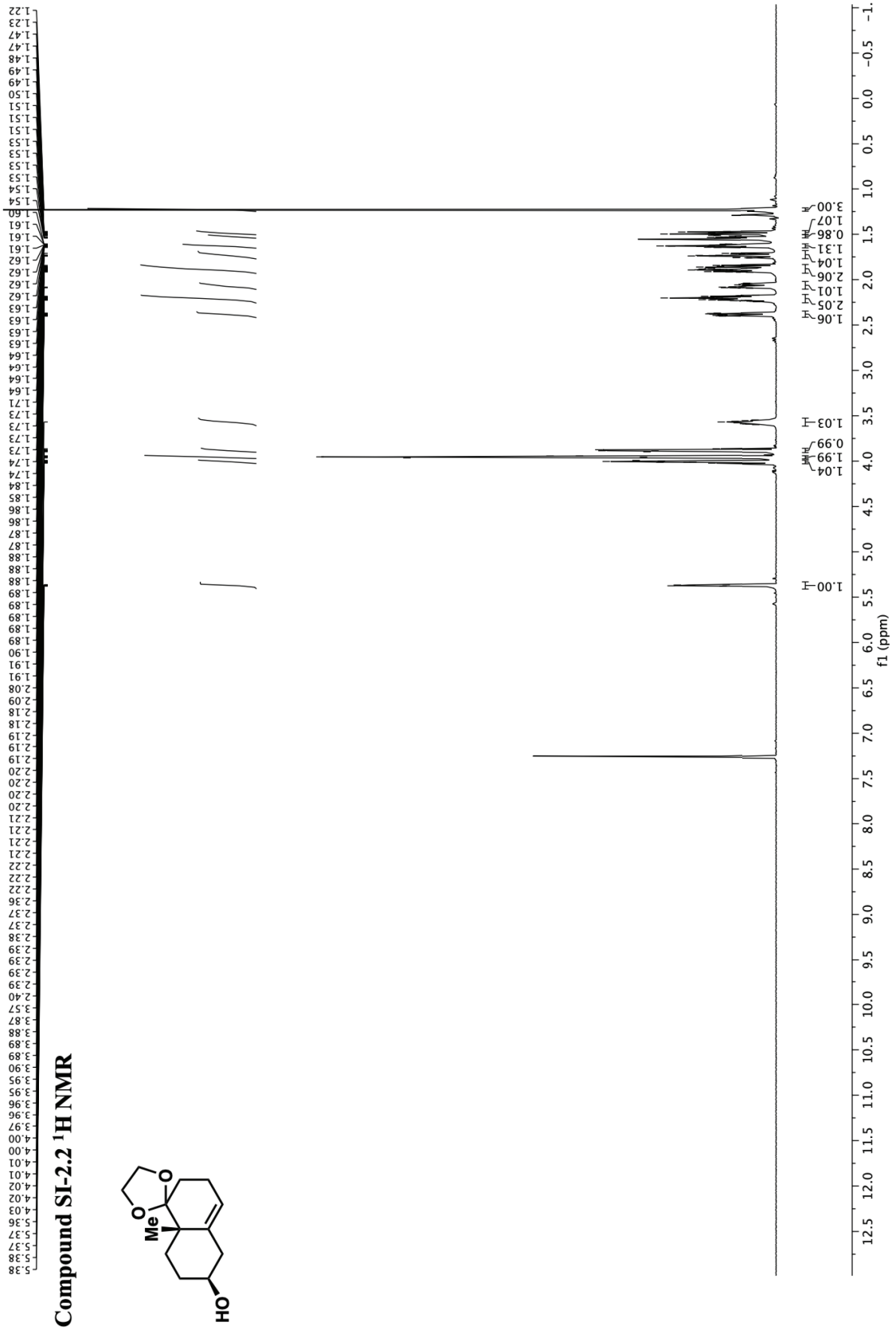
1. Gaich, T.; Baran, P. S., Aiming for the Ideal Synthesis. *J. Org. Chem.* **2010,** *75*, 4657-4673. b) Peters, D. S.; Pitts, C. R.; McClymont, K. S.; Stratton, T. P.; Bi, C.; Baran, P. S., Ideality in Context: Motivations for Total Synthesis. *Acc. Chem. Res.* **2021,** *54*, 605-617.
2. (a) Vizóquez, S. F.; Guillena, G.; Nájera, C.; Bradshaw, B.; Etxebarria-Jardi, G.; Bonjoch, J., (S a, S)-N-[2′-(4-Methylphenylsulfonamido)-1, 1′-Binaphthyl-2-Yl] Pyrrolidine-2-Carboxamide: An Organocatalyst for the Direct Aldol Reaction. *Org. Synth.* **2003,** *88*, 317-329. (b) Viózquez, S. F.; Guillena, G.; Nájera, C., Synthesis of (S)-8a-methyl-3, 4, 8, 8a-tetrahydro-1, 6-(2H, 7H)-naphthalenedione via N-tosyl-(Sa)- binam-L-prolinamide organocatalysis. *Org. Synth* **2011,** *88*, 330-341.
3. Karimov, R. R.; Tan, D. S.; Gin, D. Y., Synthesis of the hexacyclic triterpene core of the jujuboside saponins via tandem Wolff rearrangement–intramolecular ketene hetero-Diels–Alder reaction. *Tetrahedron* **2018,** *74*, 3370-3383.
4. Piers, E.; Abeysekera, B., Alkylation of enolate anions with dimethyl 3-bromo-2-ethoxypropenylphosphonate. A convergent cyclopentenone annulation method. *Can. J. Chem.* **1982,** *60*, 1114-1121.
5. Enomoto, M.; Morita, A.; Kuwahara, S., Total Synthesis of the Tremorgenic Indole Diterpene Paspalinine. *Angew. Chem. Int. Ed.* **2012,** *51*, 12833-12836.
6. (a) Baker, B. A.; Bošković, Ž. V.; Lipshutz, B. H., (BDP)CuH: A “Hot” Stryker's Reagent for Use in Achiral Conjugate Reductions. *Org. Lett.* **2008,** *10*, 289-292.

(b) Gao, A. X.; Hamada, T.; Snyder, S. A., The Enantioselective Total Synthesis of Exochomine. *Angew. Chem. Int. Ed.* **2016,** *55*, 10301-10306.

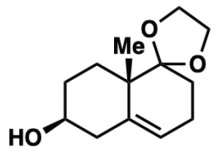
7. Kemppainen, E. K.; Sahoo, G.; Valkonen, A.; Pihko, P. M., Mukaiyama–Michael Reactions with Acrolein and Methacrolein: A Catalytic Enantioselective Synthesis of the C17–C28 Fragment of Pectenotoxins. *Org. Lett.* **2012,** *14*, 1086-1089.
8. Richard, F.; Aubert, S.; Katsina, T.; Reinalda, L.; Palomas, D.; Crespo-Otero, R.; Huang, J.; Leitch, D. C.; Mateos, C.; Arseniyadis, S., Enantioselective synthesis of γ-butenolides through Pd-catalysed C5-selective allylation of siloxyfurans. *Nat. Synth.* **2022,** *1*, 641-648.
9. Zalesskiy, S. S.; Ananikov, V. P., Pd2(dba)3 as a Precursor of Soluble Metal Complexes and Nanoparticles: Determination of Palladium Active Species for Catalysis and Synthesis. *Organometallics* **2012,** *31*, 2302-2309.
10. Feng, S.; Li, S.; Li, J.; Wei, J., Palladium-catalyzed annulation of N-alkoxy benzsulfonamides with arynes by C–H functionalization: access to dibenzosultams. *Org. Chem. Front.* **2019,** *6*, 517-522.
11. Yamamura, S.; Toda, M.; Hirata, Y., Modified Clemmensen reduction: cholestane. *Org. Synth.* **2003,** *53*, 86-86.
12. Giannis, A.; Heretsch, P.; Sarli, V.; Stößel, A., Synthesis of Cyclopamine Using a Biomimetic and Diastereoselective Approach. *Angew. Chem. Int. Ed.* **2009,** *48*, 7911-7914.
13. Hill, R. R.; Rychnovsky, S. D., Generation, Stability, and Utility of Lithium 4,4′-Di-tert-butylbiphenylide (LiDBB). *J. Org. Chem.* **2016,** *81*, 10707-10714.

NMR Spectra

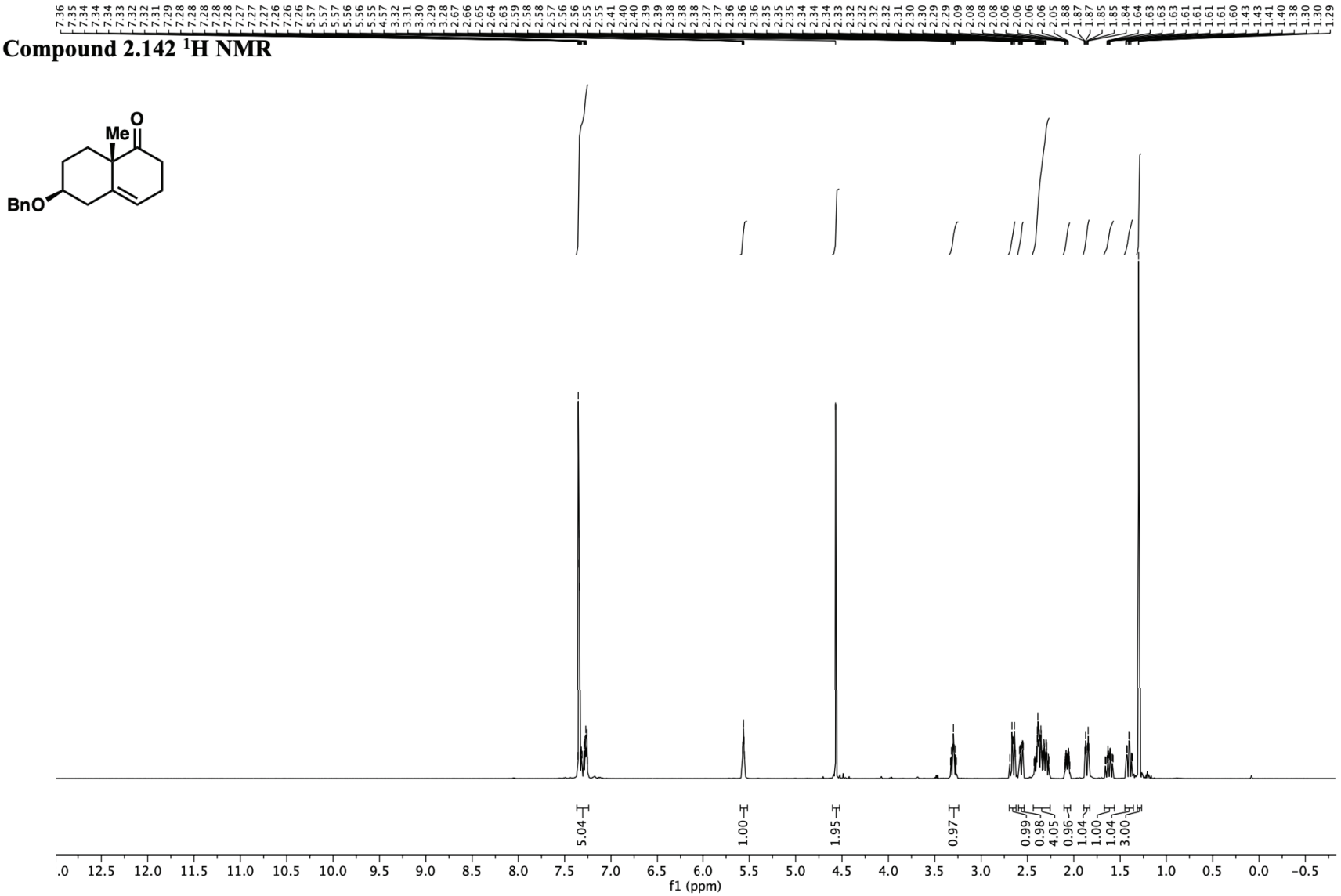
Compound SI-2.2 ^{1}H NMR



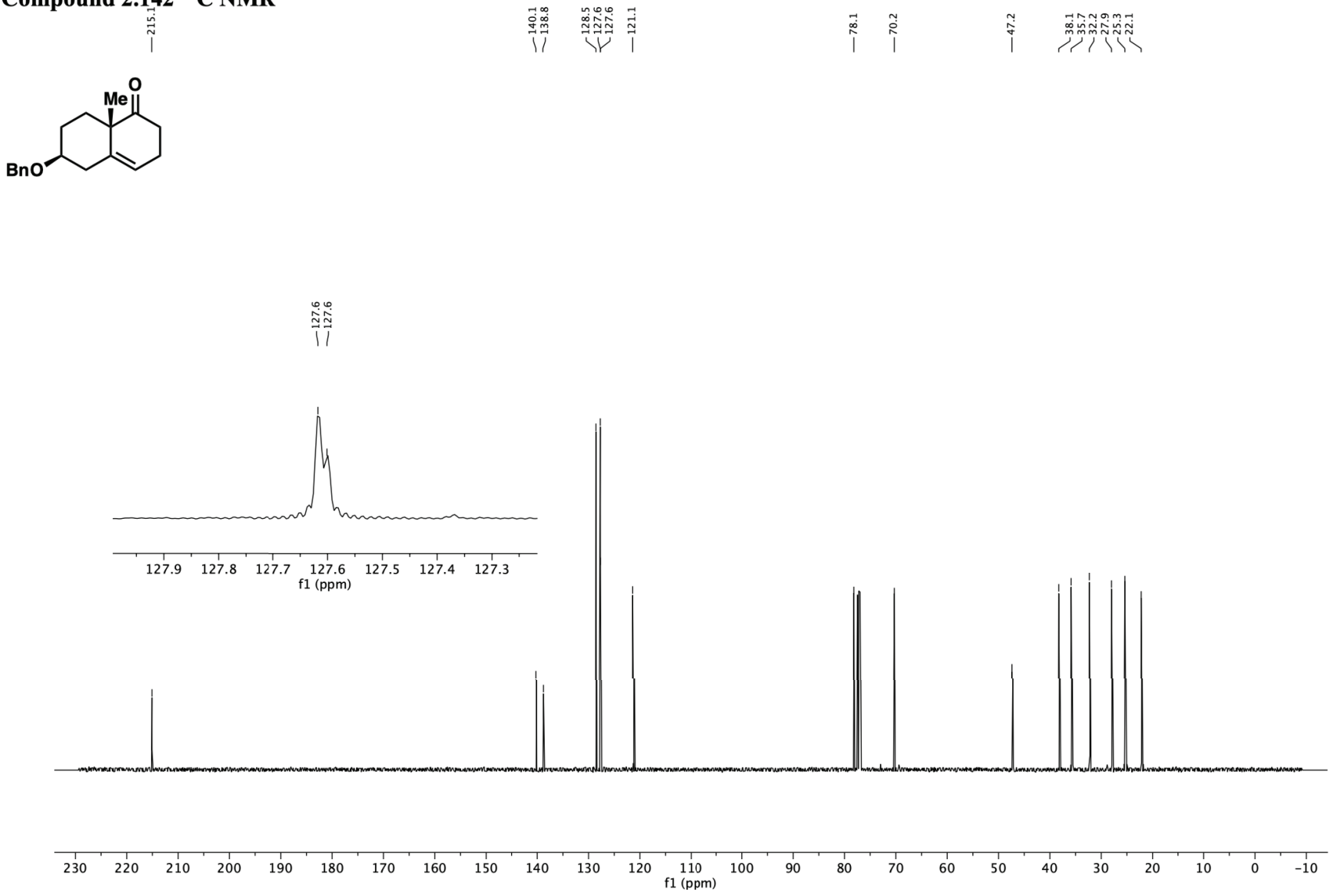
Compound SI-2.2 ^{13}C NMR



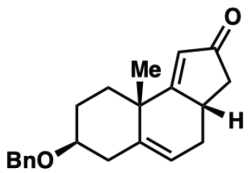
Compound 2.142 ^{1}H NMR



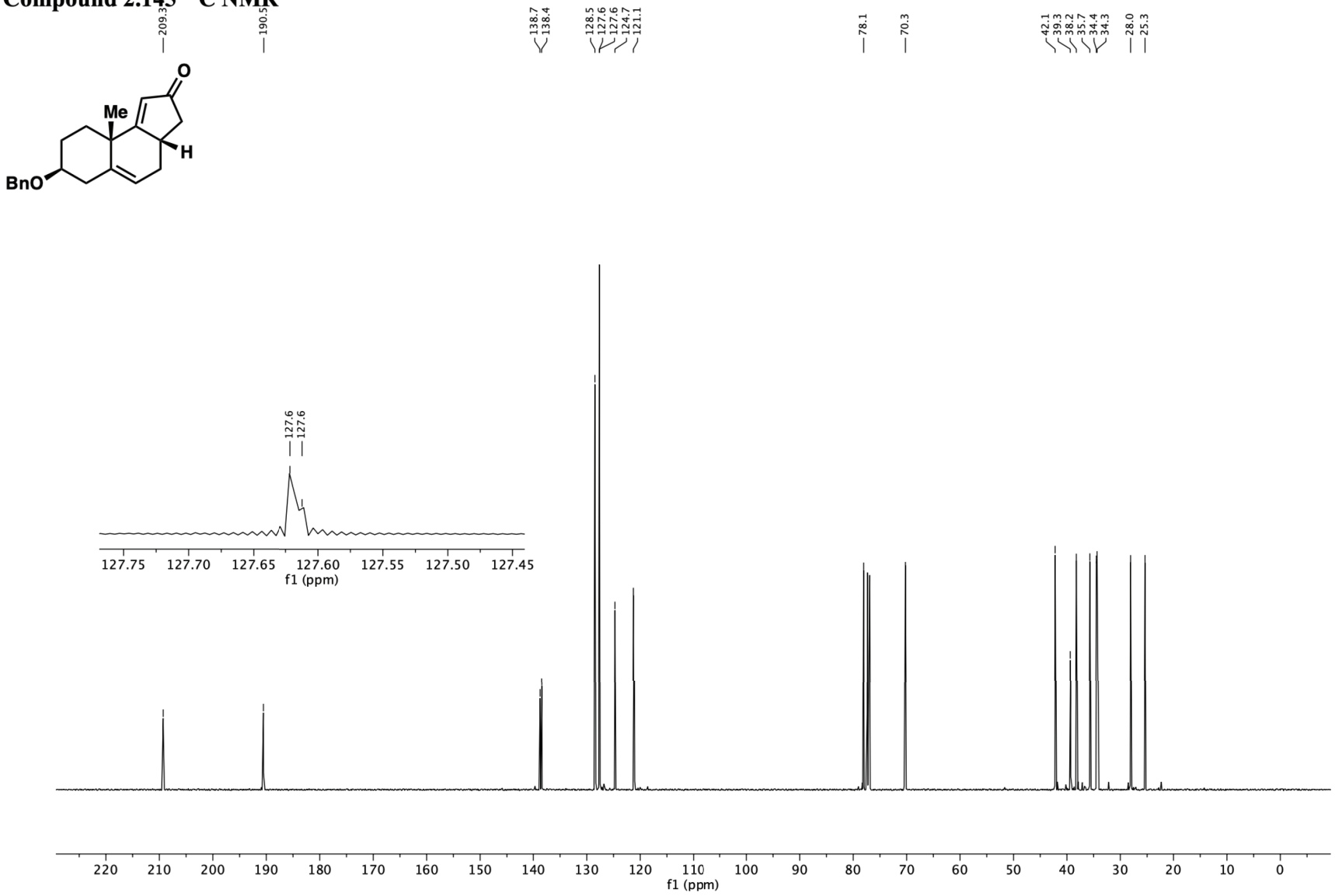
Compound 2.142 ^{13}C NMR



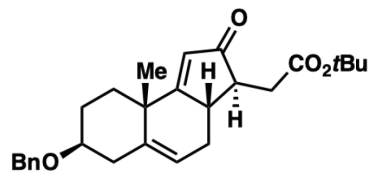
Compound 2.145 ^{1}H NMR



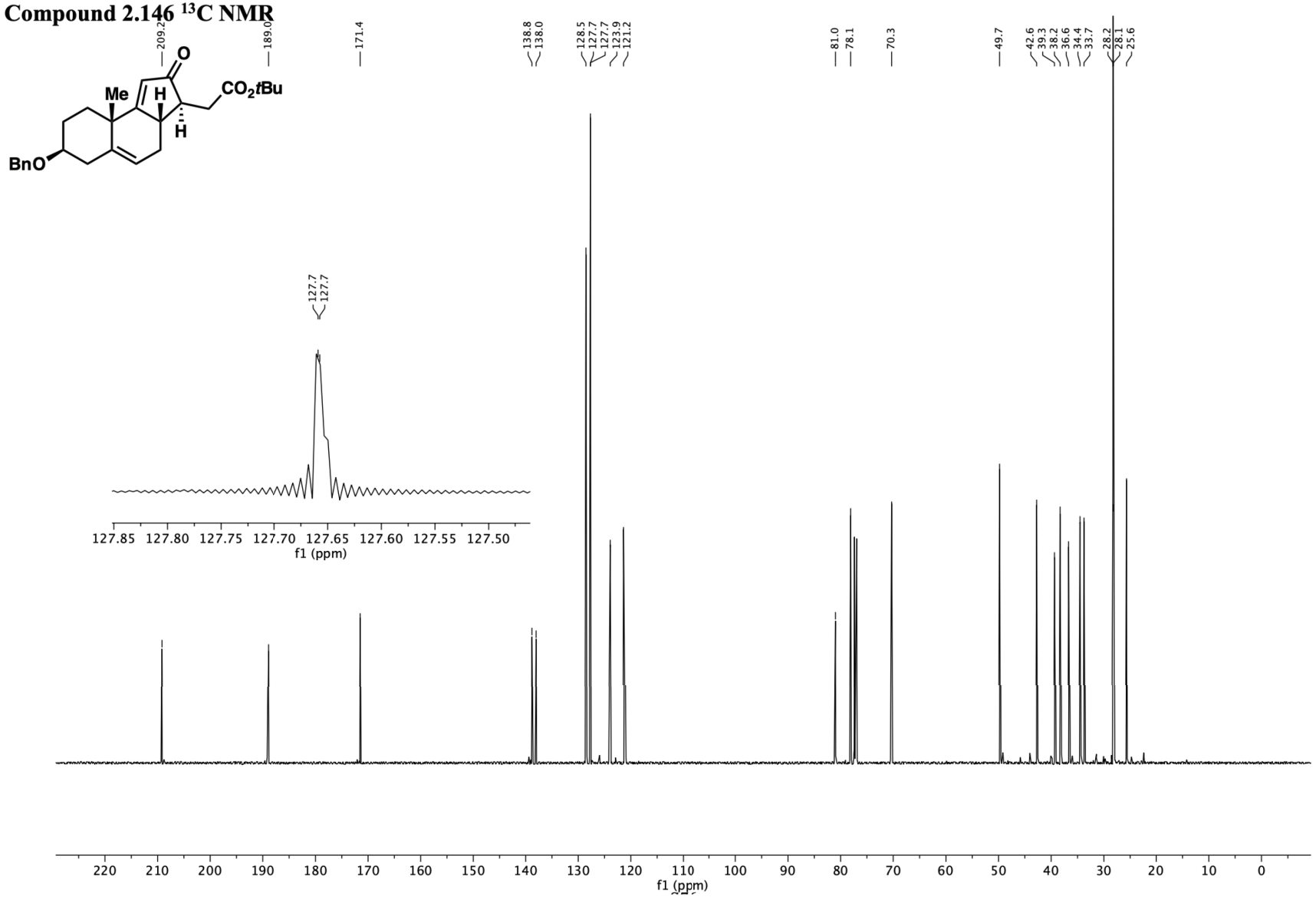
Compound 2.145 ^{13}C NMR



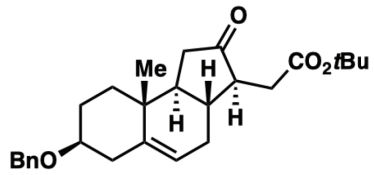
Compound 2.146 ^{1}H NMR



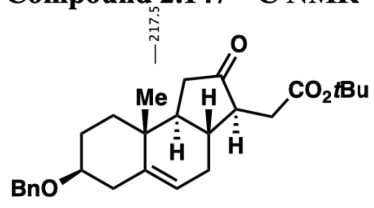
Compound 2.146 ^{13}C NMR



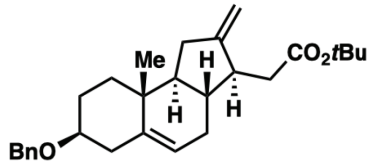
Compound 2.147 ^{1}H NMR



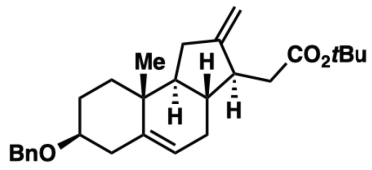
Compound 2.147 ^{13}C NMR



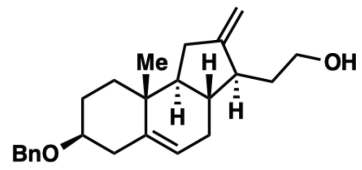
Compound SI-2.3 ^{1}H NMR



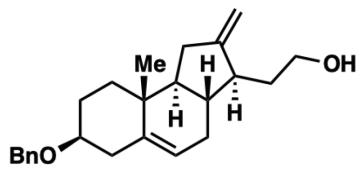
Compound SI-2.3 ^{13}C NMR



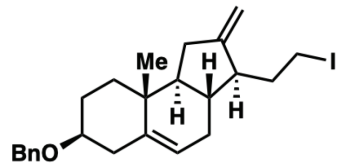
Compound SI-2.4 ^{1}H NMR



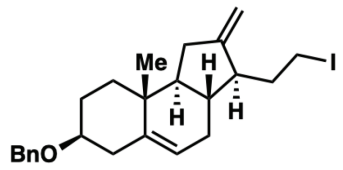
Compound SI-2.4 ^{13}C NMR



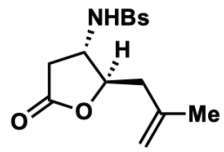
Compound 2.139 ^{1}H NMR

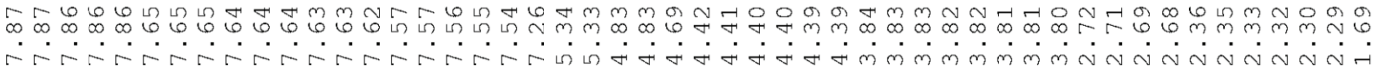


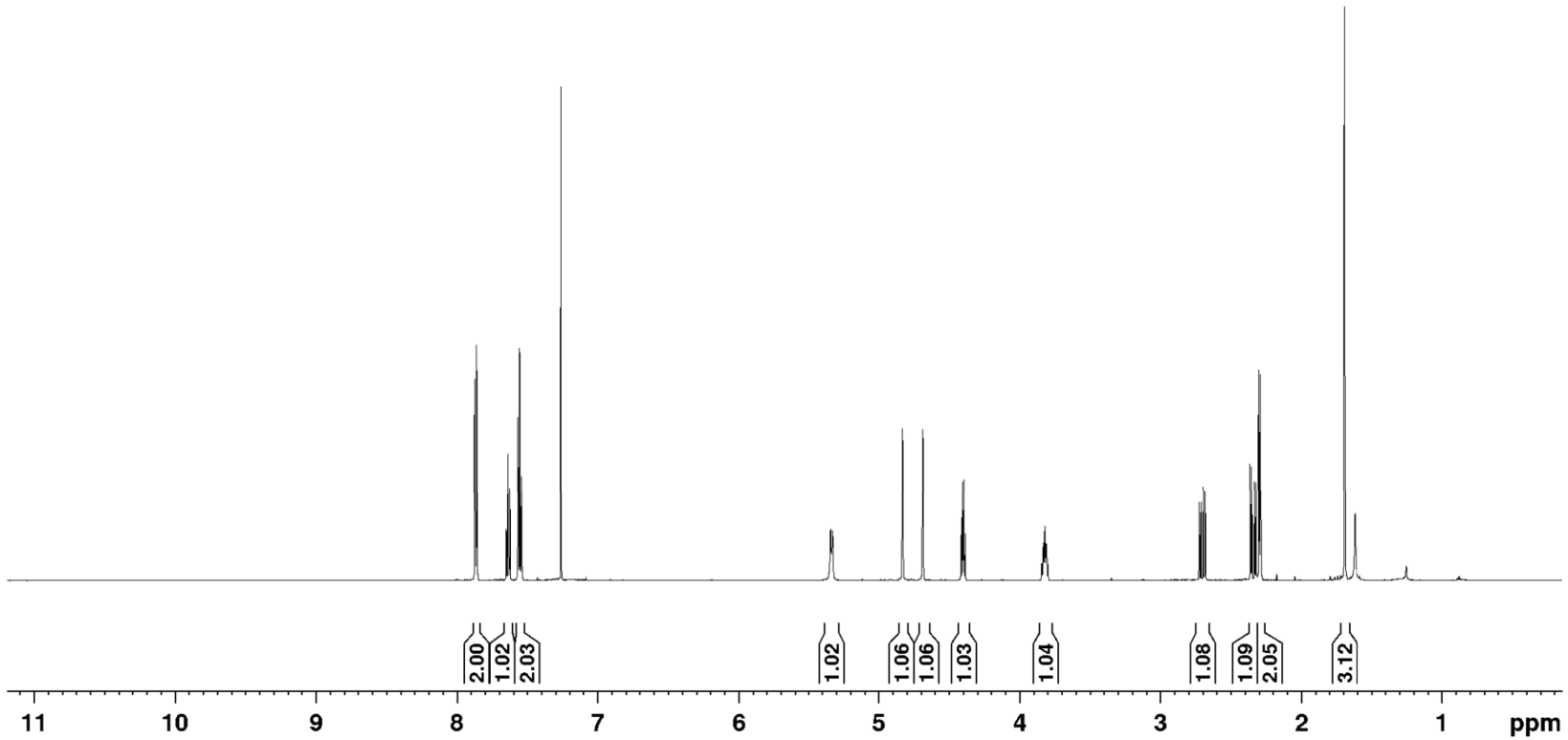
Compound 2.139 ^{13}C NMR



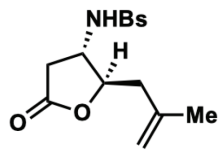
Compound 2.150 ^{1}H NMR



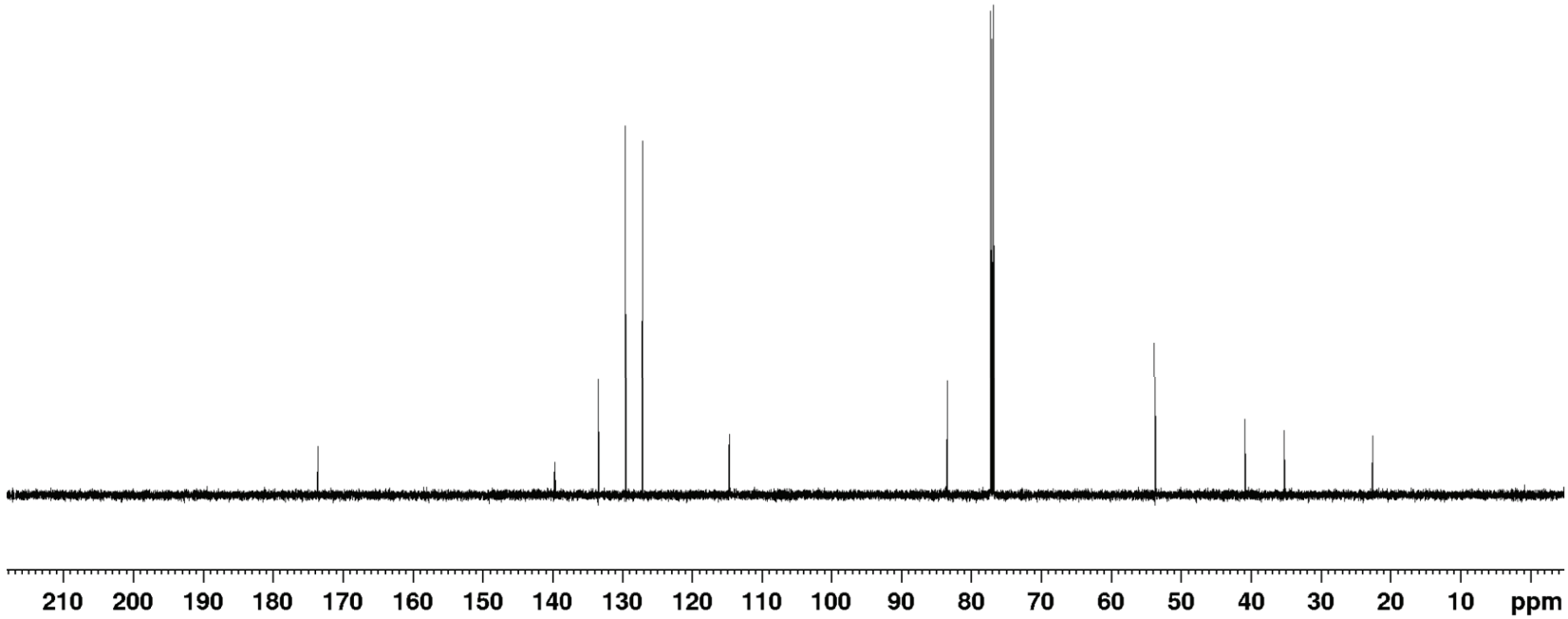




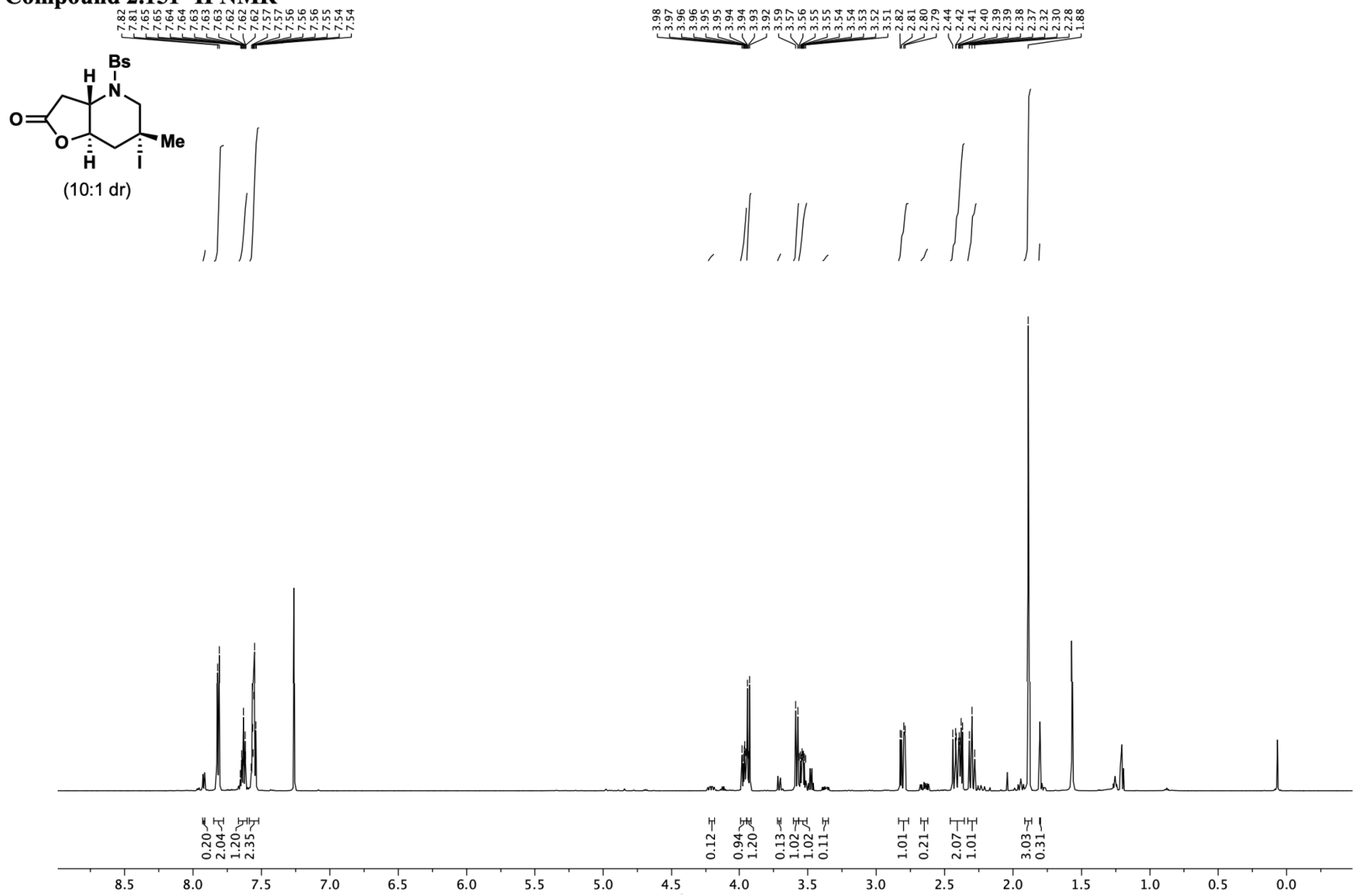
Compound 2.150 ^{13}C NMR



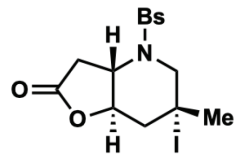
173.57
139.75
139.64
133.39
129.50
127.03
114.71
83.36
77.21
77.00
76.79
53.79
41.00
35.33
22.64



Compound 2.151 ^{1}H NMR

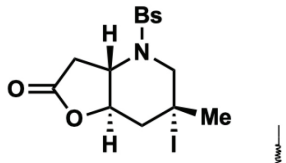


Compound 2.151 ^{13}C NMR

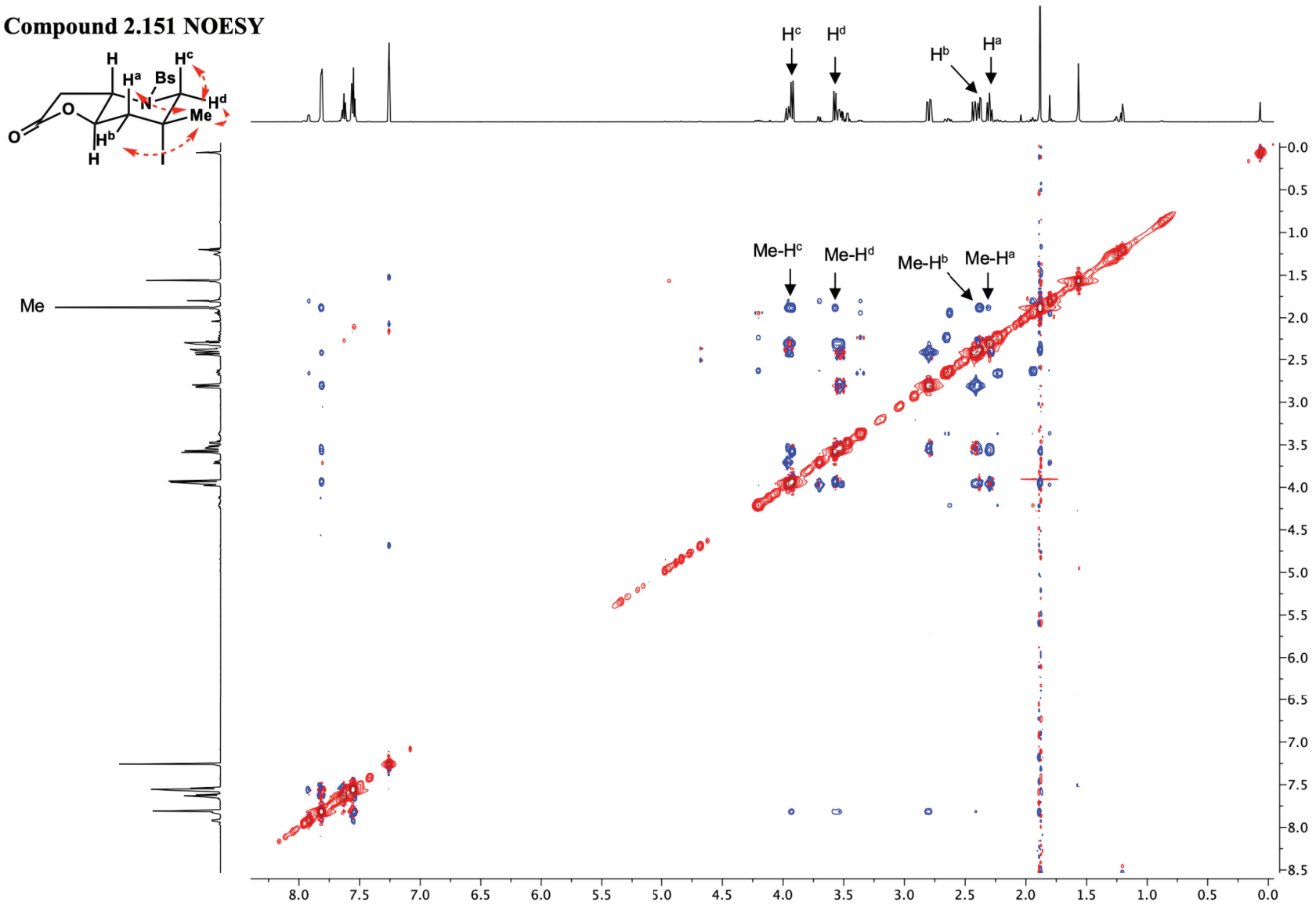


(10:1 dr)

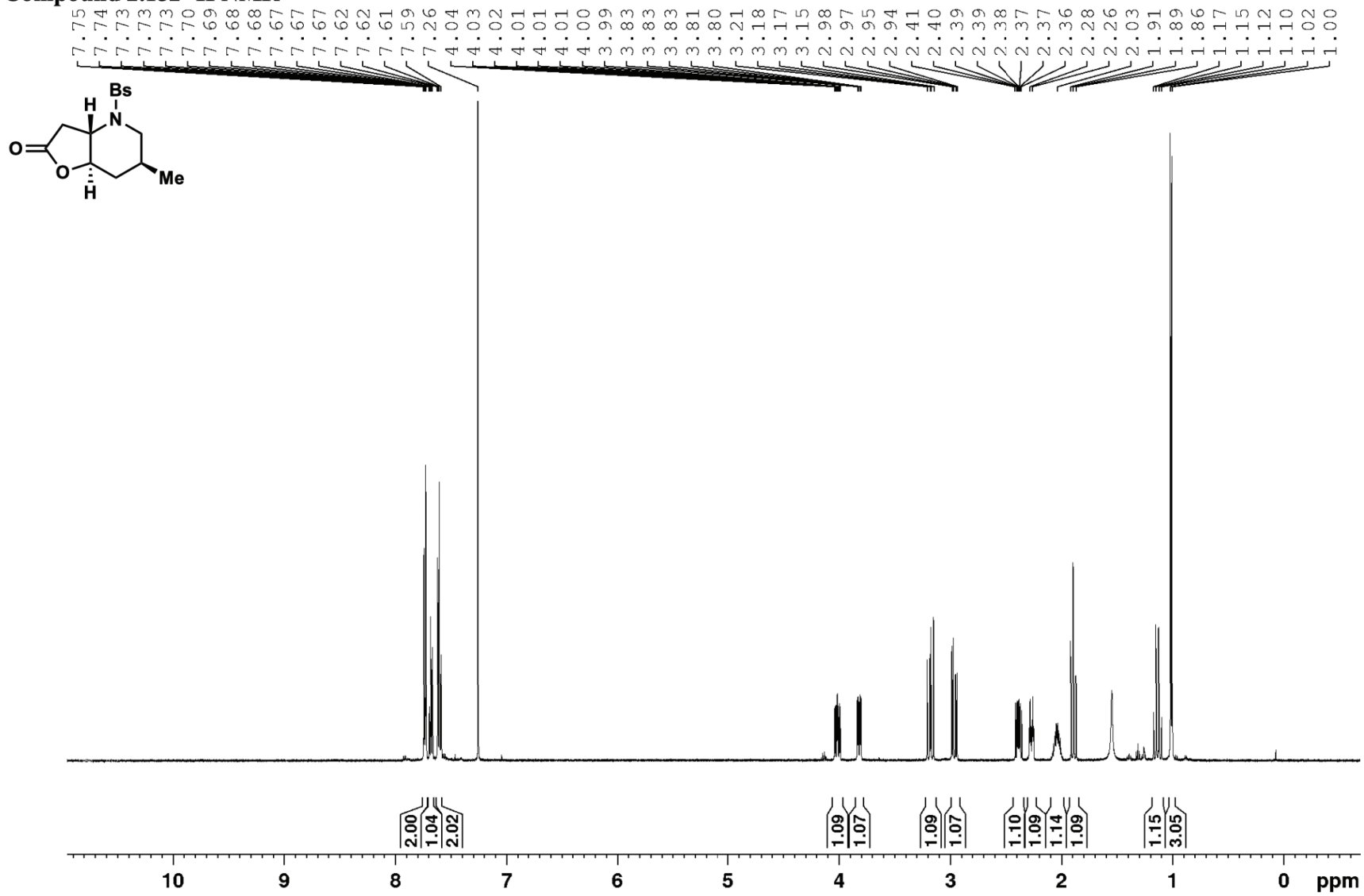
Compound 2.151 HSQC



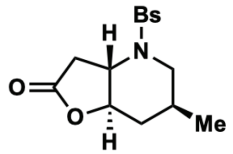
(10:1 dr)


Compound 2.151 NOESY
H
Ha
Bs
Hc
Hd
N
Me
O
O
Hb
H
I
Hc
Hd
Hb
Ha
Me
Me-Hc
Me-Hd
Me-Hb
Me-Ha
0.0
0.5
1.0
1.5
2.0
2.5
3.0
3.5
4.0
4.5
5.0
5.5
6.0
6.5
7.0
7.5
8.0
8.5
8.0
7.5
7.0
6.5
6.0
5.5
5.0
4.5
4.0
3.5
3.0
2.5
2.0
1.5
1.0
0.5
0.0

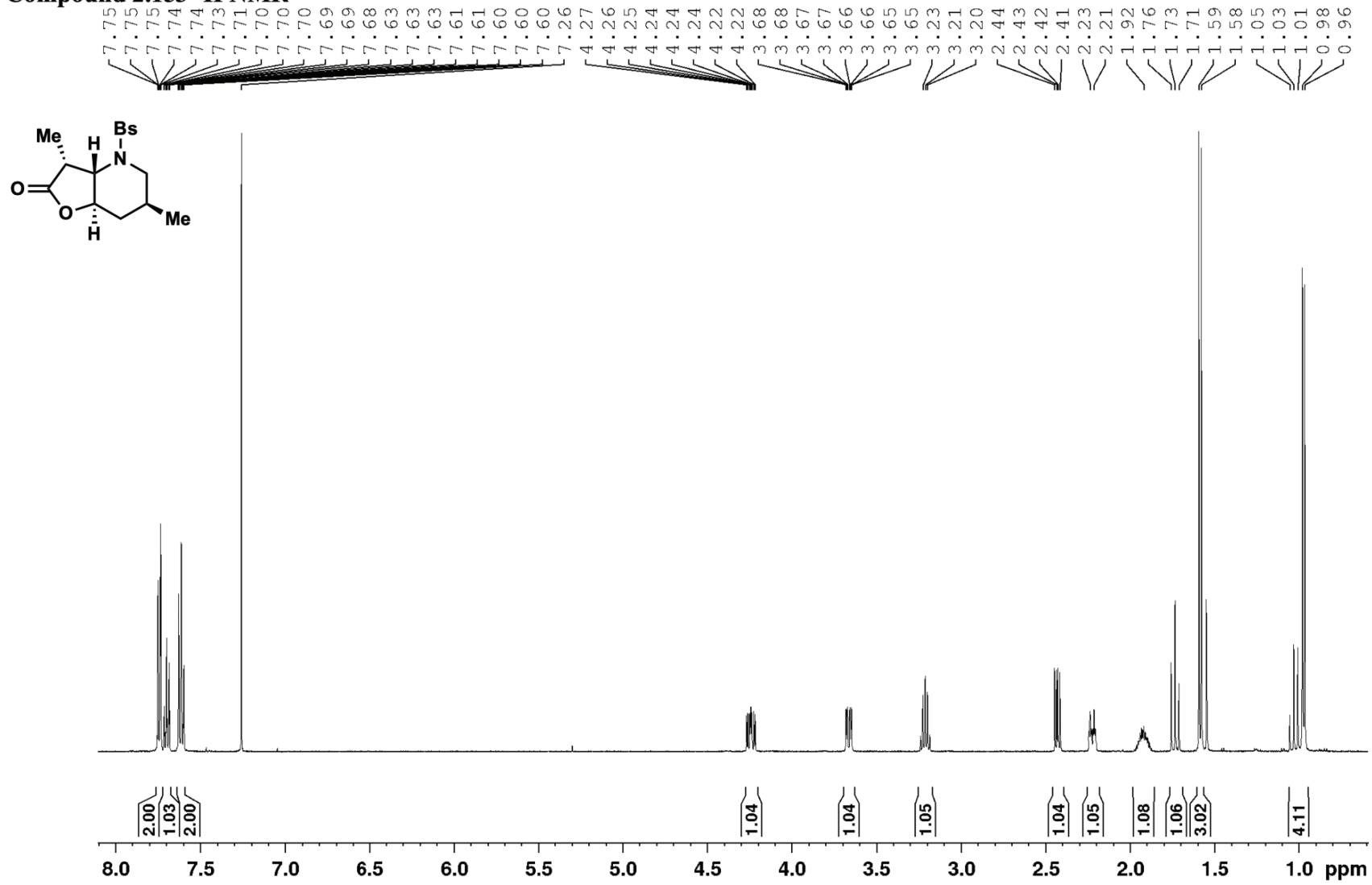
Compound 2.152 ^{1}H NMR



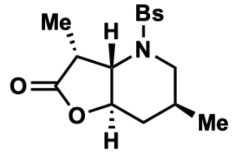
Compound 2.152 ^{13}C NMR



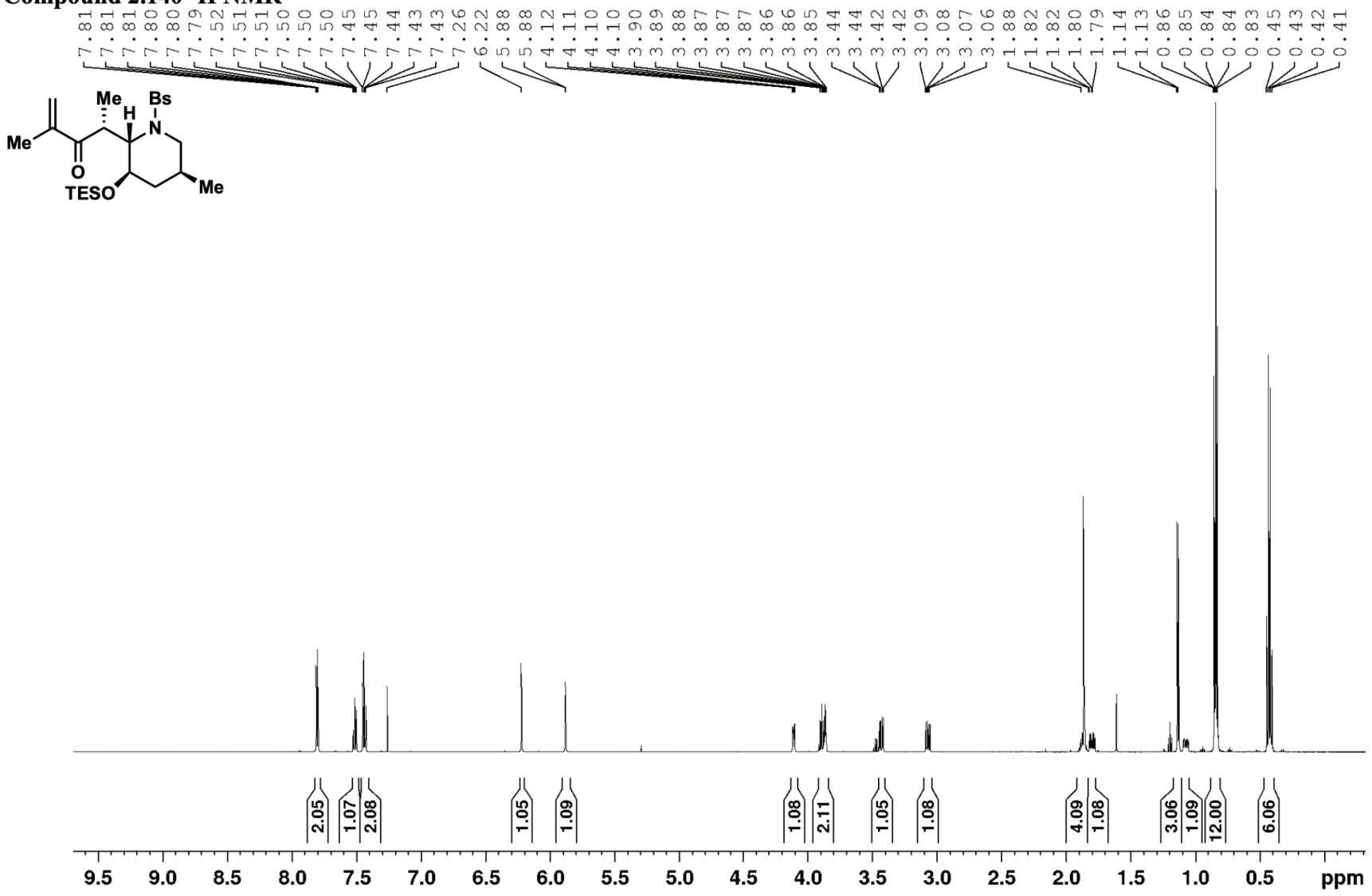
Compound 2.153 ^{1}H NMR



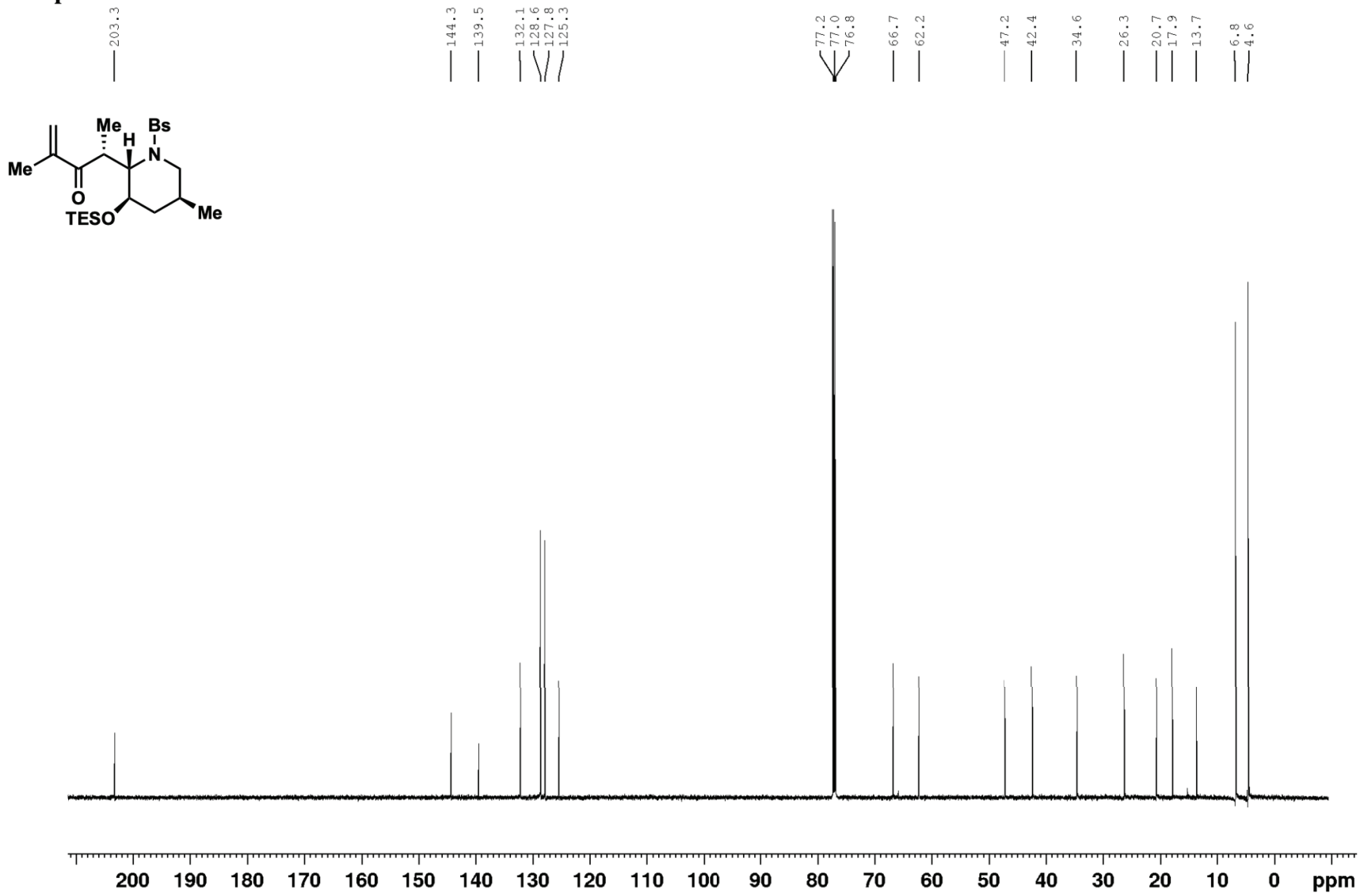
Compound 2.153 ^{13}C NMR



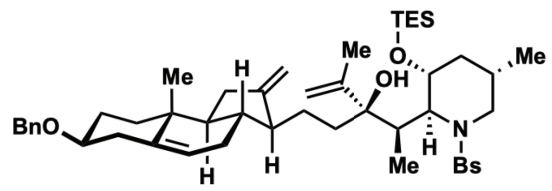
Compound 2.140 ^{1}H NMR



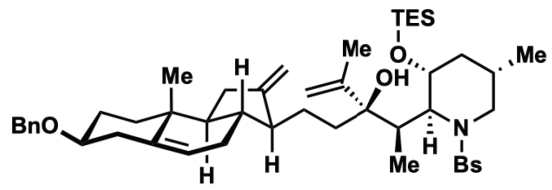
Compound 2.140 ^{13}C NMR

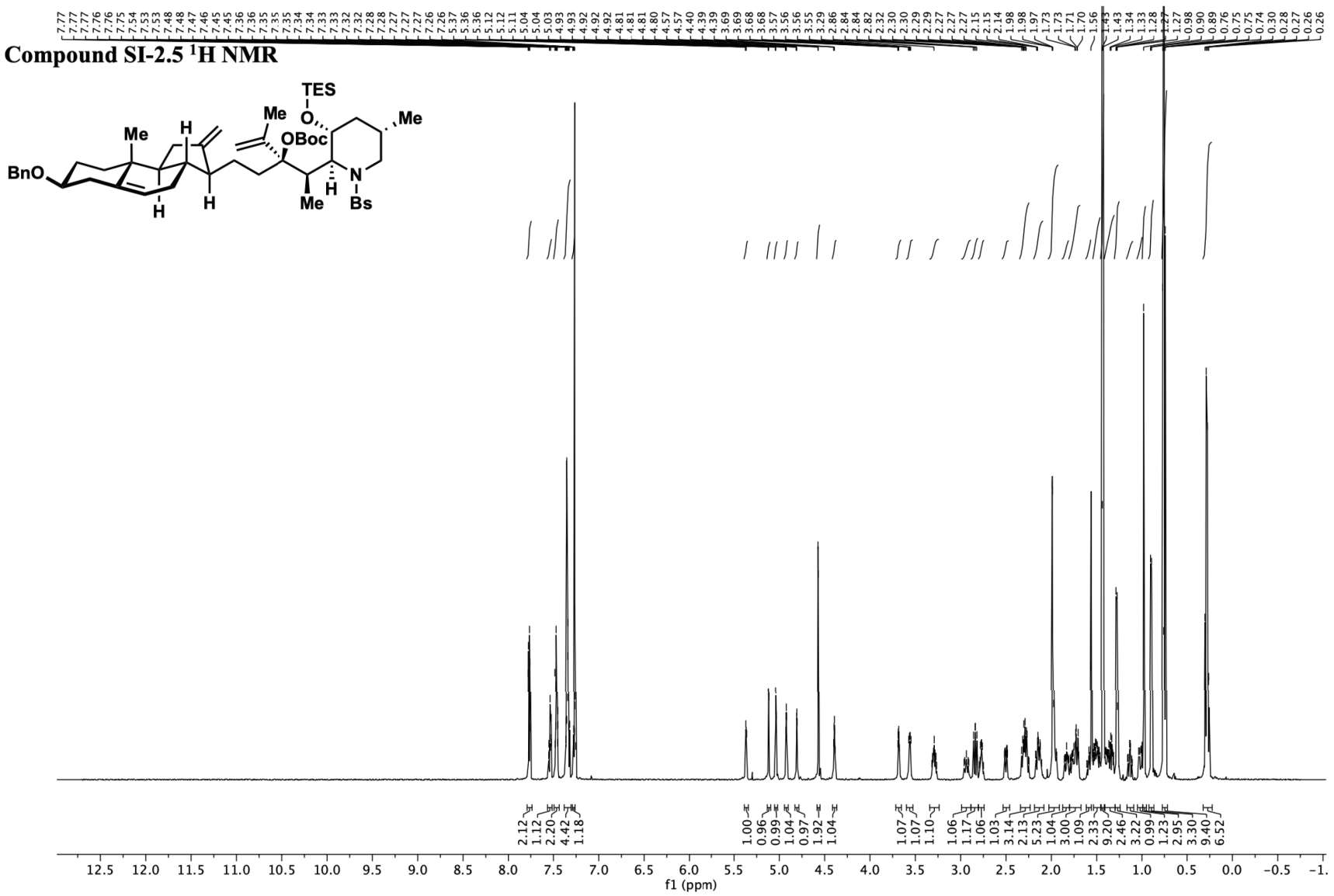


Compound 2.154 ^{1}H NMR

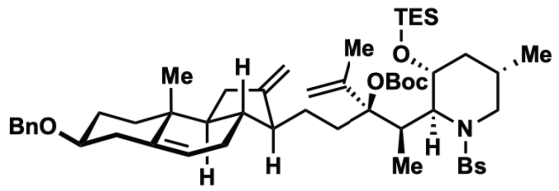


Compound 2.154 ^{13}C NMR

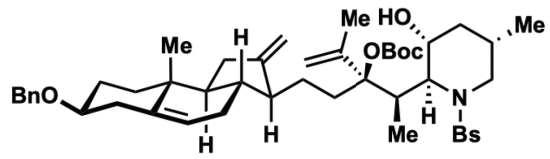



Compound SI-2.5 ^{1}H NMR
TES
O
Me
OBoc
Me
BnO
H
Me
H
H
H
Me
N
Bs
f1 (ppm)

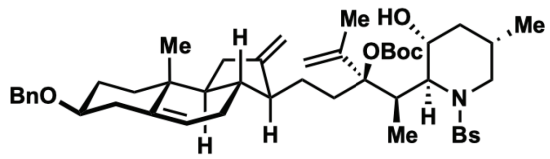
Compound SI-2.5 ^{13}C NMR



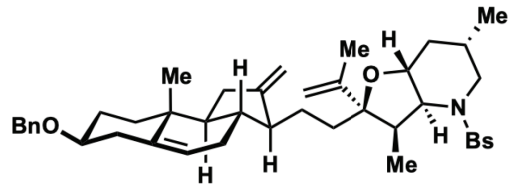
Compound 2.155 ^{1}H NMR



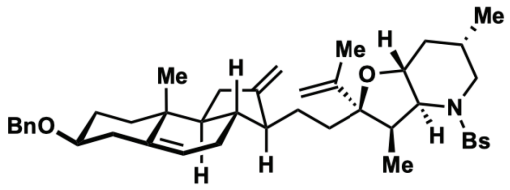
Compound 2.155 ^{13}C NMR



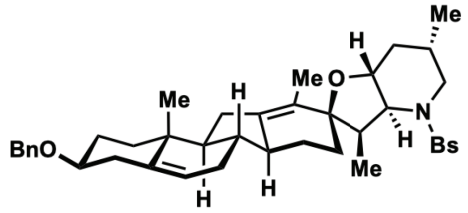
Compound 2.117 ^{1}H NMR



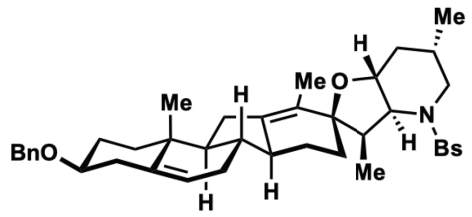
Compound 2.117 ^{13}C NMR



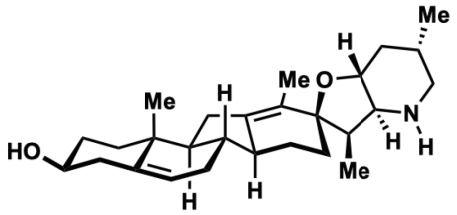
Compound 2.118 ^{1}H NMR



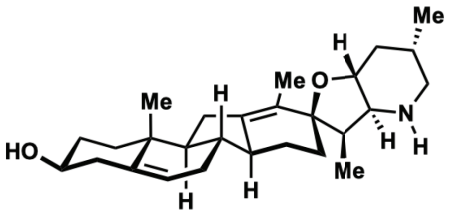
Compound 2.118 ^{13}C NMR



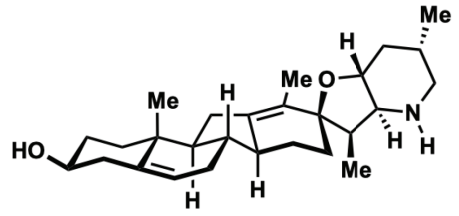
(–)-Cyclopamine (2.1) ^{1}H NMR (CD_2Cl_2)



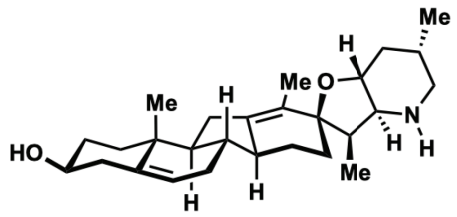
(–)-Cyclopamine (2.1) ^{13}C NMR (CD_2Cl_2)



(–)-Cyclopamine (2.1) ^{1}H NMR ($CDCl_3$)



(–)-Cyclopamine (2.1) ^{13}C NMR ($CDCl_3$)



X-Ray Crystallography Data

Crystal Structure of 2.145

Experimental Summary

The single crystal X-ray diffraction studies were carried out on a Bruker SMART Pt135 CCD diffractometer equipped with Cu K_α radiation (λ = 1.54178 Å).

Crystals of the subject compound were used as received. A 0.12 x 0.1 x 0.065 mm piece of a crystal was mounted on a Cryoloop with Paratone oil. Data were collected in a nitrogen gas stream at 100(2) K using ϕ and ω scans. Crystal-to-detector distance was 45 mm and exposure time was 5, 10, 15, or 20 seconds depending on the 2θ range per frame using a scan width of 1.25°. Data collection was 100 % complete to 67.679° in θ. A total of 36105 reflections were collected covering the indices, −11<=h<=11, −22<=k<=22, −12<=l<=12. 6376 reflections were found to be symmetry independent, with a R_{int} of 0.0438. Indexing and unit cell refinement indicated a **P**rimitive, **Monoclinic** lattice. The space group was found to be ***P*2$_1$**. The data were integrated using the Bruker SAINT Software program and scaled using the SADABS software program. Solution by direct methods (SHELXT) produced a complete phasing model consistent with the proposed structure.

All nonhydrogen atoms were refined anisotropically by full-matrix least-squares (SHELXL-2014). All carbon bonded hydrogen atoms were placed using a riding model. Their positions were constrained relative to their parent atom using the appropriate HFIX command in SHELXL-2014. Crystallographic data are summarized in Table 1.

Notes: Great data! Absolute stereochemistry was conclusively assigned (Absolute Structure Parameter = 0.01(9)). There are two copies of the compound in the asymmetric unit. The chemical formula for the compound is: $C_{21}H_{24}O_2$

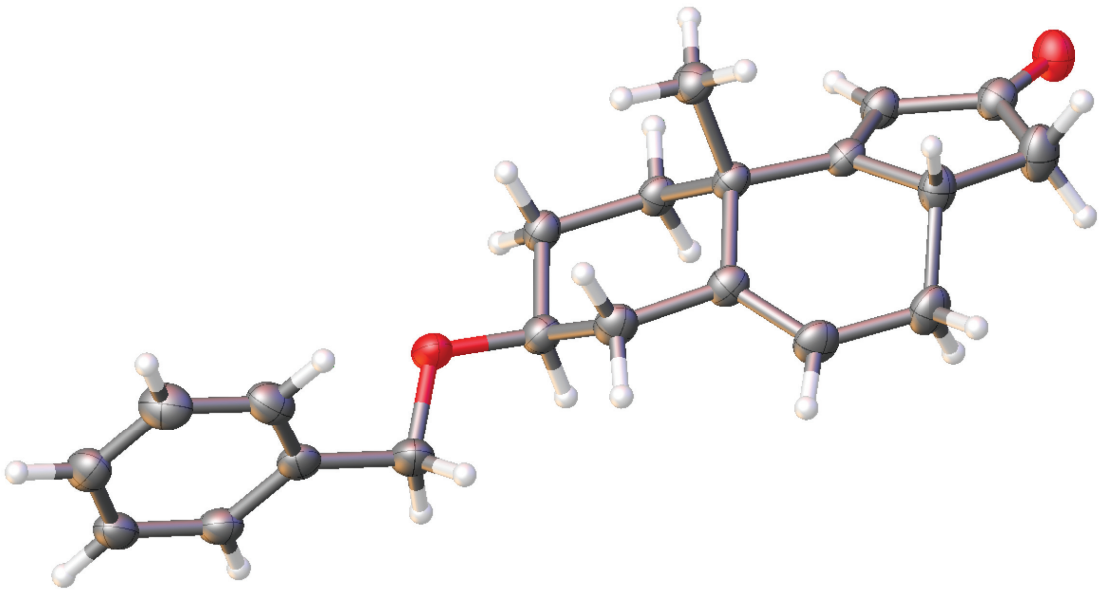


Table 1. Crystal data and structure refinement for Baran853.

Identification code	baran853	
Empirical formula	C21 H24 O2	
Formula weight	308.40	
Temperature	100.15 K	
Wavelength	1.54178 Å	
Crystal system	Monoclinic	
Space group	P 1 21 1	
Unit cell dimensions	a = 9.6112(5) Å	α= 90°.
	b = 18.4068(10) Å	β= 112.552(2)°.
	c = 10.2091(6) Å	γ = 90°.
Volume	1668.00(16) $Å^3$	
Z	4	
Density (calculated)	1.228 Mg/m^3	
Absorption coefficient	0.602 mm^{-1}	
F(000)	664	
Crystal size	0.12 x 0.1 x 0.065 mm^3	
Theta range for data collection	4.690 to 70.563°.	
Index ranges	-11<=h<=11, -22<=k<=22, -12<=l<=12	
Reflections collected	36105	
Independent reflections	6376 [R(int) = 0.0438]	
Completeness to theta = 67.679°	100.0 %	
Absorption correction	Semi-empirical from equivalents	
Max. and min. transmission	0.6617 and 0.6008	
Refinement method	Full-matrix least-squares on F^2	
Data / restraints / parameters	6376 / 1 / 417	
Goodness-of-fit on F^2	1.019	
Final R indices [I>2sigma(I)]	R1 = 0.0331, wR2 = 0.0870	
R indices (all data)	R1 = 0.0343, wR2 = 0.0880	
Absolute structure parameter	0.01(9)	
Largest diff. peak and hole	0.199 and -0.139 $e.Å^{-3}$	

Table 2. Atomic coordinates (x 10^4) and equivalent isotropic displacement parameters ($Å^2$x 10^3) for Baran853. U(eq) is defined as one third of the trace of the orthogonalized U^{ij} tensor.

	x	y	z	U(eq)
O(1)	6996(2)	3858(1)	1461(2)	31(1)
O(2)	766(2)	4401(1)	6085(2)	46(1)
C(1)	8830(3)	3002(1)	337(3)	42(1)
C(2)	9336(3)	2750(2)	-675(3)	54(1)
C(3)	10130(3)	3208(2)	-1221(3)	52(1)
C(4)	10420(2)	3915(2)	-754(2)	42(1)
C(5)	9912(2)	4169(1)	268(2)	32(1)
C(6)	9113(2)	3717(1)	817(2)	31(1)
C(7)	8576(2)	3983(1)	1932(3)	38(1)
C(8)	6367(2)	4079(1)	2463(2)	27(1)
C(9)	4675(2)	3972(1)	1719(2)	31(1)
C(10)	3859(2)	4138(1)	2705(2)	31(1)
C(11)	4430(2)	3668(1)	4068(2)	28(1)
C(12)	4044(3)	2858(1)	3698(3)	42(1)
C(13)	3679(2)	3886(1)	5055(2)	29(1)
C(14)	2306(2)	4170(1)	4743(2)	34(1)
C(15)	1967(3)	4234(1)	6025(2)	35(1)
C(16)	3395(3)	4027(2)	7277(3)	43(1)
C(17)	4501(3)	3756(1)	6628(2)	38(1)
C(18)	6021(3)	4150(2)	7113(2)	42(1)
C(19)	6811(2)	4000(2)	6118(2)	39(1)
C(20)	6134(2)	3773(1)	4785(2)	30(1)
C(21)	7000(2)	3638(1)	3849(2)	32(1)
O(1A)	7226(2)	6086(1)	7623(2)	31(1)
O(2A)	11776(2)	5775(1)	1449(2)	35(1)
C(1A)	6503(3)	6915(1)	9849(2)	36(1)
C(2A)	5487(3)	7166(1)	10414(3)	39(1)
C(3A)	4688(3)	6674(1)	10890(2)	36(1)
C(4A)	4901(2)	5937(1)	10794(2)	34(1)
C(5A)	5901(2)	5687(1)	10210(2)	31(1)
C(6A)	6712(2)	6172(1)	9727(2)	30(1)

C(7A)	7797(2)	5901(2)	9101(2)	38(1)
C(8A)	8268(2)	5936(1)	6960(2)	28(1)
C(9A)	7360(2)	5976(1)	5367(2)	27(1)
C(10A)	8365(2)	5903(1)	4518(2)	25(1)
C(11A)	9649(2)	6474(1)	4939(2)	24(1)
C(12A)	9002(2)	7251(1)	4508(2)	30(1)
C(13A)	10683(2)	6328(1)	4175(2)	25(1)
C(14A)	10367(2)	6019(1)	2906(2)	27(1)
C(15A)	11697(2)	5999(1)	2544(2)	29(1)
C(16A)	13003(3)	6328(2)	3785(3)	40(1)
C(17A)	12316(2)	6567(1)	4851(2)	31(1)
C(18A)	13028(2)	6232(1)	6335(2)	36(1)
C(19A)	12009(2)	6303(1)	7132(2)	33(1)
C(20A)	10531(2)	6423(1)	6545(2)	27(1)
C(21A)	9580(2)	6476(1)	7425(2)	31(1)

Table 3. Bond lengths [Å] and angles [°] for Baran853.

O(1)-C(7)	1.424(2)
O(1)-C(8)	1.432(2)
O(2)-C(15)	1.219(3)
C(1)-H(1)	0.9500
C(1)-C(2)	1.380(4)
C(1)-C(6)	1.393(3)
C(2)-H(2)	0.9500
C(2)-C(3)	1.389(5)
C(3)-H(3)	0.9500
C(3)-C(4)	1.376(4)
C(4)-H(4)	0.9500
C(4)-C(5)	1.392(3)
C(5)-H(5)	0.9500
C(5)-C(6)	1.388(3)
C(6)-C(7)	1.502(3)
C(7)-H(7A)	0.9900
C(7)-H(7B)	0.9900
C(8)-H(8)	1.0000
C(8)-C(9)	1.521(3)
C(8)-C(21)	1.539(3)
C(9)-H(9A)	0.9900
C(9)-H(9B)	0.9900
C(9)-C(10)	1.525(3)
C(10)-H(10A)	0.9900
C(10)-H(10B)	0.9900
C(10)-C(11)	1.548(3)
C(11)-C(12)	1.548(3)
C(11)-C(13)	1.502(3)
C(11)-C(20)	1.528(3)
C(12)-H(12A)	0.9800
C(12)-H(12B)	0.9800
C(12)-H(12C)	0.9800
C(13)-C(14)	1.339(3)
C(13)-C(17)	1.512(3)
C(14)-H(14)	0.9500
C(14)-C(15)	1.470(3)

C(15)-C(16)	1.523(3)
C(16)-H(16B)	0.9900
C(16)-H(16A)	0.9900
C(16)-C(17)	1.535(3)
C(17)-H(17)	1.0000
C(17)-C(18)	1.534(3)
C(18)-H(18A)	0.9900
C(18)-H(18B)	0.9900
C(18)-C(19)	1.508(3)
C(19)-H(19)	0.9500
C(19)-C(20)	1.331(3)
C(20)-C(21)	1.509(3)
C(21)-H(21A)	0.9900
C(21)-H(21B)	0.9900
O(1A)-C(7A)	1.434(2)
O(1A)-C(8A)	1.434(2)
O(2A)-C(15A)	1.221(3)
C(1A)-H(1A)	0.9500
C(1A)-C(2A)	1.390(4)
C(1A)-C(6A)	1.395(3)
C(2A)-H(2A)	0.9500
C(2A)-C(3A)	1.391(4)
C(3A)-H(3A)	0.9500
C(3A)-C(4A)	1.381(3)
C(4A)-H(4A)	0.9500
C(4A)-C(5A)	1.388(3)
C(5A)-H(5A)	0.9500
C(5A)-C(6A)	1.393(3)
C(6A)-C(7A)	1.502(3)
C(7A)-H(7AA)	0.9900
C(7A)-H(7AB)	0.9900
C(8A)-H(8A)	1.0000
C(8A)-C(9A)	1.524(3)
C(8A)-C(21A)	1.532(3)
C(9A)-H(9AA)	0.9900
C(9A)-H(9AB)	0.9900
C(9A)-C(10A)	1.531(3)
C(10A)-H(10C)	0.9900

C(10A)-H(10D)	0.9900
C(10A)-C(11A)	1.551(3)
C(11A)-C(12A)	1.554(3)
C(11A)-C(13A)	1.503(3)
C(11A)-C(20A)	1.533(3)
C(12A)-H(12D)	0.9800
C(12A)-H(12E)	0.9800
C(12A)-H(12F)	0.9800
C(13A)-C(14A)	1.340(3)
C(13A)-C(17A)	1.518(3)
C(14A)-H(14A)	0.9500
C(14A)-C(15A)	1.461(3)
C(15A)-C(16A)	1.526(3)
C(16A)-H(16C)	0.9900
C(16A)-H(16D)	0.9900
C(16A)-C(17A)	1.539(3)
C(17A)-H(17A)	1.0000
C(17A)-C(18A)	1.532(3)
C(18A)-H(18C)	0.9900
C(18A)-H(18D)	0.9900
C(18A)-C(19A)	1.500(3)
C(19A)-H(19A)	0.9500
C(19A)-C(20A)	1.332(3)
C(20A)-C(21A)	1.511(3)
C(21A)-H(21C)	0.9900
C(21A)-H(21D)	0.9900

C(7)-O(1)-C(8)	113.59(15)
C(2)-C(1)-H(1)	119.9
C(2)-C(1)-C(6)	120.2(2)
C(6)-C(1)-H(1)	119.9
C(1)-C(2)-H(2)	119.9
C(1)-C(2)-C(3)	120.1(3)
C(3)-C(2)-H(2)	119.9
C(2)-C(3)-H(3)	119.9
C(4)-C(3)-C(2)	120.3(3)
C(4)-C(3)-H(3)	119.9
C(3)-C(4)-H(4)	120.2

C(3)-C(4)-C(5)	119.6(3)
C(5)-C(4)-H(4)	120.2
C(4)-C(5)-H(5)	119.7
C(6)-C(5)-C(4)	120.6(2)
C(6)-C(5)-H(5)	119.7
C(1)-C(6)-C(7)	119.8(2)
C(5)-C(6)-C(1)	119.2(2)
C(5)-C(6)-C(7)	120.9(2)
O(1)-C(7)-C(6)	108.85(17)
O(1)-C(7)-H(7A)	109.9
O(1)-C(7)-H(7B)	109.9
C(6)-C(7)-H(7A)	109.9
C(6)-C(7)-H(7B)	109.9
H(7A)-C(7)-H(7B)	108.3
O(1)-C(8)-H(8)	109.2
O(1)-C(8)-C(9)	105.70(16)
O(1)-C(8)-C(21)	112.44(16)
C(9)-C(8)-H(8)	109.2
C(9)-C(8)-C(21)	111.12(16)
C(21)-C(8)-H(8)	109.2
C(8)-C(9)-H(9A)	109.3
C(8)-C(9)-H(9B)	109.3
C(8)-C(9)-C(10)	111.53(17)
H(9A)-C(9)-H(9B)	108.0
C(10)-C(9)-H(9A)	109.3
C(10)-C(9)-H(9B)	109.3
C(9)-C(10)-H(10A)	109.0
C(9)-C(10)-H(10B)	109.0
C(9)-C(10)-C(11)	112.75(17)
H(10A)-C(10)-H(10B)	107.8
C(11)-C(10)-H(10A)	109.0
C(11)-C(10)-H(10B)	109.0
C(12)-C(11)-C(10)	110.44(18)
C(13)-C(11)-C(10)	110.97(16)
C(13)-C(11)-C(12)	106.76(17)
C(13)-C(11)-C(20)	110.33(17)
C(20)-C(11)-C(10)	107.80(16)
C(20)-C(11)-C(12)	110.58(18)

C(11)-C(12)-H(12A)	109.5
C(11)-C(12)-H(12B)	109.5
C(11)-C(12)-H(12C)	109.5
H(12A)-C(12)-H(12B)	109.5
H(12A)-C(12)-H(12C)	109.5
H(12B)-C(12)-H(12C)	109.5
C(11)-C(13)-C(17)	118.74(18)
C(14)-C(13)-C(11)	128.92(19)
C(14)-C(13)-C(17)	112.3(2)
C(13)-C(14)-H(14)	124.6
C(13)-C(14)-C(15)	110.79(19)
C(15)-C(14)-H(14)	124.6
O(2)-C(15)-C(14)	127.1(2)
O(2)-C(15)-C(16)	126.0(2)
C(14)-C(15)-C(16)	106.89(19)
C(15)-C(16)-H(16B)	110.6
C(15)-C(16)-H(16A)	110.6
C(15)-C(16)-C(17)	105.64(19)
H(16B)-C(16)-H(16A)	108.7
C(17)-C(16)-H(16B)	110.6
C(17)-C(16)-H(16A)	110.6
C(13)-C(17)-C(16)	103.98(18)
C(13)-C(17)-H(17)	109.4
C(13)-C(17)-C(18)	108.25(18)
C(16)-C(17)-H(17)	109.4
C(18)-C(17)-C(16)	116.0(2)
C(18)-C(17)-H(17)	109.4
C(17)-C(18)-H(18A)	109.4
C(17)-C(18)-H(18B)	109.4
H(18A)-C(18)-H(18B)	108.0
C(19)-C(18)-C(17)	111.1(2)
C(19)-C(18)-H(18A)	109.4
C(19)-C(18)-H(18B)	109.4
C(18)-C(19)-H(19)	117.6
C(20)-C(19)-C(18)	124.8(2)
C(20)-C(19)-H(19)	117.6
C(19)-C(20)-C(11)	122.9(2)
C(19)-C(20)-C(21)	121.80(19)

C(21)-C(20)-C(11)	115.18(18)
C(8)-C(21)-H(21A)	109.2
C(8)-C(21)-H(21B)	109.2
C(20)-C(21)-C(8)	112.13(16)
C(20)-C(21)-H(21A)	109.2
C(20)-C(21)-H(21B)	109.2
H(21A)-C(21)-H(21B)	107.9
C(8A)-O(1A)-C(7A)	113.35(15)
C(2A)-C(1A)-H(1A)	119.6
C(2A)-C(1A)-C(6A)	120.7(2)
C(6A)-C(1A)-H(1A)	119.6
C(1A)-C(2A)-H(2A)	120.1
C(1A)-C(2A)-C(3A)	119.9(2)
C(3A)-C(2A)-H(2A)	120.1
C(2A)-C(3A)-H(3A)	120.1
C(4A)-C(3A)-C(2A)	119.9(2)
C(4A)-C(3A)-H(3A)	120.1
C(3A)-C(4A)-H(4A)	120.0
C(3A)-C(4A)-C(5A)	120.1(2)
C(5A)-C(4A)-H(4A)	120.0
C(4A)-C(5A)-H(5A)	119.5
C(4A)-C(5A)-C(6A)	120.9(2)
C(6A)-C(5A)-H(5A)	119.5
C(1A)-C(6A)-C(7A)	120.7(2)
C(5A)-C(6A)-C(1A)	118.5(2)
C(5A)-C(6A)-C(7A)	120.9(2)
O(1A)-C(7A)-C(6A)	108.74(17)
O(1A)-C(7A)-H(7AA)	109.9
O(1A)-C(7A)-H(7AB)	109.9
C(6A)-C(7A)-H(7AA)	109.9
C(6A)-C(7A)-H(7AB)	109.9
H(7AA)-C(7A)-H(7AB)	108.3
O(1A)-C(8A)-H(8A)	109.2
O(1A)-C(8A)-C(9A)	106.07(15)
O(1A)-C(8A)-C(21A)	111.62(17)
C(9A)-C(8A)-H(8A)	109.2
C(9A)-C(8A)-C(21A)	111.44(17)
C(21A)-C(8A)-H(8A)	109.2

C(8A)-C(9A)-H(9AA)	109.2
C(8A)-C(9A)-H(9AB)	109.2
C(8A)-C(9A)-C(10A)	111.88(15)
H(9AA)-C(9A)-H(9AB)	107.9
C(10A)-C(9A)-H(9AA)	109.2
C(10A)-C(9A)-H(9AB)	109.2
C(9A)-C(10A)-H(10C)	109.0
C(9A)-C(10A)-H(10D)	109.0
C(9A)-C(10A)-C(11A)	113.06(16)
H(10C)-C(10A)-H(10D)	107.8
C(11A)-C(10A)-H(10C)	109.0
C(11A)-C(10A)-H(10D)	109.0
C(10A)-C(11A)-C(12A)	110.78(15)
C(13A)-C(11A)-C(10A)	110.45(15)
C(13A)-C(11A)-C(12A)	106.88(16)
C(13A)-C(11A)-C(20A)	109.85(15)
C(20A)-C(11A)-C(10A)	108.03(16)
C(20A)-C(11A)-C(12A)	110.85(16)
C(11A)-C(12A)-H(12D)	109.5
C(11A)-C(12A)-H(12E)	109.5
C(11A)-C(12A)-H(12F)	109.5
H(12D)-C(12A)-H(12E)	109.5
H(12D)-C(12A)-H(12F)	109.5
H(12E)-C(12A)-H(12F)	109.5
C(11A)-C(13A)-C(17A)	119.12(16)
C(14A)-C(13A)-C(11A)	128.87(18)
C(14A)-C(13A)-C(17A)	112.00(18)
C(13A)-C(14A)-H(14A)	124.5
C(13A)-C(14A)-C(15A)	111.05(18)
C(15A)-C(14A)-H(14A)	124.5
O(2A)-C(15A)-C(14A)	127.44(19)
O(2A)-C(15A)-C(16A)	124.99(19)
C(14A)-C(15A)-C(16A)	107.57(17)
C(15A)-C(16A)-H(16C)	110.7
C(15A)-C(16A)-H(16D)	110.7
C(15A)-C(16A)-C(17A)	105.13(17)
H(16C)-C(16A)-H(16D)	108.8
C(17A)-C(16A)-H(16C)	110.7

C(17A)-C(16A)-H(16D)	110.7
C(13A)-C(17A)-C(16A)	104.20(16)
C(13A)-C(17A)-H(17A)	109.2
C(13A)-C(17A)-C(18A)	108.96(18)
C(16A)-C(17A)-H(17A)	109.2
C(18A)-C(17A)-C(16A)	115.78(19)
C(18A)-C(17A)-H(17A)	109.2
C(17A)-C(18A)-H(18C)	109.3
C(17A)-C(18A)-H(18D)	109.3
H(18C)-C(18A)-H(18D)	108.0
C(19A)-C(18A)-C(17A)	111.39(18)
C(19A)-C(18A)-H(18C)	109.3
C(19A)-C(18A)-H(18D)	109.3
C(18A)-C(19A)-H(19A)	117.4
C(20A)-C(19A)-C(18A)	125.17(19)
C(20A)-C(19A)-H(19A)	117.4
C(19A)-C(20A)-C(11A)	123.24(19)
C(19A)-C(20A)-C(21A)	121.85(18)
C(21A)-C(20A)-C(11A)	114.82(16)
C(8A)-C(21A)-H(21C)	109.0
C(8A)-C(21A)-H(21D)	109.0
C(20A)-C(21A)-C(8A)	112.79(17)
C(20A)-C(21A)-H(21C)	109.0
C(20A)-C(21A)-H(21D)	109.0
H(21C)-C(21A)-H(21D)	107.8

Symmetry transformations used to generate equivalent atoms:

Table 4. Anisotropic displacement parameters ($Å^2 x\ 10^3$) for Baran853. The anisotropic displacement factor exponent takes the form: $-2\pi^2[\ h^2\ a^{*2}U^{11} + ...\ + 2\ h\ k\ a^*\ b^*\ U^{12}]$

	U^{11}	U^{22}	U^{33}	U^{23}	U^{13}	U^{12}
O(1)	24(1)	34(1)	32(1)	-2(1)	8(1)	-2(1)
O(2)	40(1)	56(1)	47(1)	3(1)	21(1)	7(1)
C(1)	39(1)	32(1)	51(1)	4(1)	13(1)	4(1)
C(2)	52(2)	40(1)	64(2)	-14(1)	15(1)	8(1)
C(3)	41(1)	73(2)	39(1)	-7(1)	12(1)	17(1)
C(4)	25(1)	63(2)	33(1)	10(1)	6(1)	7(1)
C(5)	22(1)	34(1)	33(1)	4(1)	3(1)	4(1)
C(6)	22(1)	33(1)	32(1)	3(1)	4(1)	5(1)
C(7)	26(1)	46(1)	40(1)	-6(1)	10(1)	-7(1)
C(8)	25(1)	24(1)	28(1)	1(1)	6(1)	-1(1)
C(9)	26(1)	34(1)	27(1)	0(1)	5(1)	-2(1)
C(10)	22(1)	38(1)	26(1)	3(1)	2(1)	3(1)
C(11)	23(1)	26(1)	30(1)	3(1)	6(1)	-2(1)
C(12)	46(1)	31(1)	56(2)	-6(1)	26(1)	-12(1)
C(13)	26(1)	28(1)	30(1)	4(1)	6(1)	-3(1)
C(14)	27(1)	40(1)	30(1)	2(1)	6(1)	-1(1)
C(15)	36(1)	33(1)	35(1)	3(1)	12(1)	-1(1)
C(16)	39(1)	56(2)	32(1)	8(1)	12(1)	4(1)
C(17)	34(1)	43(1)	32(1)	9(1)	9(1)	2(1)
C(18)	31(1)	60(2)	28(1)	4(1)	1(1)	-3(1)
C(19)	26(1)	51(1)	32(1)	11(1)	2(1)	-2(1)
C(20)	24(1)	28(1)	33(1)	11(1)	5(1)	3(1)
C(21)	24(1)	32(1)	36(1)	10(1)	7(1)	5(1)
O(1A)	28(1)	41(1)	23(1)	6(1)	9(1)	8(1)
O(2A)	33(1)	39(1)	36(1)	-8(1)	16(1)	-2(1)
C(1A)	36(1)	39(1)	30(1)	4(1)	10(1)	-7(1)
C(2A)	49(1)	32(1)	35(1)	-3(1)	14(1)	-1(1)
C(3A)	38(1)	44(1)	26(1)	1(1)	13(1)	6(1)
C(4A)	31(1)	40(1)	27(1)	9(1)	8(1)	-1(1)
C(5A)	32(1)	33(1)	25(1)	6(1)	8(1)	4(1)
C(6A)	25(1)	40(1)	20(1)	5(1)	3(1)	2(1)

C(7A)	33(1)	53(1)	27(1)	12(1)	11(1)	10(1)
C(8A)	25(1)	32(1)	27(1)	2(1)	8(1)	4(1)
C(9A)	22(1)	30(1)	26(1)	-2(1)	8(1)	1(1)
C(10A)	21(1)	30(1)	22(1)	-4(1)	4(1)	0(1)
C(11A)	21(1)	26(1)	22(1)	-2(1)	5(1)	2(1)
C(12A)	31(1)	28(1)	32(1)	1(1)	12(1)	5(1)
C(13A)	22(1)	24(1)	26(1)	-1(1)	5(1)	2(1)
C(14A)	23(1)	29(1)	27(1)	-3(1)	6(1)	-1(1)
C(15A)	26(1)	26(1)	32(1)	-2(1)	10(1)	1(1)
C(16A)	27(1)	55(1)	39(1)	-12(1)	13(1)	-5(1)
C(17A)	24(1)	35(1)	34(1)	-7(1)	10(1)	-4(1)
C(18A)	22(1)	45(1)	34(1)	-6(1)	4(1)	0(1)
C(19A)	26(1)	40(1)	26(1)	-3(1)	2(1)	-2(1)
C(20A)	25(1)	27(1)	24(1)	-5(1)	5(1)	-1(1)
C(21A)	28(1)	38(1)	23(1)	-3(1)	6(1)	2(1)

Table 5. Hydrogen coordinates (x 10^4) and isotropic displacement parameters ($Å^2$x 10^{-3}) for Baran853.

	x	y	z	U(eq)
H(1)	8287	2688	708	50
H(2)	9141	2263	-999	65
H(3)	10474	3033	-1919	62
H(4)	10963	4227	-1128	50
H(5)	10114	4656	594	39
H(7A)	9109	3722	2835	45
H(7B)	8791	4509	2100	45
H(8)	6584	4606	2685	32
H(9A)	4466	3464	1382	37
H(9B)	4286	4295	882	37
H(10A)	2767	4051	2190	37
H(10B)	4000	4657	2974	37
H(12A)	4326	2575	4575	64
H(12B)	4601	2679	3137	64
H(12C)	2960	2808	3149	64
H(14)	1642	4310	3819	40
H(16B)	3184	3639	7847	51
H(16A)	3815	4453	7895	51
H(17)	4675	3224	6809	45
H(18A)	5858	4680	7148	51
H(18B)	6666	3987	8080	51
H(19)	7870	4074	6469	47
H(21A)	6957	3114	3618	38
H(21B)	8069	3771	4372	38
H(1A)	7061	7253	9542	43
H(2A)	5339	7673	10474	47
H(3A)	3998	6844	11282	43
H(4A)	4362	5600	11126	40
H(5A)	6034	5179	10140	38
H(7AA)	8797	6127	9595	46

H(7AB)	7911	5368	9216	46
H(8A)	8673	5432	7214	34
H(9AA)	6819	6446	5137	32
H(9AB)	6599	5583	5088	32
H(10C)	7735	5956	3495	31
H(10D)	8812	5411	4665	31
H(12D)	9832	7596	4699	46
H(12E)	8402	7387	5059	46
H(12F)	8363	7259	3495	46
H(14A)	9404	5836	2319	33
H(16C)	13434	6749	3468	48
H(16D)	13808	5963	4215	48
H(17A)	12360	7108	4934	38
H(18C)	13240	5712	6250	43
H(18D)	13996	6478	6871	43
H(19A)	12454	6259	8135	39
H(21C)	9174	6976	7351	37
H(21D)	10224	6386	8432	37

Crystal Structure of 2.150

Experimental Summary

The single crystal X-ray diffraction studies were carried out on a Bruker ApexII-Ultra CCD diffractometer equipped with Mo K_α radiation (λ = 0.7107 Å).
Crystals of the subject compound were used as received. A 0.26 x 0.18 x 0.04 mm piece of a crystal was mounted on a Cryoloop with Paratone oil. Data were collected in a nitrogen gas stream at 100(2) K using ϕ and ω scans. Crystal-to-detector distance was 40 mm and exposure time was 5 seconds per frame using a scan width of 0.70°. Data collection was 99.9 % complete to 25.242° in θ. A total of 10654 reflections were collected covering the indices, −6<=h<=8, −10<=k<=14, −24<=l<=24. 3091 reflections were found to be symmetry independent, with a R_{int} of 0.0390. Indexing and unit cell refinement indicated a **P**rimitive, **Orthorhombic** lattice. The space group was found to be $\boldsymbol{P2_12_12_1}$. The data were integrated using the Bruker SAINT Software program and scaled using the SADABS software program. Solution by direct methods (SHELXT) produced a complete phasing model consistent with the proposed structure.
All nonhydrogen atoms were refined anisotropically by full-matrix least-squares (SHELXL-2014). All carbon bonded hydrogen atoms were placed using a riding model. Their positions were constrained relative to their parent atom using the appropriate HFIX command in SHELXL-2014. Crystallographic data are summarized in Table 1.

Notes: Great data! Absolute stereochemistry was conclusively assigned (Absolute Structure Parameter = -0.01(5)). There is one copy of the compound in the asymmetric unit. The chemical formula for the compound is: $C_{14}H_{17}NO_4S$

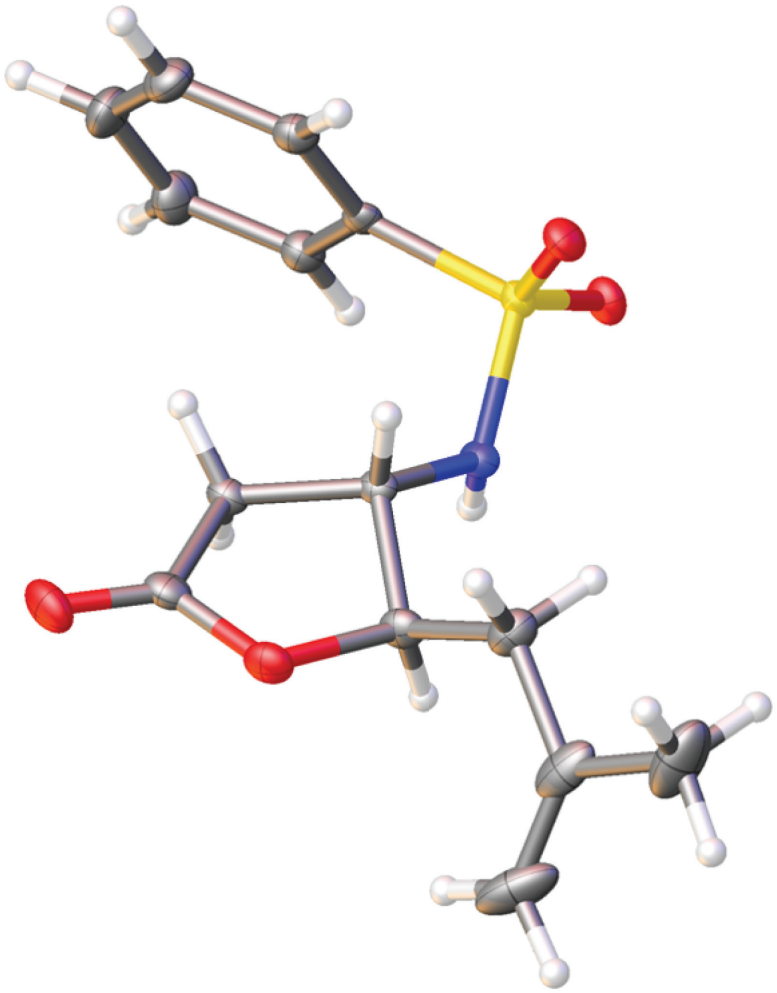


Table 1. Crystal data and structure refinement for Baran874.

Identification code	baran874b_0m_a	
Empirical formula	C14 H17 N O4 S	
Formula weight	295.34	
Temperature	100.15 K	
Wavelength	0.71073 Å	
Crystal system	Orthorhombic	
Space group	$P2_12_12_1$	
Unit cell dimensions	a = 6.7104(8) Å	α= 90°.
	b = 11.4454(12) Å	β= 90°.
	c = 19.440(2) Å	γ = 90°.
Volume	1493.1(3) $Å^3$	
Z	4	
Density (calculated)	1.314 Mg/m^3	
Absorption coefficient	0.229 mm^{-1}	
F(000)	624	
Crystal size	0.26 x 0.18 x 0.04 mm^3	
Theta range for data collection	2.065 to 26.523°.	
Index ranges	-6<=h<=8, -10<=k<=14, -24<=l<=24	
Reflections collected	10654	
Independent reflections	3091 [R(int) = 0.0390]	
Completeness to theta = 25.242°	99.9 %	
Absorption correction	Semi-empirical from equivalents	
Max. and min. transmission	0.4908 and 0.4416	
Refinement method	Full-matrix least-squares on F^2	
Data / restraints / parameters	3091 / 1 / 185	
Goodness-of-fit on F^2	1.055	
Final R indices [I>2sigma(I)]	R1 = 0.0327, wR2 = 0.0730	
R indices (all data)	R1 = 0.0379, wR2 = 0.0752	
Absolute structure parameter	-0.01(5)	
Largest diff. peak and hole	0.265 and -0.323 $e.Å^{-3}$	

Table 2. Atomic coordinates (x 10^4) and equivalent isotropic displacement parameters ($Å^2$x 10^3) for Baran874. U(eq) is defined as one third of the trace of the orthogonalized U^{ij} tensor.

	x	y	z	U(eq)
S(1)	4402(1)	1695(1)	7302(1)	14(1)
O(1)	4114(3)	470(1)	7202(1)	19(1)
O(2)	2963(3)	2512(1)	7054(1)	19(1)
O(3)	10921(3)	5057(2)	7724(1)	26(1)
O(4)	9850(3)	4466(1)	6701(1)	21(1)
N(1)	6516(3)	2004(2)	6939(1)	14(1)
C(1)	3957(4)	2957(2)	8486(1)	20(1)
C(2)	4379(4)	3190(2)	9168(1)	26(1)
C(3)	5590(5)	2446(2)	9541(1)	29(1)
C(4)	6386(4)	1460(2)	9238(1)	26(1)
C(5)	5966(4)	1208(2)	8556(1)	20(1)
C(6)	4744(4)	1958(2)	8190(1)	15(1)
C(7)	7300(4)	3182(2)	7032(1)	13(1)
C(8)	8670(3)	3396(2)	7642(1)	15(1)
C(9)	9938(4)	4385(2)	7392(1)	19(1)
C(10)	8623(4)	3514(2)	6427(1)	18(1)
C(11)	7510(4)	3923(2)	5800(1)	23(1)
C(12)	8618(5)	4032(2)	5133(1)	31(1)
C(13)	10541(6)	3816(2)	5065(2)	43(1)
C(14)	7318(6)	4400(3)	4543(2)	47(1)

Table 3. Bond lengths [Å] and angles [°] for Baran874.

S(1)-O(1)	1.4292(16)
S(1)-O(2)	1.4282(17)
S(1)-N(1)	1.623(2)
S(1)-C(6)	1.767(2)
O(3)-C(9)	1.202(3)
O(4)-C(9)	1.347(3)
O(4)-C(10)	1.466(3)
N(1)-H(1)	0.866(12)
N(1)-C(7)	1.458(3)
C(1)-H(1A)	0.9500
C(1)-C(2)	1.382(3)
C(1)-C(6)	1.385(3)
C(2)-H(2)	0.9500
C(2)-C(3)	1.382(4)
C(3)-H(3)	0.9500
C(3)-C(4)	1.380(4)
C(4)-H(4)	0.9500
C(4)-C(5)	1.386(3)
C(5)-H(5)	0.9500
C(5)-C(6)	1.384(3)
C(7)-H(7)	1.0000
C(7)-C(8)	1.522(3)
C(7)-C(10)	1.521(3)
C(8)-H(8A)	0.9900
C(8)-H(8B)	0.9900
C(8)-C(9)	1.497(3)
C(10)-H(10)	1.0000
C(10)-C(11)	1.503(3)
C(11)-H(11A)	0.9900
C(11)-H(11B)	0.9900
C(11)-C(12)	1.501(4)
C(12)-C(13)	1.320(5)
C(12)-C(14)	1.501(5)
C(13)-H(13A)	0.9500

C(13)-H(13B)	0.9500
C(14)-H(14A)	0.9800
C(14)-H(14B)	0.9800
C(14)-H(14C)	0.9800
O(1)-S(1)-N(1)	105.83(10)
O(1)-S(1)-C(6)	108.49(10)
O(2)-S(1)-O(1)	120.33(11)
O(2)-S(1)-N(1)	107.54(10)
O(2)-S(1)-C(6)	107.89(11)
N(1)-S(1)-C(6)	105.91(11)
C(9)-O(4)-C(10)	109.61(18)
S(1)-N(1)-H(1)	111.3(17)
C(7)-N(1)-S(1)	117.57(15)
C(7)-N(1)-H(1)	116.5(17)
C(2)-C(1)-H(1A)	120.7
C(2)-C(1)-C(6)	118.7(2)
C(6)-C(1)-H(1A)	120.7
C(1)-C(2)-H(2)	119.8
C(1)-C(2)-C(3)	120.3(2)
C(3)-C(2)-H(2)	119.8
C(2)-C(3)-H(3)	119.8
C(4)-C(3)-C(2)	120.5(2)
C(4)-C(3)-H(3)	119.8
C(3)-C(4)-H(4)	120.0
C(3)-C(4)-C(5)	120.0(3)
C(5)-C(4)-H(4)	120.0
C(4)-C(5)-H(5)	120.5
C(6)-C(5)-C(4)	118.9(2)
C(6)-C(5)-H(5)	120.5
C(1)-C(6)-S(1)	119.79(18)
C(5)-C(6)-S(1)	118.32(19)
C(5)-C(6)-C(1)	121.6(2)
N(1)-C(7)-H(7)	108.8
N(1)-C(7)-C(8)	117.55(19)
N(1)-C(7)-C(10)	110.30(18)
C(8)-C(7)-H(7)	108.8

C(10)-C(7)-H(7)	108.8
C(10)-C(7)-C(8)	102.10(18)
C(7)-C(8)-H(8A)	111.3
C(7)-C(8)-H(8B)	111.3
H(8A)-C(8)-H(8B)	109.2
C(9)-C(8)-C(7)	102.20(18)
C(9)-C(8)-H(8A)	111.3
C(9)-C(8)-H(8B)	111.3
O(3)-C(9)-O(4)	121.0(2)
O(3)-C(9)-C(8)	128.4(2)
O(4)-C(9)-C(8)	110.6(2)
O(4)-C(10)-C(7)	103.50(17)
O(4)-C(10)-H(10)	109.6
O(4)-C(10)-C(11)	110.0(2)
C(7)-C(10)-H(10)	109.6
C(11)-C(10)-C(7)	114.5(2)
C(11)-C(10)-H(10)	109.6
C(10)-C(11)-H(11A)	107.6
C(10)-C(11)-H(11B)	107.6
H(11A)-C(11)-H(11B)	107.1
C(12)-C(11)-C(10)	118.7(2)
C(12)-C(11)-H(11A)	107.6
C(12)-C(11)-H(11B)	107.6
C(11)-C(12)-C(14)	113.3(3)
C(13)-C(12)-C(11)	123.7(3)
C(13)-C(12)-C(14)	122.9(3)
C(12)-C(13)-H(13A)	120.0
C(12)-C(13)-H(13B)	120.0
H(13A)-C(13)-H(13B)	120.0
C(12)-C(14)-H(14A)	109.5
C(12)-C(14)-H(14B)	109.5
C(12)-C(14)-H(14C)	109.5
H(14A)-C(14)-H(14B)	109.5
H(14A)-C(14)-H(14C)	109.5
H(14B)-C(14)-H(14C)	109.5

Symmetry transformations used to generate equivalent atoms:

Table 4. Anisotropic displacement parameters ($Å^2 x\ 10^3$) for Baran874. The anisotropic displacement factor exponent takes the form: $-2\pi^2[\ h^2\ a^{*2}U^{11} + ...\ + 2\ h\ k\ a^*\ b^*\ U^{12}]$

	U^{11}	U^{22}	U^{33}	U^{23}	U^{13}	U^{12}
S(1)	13(1)	15(1)	16(1)	0(1)	-1(1)	-1(1)
O(1)	20(1)	14(1)	23(1)	0(1)	-2(1)	-6(1)
O(2)	14(1)	22(1)	22(1)	1(1)	-3(1)	1(1)
O(3)	19(1)	18(1)	40(1)	-3(1)	-3(1)	-6(1)
O(4)	19(1)	16(1)	27(1)	2(1)	4(1)	-4(1)
N(1)	14(1)	9(1)	18(1)	0(1)	1(1)	1(1)
C(1)	18(1)	18(1)	22(1)	1(1)	3(1)	-1(1)
C(2)	29(1)	25(1)	24(1)	-7(1)	6(1)	0(1)
C(3)	32(2)	37(2)	16(1)	-4(1)	0(1)	-3(2)
C(4)	29(2)	29(2)	21(1)	3(1)	-5(1)	0(1)
C(5)	18(1)	20(1)	21(1)	1(1)	0(1)	0(1)
C(6)	13(1)	15(1)	16(1)	2(1)	4(1)	-4(1)
C(7)	14(1)	9(1)	17(1)	0(1)	2(1)	1(1)
C(8)	13(1)	12(1)	20(1)	1(1)	1(1)	0(1)
C(9)	12(1)	18(1)	27(1)	1(1)	2(1)	2(1)
C(10)	19(1)	13(1)	22(1)	1(1)	4(1)	-3(1)
C(11)	31(2)	18(1)	21(1)	1(1)	4(1)	-1(1)
C(12)	56(2)	13(1)	24(1)	-3(1)	12(2)	-4(1)
C(13)	67(3)	24(2)	37(2)	3(1)	32(2)	3(2)
C(14)	85(3)	35(2)	21(1)	1(1)	4(2)	-12(2)

Table 5. Hydrogen coordinates (x 10^4) and isotropic displacement parameters ($Å^2$x 10^{-3}) for Baran874.

	x	y	z	U(eq)
H(1)	7360(30)	1436(16)	6984(13)	17
H(1A)	3142	3472	8226	24
H(2)	3834	3864	9382	31
H(3)	5877	2615	10009	34
H(4)	7222	955	9497	31
H(5)	6508	532	8344	24
H(7)	6158	3742	7056	16
H(8A)	7905	3620	8057	18
H(8B)	9485	2697	7747	18
H(10)	9494	2838	6303	22
H(11A)	6385	3378	5725	28
H(11B)	6929	4696	5908	28
H(13A)	11302	3577	5452	51
H(13B)	11163	3900	4629	51
H(14A)	6238	3832	4484	70
H(14B)	8116	4435	4121	70
H(14C)	6753	5172	4638	70

Crystal Structure of 2.153

Experimental Summary

The single crystal X-ray diffraction studies were carried out on a Bruker D8 Venture diffractometer equipped with Mo K_α radiation (λ=0.71073 Å).

Crystals of the subject compound were used as received (THF/Pentane).

A 0.200 x 0.200 x 0.200 mm colorless crystal was mounted on a Cryoloop with Paratone oil. Data were collected in a nitrogen gas stream at 100(2) K using ϕ and ϖ scans. Crystal-to-detector distance was 50 mm and exposure time was 1.0 seconds (depending on the 2θ range) per frame using a scan width of 0.70°. Data collection was 99.8% complete to 25.242° in θ.

A total of 54708 reflections were collected, 3094 reflections were found to be symmetry independent, with a R_{int} of 0.0620. Indexing and unit cell refinement indicated a **Trigonal** lattice. The space group was found to be ***P*6$_2$21**. The data were integrated using the Bruker SAINT Software program and scaled using the SADABS software program. Solution by direct methods (SHELXT) produced a complete phasing model consistent with the proposed structure.

All nonhydrogen atoms were refined anisotropically by full-matrix least-squares (SHELXL-2014). All carbon bonded hydrogen atoms were placed using a riding model. Their positions were constrained relative to their parent atom using the appropriate HFIX command in SHELXL-2014.

Crystallographic data are summarized in Table 1.

Notes: Excellent data and refinement

Absolute structure parameter -0.01(3) Conclusive

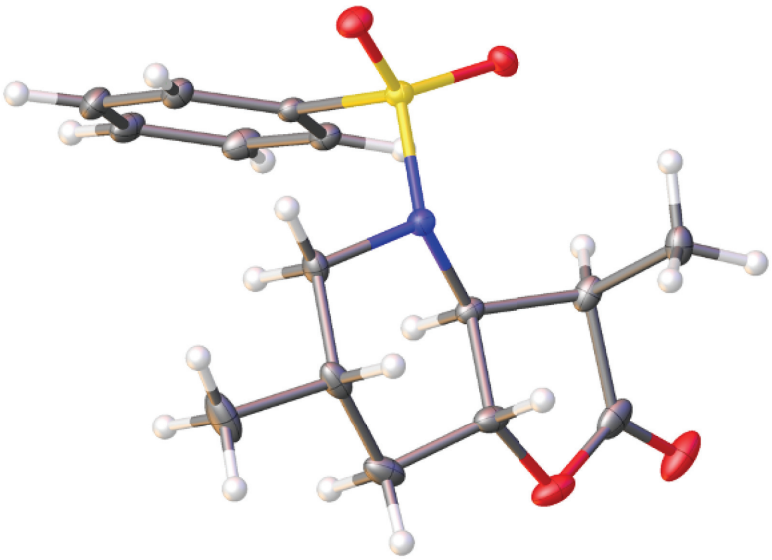


Table 1. Crystal data and structure refinement for Baran877.

Report date	2023-07-03	
Identification code	Baran877	
Empirical formula	C15 H19 N O4 S	
Molecular formula	C15 H19 N O4 S	
Formula weight	309.37	
Temperature	100.00 K	
Wavelength	0.71073 Å	
Crystal system	Trigonal	
Space group	$P3_221$	
Unit cell dimensions	a = 10.62870(10) Å	α= 90°.
	b = 10.62870(10) Å	β= 90°.
	c = 23.2385(5) Å	γ = 120°.
Volume	2273.52(6) $Å^3$	
Z	6	
Density (calculated)	1.356 Mg/m^3	
Absorption coefficient	0.229 mm^{-1}	
F(000)	984	
Crystal size	0.2 x 0.2 x 0.2 mm^3	
Crystal color, habit	colorless octahedral	
Theta range for data collection	2.629 to 26.363°.	
Index ranges	-13<=h<=13, -13<=k<=13, -29<=l<=28	
Reflections collected	54708	
Independent reflections	3094 [R(int) = 0.0620]	
Completeness to theta = 25.242°	99.8 %	
Absorption correction	Semi-empirical from equivalents	
Max. and min. transmission	0.7381 and 0.7098	
Refinement method	Full-matrix least-squares on F^2	
Data / restraints / parameters	3094 / 0 / 192	
Goodness-of-fit on F^2	1.032	
Final R indices [I>2sigma(I)]	R1 = 0.0266, wR2 = 0.0635	
R indices (all data)	R1 = 0.0294, wR2 = 0.0650	
Absolute structure parameter	-0.01(3)	
Largest diff. peak and hole	0.210 and -0.269 $e.Å^{-3}$	

Table 2. Atomic coordinates (x 10^4) and equivalent isotropic displacement parameters ($Å^2$x 10^3) for Baran877. U(eq) is defined as one third of the trace of the orthogonalized U^{ij} tensor.

	x	y	z	U(eq)
S(1)	5667(1)	8787(1)	5060(1)	16(1)
O(1)	5482(2)	9766(2)	5428(1)	24(1)
O(2)	5700(2)	7569(2)	5309(1)	21(1)
O(3)	3530(2)	3689(2)	3677(1)	38(1)
O(4)	2850(2)	5330(2)	3494(1)	30(1)
N(1)	4283(2)	8132(2)	4598(1)	16(1)
C(1)	7848(2)	11291(2)	4580(1)	22(1)
C(2)	9140(2)	12076(2)	4279(1)	27(1)
C(3)	9872(2)	11390(2)	4075(1)	26(1)
C(4)	9304(2)	9915(3)	4158(1)	25(1)
C(5)	7996(2)	9103(2)	4448(1)	20(1)
C(6)	7290(2)	9808(2)	4662(1)	17(1)
C(7)	4226(2)	7064(2)	4180(1)	16(1)
C(8)	4061(2)	5612(2)	4383(1)	21(1)
C(9)	2942(2)	4862(2)	4868(1)	24(1)
C(10)	3485(2)	4750(2)	3826(1)	27(1)
C(11)	2855(2)	6510(2)	3816(1)	22(1)
C(12)	2821(2)	7669(3)	3462(1)	28(1)
C(13)	2854(2)	8753(2)	3902(1)	24(1)
C(14)	2862(3)	10055(3)	3618(1)	40(1)
C(15)	4192(2)	9323(2)	4293(1)	20(1)

Table 3. Bond lengths [Å] and angles [°] for Baran877.

S(1)-O(1)	1.4335(14)
S(1)-O(2)	1.4348(15)
S(1)-N(1)	1.6658(16)
S(1)-C(6)	1.7710(19)
O(3)-C(10)	1.204(3)
O(4)-C(10)	1.360(3)
O(4)-C(11)	1.459(2)
N(1)-C(7)	1.472(2)
N(1)-C(15)	1.497(2)
C(1)-H(1)	0.9500
C(1)-C(2)	1.387(3)
C(1)-C(6)	1.391(3)
C(2)-H(2)	0.9500
C(2)-C(3)	1.390(3)
C(3)-H(3)	0.9500
C(3)-C(4)	1.383(3)
C(4)-H(4)	0.9500
C(4)-C(5)	1.390(3)
C(5)-H(5)	0.9500
C(5)-C(6)	1.391(3)
C(7)-H(7)	1.0000
C(7)-C(8)	1.538(3)
C(7)-C(11)	1.526(3)
C(8)-H(8)	1.0000
C(8)-C(9)	1.540(3)
C(8)-C(10)	1.526(3)
C(9)-H(9A)	0.9800
C(9)-H(9B)	0.9800
C(9)-H(9C)	0.9800
C(11)-H(11)	1.0000
C(11)-C(12)	1.497(3)
C(12)-H(12A)	0.9900
C(12)-H(12B)	0.9900
C(12)-C(13)	1.528(3)

C(13)-H(13)	1.0000
C(13)-C(14)	1.528(3)
C(13)-C(15)	1.533(3)
C(14)-H(14A)	0.9800
C(14)-H(14B)	0.9800
C(14)-H(14C)	0.9800
C(15)-H(15A)	0.9900
C(15)-H(15B)	0.9900
O(1)-S(1)-O(2)	119.20(8)
O(1)-S(1)-N(1)	105.94(8)
O(1)-S(1)-C(6)	108.15(9)
O(2)-S(1)-N(1)	107.29(8)
O(2)-S(1)-C(6)	107.92(9)
N(1)-S(1)-C(6)	107.87(8)
C(10)-O(4)-C(11)	107.98(15)
C(7)-N(1)-S(1)	115.73(12)
C(7)-N(1)-C(15)	110.11(14)
C(15)-N(1)-S(1)	111.63(12)
C(2)-C(1)-H(1)	120.5
C(2)-C(1)-C(6)	118.93(19)
C(6)-C(1)-H(1)	120.5
C(1)-C(2)-H(2)	119.9
C(1)-C(2)-C(3)	120.1(2)
C(3)-C(2)-H(2)	119.9
C(2)-C(3)-H(3)	119.8
C(4)-C(3)-C(2)	120.36(19)
C(4)-C(3)-H(3)	119.8
C(3)-C(4)-H(4)	119.8
C(3)-C(4)-C(5)	120.4(2)
C(5)-C(4)-H(4)	119.8
C(4)-C(5)-H(5)	120.6
C(4)-C(5)-C(6)	118.72(19)
C(6)-C(5)-H(5)	120.6
C(1)-C(6)-S(1)	119.91(15)
C(5)-C(6)-S(1)	118.64(16)
C(5)-C(6)-C(1)	121.44(18)

N(1)-C(7)-H(7)	108.8
N(1)-C(7)-C(8)	120.73(15)
N(1)-C(7)-C(11)	109.05(15)
C(8)-C(7)-H(7)	108.8
C(11)-C(7)-H(7)	108.8
C(11)-C(7)-C(8)	100.07(16)
C(7)-C(8)-H(8)	111.1
C(7)-C(8)-C(9)	114.52(16)
C(9)-C(8)-H(8)	111.1
C(10)-C(8)-C(7)	98.77(16)
C(10)-C(8)-H(8)	111.1
C(10)-C(8)-C(9)	109.58(17)
C(8)-C(9)-H(9A)	109.5
C(8)-C(9)-H(9B)	109.5
C(8)-C(9)-H(9C)	109.5
H(9A)-C(9)-H(9B)	109.5
H(9A)-C(9)-H(9C)	109.5
H(9B)-C(9)-H(9C)	109.5
O(3)-C(10)-O(4)	121.5(2)
O(3)-C(10)-C(8)	128.0(2)
O(4)-C(10)-C(8)	110.54(17)
O(4)-C(11)-C(7)	102.05(16)
O(4)-C(11)-H(11)	108.4
O(4)-C(11)-C(12)	115.70(17)
C(7)-C(11)-H(11)	108.4
C(12)-C(11)-C(7)	113.48(18)
C(12)-C(11)-H(11)	108.4
C(11)-C(12)-H(12A)	110.8
C(11)-C(12)-H(12B)	110.8
C(11)-C(12)-C(13)	104.56(16)
H(12A)-C(12)-H(12B)	108.9
C(13)-C(12)-H(12A)	110.8
C(13)-C(12)-H(12B)	110.8
C(12)-C(13)-H(13)	108.3
C(12)-C(13)-C(15)	111.18(17)
C(14)-C(13)-C(12)	112.40(19)

C(14)-C(13)-H(13)	108.3
C(14)-C(13)-C(15)	108.3(2)
C(15)-C(13)-H(13)	108.3
C(13)-C(14)-H(14A)	109.5
C(13)-C(14)-H(14B)	109.5
C(13)-C(14)-H(14C)	109.5
H(14A)-C(14)-H(14B)	109.5
H(14A)-C(14)-H(14C)	109.5
H(14B)-C(14)-H(14C)	109.5
N(1)-C(15)-C(13)	112.71(17)
N(1)-C(15)-H(15A)	109.0
N(1)-C(15)-H(15B)	109.0
C(13)-C(15)-H(15A)	109.0
C(13)-C(15)-H(15B)	109.0
H(15A)-C(15)-H(15B)	107.8

Crystal Structure of 2.154

Experimental Summary

The single crystal X-ray diffraction studies were carried out on a Bruker Microstar APEX II CCD diffractometer equipped with Cu K_α radiation (λ = 1.54178 Å).

Crystals of the subject compound were used as received. A 0.23 x 0.2 x 0.18 mm piece of a crystal was mounted on a Cryoloop with Paratone oil. Data were collected in a nitrogen gas stream at 100(2) K using ϕ and ω scans. Crystal-to-detector distance was 40 mm and exposure time was 1, 3, or 5 seconds depending on the 2θ range per frame using a scan width of 1.25°. Data collection was 100 % complete to 67.679° in θ. A total of 43360 reflections were collected covering the indices, −12<=h<=12, −15<=k<=13, −39<=l<=38. 8178 reflections were found to be symmetry independent, with a R_{int} of 0.0307. Indexing and unit cell refinement indicated a **P**rimitive, **Orthorhombic** lattice. The space group was found to be ***P*2$_1$2$_1$2$_1$**. The data were integrated using the Bruker SAINT Software program and scaled using the SADABS software program. Solution by direct methods (SHELXT) produced a complete phasing model consistent with the proposed structure.

All nonhydrogen atoms were refined anisotropically by full-matrix least-squares (SHELXL-2014). All carbon bonded hydrogen atoms were placed using a riding model. Their positions were constrained relative to their parent atom using the appropriate HFIX command in SHELXL-2014. Crystallographic data are summarized in Table 1.

Notes: Great data! Absolute stereochemistry was conclusively assigned (Absolute Structure Parameter = 0.023(3)). There is one copy of the compound in the asymmetric unit. The chemical formula for the compound is: $C_{48}H_{71}NO_5SSi$

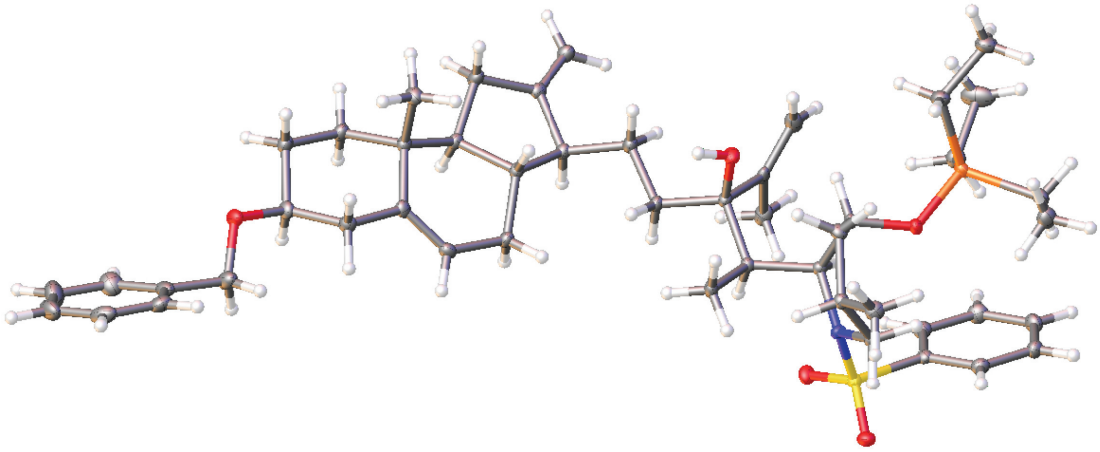


Table 1. Crystal data and structure refinement for Baran852.

Identification code	baran852_0m_a	
Empirical formula	C48 H71 N O5 S Si	
Formula weight	802.20	
Temperature	100.15 K	
Wavelength	1.54178 Å	
Crystal system	Orthorhombic	
Space group	$P2_12_12_1$	
Unit cell dimensions	a = 10.4806(2) Å	α= 90°.
	b = 12.8655(3) Å	β= 90°.
	c = 33.0312(8) Å	γ = 90°.
Volume	4453.87(17) $Å^3$	
Z	4	
Density (calculated)	1.196 Mg/m^3	
Absorption coefficient	1.257 mm^{-1}	
F(000)	1744	
Crystal size	0.23 x 0.2 x 0.18 mm^3	
Theta range for data collection	2.675 to 68.766°.	
Index ranges	-12<=h<=12, -15<=k<=13, -39<=l<=38	
Reflections collected	43360	
Independent reflections	8178 [R(int) = 0.0307]	
Completeness to theta = 67.679°	99.9 %	
Absorption correction	Semi-empirical from equivalents	
Max. and min. transmission	0.5212 and 0.4128	
Refinement method	Full-matrix least-squares on F^2	
Data / restraints / parameters	8178 / 0 / 513	
Goodness-of-fit on F^2	1.045	
Final R indices [I>2sigma(I)]	R1 = 0.0236, wR2 = 0.0589	
R indices (all data)	R1 = 0.0244, wR2 = 0.0592	
Absolute structure parameter	0.023(3)	
Largest diff. peak and hole	0.223 and -0.272 $e.Å^{-3}$	

Table 2. Atomic coordinates (x 10^4) and equivalent isotropic displacement parameters ($Å^2$x 10^3) for Baran852. U(eq) is defined as one third of the trace of the orthogonalized U^{ij} tensor.

	x	y	z	U(eq)
S(1)	5257(1)	3094(1)	2374(1)	12(1)
Si(1)	9083(1)	1414(1)	3136(1)	13(1)
O(1)	1150(1)	10344(1)	5260(1)	18(1)
O(2)	7054(1)	4294(1)	3921(1)	16(1)
O(3)	7561(1)	1731(1)	3113(1)	14(1)
O(4)	4172(1)	2589(1)	2198(1)	18(1)
O(5)	5364(1)	4205(1)	2357(1)	17(1)
N(1)	5317(1)	2759(1)	2847(1)	12(1)
C(1)	-1173(2)	11728(2)	5403(1)	28(1)
C(2)	-2125(2)	12166(2)	5636(1)	34(1)
C(3)	-3022(2)	11541(2)	5823(1)	31(1)
C(4)	-2955(2)	10479(2)	5784(1)	28(1)
C(5)	-1985(2)	10030(2)	5554(1)	24(1)
C(6)	-1093(2)	10655(2)	5358(1)	21(1)
C(7)	-93(2)	10167(2)	5094(1)	26(1)
C(8)	2163(2)	10119(1)	4977(1)	16(1)
C(9)	3414(2)	10461(1)	5165(1)	17(1)
C(10)	4531(2)	10196(1)	4884(1)	16(1)
C(11)	4624(2)	9028(1)	4773(1)	13(1)
C(12)	4946(2)	8393(1)	5154(1)	18(1)
C(13)	5628(2)	8881(1)	4439(1)	13(1)
C(14)	7046(2)	8945(2)	4551(1)	17(1)
C(15)	7709(2)	8423(1)	4198(1)	14(1)
C(16)	8944(2)	8517(1)	4114(1)	18(1)
C(17)	6753(2)	7764(1)	3965(1)	14(1)
C(18)	5522(2)	7835(1)	4219(1)	12(1)
C(19)	4249(2)	7789(1)	3995(1)	16(1)
C(20)	3181(2)	8167(1)	4262(1)	16(1)
C(21)	3330(2)	8687(1)	4608(1)	14(1)
C(22)	2186(2)	8968(1)	4864(1)	17(1)
C(23)	7258(2)	6665(1)	3881(1)	16(1)

C(24)	6298(2)	5964(1)	3665(1)	14(1)
C(25)	6809(2)	4870(1)	3558(1)	12(1)
C(26)	8077(2)	4975(1)	3331(1)	15(1)
C(27)	9156(2)	4601(1)	3482(1)	21(1)
C(28)	8041(2)	5552(2)	2936(1)	20(1)
C(29)	5805(2)	4293(1)	3292(1)	12(1)
C(30)	4531(2)	4164(1)	3511(1)	15(1)
C(31)	6328(2)	3275(1)	3097(1)	11(1)
C(32)	6926(2)	2458(1)	3376(1)	13(1)
C(33)	5967(2)	1868(1)	3636(1)	15(1)
C(34)	10053(2)	2419(2)	2863(1)	20(1)
C(35)	11477(2)	2466(2)	2959(1)	36(1)
C(36)	9174(2)	136(1)	2869(1)	18(1)
C(37)	8238(2)	-679(2)	3031(1)	23(1)
C(38)	9536(2)	1271(2)	3685(1)	20(1)
C(39)	10823(2)	752(2)	3770(1)	24(1)
C(40)	4732(2)	1580(1)	3405(1)	14(1)
C(41)	4287(2)	484(1)	3508(1)	18(1)
C(42)	4926(2)	1678(1)	2949(1)	13(1)
C(43)	6631(2)	2589(1)	2128(1)	14(1)
C(44)	6696(2)	1527(1)	2042(1)	16(1)
C(45)	7758(2)	1145(1)	1838(1)	18(1)
C(46)	8735(2)	1815(2)	1719(1)	19(1)
C(47)	8659(2)	2862(2)	1810(1)	20(1)
C(48)	7609(2)	3256(1)	2017(1)	16(1)

Table 3. Bond lengths [Å] and angles [°] forBaran852.

S(1)-O(4)	1.4338(13)
S(1)-O(5)	1.4345(12)
S(1)-N(1)	1.6226(14)
S(1)-C(43)	1.7772(18)
Si(1)-O(3)	1.6491(12)
Si(1)-C(34)	1.8766(19)
Si(1)-C(36)	1.8679(18)
Si(1)-C(38)	1.8827(19)
O(1)-C(7)	1.431(2)
O(1)-C(8)	1.443(2)
O(2)-H(2)	0.8400
O(2)-C(25)	1.434(2)
O(3)-C(32)	1.440(2)
N(1)-C(31)	1.498(2)
N(1)-C(42)	1.488(2)
C(1)-H(1)	0.9500
C(1)-C(2)	1.381(3)
C(1)-C(6)	1.390(3)
C(2)-H(2A)	0.9500
C(2)-C(3)	1.382(4)
C(3)-H(3)	0.9500
C(3)-C(4)	1.374(3)
C(4)-H(4)	0.9500
C(4)-C(5)	1.394(3)
C(5)-H(5)	0.9500
C(5)-C(6)	1.392(3)
C(6)-C(7)	1.503(3)
C(7)-H(7A)	0.9900
C(7)-H(7B)	0.9900
C(8)-H(8)	1.0000
C(8)-C(9)	1.517(3)
C(8)-C(22)	1.527(2)
C(9)-H(9A)	0.9900
C(9)-H(9B)	0.9900

C(9)-C(10)	1.533(2)
C(10)-H(10A)	0.9900
C(10)-H(10B)	0.9900
C(10)-C(11)	1.549(2)
C(11)-C(12)	1.540(2)
C(11)-C(13)	1.535(2)
C(11)-C(21)	1.526(2)
C(12)-H(12A)	0.9800
C(12)-H(12B)	0.9800
C(12)-H(12C)	0.9800
C(13)-H(13)	1.0000
C(13)-C(14)	1.534(2)
C(13)-C(18)	1.534(2)
C(14)-H(14A)	0.9900
C(14)-H(14B)	0.9900
C(14)-C(15)	1.513(2)
C(15)-C(16)	1.329(3)
C(15)-C(17)	1.523(2)
C(16)-H(16A)	0.9500
C(16)-H(16B)	0.9500
C(17)-H(17)	1.0000
C(17)-C(18)	1.543(2)
C(17)-C(23)	1.535(2)
C(18)-H(18)	1.0000
C(18)-C(19)	1.527(2)
C(19)-H(19A)	0.9900
C(19)-H(19B)	0.9900
C(19)-C(20)	1.505(2)
C(20)-H(20)	0.9500
C(20)-C(21)	1.335(3)
C(21)-C(22)	1.511(2)
C(22)-H(22A)	0.9900
C(22)-H(22B)	0.9900
C(23)-H(23A)	0.9900
C(23)-H(23B)	0.9900
C(23)-C(24)	1.527(2)

C(24)-H(24A)	0.9900
C(24)-H(24B)	0.9900
C(24)-C(25)	1.547(2)
C(25)-C(26)	1.531(2)
C(25)-C(29)	1.558(2)
C(26)-C(27)	1.326(3)
C(26)-C(28)	1.503(3)
C(27)-H(27A)	0.9500
C(27)-H(27B)	0.9500
C(28)-H(28A)	0.9800
C(28)-H(28B)	0.9800
C(28)-H(28C)	0.9800
C(29)-H(29)	1.0000
C(29)-C(30)	1.528(2)
C(29)-C(31)	1.559(2)
C(30)-H(30A)	0.9800
C(30)-H(30B)	0.9800
C(30)-H(30C)	0.9800
C(31)-H(31)	1.0000
C(31)-C(32)	1.532(2)
C(32)-H(32)	1.0000
C(32)-C(33)	1.524(2)
C(33)-H(33A)	0.9900
C(33)-H(33B)	0.9900
C(33)-C(40)	1.547(2)
C(34)-H(34A)	0.9900
C(34)-H(34B)	0.9900
C(34)-C(35)	1.528(3)
C(35)-H(35A)	0.9800
C(35)-H(35B)	0.9800
C(35)-H(35C)	0.9800
C(36)-H(36A)	0.9900
C(36)-H(36B)	0.9900
C(36)-C(37)	1.533(3)
C(37)-H(37A)	0.9800
C(37)-H(37B)	0.9800

C(37)-H(37C)	0.9800
C(38)-H(38A)	0.9900
C(38)-H(38B)	0.9900
C(38)-C(39)	1.531(3)
C(39)-H(39A)	0.9800
C(39)-H(39B)	0.9800
C(39)-H(39C)	0.9800
C(40)-H(40)	1.0000
C(40)-C(41)	1.523(2)
C(40)-C(42)	1.526(2)
C(41)-H(41A)	0.9800
C(41)-H(41B)	0.9800
C(41)-H(41C)	0.9800
C(42)-H(42A)	0.9900
C(42)-H(42B)	0.9900
C(43)-C(44)	1.397(3)
C(43)-C(48)	1.386(3)
C(44)-H(44)	0.9500
C(44)-C(45)	1.390(3)
C(45)-H(45)	0.9500
C(45)-C(46)	1.394(3)
C(46)-H(46)	0.9500
C(46)-C(47)	1.382(3)
C(47)-H(47)	0.9500
C(47)-C(48)	1.391(3)
C(48)-H(48)	0.9500

O(4)-S(1)-O(5)	119.86(8)
O(4)-S(1)-N(1)	107.51(7)
O(4)-S(1)-C(43)	106.93(8)
O(5)-S(1)-N(1)	107.43(7)
O(5)-S(1)-C(43)	106.46(8)
N(1)-S(1)-C(43)	108.21(8)
O(3)-Si(1)-C(34)	109.34(8)
O(3)-Si(1)-C(36)	104.17(7)
O(3)-Si(1)-C(38)	108.25(7)

C(34)-Si(1)-C(38)	113.24(9)
C(36)-Si(1)-C(34)	110.57(8)
C(36)-Si(1)-C(38)	110.84(8)
C(7)-O(1)-C(8)	112.93(13)
C(25)-O(2)-H(2)	109.5
C(32)-O(3)-Si(1)	125.42(10)
C(31)-N(1)-S(1)	116.10(11)
C(42)-N(1)-S(1)	117.09(11)
C(42)-N(1)-C(31)	118.98(13)
C(2)-C(1)-H(1)	119.8
C(2)-C(1)-C(6)	120.5(2)
C(6)-C(1)-H(1)	119.8
C(1)-C(2)-H(2A)	119.9
C(1)-C(2)-C(3)	120.2(2)
C(3)-C(2)-H(2A)	119.9
C(2)-C(3)-H(3)	119.9
C(4)-C(3)-C(2)	120.1(2)
C(4)-C(3)-H(3)	119.9
C(3)-C(4)-H(4)	120.0
C(3)-C(4)-C(5)	120.1(2)
C(5)-C(4)-H(4)	120.0
C(4)-C(5)-H(5)	119.9
C(6)-C(5)-C(4)	120.1(2)
C(6)-C(5)-H(5)	119.9
C(1)-C(6)-C(5)	118.98(18)
C(1)-C(6)-C(7)	121.23(19)
C(5)-C(6)-C(7)	119.76(19)
O(1)-C(7)-C(6)	110.21(15)
O(1)-C(7)-H(7A)	109.6
O(1)-C(7)-H(7B)	109.6
C(6)-C(7)-H(7A)	109.6
C(6)-C(7)-H(7B)	109.6
H(7A)-C(7)-H(7B)	108.1
O(1)-C(8)-H(8)	108.5
O(1)-C(8)-C(9)	108.22(14)
O(1)-C(8)-C(22)	111.37(15)

C(9)-C(8)-H(8)	108.5
C(9)-C(8)-C(22)	111.56(15)
C(22)-C(8)-H(8)	108.5
C(8)-C(9)-H(9A)	109.6
C(8)-C(9)-H(9B)	109.6
C(8)-C(9)-C(10)	110.29(14)
H(9A)-C(9)-H(9B)	108.1
C(10)-C(9)-H(9A)	109.6
C(10)-C(9)-H(9B)	109.6
C(9)-C(10)-H(10A)	108.7
C(9)-C(10)-H(10B)	108.7
C(9)-C(10)-C(11)	114.05(14)
H(10A)-C(10)-H(10B)	107.6
C(11)-C(10)-H(10A)	108.7
C(11)-C(10)-H(10B)	108.7
C(12)-C(11)-C(10)	109.52(14)
C(13)-C(11)-C(10)	109.43(14)
C(13)-C(11)-C(12)	111.83(14)
C(21)-C(11)-C(10)	107.90(14)
C(21)-C(11)-C(12)	109.52(14)
C(21)-C(11)-C(13)	108.56(14)
C(11)-C(12)-H(12A)	109.5
C(11)-C(12)-H(12B)	109.5
C(11)-C(12)-H(12C)	109.5
H(12A)-C(12)-H(12B)	109.5
H(12A)-C(12)-H(12C)	109.5
H(12B)-C(12)-H(12C)	109.5
C(11)-C(13)-H(13)	106.8
C(14)-C(13)-C(11)	119.00(14)
C(14)-C(13)-H(13)	106.8
C(18)-C(13)-C(11)	113.47(14)
C(18)-C(13)-H(13)	106.8
C(18)-C(13)-C(14)	103.33(14)
C(13)-C(14)-H(14A)	111.0
C(13)-C(14)-H(14B)	111.0
H(14A)-C(14)-H(14B)	109.0

C(15)-C(14)-C(13)	103.68(14)
C(15)-C(14)-H(14A)	111.0
C(15)-C(14)-H(14B)	111.0
C(14)-C(15)-C(17)	109.53(14)
C(16)-C(15)-C(14)	124.59(16)
C(16)-C(15)-C(17)	125.86(16)
C(15)-C(16)-H(16A)	120.0
C(15)-C(16)-H(16B)	120.0
H(16A)-C(16)-H(16B)	120.0
C(15)-C(17)-H(17)	108.1
C(15)-C(17)-C(18)	103.96(13)
C(15)-C(17)-C(23)	112.16(14)
C(18)-C(17)-H(17)	108.1
C(23)-C(17)-H(17)	108.1
C(23)-C(17)-C(18)	116.22(14)
C(13)-C(18)-C(17)	104.46(13)
C(13)-C(18)-H(18)	108.4
C(17)-C(18)-H(18)	108.4
C(19)-C(18)-C(13)	109.06(14)
C(19)-C(18)-C(17)	117.67(14)
C(19)-C(18)-H(18)	108.4
C(18)-C(19)-H(19A)	109.5
C(18)-C(19)-H(19B)	109.5
H(19A)-C(19)-H(19B)	108.1
C(20)-C(19)-C(18)	110.73(14)
C(20)-C(19)-H(19A)	109.5
C(20)-C(19)-H(19B)	109.5
C(19)-C(20)-H(20)	117.4
C(21)-C(20)-C(19)	125.23(16)
C(21)-C(20)-H(20)	117.4
C(20)-C(21)-C(11)	123.60(16)
C(20)-C(21)-C(22)	120.49(16)
C(22)-C(21)-C(11)	115.91(14)
C(8)-C(22)-H(22A)	109.1
C(8)-C(22)-H(22B)	109.1
C(21)-C(22)-C(8)	112.41(15)

C(21)-C(22)-H(22A)	109.1
C(21)-C(22)-H(22B)	109.1
H(22A)-C(22)-H(22B)	107.9
C(17)-C(23)-H(23A)	108.8
C(17)-C(23)-H(23B)	108.8
H(23A)-C(23)-H(23B)	107.7
C(24)-C(23)-C(17)	113.60(14)
C(24)-C(23)-H(23A)	108.8
C(24)-C(23)-H(23B)	108.8
C(23)-C(24)-H(24A)	108.6
C(23)-C(24)-H(24B)	108.6
C(23)-C(24)-C(25)	114.60(14)
H(24A)-C(24)-H(24B)	107.6
C(25)-C(24)-H(24A)	108.6
C(25)-C(24)-H(24B)	108.6
O(2)-C(25)-C(24)	109.83(13)
O(2)-C(25)-C(26)	107.42(13)
O(2)-C(25)-C(29)	110.25(13)
C(24)-C(25)-C(29)	109.23(13)
C(26)-C(25)-C(24)	109.42(14)
C(26)-C(25)-C(29)	110.67(13)
C(27)-C(26)-C(25)	121.68(16)
C(27)-C(26)-C(28)	121.79(17)
C(28)-C(26)-C(25)	116.51(15)
C(26)-C(27)-H(27A)	120.0
C(26)-C(27)-H(27B)	120.0
H(27A)-C(27)-H(27B)	120.0
C(26)-C(28)-H(28A)	109.5
C(26)-C(28)-H(28B)	109.5
C(26)-C(28)-H(28C)	109.5
H(28A)-C(28)-H(28B)	109.5
H(28A)-C(28)-H(28C)	109.5
H(28B)-C(28)-H(28C)	109.5
C(25)-C(29)-H(29)	105.4
C(25)-C(29)-C(31)	113.31(13)
C(30)-C(29)-C(25)	112.06(14)

C(30)-C(29)-H(29)	105.4
C(30)-C(29)-C(31)	114.34(13)
C(31)-C(29)-H(29)	105.4
C(29)-C(30)-H(30A)	109.5
C(29)-C(30)-H(30B)	109.5
C(29)-C(30)-H(30C)	109.5
H(30A)-C(30)-H(30B)	109.5
H(30A)-C(30)-H(30C)	109.5
H(30B)-C(30)-H(30C)	109.5
N(1)-C(31)-C(29)	110.58(13)
N(1)-C(31)-H(31)	106.3
N(1)-C(31)-C(32)	108.44(13)
C(29)-C(31)-H(31)	106.3
C(32)-C(31)-C(29)	118.11(14)
C(32)-C(31)-H(31)	106.3
O(3)-C(32)-C(31)	105.77(13)
O(3)-C(32)-H(32)	109.3
O(3)-C(32)-C(33)	108.73(13)
C(31)-C(32)-H(32)	109.3
C(33)-C(32)-C(31)	114.28(14)
C(33)-C(32)-H(32)	109.3
C(32)-C(33)-H(33A)	108.9
C(32)-C(33)-H(33B)	108.9
C(32)-C(33)-C(40)	113.15(14)
H(33A)-C(33)-H(33B)	107.8
C(40)-C(33)-H(33A)	108.9
C(40)-C(33)-H(33B)	108.9
Si(1)-C(34)-H(34A)	108.0
Si(1)-C(34)-H(34B)	108.0
H(34A)-C(34)-H(34B)	107.3
C(35)-C(34)-Si(1)	117.11(14)
C(35)-C(34)-H(34A)	108.0
C(35)-C(34)-H(34B)	108.0
C(34)-C(35)-H(35A)	109.5
C(34)-C(35)-H(35B)	109.5
C(34)-C(35)-H(35C)	109.5

H(35A)-C(35)-H(35B)	109.5
H(35A)-C(35)-H(35C)	109.5
H(35B)-C(35)-H(35C)	109.5
Si(1)-C(36)-H(36A)	108.8
Si(1)-C(36)-H(36B)	108.8
H(36A)-C(36)-H(36B)	107.7
C(37)-C(36)-Si(1)	113.93(13)
C(37)-C(36)-H(36A)	108.8
C(37)-C(36)-H(36B)	108.8
C(36)-C(37)-H(37A)	109.5
C(36)-C(37)-H(37B)	109.5
C(36)-C(37)-H(37C)	109.5
H(37A)-C(37)-H(37B)	109.5
H(37A)-C(37)-H(37C)	109.5
H(37B)-C(37)-H(37C)	109.5
Si(1)-C(38)-H(38A)	108.2
Si(1)-C(38)-H(38B)	108.2
H(38A)-C(38)-H(38B)	107.4
C(39)-C(38)-Si(1)	116.19(13)
C(39)-C(38)-H(38A)	108.2
C(39)-C(38)-H(38B)	108.2
C(38)-C(39)-H(39A)	109.5
C(38)-C(39)-H(39B)	109.5
C(38)-C(39)-H(39C)	109.5
H(39A)-C(39)-H(39B)	109.5
H(39A)-C(39)-H(39C)	109.5
H(39B)-C(39)-H(39C)	109.5
C(33)-C(40)-H(40)	108.2
C(41)-C(40)-C(33)	111.60(14)
C(41)-C(40)-H(40)	108.2
C(41)-C(40)-C(42)	109.82(14)
C(42)-C(40)-C(33)	110.80(14)
C(42)-C(40)-H(40)	108.2
C(40)-C(41)-H(41A)	109.5
C(40)-C(41)-H(41B)	109.5
C(40)-C(41)-H(41C)	109.5

H(41A)-C(41)-H(41B)	109.5
H(41A)-C(41)-H(41C)	109.5
H(41B)-C(41)-H(41C)	109.5
N(1)-C(42)-C(40)	109.74(13)
N(1)-C(42)-H(42A)	109.7
N(1)-C(42)-H(42B)	109.7
C(40)-C(42)-H(42A)	109.7
C(40)-C(42)-H(42B)	109.7
H(42A)-C(42)-H(42B)	108.2
C(44)-C(43)-S(1)	119.39(13)
C(48)-C(43)-S(1)	119.56(13)
C(48)-C(43)-C(44)	121.04(16)
C(43)-C(44)-H(44)	120.6
C(45)-C(44)-C(43)	118.88(16)
C(45)-C(44)-H(44)	120.6
C(44)-C(45)-H(45)	119.8
C(44)-C(45)-C(46)	120.38(16)
C(46)-C(45)-H(45)	119.8
C(45)-C(46)-H(46)	120.0
C(47)-C(46)-C(45)	119.95(17)
C(47)-C(46)-H(46)	120.0
C(46)-C(47)-H(47)	119.8
C(46)-C(47)-C(48)	120.44(17)
C(48)-C(47)-H(47)	119.8
C(43)-C(48)-C(47)	119.30(16)
C(43)-C(48)-H(48)	120.4
C(47)-C(48)-H(48)	120.4

Symmetry transformations used to generate equivalent atoms:

Table 4. Anisotropic displacement parameters ($Å^2 x\ 10^3$) for Baran852. The anisotropic displacement factor exponent takes the form: $-2\pi^2[\ h^2\ a^{*2}U^{11} + ...\ + 2\ h\ k\ a^*\ b^*\ U^{12}]$

	U^{11}	U^{22}	U^{33}	U^{23}	U^{13}	U^{12}
S(1)	13(1)	14(1)	11(1)	0(1)	-1(1)	2(1)
Si(1)	10(1)	14(1)	16(1)	-1(1)	-1(1)	2(1)
O(1)	13(1)	26(1)	15(1)	-5(1)	1(1)	3(1)
O(2)	20(1)	18(1)	11(1)	0(1)	-1(1)	4(1)
O(3)	12(1)	14(1)	17(1)	-4(1)	-1(1)	3(1)
O(4)	15(1)	22(1)	15(1)	-2(1)	-4(1)	2(1)
O(5)	22(1)	14(1)	15(1)	2(1)	0(1)	4(1)
N(1)	13(1)	11(1)	12(1)	-1(1)	-1(1)	-1(1)
C(1)	31(1)	31(1)	23(1)	4(1)	3(1)	3(1)
C(2)	38(1)	31(1)	32(1)	-2(1)	1(1)	15(1)
C(3)	20(1)	48(1)	26(1)	-9(1)	-1(1)	13(1)
C(4)	18(1)	47(1)	19(1)	-3(1)	0(1)	-6(1)
C(5)	24(1)	28(1)	21(1)	-6(1)	-7(1)	-2(1)
C(6)	15(1)	32(1)	15(1)	-5(1)	-3(1)	5(1)
C(7)	18(1)	38(1)	24(1)	-11(1)	-2(1)	3(1)
C(8)	16(1)	20(1)	14(1)	-2(1)	3(1)	3(1)
C(9)	18(1)	16(1)	17(1)	-4(1)	1(1)	0(1)
C(10)	16(1)	16(1)	16(1)	-4(1)	1(1)	-1(1)
C(11)	14(1)	12(1)	13(1)	-1(1)	0(1)	0(1)
C(12)	18(1)	22(1)	14(1)	1(1)	1(1)	2(1)
C(13)	15(1)	12(1)	13(1)	-1(1)	0(1)	-1(1)
C(14)	15(1)	20(1)	16(1)	-6(1)	0(1)	-2(1)
C(15)	17(1)	11(1)	14(1)	1(1)	-1(1)	0(1)
C(16)	16(1)	20(1)	17(1)	-3(1)	1(1)	-2(1)
C(17)	14(1)	14(1)	12(1)	-1(1)	1(1)	0(1)
C(18)	13(1)	12(1)	12(1)	-1(1)	1(1)	0(1)
C(19)	15(1)	16(1)	15(1)	-5(1)	-1(1)	0(1)
C(20)	12(1)	17(1)	20(1)	-1(1)	-2(1)	0(1)
C(21)	14(1)	11(1)	17(1)	0(1)	1(1)	1(1)
C(22)	15(1)	19(1)	18(1)	-2(1)	1(1)	-2(1)
C(23)	15(1)	16(1)	17(1)	-4(1)	0(1)	1(1)

C(24)	14(1)	14(1)	15(1)	-4(1)	-1(1)	1(1)
C(25)	14(1)	12(1)	11(1)	-1(1)	0(1)	1(1)
C(26)	14(1)	12(1)	18(1)	-6(1)	1(1)	-2(1)
C(27)	14(1)	18(1)	30(1)	-5(1)	1(1)	-1(1)
C(28)	18(1)	22(1)	20(1)	-3(1)	6(1)	-4(1)
C(29)	11(1)	12(1)	13(1)	0(1)	-1(1)	1(1)
C(30)	12(1)	14(1)	20(1)	-4(1)	1(1)	1(1)
C(31)	9(1)	13(1)	12(1)	-1(1)	0(1)	-1(1)
C(32)	11(1)	12(1)	14(1)	-3(1)	0(1)	2(1)
C(33)	16(1)	15(1)	14(1)	2(1)	-1(1)	2(1)
C(34)	19(1)	21(1)	21(1)	0(1)	1(1)	-1(1)
C(35)	20(1)	59(2)	29(1)	12(1)	-1(1)	-12(1)
C(36)	16(1)	19(1)	18(1)	-1(1)	0(1)	5(1)
C(37)	22(1)	19(1)	29(1)	-4(1)	-1(1)	-2(1)
C(38)	16(1)	24(1)	18(1)	-2(1)	-4(1)	1(1)
C(39)	20(1)	27(1)	24(1)	1(1)	-6(1)	1(1)
C(40)	13(1)	15(1)	14(1)	0(1)	0(1)	0(1)
C(41)	20(1)	17(1)	18(1)	2(1)	1(1)	-2(1)
C(42)	13(1)	12(1)	16(1)	0(1)	-1(1)	-2(1)
C(43)	14(1)	18(1)	9(1)	-1(1)	-1(1)	1(1)
C(44)	15(1)	17(1)	16(1)	0(1)	-1(1)	-2(1)
C(45)	19(1)	16(1)	19(1)	-4(1)	-2(1)	2(1)
C(46)	15(1)	23(1)	18(1)	-1(1)	2(1)	3(1)
C(47)	18(1)	22(1)	18(1)	2(1)	3(1)	-3(1)
C(48)	19(1)	15(1)	14(1)	1(1)	-1(1)	-1(1)

Table 5. Hydrogen coordinates (x 10^4) and isotropic displacement parameters ($Å^2$x 10^{-3}) for Baran852.

	x	y	z	U(eq)
H(2)	6587	4520	4108	24
H(1)	-569	12163	5272	34
H(2A)	-2164	12899	5668	40
H(3)	-3686	11846	5978	38
H(4)	-3570	10051	5913	34
H(5)	-1932	9295	5531	29
H(7A)	-251	9411	5072	32
H(7B)	-141	10469	4818	32
H(8)	2017	10534	4725	20
H(9A)	3533	10107	5429	20
H(9B)	3394	11220	5215	20
H(10A)	5336	10410	5016	19
H(10B)	4443	10605	4631	19
H(12A)	4247	8453	5350	27
H(12B)	5734	8661	5276	27
H(12C)	5064	7662	5080	27
H(13)	5468	9434	4232	16
H(14A)	7324	9677	4579	20
H(14B)	7220	8572	4807	20
H(16A)	9474	8935	4281	21
H(16B)	9296	8166	3887	21
H(17)	6590	8109	3698	16
H(18)	5537	7268	4426	15
H(19A)	4295	8226	3749	19
H(19B)	4076	7064	3910	19
H(20)	2333	8023	4177	20
H(22A)	2197	8547	5115	20
H(22B)	1397	8795	4714	20
H(23A)	8038	6717	3713	19
H(23B)	7501	6338	4141	19
H(24A)	6021	6312	3413	17
H(24B)	5538	5885	3840	17
H(27A)	9934	4695	3339	25
H(27B)	9151	4239	3732	25
H(28A)	7430	5216	2753	30
H(28B)	8891	5543	2812	30
H(28C)	7778	6272	2984	30
H(29)	5626	4771	3060	15
H(30A)	4660	3762	3760	23
H(30B)	3929	3798	3335	23
H(30C)	4186	4850	3580	23
H(31)	7013	3493	2904	14
H(32)	7570	2800	3555	15
H(33A)	5741	2300	3873	18
H(33B)	6372	1224	3737	18
H(34A)	9958	2297	2568	24
H(34B)	9680	3110	2922	24
H(35A)	11890	2976	2782	54
H(35B)	11860	1780	2915	54
H(35C)	11595	2671	3243	54

H(36A)	9003	249	2578	21
H(36B)	10053	-138	2895	21
H(37A)	8392	-1345	2895	35
H(37B)	7361	-452	2977	35
H(37C)	8361	-763	3323	35
H(38A)	9544	1971	3809	23
H(38B)	8862	863	3822	23
H(39A)	10839	61	3645	36
H(39B)	10942	683	4063	36
H(39C)	11510	1178	3657	36
H(40)	4047	2077	3488	17
H(41A)	4951	-16	3433	28
H(41B)	3503	329	3358	28
H(41C)	4121	436	3800	28
H(42A)	5593	1185	2859	16
H(42B)	4123	1505	2806	16
H(44)	6027	1073	2121	19
H(45)	7818	424	1779	22
H(46)	9452	1551	1576	23
H(47)	9329	3316	1731	24
H(48)	7562	3974	2081	19

Crystal Structure of 2.118

Experimental Summary

The single crystal X-ray diffraction studies were carried out on a Bruker D8-Venture 3-circle diffractometer equipped with a Photon3 detector and Mo K_α radiation (λ = 0.7107 Å).

Crystals of the subject compound were used as received. A 0.24 x 0.24 x 0.1 mm piece of a crystal was mounted on a Cryoloop with Paratone oil. Data were collected in a nitrogen gas stream at 100(2) K using ω scans. Crystal-to-detector distance was 50 mm and exposure time was 1 or 5 seconds depending on the 2θ range per frame using a scan width of 0.70°. Data collection was 99.3 % complete to 25.242° in θ. A total of 44834 reflections were collected covering the indices, −16<=h<=16, −10<=k<=10, −22<=l<=22. 7651 reflections were found to be symmetry independent, with a R_{int} of 0.0566. Indexing and unit cell refinement indicated a **P**rimitive, **Monoclinic** lattice. The space group was found to be ***P*2$_1$**. The data were integrated using the Bruker SAINT Software program and scaled using the SADABS software program. Solution by direct methods (SHELXT) produced a complete phasing model consistent with the proposed structure.

All nonhydrogen atoms were refined anisotropically by full-matrix least-squares (SHELXL-2014). All carbon bonded hydrogen atoms were placed using a riding model. Their positions were constrained relative to their parent atom using the appropriate HFIX command in SHELXL-2014. Crystallographic data are summarized in Table 1.

Notes: Great data! Absolute stereochemistry was conclusively assigned (Absolute Structure Parameter = 0.02(3)). There is one copy of the compound and one copy of THF in the asymmetric unit. The chemical formula for the compound is: $C_{40}H_{51}NO_4S$

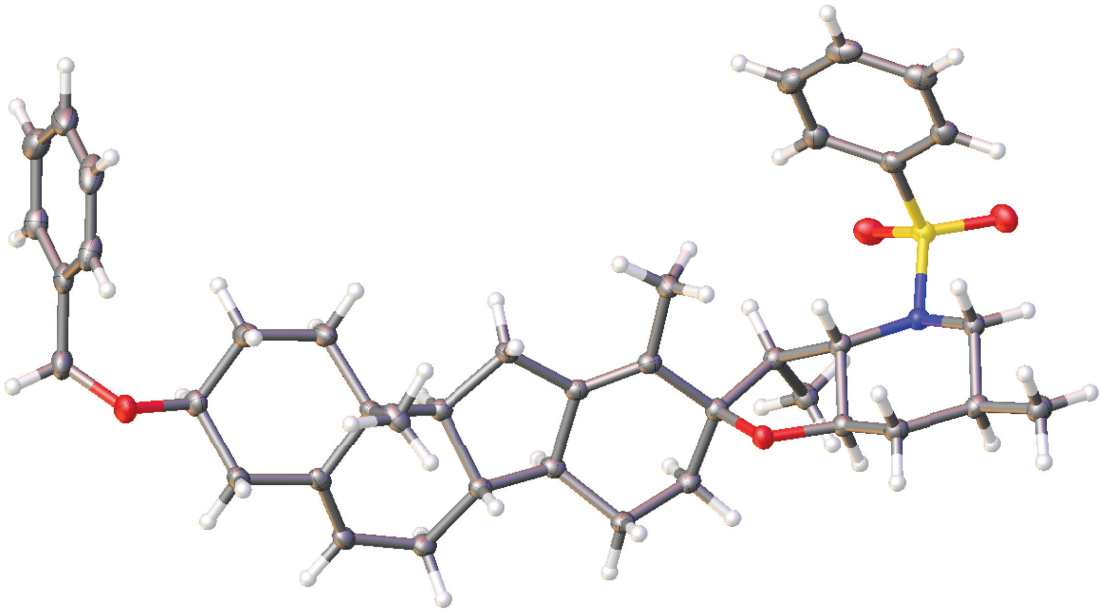


Table 1. Crystal data and structure refinement for Baran859.

Identification code	baran859_0m_a	
Empirical formula	C44 H59 N O5 S	
Formula weight	713.98	
Temperature	100 K	
Wavelength	0.71073 Å	
Crystal system	Monoclinic	
Space group	P 1 21 1	
Unit cell dimensions	a = 12.8896(13) Å	α= 90°.
	b = 8.2945(9) Å	β= 95.520(4)°.
	c = 17.6195(15) Å	γ = 90°.
Volume	1875.0(3) $Å^3$	
Z	2	
Density (calculated)	1.265 Mg/m^3	
Absorption coefficient	0.134 mm^{-1}	
F(000)	772	
Crystal size	0.24 x 0.24 x 0.1 mm^3	
Theta range for data collection	2.716 to 26.490°.	
Index ranges	-16<=h<=16, -10<=k<=10, -22<=l<=22	
Reflections collected	44834	
Independent reflections	7651 [R(int) = 0.0566]	
Completeness to theta = 25.242°	99.3 %	
Absorption correction	Semi-empirical from equivalents	
Max. and min. transmission	0.4908 and 0.4594	
Refinement method	Full-matrix least-squares on F^2	
Data / restraints / parameters	7651 / 1 / 474	
Goodness-of-fit on F^2	1.031	
Final R indices [I>2sigma(I)]	R1 = 0.0319, wR2 = 0.0710	
R indices (all data)	R1 = 0.0365, wR2 = 0.0738	
Absolute structure parameter	0.02(3)	
Largest diff. peak and hole	0.224 and -0.225 $e.Å^{-3}$	

Table 2. Atomic coordinates (x 10^4) and equivalent isotropic displacement parameters ($Å^2$x 10^3) for Baran859. U(eq) is defined as one third of the trace of the orthogonalized U^{ij} tensor.

	x	y	z	U(eq)
S(1)	2424(1)	10607(1)	3964(1)	19(1)
O(1)	8195(1)	1588(2)	10081(1)	27(1)
O(2)	2282(1)	9025(2)	6664(1)	18(1)
O(3)	3468(1)	11144(2)	4168(1)	25(1)
O(4)	1779(1)	11452(2)	3389(1)	26(1)
N(1)	1799(1)	10649(2)	4746(1)	17(1)
C(1)	3814(2)	6701(3)	5987(1)	21(1)
C(2)	3992(2)	7875(3)	6643(1)	17(1)
C(3)	4632(2)	7498(3)	7258(1)	17(1)
C(4)	5190(2)	5895(3)	7402(1)	19(1)
C(5)	5772(2)	6099(3)	8202(1)	17(1)
C(6)	6049(2)	4575(3)	8676(1)	17(1)
C(7)	5099(2)	3465(3)	8715(1)	24(1)
C(8)	6921(2)	3662(3)	8313(1)	23(1)
C(9)	7407(2)	2293(3)	8802(1)	26(1)
C(10)	7844(2)	2896(3)	9582(1)	22(1)
C(11)	9248(2)	1097(3)	10029(1)	29(1)
C(12)	9411(2)	-8(3)	9370(1)	23(1)
C(13)	10315(2)	92(3)	9003(1)	26(1)
C(14)	10487(2)	-922(3)	8399(2)	33(1)
C(15)	9746(2)	-2053(3)	8152(2)	37(1)
C(16)	8849(2)	-2185(3)	8514(2)	37(1)
C(17)	8682(2)	-1191(3)	9124(2)	29(1)
C(18)	7008(2)	3788(3)	9976(1)	21(1)
C(19)	6456(2)	5092(3)	9486(1)	17(1)
C(20)	6326(2)	6581(3)	9749(1)	19(1)
C(21)	5755(2)	7941(3)	9317(1)	20(1)
C(22)	5124(2)	7318(3)	8602(1)	17(1)
C(23)	4817(2)	8541(3)	7966(1)	18(1)
C(24)	3887(2)	9643(3)	8025(1)	19(1)
C(25)	3718(2)	10571(3)	7273(1)	20(1)

C(26)	3383(2)	9459(3)	6599(1)	17(1)
C(27)	3381(2)	10321(3)	5797(1)	18(1)
C(28)	3499(2)	12162(3)	5826(1)	21(1)
C(29)	2305(2)	9778(3)	5420(1)	16(1)
C(30)	2491(2)	8563(3)	3678(1)	20(1)
C(31)	3382(2)	7670(3)	3892(1)	23(1)
C(32)	3436(2)	6076(3)	3658(1)	28(1)
C(33)	2604(2)	5386(3)	3211(1)	30(1)
C(34)	1718(2)	6287(3)	2998(1)	27(1)
C(35)	1652(2)	7884(3)	3231(1)	23(1)
C(36)	690(2)	10116(3)	4584(1)	18(1)
C(37)	61(2)	10303(3)	5271(1)	18(1)
C(38)	-1074(2)	9845(3)	5039(1)	23(1)
C(39)	561(2)	9311(3)	5942(1)	19(1)
C(40)	1661(2)	9927(3)	6099(1)	17(1)
C(1S)	905(3)	3277(5)	7860(2)	66(1)
C(2S)	1892(2)	3647(3)	8357(2)	36(1)
C(3S)	2185(2)	5290(3)	8065(2)	37(1)
C(4S)	1774(2)	5224(4)	7239(2)	40(1)
O(1S)	820(10)	4333(17)	7222(6)	48(3)
O(1S')	1170(20)	3850(30)	7097(9)	44(4)

Table 3. Bond lengths [Å] and angles [°] for Baran859.

S(1)-O(3)	1.4304(16)
S(1)-O(4)	1.4309(16)
S(1)-N(1)	1.6606(17)
S(1)-C(30)	1.774(2)
O(1)-C(10)	1.441(3)
O(1)-C(11)	1.429(3)
O(2)-C(26)	1.480(2)
O(2)-C(40)	1.427(2)
N(1)-C(29)	1.486(3)
N(1)-C(36)	1.498(3)
C(1)-H(1A)	0.9800
C(1)-H(1B)	0.9800
C(1)-H(1C)	0.9800
C(1)-C(2)	1.511(3)
C(2)-C(3)	1.334(3)
C(2)-C(26)	1.528(3)
C(3)-C(4)	1.521(3)
C(3)-C(23)	1.519(3)
C(4)-H(4A)	0.9900
C(4)-H(4B)	0.9900
C(4)-C(5)	1.540(3)
C(5)-H(5)	1.0000
C(5)-C(6)	1.539(3)
C(5)-C(22)	1.528(3)
C(6)-C(7)	1.539(3)
C(6)-C(8)	1.545(3)
C(6)-C(19)	1.533(3)
C(7)-H(7A)	0.9800
C(7)-H(7B)	0.9800
C(7)-H(7C)	0.9800
C(8)-H(8A)	0.9900
C(8)-H(8B)	0.9900
C(8)-C(9)	1.523(3)
C(9)-H(9A)	0.9900

C(9)-H(9B)	0.9900
C(9)-C(10)	1.519(3)
C(10)-H(10)	1.0000
C(10)-C(18)	1.526(3)
C(11)-H(11A)	0.9900
C(11)-H(11B)	0.9900
C(11)-C(12)	1.510(3)
C(12)-C(13)	1.388(3)
C(12)-C(17)	1.397(3)
C(13)-H(13)	0.9500
C(13)-C(14)	1.390(4)
C(14)-H(14)	0.9500
C(14)-C(15)	1.379(4)
C(15)-H(15)	0.9500
C(15)-C(16)	1.378(4)
C(16)-H(16)	0.9500
C(16)-C(17)	1.388(4)
C(17)-H(17)	0.9500
C(18)-H(18A)	0.9900
C(18)-H(18B)	0.9900
C(18)-C(19)	1.517(3)
C(19)-C(20)	1.336(3)
C(20)-H(20)	0.9500
C(20)-C(21)	1.512(3)
C(21)-H(21A)	0.9900
C(21)-H(21B)	0.9900
C(21)-C(22)	1.523(3)
C(22)-H(22)	1.0000
C(22)-C(23)	1.535(3)
C(23)-H(23)	1.0000
C(23)-C(24)	1.519(3)
C(24)-H(24A)	0.9900
C(24)-H(24B)	0.9900
C(24)-C(25)	1.529(3)
C(25)-H(25A)	0.9900
C(25)-H(25B)	0.9900

C(25)-C(26)	1.534(3)
C(26)-C(27)	1.584(3)
C(27)-H(27)	1.0000
C(27)-C(28)	1.535(3)
C(27)-C(29)	1.546(3)
C(28)-H(28A)	0.9800
C(28)-H(28B)	0.9800
C(28)-H(28C)	0.9800
C(29)-H(29)	1.0000
C(29)-C(40)	1.527(3)
C(30)-C(31)	1.388(3)
C(30)-C(35)	1.393(3)
C(31)-H(31)	0.9500
C(31)-C(32)	1.388(4)
C(32)-H(32)	0.9500
C(32)-C(33)	1.392(4)
C(33)-H(33)	0.9500
C(33)-C(34)	1.386(4)
C(34)-H(34)	0.9500
C(34)-C(35)	1.392(3)
C(35)-H(35)	0.9500
C(36)-H(36A)	0.9900
C(36)-H(36B)	0.9900
C(36)-C(37)	1.527(3)
C(37)-H(37)	1.0000
C(37)-C(38)	1.529(3)
C(37)-C(39)	1.532(3)
C(38)-H(38A)	0.9800
C(38)-H(38B)	0.9800
C(38)-H(38C)	0.9800
C(39)-H(39A)	0.9900
C(39)-H(39B)	0.9900
C(39)-C(40)	1.507(3)
C(40)-H(40)	1.0000
C(1S)-H(1SA)	0.9900
C(1S)-H(1SB)	0.9900

C(1S)-H(1SC)	0.9900
C(1S)-H(1SD)	0.9900
C(1S)-C(2S)	1.504(4)
C(1S)-O(1S)	1.422(7)
C(1S)-O(1S')	1.497(18)
C(2S)-H(2SA)	0.9900
C(2S)-H(2SB)	0.9900
C(2S)-C(3S)	1.517(4)
C(3S)-H(3SA)	0.9900
C(3S)-H(3SB)	0.9900
C(3S)-C(4S)	1.500(4)
C(4S)-H(4SA)	0.9900
C(4S)-H(4SB)	0.9900
C(4S)-H(4SC)	0.9900
C(4S)-H(4SD)	0.9900
C(4S)-O(1S)	1.432(7)
C(4S)-O(1S')	1.389(14)

O(3)-S(1)-O(4)	119.59(10)
O(3)-S(1)-N(1)	107.76(9)
O(3)-S(1)-C(30)	107.39(10)
O(4)-S(1)-N(1)	106.37(9)
O(4)-S(1)-C(30)	107.91(10)
N(1)-S(1)-C(30)	107.26(10)
C(11)-O(1)-C(10)	114.87(17)
C(40)-O(2)-C(26)	107.27(15)
C(29)-N(1)-S(1)	116.19(13)
C(29)-N(1)-C(36)	110.28(16)
C(36)-N(1)-S(1)	111.49(13)
H(1A)-C(1)-H(1B)	109.5
H(1A)-C(1)-H(1C)	109.5
H(1B)-C(1)-H(1C)	109.5
C(2)-C(1)-H(1A)	109.5
C(2)-C(1)-H(1B)	109.5
C(2)-C(1)-H(1C)	109.5
C(1)-C(2)-C(26)	118.36(18)

C(3)-C(2)-C(1)	120.4(2)
C(3)-C(2)-C(26)	121.19(19)
C(2)-C(3)-C(4)	125.9(2)
C(2)-C(3)-C(23)	124.7(2)
C(23)-C(3)-C(4)	109.02(17)
C(3)-C(4)-H(4A)	111.0
C(3)-C(4)-H(4B)	111.0
C(3)-C(4)-C(5)	103.78(17)
H(4A)-C(4)-H(4B)	109.0
C(5)-C(4)-H(4A)	111.0
C(5)-C(4)-H(4B)	111.0
C(4)-C(5)-H(5)	106.5
C(6)-C(5)-C(4)	118.32(18)
C(6)-C(5)-H(5)	106.5
C(22)-C(5)-C(4)	104.77(16)
C(22)-C(5)-H(5)	106.5
C(22)-C(5)-C(6)	113.65(17)
C(5)-C(6)-C(7)	111.79(18)
C(5)-C(6)-C(8)	108.48(17)
C(7)-C(6)-C(8)	109.79(19)
C(19)-C(6)-C(5)	108.50(18)
C(19)-C(6)-C(7)	109.23(17)
C(19)-C(6)-C(8)	108.99(17)
C(6)-C(7)-H(7A)	109.5
C(6)-C(7)-H(7B)	109.5
C(6)-C(7)-H(7C)	109.5
H(7A)-C(7)-H(7B)	109.5
H(7A)-C(7)-H(7C)	109.5
H(7B)-C(7)-H(7C)	109.5
C(6)-C(8)-H(8A)	108.8
C(6)-C(8)-H(8B)	108.8
H(8A)-C(8)-H(8B)	107.6
C(9)-C(8)-C(6)	114.01(18)
C(9)-C(8)-H(8A)	108.8
C(9)-C(8)-H(8B)	108.8
C(8)-C(9)-H(9A)	109.4

C(8)-C(9)-H(9B)	109.4
H(9A)-C(9)-H(9B)	108.0
C(10)-C(9)-C(8)	111.28(19)
C(10)-C(9)-H(9A)	109.4
C(10)-C(9)-H(9B)	109.4
O(1)-C(10)-C(9)	111.75(19)
O(1)-C(10)-H(10)	109.3
O(1)-C(10)-C(18)	106.39(17)
C(9)-C(10)-H(10)	109.3
C(9)-C(10)-C(18)	110.74(18)
C(18)-C(10)-H(10)	109.3
O(1)-C(11)-H(11A)	108.5
O(1)-C(11)-H(11B)	108.5
O(1)-C(11)-C(12)	115.15(19)
H(11A)-C(11)-H(11B)	107.5
C(12)-C(11)-H(11A)	108.5
C(12)-C(11)-H(11B)	108.5
C(13)-C(12)-C(11)	120.4(2)
C(13)-C(12)-C(17)	117.9(2)
C(17)-C(12)-C(11)	121.7(2)
C(12)-C(13)-H(13)	119.2
C(12)-C(13)-C(14)	121.5(2)
C(14)-C(13)-H(13)	119.2
C(13)-C(14)-H(14)	120.1
C(15)-C(14)-C(13)	119.8(2)
C(15)-C(14)-H(14)	120.1
C(14)-C(15)-H(15)	120.2
C(16)-C(15)-C(14)	119.6(3)
C(16)-C(15)-H(15)	120.2
C(15)-C(16)-H(16)	119.7
C(15)-C(16)-C(17)	120.7(2)
C(17)-C(16)-H(16)	119.7
C(12)-C(17)-H(17)	119.8
C(16)-C(17)-C(12)	120.5(2)
C(16)-C(17)-H(17)	119.8
C(10)-C(18)-H(18A)	108.8

C(10)-C(18)-H(18B)	108.8
H(18A)-C(18)-H(18B)	107.7
C(19)-C(18)-C(10)	113.58(17)
C(19)-C(18)-H(18A)	108.8
C(19)-C(18)-H(18B)	108.8
C(18)-C(19)-C(6)	115.45(18)
C(20)-C(19)-C(6)	122.58(19)
C(20)-C(19)-C(18)	121.97(19)
C(19)-C(20)-H(20)	117.1
C(19)-C(20)-C(21)	125.90(19)
C(21)-C(20)-H(20)	117.1
C(20)-C(21)-H(21A)	109.4
C(20)-C(21)-H(21B)	109.4
C(20)-C(21)-C(22)	111.06(19)
H(21A)-C(21)-H(21B)	108.0
C(22)-C(21)-H(21A)	109.4
C(22)-C(21)-H(21B)	109.4
C(5)-C(22)-H(22)	109.1
C(5)-C(22)-C(23)	102.37(16)
C(21)-C(22)-C(5)	109.52(17)
C(21)-C(22)-H(22)	109.1
C(21)-C(22)-C(23)	117.37(19)
C(23)-C(22)-H(22)	109.1
C(3)-C(23)-C(22)	103.45(17)
C(3)-C(23)-H(23)	107.8
C(22)-C(23)-H(23)	107.8
C(24)-C(23)-C(3)	109.64(17)
C(24)-C(23)-C(22)	119.84(18)
C(24)-C(23)-H(23)	107.8
C(23)-C(24)-H(24A)	110.3
C(23)-C(24)-H(24B)	110.3
C(23)-C(24)-C(25)	106.95(17)
H(24A)-C(24)-H(24B)	108.6
C(25)-C(24)-H(24A)	110.3
C(25)-C(24)-H(24B)	110.3
C(24)-C(25)-H(25A)	109.2

C(24)-C(25)-H(25B)	109.2
C(24)-C(25)-C(26)	111.98(19)
H(25A)-C(25)-H(25B)	107.9
C(26)-C(25)-H(25A)	109.2
C(26)-C(25)-H(25B)	109.2
O(2)-C(26)-C(2)	106.20(17)
O(2)-C(26)-C(25)	106.69(16)
O(2)-C(26)-C(27)	105.00(16)
C(2)-C(26)-C(25)	111.86(17)
C(2)-C(26)-C(27)	113.02(17)
C(25)-C(26)-C(27)	113.35(18)
C(26)-C(27)-H(27)	109.4
C(28)-C(27)-C(26)	115.35(17)
C(28)-C(27)-H(27)	109.4
C(28)-C(27)-C(29)	112.74(18)
C(29)-C(27)-C(26)	100.19(16)
C(29)-C(27)-H(27)	109.4
C(27)-C(28)-H(28A)	109.5
C(27)-C(28)-H(28B)	109.5
C(27)-C(28)-H(28C)	109.5
H(28A)-C(28)-H(28B)	109.5
H(28A)-C(28)-H(28C)	109.5
H(28B)-C(28)-H(28C)	109.5
N(1)-C(29)-C(27)	120.57(17)
N(1)-C(29)-H(29)	108.3
N(1)-C(29)-C(40)	110.92(16)
C(27)-C(29)-H(29)	108.3
C(40)-C(29)-C(27)	99.91(16)
C(40)-C(29)-H(29)	108.3
C(31)-C(30)-S(1)	119.63(18)
C(31)-C(30)-C(35)	121.0(2)
C(35)-C(30)-S(1)	119.40(18)
C(30)-C(31)-H(31)	120.3
C(30)-C(31)-C(32)	119.5(2)
C(32)-C(31)-H(31)	120.3
C(31)-C(32)-H(32)	120.0

C(31)-C(32)-C(33)	120.1(2)
C(33)-C(32)-H(32)	120.0
C(32)-C(33)-H(33)	119.9
C(34)-C(33)-C(32)	120.1(2)
C(34)-C(33)-H(33)	119.9
C(33)-C(34)-H(34)	119.8
C(33)-C(34)-C(35)	120.4(2)
C(35)-C(34)-H(34)	119.8
C(30)-C(35)-H(35)	120.5
C(34)-C(35)-C(30)	119.0(2)
C(34)-C(35)-H(35)	120.5
N(1)-C(36)-H(36A)	109.0
N(1)-C(36)-H(36B)	109.0
N(1)-C(36)-C(37)	112.89(17)
H(36A)-C(36)-H(36B)	107.8
C(37)-C(36)-H(36A)	109.0
C(37)-C(36)-H(36B)	109.0
C(36)-C(37)-H(37)	108.1
C(36)-C(37)-C(38)	109.33(17)
C(36)-C(37)-C(39)	110.00(17)
C(38)-C(37)-H(37)	108.1
C(38)-C(37)-C(39)	113.17(18)
C(39)-C(37)-H(37)	108.1
C(37)-C(38)-H(38A)	109.5
C(37)-C(38)-H(38B)	109.5
C(37)-C(38)-H(38C)	109.5
H(38A)-C(38)-H(38B)	109.5
H(38A)-C(38)-H(38C)	109.5
H(38B)-C(38)-H(38C)	109.5
C(37)-C(39)-H(39A)	110.5
C(37)-C(39)-H(39B)	110.5
H(39A)-C(39)-H(39B)	108.7
C(40)-C(39)-C(37)	106.14(17)
C(40)-C(39)-H(39A)	110.5
C(40)-C(39)-H(39B)	110.5
O(2)-C(40)-C(29)	101.15(16)

O(2)-C(40)-C(39)	113.87(17)
O(2)-C(40)-H(40)	109.3
C(29)-C(40)-H(40)	109.3
C(39)-C(40)-C(29)	113.68(17)
C(39)-C(40)-H(40)	109.3
H(1SA)-C(1S)-H(1SB)	108.3
H(1SC)-C(1S)-H(1SD)	109.3
C(2S)-C(1S)-H(1SA)	109.8
C(2S)-C(1S)-H(1SB)	109.8
C(2S)-C(1S)-H(1SC)	111.4
C(2S)-C(1S)-H(1SD)	111.4
O(1S)-C(1S)-H(1SA)	109.8
O(1S)-C(1S)-H(1SB)	109.8
O(1S)-C(1S)-C(2S)	109.3(3)
O(1S')-C(1S)-H(1SC)	111.4
O(1S')-C(1S)-H(1SD)	111.4
O(1S')-C(1S)-C(2S)	101.9(9)
C(1S)-C(2S)-H(2SA)	111.3
C(1S)-C(2S)-H(2SB)	111.3
C(1S)-C(2S)-C(3S)	102.1(2)
H(2SA)-C(2S)-H(2SB)	109.2
C(3S)-C(2S)-H(2SA)	111.3
C(3S)-C(2S)-H(2SB)	111.3
C(2S)-C(3S)-H(3SA)	111.2
C(2S)-C(3S)-H(3SB)	111.2
H(3SA)-C(3S)-H(3SB)	109.1
C(4S)-C(3S)-C(2S)	102.7(2)
C(4S)-C(3S)-H(3SA)	111.2
C(4S)-C(3S)-H(3SB)	111.2
C(3S)-C(4S)-H(4SA)	110.7
C(3S)-C(4S)-H(4SB)	110.7
C(3S)-C(4S)-H(4SC)	109.6
C(3S)-C(4S)-H(4SD)	109.6
H(4SA)-C(4S)-H(4SB)	108.8
H(4SC)-C(4S)-H(4SD)	108.1
O(1S)-C(4S)-C(3S)	105.2(4)

O(1S)-C(4S)-H(4SA)	110.7
O(1S)-C(4S)-H(4SB)	110.7
O(1S')-C(4S)-C(3S)	110.2(6)
O(1S')-C(4S)-H(4SC)	109.6
O(1S')-C(4S)-H(4SD)	109.6
C(1S)-O(1S)-C(4S)	107.5(5)
C(4S)-O(1S')-C(1S)	105.7(11)

Symmetry transformations used to generate equivalent atoms:

Table 4. Anisotropic displacement parameters ($Å^2 x\ 10^3$) for Baran859. The anisotropic displacement factor exponent takes the form: $-2\pi^2[\ h^2\ a^{*2}U^{11} + ...\ + 2\ h\ k\ a^*\ b^*\ U^{12}]$

	U^{11}	U^{22}	U^{33}	U^{23}	U^{13}	U^{12}
S(1)	21(1)	19(1)	16(1)	1(1)	4(1)	-2(1)
O(1)	28(1)	32(1)	21(1)	6(1)	1(1)	9(1)
O(2)	16(1)	21(1)	17(1)	3(1)	1(1)	0(1)
O(3)	24(1)	29(1)	24(1)	-1(1)	7(1)	-7(1)
O(4)	33(1)	24(1)	20(1)	6(1)	2(1)	1(1)
N(1)	16(1)	18(1)	16(1)	0(1)	2(1)	1(1)
C(1)	26(1)	18(1)	19(1)	-1(1)	-1(1)	4(1)
C(2)	16(1)	18(1)	18(1)	-2(1)	3(1)	-1(1)
C(3)	16(1)	18(1)	17(1)	-1(1)	4(1)	-1(1)
C(4)	23(1)	19(1)	14(1)	-2(1)	0(1)	3(1)
C(5)	16(1)	18(1)	16(1)	-1(1)	2(1)	-1(1)
C(6)	20(1)	19(1)	13(1)	1(1)	0(1)	0(1)
C(7)	27(1)	24(1)	18(1)	2(1)	-3(1)	-8(1)
C(8)	30(1)	23(1)	16(1)	1(1)	3(1)	5(1)
C(9)	34(1)	23(1)	20(1)	-1(1)	2(1)	8(1)
C(10)	24(1)	23(1)	20(1)	4(1)	1(1)	4(1)
C(11)	24(1)	31(1)	29(1)	0(1)	-7(1)	7(1)
C(12)	21(1)	20(1)	26(1)	5(1)	-4(1)	4(1)
C(13)	23(1)	22(1)	32(1)	5(1)	-2(1)	0(1)
C(14)	32(1)	36(2)	33(1)	5(1)	5(1)	10(1)
C(15)	41(2)	32(1)	34(1)	-7(1)	-9(1)	14(1)
C(16)	32(1)	22(1)	52(2)	-5(1)	-17(1)	3(1)
C(17)	19(1)	24(1)	43(1)	4(1)	-4(1)	2(1)
C(18)	19(1)	28(1)	16(1)	1(1)	0(1)	1(1)
C(19)	15(1)	24(1)	14(1)	2(1)	3(1)	-3(1)
C(20)	17(1)	24(1)	15(1)	-2(1)	-1(1)	-1(1)
C(21)	19(1)	22(1)	19(1)	-5(1)	0(1)	0(1)
C(22)	17(1)	19(1)	16(1)	-2(1)	2(1)	-1(1)
C(23)	18(1)	19(1)	16(1)	-2(1)	1(1)	-3(1)
C(24)	21(1)	18(1)	18(1)	-3(1)	2(1)	0(1)
C(25)	21(1)	17(1)	21(1)	-2(1)	1(1)	2(1)

C(26)	16(1)	17(1)	18(1)	0(1)	2(1)	-1(1)
C(27)	17(1)	18(1)	18(1)	-1(1)	2(1)	0(1)
C(28)	23(1)	20(1)	21(1)	0(1)	-1(1)	-3(1)
C(29)	16(1)	14(1)	18(1)	0(1)	3(1)	0(1)
C(30)	25(1)	21(1)	15(1)	1(1)	6(1)	0(1)
C(31)	22(1)	28(1)	19(1)	2(1)	5(1)	1(1)
C(32)	32(1)	29(1)	24(1)	4(1)	10(1)	8(1)
C(33)	43(1)	22(1)	26(1)	0(1)	16(1)	-2(1)
C(34)	32(1)	28(1)	22(1)	-2(1)	10(1)	-9(1)
C(35)	23(1)	27(1)	20(1)	1(1)	6(1)	-1(1)
C(36)	17(1)	18(1)	18(1)	0(1)	0(1)	0(1)
C(37)	17(1)	17(1)	22(1)	-1(1)	3(1)	1(1)
C(38)	19(1)	24(1)	25(1)	-1(1)	2(1)	1(1)
C(39)	17(1)	20(1)	20(1)	-1(1)	3(1)	-1(1)
C(40)	18(1)	16(1)	16(1)	1(1)	2(1)	1(1)
C(1S)	80(3)	66(2)	46(2)	29(2)	-22(2)	-40(2)
C(2S)	42(2)	35(2)	31(1)	1(1)	-2(1)	4(1)
C(3S)	28(1)	36(2)	47(2)	-1(1)	0(1)	-5(1)
C(4S)	51(2)	35(2)	37(2)	1(1)	13(1)	-7(1)
O(1S)	47(4)	54(5)	38(3)	19(3)	-16(2)	-21(3)
O(1S')	56(10)	39(7)	36(5)	8(5)	-5(5)	-15(6)

Table 5. Hydrogen coordinates (x 10^4) and isotropic displacement parameters ($Å^2$x 10^{-3}) for Baran859.

	x	y	z	U(eq)
H(1A)	3070	6441	5902	32
H(1B)	4212	5713	6109	32
H(1C)	4043	7189	5525	32
H(4A)	5683	5691	7016	23
H(4B)	4685	4994	7394	23
H(5)	6447	6643	8127	20
H(7A)	5285	2568	9063	36
H(7B)	4881	3041	8205	36
H(7C)	4524	4080	8900	36
H(8A)	6630	3215	7816	27
H(8B)	7475	4438	8212	27
H(9A)	6873	1457	8864	31
H(9B)	7974	1793	8542	31
H(10)	8440	3643	9523	26
H(11A)	9503	545	10509	34
H(11B)	9681	2073	9986	34
H(13)	10827	872	9168	31
H(14)	11112	-836	8158	40
H(15)	9854	-2738	7734	44
H(16)	8338	-2965	8344	44
H(17)	8068	-1315	9377	35
H(18A)	6485	2998	10119	25
H(18B)	7336	4283	10451	25
H(20)	6619	6806	10254	23
H(21A)	6265	8750	9173	24
H(21B)	5283	8475	9651	24
H(22)	4481	6775	8751	21
H(23)	5438	9236	7906	21
H(24A)	4026	10399	8457	22
H(24B)	3260	9001	8107	22

H(25A)	4373	11126	7178	24
H(25B)	3177	11404	7315	24
H(27)	3942	9849	5511	21
H(28A)	2932	12631	6086	32
H(28B)	3472	12589	5305	32
H(28C)	4169	12444	6104	32
H(29)	2351	8610	5285	19
H(31)	3949	8145	4196	27
H(32)	4043	5456	3803	34
H(33)	2643	4296	3051	36
H(34)	1152	5812	2692	32
H(35)	1045	8503	3087	27
H(36A)	677	8971	4425	21
H(36B)	354	10757	4154	21
H(37)	81	11464	5424	22
H(38A)	-1114	8702	4898	34
H(38B)	-1348	10503	4603	34
H(38C)	-1489	10037	5468	34
H(39A)	173	9457	6396	23
H(39B)	562	8151	5810	23
H(40)	1643	11082	6261	20
H(1SA)	917	2144	7684	79
H(1SB)	296	3418	8156	79
H(1SC)	751	2108	7854	79
H(1SD)	304	3873	8031	79
H(2SA)	2440	2838	8289	44
H(2SB)	1766	3693	8902	44
H(3SA)	1849	6166	8334	45
H(3SB)	2950	5449	8124	45
H(4SA)	1645	6323	7033	48
H(4SB)	2275	4672	6935	48
H(4SC)	1350	6196	7106	48
H(4SD)	2364	5209	6918	48

Distribution of Credit

Cyclopamine was truly a team effort. At the risk of sounding redundant, I would like to express my gratitude towards my amazing collaborators, Dr. Manolis Sofiadis (M.S.), Anthony J. Rodriguez (A.J.R.), Benedikt Nissl (B.N.), and of course my supervisor Prof. Phil S. Baran (P.S.B.). I would also like to thank my industry collaborators from LEO Pharma, Dr. Lars Jørgensen (L.J.), Dr. Sebastian Clementson (S.C.), and Dr. Nadia Nasser Petersen (N.N.P.). This achievement would certainly not be possible without their insight, creativity, and hard work.

Credit for this project is distributed as follow: the cyclopamine project was initially conceived by P.S.B., L.J. and me. I was responsible for early-stage exploration of the 1st generation route (cross metathesis and enolate addition), whereas M.S. was responsible for the majority of the follow up studies (the β-lactone approach and beyond). I was responsible for the synthesis of the ABC fragment (both the HAT and the phosphonate approaches) for the 2nd generation route as well as the endgame model studies. M.S. was responsible for reproducing and optimizing Taber's approach towards the EF lactone, as well as development of the route from the lactone to the alkyl triflate EF fragment. Scale up of this sequence was performed by M.S. and A.J.R. I developed the endgame sequence of the 2nd generation route based on results from the model studies. A.J.R. was responsible for a pyridine hydrogenation approach that simplified synthesis of the EF lactone (not included in this thesis). I was responsible for the initial screening of the DDCC coupling, but later with extensive assistance from M.S., A.J.R. and B.N. The Prins approach was explored by M.S., A.J.R. and me. M.S. and A.J.R. were also responsible for a number of approaches towards a shorter synthesis of the EF fragment (not included in this thesis).

A.J.R. was responsible for a few potential approaches towards the related natural product jervine (not included in this thesis). With respect to the final route, I was responsible for the synthesis of the ABC fragment, including the simplified synthesis of the benzyl protected decalin intermediate. M.S. and A.J.R. conceived the novel furan-based approach towards the EF fragment. M.S. successfully reproduced and scaled up the AAA reaction with NH_4OAc as an additive. A.J.R. performed optimization and scale up of the aza-Michael step. M.S. and A.J.R. optimized the halocyclization step, and A.J.R. performed the scale up. A.J.R. piloted, optimized, and scaled up the dehalogenation step. M.S. was responsible for methylation of the EF lactone and its elaboration to the enone. Initial studies on the 1,2-addition were performed by M.S. and me, and I was responsible for developing and scaling up the reaction protocol on the real system. The Tsuji-Trost cyclization was optimized by M.S. and me. I was responsible for optimization of the RCM reaction, as well as the final deprotection step with LiDBB. I was responsible for isolation of the final natural product and studying its behavior under different NMR parameters. The manuscript was prepared by P.S.B., M.S., A.J.R. and me, with valuable inputs and suggestions provided by B.N., S.C., and N.N.P.

Dongmin Xu

The Scripps Research Institute, 10550 N. Torrey Pines Rd, La Jolla, CA 92130
Phone: 858-784-8446 | Email: dongminxu@scripps.edu

EDUCATION

- **Scripps Research, San Diego, CA** **08/2018 – present**
  - Graduate student
- **Boston College, Chestnut Hill, MA** **09/2014 – 05/2018**
  - B.S. in Chemistry, *summa cum laude*

RESEARCH EXPERIENCE

- **Graduate Student** **08/2018 – Present**
  - Baran Lab, Department of Chemistry, Scripps Research
- **Undergraduate Research Assistant** **01/2016 – 05/2018**
  - Hoveyda Lab, Chemistry Department, Boston College

PUBLICATIONS

- "Convergent Total Synthesis of (–)-Cyclopamine," Sofiadis, M.[†]; Xu, D.[†]; Rodriguez, A. J.[†]; Nissl, B.; Clementson, S.; Petersen, N. N.; Baran, P.S. *J. Am. Chem. Soc.* **2023**, *145*, 21760-21765.
  [†] These authors contributed equally.
- "Enantiodivergent Formation of C–P Bonds: Synthesis of P-Chiral Phosphines and Methylphosphonate Oligonucleotides," Xu, D.; Rivas-Bascón, N.; Padial, N. M.; Knouse, K. W.; Zheng, B.; Vantourout, J. C.; Schmidt, M. A.; Eastgate, M. D.; Baran, P. S. *J. Am. Chem. Soc.* **2020**, *142*, 5785-5792.
- "*Z*- or *E*-Trisubstituted Allylic Alcohols and Ethers through Kinetically Controlled Cross-Metathesis with a Ru Catechothiolate Complex," Xu, C.; Liu, Z.; Torker, S.; Shen, X.; Xu, D.; Hoveyda, A. H. *J. Am. Chem. Soc.* **2017**, *139*, 15640.
- "Kinetically *E*-Selective Macrocyclic Ring-Closing Metathesis," Shen, X.; Nguyen, T. T.; Koh, M. J.; Xu, D.; Speed, A. W. H.; Schrock, R. R.; Hoveyda, A. H. *Nature* **2017**, *541*, 380.

HONORS AND AWARDS

- **RSC Horizon Prize, 2022 Organic Division** **June 2022**
- **Dean's Fellowship** **August 2018**
  - Graduate Program, Scripps Research
- **Scholar of College** **May 2018**
  - Morrissey College of Arts and Sciences, Boston College
- **The Boston College Excellence in Chemistry Award** **May 2018**
- **Phi Beta Kappa** **May 2018**
- **John Kozarich Summer Undergraduate Research Fellowship** **May 2017**
- **Dean's Scholar** **Apr. 2017**
  - Morrissey College of Arts and Sciences, Boston College
- **Brian Lawrence Gray Prize** **May 2016**
  - Chemistry Department, Boston College
- **Dean's List, First Honors** **2014 – 2018**
  - Morrissey College of Arts and Sciences, Boston College

ProQuest Number: 30813510

INFORMATION TO ALL USERS
The quality and completeness of this reproduction is dependent on the quality
and completeness of the copy made available to ProQuest.



Distributed by ProQuest LLC (2024).
Copyright of the Dissertation is held by the Author unless otherwise noted.

This work may be used in accordance with the terms of the Creative Commons license
or other rights statement, as indicated in the copyright statement or in the metadata
associated with this work. Unless otherwise specified in the copyright statement
or the metadata, all rights are reserved by the copyright holder.

This work is protected against unauthorized copying under Title 17,
United States Code and other applicable copyright laws.

Microform Edition where available © ProQuest LLC. No reproduction or digitization
of the Microform Edition is authorized without permission of ProQuest LLC.

ProQuest LLC
789 East Eisenhower Parkway
P.O. Box 1346
Ann Arbor, MI 48106 - 1346 USA